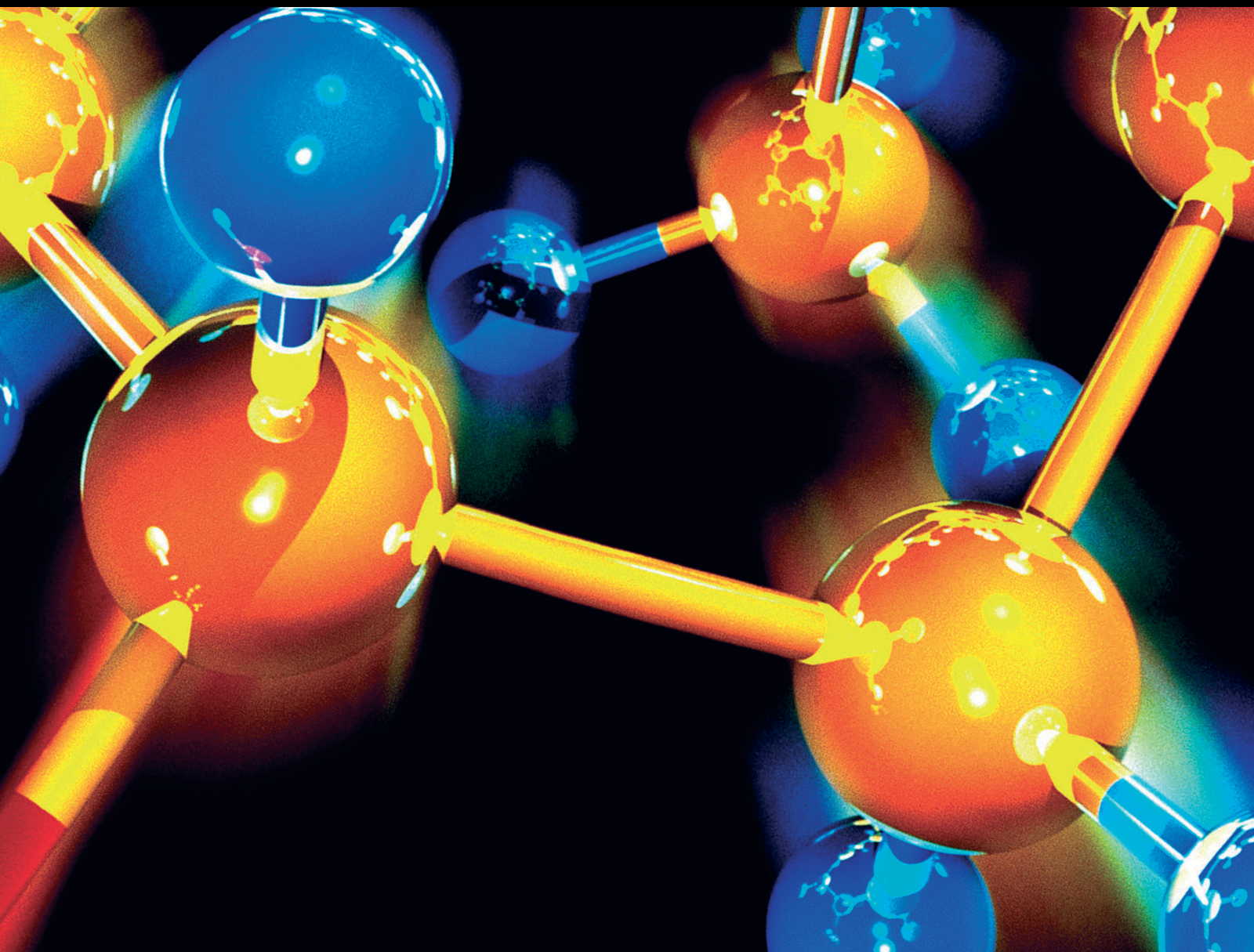


# Application of Molecular Topological Descriptors in Chemistry

Lead Guest Editor: Muhammad Imran

Guest Editors: Syed Ahtsham Ul Haq Bokhary and Muhammad Kamran Jamil





---

# **Application of Molecular Topological Descriptors in Chemistry**

# **Application of Molecular Topological Descriptors in Chemistry**

Lead Guest Editor: Muhammad Imran

Guest Editors: Syed Ahtsham Ul Haq Bokhary and  
Muhammad Kamran Jamil



---

Copyright © 2022 Hindawi Limited. All rights reserved.

This is a special issue published in "Journal of Chemistry." All articles are open access articles distributed under the Creative Commons Attribution License, which permits unrestricted use, distribution, and reproduction in any medium, provided the original work is properly cited.

# Chief Editor

Kaustubha Mohanty, India

## Associate Editors

Mohammad Al-Ghouthi, Qatar

Tingyue Gu , USA

Teodorico C. Ramalho , Brazil

Artur M. S. Silva , Portugal

## Academic Editors

Jinwei Duan, China

Luqman C. Abdullah , Malaysia

Dr Abhilash , India

Amitava Adhikary, USA

Amitava Adhikary , USA

Mozhgan Afshari, Iran

Daryoush Afzali , Iran

Mahmood Ahmed, Pakistan

Islam Al-Akraa , Egypt

Juan D. Alché , Spain

Gomaa A. M. Ali , Egypt

Mohd Sajid Ali , Saudi Arabia

Shafaqat Ali , Pakistan

Patricia E. Allegretti , Argentina

Marco Anni , Italy

Alessandro Arcovito, Italy

Hassan Arida , Saudi Arabia

Umair Ashraf, Pakistan

Narcis Avarvari , France

Davut Avci , Turkey

Chandra Azad , USA

Mohamed Azaroual, France

Rasha Azzam , Egypt

Hassan Azzazy , Egypt

Renal Backov, France

Suresh Kannan Balasingam , Republic of Korea

Sukanta Bar , USA

Florent Barbault , France

Maurizio Barbieri , Italy

James Barker , United Kingdom

Salvatore Barreca , Italy

Jorge Barros-Velázquez , Spain

THANGAGIRI Baskaran , India

Haci Baykara, Ecuador

Michele Benedetti, Italy

Laurent Billon, France

Marek Biziuk, Poland

Jean-Luc Blin , France

Tomislav Bolanca , Croatia

Ankur Bordoloi , India

Cato Brede , Norway

Leonid Breydo , USA

Wybren J. Buma , The Netherlands

J. O. Caceres , Spain

Patrizia Calaminici , Mexico

Claudio Cameselle , Spain

Joaquin Campos , Spain

Dapeng Cao , China

Domenica Capasso , Italy

Stefano Caporali , Italy

Zenilda Cardeal , Brazil

Angela Cardinali , Italy

Stefano Carli , Italy

Maria F. Carvalho , Portugal

Susana Casal , Portugal

David E. Chavez, USA

Riccardo Chelli , Italy

Zhongfang Chen , Puerto Rico

Vladislav Chrastny , Czech Republic

Roberto Comparelli , Italy

Filomena Conforti , Italy

Luca Conti , Italy

Christophe Coquelet, France

Filomena Corbo , Italy

Jose Corchado , Spain

Maria N. D.S. Cordeiro , Portugal

Claudia Crestini, Italy

Gerald Culioli , France

Nguyen Duc Cuong , Vietnam

Stefano D'Errico , Italy

Matthias D'hooghe , Belgium

Samuel B. Dampare, Ghana

Umashankar Das, Canada

Victor David, Romania

Annalisa De Girolamo, Italy

Antonio De Lucas-Consuegra , Spain

Marcone A. L. De Oliveira , Brazil

Paula G. De Pinho , Portugal

Damião De Sousa , Brazil

Francisco Javier Deive , Spain

Tianlong Deng , China

Fatih Deniz , Turkey  
Claudio Di Iaconi, Italy  
Irene Dini , Italy  
Daniele Dondi, Italy  
Yingchao Dong , China  
Dennis Douroumis , United Kingdom  
John Drexler, USA  
Qizhen Du, China  
Yuanyuan Duan , China  
Philippe Dugourd, France  
Frederic Dumur , France  
Grégory Durand , France  
Mehmet E. Duru, Turkey  
Takayuki Ebata , Japan  
Arturo Espinosa Ferao , Spain  
Valdemar Esteves , Portugal  
Cristina Femoni , Italy  
Gang Feng, China  
Dieter Fenske, Germany  
Jorge F. Fernandez-Sanchez , Spain  
Alberto Figoli , Italy  
Elena Forte, Italy  
Sylvain Franger , France  
Emiliano Fratini , Italy  
Franco Frau , Italy  
Bartolo Gabriele , Italy  
Guillaume Galliero , France  
Andrea Gambaro , Italy  
Vijay Kumar Garlapati, India  
James W. Gauld , Canada  
Barbara Gawdzik , Poland  
Pier Luigi Gentili , Italy  
Beatrice Giannetta , Italy  
Dimosthenis L. Giokas , Greece  
Alejandro Giorgetti , Italy  
Alexandre Giuliani , France  
Elena Gomez , Spain  
Yves Grohens, France  
Katharina Grupp, Germany  
Luis F. Guido , Portugal  
Maolin Guo, USA  
Wenshan Guo , Australia  
Leena Gupta , India  
Muhammad J. Habib, USA  
Jae Ryang Hahn, Republic of Korea

Christopher G. Hamaker , USA  
Ashanul Haque , Saudi Arabia  
Yusuke Hara, Japan  
Naoki Haraguchi, Japan  
Serkos A. Haroutounian , Greece  
Rudi Hendra , Indonesia  
Javier Hernandez-Borges , Spain  
Miguel Herrero, Spain  
Mark Hoffmann , USA  
Hanmin Huang, China  
Doina Humelnicu , Romania  
Charlotte Hurel, France  
Nenad Ignjatović , Serbia  
Ales Imramovsky , Czech Republic  
Muhammad Jahangir, Pakistan  
Philippe Jeandet , France  
Sipak Joyasawal, USA  
Sławomir M. Kaczmarek, Poland  
Ewa Kaczorek, Poland  
Mostafa Khajeh, Iran  
Srećko I. Kirin , Croatia  
Anton Kokalj , Slovenia  
Sevgi Kolaylı , Turkey  
Takeshi Kondo , Japan  
Christos Kordulis, Greece  
Ioannis D. Kostas , Greece  
Yiannis Kourkoutas , Greece  
Henryk Kozłowski, Poland  
Yoshihiro Kudo , Japan  
Avvaru Praveen Kumar , Ethiopia  
Dhanaji Lade, USA  
Isabel Lara , Spain  
Jolanta N. Latosinska , Poland  
João Paulo Leal , Portugal  
Woojin Lee, Kazakhstan  
Yuan-Pern Lee , Taiwan  
Matthias Lein , New Zealand  
Huabing Li, China  
Jinan Li , USA  
Kokhwa Lim , Singapore  
Teik-Cheng Lim , Singapore  
Jianqiang Liu , China  
Xi Liu , China  
Xinyong Liu , China  
Zhong-Wen Liu , China

Eulogio J. Llorent-Martínez , Spain  
Pasquale Longo , Italy  
Pablo Lorenzo-Luis , Spain  
Zhang-Hui Lu, China  
Devanand Luthria, USA  
Konstantin V. Luzyanin , United Kingdom  
Basavarajaiah S M, India  
Mari Maeda-Yamamoto , Japan  
Isabel Mafra , Portugal  
Dimitris P. Makris , Greece  
Pedro M. Mancini, Argentina  
Marcelino Maneiro , Spain  
Giuseppe F. Mangiatordi , Italy  
Casimiro Mantell , Spain  
Carlos A Martínez-Huitle , Brazil  
José M. G. Martinho , Portugal  
Andrea Mastinu , Italy  
Cesar Mateo , Spain  
Georgios Matthaiolampakis, USA  
Mehrab Mehrvar, Canada  
Saurabh Mehta , India  
Oinam Romesh Meitei , USA  
Saima Q. Memon , Pakistan  
Morena Miciaccia, Italy  
Maurice Millet , France  
Angelo Minucci, Italy  
Liviu Mitu , Romania  
Hideto Miyabe , Japan  
Ahmad Mohammad Alakraa , Egypt  
Kaustubha Mohanty, India  
Subrata Mondal , India  
José Morillo, Spain  
Giovanni Morrone , Italy  
Ahmed Mourran, Germany  
Nagaraju Mupparapu , USA  
Markus Muschen, USA  
Benjamin Mwashote , USA  
Mallikarjuna N. Nadagouda , USA  
Lutfun Nahar , United Kingdom  
Kamala Kanta Nanda , Peru  
Senthilkumar Nangan, Thailand  
Mu. Naushad , Saudi Arabia  
Gabriel Navarrete-Vazquez , Mexico  
Jean-Marie Nedelec , France  
Sridhar Goud Nerella , USA  
Nagatoshi Nishiwaki , Japan  
Tzortzis Nomikos , Greece  
Beatriz P. P. Oliveira , Portugal  
Leonardo Palmisano , Italy  
Mohamed Afzal Pasha , India  
Dario Pasini , Italy  
Angela Patti , Italy  
Massimiliano F. Peana , Italy  
Andrea Penoni , Italy  
Franc Perdih , Slovenia  
Jose A. Pereira , Portugal  
Pedro Avila Pérez , Mexico  
Maria Grazia Perrone , Italy  
Silvia Persichilli , Italy  
Thijs A. Peters , Norway  
Christophe Petit , France  
Marinos Pitsikalis , Greece  
Rita Rosa Plá, Argentina  
Fabio Polticelli , Italy  
Josefina Pons, Spain  
V. Prakash Reddy , USA  
Thathan Premkumar, Republic of Korea  
Maciej Przybyłek , Poland  
María Quesada-Moreno , Germany  
Maurizio Quinto , Italy  
Franck Rabilloud , France  
C.R. Raj, India  
Sanchayita Rajkhowa , India  
Manzoor Rather , India  
Enrico Ravera , Italy  
Julia Revuelta , Spain  
Muhammad Rizwan , Pakistan  
Manfredi Rizzo , Italy  
Maria P. Robalo , Portugal  
Maria Roca , Spain  
Nicolas Roche , France  
Samuel Rokhum , India  
Roberto Romeo , Italy  
Antonio M. Romerosa-Nievas , Spain  
Arpita Roy , India  
Eloy S. Sanz P rez , Spain  
Nagaraju Sakkani , USA  
Diego Sampedro , Spain  
Shengmin Sang , USA

Vikram Sarpe , USA  
Adrian Saura-Sanmartin , Spain  
Stéphanie Sayen, France  
Ewa Schab-Balcerzak , Poland  
Hartwig Schulz, Germany  
Gulaim A. Seisenbaeva , Sweden  
Serkan Selli , Turkey  
Murat Senturk , Turkey  
Beatrice Severino , Italy  
Sunil Shah Shah , USA  
Ashutosh Sharma , USA  
Hideaki Shirota , Japan  
Cláudia G. Silva , Portugal  
Ajaya Kumar Singh , India  
Vijay Siripuram, USA  
Ponnurengam Malliappan Sivakumar ,  
Japan  
Tomás Sobrino , Spain  
Raquel G. Soengas , Spain  
Yujiang Song , China  
Olivier Soppera, France  
Radhey Srivastava , USA  
Vivek Srivastava, India  
Theocharis C. Stamatatos , Greece  
Athanasios Stavrakoudis , Greece  
Darren Sun, Singapore  
Arun Suneja , USA  
Kamal Swami , USA  
B.E. Kumara Swamy , India  
Elad Tako , USA  
Shoufeng Tang, China  
Zhenwei Tang , China  
Vijai Kumar Reddy Tangadanchu , USA  
Franco Tassi, Italy  
Alexander Tatarinov, Russia  
Lorena Tavano, Italy  
Tullia Tedeschi, Italy  
Vinod Kumar Tiwari , India  
Augusto C. Tome , Portugal  
Fernanda Tonelli , Brazil  
Naoki Toyooka , Japan  
Andrea Trabocchi , Italy  
Philippe Trens , France  
Ekaterina Tsipis, Russia  
Esteban P. Urriolabeitia , Spain

Toyonobu Usuki , Japan  
Giuseppe Valacchi , Italy  
Ganga Reddy Velma , USA  
Marco Viccaro , Italy  
Jaime Villaverde , Spain  
Marc Visseaux , France  
Balaga Viswanadham , India  
Alessandro Volonterio , Italy  
Zoran Vujcic , Serbia  
Chun-Hua Wang , China  
Leiming Wang , China  
Carmen Wängler , Germany  
Wieslaw Wiczowski , Poland  
Bryan M. Wong , USA  
Frank Wuest, Canada  
Yang Xu, USA  
Dharmendra Kumar Yadav , Republic of  
Korea  
Maria C. Yebra-Biurrún , Spain  
Dr Nagesh G Yernale, India  
Tomokazu Yoshimura , Japan  
Maryam Yousaf, China  
Sedat Yurdakal , Turkey  
Shin-ichi Yusa , Japan  
Claudio Zaccone , Italy  
Ronen Zangi, Spain  
John CG Zhao , USA  
Zhen Zhao, China  
Antonio Zizzi , Italy  
Mire Zloh , United Kingdom  
Grigoris Zoidis , Greece  
Deniz ŞAHİN , Turkey

## Contents

### **Degree-Based Topological Indices and QSPR Analysis of Antituberculosis Drugs**

Mr. Adnan , Syed Ahtsham Ul Haq Bokhary , Ghulam Abbas, and Tanveer Iqbal 

Research Article (17 pages), Article ID 5748626, Volume 2022 (2022)

### **Study of Vanadium Carbide Structures Based on $V_e$ and $E_v$ -Degree Topological Indices**

Abdul Rauf , Saba Maqbool, Muhammad Naeem , Adnan Aslam , Hamideh Aram, and Kraidi Anoh Yannick 

Research Article (12 pages), Article ID 7189918, Volume 2021 (2021)

### **On Wiener Polarity Index and Wiener Index of Certain Triangular Networks**

Mr. Adnan, Syed Ahtsham Ul Haq Bokhary , and Muhammad Imran 

Research Article (20 pages), Article ID 2757925, Volume 2021 (2021)

### **Computation of Polynomial Degree-Based Topological Descriptors of Indu-Bala Product of Two Paths**

Ghazanfar Abbas  and Muhammad Ibrahim 

Research Article (19 pages), Article ID 6281596, Volume 2021 (2021)

### **Computing the Hosoya Polynomial of $M$ -th Level Wheel and Its Subdivision Graph**

Peng Xu , Muhammad Numan, Aamra Nawaz, Saad Ihsan Butt , Adnan Aslam , and Asfand Fahad 

Research Article (7 pages), Article ID 1078792, Volume 2021 (2021)

### **The Second Hyper-Zagreb Coindex of Chemical Graphs and Some Applications**

Ahmed Ayache , Abdu Alameri , Mohammed Alsharafi , and Hanan Ahmed 

Research Article (8 pages), Article ID 3687533, Volume 2021 (2021)

### **Vertex-Based Topological Indices of Double and Strong Double Graph of Dutch Windmill Graph**

Muhammad Asad Ali, Muhammad Shoaib Sardar , Imran Siddique , and Dalal Alrowaili 

Review Article (12 pages), Article ID 7057412, Volume 2021 (2021)

### **Eccentricity-Based Topological Invariants of Dominating David-Derived Networks**

Muhammad Imran , Mian Muhammad Zobair , and Hani Shaker 

Research Article (10 pages), Article ID 8944080, Volume 2021 (2021)

### **Topological Descriptors on Some Families of Graphs**

Iftikhar Ahmad , Maqbool Ahmad Chaudhry, Muhammad Hussain , and Tariq Mahmood

Research Article (12 pages), Article ID 6018893, Volume 2021 (2021)

### **Topological Descriptors of $M$ -Carbon $M[r, s, t]$**

Hong Yang  and Muhammad Naeem 

Research Article (14 pages), Article ID 8792585, Volume 2021 (2021)

**Comparing Zinc Oxide- and Zinc Silicate-Related Metal-Organic Networks via Connection-Based Zagreb Indices**

Muhammad Tanveer Hussain, Muhammad Javaid , Usman Ali, Ali Raza, and Md Nur Alam   
Research Article (16 pages), Article ID 5066394, Volume 2021 (2021)

**Forgotten Coindex for the Derived Sum Graphs under Cartesian Product**

Muhammad Ibraheem, Meshari M. Aljohani, Muhammad Javaid , and Abdulaziz Mohammed Alanazi   
Research Article (13 pages), Article ID 3235068, Volume 2021 (2021)

**Novel Degree-Based Topological Descriptors of Carbon Nanotubes**

M. C. Shanmukha, A. Usha, M. K. Siddiqui, K. C. Shilpa, and A. Asare-Tuah   
Research Article (15 pages), Article ID 3734185, Volume 2021 (2021)

**On Analysis of Topological Properties for Terbium IV Oxide via Enthalpy and Entropy Measurements**

Muhammad Kamran Siddiqui , Sana Javed, Lubna Sherin, Sadia Khalid, Muhammad Mathar Bashir, Amir Hassan, and Mlamuli Dhlamini   
Research Article (16 pages), Article ID 5351776, Volume 2021 (2021)

**Molecular Descriptor Analysis of Certain Isomeric Natural Polymers**

Maqsood Ahmad, Muhammad Saeed , Muhammad Javaid , and Ebenezer Bonyah   
Research Article (26 pages), Article ID 9283246, Volume 2021 (2021)

**Study of Generalized Hourglass Section in Carbon Nanocone via Connection Number**

Muhammad Mubashar , Muhammad Hussain , Fatimah Abdulrahman Alrawajeh , and Sultan Almotairi   
Research Article (8 pages), Article ID 7311757, Volume 2021 (2021)

**On Degree-Based Topological Indices for Strong Double Graphs**

Muhammad Rafiullah , Hafiz Muhammad Afzal Siddiqui , Muhammad Kamran Siddiqui, and Mlamuli Dhlamini   
Research Article (12 pages), Article ID 4852459, Volume 2021 (2021)

**Study of Hardness of Superhard Crystals by Topological Indices**

Xiujun Zhang , Muhammad Naeem , Abdul Qudair Baig , and Manzoor Ahmad Zahid   
Research Article (10 pages), Article ID 9604106, Volume 2021 (2021)

**On Analysis and Computation of Degree-Based Topological Invariants for Cyclic Mesh Network**

Nida Zahra, Muhammad Ibrahim, Muhammad Kamran Siddiqui, and Hajar Shooshtri   
Research Article (8 pages), Article ID 1290881, Volume 2021 (2021)

## Research Article

# Degree-Based Topological Indices and QSPR Analysis of Antituberculosis Drugs

Mr. Adnan <sup>1,2</sup> Syed Ahtsham Ul Haq Bokhary <sup>1</sup> Ghulam Abbas,<sup>1</sup> and Tanveer Iqbal <sup>1,3</sup>

<sup>1</sup>Centre for Advanced Studies in Pure and Applied Mathematics, Bahauddin Zakariya University, Multan, Pakistan

<sup>2</sup>Allama Iqbal Open University, Islamabad, Pakistan

<sup>3</sup>Emersen University, Multan, Pakistan

Correspondence should be addressed to Syed Ahtsham Ul Haq Bokhary; [sihtsham@gmail.com](mailto:sihtsham@gmail.com)

Received 18 August 2021; Revised 25 December 2021; Accepted 5 February 2022; Published 25 February 2022

Academic Editor: Ajaya Kumar Singh

Copyright © 2022 Mr. Adnan et al. This is an open access article distributed under the Creative Commons Attribution License, which permits unrestricted use, distribution, and reproduction in any medium, provided the original work is properly cited.

A topological index of graph  $G$  is a numerical quantity which describes its topology. If it is applied to molecular structure of a chemical compounds, then it reflects the theoretical properties of the chemical compounds. In this paper, well-known degree-based topological indices are applied on chemical structures of antituberculosis drugs. Chemical structure is considered as graph, where elements are taken as vertices and bounds between them are taken as edges. Furthermore, QSPR analysis of the said topological indices are discussed, and it is shown that these topological indices are highly correlated with the physical properties of antituberculosis drugs. This theoretical analysis may help the chemist and people working in pharmaceutical industry to predict properties of antituberculosis drugs without experimenting.

## 1. Introduction

Before discovery/invention of antibiotics, lives of humans and animals were on great threat of being infected by some bacteria. In previous century, different bacterial infections were the most common causes of death until Alexander Flemings discovered Penicillin in 1929, the first antibiotic which was introduced to the world in 1940.

Tuberculosis (TB) is a contagious infection caused by bacteria “*Mycobacterium tuberculosis*” that usually attacks lungs. It can also spread to other parts of body, like brain and spine.

A molecular graph is a representation of the structural formula of a chemical compound in terms of graph theory, whose vertices correspond to the atoms of the compound and edges correspond to chemical bonds between atoms. *Cheminformatics* is a new subject which is a combination of chemistry, mathematics, and information science. It studies quantitative structure-activity (QSAR) and structure-property (QSPR) relationships that are used to predict the biological activities and properties of different chemical compounds. The molecular topological indices or simply the topological indices are used in chemistry. Wiener was the

first who first showed that the Wiener index number is closely correlated with the boiling points of alkane molecules [18]. Later, work on quantitative structure-activity relationships showed that it is also correlated with other quantities including the parameters of its critical point [16], density, surface tension, viscosity of its liquid phase [14], and the van der Waals surface area of the molecule [10]. In the QSAR/QSPR study, physico-chemical properties and topological indices are used to predict bioactivity of the chemical compounds. In this work, it is shown that no single topological index exists that correlates with all the physical properties of chemical compounds.

A graph  $G(V, E)$  with vertex set  $V(G)$  and edge set  $E(G)$  is connected if there exists a connection between any pair of vertices in  $G$ . The distance between two vertices  $u$  and  $v$  is denoted as  $d(u, v) = d_G(u, v)$  and is defined as the length of shortest path between  $u$  and  $v$  in graph  $G$ . The number of vertices of  $G$  adjacent to a given vertex  $v$  is the “degree” of this vertex and will be denoted by  $d_v(G)$  or if misunderstanding is not possible simply by  $d_v$ . The concept of degree is somewhat closely related to the concept of valence in chemistry.

Some of the degree-based topological indices which we use in this work are defined as follows.

*Definition 1.* ABC index is proposed by Estrada et al. in [7], as

$$ABC(G) = \sum_{e=uv \in E(G)} \sqrt{\frac{d_u + d_v - 2}{d_u d_v}}. \quad (1)$$

*Definition 2.* The Randić index is proposed by Milan Randić in [13], as

$$R(G) = \sum_{e=uv \in E(G)} \sqrt{\frac{1}{d_u d_v}}. \quad (2)$$

*Definition 3.* The sum connectivity index is proposed by Zhou and Trinajstić in [19], as

$$S(G) = \sum_{e=uv \in E(G)} \sqrt{\frac{1}{d_u + d_v}}. \quad (3)$$

*Definition 4.* The GA index is proposed by Vukicević et al. in [17], as

$$GA(G) = \sum_{e=uv \in E(G)} \frac{2\sqrt{d_u d_v}}{d_u + d_v}. \quad (4)$$

*Definition 5.* The first and second Zagreb indices are proposed by Gutman and Trinajstić in [11], as

$$\begin{aligned} M_1(G) &= \sum_{e=uv \in E(G)} (d_u + d_v), \\ M_2(G) &= \sum_{e=uv \in E(G)} (d_u d_v). \end{aligned} \quad (5)$$

*Definition 6.* The Harmonic index is proposed by Fajtlowicz et al. in [9], as

$$H(G) = \sum_{e=uv \in E(G)} \frac{2}{d_u + d_v}. \quad (6)$$

*Definition 7.* The hyper-Zagreb index is proposed by Shirdel et al. in [15], as

$$HM(G) = \sum_{e=uv \in E(G)} (d_u + d_v)^2. \quad (7)$$

*Definition 8.* The third Zagreb index is proposed by Fath-Tabar et al. in [1], as

$$ZG_3(G) = \sum_{e=uv \in E(G)} |d_u - d_v|. \quad (8)$$

*Definition 9.* The forgotten index is proposed by Furtula et al. in [8], as

$$F(G) = \sum_{e=uv \in E(G)} [(d_u)^2 + (d_v)^2]. \quad (9)$$

*Definition 10.* The symmetric division index is proposed in [2], as

$$SSD(G) = \sum_{e=uv \in E(G)} \left[ \frac{P}{Q} + \frac{Q}{P} \right], \quad (10)$$

where  $P = \min[d_u, d_v]$  and  $Q = \max[d_u, d_v]$ .

Some of the work in this area can be seen in [3–6, 12].

## 2. Results and Discussion

The above defined 11 topological indices are used for the modeling of six physical properties: boiling point (BP), enthalpy of vaporization (E), flash point (F), molar refractivity (MR), molar volume (MV), and polarizability (P) of 15 antituberculosis drugs: amikacin, bedaquiline, clofazimine, delamanid, ethambutol, ethionamide, imipenem-cilastatin, isoniazid, levofloxacin, linezolid, moxifloxacin, p-aminosalicylic acid, pyrazinamide, rifampin, and terizidone.

*2.1. Regression Models.* The following equation is used to correlate the various physical properties of various drugs used for the treatment of tuberculosis with some topological indices. We have used the following linear regression model:

$$P = A + b[TI], \quad (11)$$

where  $P$  is physical property of drug,  $A$  is constant,  $b$  is regression coefficient, and  $TI$  is topological index. Constant  $A$  and regression coefficient  $b$  is calculated from SPSS software for seven physical properties and eleven degree-based topological indices of molecular structure of fourteen drugs. Using equation (11), following are the linear regression model for the defined degree-based topological indices:

- (1) Regression models for atom bond connectivity index:  $ABC(G)$ 
  - Boiling point =  $142.94 + 19.699[ABC(G)]$
  - Enthalpy =  $38.04 + 2.605[ABC(G)]$
  - Flash point =  $67.648 + 11.254[ABC(G)]$
  - Molar refraction =  $1.797 + 4.588[ABC(G)]$
  - Molar volume =  $8.698 + 12.686[ABC(G)]$
  - Polarizability =  $0.685 + 1.82[ABC(G)]$
- (2) Regression models for Randić index:  $R(G)$ 
  - Boiling point =  $124.752 + 33.178[R(G)]$
  - Enthalpy =  $35.127 + 4.424[R(G)]$
  - Flash point =  $59.012 + 18.814[R(G)]$
  - Molar refraction =  $-2.76 + 7.757[R(G)]$
  - Molar volume =  $-5.066 + 21.541[R(G)]$
  - Polarizability =  $-1.122 + 3.077[R(G)]$

TABLE 1: Physical properties of drugs used for the treatment of tuberculosis.

Name of medicine	Boiling point	Melting point	Flash point	Enthalpy of vaporization	Molar refractivity	Polarizability	Surface tension	Molar volume
Amikacin	981.8	203.5	547.6	162.2	134.9	53.5	103.3	363.9
Bedaquiline	702.7	176	378.8	108	156.2	61.9	52.6	420.1
Clofazimine	566.9	210	296.7	85.1	136.2	54	47.1	366.1
Delamanid	653.7	193	349.1	96.3	127.7	50.6	50	368
Ethambutol	345.3	89	113.7	68.3	58.6	23.2	38.1	207
Ethionamide	247.9	163	103.7	46.5	49	19.4	39.8	142
Imipenem-cilastatin	530.2		274.5	92.7	72.7	28.8	71	183.9
Isoniazid	251.97	172	251		36.9	14.6	57.8	110.2
Levofloxacin	571.5	224	299.4	90.1	91.1	36.1	70.3	244
Linezolid	585.5	177	307.9	87.5	83	32.9	47.7	259
Moxifloxacin	636	270	338.7	98.8	101.8	40.4	60.6	285
p-Aminosalicylic acid	380.8	145	184.1	66.3	39.3	15.6	83.4	102.7
Pyrazinamide	173.3	190	119.1	54.1	31.9	12.6	60.7	87.7
Rifampin	937.4	183	561.3	153.5	213.1	84.5	48	611.7
Terizidone		175			76.1	30.2	62.5	198.9

Physical properties are taken from ChemSpider.

(3) . Regression models for sum-connectivity index.

$S(G)$

$$\text{Boiling point} = 133.839 + 31.497[S(G)]$$

$$\text{Enthalpy} = 36.755 + 4.169[S(G)]$$

$$\text{Flash point} = 63.724 + 17.895[S(G)]$$

$$\text{Molar refraction} = -0.81 + 7.373[S(G)]$$

$$\text{Molar volume} = 1.064 + 20.419[S(G)]$$

$$\text{Polarizability} = -0.348 + 2.925[S(G)]$$

(4) Regression models for geometric-arithmetic index ( $GA(G)$ )

$$\text{Boiling point} = 197.225 + 14.102[GA(G)]$$

$$\text{Enthalpy} = 45.041 + 1.89[GA(G)]$$

$$\text{Flash point} = 97.24 + 8.114[GA(G)]$$

$$\text{Molar refraction} = 21.849 + 3.067[GA(G)]$$

$$\text{Molar volume} = 60.81 + 8.621[GA(G)]$$

$$\text{Polarizability} = 8.648 + 1.216[GA(G)]$$

(5) Regression models for first Zagreb index:  $M_1(G)$

$$\text{Boiling point} = 159.511 + 2.802[M_1(G)]$$

$$\text{Enthalpy} = 40.359 + 0.37[M_1(G)]$$

$$\text{Flash point} = 75.639 + 1.611[M_1(G)]$$

$$\text{Molar refraction} = 4.118 + 0.664[M_1(G)]$$

$$\text{Molar volume} = 15.714 + 1.3[M_1(G)]$$

$$\text{Polarizability} = 1.606 + 0.264[M_1(G)]$$

(6) Regression models for second Zagreb index:  $M_2(G)$

$$\text{Boiling point} = 176.377 + 2.294[M_2(G)]$$

$$\text{Enthalpy} = 42.366 + 0.304[M_2(G)]$$

$$\text{Flash point} = 85.303 + 1.32[M_2(G)]$$

$$\text{Molar refraction} = 11.967 + 0.52[M_2(G)]$$

$$\text{Molar volume} = 37.688 + 1.431[M_2(G)]$$

$$\text{Polarizability} = 4.716 + 0.206[M_2(G)]$$

(7) Regression models for harmonic index:  $H(G)$

$$\text{Boiling point} = 124.25 + 34.754[H(G)]$$

$$\text{Enthalpy} = 35.279 + 4.616[H(G)]$$

$$\text{Flash point} = 59.249 + 19.664[H(G)]$$

$$\text{Molar refraction} = -3.359 + 8.161[H(G)]$$

$$\text{Molar volume} = -6.627 + 22.655[H(G)]$$

$$\text{Polarizability} = -1.359 + 3.237[H(G)]$$

(8) Regression models for hyper-Zagreb index:  $HM(G)$

$$\text{Boiling point} = 175.29 + 0.538[HM(G)]$$

$$\text{Enthalpy} = 42.25 + 0.071[HM(G)]$$

$$\text{Flash point} = 84.694 + 0.31[HM(G)]$$

$$\text{Molar refraction} = 10.754 + 0.123[HM(G)]$$

$$\text{Molar volume} = 34.659 + 0.34[HM(G)]$$

$$\text{Polarizability} = 4.237 + 0.049[HM(G)]$$

(9) Regression models for third Zagreb index:  $ZG_3(G)$

$$\text{Boiling point} = 188.731 + 14.187[ZG_3(G)]$$

$$\text{Enthalpy} = 45.595 + 1.819[ZG_3(G)]$$

$$\text{Flash point} = 96.444 + 7.998[ZG_3(G)]$$

$$\text{Molar refraction} = 18.618 + 3.077[ZG_3(G)]$$

$$\text{Molar volume} = 49.304 + 8.748[ZG_3(G)]$$

$$\text{Polarizability} = 7.358 + 1.221[ZG_3(G)]$$

(10) Regression models for forgotten index:  $F(G)$

$$\text{Boiling point} = 174.862 + 1.017[F(G)]$$

$$\text{Enthalpy} = 42.93 + 0.134[F(G)]$$

$$\text{Flash point} = 81.722 + 0.593[F(G)]$$

$$\text{Molar refraction} = 10.095 + 0.235[F(G)]$$

$$\text{Molar volume} = 32.425 + 0.648[F(G)]$$

TABLE 2: Various drugs and topological indices values.

Name of medicine	ABC(G)	R(G)	S(G)	GA(G)	M1(G)	M2(G)	H(G)	HM(G)	ZG3(G)	F(G)	SSD(G)
Amikacin	30.266	18.85	19.24	40.18	191	247	17.83	1046	38	542	101.33
Bedaquiline	28.46	17.61	18.41	38.95	190	197	17.08	959	29	501	90
Clofazimine	27.06	16.68	17.47	18.97	186	216	16.16	901	29	469	85.16
Delamanid	30.38	18.29	19.15	40.43	204	234	17.53	1004	42	536	99.41
Ethambutol	10.6	8.19	7.64	14.53	60	60	7.9	252	12	132	34
Ethionamide	7.95	5.23	5.22	10.57	50	54	5	234	10	124	26
Imipenem-cilastatin	15.88	9.87	10.07	21.03	108	130	9.33	550	18	290	53.33
Isoniazid	8.02	5.21	5.21	10.55	50	55	4.966	234	8	156	26.33
Levofloxacin	20.75	12.37	13.05	27.99	146	186	11.83	754	22	394	67.66
Linezolid	19.43	11.95	12.4	26.08	130	152	11.46	640	42	336	62.66
Moxifloxacin	24.1	14.4	15.29	16.97	172	215	13.866	894	24	464	77.33
p-Aminosalicylic acid	8.13	5.1	5.1	10.38	52	58	4.76	252	12	136	28
Pyrazinamide	6.54	4.3	4.3	4.84	55	43	4.13	182	6	96	21
Rifampin	44.87	27.32	28.14	59.19	309	374	25.78	1593	55	855	151.5
Terizidone	18.66	11.54	11.99	11.74	124	144	11.13	604	20	316	50.33

TABLE 3: Correlation coefficients.

Topological index	Correlation coefficients of boiling point	Correlation coefficients of enthalpy	Correlation coefficients of flash point	Correlation coefficients of molar refraction	Correlation coefficients of molar volume	Correlation coefficients of polarizability
ABC(G)	0.921	0.866	0.903	0.980	0.973	0.980
R(G)	0.921	0.872	0.896	0.984	0.981	0.984
S(G)	0.919	0.864	0.897	0.983	0.978	0.984
GA(G)	0.894	0.865	0.883	0.909	0.917	0.908
M1(G)	0.899	0.840	0.887	0.974	0.965	0.974
M2(G)	0.921	0.869	0.910	0.953	0.943	0.954
H(G)	0.918	0.865	0.891	0.985	0.982	0.985
HM(G)	0.925	0.872	0.914	0.971	0.959	0.971
ZG3(G)	0.877	0.796	0.849	0.872	0.890	0.872
F(G)	0.917	0.868	0.917	0.970	0.959	0.970
SSD(G)	0.925	0.879	0.912	0.978	0.974	0.978

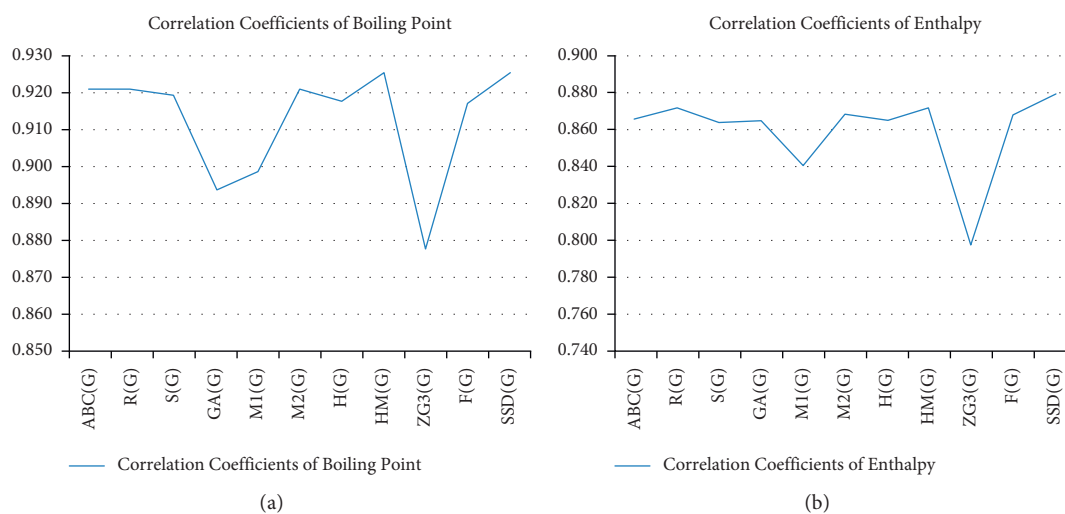


FIGURE 1: Continued.

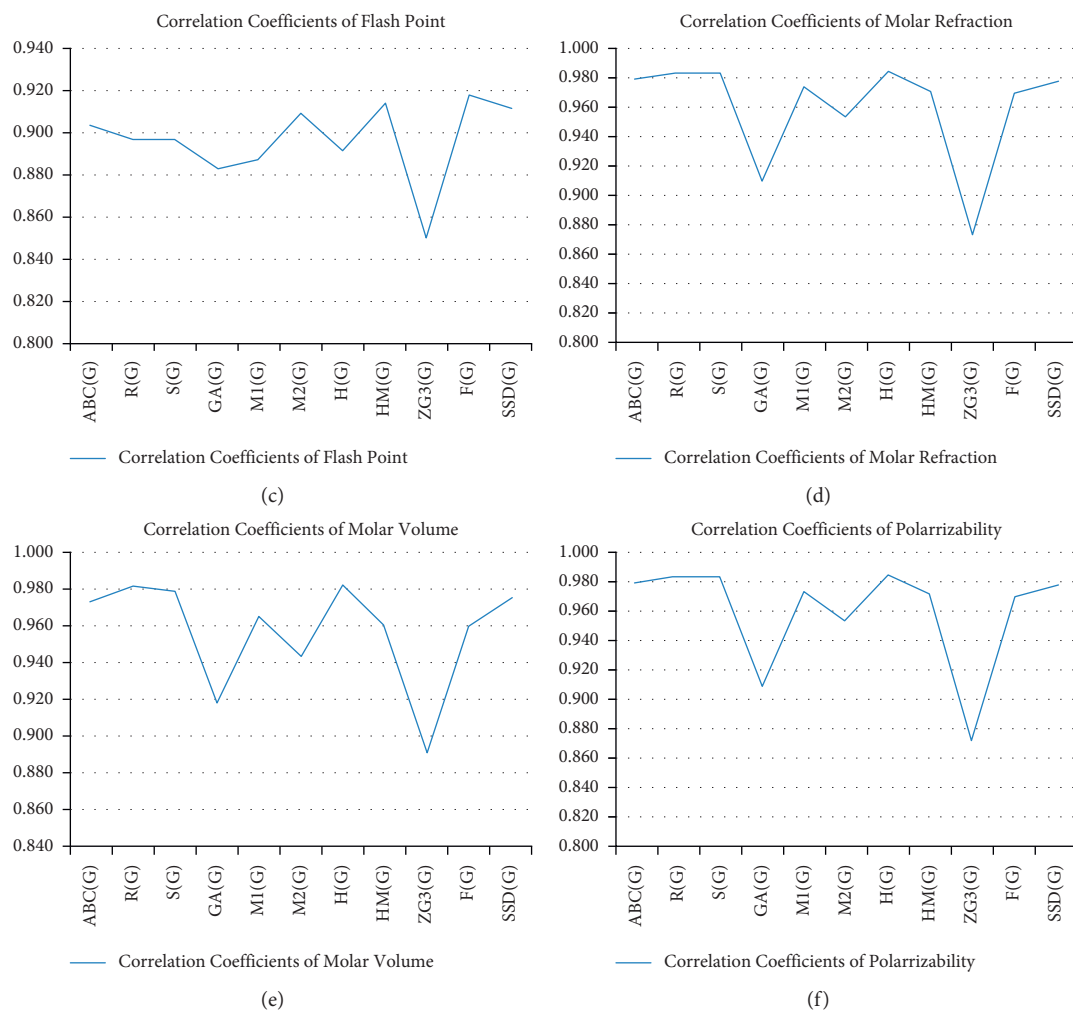


FIGURE 1: Physical properties and topological indices. (a) Boiling Point on TI. (b) Enthalpy on TI. (c) Flash point on TI. (d) Molar Refraction on TI. (e) Molar Volume on TI. (f) Polarizability on TI.

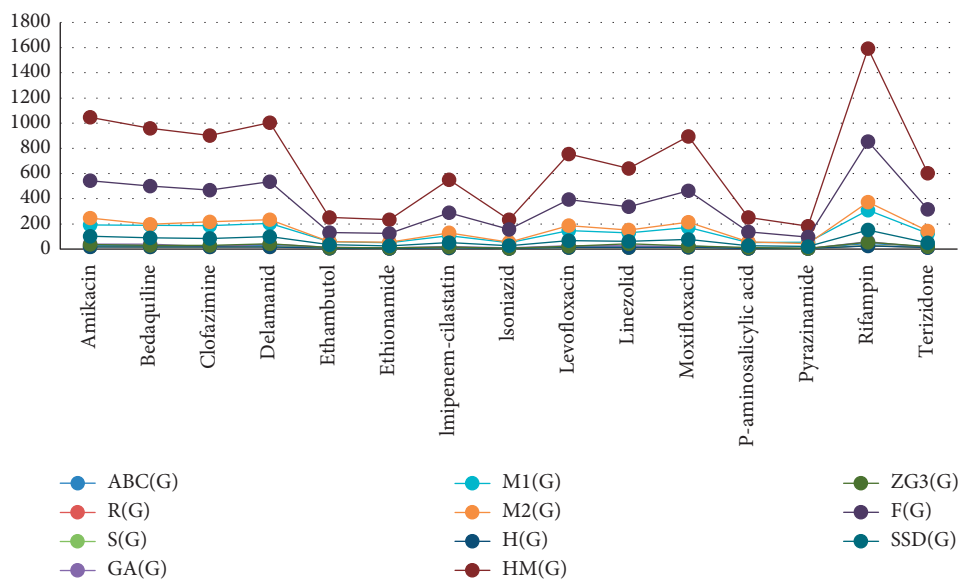


FIGURE 2: Medicine with topological indices.

TABLE 4: Statistical parameters for the linear QSPR model for  $ABC(G)$ .

Physical property	$N$	$A$	$b$	$r$	$r^2$	$F$	$p$	Indicator
Boiling point	14	142.940	19.699	0.921	0.848	67.034	$\leq 0.0001$	Significant
Enthalpy	13	38.040	2.605	0.866	0.750	33.027	$\leq 0.0001$	Significant
Flash point	14	67.648	11.254	0.903	0.816	53.137	$\leq 0.0001$	Significant
Molar refraction	14	1.797	4.588	0.980	0.961	320.196	$\leq 0.0001$	Significant
Molar volume	15	8.698	12.686	0.973	0.947	233.580	$\leq 0.0001$	Significant
Polarizability	15	0.685	1.820	0.980	0.961	322.025	$\leq 0.0001$	Significant

TABLE 5: Statistical parameters for the linear QSPR model for  $R(G)$ .

Physical property	$N$	$A$	$b$	$r$	$r^2$	$F$	$p$	Indicator
Boiling point	14	124.752	33.178	0.921	0.848	66.986	$\leq 0.0001$	Significant
Enthalpy	13	35.127	4.424	0.872	0.760	34.889	$\leq 0.0001$	Significant
Flash point	14	59.012	18.814	0.896	0.804	49.123	$\leq 0.0001$	Significant
Molar refraction	14	-2.760	7.757	0.984	0.968	398.969	$\leq 0.0001$	Significant
Molar volume	15	-5.066	21.541	0.981	0.963	338.102	$\leq 0.0001$	Significant
Polarizability	15	-1.122	3.077	0.984	0.969	401.220	$\leq 0.0001$	Significant

TABLE 6: Statistical parameters for the linear QSPR model for  $S(G)$ .

Physical property	$N$	$A$	$b$	$r$	$r^2$	$F$	$p$	Indicator
Boiling point	14	133.839	31.497	0.919	0.845	65.492	$\leq 0.0001$	Significant
Enthalpy	13	36.755	4.169	0.864	0.747	32.410	$\leq 0.0001$	Significant
Flash point	14	63.724	17.895	0.897	0.804	49.215	$\leq 0.0001$	Significant
Molar refraction	14	-0.810	7.373	0.983	0.967	382.171	$\leq 0.0001$	Significant
Molar volume	15	1.064	20.419	0.978	0.956	285.344	$\leq 0.0001$	Significant
Polarizability	15	-0.348	2.925	0.984	0.967	384.473	$\leq 0.0001$	Significant

TABLE 7: Statistical parameters for the linear QSPR model for  $GA(G)$ .

Physical property	$N$	$A$	$b$	$r$	$r^2$	$F$	$p$	Indicator
Boiling point	14	197.225	14.102	0.894	0.799	47.624	$\leq 0.0001$	Significant
Enthalpy	13	45.041	1.890	0.865	0.748	32.691	$\leq 0.0001$	Significant
Flash point	14	97.240	8.114	0.883	0.779	42.398	$\leq 0.0001$	Significant
Molar refraction	14	21.849	3.067	0.909	0.826	61.559	$\leq 0.0001$	Significant
Molar volume	15	60.810	8.621	0.917	0.841	68.909	$\leq 0.0001$	Significant
Polarizability	15	8.648	1.216	0.908	0.825	61.422	$\leq 0.0001$	Significant

TABLE 8: Statistical parameters for the linear QSPR model for  $M_1(G)$ .

Physical property	$N$	$A$	$b$	$r$	$r^2$	$F$	$p$	Indicator
Boiling point	14	159.511	2.802	0.899	0.808	50.411	$\leq 0.0001$	Significant
Enthalpy	13	40.359	0.370	0.840	0.706	26.417	$\leq 0.0001$	Significant
Flash point	14	75.639	1.611	0.887	0.787	44.458	$\leq 0.0001$	Significant
Molar refraction	14	4.118	0.664	0.974	0.949	241.578	$\leq 0.0001$	Significant
Molar volume	15	15.714	1.833	0.965	0.931	175.131	$\leq 0.0001$	Significant
Polarizability	15	1.606	0.264	0.974	0.949	242.643	$\leq 0.0001$	Significant

TABLE 9: Statistical parameters for the linear QSPR model for  $M_2(G)$ .

Physical property	$N$	$A$	$b$	$r$	$r^2$	$F$	$p$	Indicator
Boiling point	14	176.377	2.294	0.921	0.848	67.069	$\leq 0.0001$	Significant
Enthalpy	13	42.366	0.304	0.869	0.755	33.832	$\leq 0.0001$	Significant
Flash point	14	85.303	1.320	0.910	0.827	57.458	$\leq 0.0001$	Significant
Molar refraction	14	11.967	0.520	0.953	0.909	130.015	$\leq 0.0001$	Significant
Molar volume	15	37.688	1.431	0.943	0.889	104.388	$\leq 0.0001$	Significant
Polarizability	15	4.716	0.206	0.954	0.909	130.608	$\leq 0.0001$	Significant

TABLE 10: Statistical parameters for the linear QSPR model for  $H(G)$ .

Physical property	$N$	$A$	$b$	$r$	$r^2$	$F$	$p$	Indicator
Boiling point	14	124.250	34.754	0.918	0.842	0.842	$\leq 0.0001$	Significant
Enthalpy	13	35.279	4.616	0.865	0.748	32.682	$\leq 0.0001$	Significant
Flash point	14	59.249	19.664	0.891	0.795	46.457	$\leq 0.0001$	Significant
Molar refraction	14	-3.359	8.161	0.985	0.970	422.174	$\leq 0.0001$	Significant
Molar volume	15	-6.627	22.655	0.982	0.964	347.348	$\leq 0.0001$	Significant
Polarizability	15	-1.359	3.237	0.985	0.970	424.568	$\leq 0.0001$	Significant

TABLE 11: Statistical parameters for the linear QSPR model for  $HM(G)$ .

Physical property	$N$	$A$	$b$	$r$	$r^2$	$F$	$p$	Indicator
Boiling point	14	175.290	0.538	0.925	0.857	71.653	$\leq 0.0001$	Significant
Enthalpy	13	42.250	0.071	0.872	0.761	34.961	$\leq 0.0001$	Significant
Flash point	14	84.694	0.310	0.914	0.835	60.823	$\leq 0.0001$	Significant
Molar refraction	14	10.754	0.123	0.971	0.943	213.272	$\leq 0.0001$	Significant
Molar volume	15	34.659	0.340	0.959	0.919	148.407	$\leq 0.0001$	Significant
Polarizability	15	4.237	0.049	0.971	0.943	214.463	$\leq 0.0001$	Significant

TABLE 12: Statistical parameters for the linear QSPR model for  $ZG_3(G)$ .

Physical property	$N$	$A$	$b$	$r$	$r^2$	$F$	$p$	Indicator
Boiling point	14	188.731	14.187	0.877	0.770	40.068	$\leq 0.0001$	Significant
Enthalpy	13	45.595	1.819	0.796	0.634	19.044	$\leq 0.0012$	Significant
Flash point	14	96.444	7.998	0.849	0.721	30.987	$\leq 0.0001$	Significant
Molar refraction	14	18.618	3.077	0.872	0.761	41.284	$\leq 0.0001$	Significant
Molar volume	15	49.304	8.748	0.890	0.793	49.736	$\leq 0.0001$	Significant
Polarizability	15	7.358	1.221	0.872	0.761	41.320	$\leq 0.0001$	Significant

TABLE 13: Statistical parameters for the linear QSPR model for  $F(G)$ .

Physical property	$N$	$A$	$b$	$r$	$r^2$	$F$	$p$	Indicator
Boiling point	14	174.862	1.017	0.917	0.841	63.583	$\leq 0.0001$	Significant
Enthalpy	13	42.930	0.134	0.868	0.753	33.540	$\leq 0.0001$	Significant
Flash point	14	81.722	0.593	0.917	0.842	63.799	$\leq 0.0001$	Significant
Molar refraction	14	10.095	0.235	0.970	0.940	204.155	$\leq 0.0001$	Significant
Molar volume	15	32.425	0.648	0.959	0.920	150.473	$\leq 0.0001$	Significant
Polarizability	15	3.976	0.093	0.970	0.940	205.151	$\leq 0.0001$	Significant

TABLE 14: Standard error of estimate.

Topological index	Std. error of the estimate for boiling point	Std. error of the estimate for enthalpy	Std. error of the estimate for molar refraction	Std. error of the estimate for flash point	Std. error of the estimate for molar volume	Std. error of the estimate for polarizability
$ABC(G)$	98.80842	17.71587	10.53701	63.40101	34.10937	4.16784
$R(G)$	98.83840	17.35274	9.47621	65.44951	28.58485	3.74830
$S(G)$	99.78636	17.84127	9.67553	65.40054	31.00944	3.82645
$GA(G)$	113.75977	17.78385	22.27504	69.37762	59.18170	8.84300
$MI(G)$	111.19073	19.21715	12.05471	68.10000	39.05016	4.77125
$M2(G)$	98.78608	17.55617	16.08332	61.39726	49.43571	6.36590
$H(G)$	100.68522	17.78575	9.22010	66.92575	28.21576	3.64692
$HM(G)$	96.04169	17.33909	12.78650	59.96174	42.15912	5.05818
$ZG3(G)$	121.73452	21.44588	26.10552	78.04393	67.62305	10.35071
$F(G)$	76.32456	11.75776	17.41567	93.39236	73.68525	6.90532
$SSD(G)$	96.18479	16.88420	11.19841	60.73508	33.75294	4.43398

TABLE 15: Comparison of actual and computed values for boiling point from regression models.

Name of drug	Boiling point of drug	Boiling point computed from regression model for ABC index	Boiling point computed from regression model for R(G) index	Boiling point computed from regression model for S(G) index	Boiling point computed from regression model for GA(G) index	Boiling point computed from regression model for M1(G) index	Boiling point computed from regression model for M2(G) index	Boiling point computed from regression model H(G) index	Boiling point computed from regression model of HM(G) index	Boiling point computed from regression model for ZG3(G) index	Boiling point computed from regression model of F(G) index	Boiling point computed from regression model of SSD(G) index
Amikacin	981.8	739.16	750.16	739.84	763.82	694.65	743.07	743.91	738.32	727.82	726.12	751.10
Bedaquiline	702.7	703.58	709.02	713.70	746.48	691.85	628.36	717.84	691.49	600.14	684.42	683.56
Clofazimine	566.9	676.00	678.16	684.09	464.73	680.64	671.95	685.87	660.27	600.14	651.87	654.70
Delamanid	653.7	741.41	731.58	737.01	767.35	731.08	713.25	733.48	715.72	784.57	720.01	739.65
Ethambutol	345.3	351.75	396.48	374.48	402.12	327.62	314.04	398.80	310.94	358.97	309.12	349.71
Ethionamide	247.9	299.55	298.27	298.25	346.28	299.60	300.27	298.02	301.25	330.60	300.98	302.02
Imipenem-cilastatin	530.2	455.77	452.22	451.02	493.78	462.10	474.64	448.50	471.34	444.09	469.81	464.95
Isoniazid	251.97	300.93	297.61	297.94	346.00	299.60	302.56	296.84	301.25	302.22	333.53	303.98
Levofloxacin	571.5	551.70	535.16	544.88	591.93	568.57	603.12	535.39	581.15	500.84	575.59	550.37
Linezolid	585.5	525.70	521.23	524.40	564.99	523.74	525.11	522.53	519.79	784.57	516.60	520.57
Moxifloxacin	636	617.69	602.52	615.43	436.53	641.42	669.66	606.14	656.51	529.21	646.78	608.02
P-Aminosalicylic acid	380.8	303.10	293.96	294.47	343.60	305.20	309.45	289.68	310.94	358.97	313.18	313.94
Pyrazinamide	173.3	271.77	267.42	269.28	265.48	313.61	275.03	267.78	273.26	273.85	272.50	272.21

TABLE 16: Comparison of actual values computed values for enthalpy from regression models.

Name of drug	Boiling point of drug	Boiling point computed from regression model for ABC index	Boiling point computed from regression model for R(G) index	Boiling point computed from regression model for S(G) index	Boiling point computed from regression model for GA(G) index	Boiling point computed from regression model for M1(G) index	Boiling point computed from regression model for M2(G) index	Boiling point computed from regression model H(G) index	Boiling point computed from regression of HM(G) index	Boiling point computed from regression model for ZG3(G) index	Boiling point computed from regression model of F(G) index	Boiling point computed from regression model of SSD(G) index
Amikacin	981.8	739.16	750.16	739.84	763.82	694.65	743.07	743.91	738.32	727.82	726.12	751.10
Bedaquiline	702.7	703.58	709.02	713.70	746.48	691.85	628.36	717.84	691.49	600.14	684.42	683.56
Clofazimine	566.9	676.00	678.16	684.09	464.73	680.64	671.95	685.87	660.27	600.14	651.87	654.70
Delamanid	653.7	741.41	731.58	737.01	767.35	731.08	713.25	733.48	715.72	784.57	720.01	739.65
Ethambutol	345.3	351.75	396.48	374.48	402.12	327.62	314.04	398.80	310.94	358.97	309.12	349.71
Ethionamide	247.9	299.55	298.27	298.25	346.28	299.60	300.27	298.02	301.25	330.60	300.98	302.02
Imipenem-cilastatin	530.2	455.77	452.22	451.02	493.78	462.10	474.64	448.50	471.34	444.09	469.81	464.95
Isoniazid	251.97	300.93	297.61	297.94	346.00	299.60	302.56	296.84	301.25	302.22	333.53	303.98
Levofloxacin	571.5	551.70	535.16	544.88	591.93	568.57	603.12	535.39	581.15	500.84	575.59	550.37
Linezolid	585.5	525.70	521.23	524.40	564.99	523.74	525.11	522.53	519.79	784.57	516.60	520.57
Moxifloxacin	636	617.69	602.52	615.43	436.53	641.42	669.66	606.14	656.51	529.21	646.78	608.02
p-Aminosalicylic acid	380.8	303.10	293.96	294.47	343.60	305.20	309.45	289.68	310.94	358.97	313.18	313.94
Pyrazinamide	173.3	271.77	267.42	269.28	265.48	313.61	275.03	267.78	273.26	273.85	272.50	272.21

TABLE 17: Comparison of actual values computed values for Flash point from regression models.

Name of drug	Boiling point of drug	Boiling point computed from regression model for ABC index	Boiling point computed from regression model for R(G) index	Boiling point computed from regression model for S(G) index	Boiling point computed from regression model for GA(G) index	Boiling point computed from regression model for M1(G) index	Boiling point computed from regression model for M2(G) index	Boiling point computed from regression model H(G) index	Boiling point computed from regression of HM(G) index	Boiling point computed from regression model for ZG3(G) index	Boiling point computed from regression model of F(G) index	Boiling point computed from regression model of SSD(G) index
Amikacin	981.8	739.16	750.16	739.84	763.82	694.65	743.07	743.91	738.32	727.82	726.12	751.10
Bedaquiline	702.7	703.58	709.02	713.70	746.48	691.85	628.36	717.84	691.49	600.14	684.42	683.56
Clofazimine	566.9	676.00	678.16	684.09	464.73	680.64	671.95	685.87	660.27	600.14	651.87	654.70
Delamanid	653.7	741.41	731.58	737.01	767.35	731.08	713.25	733.48	715.72	784.57	720.01	739.65
Ethambutol	345.3	351.75	396.48	374.48	402.12	327.62	314.04	398.80	310.94	358.97	309.12	349.71
Ethionamide	247.9	299.55	298.27	298.25	346.28	299.60	300.27	298.02	301.25	330.60	300.98	302.02
Imipenem-cilastatin	530.2	455.77	452.22	451.02	493.78	462.10	474.64	448.50	471.34	444.09	469.81	464.95
Isoniazid	251.97	300.93	297.61	297.94	346.00	299.60	302.56	296.84	301.25	302.22	333.53	303.98
Levofloxacin	571.5	551.70	535.16	544.88	591.93	568.57	603.12	535.39	581.15	500.84	575.59	550.37
Linezolid	585.5	525.70	521.23	524.40	564.99	523.74	525.11	522.53	519.79	784.57	516.60	520.57
Moxifloxacin	636	617.69	602.52	615.43	436.53	641.42	669.66	606.14	656.51	529.21	646.78	608.02
p-Aminosalicylic acid	380.8	303.10	293.96	294.47	343.60	305.20	309.45	289.68	310.94	358.97	313.18	313.94
Pyrazinamide	173.3	271.77	267.42	269.28	265.48	313.61	275.03	267.78	273.26	273.85	272.50	272.21

TABLE 18: Comparison of actual values computed values for molar refraction from regression models.

Name of drug	Molar refraction of drug	Molar refraction computed from regression model for ABC index	Molar refraction computed from regression model for R(G) index	Molar refraction computed from regression model for S(G) index	Molar refraction computed from regression model for GA(G) index	Molar refraction computed from regression model for M1(G) index	Molar refraction computed from regression model for M2(G) index	Molar refraction computed from regression model for H(G) index	Molar refraction computed from regression model of HIM(G) index	Molar refraction computed from regression model for ZG3(G)	Molar refraction computed from regression model of F(G) index	Molar refraction computed from regression model of SSD(G)
Amikacin	134.9	140.67	143.46	141.05	145.08	131.02	140.32	142.16	139.93	135.54	137.52	143.79
Bedaquiline	156.2	132.38	133.84	134.93	141.30	130.35	114.34	136.04	129.19	107.85	127.88	128.26
Clofazimine	136.2	125.96	126.63	128.00	80.03	127.70	124.21	128.53	122.02	107.85	120.36	121.63
Delamanid	127.7	141.19	139.12	140.38	145.84	139.65	133.57	139.71	134.74	147.85	136.11	141.16
Ethambutol	58.6	50.43	60.77	55.52	66.41	43.98	43.15	61.12	41.87	55.54	41.13	51.49
Ethionamide	49	38.27	37.81	37.68	54.27	37.34	40.03	37.45	39.65	49.39	39.25	40.52
Imipenem-cilastatin	72.7	74.66	73.80	73.44	86.35	75.87	79.52	72.79	78.68	74.00	78.27	77.99
Isoniazid	36.9	38.60	37.65	37.60	54.20	37.34	40.55	37.17	39.65	43.23	46.77	40.97
Levofloxacin	91.1	97.01	93.20	95.41	107.69	101.12	108.62	93.19	103.87	86.31	102.72	97.63
Linezolid	83	90.95	89.94	90.62	101.83	90.49	90.96	90.17	89.79	147.85	89.09	90.78
Moxifloxacin	101.8	112.38	108.94	111.92	73.89	118.39	123.69	109.81	121.16	92.46	119.18	110.89
p-Aminosalicylic acid	39.3	39.10	36.80	36.79	53.68	38.67	42.11	35.49	41.87	55.54	42.07	43.26
Pyrazinamide	31.9	31.80	30.60	30.89	36.69	40.66	34.31	30.35	33.23	37.08	32.66	33.67
Rifampin	213.1	207.68	209.17	206.67	203.38	209.42	206.32	207.04	207.48	187.85	211.10	212.57

TABLE 19: Comparison of actual values computed values for molar volume from regression models.

Name of drug	Molar volume of drug	Molar volume computed from regression model for ABC index	Molar volume computed from regression model for R(G) index	Molar volume computed from regression model for S(G) index	Molar volume computed from regression model for GA(G) index	Molar volume computed from regression model for M1(G) index	Molar volume computed from regression model for M2(G) index	Molar volume computed from regression model for H(G) index	Molar volume computed from regression of HM(G) Index	Molar volume computed from regression model for ZG3(G)	Molar volume computed from regression model of F(G) index	Molar volume computed from regression model of SSD(G)
Amikacin	363.9	392.65	400.98	393.92	407.20	365.72	391.20	397.31	389.95	381.74	383.54	401.74
Bedaquiline	420.1	369.74	374.27	376.97	396.60	363.89	319.64	380.32	360.40	303.01	356.98	358.65
Clofazimine	366.1	351.98	354.23	357.78	224.35	356.56	346.84	359.48	340.70	303.01	336.25	340.25
Delamanid	368	394.10	388.92	392.08	409.36	389.54	372.60	390.51	375.69	416.73	379.65	394.44
Ethambutol	207	143.17	171.35	157.06	186.07	125.66	123.56	172.35	120.26	154.28	117.94	145.71
Ethionamide	142	109.55	107.59	107.65	151.93	107.34	114.97	106.65	114.14	136.79	112.75	115.29
Imipenem-cilastatin	183.9	210.15	207.54	206.68	242.11	213.62	223.75	204.74	221.48	206.77	220.29	219.21
Isoniazid	110.2	110.44	107.16	107.44	151.76	107.34	116.41	105.88	114.14	119.29	133.48	116.54
Levofloxacin	244	271.93	261.39	267.53	302.11	283.26	303.90	261.38	290.77	241.77	287.66	273.70
Linezolid	259	255.19	252.35	254.25	285.65	253.94	255.24	253.00	252.05	416.73	250.09	254.69
Moxifloxacin	285	314.43	305.12	313.26	207.11	330.90	345.40	307.51	338.32	259.26	333.01	310.48
p-Aminosalicylic acid	102.7	111.84	104.79	105.20	150.30	111.00	120.70	101.21	120.26	154.28	120.53	122.89
Pyrazinamide	87.7	91.66	87.56	88.86	102.54	116.50	99.23	86.94	96.48	101.79	94.61	96.28
Rifampin	611.7	577.92	583.43	575.64	571.09	581.96	572.97	577.42	575.75	530.46	586.30	592.51

TABLE 20: Comparison of actual values computed values for polarizability from regression models.

Name of drug	Molar volume of drug	Molar volume computed from regression model for ABC index	Molar volume computed from regression model for $R(G)$ index	Molar volume computed from regression model for $S(G)$ index	Molar volume computed from regression model for $GA(G)$ index	Molar volume computed from regression model for $MI(G)$ index	Molar volume computed from regression model for $M2(G)$ index	Molar volume computed from regression model H(G) index	Molar volume computed from regression of HM(G) index	Molar volume computed from regression model for ZG3(G)	Molar volume computed from regression model of F(G) index	Molar volume computed from regression model of SSD(G)
Amikacin	363.9	392.65	400.98	393.92	407.20	365.72	391.20	397.31	389.95	381.74	383.54	401.74
Bedaquiline	420.1	369.74	374.27	376.97	396.60	363.89	319.64	380.32	360.40	303.01	356.98	358.65
Clofazimine	366.1	351.98	354.23	357.78	224.35	356.56	346.84	359.48	340.70	303.01	336.25	340.25
Delamanid	368	394.10	388.92	392.08	409.36	389.54	372.60	390.51	375.69	416.73	379.65	394.44
Ethambutol	207	143.17	171.35	157.06	186.07	125.66	123.56	172.35	120.26	154.28	117.94	145.71
Ethionamide	142	109.55	107.59	107.65	151.93	107.34	114.97	106.65	114.14	136.79	112.75	115.29
Imipenem-cilastatin	183.9	210.15	207.54	206.68	242.11	213.62	223.75	204.74	221.48	206.77	220.29	219.21
Isoniazid	110.2	110.44	107.16	107.44	151.76	107.34	116.41	105.88	114.14	119.29	133.48	116.54
Levofloxacin	244	271.93	261.39	267.53	302.11	283.26	303.90	261.38	290.77	241.77	287.66	273.70
Linezolid	259	255.19	252.35	254.25	285.65	253.94	255.24	253.00	252.05	416.73	250.09	254.69
Moxifloxacin	285	314.43	305.12	313.26	207.11	330.90	345.40	307.51	338.32	259.26	333.01	310.48
p-Aminosalicylic acid	102.7	111.84	104.79	105.20	150.30	111.00	120.70	101.21	120.26	154.28	120.53	122.89
Pyrazinamide	87.7	91.66	87.56	88.86	102.54	116.50	99.23	86.94	96.48	101.79	94.61	96.28
Rifampin	611.7	577.92	583.43	575.64	571.09	581.96	572.97	577.42	575.75	530.46	586.30	592.51

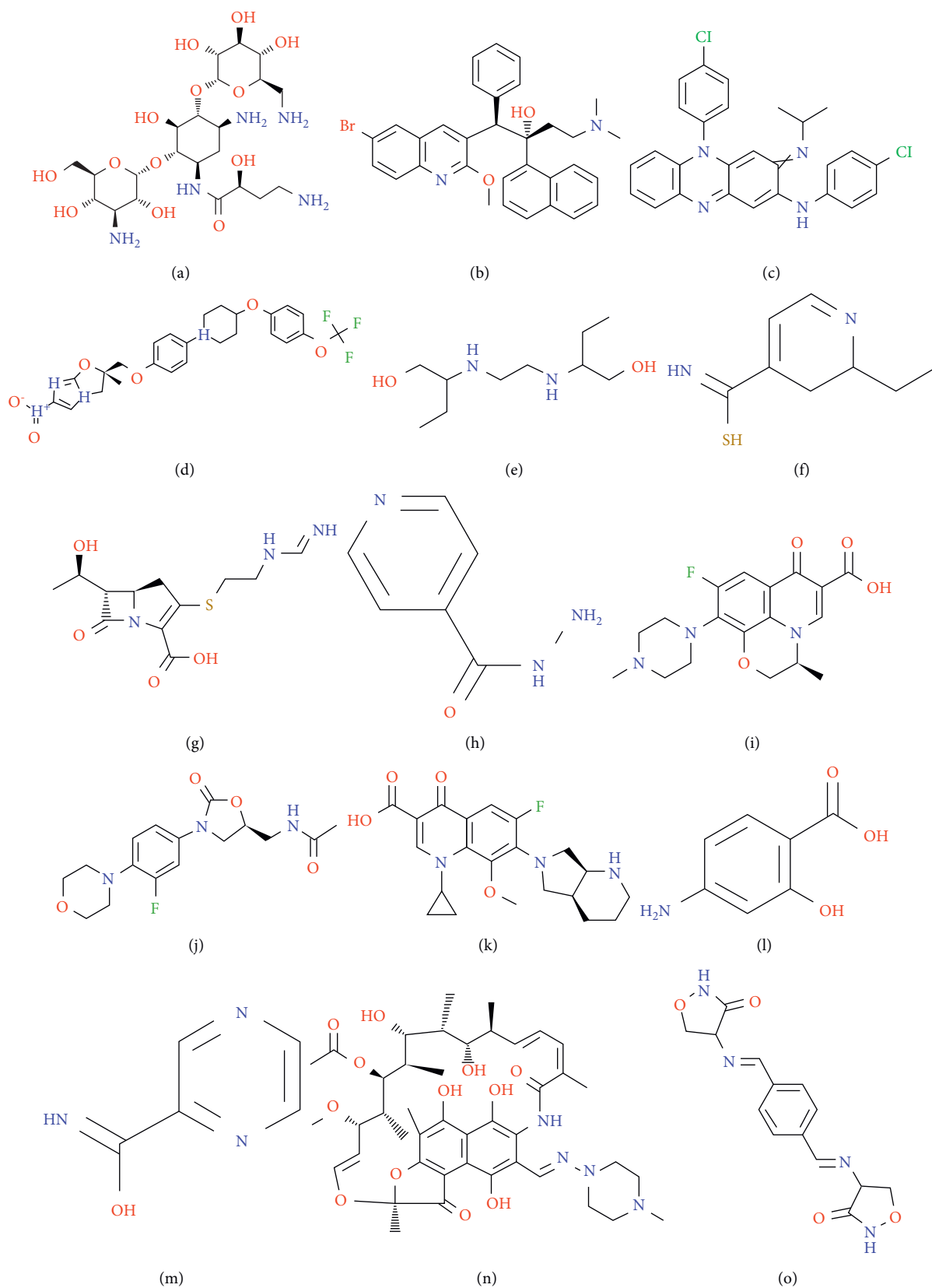


FIGURE 3: Molecular structure of drugs. (a) Amikacin. (b) Bedaquiline. (c) Clofazimine. (d) Delamanid. (e) Ethambutol. (f) Ethionamide. (g) Imipenem-cilastatin. (h) Isoniazid. (i) Levofloxacin. (j) Linezolid. (k) Moxifloxacin. (l) *p*-aminosalicylic acid. (m) Pyrazinamide. (n) Rifampin. (o) Terizidone.

TABLE 21: Correlation determination.

Topological index	Coefficient of determination of boiling point	Coefficient of determination of enthalpy	Coefficient of determination of flash point	Coefficient of determination of molar refraction	Coefficient of determination of molar volume	Coefficient of determination of polarizability
$ABC(G)$	0.848	0.750	0.816	0.961	0.947	0.961
$R(G)$	0.848	0.760	0.804	0.968	0.963	0.969
$S(G)$	0.845	0.747	0.804	0.967	0.956	0.967
$GA(G)$	0.799	0.748	0.779	0.826	0.841	0.825
$M1(G)$	0.808	0.706	0.787	0.949	0.931	0.949
$M2(G)$	0.848	0.755	0.827	0.909	0.889	0.909
$H(G)$	0.842	0.748	0.795	0.970	0.964	0.970
$HM(G)$	0.857	0.761	0.835	0.943	0.919	0.943
$ZG3(G)$	0.770	0.634	0.721	0.761	0.793	0.761
$F(G)$	0.841	0.753	0.842	0.940	0.920	0.940
$SSD(G)$	0.844	0.773	0.831	0.956	0.948	0.956

TABLE 22: Statistical parameters for the linear QSPR model for  $SS D(G)$ .

Physical property	$N$	$A$	$b$	$r$	$r^2$	$F$	$p$	Indicator
Boiling point	14	147.016	5.962	0.925	0.844	71.404	$\leq 0.0001$	Significant
Enthalpy	13	38.141	0.795	0.879	0.773	37.471	$\leq 0.0001$	Significant
Flash point	14	68.953	3.421	0.912	0.831	58.981	$\leq 0.0001$	Significant
Molar refraction	14	4.877	1.371	0.978	0.956	282.000	$\leq 0.0001$	Significant
Molar volume	15	16.421	3.803	0.974	0.948	238.815	$\leq 0.0001$	Significant
Polarizability	15	1.908	0.544	0.978	0.956	283.014	$\leq 0.0001$	Significant

$$\text{Polarizability} = 3.976 + 0.093[F(G)]$$

(11) Regression models for symmetric division index:  $SS D(G)$

$$\text{Boiling point} = 147.016 + 5.962[SS D(G)]$$

$$\text{Enthalpy} = 38.141 + 0.795[SS D(G)]$$

$$\text{Flash point} = 68.953 + 3.421[SS D(G)]$$

$$\text{Molar refraction} = 4.877 + 1.371[SS D(G)]$$

$$\text{Molar volume} = 16.421 + 3.803[SS D(G)]$$

$$\text{Polarizability} = 1.908 + 0.544[SS D(G)]$$

**2.2. Computation of Topological Indices and Their Comparison with Correlation Coefficients of Some Physical Properties.** Table 1 shows the abovementioned physical properties of 15 drugs used for the treatment of tuberculosis.

In Table 2, the 12 topological indices are computed of the graphs constructed from the molecular structures of the drugs.

In Table 3, the correlation coefficients of the 6 physical properties with respect to each topological index are computed. The graph of the correlation coefficient of all the physical properties such as boiling point, enthalpy, flash point, molar refraction, molar volume, and polarizability on different topological indices are shown in Figure 1. The graphical representation of topological indices of the different medicine is shown in Figure 2.

**2.3. Computation of Statistical Parameters.** In this section, regression parameters have been computed.  $N$  is the sample size,  $A$  is constant or  $Y$ -intercept,  $b$  is slope,  $r$  is correlation coefficient, and  $r^2$  is the percentage of the

dependent variable variation that a linear model explains. The  $p$  value for each term tests the null hypothesis that the coefficient is equal to zero (no effect), whereas a larger (insignificant)  $p$  value suggests that changes in the predictor are not associated with changes in the response. Suppose we are doing a test in which the null hypothesis is that all of the regression coefficients are zero. The result of this kind of a test gives us a value called  $F$  value. In this case, the model has no predictive capability. With the help of this test, one can compare their model with zero predictor variables and decides whether their added coefficients have improved the model. In Tables 4–13, these statistical parameters are computed for linear QSPR models for different topological indices. All of these analyses show that the  $p$  value in each of the model is zero that indicates the significance of the results.

**2.4. Standard Error of Estimate.** The Standard error of estimate is the measure of variation of an observation made around the computed regression line. Table 14 shows the standard error of estimate for six physical properties corresponding to each topological index.

**2.5. Correlation Determination.** The correlation determination describes the percentage of relation which gives you more information about the relationship between variables. When you square the correlation coefficient, you end up with the correlation of determination  $r^2$ .

**2.6. Comparison.** In this section, the comparison for known values and computed values from our regression models is

drawn. In Tables 15–20, the comparison of each physical property is shown.

### 3. Conclusion and Future Study

**3.1. Conclusion.** Tuberculosis (TB) is a disease and its infection is caused by bacteria “*Mycobacterium tuberculosis*” that usually attacks lungs. It can also spread to other parts of body, like brain and spine and cause death.

A *molecular descriptor* is actually a mathematical formula that can be applied to any graph which models some molecular structure. More precisely, a single number represents a chemical structure. In graph theory, this number is called *topological descriptor*. When a topological descriptor correlates with a molecular property, it is called molecular index or topological index (*TI*). Thus, a topological graph index is also called a *molecular descriptor*. Mathematically, a *topological index* is a numeric quantity associated with a graph which characterizes the topology of a graph. By computing these topological indices, it is possible to analyze mathematical values and further investigate some physico-chemical properties of a molecule. Actually topological indices are designed on the ground of transformation of molecular graph into a number which characterizes the topology of graph.

Molecular topological indices play a significant role in mathematical chemistry, especially in quantitative structure-property relationship (QSPR) and quantitative structure-activity relationship (QSAR) investigations. (11) is used to correlate the various physical properties of various drugs used for the treatment of tuberculosis with some topological indices. Therefore, it is an efficient way to avoid expensive and time-consuming laboratory experiments. The purpose of computing these 11 topological indices is that no single topological index is found yet that can be efficient (given in various tables) for all physical properties of these drugs.

Tables 1 and 2 gives the values of physical properties and topological indices of medicines (Figure 3), respectively. Table 3 and graphs (Figure 1) shows how degree-based topological indices and physical properties of medicine correlate. Upon examining correlation coefficients horizontally for physical properties under consideration, we see that  $H(G)$  index gives highest correlation coefficient for molar refraction ( $r = 0.985$ ), molar volume ( $r = 0.982$ ), and polarizability ( $r = 0.985$ ).  $HM(G)$  index gives highest correlation coefficient for boiling point ( $r = 0.925$ ).  $F(G)$  has highest correlation coefficient for flash point ( $r = 0.925$ ).  $SSD$  gives highest correlation coefficient for boiling point and enthalpy. When we look vertically, boiling point has also good correlation with  $ABC(G)$  and  $R(G)$ , i.e., ( $r = .921$ ) for both. Enthalpy has also good correlation with  $R(G)$  and  $HM(G)$ , i.e., ( $r = 0.872$ ). Flash point has also good correlation with  $SSD(G)$ , i.e., ( $r = 0.812$ ). Molar refraction has also good correlation with  $R(G)$ , i.e., ( $r = 0.984$ ). Molar volume has also good correlation with  $R(G)$ , i.e., ( $r = 0.981$ ). Polarizability has also good correlation with  $R(G)$  and  $S(G)$ , i.e.,  $r = .984$ .

While examining correlation determination (Table 21) horizontally for physical properties under consideration, we see that  $H(G)$  index gives highest correlation determination for molar refraction ( $r^2 = 0.970$ ), molar volume ( $r^2 = 0.964$ ), and polarizability ( $r^2 = 0.970$ ).  $HM(G)$  index gives highest correlation determination for boiling point ( $r^2 = 0.857$ ).  $F(G)$  has highest correlation determination for flash point ( $r^2 = 0.842$ ).  $SSD$  gives highest correlation determination for boiling point and enthalpy ( $r^2 = 0.773$ ). When we look vertically, boiling point has also good correlation with  $ABC(G)$  and  $R(G)$ , i.e., ( $r^2 = 0.848$ ) for both. Enthalpy has also good correlation with  $R(G)$  and  $HM(G)$ , i.e., ( $r \geq 0.760$ ). Flash point has also good correlation with  $SSD(G)$  and  $HM(G)$ , i.e., ( $r^2 = .0.831$ ). Molar refraction has also good correlation with  $R(G)$ , i.e., ( $r^2 = 0.968$ ). Molar volume has also good correlation with  $R(G)$ , i.e., ( $r^2 = 0.963$ ). Polarizability has also good correlation with  $R(G)$  and  $S(G)$ , i.e.,  $r^2 = 0.969$ . One can easily gather from the table of statistical parameters for the linear QSPR models for different degree-based topological indices that are as follows:

Harmonic index  $H(G)$  has positive and highly significant correlation coefficient for molar refraction ( $r = 0.985$ ), molar volume ( $r = 0.982$ ), and polarizability ( $r = 0.985$ ).

Sum-connectivity  $S(G)$  index and hyper-Zagreb index  $HM(G)$  has highly significant correlation coefficient for boiling point, i.e., ( $r = 0.925$ ).

Sum-connectivity  $S(G)$  index also has highly significant correlation coefficient for enthalpy.

Forgotten topological index  $F(G)$  has highly significant correlation coefficient for flash point ( $r = 0.917$ ).

From Table 21, we can also see high percentage correlation between degree-based topological index and physical properties of medicines.

Harmonic index  $H(G)$  has positive and high percentage of correlation for molar refraction ( $r^2 = 0.970$ ), molar volume ( $r^2 = 0.964$ ), and polarizability ( $r^2 = 0.970$ ).

Hyper-Zagreb index  $HM(G)$  has high percentage of correlation for boiling point, i.e., ( $r^2 = 0.857$ ).

Sum-connectivity  $S(G)$  index also has high percentage of correlation for enthalpy ( $r^2 = 0.773$ ).

Forgotten topological index  $F(G)$  has high percentage of correlation for flash point ( $r^2 = 0.842$ ).

Tables 4–13 and 22 show different statistical parameters of correlation between values of eleven degree based topological indices and six physical properties of medicine. We could not find any correlation between degree-based topological index and melting point of antituberculosis drugs.

This work indicated that this theoretical analysis may help the chemist and people working in pharmaceutical industry to predict properties of antituberculosis drugs

without experimenting. It is also possible that different composition of these drugs may be used for different diseases; of course it depends on the range of the topological indices which are computed in this work. In this work, we have found the correlation coefficient for different topological indices; this will help the chemist to design new drugs based on the combination of positively high correlated drugs.

**3.2. Future Study.** In a similar pattern, relation between physical properties for different drugs/medicine for the treatment/preventive measures of a particular disease and Topological indices can be established to estimate physical properties of newly discovered medicine or candidate drug(s) of particular disease.

It will be very important to find a topological index that can correlate with all the physical properties.

### Data Availability

The physical property data used to support the findings of this study are included within the article.

### Conflicts of Interest

The authors have no conflicts of interest.

### References

- [1] A. Astanesh-Asl and G. H Fath-Tabar, "Computing the first and third Zagreb polynomials of certain product of graphs, Iran," *Journal of Mathematical Chemistry*, vol. 2, no. 2, pp. 73–78, 2011.
- [2] V. Alexander, "Upper and lower bounds of symmetric division deg index, Iran," *Journal of Mathematical Chemistry*, vol. 5, no. 2, p. 9198, 2014.
- [3] Adnan and S. Ahtsham Ul Haq Bokhary, "On vertex PI index of certain triangular tessellation networks," *Main Group Met. Chem.* vol. 44, pp. 203–212, 2021.
- [4] M. Imran, S. Akhter, and S. Manzoor, "Molecular, topological invariants of certain chemical networks," *Main Group Met. Chem.* vol. 44, pp. 141–149, 2021.
- [5] M. Imran, Syed Ahtsham Ul Haq Bokhary, and S. Manzoor, "On molecular topological properties of dendrimers," *Canadian Journal of Chemistry*, vol. 94, pp. 120–125, 2016.
- [6] Adnan, S. Ahtsham Ul Haq Bokhary, M. K. Siddiqui, and M. Cancan, "On topological indices and QSPR analysis of drugs used for the treatment of breast cancer," *Polycyclic Aromatic Compounds*, vol. 23, 2021.
- [7] E. Estrada, L. Torres, L. Rodriguez, and I. Gutman, "An atom-bond connectivity index: modeling the enthalpy of formation of alkanes," *Indian Journal of Chemistry*, vol. 37, pp. 849–855, 1998.
- [8] B. Furtula and I. Gutman, "A forgotten topological index," *Journal of Mathematical Chemistry*, vol. 53, pp. 213–220, 2015.
- [9] S. Fajtlowicz, "On conjectures of grafitti II," *Congressus Numerantium*, vol. 60, pp. 189–197, 1987.
- [10] I. Gutman and T. Krtvlyesi, "Wiener indices and molecular surfaces," *Zeitschrift fr Naturforschung*, vol. 50, Article ID 6696671, 1995.
- [11] I. Gutman, "Degree based topological indices," *Croatica Chemica Acta*, vol. 86, pp. 351–361, 2013.
- [12] V. Loksha, S. Suvarna, and A. Sinan Cevik, "Status index and co-index of connected graphs," *Proc of the Jangjeon Mathematical society*, vol. 24, no. 3, pp. 285–295, 2021.
- [13] M. Randi, "On Characterization of molecular branching," *Journal of the American Chemical Society*, vol. 97, pp. 6609–6615, 1975.
- [14] D. H. Rouvray and B. C. Crafford, "The dependence of physical-chemical properties on topological factors," *South African Journal of Science*, vol. 72, p. 47, 1976.
- [15] G. H. Shirdel, H. RezaPour, and A. M. Sayadi, "The hyperzagreb index of graph operations, Iran," *Journal of Mathematical Chemistry*, vol. 4, no. 2, pp. 213–220, 2013.
- [16] L. I. Stiel and G. Thodos, "The normal boiling points and critical constants of saturated aliphatic hydrocarbons," *AICHE Journal*, vol. 8, no. 4, Article ID 5276529, 1962.
- [17] D. V.-B. Furtula, "Topological index based on the ratios of geometrical and arithmetical means of end-vertex degrees of edges," *Journal of Mathematical Chemistry*, vol. 46, pp. 1369–1376, 2009.
- [18] H. Wiener, "Structural determination of paraffin boiling points," *Journal of the American Chemical Society*, vol. 69, pp. 17–20, 1947.
- [19] B. Zhou and N. Trinajstic, "On general sum-connectivity index," *Journal of Mathematical Chemistry*, vol. 47, pp. 210–218, 2010.

## Research Article

# Study of Vanadium Carbide Structures Based on Ve and Ev-Degree Topological Indices

Abdul Rauf <sup>1</sup>, Saba Maqbool,<sup>1</sup> Muhammad Naeem <sup>1</sup>, Adnan Aslam <sup>2</sup>, Hamideh Aram,<sup>3</sup> and Kraidi Anoh Yannick <sup>4</sup>

<sup>1</sup>Department of Mathematics, Air University Multan Campus, Multan, Pakistan

<sup>2</sup>Department of Natural Sciences and Humanities, University of Engineering and Technology, Lahore, Pakistan (RCET), Pakistan

<sup>3</sup>Department of Mathematics, Gareziaeddin Center, Khoy Branch, Islamic Azad University Khoy, Iran

<sup>4</sup>UFR of Mathematics and Informatics, University Felix Houphouet Boigny of Cocody, Abidjan, Côte d'Ivoire

Correspondence should be addressed to Kraidi Anoh Yannick; kayanoh2000@yahoo.fr

Received 13 June 2021; Accepted 7 December 2021; Published 27 December 2021

Academic Editor: Muhammad Imran

Copyright © 2021 Abdul Rauf et al. This is an open access article distributed under the Creative Commons Attribution License, which permits unrestricted use, distribution, and reproduction in any medium, provided the original work is properly cited.

Vanadium is a biologically active product with significant industrial and biological applications. Vanadium is found in a variety of minerals and fossil fuels, the most common of which are sandstones, crude oil, and coal. Topological descriptors are numerical numbers assigned to the molecular structures and have the ability to predict certain of their physical/chemical properties. In this paper, we have studied topological descriptors of vanadium carbide structure based on ev and ve degrees. In particular, we have computed the closed forms of Zagreb, Randic, geometric-arithmetic, and atom-bond connectivity (ABC) indices of vanadium carbide structure based on ev and ve degrees. This kind of study may be useful for understanding the biological and chemical behavior of the structure.

## 1. Introduction

Vertex degree concept has devised many topological indices that are applicable in QSPR/QSAR studies. Topological indices are widely used in theoretical and mathematical chemistry as they are associated with the topology of a chemical structure along with its other identical properties such as boiling points, strain energy, and stability [1]. In chemical graph theory, a chemical graph is referred as a molecular structure with atoms as its vertices and chemical bonds as its edges. A topological index is a numerical parameter that creates a link between the physical and chemical properties of a molecule [2]. Many topological descriptors based on degree have been introduced. These topological indices have provided assistance in calculating different parametric calculations related to molecular structures to make them understandable and beneficial. A lot of topological descriptors have been defined and studied so far, but Zagreb indices [3], Wiener index [4], and Randic index [5] are the most

studied among all of them. To read more about the chemical applicability of topological descriptors, see [5–12].

Researchers have attempted to study the varying behavior of transition metal carbides due to their complex structures. Such mineral metals are available in commercial places, and their salts are broadly utilized in our enterprises related to electrochemistry and material science. Among these, vanadium carbide complexes have shown crystal morphologies and stoichiometrics and display a great variety of superstructures. Very recently, many attempts have been done to purify high quality vanadium carbide by presenting different binary model system such as VC, V<sub>2</sub>C, V<sub>4</sub>C<sub>3</sub>, V<sub>6</sub>C<sub>5</sub>, and V<sub>8</sub>C<sub>7</sub>. For more details, see [13–16].

Let  $G$  be a simple connected graph with its edge set and vertex set denoted by  $E$  and  $V$ , respectively. The neighbor set  $N(v)$  of a vertex  $v$  contains those vertices  $v_1$  such that  $vv_1 \in E$ . The degree of vertex  $v$  is denoted by  $d_v$ , and is the cardinality of the set  $N(v)$ . Let  $N[v] = \{v_1 \in V: vv_1 \in E\}$

$\cup \{v\}$  be the closed neighborhood of  $v$ . To read more about the basic concepts related to graph, see [17].

M. Chellali et al. [18] first introduced the concept of  $ev$  degree of an edge  $e$  and  $ve$  degree of a vertex  $v$ . The  $ev$  degree of an edge  $e$  is denoted by  $d_{ev}(e)$  and is defined as the total number of vertices in the closed neighborhoods of the end vertices of an edge  $e$ . The  $ve$  degree of a vertex  $v$  is denoted by  $d_{ve}(v)$  and is the total number of edges that are adjacent with  $v$  and the first neighbor of  $v$ . Ediz [3] first introduced the concept of  $ve$  degree and  $ev$  degree Zagreb and Randic indices. The mathematical formulas of these indices are presented in Table 1. These newly defined indices were compared with Zagreb, Weiner, and Randic indices by modeling some of the physical/chemical properties of octane isomers. These indices have been observed to provide better correlation than the Randic, Weiner, and Zagreb indices for predicting some specific physical and chemical properties of octane isomers. Recently, a lot of work is done in the direction of computing newly defined  $ve$  degree and  $ev$  degree-based indices [19–23].

## 2. Vanadium Carbide

Vanadium carbide belongs to the family of group IV to VI transition metal carbides and shows homogeneity to metal nitrides, monocarbides, and carbonitrides. They possess unique associations between physio-chemical properties such as high melting points, high temperature resistivity, strength, and hardness which are associated with good electrical and thermal conductivity. These rare combinations of properties make such compounds very interesting for the researchers. These materials can be used as wear-resistant

hard alloys and as hard coatings for protection purposes, due to their nanochemical properties [24, 25].

Vanadium carbide is the hardest inorganic metal-carbide with the formula VC. VC is an incredibly hard refractory ceramic with exceptional wear resistance, high modulus of elasticity (400 GPa), and good strength retention even at high temperatures [26–28]. VC coatings are used in corrosion prevention, cutting tool application, machining, drilling, and dyeing. Some industrial uses of VC are given in [27, 29–31]. We denote the crystallographic structure of vanadium carbide by  $VC[m, n]$ . The molecular structure of vanadium carbide for  $m = 5 = n$  is depicted in Figure 1. The structure of  $VC[m, n]$  has total number of  $3mn + m + n$  vertices and  $6mn - m - n$  edges. Let  $V_i$  denote the vertex set containing the vertices of  $VC[m, n]$  of degree  $i$ . Then, the vertex set  $V(VC[m, n])$  can be partitioned into six sets with  $|V_1| = m + n + 2$ ,  $|V_2| = 2m + 2n - 4$ ,  $|V_3| = 4m - 2n + 2$ ,  $|V_4| = 1$ ,  $|V_5| = m + n - 2$ , and  $|V_6| = mn - m - n + 1$ . Let  $E_{(i,j)}$  denote the edge set containing the edges of  $VC[m, n]$  with end vertices of degree  $i$  and degree  $j$ . The edge set of  $VC[m, n]$  can be partitioned based on the degree of end vertices as follows:  $E_{(1,4)}$  with 1 edge,  $E_{(1,5)}$  with 2 edges,  $E_{(1,6)}$  with  $m + n - 1$  edges,  $E_{(2,4)}$  with 2 edges,  $E_{(2,5)}$  with  $2m + 2n - 4$  edges,  $E_{(2,6)}$  with  $2m + 2n - 6$  edges,  $E_{(3,4)}$  with 1 edge,  $E_{(3,5)}$  with  $3m + 3n - 8$  edges, and  $E_{(3,6)}$  having  $6mn - 9m - 9n + 13$  edges. In Theorem 1, we compute the  $ev$  degree Randic and  $ev$  degree Zagreb index of  $VC[m, n]$ .

## 3. Main Results

**Theorem 1.** Let  $m, n \geq 2$ , then

$$\begin{aligned}
 M^{ev}(VC[m, n]) &= 486mn - 262m - 262n + 130, \\
 R^{ev}(VC[m, n]) &= \frac{1}{\sqrt{7}}mn + \left( \frac{1}{\sqrt{7}} + \frac{2}{\sqrt{7}} + \frac{2}{\sqrt{8}} + \frac{3}{\sqrt{8}} - \frac{9}{\sqrt{9}} \right)m \\
 &\quad + \left( \frac{1}{\sqrt{7}} + \frac{2}{\sqrt{7}} + \frac{2}{\sqrt{8}} + \frac{3}{\sqrt{8}} - \frac{9}{\sqrt{9}} \right)n + \left( \frac{1}{\sqrt{5}} + \frac{4}{\sqrt{6}} - \frac{4}{\sqrt{7}} - \frac{6}{\sqrt{8}} - \frac{8}{\sqrt{8}} + \frac{13}{\sqrt{9}} \right).
 \end{aligned} \tag{1}$$

*Proof.* To compute the  $ev$  degree Zagreb and  $ev$  degree Randic index of  $VC[m, n]$ , we need to compute the  $ev$  degree of the edges in each partition set  $E_{(i,j)}$ . This calculation is

presented in Table 2. Now, using the information presented in Table 2 and the definition of  $ev$  degree Zagreb and  $ev$  degree Randic index, we get

$$\begin{aligned}
 M^{ev}(VC[m, n]) &= \sum_{e \in E(Z)} d_{ev}(e)^2 \\
 &= (5)^2 |E_{(1,4)}| + (6)^2 |E_{(1,5)}| + (7)^2 |E_{(1,6)}| + (6)^2 |E_{(2,4)}| + (7)^2 |E_{(2,5)}| \\
 &\quad + (8)^2 |E_{(2,6)}| + (7)^2 |E_{(3,4)}| + (8)^2 |E_{(3,5)}| + (9)^2 |E_{(3,6)}| \\
 &= (5)^2 (1) + (6)^2 (2) + (7)^2 (m + n - 1) + (6)^2 (2) + (7)^2 (2m + 2n - 4)
 \end{aligned}$$

TABLE 1: Mathematical formula of topological indices.

Topological indices	Notation	Mathematical formula
Ev degree Randic index	$R^{ev}(G)$	$\sum_{e \in E(G)} d_{ev}(e)^{-1/2}$
First Zagreb $\beta$ -index	$M_1^{\beta ve}(G)$	$\sum_{uv \in E(G)} (d_{ve}(u) + d_{ve}(v))$
Ev degree Zagreb index	$M^{ev}(G)$	$\sum_{e \in E(G)} d_{ev}(e)^2$
Second Zagreb $\beta$ -index	$M_2^{\beta ve}(G)$	$\sum_{uv \in E(G)} (d_{ve}(u) \times d_{ve}(v))$
Ve degree harmonic index	$H^{ve}(G)$	$\sum_{uv \in E(G)} ((2)/(d_{ve}(u) + d_{ve}(v)))$
Ve degree sum connectivity index	$\chi^{ve}(G)$	$\sum_{uv \in E(G)} (d_{ve}(u) + d_{ve}(v))^{-1/2}$
Ve degree geometric arithmetic index	$GA^{ve}(G)$	$\sum_{uv \in E(G)} (2\sqrt{d_{ve}(u) \times d_{ve}(v)})/(d_{ve}(u) + d_{ve}(v))$
Ve degree atom bond connectivity index	$ABC^{ve}(G)$	$\sum_{uv \in E(G)} \sqrt{(d_{ve}(u) + d_{ve}(v) - 2)/(d_{ve}(u) \times d_{ve}(v))}$

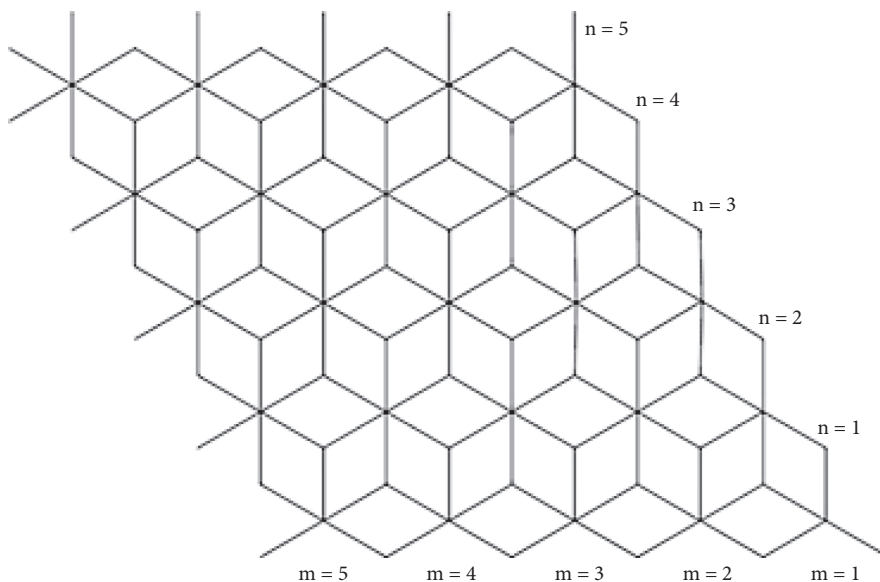
FIGURE 1: Molecular structure of vanadium carbide for  $m = 5$  and  $n = 5$ .

TABLE 2: Ev-degrees of edges of vanadium carbide.

$(d(u), d(v))$	$d_{ev}(e)$	Frequency
$E_{(1,4)}$	5	1
$E_{(1,5)}$	6	2
$E_{(1,6)}$	7	$m + n - 1$
$E_{(2,4)}$	6	2
$E_{(2,5)}$	7	$2m + 2n - 4$
$E_{(2,6)}$	8	$2m + 2n - 6$
$E_{(3,4)}$	7	1
$E_{(3,5)}$	8	$3m + 3n - 8$
$E_{(3,6)}$	9	$6mn - 9m - 9n + 13$

$$\begin{aligned}
& + (8)^2 (2m + 2n - 6) + (9)^2 (1) + (7)^2 (3m + 3n - 8) \\
& + (8)^2 (6mn - 9m - 9n + 13) \\
& = 486mn - 262m - 262n + 130. \\
R^{ev}(VC[m, n]) &= \sum_{e \in E(Z)} d_{ev}(e)^{-1/2}, \\
&= (5)^{-1/2} |E_{(1,4)}| + (6)^{-1/2} |E_{(1,5)}| + (7)^{-1/2} |E_{(1,6)}| + (6)^{-1/2} |E_{(2,4)}| + (7)^{-1/2} |E_{(2,5)}| \\
& + (8)^{-1/2} |E_{(2,6)}| + (7)^{-1/2} |E_{(3,4)}| + (8)^{-1/2} |E_{(3,5)}| + (9)^{-1/2} |E_{(3,6)}|
\end{aligned}$$

$$\begin{aligned}
&= (5)^{-1/2} (1) + (6)^{-1/2} (2) + (7)^{-1/2} (m+n-1) + (6)^{-1/2} (2) + (7)^{-1/2} (2m+2n-4) \\
&+ (8)^{-1/2} (2m+2n-6) + (9)^{-1/2} (1) + (7)^{-1/2} (3m+3n-8) \\
&+ (8)^{-1/2} (6mn-9m-9n+13) \\
&= \frac{1}{\sqrt{7}} mn + \left( \frac{1}{\sqrt{7}} + \frac{2}{\sqrt{7}} + \frac{2}{\sqrt{8}} + \frac{3}{\sqrt{8}} - \frac{9}{\sqrt{9}} \right) m + \left( \frac{1}{\sqrt{7}} + \frac{2}{\sqrt{7}} + \frac{2}{\sqrt{8}} + \frac{3}{\sqrt{8}} - \frac{9}{\sqrt{9}} \right) n \\
&+ \left( \frac{1}{\sqrt{5}} + \frac{4}{\sqrt{6}} - \frac{4}{\sqrt{7}} - \frac{6}{\sqrt{8}} - \frac{8}{\sqrt{8}} + \frac{13}{\sqrt{9}} \right). \tag{2}
\end{aligned}$$

□

**Theorem 2.** Let  $m, n \geq 3$ , then

$$\begin{aligned}
M_1^{bve} (VC[m, n]) &= 216mn + 76m + 20n + 54, \\
M_2^{bve} (VC[m, n]) &= 1944mn - 51m - 1887n + 1798, \\
ABC^{ve} (VC[m, n]) &= \left( 6\sqrt{\frac{34}{324}} \right) mn + \left( \sqrt{\frac{18}{84}} + 2\sqrt{\frac{21}{130}} + 2\sqrt{\frac{24}{168}} + \sqrt{\frac{28}{121}} + 2\sqrt{\frac{27}{208}} + 3\sqrt{\frac{30}{252}} \right. \\
&+ \left. \sqrt{\frac{32}{288}} + 8\sqrt{\frac{33}{306}} - 15\sqrt{\frac{34}{324}} \right) m + \left( \sqrt{\frac{18}{84}} + 2\sqrt{\frac{21}{130}} + 2\sqrt{\frac{24}{168}} + \sqrt{\frac{28}{121}} \right. \\
&+ \left. 2\sqrt{\frac{27}{208}} + 3\sqrt{\frac{30}{252}} + \sqrt{\frac{32}{288}} + 2\sqrt{\frac{33}{306}} - 15\sqrt{\frac{34}{324}} \right) n + \left( \sqrt{\frac{10}{32}} + 2\sqrt{\frac{14}{55}} \right. \\
&+ \left. 3\sqrt{\frac{14}{60}} - 4\sqrt{\frac{18}{84}} + 2\sqrt{\frac{15}{72}} + 2\sqrt{\frac{19}{110}} + 2\sqrt{\frac{20}{121}} - 10\sqrt{\frac{21}{130}} + 2\sqrt{\frac{22}{117}} \right. \\
&+ \left. 2\sqrt{\frac{23}{154}} + 2\sqrt{\frac{20}{120}} - 10\sqrt{\frac{24}{168}} \sqrt{\frac{22}{112}} - 6\sqrt{\frac{28}{121}} + 2\sqrt{\frac{25}{182}} - 8\sqrt{\frac{27}{208}} + 2\sqrt{\frac{25}{176}} \right. \\
&+ \left. 2\sqrt{\frac{26}{187}} + 2\sqrt{\frac{29}{238}} - 14\sqrt{\frac{30}{252}} - 3\sqrt{\frac{32}{288}} - 10\sqrt{\frac{33}{306}} + \sqrt{\frac{26}{180}} + 37\sqrt{\frac{34}{324}} \right), \\
GA^{ve} (VC[m, n]) &= \frac{12\sqrt{324}}{36} mn + \left( \frac{2\sqrt{84}}{20} + \frac{4\sqrt{130}}{23} + \frac{4\sqrt{168}}{26} + \frac{2\sqrt{121}}{30} + \frac{4\sqrt{208}}{29} + \frac{6\sqrt{252}}{32} \right. \\
&+ \left. \frac{2\sqrt{288}}{34} + \frac{16\sqrt{306}}{35} - \frac{30\sqrt{324}}{36} \right) m + \left( \frac{2\sqrt{84}}{20} + \frac{4\sqrt{130}}{23} + \frac{4\sqrt{168}}{26} + \frac{2\sqrt{121}}{30} \right. \\
&+ \left. \frac{4\sqrt{208}}{29} + \frac{6\sqrt{252}}{32} + \frac{2\sqrt{288}}{34} + \frac{4\sqrt{306}}{35} - \frac{30\sqrt{324}}{36} \right) n + \left( \frac{2\sqrt{32}}{12} + \frac{4\sqrt{55}}{16} \right. \\
&+ \left. \frac{6\sqrt{60}}{16} - \frac{8\sqrt{84}}{20} + \frac{4\sqrt{72}}{17} + \frac{4\sqrt{110}}{21} + \frac{4\sqrt{121}}{22} - \frac{20\sqrt{130}}{23} + \frac{4\sqrt{117}}{22} + \frac{4\sqrt{154}}{25} \right. \\
&+ \left. \frac{4\sqrt{120}}{22} - \frac{20\sqrt{168}}{26} + \frac{2\sqrt{112}}{22} - \frac{12\sqrt{121}}{30} + \frac{4\sqrt{182}}{27} - \frac{16\sqrt{208}}{29} + \frac{4\sqrt{176}}{27} \right. \\
&+ \left. \frac{4\sqrt{187}}{28} + \frac{4\sqrt{238}}{31} - \frac{28\sqrt{252}}{32} - \frac{6\sqrt{288}}{34} - \frac{20\sqrt{306}}{35} + \frac{2\sqrt{180}}{28} + \frac{74\sqrt{324}}{36} \right), \\
H^{ve} (VC[m, n]) &= \frac{1}{3} mn + \frac{10974905939}{29469607440} m + \frac{39532069}{247643760} n + \frac{801297510323}{950023374300}, \tag{3a}
\end{aligned}$$

$$\begin{aligned}
\chi^{ve} (Z) &= mn + \left( \frac{1}{\sqrt{20}} + \frac{2}{\sqrt{23}} + \frac{2}{\sqrt{26}} + \frac{1}{\sqrt{30}} + \frac{2}{\sqrt{29}} + \frac{3}{\sqrt{32}} + \frac{1}{\sqrt{34}} + \frac{8}{\sqrt{35}} - \frac{15}{\sqrt{36}} \right) m + \left( \frac{1}{\sqrt{20}} \right. \\
&+ \left. \frac{2}{\sqrt{23}} + \frac{2}{\sqrt{26}} + \frac{1}{\sqrt{30}} + \frac{2}{\sqrt{29}} + \frac{3}{\sqrt{32}} + \frac{1}{\sqrt{34}} + \frac{2}{\sqrt{35}} - \frac{15}{\sqrt{36}} \right) n + \left( \frac{1}{\sqrt{12}} + \frac{2}{\sqrt{16}} + \frac{3}{\sqrt{16}} \right. \\
&- \left. \frac{4}{\sqrt{20}} + \frac{2}{\sqrt{17}} + \frac{2}{\sqrt{21}} + \frac{2}{\sqrt{22}} - \frac{10}{\sqrt{23}} + \frac{2}{\sqrt{22}} + \frac{2}{\sqrt{25}} - \frac{10}{\sqrt{26}} + \frac{1}{\sqrt{22}} - \frac{6}{\sqrt{30}} + \frac{2}{\sqrt{27}} \right)
\end{aligned}$$

$$\begin{aligned}
R^{ve}(VC[m, n]) = & \left( -\frac{8}{\sqrt{29}} + \frac{2}{\sqrt{27}} + \frac{2}{\sqrt{28}} + \frac{2}{\sqrt{31}} - \frac{14}{\sqrt{32}} - \frac{3}{\sqrt{34}} - \frac{10}{\sqrt{35}} + \frac{1}{\sqrt{28}} + \frac{37}{\sqrt{36}} \right), \\
= & \frac{6}{\sqrt{324}}mn + \left( \frac{1}{\sqrt{84}} + \frac{2}{\sqrt{130}} + \frac{2}{\sqrt{168}} + \frac{1}{\sqrt{221}} + \frac{2}{\sqrt{208}} + \frac{3}{\sqrt{252}} + \frac{1}{\sqrt{288}} \right. \\
& \left. + \frac{8}{\sqrt{306}} - \frac{15}{\sqrt{324}} \right)m + \left( \frac{1}{\sqrt{84}} + \frac{2}{\sqrt{130}} + \frac{2}{\sqrt{168}} + \frac{1}{\sqrt{221}} + \frac{2}{\sqrt{208}} + \frac{3}{\sqrt{252}} \right. \\
& \left. + \frac{1}{\sqrt{288}} + \frac{2}{\sqrt{306}} - \frac{15}{\sqrt{324}} \right)n + \left( \frac{1}{\sqrt{32}} + \frac{2}{\sqrt{55}} + \frac{3}{\sqrt{60}} - \frac{4}{\sqrt{72}} + \frac{2}{\sqrt{110}} + \frac{2}{\sqrt{121}} \right. \\
& \left. - \frac{4}{\sqrt{84}} - \frac{10}{\sqrt{130}} + \frac{2}{\sqrt{117}} + \frac{2}{\sqrt{154}} - \frac{10}{\sqrt{168}} + \frac{1}{\sqrt{112}} + \frac{6}{\sqrt{221}} + \frac{2}{\sqrt{182}} - \frac{8}{\sqrt{208}} \right. \\
& \left. + \frac{2}{\sqrt{176}} + \frac{2}{\sqrt{187}} + \frac{2}{\sqrt{238}} - \frac{14}{\sqrt{252}} - \frac{3}{\sqrt{288}} - \frac{10}{\sqrt{300}} + \frac{1}{\sqrt{180}} + \frac{37}{\sqrt{324}} \right). \tag{3b}
\end{aligned}$$

*Proof.* To compute the ve degree-based indices, we need to find the edge partition of  $E(VC[m, n])$  based on the ve degree of end vertices of each edge. This partition is

presented in Table 3. Now, using the values from Table 3 and the definition of ve degree indices, we get

$$\begin{aligned}
M_1^{\beta_{ve}}(VC[m, n]) &= \sum_{uv \in E(VC[m, n])} (d_{ve}(u) + d_{ve}(v)) \\
&= (12)|E_1| + (16)|E_2| + (16)|E_3| + (20)|E_4| + (17)|E_5| + (21)|E_6| \\
&\quad + (22)|E_7| + (23)|E_8| + (22)|E_9| + (25)|E_{10}| + (22)|E_{11}| + (26)|E_{12}| + (22)|E_{13}| \\
&\quad + (30)|E_{14}| + (27)|E_{15}| + (29)|E_{16}| + (27)|E_{17}| + (28)|E_{18}| \\
&\quad + (31)|E_{19}| + (32)|E_{20}| + (34)|E_{21}| + (35)|E_{22}| \\
&\quad + (28)|E_{23}| + (36)|E_{24}| \\
&= (12)(1) + (16)(2) + (16)(3) + (20)(m+n-4) + (17)(2) + (21)(2) + (22)(2) \\
&\quad + (23)(2m+2n-10) + (22)(2) + (25)(2) + (22)(2) + (26)(2m+2n-10) \\
&\quad + (22)(1) + (30)(m+n-6) + (27)(2) + (29)(2m+2n-8) + (27)(2) + (28)(2) \\
&\quad + (31)(2) + (32)(3m+3n-14) + (34)(m+n-3) + (35)(8m+2n-10) \\
&\quad + (28)(1) + (36)(6mn-15m-15n+37) \\
&= 216mn + 76m + 20n + 54,
\end{aligned}$$

$$\begin{aligned}
M_2^{\beta_{ve}}(VC[m, n]) &= \sum_{uv \in E(VC[m, n])} (d_{ve}(u) \times d_{ve}(v)) \\
&= (32)|E_1| + (55)|E_2| + (60)|E_3| + (84)|E_4| + (72)|E_5| + (110)|E_6| \\
&\quad + (168)|E_{12}| + (112)|E_{13}| + (121)|E_7| + (130)|E_8| + (117)|E_9| \\
&\quad + (154)|E_{10}| + (120)|E_{11}| + (121)|E_{14}| + (182)|E_{15}| + (208)|E_{16}| \\
&\quad + (176)|E_{17}| + (187)|E_{18}| + (238)|E_{19}| + (252)|E_{20}| + (288)|E_{21}|
\end{aligned}$$

TABLE 3: Edge Partition of vanadium carbide.

Edge	$(d_{ve}(u), d_{ve}(v))$	Frequency
$E_1$	(4, 8)	1
$E_2$	(5, 11)	2
$E_3$	(6, 10)	3
$E_4$	(6, 14)	$m + n - 4$
$E_5$	(9, 8)	2
$E_6$	(10, 11)	2
$E_7$	(11, 11)	2
$E_8$	(10, 13)	$2m + 2n - 10$
$E_9$	(9, 13)	2
$E_{10}$	(11, 14)	2
$E_{11}$	(12, 10)	2
$E_{12}$	(12, 14)	$2m + 2n - 10$
$E_{13}$	(8, 14)	1
$E_{14}$	(17, 13)	$m + n - 6$
$E_{15}$	(14, 13)	2
$E_{16}$	(16, 13)	$2m + 2n - 8$
$E_{17}$	(16, 11)	2
$E_{18}$	(17, 11)	2
$E_{19}$	(17, 14)	2
$E_{20}$	(18, 14)	$3m + 3n - 14$
$E_{21}$	(16, 18)	$m + n - 3$
$E_{22}$	(17, 18)	$2m + 2n - 10$
$E_{23}$	(18, 10)	1
$E_{24}$	(18, 18)	$6mn - 15m - 15n + 37$

$$\begin{aligned}
& + (306)|E_{22}| + (180)|E_{23}| + (324)|E_{24}| \\
= & (32)(1) + (55)(2) + (60)(3) + (84)(m + n - 4) + (72)(2) + (110)(2) + (121)(2) \\
& + (130)(2m + 2n - 10) + (117)(2) + (154)(2) + (120)(2) + (168)(2m + 2n - 10) \\
& + (112)(1) + (121)(m + n - 6) + (182)(2) + (208)(2m + 2n - 8) + (176)(2) \\
& + (187)(2) + (238)(2) + (252)(3m + 3n - 14) + (288)(m + n - 3) \\
& + (306)(8m + 2n - 10) + (180)(1) + (324)(6mn - 15m - 15n + 37) \\
= & 1944mn - 51m - 1887n + 1798. \tag{4}
\end{aligned}$$

$$\begin{aligned}
ABC^{ve}(VC[m, n]) &= \sum_{uv \in E(VC[m, n])} \sqrt{\frac{d_{ve}(u) + d_{ve}(v) - 2}{d_{ve}(u) \times d_{ve}(v)}} \\
&= \left(\sqrt{\frac{10}{32}}\right)|E_1| + \left(\sqrt{\frac{14}{55}}\right)|E_2| + \left(\sqrt{\frac{14}{60}}\right)|E_3| + \left(\sqrt{\frac{18}{84}}\right)|E_4| + \left(\sqrt{\frac{21}{130}}\right)|E_8| \\
&+ \left(\sqrt{\frac{15}{72}}\right)|E_5| + \left(\sqrt{\frac{19}{110}}\right)|E_6| + \left(\sqrt{\frac{20}{121}}\right)|E_7| + \left(\sqrt{\frac{22}{117}}\right)|E_9| \\
&+ \left(\sqrt{\frac{23}{154}}\right)|E_{10}| + \left(\sqrt{\frac{20}{120}}\right)|E_{11}| + \left(\sqrt{\frac{24}{168}}\right)|E_{12}| + \left(\sqrt{\frac{22}{112}}\right)|E_{13}| \\
&+ \left(\sqrt{\frac{28}{121}}\right)|E_{14}| + \left(\sqrt{\frac{25}{182}}\right)|E_{15}| + \left(\sqrt{\frac{27}{208}}\right)|E_{16}| + \left(\sqrt{\frac{25}{176}}\right)|E_{17}| \\
&+ \left(\sqrt{\frac{26}{187}}\right)|E_{18}| + \left(\sqrt{\frac{29}{238}}\right)|E_{19}| + \left(\sqrt{\frac{30}{252}}\right)|E_{20}| + \left(\sqrt{\frac{32}{288}}\right)|E_{21}| \\
&+ \left(\sqrt{\frac{33}{306}}\right)|E_{22}| + \left(\sqrt{\frac{26}{180}}\right)|E_{23}| + \left(\sqrt{\frac{34}{324}}\right)|E_{24}| \\
&= \left(6\sqrt{\frac{34}{324}}\right)mn + \left(\sqrt{\frac{18}{84}} + 2\sqrt{\frac{21}{130}} + 2\sqrt{\frac{24}{168}} + \sqrt{\frac{28}{121}} + 2\sqrt{\frac{27}{208}} + 3\sqrt{\frac{30}{252}}\right)
\end{aligned}$$

$$\begin{aligned}
& + \sqrt{\frac{32}{288}} + 8\sqrt{\frac{33}{306}} - 15\sqrt{\frac{34}{324}} \Big) m + \left( \sqrt{\frac{18}{84}} + 2\sqrt{\frac{21}{130}} + 2\sqrt{\frac{24}{168}} + \sqrt{\frac{28}{121}} \right. \\
& + 2\sqrt{\frac{27}{208}} + 3\sqrt{\frac{30}{252}} + \sqrt{\frac{32}{288}} + 2\sqrt{\frac{33}{306}} - 15\sqrt{\frac{34}{324}} \Big) n + \left( \sqrt{\frac{10}{32}} + 2\sqrt{\frac{14}{55}} \right. \\
& + 3\sqrt{\frac{14}{60}} - 4\sqrt{\frac{18}{84}} + 2\sqrt{\frac{15}{72}} + 2\sqrt{\frac{19}{110}} + 2\sqrt{\frac{20}{121}} - 10\sqrt{\frac{21}{130}} + 2\sqrt{\frac{22}{117}} \\
& + 2\sqrt{\frac{23}{154}} + 2\sqrt{\frac{20}{120}} - 10\sqrt{\frac{24}{168}} + \sqrt{\frac{22}{112}} - 6\sqrt{\frac{28}{121}} + 2\sqrt{\frac{25}{182}} - 8\sqrt{\frac{27}{208}} \\
& + 2\sqrt{\frac{25}{176}} + 2\sqrt{\frac{26}{187}} + 2\sqrt{\frac{29}{238}} - 14\sqrt{\frac{30}{252}} - 3\sqrt{\frac{32}{288}} - 10\sqrt{\frac{33}{306}} + \sqrt{\frac{26}{180}} \\
& \left. + 37\sqrt{\frac{34}{324}} \right), \tag{5a}
\end{aligned}$$

$$\begin{aligned}
\text{GA}^{ve}(\text{VC}[m, n]) &= \sum_{uv \in E(\text{VC}[m, n])} \frac{2\sqrt{d_{ve}(u)} \times d_{ve}(v)}{(d_{ve}(u) + d_{ve}(v))} \\
&= \left( \frac{2\sqrt{32}}{12} \right) |E_1| + \left( \frac{2\sqrt{55}}{16} \right) |E_2| + \left( \frac{2\sqrt{60}}{16} \right) |E_3| + \left( \frac{2\sqrt{84}}{20} \right) |E_4| + \left( \frac{2\sqrt{72}}{17} \right) |E_5| \\
&+ \left( \frac{2\sqrt{110}}{21} \right) |E_6| + \left( \frac{2\sqrt{121}}{22} \right) |E_7| + \left( \frac{2\sqrt{130}}{23} \right) |E_8| + \left( \frac{2\sqrt{117}}{22} \right) |E_9| \\
&+ \left( \frac{2\sqrt{154}}{25} \right) |E_{10}| + \left( \frac{2\sqrt{120}}{22} \right) |E_{11}| + \left( \frac{2\sqrt{168}}{26} \right) |E_{12}| + \left( \frac{2\sqrt{112}}{22} \right) |E_{13}| \\
&+ \left( \frac{2\sqrt{121}}{30} \right) |E_{14}| + \left( \frac{2\sqrt{182}}{27} \right) |E_{15}| + \left( \frac{2\sqrt{208}}{29} \right) |E_{16}| + \left( \frac{2\sqrt{176}}{27} \right) |E_{17}| \\
&+ \left( \frac{2\sqrt{187}}{28} \right) |E_{18}| + \left( \frac{2\sqrt{238}}{31} \right) |E_{19}| + \left( \frac{2\sqrt{252}}{32} \right) |E_{20}| + \left( \frac{2\sqrt{288}}{34} \right) |E_{21}| \\
&+ \left( \frac{2\sqrt{306}}{35} \right) |E_{22}| + \left( \frac{2\sqrt{180}}{28} \right) |E_{23}| + \left( \frac{2\sqrt{324}}{36} \right) |E_{24}| \tag{5b} \\
&= \frac{12\sqrt{324}}{36} mn + \left( \frac{2\sqrt{84}}{20} + \frac{4\sqrt{130}}{23} + \frac{4\sqrt{168}}{26} + \frac{2\sqrt{121}}{30} + \frac{4\sqrt{208}}{29} + \frac{6\sqrt{252}}{32} \right. \\
&+ \left. \frac{2\sqrt{288}}{34} + \frac{16\sqrt{306}}{35} - \frac{30\sqrt{324}}{36} \right) m + \left( \frac{2\sqrt{84}}{20} + \frac{4\sqrt{130}}{23} + \frac{4\sqrt{168}}{26} + \frac{2\sqrt{121}}{30} \right. \\
&+ \left. \frac{4\sqrt{208}}{29} + \frac{6\sqrt{252}}{32} + \frac{2\sqrt{288}}{34} + \frac{4\sqrt{306}}{35} - \frac{30\sqrt{324}}{36} \right) n + \left( \frac{2\sqrt{32}}{12} + \frac{4\sqrt{55}}{16} \right. \\
&+ \frac{6\sqrt{60}}{16} - \frac{8\sqrt{84}}{20} + \frac{4\sqrt{72}}{17} + \frac{4\sqrt{110}}{21} + \frac{4\sqrt{121}}{22} - \frac{20\sqrt{130}}{23} + \frac{4\sqrt{117}}{22} + \frac{4\sqrt{154}}{25} \\
&+ \frac{4\sqrt{120}}{22} - \frac{20\sqrt{168}}{26} + \frac{2\sqrt{112}}{22} - \frac{12\sqrt{121}}{30} + \frac{4\sqrt{182}}{27} - \frac{16\sqrt{208}}{29} + \frac{4\sqrt{176}}{27} \\
&\left. + \frac{4\sqrt{187}}{28} + \frac{4\sqrt{238}}{31} - \frac{28\sqrt{252}}{32} - \frac{6\sqrt{288}}{34} - \frac{20\sqrt{306}}{35} + \frac{2\sqrt{180}}{28} + \frac{74\sqrt{324}}{36} \right).
\end{aligned}$$

$$\begin{aligned}
\text{H}^{ve}(\text{VC}[m, n]) &= \sum_{uv \in E(\text{VC}[m, n])} \frac{2}{d_{ve}(u) + d_{ve}(v)} \\
&= \left( \frac{2}{12} \right) |E_1| + \left( \frac{2}{16} \right) |E_2| + \left( \frac{2}{16} \right) |E_3| + \left( \frac{2}{20} \right) |E_4| + \left( \frac{2}{17} \right) |E_5| + \left( \frac{2}{21} \right) |E_6| \\
&+ \left( \frac{2}{22} \right) |E_7| + \left( \frac{2}{23} \right) |E_8| + \left( \frac{2}{22} \right) |E_9| + \left( \frac{2}{25} \right) |E_{10}| + \left( \frac{2}{22} \right) |E_{11}| + \left( \frac{2}{26} \right) |E_{12}| \\
&+ \left( \frac{2}{22} \right) |E_{13}| + \left( \frac{2}{30} \right) |E_{14}| + \left( \frac{2}{27} \right) |E_{15}| + \left( \frac{2}{29} \right) |E_{16}| + \left( \frac{2}{27} \right) |E_{17}|
\end{aligned}$$

$$\begin{aligned}
& + \left(\frac{2}{28}\right)|E_{18}| + \left(\frac{2}{31}\right)|E_{19}| + \left(\frac{2}{32}\right)|E_{20}| + \left(\frac{2}{34}\right)|E_{21}| + \left(\frac{2}{35}\right)|E_{22}| \\
& + \left(\frac{2}{28}\right)|E_{23}| + \left(\frac{2}{36}\right)|E_{24}| \\
& = \frac{1}{3}mn + \frac{10974905939}{29469607440}m + \frac{39532069}{247643760}n + \frac{801297510323}{950023374300}
\end{aligned} \tag{6a}$$

$$\begin{aligned}
\chi^{ve}(VC[m, n]) &= \sum_{uv \in E(VC[m, n])} (d_{ve}(u) + d_{ve}(v))^{-1/2} \\
&= (12)^{-1/2}|E_1| + (16)^{-1/2}|E_2| + (16)^{-1/2}|E_3| + (20)^{-1/2}|E_4| + (17)^{-1/2}|E_5| \\
&+ (21)^{-1/2}|E_6| + (22)^{-1/2}|E_7| + (23)^{-1/2}|E_8| + (22)^{-1/2}|E_9| + (25)^{-1/2}|E_{10}| \\
&+ (22)^{-1/2}|E_{11}| + (26)^{-1/2}|E_{12}| + (22)^{-1/2}|E_{13}| + (30)^{-1/2}|E_{14}| \\
&+ (27)^{-1/2}|E_{15}| + (29)^{-1/2}|E_{16}| + (27)^{-1/2}|E_{17}| + (28)^{-1/2}|E_{18}| \\
&+ (31)^{-1/2}|E_{19}| + (32)^{-1/2}|E_{20}| + (34)^{-1/2}|E_{21}| + (35)^{-1/2}|E_{22}| \\
&+ (28)^{-1/2}|E_{23}| + (36)^{-1/2}|E_{24}| \\
&= mn + \left( \frac{1}{\sqrt{20}} + \frac{2}{\sqrt{23}} + \frac{2}{\sqrt{26}} + \frac{1}{\sqrt{30}} + \frac{2}{\sqrt{29}} + \frac{3}{\sqrt{32}} + \frac{1}{\sqrt{34}} + \frac{8}{\sqrt{35}} - \frac{15}{\sqrt{36}} \right)m \\
&+ \left( \frac{1}{\sqrt{20}} + \frac{2}{\sqrt{23}} + \frac{2}{\sqrt{26}} + \frac{1}{\sqrt{30}} + \frac{2}{\sqrt{29}} + \frac{3}{\sqrt{32}} + \frac{1}{\sqrt{34}} + \frac{2}{\sqrt{35}} - \frac{15}{\sqrt{36}} \right)n \\
&+ \left( \frac{1}{\sqrt{12}} + \frac{2}{\sqrt{16}} + \frac{3}{\sqrt{16}} - \frac{4}{\sqrt{20}} + \frac{2}{\sqrt{17}} + \frac{2}{\sqrt{21}} + \frac{2}{\sqrt{22}} - \frac{10}{\sqrt{23}} + \frac{2}{\sqrt{22}} + \frac{2}{\sqrt{25}} \right. \\
&- \frac{10}{\sqrt{26}} + \frac{1}{\sqrt{22}} - \frac{6}{\sqrt{30}} + \frac{2}{\sqrt{27}} - \frac{8}{\sqrt{29}} + \frac{2}{\sqrt{27}} + \frac{2}{\sqrt{28}} + \frac{2}{\sqrt{31}} - \frac{14}{\sqrt{32}} - \frac{3}{\sqrt{34}} \\
&\left. - \frac{10}{\sqrt{35}} + \frac{1}{\sqrt{28}} + \frac{37}{\sqrt{36}} \right).
\end{aligned} \tag{6b}$$

$$\begin{aligned}
R^{ve}(VC[m, n]) &= \sum_{uv \in E(VC[m, n])} (d_{ve}(u) \times d_{ve}(v))^{-1/2} \\
&= (32)^{-1/2}|E_1| + (55)^{-1/2}|E_2| + (60)^{-1/2}|E_3| + (84)^{-1/2}|E_4| + (72)^{-1/2}|E_5| \\
&+ (110)^{-1/2}|E_6| + (121)^{-1/2}|E_7| + (130)^{-1/2}|E_8| + (117)^{-1/2}|E_9| \\
&+ (154)^{-1/2}|E_{10}| + (120)^{-1/2}|E_{11}| + (168)^{-1/2}|E_{12}| + (112)^{-1/2}|E_{13}| \\
&+ (121)^{-1/2}|E_{14}| + (182)^{-1/2}|E_{15}| + (208)^{-1/2}|E_{16}| + (176)^{-1/2}|E_{17}| \\
&+ (187)^{-1/2}|E_{18}| + (238)^{-1/2}|E_{19}| + (252)^{-1/2}|E_{20}| + (288)^{-1/2}|E_{21}| \\
&+ (306)^{-1/2}|E_{22}| + (180)^{-1/2}|E_{23}| + (324)^{-1/2}|E_{24}| \\
&= \frac{6}{\sqrt{324}}mn + \left( \frac{1}{\sqrt{84}} + \frac{2}{\sqrt{130}} + \frac{2}{\sqrt{168}} + \frac{1}{\sqrt{221}} + \frac{2}{\sqrt{208}} + \frac{3}{\sqrt{252}} + \frac{1}{\sqrt{288}} \right. \\
&+ \frac{8}{\sqrt{306}} - \frac{15}{\sqrt{324}} \left. \right)m + \left( \frac{1}{\sqrt{84}} + \frac{2}{\sqrt{130}} + \frac{2}{\sqrt{168}} + \frac{1}{\sqrt{221}} + \frac{2}{\sqrt{208}} + \frac{3}{\sqrt{252}} \right. \\
&+ \frac{1}{\sqrt{288}} + \frac{2}{\sqrt{306}} - \frac{15}{\sqrt{324}} \left. \right)n + \left( \frac{1}{\sqrt{32}} + \frac{2}{\sqrt{55}} + \frac{3}{\sqrt{60}} - \frac{4}{\sqrt{72}} + \frac{2}{\sqrt{110}} \right. \\
&+ \frac{2}{\sqrt{121}} - \frac{4}{\sqrt{84}} - \frac{10}{\sqrt{130}} + \frac{2}{\sqrt{117}} + \frac{2}{\sqrt{154}} - \frac{10}{\sqrt{168}} + \frac{1}{\sqrt{112}} + \frac{6}{\sqrt{221}} \\
&+ \frac{2}{\sqrt{182}} - \frac{8}{\sqrt{208}} + \frac{2}{\sqrt{176}} + \frac{2}{\sqrt{187}} + \frac{2}{\sqrt{238}} - \frac{14}{\sqrt{252}} - \frac{3}{\sqrt{288}} - \frac{10}{\sqrt{300}} \\
&\left. + \frac{1}{\sqrt{180}} + \frac{37}{\sqrt{324}} \right).
\end{aligned} \tag{7}$$

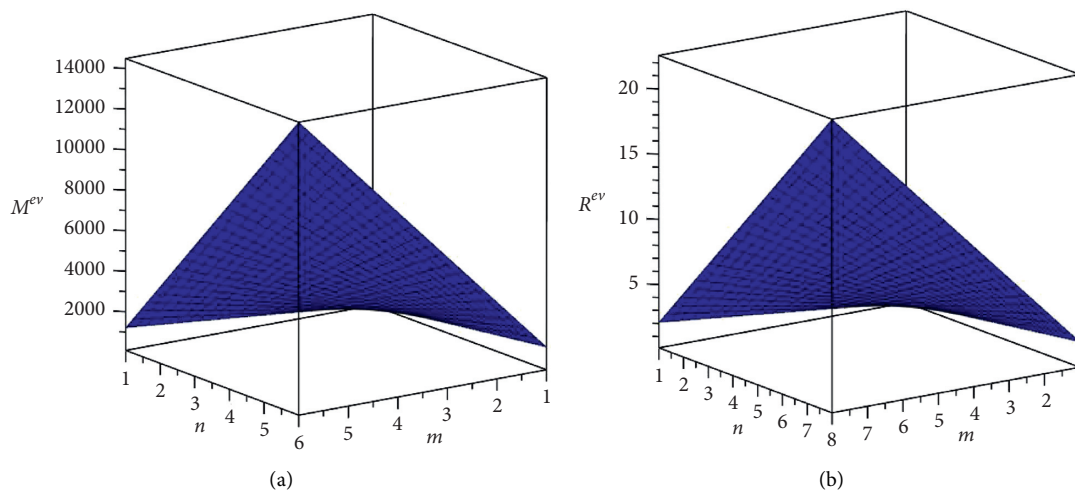
□

TABLE 4: Numerical results of indices for vanadium carbide.

$[m, n]$	$M^{ev}(H)$	$R^{ev}(H)$	$M_1^{\alpha ve}(H)$	$M_1^{\beta ve}(H)$	$M_2^{\beta ve}(H)$
[1, 1]	92	0.133 2	1324	2110	1804
[2, 2]	1026	1.070 4	2732	2854	5698
[3, 3]	2932	2.763 6	4788	4030	13 480
[4, 4]	5810	5.212 6	7492	5638	25 150
[5, 5]	9660	8.417 7	10 844	7678	40 708
[6, 6]	14 482	12.378 6	14 844	10 150	60 154
[7, 7]	20 276	17.095 4	19 492	13 054	83 488
[8, 8]	27 042	22.568 2	24 788	16 390	110 710
[9, 9]	34 780	28.796 9	30 732	20 158	141 820
[10, 10]	43 490	35.781 6	37 324	24 358	176 818

TABLE 5: Numerical results of indices for vanadium carbide.

$[m, n]$	$ABC^{ve}(H)$	$GA^{ve}(H)$	$H^{ve}(H)$	$\chi^{ve}(H)$	$R^{ve}(H)$
[1, 1]	4.707 4	10.857 0	1.708 8	1.855 0	1.031 9
[2, 2]	13.289 6	32.034 6	3.240 9	6.122 7	2.722 3
[3, 3]	25.759 0	65.212 2	5.439 6	12.390 3	5.079 3
[4, 4]	42.115 7	110.389 8	8.305 0	20.657 9	8.103 0
[5, 5]	62.359 7	167.567 4	11.837 0	30.925 5	11.793 3
[6, 6]	86.491 0	236.745 0	16.035 7	43.193 2	16.150 3
[7, 7]	114.509 6	317.922 6	20.901 1	57.460 8	21.174 0
[8, 8]	146.415 5	411.100 2	26.433 2	73.728 4	26.864 3
[9, 9]	182.208 7	516.277 9	32.631 9	91.996 1	33.221 3
[10, 10]	221.889 3	633.455 5	39.497 3	112.263 7	40.245 0

FIGURE 2: 3D plot of (a)  $M^{ev}(VC[m, n])$  (b)  $R^{ev}(VC[m, n])$ .

#### 4. Numerical Results and Discussion

Topological indices are used as vital tools for the analysis of chemicals, given the essential topology of chemical structures. Zagreb-type indices are used to calculate the total  $\pi$ -electronic energy of molecules [32]. The Randich index is commonly used to determine the chemical similarity of molecular compounds, as well as to calculate

the boiling point and Kovaz constants of molecules [33]. The atom-bond connectivity index (ABC) provides a very good correlation for calculating strain energies as well as for the stability of linear and branched chemical structures [34]. It can be seen from Table 4 and 5 and Figures 2–6 of indices, an increase in the value of  $m$  and  $n$  raises the values of topological descriptors for vanadium carbide structure.

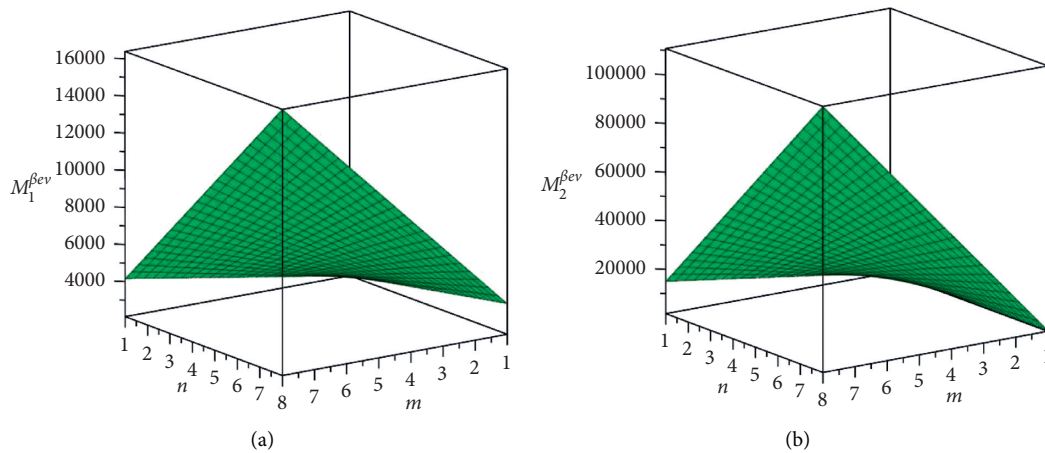


FIGURE 3: 3D plot of (a)  $M_1^{\beta ev}(VC[m, n])$  (b)  $M_2^{\beta ev}(VC[m, n])$ .

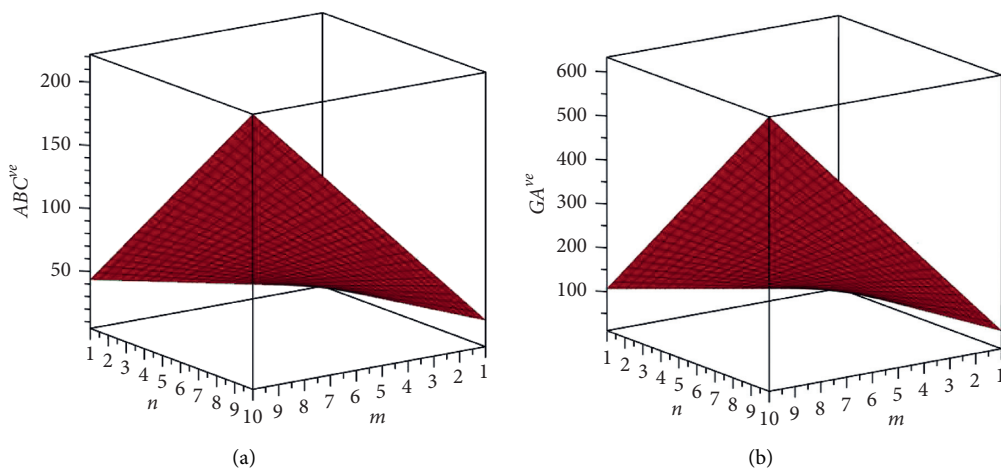


FIGURE 4: 3D plot of (a)  $ABC^{ve}(VC[m, n])$  (b)  $GA^{ve}(VC[m, n])$ .

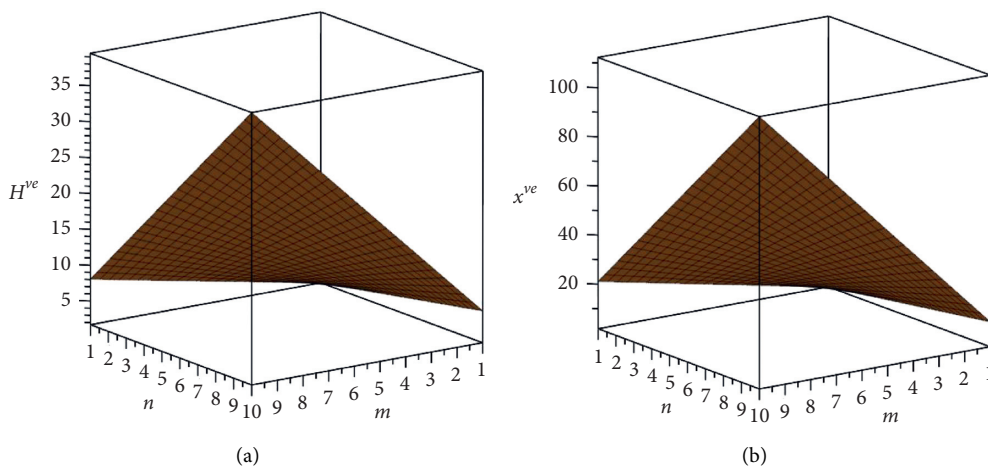


FIGURE 5: 3D plot of (a)  $H^{ve}(VC[m, n])$  (b)  $\chi^{ve}(VC[m, n])$ .

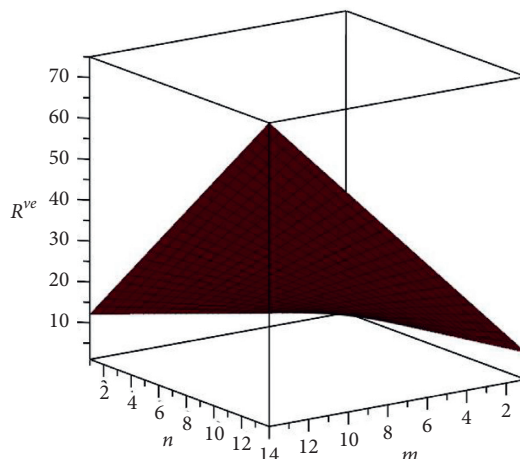


FIGURE 6: Graphical representation of  $R^{ve}(VC[m, n])$ .

## 5. Conclusion

Graphs invariants are calculated by some well-known topological indices which are important tools for resembling and forecasting the properties of chemical compounds in QSPRs and the QSARs. The TI is a numerical measure that represents the biological, physical, and chemical properties of molecules such as boiling, melting, and flickering point; moisture; and forming heat. In this paper, we have computed the  $ev$  degree and  $ve$  degree-based topological indices with graphical representations for the molecular structure of vanadium carbide for a better understanding of pharmaceutical, physical, chemical, and biological properties.

## Data Availability

No data were used to support this study.

## Disclosure

This research was carried out as a part of employment of the authors.

## Conflicts of Interest

The authors hereby declare that there are no conflicts of interest regarding the publication of this paper.

## References

- [1] B. . Sahin and S. Ediz, "On  $ev$ -degree and  $ve$ -degree topological indices," *Iranian Journal of Mathematical Chemistry*, vol. 9, no. 4, pp. 263–277, 2018.
- [2] S. Hosamani, D. Perigidad, S. Jamagoud, Y. Maled, and S. Gavade, "QSPR analysis of certain degree based topological indices," *Journal of Statistics Applications & Probability*, vol. 6, no. 2, pp. 361–371, 2017.
- [3] S. Ediz, "Predicting some physicochemical properties of octane isomers: a topological approach using  $ev$ -degree and  $ve$ -degree Zagreb indices," 2017, [https://ui.adsabs.harvard.edu/link\\_gateway/2017arXiv170102859E/arXiv:1701.02859](https://ui.adsabs.harvard.edu/link_gateway/2017arXiv170102859E/arXiv:1701.02859).
- [4] H. Wiener, "Structural determination of paraffin boiling points," *Journal of the American Chemical Society*, vol. 69, no. 1, pp. 17–20, 1947.
- [5] M. Randic, "Characterization of molecular branching," *Journal of the American Chemical Society*, vol. 97, no. 23, pp. 6609–6615, 1975.
- [6] I. Gutman and N. Trinajstić, "Graph theory and molecular orbitals. Total  $\phi$ -electron energy of alternant hydrocarbons," *Chemical Physics Letters*, vol. 17, no. 4, pp. 535–538, 1972.
- [7] S. . Ediz, "Predicting some physicochemical properties of octane isomers: a topological approach using  $ev$ -degree and  $ve$ -degree Zagreb indices," 2017.
- [8] Y.-X. Li, A. Rauf, M. Naeem, M. Ahsan Binyamin, and A. Aslam, "Valency-based topological properties of linear hexagonal chain and hammer-like benzenoid," *Complexity*, p. 2021, 2021.
- [9] S.-B. Chen, A. Rauf, M. Ishtiaq, M. Naeem, and A. Aslam, "On  $ve$ -degree- and  $ev$ -degree-based topological properties of crystallographic structure of cuprite  $Cu_2O$ ," *Open Chemistry*, vol. 19, no. 1, pp. 576–585, 2021.
- [10] S. Shirakol, M. Kalyanshetti, M. Sunilkumar, and Hosaman, "QSPR analysis of certain distance based topological indices," *Applied Mathematics and Nonlinear Sciences*, vol. 4, no. 2, pp. 371–386, 2019.
- [11] S. J. Patel, D. Ng, and M. S. Mannan, "QSPR flash point prediction of solvents using topological indices for application in computer aided molecular design," *Industrial & Engineering Chemistry Research*, vol. 48, no. 15, pp. 7378–7387, 2009.
- [12] J. C. Dearden, "The use of topological indices in QSAR and QSPR modeling," in *Advances in QSAR Modeling, Challenges and Advances in Computational Chemistry and Physics*, pp. 57–88, Springer, Cham, Switzerland, 2017.
- [13] W. Xing, F. Meng, and R. Yu, "A new type of vanadium carbide  $V_5C_3$  and its hardening by tuning Fermi energy," *Scientific Reports*, vol. 6, no. 1, pp. 21794–21799, 2016.
- [14] A. VahidMohammadi, A. Hadjikhani, S. Shahbazmohamadi, and M. Beidaghi, "Two-dimensional vanadium carbide (MXene) as a high-capacity cathode material for rechargeable aluminum batteries," *ACS Nano*, vol. 11, no. 11, pp. 11135–11144, 2017.
- [15] Y. Guan, S. Jiang, Y. Cong et al., "A hydrofluoric acid-free synthesis of 2D vanadium carbide ( $V_2C$ ) MXene for

- supercapacitor electrodes," *2D Materials*, vol. 7, no. 2, Article ID 025010, 2020.
- [16] D. Huang, Y. Xie, D. Lu et al., "Demonstration of a white laser with V2C MXene-based quantum dots," *Advanced Materials*, vol. 31, pp. 1901117–24, 2019.
- [17] D. B. West, *Introduction to Graph Theory*, Vol. 2, Prentice-Hall, Upper Saddle River, NJ, USA, 2001.
- [18] M. Chellali, T. W. Haynes, S. T. Hedetniemi, and T. M. Lewis, "On ve-degrees and ev-degrees in graphs," *Discrete Mathematics*, vol. 340, no. 2, pp. 31–38, 2017.
- [19] A. N. A. Koam, A. Ahmad, and A. A. Ahamdini, "Computation of vertex-edge degree based topological descriptors for hex-derived networks," *IEEE Access*, 2021.
- [20] E. A. Refaee and A. Ahmad, "A study of hexagon star network with vertex-edge-based topological descriptors," *Complexity*, vol. 2021, 2021.
- [21] A. Ahmad, "Comparative study of ve-degree and ev-degree topological descriptors for benzene ring embedded in P-Type-Surface in 2D network," *Polycyclic Aromatic Compounds*, pp. 1–10, 2020.
- [22] J. Zhang, M. K. Siddiqui, A. Rauf, and M. Ishtiaq, "On ve-degree and ev-degree based topological properties of single walled titanium dioxide nanotube," *Journal of Cluster Science*, pp. 1–12, 2020.
- [23] B. Horoldagva, K. Ch Das, and T.-A. Selenge, "On ve-Degree and ev-Degree of Graphs," *Discrete Optimization*, vol. 31, pp. 1–7, 2019.
- [24] Te-H. Fang, S.-R. Jian, and D.-S. Chuu, "Nanomechanical properties of TiC, TiN and TiCN thin films using scanning probe microscopy and nanoindentation," *Applied Surface Science*, vol. 228, no. 1–4, pp. 365–372, 2004.
- [25] H. G. Prengel, W. R. Pfouts, and A. T. Santhanam, "State of the art in hard coatings for carbide cutting tools," *Surface and Coatings Technology*, vol. 102, no. 3, pp. 183–190, 1998.
- [26] K. H. Lo, F. T. Cheng, C. T. Kwok, and H. Chung Man, "Improvement of cavitation erosion resistance of AISI 316 stainless steel by laser surface alloying using fine WC powder," *Surface and Coatings Technology*, vol. 165, no. 3, pp. 258–267, 2003.
- [27] B. Chicco, W. E. Borbidge, and E. Summerville, "Experimental study of vanadium carbide and carbonitride coatings," *Materials Science and Engineering: A*, vol. 266, no. 1-2, pp. 62–72, 1999.
- [28] S. A. Hassanzadeh-Tabrizi, "Homa Hosseini Badr, and Sara Alizadeh. "In situ synthesis of vanadium carbide-copper nanocomposite by a modified mechanochemical combustion method," *Ceramics International*, vol. 42, no. 8, pp. 9371–9374, 2016.
- [29] D. Ferro, J. V. Rau, A. Generosi, V. Rossi Albertini, A. Latini, and S. M. Barinov, "Electron beam deposited VC and NbC thin films on titanium: hardness and energy-dispersive X-ray diffraction study," *Surface and Coatings Technology*, vol. 202, no. 10, pp. 2162–2168, 2008.
- [30] L. B. Wang, Z. F. Chen, Y. Zhang, and W. P. Wu, *International Journal of Refractory Metals and Hard Materials*, p. 2004, 2009.
- [31] A. Aouni, P. Weisbecker, T. Huu Loi, and E. Bauer-Grosse, "Search for new materials in sputtered V1-xCx films," *Thin Solid Films*, vol. 469, pp. 315–321, 2004.
- [32] I. Gutman, B. Ruščić, N. Trinajstić, and C. F. Wilcox Jr., "Graph theory and molecular orbitals. XII. Acyclic polyenes," *The Journal of Chemical Physics*, vol. 62, no. 9, pp. 3399–3405, 1975.
- [33] N. Nikolova and J. Jaworska, "Approaches to measure chemical similarity—a review," *QSAR & Combinatorial Science*, vol. 22, no. 9-10, pp. 1006–1026, 2003.
- [34] E. Estrada, L. Torres, L. Rodriguez, and I. Gutman, "An atom-bond connectivity index: modelling the enthalpy of formation of alkanes," 1998.

## Research Article

# On Wiener Polarity Index and Wiener Index of Certain Triangular Networks

Mr. Adnan,<sup>1,2</sup> Syed Ahtsham Ul Haq Bokhary <sup>1</sup> and Muhammad Imran <sup>3</sup>

<sup>1</sup>Centre for Advanced Studies in Pure and Applied Mathematics, Bahauddin Zakariya University, Multan, Pakistan

<sup>2</sup>Allama Iqbal Open University, Islamabad, Pakistan

<sup>3</sup>Department of Mathematical Sciences, United Arab Emirates University, P. O. Box, Al Ain 15551, UAE

Correspondence should be addressed to Syed Ahtsham Ul Haq Bokhary; [sihtsham@gmail.com](mailto:sihtsham@gmail.com)

Received 16 June 2021; Revised 30 August 2021; Accepted 16 November 2021; Published 20 December 2021

Academic Editor: Alberto Figoli

Copyright © 2021 Mr. Adnan et al. This is an open access article distributed under the Creative Commons Attribution License, which permits unrestricted use, distribution, and reproduction in any medium, provided the original work is properly cited.

A topological index of graph  $G$  is a numerical quantity which describes its topology. If it is applied to the molecular structure of chemical compounds, it reflects the theoretical properties of the chemical compounds. A number of topological indices have been introduced so far by different researchers. The Wiener index is one of the oldest molecular topological indices defined by Wiener. The Wiener index number reflects the index boiling points of alkane molecules. Quantitative structure activity relationships (QSAR) showed that they also describe other quantities including the parameters of its critical point, density, surface tension, viscosity of its liquid phase, and the van der Waals surface area of the molecule. The Wiener polarity index has been introduced by Wiener and known to be related to the cluster coefficient of networks. In this paper, the Wiener polarity index  $W_p(G)$  and Wiener index  $W(G)$  of certain triangular networks are computed by using graph-theoretic analysis, combinatorial computing, and vertex-dividing technology.

## 1. Introduction

The Wiener index is originally the first and most studied topological index (see for details in [1]). It was the first molecular topological index that was used in chemistry. Since then, a lot of indices were introduced that relate the topological indices to different physical properties, and some of the recent results can be found in [3–6]. Wiener shows that the Wiener index number is closely correlated with the boiling points of alkane molecules [2]. Later work on quantitative structure activity relationships showed that it is also correlated with other quantities including the parameters of its critical point [7], the density, surface tension, and viscosity of its liquid phase [8], and the van der Waals surface area of the molecule [9].

Mathematically, the Wiener index is sum of all the distances between every vertex of the graph, denoted by  $W(G)$ , and is

$$W(G) = \sum_{p,q \in V(G)} d(p,q). \quad (1)$$

Later on, Wiener introduced another descriptor known as Wiener polarity index that is known to be related to the cluster coefficient of networks. The Wiener polarity index is denoted by  $W_p(G)$  and is defined as the number of unordered pairs of vertices that are at distance 3 in  $G$ . That is,

$$W_p(G) = |\{(p,q) | d_G(p,q) = 3, p, q \in V(G)\}|. \quad (2)$$

In organic compounds, say paraffin, the Wiener polarity index is the number of pairs of carbon atoms which are separated by three carbon-carbon bonds. Based on the Wiener index and the Wiener polarity index, the formula

$$t_B = aW(G) + bW_p(G) + c \quad (3)$$

was used to calculate the boiling points  $t_B$  of the paraffins, where  $a$ ,  $b$ , and  $c$  are constants for a given isomeric group.

By using the Wiener polarity index, Lukovits and Linert demonstrated quantitative structure-property relationships in a series of acyclic and cycle-containing hydrocarbons in [10]. Hosoya in [11] found a physical-chemical interpretation of  $W_p(G)$ . Actually, the Wiener polarity index of many kinds of graphs is studied, such as trees [12], unicyclic and bicyclic graphs [13], hexagonal systems, fullerenes, and polyphenylene chains [14], and lattice networks [15]. For more results on the Wiener polarity index, we refer some recent papers [16–19] and the survey paper [20].

## 2. The Wiener Polarity Index and Wiener Index of Networks Obtained from Triangular Mesh

The graph of the triangular mesh network, denoted by  $T_n$ , is obtained inductively by the triangulation of the graph  $T_{n-1}$ . The procedure to construct this network is as follows:

- (i) Consider a basic graph  $T_3$  which is a cycle  $C_3$  of length 3.
- (ii) Subdivide each edge of  $T_3$ , and then join them to form a triangle; the resulting graph is  $T_4$ .
- (iii) Continuing in this way, construct a graph  $T_n$  from  $T_{n-1}$  by subdividing each edge of  $T_{n-1}$  and then connect them to form triangles.
- (iv) The graph  $T_n$  has  $n$  vertices on each of its side:

The graph of triangular mesh network  $T_5$  is shown in Figure 1.

The vertices and edges of  $T_n$  are defined as follows:  
 $V(T_n) = \{x_{l,m} : 1 \leq l \leq n, 1 \leq m \leq l\}$ .  
 $E(T_n) = \{x_{l,m}x_{l,m+1} : m+1 : 2 \leq l \leq n, 1 \leq m \leq l-1\} \cup \{x_{l,m}, x_{l+1,m} : 1 \leq l \leq n-1, 1 \leq m \leq l\} \cup \{x_{l,m}, x_{l+1,m+1} : 1 \leq l \leq n-1, 2 \leq m \leq l+1\}$ .

The count of vertices of the graph  $T_n$  is  $n(n+1)/2$  and edges of  $T_n$  is  $3n(n-1)/2$ .

Furthermore, we partition the vertex set  $V(T_n)$  as follows:  $V(T_n) = \cup_{l=1}^n V_l$ , where  $V_l = \{x_{l,m} : 1 \leq l \leq n, 1 \leq m \leq l\}$ .

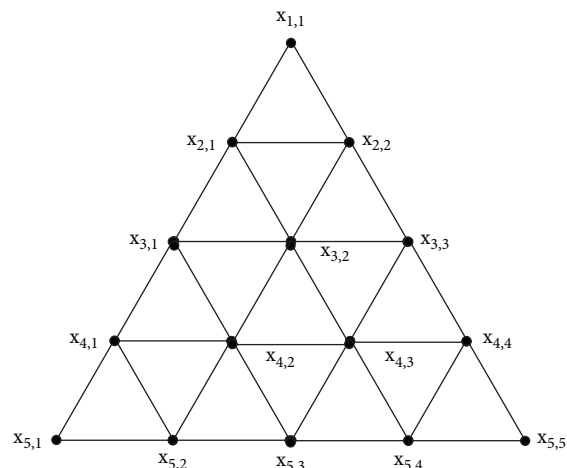


FIGURE 1: Triangular mesh.

Thus, the graph is divided into  $n$  sets. This will help us in calculating the Wiener and Wiener polarity indices of  $T_n$ . The first main result of this chapter is proved in the following.

**Theorem 1.**  $W_p(T_n) = 9(n-2)(n-3)/2$ , for  $n \geq 3$ .

*Proof.* Now, we find a number of pair  $(p, q)$  of vertices of  $T_n$  which are connected through a path of length 3.

However,

$$W_p(V_l) = |\{(p, q) | d(p, q) = 3; p, q \in V_l\}| \quad (4)$$

$$W_p(V_l, V_m) = |\{(p, q) | d(p, q) = 3; p \in V_l, q \in V_m\}|$$

is the cardinality of the set of vertices in  $V_m$  that are at distance 3 from  $V_l$ . From the construction of  $T_n$ , it is important to note that there is no vertex  $p \in V_l$  and  $q \in V_m$  such that  $d(p, q) = 3$  where  $l, m \in \{1, 2, 3\}$ . It implies that for  $x \in V_l$  and  $y \in V_m$ , we have 4 cases to consider.

$$W_p(T_n) = \sum_{l=4}^{l=n} W_p(V_l) + \sum_{l=4}^{l=n} W_p(V_l, V_{l-1}) + \sum_{l=4}^{l=n} W_p(V_l, V_{l-2}) + \sum_{l=4}^{l=n} W_p(V_l, V_{l-2}). \quad (5)$$

*Case 1.* Let  $x_{lm} \in V_l$ , where  $4 \leq l \leq n$ . If  $d(x, y) < 3$ , then  $|l-m| \leq 3$ ; then, for each  $l$ , there is only one vertex  $x_{l,m+3}$  which is at distance 3 from  $x_{l,m}$ .

Since  $l \leq m \leq n-3$ ,

$$W_p(V_l) = \{(p, q) | d(p, q) = 3; p, q \in V_l\} = l-3$$

$$\sum_{l=4}^{l=n} W_p(V_l) = \sum_{l=4}^{l=n} (l-3) = \frac{(n-3)(n-2)}{2}. \quad (6)$$

*Case 2.* Let  $u \in V_l$  and  $v \in V_{l-1}$  where  $4 \leq l \leq n$ . In this case, there are  $2l-6$  vertices in  $V_{l-1}$  that are at distance 3 from  $V_l$  for each  $l$ . Since  $i \leq m \leq n-3$ ,

$$W_p(V_l, V_{l-1}) = 2l-6$$

$$\sum_{l=4}^{l=n} W_p(V_l, V_{l-1}) = \sum_{l=4}^{l=n} 2l-6 = (n-2)(n-3). \quad (7)$$

Case 3. Let  $u \in V_l$  and  $v \in V_{l-2}$  where  $4 \leq l \leq n$ ; in this case, there are  $2l - 6$  vertices in  $V_{l-2}$  that are at distance 3 from  $V_l$  for each  $i$ . Since  $i \leq m \leq n - 3$ ,

$$W_p(V_l, V_{l-2}) = 2l - 6$$

$$\sum_{l=4}^{l=n} W_p(V_l, V_{l-2}) = \sum_{l=4}^{l=n} 2l - 6 = (n - 2)(n - 3). \quad (8)$$

Case 4. Let  $u \in V_l$  and  $v \in V_{l-3}$  where  $4 \leq l \leq n$ . In this case, there are  $4l + 6$  vertices in  $V_{l-3}$  that are at distance 3 from  $V_l$  for each  $i$ . Since  $i \leq m \leq n - 3$ ,

$$W_p(V_l, V_{l-3}) = 4l + 6$$

$$\sum_{l=4}^{l=n} W_p(V_l, V_{l-3}) = \sum_{l=4}^{l=n} 4l + 6 = 2(n - 2)(n - 3). \quad (9)$$

Putting equations (6) and (7) and (31) and (9) in (5), we get

$$W_p(T_n) = \frac{(n - 2)(n - 3)}{2} + (n - 2)(n - 3) + (n - 2)(n - 3)$$

$$+ 2(n - 2)(n - 3)$$

$$= \frac{9(n - 2)(n - 3)}{2}. \quad (10)$$

In the next result, the Wiener index of the graph  $T_n$  is computed.

**Theorem 2.**  $W(T_n) = W(T_{n-1}) + n^4 - n^2/4$ .

*Proof.* Let  $W(V_n, T_{n-1})$  be the distance between the vertices of  $V_n$  and  $T_{n-1}$ , where  $V_n = \{x_{n,1}, x_{n,2}, x_{n,3}, \dots, x_{n,n}\}$ . For  $x_{lm} \in V(T_{n-1})$ ,

$$W(V_n, T_{n-1}) = \sum_{\theta=1}^{\theta=n} W(x_{n,\theta}, T_{n-1}) + W(V_n). \quad (11)$$

This can be computed by finding the distance between each vertex  $x_{n,\theta}$  from the vertices of  $T_{n-1}$ . These distances are listed in the following.

For  $2 \leq \theta \leq n$  and  $1 \leq m \leq \theta - 1$ ,

$$d(x_{n,\theta}, x_{lm}) = \begin{cases} n - 1, & \text{for } m \leq l \leq n + m - \theta - 1, \\ \theta - m, & \text{for } n + m - \theta \leq l \leq n - 1. \end{cases} \quad (12)$$

For  $1 \leq \theta \leq n$  and  $\theta \leq m \leq n$ ,

$$d(x_{n,\theta}, x_{lm}) = \{n + m - l - \theta \quad \text{for } m \leq l \leq n - 1. \quad (13)$$

Thus, we get

$$\sum_{\theta=1}^{\theta=n} W(x_{n,\theta}, T_{n-1}) = \sum_{\theta=1}^{\theta=n} \sum_{m=1}^{m=\theta-1} \sum_{l=m}^{l=n-1} d(x_{n,\theta}, x_{lm})$$

$$= \sum_{\theta=2}^{\theta=n} \sum_{m=1}^{m=\theta-1} \sum_{l=m}^{l=n-1} d(x_{n,\theta}, x_{lm}) + \sum_{\theta=1}^{\theta=n} \sum_{m=\theta}^{m=n-1} \sum_{l=m}^{l=n-1} d(x_{n,\theta}, x_{lm})$$

$$= \sum_{\theta=2}^{\theta=n} \sum_{m=1}^{m=\theta-1} \sum_{l=n+m-\theta-1}^{l=n-1} d(x_{n,\theta}, x_{lm}) + \sum_{\theta=2}^{\theta=n} \sum_{m=1}^{m=\theta-1} \sum_{l=n+m-\theta}^{l=n-1} d(x_{n,\theta}, x_{lm})$$

$$+ \sum_{\theta=1}^{\theta=n} \sum_{m=\theta}^{m=n-1} \sum_{l=m}^{l=n-1} d(x_{n,\theta}, x_{lm}) \quad (14)$$

$$= \sum_{\theta=2}^{\theta=n} \sum_{m=1}^{m=\theta-1} \sum_{l=m}^{l=n+m-\theta-1} (n - l) + \sum_{\theta=2}^{\theta=n} \sum_{m=1}^{m=\theta-1} \sum_{l=n+m-\theta}^{l=n-1} (\theta - m)$$

$$+ \sum_{\theta=1}^{\theta=n} \sum_{m=\theta}^{m=n-1} \sum_{l=m}^{l=n-1} (n + m - l - \theta)$$

$$= \frac{1}{12} [n^4 - 2n^3 - n^2 + 2n] + \frac{1}{12} [n^4 - n^2] + \frac{1}{12} [n^4 - n^2],$$

$$W(V_n) = \sum_{\theta=1}^{\theta=n} W(x_{n,\theta}) = \sum_{l=1}^{l=n-1} \sum_{m=l}^{m=n-l} m = \frac{1}{6} [n^3 - n]. \quad (15)$$

By replacing the values of  $\sum_{\theta=1}^{\theta=n} W(x_{n,\theta}, T_{n-1})$  and  $W(V_n)$  in equation (11), we get

$$W(V_n, T_{n-1}) = \frac{1}{12} [n^4 - 2n^3 + 2n - n^2] + \frac{1}{12} [n^4 - n^2] + \frac{1}{12} [n^4 - n^2] + \frac{1}{6} [n^3 - n]. \quad (16)$$

This after simplification implies

$$W(V_n, T_{n-1}) = \frac{1}{4} [n^4 - n^2]. \quad (17)$$

However, the Wiener index of  $T_n$  is  $W(T_n) = W(T_{n-1}) + W(V_n, T_{n-1})$ . Therefore,

$$W(T_n) = W(T_{n-1}) + \frac{1}{4} [n^4 - n^2]. \quad (18)$$

### 3. The Wiener Polarity Index and Wiener Index of the Equilateral Triangular Tetra Sheet

This section will start with the definition and properties of the equilateral triangular tetra sheet network. The graph of equilateral triangular tetra sheet network denoted by  $ET_n$  is obtained from the graph of triangular mesh network by replacing each triangle by the complete graph  $K_4$ . This can be done by inserting a vertex in each triangle of the graph  $T_n$  and then connecting all the adjacent vertices to form  $K_4$ . These new vertices will be denoted by  $u_i$  and  $w_j$ , where  $1 \leq i \leq n-1$  and  $1 \leq j \leq n-2$ .

The order and size of the graph  $ET(n)$  are

$$|V(ET_n)| = \frac{(3n^2 - 3n + 2)}{2}, \quad (19)$$

$$|E(ET(n))| = \frac{(9n^2 - 15n + 6)}{2}.$$

The graph of equilateral triangular tetra sheet is shown in Figure 2.

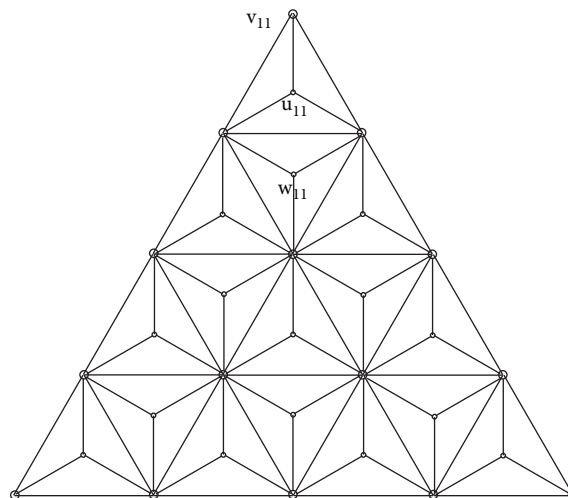


FIGURE 2: The graph of equilateral triangular tetra sheet.

In order to compute the Wiener and Wiener polarity indices, we want to find the distance between each pair of vertices of  $ET_n$ . For this purpose, we define partition of the vertex set as follows:  $V(ET_n) = \cup_{l=1}^{l=n} V_l \cup \cup_{l=1}^{l=n-1} U_l \cup \cup_{l=1}^{l=n-2} W_l$ , where  $V_l = \{x_{lm} | 1 \leq m \leq l \leq n\}$ ,  $U_l = \{u_{lm} | 1 \leq m \leq l \leq n-1\}$ , and  $W_l = \{w_{lm} | 1 \leq m \leq l \leq n-2\}$ .

Furthermore, define  $V'_l = V(ET_l) \setminus V_l$ ,  $U'_l = V(ET_l) \setminus \{V_l \cup U_l\}$ , and  $W'_l = V(ET_l) \setminus \{V_{l+2} \cup U_{l+1} \cup W_l\}$ .

In the next result, the Wiener polarity index of the graph  $ET_n$  is computed.

**Theorem 3.** For  $n \geq 3$ ,  $W_p(ET_n) = 63n^2 - 357n + 504/2$ .

*Proof.* In order to find the Wiener polarity index, we have to compute all those pairs of vertices that are at distance 3 to each other. Since the vertex set of the graph  $ET_n$  is divided into three parts, we first find the number of such pairs in each possible set. Define  $W_p(A, B)$  as the set of those vertices of  $A$  that are at distance 3 from the vertices of  $B$ . For simplicity,  $W_p(A, A) = W_p(A)$ . Thus, we have

$$W_p(V_l) = \left| \left\{ (v, vt) \mid d(v, vt) = 3; v, vt \in V_l \right\} \right|$$

$$W_p(U_l) = \left| \left\{ (u, ut) \mid d(u, ut) = 3; u, ut \in U_l \right\} \right|$$

$$W_p(W_l) = \left| \left\{ (w, wt) \mid d(w, wt) = 3; w, wt \in W_l \right\} \right|$$

$$W_p(V_l, V'_l) = \left| \left\{ (v, x) \mid d(v, x) = 3; v \in V_l, x \in V'_l; 4 \leq l \leq n \right\} \right|$$

$$W_p(U_l, U'_l) = \left| \left\{ (u, x) \mid d(u, x) = 3; u \in U_l, x \in U'_l; 3 \leq l \leq n-1 \right\} \right|$$

$$W_p(W_l, W'_l) = \left| \left\{ (w, x) \mid d(w, x) = 3; w \in W_l, x \in W'_l; 2 \leq l \leq n-2 \right\} \right|$$

$$W_p(ET(n)) = \sum_{l=4}^{l=n} (W_p(V_l) + W_p(V_l, V'_l)) + \sum_{l=3}^{l=n-1} (W_p(U_l) + W_p(U_l, U'_l)) + \sum_{l=2}^{l=n-2} (W_p(W_l) + W_p(W_l, W'_l)). \quad (20)$$

For simplicity, we compute the three factors separately:

- (i) Let  $v \in V_l$  and  $x \in V'_l$ . From the construction of  $ET_n$ , there does not exist any  $x \in V_{l-\theta}$ ,  $4 \leq \theta \leq n-1$

s.t.  $d(v, x) = 3$  which implies  $x \in \{V_{l-1} \cup V_{l-2} \cup V_{l-3} \cup U_{l-1} \cup U_{l-2} \cup U_{l-3} \cup W_{l-2} \cup W_{l-3} \cup W_{l-4}\}$   
The value of  $\sum_{l=1}^{l=n-1} W_p(V_l)$  is already calculated in Theorem 1. Furthermore,

$$W_p(V_l, V'_l) = W_p(V_l, U_{l-1}) + W_p(V_l, W_{l-2}) + W_p(V_l, V_{l-1}) + W_p(V_l, U_{l-2}) + W_p(V_l, W_{l-3}) + W_p(V_l, V_{l-3}) + W_p(V_l, U_{l-3}) + W_p(V_l, W_{l-4}). \quad (21)$$

If  $x \in U_{l-1} \cup W_{l-2} \cup U_{l-2} \cup W_{l-3}$ , then there are  $2l-6$  vertices that are at distance 3 from  $V_l$ . Thus,

$$\begin{aligned} W_p(V_l, U_{l-1}) &= W_p(V_l, W_{l-2}) = W_p(V_l, U_{l-2}) = W_p(V_l, W_{l-3}) = 2l-6 \\ \sum_{l=4}^{l=n} W_p(V_l, U_{l-1}) &= \sum_{l=4}^{l=n} W_p(V_l, W_{l-2}) = \sum_{l=4}^{l=n} W_p(V_l, U_{l-2}) = \sum_{l=4}^{l=n} W_p(V_l, W_{l-3}) \sum_{l=4}^{l=n} 2l-6 \\ &= (n-2)(n-3). \end{aligned} \quad (22)$$

- (ii) If  $x \in U_{l-3} \cup W_{l-4}$ , there are  $3l-12$  vertices that are at distance 3 from  $V_l$ .

$$\begin{aligned} W_p(V_l, U_{l-3}) &= W_p(V_l, W_{l-4}) = 3l-12 \\ \sum_{l=4}^{l=n} W_p(V_l, U_{l-3}) &= \sum_{l=4}^{l=n} W_p(V_l, W_{l-4}) = \sum_{l=4}^{l=n} 3l-12 = \frac{3n^2 - 21n + 36}{2}. \end{aligned} \quad (23)$$

From Theorem 1 and equations (22) and (23), we get after simplification

$$\sum_{l=4}^{l=n} (W_p(V_l) + W_p(V_l, V'_l)) = 3(n-3)(4n-9). \quad (24)$$

- (iii) Let  $u \in U_{l-1}$  and  $x \in U_{l-1}'$ . From the construction of  $ET_n$  there does not exist any  $x \in U_{l-\theta}$ ,  $4 \leq \theta \leq n-1$ , s.t.  $d(u, x) = 3$  which implies  $x \in \{V_i \cup V_{l-1} \cup V_{l-2} \cup U_{l-1} \cup U_{l-2} \cup U_{l-3} \cup W_{l-2} \cup W_{l-3} \cup W_{l-4}\}$ . Thus, we get

$$\begin{aligned} W_p(U_{l-1}, U_{l-1}') &= W_p(U_{l-1}, W_{l-2}) + W_p(U_{l-1}, V_{l-1}) + W_p(U_{l-1}, U_{l-2}) \\ &+ W_p(U_{l-1}, W_{l-3}) + W_p(U_{l-1}, V_{l-2}) + W_p(U_{l-1}, U_{l-3}) \\ &+ W_p(U_{l-1}, W_{l-4}) + W_p(U_{l-1}, V_{l-3}). \end{aligned} \quad (25)$$

We compute each of these factors as follows:

(iv) If  $x \in W_{l-2} \cup V_{l-1} \cup U_{l-2} \cup W_{l-3} \cup V_{l-2}$ , then there are  $2l - 4$  vertices  $x$  that are at distance 3 from  $U_{l-1}$ . Thus,

$$\begin{aligned}
 W_p(U_{l-1}, W_{l-2}) &= W_p(U_{l-1}, V_{l-1}) = W_p(U_{l-1}, U_{l-2}) \\
 &= W_p(U_{l-1}, W_{l-3}) = W_p(U_{l-1}, V_{l-2}) \\
 &= 2l - 4, \\
 \sum_{l=3}^{l=n-1} W_p(U_l, W_{l-2}) &= \sum_{l=3}^{l=n-1} W_p(U_{l-1}, V_{l-1}) \\
 &= \sum_{l=3}^{l=n-1} W_p(U_{l-1}, U_{l-2}) \\
 &= \sum_{l=3}^{l=n-1} W_p(U_{l-1}, W_{l-3}) \\
 &= \sum_{l=3}^{l=n-1} W_p(U_{l-1}, V_{l-2}) \\
 &= \sum_{l=3}^{l=n-1} 2l - 4 = (n-2)(n-3).
 \end{aligned} \tag{26}$$

If  $x \in U_{l-3} \cup V_{l-3}$ , then there are  $3l - 6$  vertices of  $x$  that are at distance 3 from  $U_{l-1}$ .

$$\begin{aligned}
 W_p(U_{l-1}, U_{l-3}) &= W_p(U_{l-1}, V_{l-3}) = 2l - 6 \\
 \sum_{l=3}^{l=n-1} W_p(U_{l-1}, U_{l-3}) &= \sum_{l=3}^{l=n-1} W_p(U_{l-1}, V_{l-3}) = \sum_{l=3}^{l=n-1} 2l - 6 = \frac{1}{2} [3n^2 - 15n + 18].
 \end{aligned} \tag{27}$$

If  $x \in W_{l-4}$ , then there are  $2l - 6$  vertices that are at distance 3 from  $U_{l-1}$ .

$$\begin{aligned}
 W_p(U_{l-1}, W_{l-4}) &= 2l - 6 \\
 \sum_{l=4}^{l=n-1} W_p(U_{l-1}, W_{l-4}) &= \sum_{l=4}^{l=n-1} 2l - 6 = n^2 - 7n + 12.
 \end{aligned} \tag{28}$$

For every  $u \in U_{l-1}$ , there are  $l - 2$   $u' \in U_{l-1}$  that are at distance 3 from  $u$ .

$$\begin{aligned}
 W_p(U_{l-1}) &= l - 2 \\
 \sum_{l=3}^{l=n-1} W_p(U_{l-1}) &= \sum_{l=3}^{l=n-1} l - 2 = \frac{n^2 - 5n + 6}{2}.
 \end{aligned} \tag{29}$$

Substituting each of these values in the second factor, we get after simplification

$$\sum_{l=4}^{l=n-1} (W_p(U_{l-1}) + W_p(U_{l-1}, U_{l-1}')) = \left(\frac{19}{2}n - 21\right)(n-3). \tag{30}$$

Let  $w \in W_{l-2}$  and  $x \in W_{l-2}'$ . From the construction of  $ET_n$ , there does not exist any  $x \in U_{l-\theta}'$ ,  $4 \leq \theta \leq n-1$  s.t.  $d(u, x) = 3$ . This implies that  $x \in \{V_{l-1} \cup V_{l-2} \cup U_{l-2} \cup U_{l-3} \cup W_{l-3} \cup W_{l-4}\}$ , and we get

$$\begin{aligned}
 W_p(W_{l-2}, W_{l-2}') &= W_p(W_{l-2}, V_{l-1}) + W_p(W_{l-2}, U_{l-2}) + W_p(W_{l-2}, W_{l-3}) \\
 &\quad + W_p(W_{l-2}, V_{l-2}) + W_p(W_{l-2}, U_{l-3}) + W_p(W_{l-2}, W_{l-4}) \\
 &\quad + W_p(W_{l-2}, V_{l-3}).
 \end{aligned} \tag{31}$$

We compute each of the factors in the following.

If  $x \in V_{l-1} \cap U_{l-2} \cup W_{l-3} \cup V_{l-2}$ , then there are  $2l - 4$  vertices that are at distance 3 from  $W_{l-2}$ . This follows that

$$\begin{aligned}
 W_p(W_{l-2}, V_{l-1}) &= W_p(W_{l-2}, U_{l-2}) = W_p(W_{l-2}, W_{l-3}) = W_p(W_{l-2}, V_{l-2}) \\
 &= 2l - 4, \\
 \sum_{l=3}^{l=n-2} W_p(W_{l-2}, V_{l-1}) &= \sum_{l=3}^{l=n-2} W_p(W_{l-2}, U_{l-2}) \\
 &= \sum_{l=3}^{l=n-2} W_p(W_{l-2}, W_{l-3}) \\
 &= \sum_{l=3}^{l=n-2} W_p(W_{l-2}, V_{l-2}) \\
 &= \sum_{l=3}^{l=n-2} (2l - 4) = n^2 - 7n + 12.
 \end{aligned} \tag{32}$$

If  $x \in U_{l-3} \cup V_{l-3}$ , then there are  $4l - 6$  vertices that are at distance 3 from  $W_{l-2}$ . This follows that

$$\begin{aligned}
 W_p(W_{l-2}, U_{l-3}) &= W_p(W_{l-2}, V_{l-3}) = 4l - 6, \\
 \sum_{l=3}^{l=n-2} W_p(W_{l-2}, U_{l-3}) &= \sum_{l=3}^{l=n-2} W_p(W_{l-2}, V_{l-3}) = \sum_{l=3}^{l=n-2} 4l - 6 = [2n^2 - 12n + 18].
 \end{aligned} \tag{33}$$

If  $x \in W_{l-4}$ , then there are  $3l - 6$  vertices that are at distance 3 from  $W_{l-2}$ . This follows that

$$\begin{aligned}
 W_p(W_{l-2}, W_{l-4}) &= 3l - 6 \\
 \sum_{l=3}^{l=n-2} W_p(W_{l-2}, W_{l-4}) &= \sum_{l=3}^{l=n-2} 3l - 6 = \frac{3n^2 - 21n + 36}{2}.
 \end{aligned} \tag{34}$$

For every  $w \in W_{l-2}$ , there are  $l - 2$  vertices  $x$  in  $w' \in W_{l-2}$  that are at distance 3 from  $w$ .

$$\begin{aligned}
 W_p(W_{l-1}) &= l - 2, \\
 \sum_{l=3}^{l=n-2} W_p(W_{l-1}) &= \sum_{l=3}^{l=n-2} l - 2 = \frac{n^2 - 7n + 12}{2}.
 \end{aligned} \tag{35}$$

Replace all these values in the third factor, and we get after simplification

$$\sum_{l=4}^{l=n-2} (W_p(W_{l-2}) + W_p(W_{l-2}, W_{l-2}')) = 10n^2 - 66n + 108. \tag{36}$$

By combining the values of all three factors in equation (20), we found that the Wiener polarity index of the graph  $ET_n$  is

$$W_p(ET_n) = \frac{63n^2 - 357n + 504}{2}. \tag{37}$$

#### Theorem

4.  $W(ET_n) = W(ET_{n-1}) + 1/12[28n^4 - 86n^3 + 134n^2 - 172n + 120]$ .

*Proof.* Let  $W(V_n, ET_{n_l})$  be the distance between the vertices of  $V_n$  from itself and from  $U_{n-1}$ ,  $W_{n-2}$ , and  $ET_{n-1}$ , where  $V_n = \{x_{n,1}, x_{n,2}, x_{n,3}, \dots, x_{n,n}\}$ ,  $U_{n-1} = \{u_{n,1}, u_{n,2}, u_{n,3}, \dots, u_{n,n-1}\}$ , and  $W_{n-1} = \{w_{n,1}, w_{n,2}, w_{n,3}, \dots, w_{n,n-2}\}$ . Thus, for any vertex in  $V_n$ , we have

$$\begin{aligned}
 W(V_n, ET_{n_l}) &= \sum_{\theta=1}^{\theta=n} W(x_{n,\theta}, ET_{n-1}) + \sum_{\theta=1}^{\theta=n} W(x_{n,\theta}, U_{n-1}) \\
 &\quad + \sum_{\theta=1}^{\theta=n} W(x_{n,\theta}, W_{n-2}) + W(V_n).
 \end{aligned} \tag{38}$$

This can further reduce to the following equation:

$$W(V_n, ET_{n_l}) = \sum_{\theta=1}^{\theta=n} W(x_{n,\theta}, \bigcup_{l=1}^{l=n-1} V_l) + \sum_{\theta=1}^{\theta=n} W(x_{n,\theta}, \bigcup_{l=1}^{l=n-2} U_l) + \sum_{\theta=1}^{\theta=n} W(x_{n,\theta}, \bigcup_{l=1}^{l=n-3} W_l) + \sum_{\theta=1}^{\theta=n} W(x_{n,\theta}). \quad (39)$$

We compute each of the factors in equation (39) separately.

The first factor is computed with the help of following distances:

For  $2 \leq \theta \leq n$  and  $1 \leq m \leq \theta - 1$ ,

$$d(x_{n,\theta}, x_{l,m}) = \begin{cases} n-l, & \text{for } m \leq l \leq n+m-\theta-1, \\ \theta-m, & \text{for } n+m-\theta \leq l \leq n-1. \end{cases} \quad (40)$$

For  $1 \leq \theta \leq n$  and  $\theta \leq m \leq n$ ,

$$d(x_{n,\theta}, x_{l,m}) = \{n+m-l-\theta \quad \text{for } m \leq l \leq n-1. \quad (41)$$

Thus, we get

$$\begin{aligned} \sum_{\theta=1}^{\theta=n} W(x_{n,\theta}, \bigcup_{l=1}^{l=n-1} V_l) &= \sum_{\theta=1}^{\theta=n} \sum_{m=1}^{m=\theta-1} \sum_{l=m}^{l=n-1} d(x_{n,\theta}, x_{lm}) \\ &= \sum_{\theta=2}^{\theta=n} \sum_{m=1}^{m=\theta-1} \sum_{l=m}^{l=n-1} d(x_{n,\theta}, x_{lm}) + \sum_{\theta=1}^{\theta=n} \sum_{m=\theta}^{m=n-1} \sum_{l=m}^{l=n-1} d(x_{n,\theta}, x_{lm}) \\ &= \sum_{\theta=2}^{\theta=n} \sum_{m=1}^{m=\theta-1} \sum_{l=m}^{l=n+m-\theta-1} d(x_{n,\theta}, x_{lm}) + \sum_{\theta=2}^{\theta=n} \sum_{m=1}^{m=\theta-1} \sum_{l=n+m-\theta}^{l=n-1} d(x_{n,\theta}, x_{lm}) \\ &\quad + \sum_{\theta=1}^{\theta=n} \sum_{m=\theta}^{m=n-1} \sum_{l=m}^{l=n-1} d(x_{n,\theta}, x_{lm}) \\ &= \sum_{\theta=2}^{\theta=n} \sum_{m=1}^{m=\theta-1} \sum_{l=m}^{l=n+m-\theta-1} (n-l) + \sum_{\theta=2}^{\theta=n} \sum_{m=1}^{m=\theta-1} \sum_{l=n+m-\theta}^{l=n-1} (\theta-m) \\ &\quad + \sum_{\theta=1}^{\theta=n} \sum_{m=\theta}^{m=n-1} \sum_{l=m}^{l=n-1} (n+m-l-\theta) \\ &= \frac{1}{12} [n^4 - 2n^3 - n^2 + 2n] + \frac{1}{12} [n^4 - n^2] + \frac{1}{12} [n^4 - n^2] \\ &= \frac{1}{12} [3n^4 - 2n^3 - 3n^2 + 2n]. \end{aligned} \quad (42)$$

The second factor is computed with the help of following distances:

For  $2 \leq \theta \leq n$  and  $1 \leq m \leq \theta - 1$ ,

$$d(x_{n,\theta}, u_{l,m}) = \begin{cases} n-l, & \text{for } m \leq l \leq n+m-\theta-1, \\ \theta-m, & \text{for } n+m-\theta \leq l \leq n-1. \end{cases} \quad (43)$$

For  $1 \leq \theta \leq n$  and  $\theta \leq m \leq n$ ,

$$\begin{aligned}
 d(x_{n,\theta}, u_{l,m}) &= \{n + m - l - \theta, \text{ for } m \leq l \leq n - 1, \\
 \sum_{\theta=1}^{\theta=n} W\left(x_{n,\theta}, \bigcup_{l=1}^{l=n-1} U_l\right) &= \sum_{\theta=1}^{\theta=n} \sum_{m=1}^{m=\theta-1} \sum_{l=m}^{l=n-1} d(x_{n,\theta}, u_{lm}) \\
 &= \sum_{\theta=2}^{\theta=n} \sum_{m=1}^{m=\theta-1} \sum_{l=m}^{l=n-1} d(x_{n,\theta}, u_{lm}) + \sum_{\theta=1}^{\theta=n} \sum_{m=\theta}^{m=n-1} \sum_{l=m}^{l=n-1} d(x_{n,\theta}, u_{lm}) \\
 &= \sum_{\theta=2}^{\theta=n} \sum_{m=1}^{m=\theta-1} \sum_{l=m}^{l=n+m-\theta-1} d(x_{n,\theta}, u_{lm}) + \sum_{\theta=2}^{\theta=n} \sum_{m=1}^{m=\theta-1} \sum_{l=n+m-\theta}^{l=n-1} d(x_{n,\theta}, u_{lm}) \\
 &\quad + \sum_{\theta=1}^{\theta=n} \sum_{m=\theta}^{m=n-1} \sum_{l=m}^{l=n-1} d(x_{n,\theta}, u_{lm}) \tag{44} \\
 &= \sum_{\theta=2}^{\theta=n} \sum_{m=1}^{m=\theta-1} \sum_{l=m}^{l=n+m-\theta-1} (n-l) + \sum_{\theta=2}^{\theta=n} \sum_{m=1}^{m=\theta-1} \sum_{l=n+m-\theta}^{l=n-1} (\theta-m) \\
 &\quad + \sum_{\theta=1}^{\theta=n} \sum_{m=\theta}^{m=n-1} \sum_{l=m}^{l=n-1} (n+m-l-\theta) \\
 &= \frac{1}{12} [n^4 - 2n^3 - n^2 + 2n] + \frac{1}{12} [n^4 - n^2] + \frac{1}{12} [n^4 - n^2] \\
 &= \frac{1}{12} [3n^4 - 2n^3 - 3n^2 + 2n].
 \end{aligned}$$

The third factor is computed with the help of following distances:

For  $2 \leq \theta \leq n - 1$  and  $1 \leq m \leq \theta - 1$ ,

$$d(x_{n,\theta}, w_{l,m}) = \begin{cases} n-l+1, & \text{for } m \leq l \leq n+m-\theta-2, \\ \theta-m, & \text{for } n+m-\theta-1 \leq l \leq n-2. \end{cases} \tag{45}$$

For  $\theta = n$  and  $1 \leq m \leq \theta - 2$ ,

$$d(x_{n,\theta}, w_{l,m}) = \{n - m \text{ for } m \leq l \leq n - 2. \tag{46}$$

For  $1 \leq \theta \leq n - 2$  and  $\theta \leq m \leq n - 2$ ,

$$\begin{aligned}
d(x_{n,\theta}, w_{l,m}) &= \{n + m - l - \theta \quad \text{for } m \leq l \leq n - 2, \\
\sum_{\theta=1}^{\theta=n} W\left(x_{n,\theta}, \bigcup_{l=1}^{l=n-1} W_l\right) &= \sum_{\theta=1}^{\theta=n} \sum_{m=1}^{m=\theta-1} \sum_{l=m}^{l=n-1} d(x_{n,\theta}, w_{lm}) \\
&= \sum_{\theta=2}^{\theta=n} \sum_{m=1}^{m=\theta-1} \sum_{l=m}^{l=n-1} d(x_{n,\theta}, w_{lm}) + \sum_{\theta=1}^{\theta=n} \sum_{m=\theta}^{m=n-1} \sum_{l=m}^{l=n-1} d(x_{n,\theta}, w_{lm}) \\
&= \sum_{\theta=2}^{\theta=n-1} \sum_{m=1}^{m=\theta-1} \sum_{l=m}^{l=n+m-\theta-2} d(x_{n,\theta}, w_{lm}) + \sum_{\theta=2}^{\theta=n-1} \sum_{m=1}^{m=\theta-1} \sum_{l=n+m-\theta-1}^{l=n-2} d(x_{n,\theta}, w_{lm}) \\
&\quad + \sum_{\theta=1}^{\theta=n-2} \sum_{m=\theta}^{m=n-2} \sum_{l=m}^{l=n-2} d(x_{n,\theta}, w_{lm}) + \sum_{m=1}^{m=n-2} \sum_{l=m}^{l=n-2} d(x_{m,\theta}, w_{lm}) \\
&= \sum_{\theta=2-1}^{\theta=n} \sum_{m=1}^{m=\theta-1} \sum_{l=m}^{l=n+m-\theta-2} (n-l+1) + \sum_{\theta=2}^{\theta=n-1} \sum_{m=1}^{m=\theta-1} \sum_{l=n+m-\theta-1}^{l=n-2} (\theta-m) \\
&\quad + \sum_{m=1}^{m=n-2} \sum_{l=m}^{l=n-2} (n-m) + \sum_{\theta=1}^{\theta=n-2} \sum_{m=\theta}^{m=n-2} \sum_{l=m}^{l=n-2} (n+m-l-\theta) \\
&= \frac{1}{12} [n^4 - 6n^3 + 11n^2 - 6n] + \frac{1}{12} [n^4 - 4n^3 + 5n^2 - 2n] \\
&\quad + \frac{1}{12} [4n^3 - 12n^2 + 8n] + \frac{1}{12} [n^4 - 2n^3 - n^2 + 2n] \\
&= \frac{1}{12} [3n^4 - 8n^3 + 3n^2 + 2n].
\end{aligned} \tag{47}$$

The fourth factor is

$$W(V_n) = \sum_{\theta=1}^{\theta=n} W(x_{n,\theta}) = \sum_{l=1}^{l=n-1} \sum_{m=1}^{m=n-l} m = \frac{1}{6} [n^3 - n]. \tag{48}$$

Putting equations (42), (44), (47), and (48) in (39), we get

$$W(V_n, ET_{n'}) = \frac{1}{12} [9n^4 - 10n^3 - 9n^2 + 4n]. \tag{49}$$

Let  $W(U_{n-1}, ET_{n''})$  be the distance between the vertices of  $U_{n-1}$  to itself and from  $ET_{n-1}$ , and  $W_{n-2}$ , where  $U_{n-1} = \{u_{n-1,1}, u_{n-1,2}, u_{n-1,3}, \dots, u_{n-1,n-1}\}$ , is

$$\begin{aligned}
W(U_{n-1}, ET_{n''}) &= \sum_{\theta=1}^{\theta=n-1} W(u_{n-1,\theta}, ET_{n-1}) + \sum_{\theta=1}^{\theta=n-1} W(u_{n-1,\theta}, W_{n-2}) + W(U_{n-1}), \\
W(U_{n-1}, ET_{n''}) &= \sum_{\theta=1}^{\theta=n-1} W\left(u_{n-1,\theta}, \bigcup_{l=1}^{l=n-2} W_l\right) + \sum_{\theta=1}^{\theta=n} W\left(u_{n-1,\theta}, \bigcup_{l=1}^{l=n-1} V_l\right) \\
&\quad + \sum_{\theta=1}^{\theta=n} W\left(u_{n-1,\theta}, \bigcup_{l=1}^{l=n-3} U_l\right) + \sum_{\theta=1}^{\theta=n-1} W(u_{n-1,\theta}).
\end{aligned} \tag{50}$$

Again, we compute each of the factors separately.

The first factor is computed with the help of following distances:

For  $2 \leq \theta \leq n - 2$  and  $1 \leq m \leq \theta - 1$ ,

$$d(u_{n,\theta}, w_{l,m}) = \begin{cases} n - l - 1, & \text{for } m \leq l \leq n + m - \theta - 2, \\ \theta - m + 1, & \text{for } n + m - \theta - 1 \leq l \leq n - 2. \end{cases} \tag{51}$$

For  $1 \leq \theta \leq n - 1$  and  $\theta \leq m \leq n - 2$ ,

$$\begin{aligned}
d(u_{n,\theta}, w_{l,m}) &= \{n + m - l - \theta \quad \text{for } m \leq l \leq n - 2, \\
\sum_{\theta=1}^{\theta=n-1} W\left(u_{n-1,\theta}, \bigcup_{l=1}^{l=n-2} W_l\right) &= \sum_{\theta=1}^{\theta=n-1} \sum_{m=1}^{m=n-1} \sum_{l=m}^{l=n-1} d(u_{n-1,\theta}, w_{lm}) \\
&= \sum_{\theta=2}^{\theta=n-2} \sum_{m=1}^{m=\theta-1} \sum_{l=m}^{l=n-1} d(u_{n-1,\theta}, w_{lm}) + \sum_{\theta=1}^{\theta=n} \sum_{m=\theta}^{m=n-1} \sum_{l=m}^{l=n-2} d(u_{n-1,\theta}, w_{lm}) \\
&= \sum_{\theta=2}^{\theta=n-2} \sum_{m=1}^{m=\theta-1} \sum_{l=m}^{l=n+m-\theta-2} d(u_{n-1,\theta}, w_{lm}) \\
&\quad + \sum_{\theta=2}^{\theta=n-2} \sum_{m=1}^{m=\theta-1} \sum_{l=n+m-\theta-1}^{l=n-2} d(u_{n-1,\theta}, w_{lm}) + \sum_{\theta=1}^{\theta=n-1} \sum_{m=\theta}^{m=n-2} \sum_{l=m}^{l=n-2} d(u_{n-1,\theta}, w_{lm}) \\
&= \sum_{\theta=2}^{\theta=n-2} \sum_{m=1}^{m=\theta-1} \sum_{l=m}^{l=n+m-\theta-2} (n-l-1) + \sum_{\theta=2}^{\theta=n-2} \sum_{m=1}^{m=\theta-1} \sum_{l=n+m-\theta-1}^{l=n-2} (\theta-m+1) \\
&\quad + \sum_{\theta=1}^{\theta=n-1} \sum_{m=\theta}^{m=n-2} \sum_{l=m}^{l=n-2} (n+m-l-\theta) \\
&= \frac{1}{12} [n^4 - 6n^3 + 11n^2 - 6n] + \frac{1}{12} [n^4 - 2n^3 - n^2 + 2n] \\
&\quad + \frac{1}{12} [n^4 - 2n^3 - n^2 + 2n] \\
&= \frac{1}{12} [3n^4 - 10n^3 + 9n^2 - 2n].
\end{aligned} \tag{52}$$

The second factor is computed with the help of following distances:

For  $2 \leq \theta \leq n - 2$  and  $1 \leq m \leq \theta - 1$ ,

$$d(u_{n,\theta}, w_{l,m}) = \begin{cases} n - l, & \text{for } m \leq l \leq n + m - \theta - 2, \\ \theta - m + 1, & \text{for } n + m - \theta - 1 \leq l \leq n - 2. \end{cases} \tag{53}$$

For  $1 \leq \theta \leq n - 2$  and  $\theta \leq m \leq n - 2$ ,

$$\begin{aligned}
d(u_{n,\theta}, w_{l,m}) &= \{n + m - l - \theta, \text{ for } m \leq l \leq n - 2, \\
\sum_{\theta=1}^{\theta=n-1} W(u_{n-1,\theta}, \bigcup_{l=1}^{l=n-2} U_l) &= \sum_{\theta=1}^{\theta=n-1} \sum_{m=1}^{m=n-1} \sum_{l=m}^{l=n-1} d(u_{n-1,\theta}, u_{lm}) \\
&= \sum_{\theta=2}^{\theta=n-1} \sum_{m=1}^{m=\theta-1} \sum_{l=m}^{l=n-2} d(u_{n-1,\theta}, u_{lm}) + \sum_{\theta=1}^{\theta=n} \sum_{m=\theta}^{m=n-1} \sum_{l=m}^{l=n-2} d(u_{n-1,\theta}, u_{lm}) \\
&= \sum_{\theta=2}^{\theta=n-2} \sum_{m=1}^{m=\theta-1} \sum_{l=m}^{l=n+m-\theta-2} d(u_{n-1,\theta}, u_{lm}) \\
&\quad + \sum_{\theta=2}^{\theta=n-1} \sum_{m=1}^{m=\theta-1} \sum_{l=n+m-\theta-1}^{l=n-2} d(u_{n-1,\theta}, u_{lm}) \\
&\quad + \sum_{\theta=1}^{\theta=n-1} \sum_{m=\theta}^{m=n-2} \sum_{l=m}^{l=n-2} d(u_{n-1,\theta}, u_{lm}) \tag{54} \\
&= \sum_{\theta=2}^{\theta=n-2} \sum_{m=1}^{m=\theta-1} \sum_{l=m}^{l=n+m-\theta-2} (n-l) + \sum_{\theta=2}^{\theta=n-2} \sum_{m=1}^{m=\theta-1} \sum_{l=n+m-\theta-1}^{l=n-2} (\theta-m+1) \\
&\quad + \sum_{\theta=1}^{\theta=n-1} \sum_{m=\theta}^{m=n-2} \sum_{l=m}^{l=n-2} (n-l+j-\theta) \\
&= \frac{1}{12} [n^4 - 4n^3 - n^2 - 12] + \frac{1}{12} [n^4 - 2n^3 - n^2 + 2n] \\
&\quad + \frac{1}{12} [n^4 - 2n^3 - n^2 + 2n] \\
&= \frac{1}{12} [3n^4 - 8n^3 - 3n^2 + 20n - 12].
\end{aligned}$$

The third factor is computed with the help of following distances:

For  $2 \leq \theta \leq n-1$  and  $1 \leq m \leq \theta-1$ ,

$$d(u_{n,\theta}, w_{l,m}) = \begin{cases} n-l, & \text{for } m \leq l \leq n+m-\theta-1, \\ \theta-m+1, & \text{for } n+m-\theta \leq l \leq n-1. \end{cases} \tag{55}$$

For  $1 \leq \theta \leq n-2$  and  $\theta \leq m \leq n-2$ ,

$$d(u_{n,\theta}, w_{l,m}) = \{n + m - l - \theta \text{ for } m \leq l \leq n - 1,$$

$$\begin{aligned} \sum_{\theta=1}^{\theta=n-1} W\left(u_{n-1,\theta}, \bigcup_{l=1}^{l=n-1} V_l\right) &= \sum_{\theta=1}^{\theta=n-1} \sum_{m=1}^{m=n-1} \sum_{l=m}^{l=n-1} d(u_{n-1,\theta}, x_{lm}) \\ &= \sum_{\theta=2}^{\theta=n-1} \sum_{m=1}^{m=\theta-1} \sum_{l=m}^{l=n-1} d(u_{n-1,\theta}, x_{lm}) + \sum_{\theta=1}^{\theta=n-1} \sum_{m=\theta}^{m=n-1} \sum_{l=m}^{l=n-1} d(u_{n-1,\theta}, x_{lm}) \\ &= \sum_{\theta=2}^{\theta=n-2} \sum_{m=1}^{m=\theta-1} \sum_{l=n+m-\theta-2}^{l=n-1} d(u_{n-1,\theta}, x_{lm}) \\ &\quad + \sum_{\theta=2}^{\theta=n-1} \sum_{m=1}^{m=\theta-1} \sum_{l=n+m-\theta}^{l=n-1} d(u_{n-1,\theta}, x_{lm}) + \sum_{\theta=1}^{\theta=n-1} \sum_{m=\theta}^{m=n-1} \sum_{l=m}^{l=n-1} d(u_{n-1,\theta}, x_{lm}) \quad (56) \\ &= \sum_{\theta=2}^{\theta=n-1} \sum_{m=1}^{m=\theta-1} \sum_{l=n+m-\theta-1}^{l=n-1} (n-l) + \sum_{\theta=2}^{\theta=n-1} \sum_{m=1}^{m=\theta-1} \sum_{l=n+m-\theta}^{l=n-1} (\theta-m+1) \\ &\quad + \sum_{\theta=1}^{\theta=n-1} \sum_{m=\theta}^{m=n-1} \sum_{l=m}^{l=n-1} (n-l+j-\theta) \\ &= \frac{1}{12} [n^4 - 2n^3 - n^2 + 2n] + \frac{1}{12} [n^4 - 2n^3 - n^2 + 2n] + \frac{1}{12} [n^4 - 2n^2] \\ &= \frac{1}{12} [3n^4 - 4n^3 - 3n^2 + 4n]. \end{aligned}$$

The fourth factor is

$$W(U_{n-1}) = \sum_{\theta=1}^{\theta=n-1} W(u_{n-1,\theta}) = \sum_{l=1}^{l=n-2} \sum_{m=2}^{m=n-1} m = \frac{1}{12} [2n^3 - 14n + 12]. \quad (57)$$

Putting equations (52), (54), (56), and (57) in (50), we get

$$W(U_{n-1}, ET_{n''}) = \frac{1}{12} [9n^9 - 20n^3 + 3n^2 + 8n]. \quad (58)$$

Now, let  $W(W_{n-2}, ET_{n''})$  be the distance between the vertices of  $W_{n-2}$  to itself and from  $ET_{n-1}$ , where  $W_{n-2} = \{w_{n-2,1}, w_{n-2,2}, w_{n-2,3}, \dots, w_{n-2,n-2}\}$ ; then,  $W(W_{n-2}, ET_{n''}) = \sum_{\theta=1}^{\theta=n-2} W(w_{n-2,\theta}, ET_{n-1}) + (W_{n-2})$ .

This is equivalent to

$$\begin{aligned} W(w_{n-2}, ET_{n''}) &= \sum_{\theta=1}^{\theta=n-2} W\left(w_{n-2,\theta}, \bigcup_{l=1}^{l=n-1} V_l\right) + \sum_{\theta=1}^{\theta=n} W\left(w_{n-2,\theta}, \bigcup_{l=1}^{l=n-1} U_l\right) \\ &\quad + \sum_{\theta=1}^{\theta=n} W\left(w_{n-2,\theta}, \bigcup_{l=1}^{l=n-3} W_l\right) + \sum_{\theta=1}^{\theta=n-2} W(w_{n-1,\theta}). \end{aligned} \quad (59)$$

Again, we find each factor separately.

The first factor is computed with the help of following distances:

For  $1 \leq \theta \leq n - 2$  and  $1 \leq m \leq \theta$ ,

$$d(u_{n,\theta}, w_{l,m}) = \begin{cases} n-l, & \text{for } m \leq l \leq n+m-\theta-2, \\ \theta-m+1, & \text{for } n+m-\theta-1 \leq l \leq n-1. \end{cases} \quad (60)$$

For  $1 \leq \theta \leq n - 2$  and  $\theta \leq m \leq n - 2$ ,

$$\begin{aligned}
d(u_{n,\theta}, w_{l,m}) &= \{n+m-l-\theta \quad \text{for } m \leq l \leq n-1, \\
\sum_{\theta=1}^{\theta=n-2} W\left(w_{n-2,\theta}, \bigcup_{l=1}^{l=n-1} V_l\right) &= \sum_{\theta=1}^{\theta=n-2} \sum_{m=1}^{m=n-1} \sum_{l=m}^{l=n-1} d(w_{n-2,\theta}, x_{lm}) \\
&= \sum_{\theta=2}^{\theta=n-2} \sum_{m=1}^{m=\theta} \sum_{l=m}^{l=n-1} d(w_{n-2,\theta}, x_{lm}) + \sum_{\theta=1}^{\theta=n-2} \sum_{m=\theta+1}^{m=n-1} \sum_{l=m}^{l=n-1} d(w_{n-2,\theta}, x_{lm}) \\
&= \sum_{\theta=2}^{\theta=n-2} \sum_{m=1}^{m=\theta} \sum_{l=n+m-\theta-2}^{l=n-1} d(w_{n-2,\theta}, x_{lm}) + \sum_{\theta=2}^{\theta=n-2} \sum_{m=\theta}^{m=n-1} \sum_{l=n+m-\theta-1}^{l=n-1} d(w_{n-2,\theta}, x_{lm}) \\
&\quad + \sum_{\theta=1}^{\theta=n-1} \sum_{m=\theta+1}^{m=n-1} \sum_{l=m}^{l=n-1} d(w_{n-2,\theta}, x_{lm}) \\
&= \sum_{\theta=2}^{\theta=n-2} \sum_{m=1}^{m=\theta} \sum_{l=n+m-\theta-2}^{l=n-1} (n-l) + \sum_{\theta=2}^{\theta=n-2} \sum_{m=1}^{m=\theta} \sum_{l=n+m-\theta-1}^{l=n-1} (\theta-m+1) \\
&\quad + \sum_{\theta=1}^{\theta=n-1} \sum_{m=\theta+1}^{m=n-1} \sum_{l=m}^{l=n-1} (n+m-l-\theta-1) \\
&= \frac{1}{12} [n^4 - 2n^3 - n^2 + 2n] + \frac{1}{12} [n^4 - 4n^3 + 5n^2 - 2n] \\
&\quad + \frac{1}{12} [n^4 - 4n^3 + 5n^2 - 2n] \\
&= \frac{1}{12} [3n^4 - 10n^3 + 9n^2 - 2n].
\end{aligned} \tag{61}$$

The second factor is computed with the help of following distances:

For  $1 \leq \theta \leq n-2$  and  $1 \leq m \leq \theta-1$ ,

$$d(u_{n,\theta}, w_{l,m}) = \begin{cases} n-l, & \text{for } m \leq l \leq n+m-\theta-2, \\ \theta-m+1, & \text{for } n+m-\theta-1 \leq l \leq n-1. \end{cases} \tag{62}$$

For  $1 \leq \theta \leq n-1$ ,

$$d(u_{n,\theta}, w_{l,m}) = \{n-l \quad \text{for } \theta \leq l \leq n-2. \tag{63}$$

For  $1 \leq \theta \leq n-2$  and  $\theta \leq m \leq n-2$ ,

$$\begin{aligned}
 d(u_{n,\theta}, w_{l,m}) &= \{n+m-l-\theta \quad \text{for } m \leq l \leq n-1, \\
 \sum_{\theta=1}^{\theta=n-2} W(w_{n-2,\theta}, \bigcup_{l=1}^{l=n-2} U_l) &= \sum_{\theta=1}^{\theta=n-2} \sum_{m=1}^{m=n-2} \sum_{l=m}^{l=n-2} d(w_{n-2,\theta}, u_{lm}) \\
 &= \sum_{\theta=2}^{\theta=n-2} \sum_{m=1}^{m=\theta-1} \sum_{l=m}^{l=n-2} d(w_{n-2,\theta}, u_{lm}) + \sum_{\theta=1}^{\theta=n-2} \sum_{l=\theta}^{l=n-2} d(w_{n-2,\theta}, u_{lm}) \\
 &\quad + \sum_{\theta=1}^{\theta=n-2} \sum_{m=\theta+1}^{m=n-2} \sum_{l=m}^{l=n-2} d(w_{n-2,\theta}, u_{lm}) \\
 &= \sum_{\theta=2}^{\theta=n-2} \sum_{m=1}^{m=\theta-1} \sum_{l=n+m-\theta-2}^{l=n-2} d(w_{n-2,\theta}, u_{lm}) + \sum_{\theta=2}^{\theta=n-2} \sum_{m=1}^{m=\theta-1} \sum_{l=n+m-\theta-1}^{l=n-2} d(w_{n-2,\theta}, u_{lm}) \\
 &\quad + \sum_{\theta=1}^{\theta=n-2} \sum_{l=\theta}^{l=n-2} d(w_{n-2,\theta}, u_{lm}) + \sum_{\theta=1}^{\theta=n-2} \sum_{m=\theta+1}^{m=n-2} \sum_{l=m}^{l=n-2} d(w_{n-2,\theta}, u_{lm}) \\
 &= \sum_{\theta=2}^{\theta=n-2} \sum_{m=1}^{m=\theta-1} \sum_{l=m}^{l=n+m-\theta-2} (n-l) + \sum_{\theta=2}^{\theta=n-2} \sum_{m=1}^{m=\theta-1} \sum_{l=n+m-\theta-1}^{l=n-2} (\theta-m+1) \\
 &\quad + \sum_{\theta=1}^{\theta=n-2} \sum_{l=\theta}^{l=n-2} (n-l) + \sum_{\theta=1}^{\theta=n-2} \sum_{m=\theta+1}^{m=n-2} \sum_{l=m}^{l=n-2} (n-l+m+\theta-1) \\
 &= \frac{1}{12} [n^4 - 4n^3 - n^2 + 16n - 12] + \frac{1}{12} [n^4 - 6n^3 + 11n^2 - 6n] \\
 &\quad + \frac{1}{12} [2n^3 - 14n + 12] + \frac{1}{12} [n^4 - 6n^3 + 11n^2 - 6n] \\
 &= \frac{1}{12} [3n^4 - 14n^3 + 21n^2 - 10n].
 \end{aligned} \tag{64}$$

The third factor is computed with the help of following distances:

For  $2 \leq \theta \leq n-2$  and  $1 \leq m \leq \theta-1$ ,

$$d(u_{n,\theta}, w_{l,m}) = \begin{cases} n-l-1, & \text{for } m \leq l \leq n+m-\theta-3, \\ \theta-m-1, & \text{for } n+m-\theta-2 \leq l \leq n-3. \end{cases} \tag{65}$$

For  $1 \leq \theta \leq n-2$  and  $\theta \leq m \leq n-3$ ,

$$\begin{aligned}
d(u_{n,\theta}, w_{l,m}) &= \{n + m - l - \theta - 1 \quad \text{for } m \leq l \leq n - 3, \\
\sum_{\theta=1}^{\theta=n-2} W\left(w_{n-2,\theta}, \bigcup_{l=1}^{l=n-2} W_l\right) &= \sum_{\theta=1}^{\theta=n-2} \sum_{m=1}^{m=n-3} \sum_{l=m}^{l=n-3} d(w_{n-2,\theta}, w_{lm}) \\
&= \sum_{\theta=2}^{\theta=n-2} \sum_{m=1}^{m=\theta-1} \sum_{l=m}^{l=n-3} d(w_{n-2,\theta}, w_{lm}) + \sum_{\theta=1}^{\theta=n-2} \sum_{m=\theta}^{m=n-3} \sum_{l=m}^{l=n-3} d(w_{n-2,\theta}, w_{lm}) \\
&= \sum_{\theta=2}^{\theta=n-2} \sum_{m=1}^{m=\theta-1} \sum_{l=m}^{l=n+m-\theta-3} d(w_{n-2,\theta}, w_{lm}) \\
&\quad + \sum_{\theta=2}^{\theta=n-2} \sum_{m=1}^{m=\theta-1} \sum_{l=n+m-\theta-2}^{l=n-3} d(w_{n-2,\theta}, w_{lm}) \\
&\quad + \sum_{\theta=1}^{\theta=n-2} \sum_{m=\theta}^{m=n-3} \sum_{l=m}^{l=n-3} d(w_{n-2,\theta}, w_{lm}) \\
&= \sum_{\theta=2}^{\theta=n-2} \sum_{m=1}^{m=\theta-1} \sum_{l=m}^{l=n+m-\theta-3} (n-l-1) \\
&\quad + \sum_{\theta=2}^{\theta=n-2} \sum_{m=1}^{m=\theta-1} \sum_{l=n+m-\theta-2}^{l=n-3} (\theta-m-1) \\
&\quad + \sum_{\theta=1}^{\theta=n-2} \sum_{m=\theta}^{m=n-3} \sum_{l=m}^{l=n-3} (n+m-l-\theta-1) \\
&= \frac{1}{12} [n^4 - 8n^3 + 17n^2 + 2n - 24] + \frac{1}{12} [n^4 - 6n^3 + 11n^2 - 6n] \\
&\quad + \frac{1}{12} [2n^4 - 20n^3 + 82n^2 - 160n + 120] \\
&= \frac{1}{12} [4n^4 - 34n^3 + 110n^2 - 164n + 96].
\end{aligned} \tag{66}$$

The fourth factor is

$$W(W_{n-2}) = \sum_{\theta=1}^{\theta=n-2} W(w_{n-2,\theta}) = \sum_{l=2}^{l=n-2} \sum_{m=2}^{m=n-l} m = \frac{1}{12} [2n^3 - 6n^2 - 8n + 24]. \tag{67}$$

Putting equations (61), (64), (66), and (67) in (59), we get

$$W(w_{n-2}, ET_{n''}) = \frac{1}{12} [10n^4 - 56n^3 + 134n^2 - 184n + 120]. \tag{68}$$

Now, the Wiener index of the graph  $ET_n$  is  $W(ET_n) = W(ET_{n-1}) + W(V_n, ET_{n'}) + W(U_{n-1}, ET_{n''}) + W(W_{n-2}, ET_{n''})$ . Hence, by using (49), (58), and (68), we get  $W(ET_n) = W(ET_{n-1}) + 1/12 [28n^4 - 86n^3 + 134n^2 - 172n + 120]$ .

#### 4. The Wiener Polarity Index of the Graph Derived from Hexagonal Networks

The graphs derived from hexagonal networks are finite subgraphs of the triangular grid. In this section, Wiener polarity index of the graph derived from the hexagonal network is computed.

The graph of hexagonal network of dimension  $n$  is denoted by  $HX_n$  (Figure 3). The graph contains  $3n^2 - 3n + 1$  vertices and  $9n^2 - 15n + 6$  edges, where  $n$  is the number of

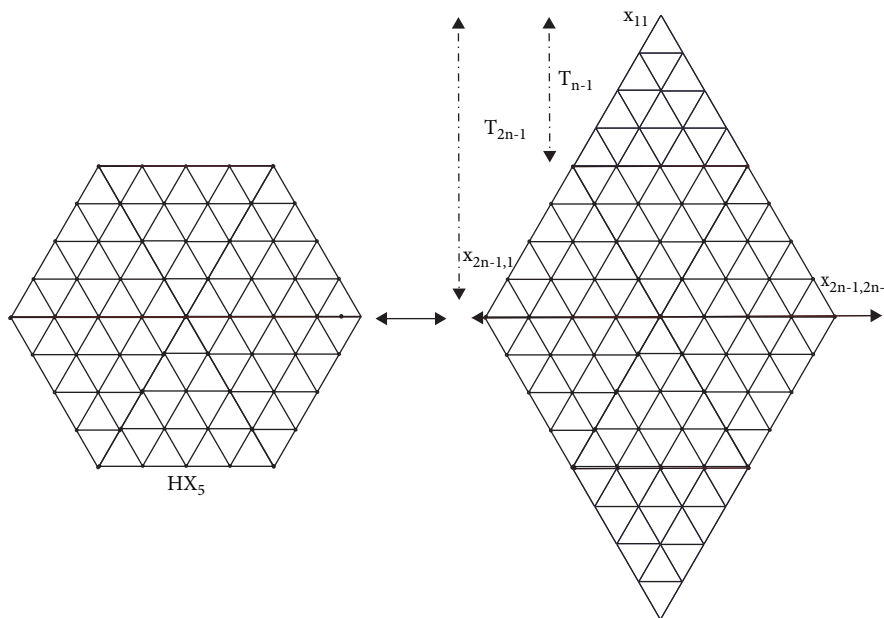


FIGURE 3: Hexagonal network  $HX_n$  and its extension.

vertices on one side of the hexagon [5]. There is only one vertex  $v$  which is at distance  $n - 1$  from every other corner vertices. This vertex is said to be the center of  $HX_n$  and is represented by  $O$ .

**Theorem 5.**  $W_p(HX_n) = 27n^2 - 81n + 48$ .

*Proof.* In order to find the vertex  $PI$  index of  $HX_n$ , firstly, we will divide the graph into two parts by drawing a line passing through the central vertex and parallel to  $x$ -axis. Now,

extend the upper and lower part of the graph  $HX_n$  to form triangular mesh networks  $T_{2n-1}$  and  $T'_{2n-1}$  of dimension  $2n - 1$ , respectively. Define the vertex set of  $T_{2n-1}$  and  $T'_{2n-1}$  as follows:  $V_l = \{x_{lm} : 1 \leq l \leq 2n - 1, 1 \leq m \leq l\}$  and  $V'_l = \{v'_{lm} : 1 \leq l \leq 2n - 1, 1 \leq m \leq l\}$ .

It is easy to see that  $V(T_{2n-1}) \cap V(T'_{2n-1}) = V_{2n-1}$  and  $d(x_{lm}, v'_{lm}) > 3$  for  $l < 2n - 3$ . This implies that the Wiener polarity index of  $HX_n$  can now be written in the following form:

$$W_p(HX_n) = 2(W_p(T_{2n-1}) - W_p(HX_n, T_{n-1}) - W_p(T_{n-1})) + W_p(V_{2n-2}, V_{2n-2}') + W_p(V_{2n-2}, V_{2n-3}') + W_p(V_{2n-3}, V_{2n-2}') - W_p(V_{2n-1}). \tag{69}$$

From Theorem 1, we know that  $W_p(T_n) = 9(n^2 - 5n + 6)/2$ . This implies that

$$W_p(T_{2n-1}) = 18n^2 - 63n + 54. \tag{70}$$

Now, we calculate the terms  $W_p(V_{2n-2}, V_{2n-2}')$ ,  $W_p(V_{2n-2}, V_{2n-3}')$ , and  $W_p(V_{2n-3}, V_{2n-2}')$ , which are equal to the number of vertices of the lower triangle that are at distance 3 from the vertices of the upper triangle. However, for every  $v \in V_{2n-2}$  and  $v' \in V_{2n-2}'$ ,  $|\{(v, v') | d(v, v') = 3\}| = 4n - 8$ . Therefore,

$$W_p(V_{2n-2}, V_{n-2}') = 4n - 8. \tag{71}$$

Similarly, for every  $v \in V_{2n-2}$  and  $v' \in V_{2n-3}'$ , we have  $|\{(v, v') | d(v, v') = 3\}| = 8n - 14$ .

And, for every  $v \in V_{2n-3}$  and  $v' \in V_{2n-2}'$ , we have

$$|\{(v, v') | d(v, v') = 3\}| = 8n - 14. \tag{72}$$

This implies that

$$W_p(V_{2n-2}, V_{2n-3}') = 4n - 8, \tag{73}$$

$$W_p(V_{2n-2}, V_{2n-2}') = 4n - 8.$$

TABLE 1: Comparison of Wiener and Wiener polarity indices of the graph of triangular mesh network.

$n$	$W_p(T_n)$	$W(T_n)$
2	0	3
3	0	39
4	9	159
5	27	459
6	54	1089
7	90	2265
8	135	4281
9	189	7521
10	252	12471
11	324	19731
12	405	30027
13	495	44223
14	594	63333
15	702	88533
16	819	121173
17	945	162789
18	1080	215115
19	1214	280095
20	1377	359895

TABLE 2: Comparison of Wiener and Wiener polarity indices of  $ET_n$ .

Comparison of Wiener and Wiener polarity index of $ET_n$		
$N$	$W_p(ETT_n)$	$W(ETT_n)$
4	42	339
5	147	1119
6	315	2921
7	546	6522
8	840	13020
9	1197	23890
10	1617	41040
11	2100	66867
12	2646	104313
13	3255	156921
14	3927	228891
15	4662	325136
16	5460	451338
17	6321	614004
18	7245	820522
19	8232	1079217
20	9282	1399407

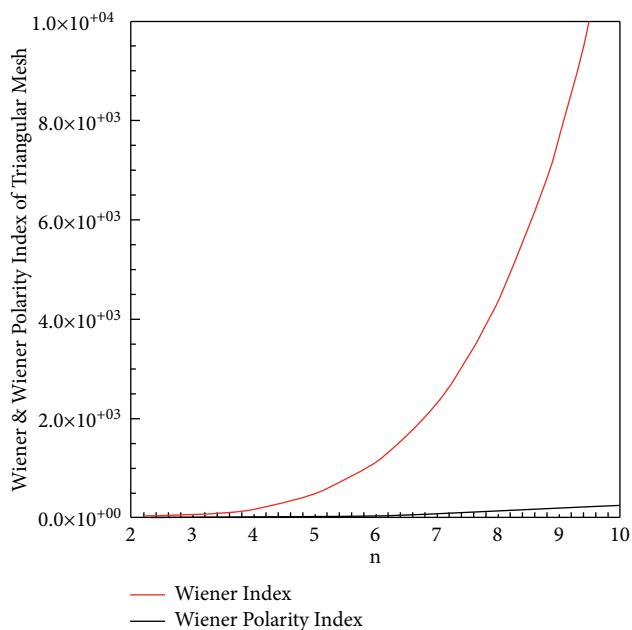
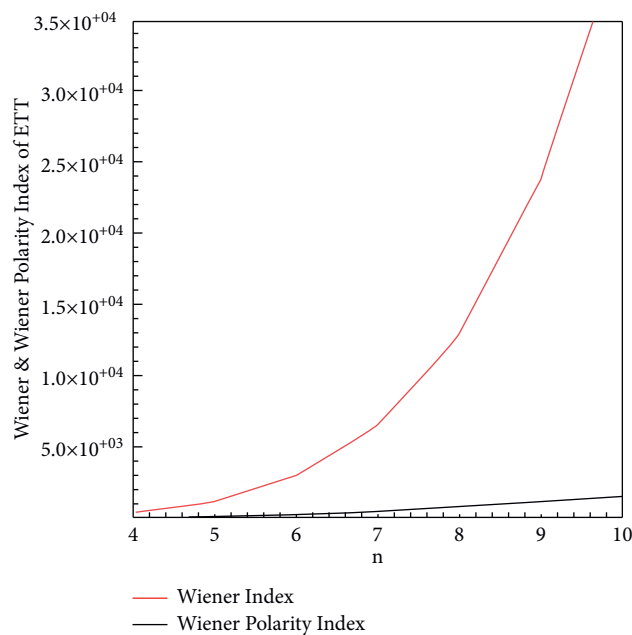
FIGURE 4: Comparison of Wiener and Wiener polarity indices of graph  $T_n$ .

FIGURE 5: Comparison of Wiener and Wiener polarity index of the equilateral triangular tetra sheet.

The term  $W_p(HX_n, T_{n-1})$  is the cardinality of set of vertices of  $T_{n-1}$  that are connected through a path of length 3 from the vertices of  $HX_n$ . It is easy to see that

$$\begin{aligned}
 W_p(HX_n, T_{n-1}) &= \sum_{l=n}^{l=n+2} W_p(V_l, V_{n-1}) + \sum_{l=n}^{l=n+1} W_p(V_l, V_{n-2}) + W_p(V_n, V_{n-3}) \\
 &= \sum_{l=n}^{l=n+2} W_p(V_l, V_{l-3}) + \sum_{l=n}^{l=n+1} W_p(V_l, V_{l-2}) + W_p(V_n, V_{n-1}) \\
 &= \sum_{l=n}^{l=n+2} 4l - 12 + \sum_{l=n}^{l=n+1} 2l - 6 + 2n - 6 \\
 &= \sum_{l=n}^{l=n+2} (4l - 12) + \sum_{l=n}^{l=n+1} (2l - 6) + 2n - 6 \\
 &= 18n - 40.
 \end{aligned} \tag{74}$$

The distance between the set of vertices of the set  $V_{2n-1}$  is equal to  $W_p(V_{2n-1})$  and it is easy to see that

$$W_p(V_{2n-1}) = 2n - 4. \tag{75}$$

Now, by replacing the values of all these factors in equation (69) and simplifying, we get

$$\begin{aligned}
 W_p(HX_n) &= 2(W_p(T_{2n-1}) - W_p(HX_n, T_{n-1}) - W_p(T_{n-1})) + W_p(V_{2n-2}, V_{2n-2}') \\
 &\quad + W_p(V_{2n-2}, V_{2n-3}') + W_p(V_{2n-3}, V_{2n-2}') - W_p(V_{2n-1}) \\
 &= 27n^2 - 81n + 48.
 \end{aligned} \tag{76}$$

## 5. Conclusion

First of all, we will present comparison between two topological indices analytically and graphically.

**5.1. Comparison of Wiener and Wiener Polarity Indices of the Triangular Mesh Network.** The comparison between the Wiener and Wiener polarity indices of triangular mesh network  $T_n$  for different values of  $n$  is shown in Table 1. The values show that the Wiener index increases rapidly compared to Wiener polarity index as  $n$  increases. The graphical representation of both indices is also presented. In Figure 4, the black curve denotes the behavior of the Wiener polarity index and red line shows the behavior of the Wiener index.

**5.2. Comparison of Wiener and Wiener Polarity Indices of the Graph of Equilateral Triangular Tetra Sheet Networks.** The comparison between the Wiener and Wiener polarity indices of equilateral triangular tetra sheet network  $ET_n$  for different values of  $n$  is shown in Table 2. The values show that the Wiener index increases rapidly compared to Wiener polarity index as  $n$  increases. The graphical representation of both indices is also presented. In Figure 5, the black curve

denotes the behavior of Wiener polarity index and red line shows the behavior of Wiener index.

In this work, we have derived the Wiener polarity index and Wiener index of certain triangular networks. We have considered triangular grids, equilateral triangular tetra sheets, and hexagonal networks to formulate closed formulas to find the Wiener polarity index and Wiener index. Comparisons of these indices with the help of tables and graphs are also included for two families of the graph. These results will be useful to understand the molecular topology of these important classes of networks.

## Data Availability

No data were used for this study.

## Conflicts of Interest

The authors declare that they have no conflicts of interest.

## Acknowledgments

This research is supported by the University Program of Advanced Research (UPAR) and UAEU-AUA grants of United Arab Emirates University (UAEU) via Grant No. G00003271 and Grant No. G00003461.

## References

- [1] A. A. Dobrynin, R. Entringer, and I. Gutman, "Wiener index of trees: theory and applications," *Acta Applicandae Mathematica*, vol. 66, no. 3, pp. 211–249, 2001.
- [2] H. Wiener, "Structural determination of paraffin boiling points," *Journal of the American Chemical Society*, vol. 69, no. 1, pp. 17–20, 1947.
- [3] S. A. U. H. Bokhary, Adnan, M. K. Siddiqui, and M. Cancan, "On topological indices and QSPR analysis of drugs used for the treatment of breast cancer," *Polycyclic Aromatic Compounds*, vol. 1, p. 21, 2021.
- [4] S. A. Bokhary, M. Imran, S. Akhter, and S. Manzoor, "Molecular, topological invariants of certain chemical networks," *Main Group Metal Chemistry*, vol. 44, Article ID 141149, 2021.
- [5] S. A. U. H. Bokhary and F. Adnan, "On vertex PI index of certain triangular tessellation networks," *Main Group Metal Chemistry*, vol. 44, no. 1, pp. 203–212, 2021.
- [6] S. A. U. H. Bokhary, M. Imran, and S. Manzoor, "On molecular topological properties of dendrimers," *Canadian Journal of Chemistry*, vol. 94, no. 2, pp. 120–125, 2016.
- [7] L. I. Stiel and G. Thodos, "The normal boiling points and critical constants of saturated aliphatic hydrocarbons," *AIChE Journal*, vol. 8, no. 4, pp. 527–529, 1962.
- [8] D. H. Rouvray and B. C. Crafford, "The dependence of physical-chemical properties on topological factors," *South African Journal of Science*, vol. 72, p. 47, 1976.
- [9] I. Gutman and T. Krtvlyesi, "Wiener indices and molecular surfaces," *Zeitschrift fr Naturforschung*, vol. 50a, p. 669671, 1995.
- [10] I. Lukovits and W. Linert, "Polarity-numbers of cycle-containing structures," *Journal of Chemical Information and Computer Sciences*, vol. 38, no. 4, pp. 715–719, 1998.
- [11] H. Hosoya, "Mathematical and chemical analysis of Wieners polarity number," in *Topology in Chemistry-Discrete Mathematics of Molecules*, D. H. Rouvray and R. B. King, Eds., Horwood, Chichester, UK, 2002.
- [12] P. V. Khadikar, S. Karmarkar, and V. K. Agrawal, "A novel PI index and its applications to QSPR/QSAR studies," *Journal of Chemical Information and Computer Sciences*, vol. 41, no. 4, pp. 934–949, 2001.
- [13] J. Ma, Y. Shi, Z. Wang, and J. Yue, "On Wiener polarity index of bicyclic networks," *Scientific Reports*, vol. 6, no. 1, 2016.
- [14] A. Alochukwu and P. Dankelmann, "Wiener index in graphs with given minimum degree and maximum degree," *Discrete Mathematics & Theoretical Computer Science*, vol. 23, no. 1, 2021, <https://dmtcs.episciences.org/7533/pdf>.
- [15] L. Chen, T. Li, J. Liu, Y. Shi, and H. Wang, "On the Wiener polarity index of lattice networks," *PLoS One*, vol. 1112 pages, 2016.
- [16] A. Behmaram, H. Yousefi-Azari, and A. R. Ashrafi, "Wiener polarity index of fullerenes and hexagonal systems," *Applied Mathematics Letters*, vol. 25, Article ID 15101513, 2012.
- [17] H. Lei, T. Li, Y. Shi, and H. Wang, "Wiener polarity index and its generalization in trees," *MATCH Communications in Mathematical and in Computer Chemistry*, vol. 78, no. 1, pp. 199–212, 2017.
- [18] J. Ma, Y. Shi, and J. Yue, "The Wiener polarity index of graph products," *Ars Combinatoria*, vol. 116, Article ID 235244, 2016.
- [19] Y. Zhang and Y. Hu, "The Nordhaus-Gaddum-type inequality for the Wiener polarity index," *Applied Mathematics and Computation*, vol. 273, Article ID 880884, 2016.
- [20] J. Yue, Y. Shi, and Y. Wang, "Bounds of the Wiener polarity index," in *Bounds in Chemical Graph Theory Basics (MCM No. 19)*, K. C. Das, B. Furtula, I. Gutman, E. I. Milovanovic, and I. Z. Milovanovic, Eds., p. 283302, University of Kragujevac and Faculty of Science Kragujevac, Kragujevac, Serbia, 2017.

## Research Article

# Computation of Polynomial Degree-Based Topological Descriptors of Indu-Bala Product of Two Paths

Ghazanfar Abbas  and Muhammad Ibrahim 

Centre for Advanced Studies in Pure and Applied Mathematics, Bahauddin Zakariya University, Multan, Pakistan

Correspondence should be addressed to Muhammad Ibrahim; mibtufail@gmail.com

Received 10 September 2021; Accepted 28 October 2021; Published 28 November 2021

Academic Editor: Muhammad Kamran Jamil

Copyright © 2021 Ghazanfar Abbas and Muhammad Ibrahim. This is an open access article distributed under the Creative Commons Attribution License, which permits unrestricted use, distribution, and reproduction in any medium, provided the original work is properly cited.

Cheminformatics is entirely a newly coined term that encompasses a field that includes engineering computer sciences along with basic sciences. As we all know, vertices and edges form a network whereas vertex and its degrees contribute to joining edges. The degree of vertex is very much dependent on a reasonable proportion of network properties. There is no doubt that a network has to have a reliance of different kinds of hub buses, serials, and other connecting points to constitute a system that is the backbone of cheminformatics. The Indu-Bala product of two graphs  $G_1$  and  $G_2$  has a special notation as described in Section 2. The attainment of this product is very much due to related vertices at to different places of  $G_1 \vee G_2$ . This study states we have found M-polynomial and degree-based topological indices for Indu-Bala product of two paths  $P_k$  and  $P_j$  for  $j, k \geq 2$ . We also give some graphical representation of these indices and analyzed them graphically.

## 1. Introduction

Let  $G = (V(G), E(G))$  be a simple and finite graph of order  $n$ . We denote the nonempty vertex set by  $V(G)$  and edge set by  $E(G)$ . The fields of chemistry information sciences and mathematics have undoubtedly revolutionized by cheminformatics. It is a new subject that is very much helpful in keeping the data and getting information about chemicals. For this purpose, i.e., keeping the data and storing information, a significant help can be taken from the theory represented by graph in order to make index factors. The study of molecules according to their structures and their different functions based on QSAR models is also called a biological activity. The indicators that represent topology are also known as a subsidiary of the biological activity. Topological indices can be calculated using simply points (atoms) and linkages (chemical bonds) in a graphical representation. A polynomial, numeric number, a sequence of numbers, or an array representing the full graph can be used to identify it, and these representations are meant to be calculated particularly for that graph. The values in mathematics serve as indicators that have a logical connection to

the graph and its topology. These are the indicators that give various dimensions and kinds to topological indices from distance based to degree based, counting conjugal polynomials and graphs. In chemistry and especially in graph theory, the degree-based topological indices play an essential role. Precisely, we can say that  $\Sigma$  gives new shape to the index connected with topology from real numbers to its zenith. Various indicator networks are always present in an entangled form of links nodes and hubs in a network. For example, various networks have similarities in atomic structure or molecular structure, such as honeycomb, grid networks, and hexagonal. Topological properties of these networks are very interesting, which are studied in various aspects, such as minimum metric dimension of a honeycomb network in [1] and silicate network in [2], topological properties of this network in [3], and topological indicators of honeycomb, silicate, and hexagonal networks in [4]. As we study the evolution of the things biologically, different kinds of structures having six dimensions and beehive shapes come into our contact. Many authors have researched on this topic; Hayat et al. computed topological indices of some networks in [5] and for some interconnection networks in

[6]. On organized populations, Perc et al. studied the evolutionary dynamics of group interactions in [7] and on coevolutionary games in [8], and Szolnoki et al. further worked on the impact of noise on cooperation in spatial public goods games in topology-independent ways in [9] and on importance of percolation for evolution of cooperation in [10]. Mathematical references have also been found in research of paraffin, Wiener's approach [11]. Wiener invented the index that is also known as the route number. This topological descriptor formed the basis for the topological indices, in terms of theory and application in [12, 13]. Therefore, the topological indices in the chemical and quantitative literature are Weiner in [14], Zagreb in [15], and Randic in [16]. The Indu-Bala product  $G_1 \blacktriangledown G_2$  of graphs  $G_1$  and  $G_2$  is obtained from two disjoint copies of the join  $G_1 \vee G_2$  of  $G_1$  and  $G_2$  by joining the corresponding vertices in the two copies of  $G_2$ .

In this paper, we calculated some well-known topological indicators based on M-polynomial and degree based indices for Indu-Bala product of two paths.

$$M(G, z_1, z_2) = \sum_{\theta \leq i \leq j \leq \vartheta} m_{ij}(G) z_1^i z_2^j. \quad (1)$$

As in [17],  $\theta = \min\{d_s | s \in V(G)\}$ ,  $\vartheta = \max\{d_s | s \in V(G)\}$ ;  $m_{ij}(G)$  is the edge  $z_1 z_2 \in E(G)$ ;  $s \leq t$ .

Milan Randic in 1975 established the concept of Randic index [18–20], which is represented as  $R_{-1/2}(G)$ :

$$R_{-1/2}(G) = \sum_{z_1 z_2 \in E(G)} \left( \frac{1}{\sqrt{d_{z_1} d_{z_2}}} \right). \quad (2)$$

The generalized Randic index is defined as [21–28]

$$R_\alpha(G) = \sum_{z_1 z_2 \in E(G)} \left( \frac{1}{(d_{z_1} d_{z_2})^\alpha} \right). \quad (3)$$

Two indices  $M_1(G)$ ,  $M_2(G)$  were established by Gutman and Trinajstić defined as follows:

$$M_1(G) = \sum_{z_1 z_2 \in E(G)} (d_{z_1} + d_{z_2}), M_2(G) = \sum_{z_1 z_2 \in E(G)} (d_{z_1} d_{z_2}). \quad (4)$$

Another form of index is which is known as second Zagreb is define as follows [11, 29–32]:

$${}^m M_2(G) = \sum_{z_1 z_2 \in G} \left( \frac{1}{d(z_1) d(z_2)} \right). \quad (5)$$

The symmetric division index is defined as

$$\text{SDD}(G) = \sum_{z_1 z_2 \in E(G)} \left\{ \frac{(\min(d_{z_1}, d_{z_2}) + \max(d_{z_1}, d_{z_2}))}{\max(d_{z_1}, d_{z_2})} + \frac{(\min(d_{z_1}, d_{z_2}) + \max(d_{z_1}, d_{z_2}))}{\min(d_{z_1}, d_{z_2})} \right\}. \quad (6)$$

The harmonic index is defined as

$$H(G) = \sum_{z_1 z_2 \in E(G)} \left( \frac{2}{d_{z_1} + d_{z_2}} \right). \quad (7)$$

“The inverse sum index is defined as

$$I(G) = \sum_{z_1 z_2 \in E(G)} \left( \frac{d_{z_1} d_{z_2}}{d_{z_1} + d_{z_2}} \right). \quad (8)$$

The augmented Zagreb index is defined as

$$A(G) = \sum_{z_1 z_2 \in E(G)} \left\{ \frac{d_{z_1} d_{z_2}}{d_{z_1} + d_{z_2} - 2} \right\}^3. \quad (9)$$

These indices and deliberations which various researchers laboriously worked on can be seen in [33–37] as authentic references.

$$\begin{aligned} D_\gamma &= \gamma \frac{\partial(f(\gamma, \varepsilon))}{\partial \gamma}, \\ D_\varepsilon &= \varepsilon \frac{\partial(f(\gamma, \varepsilon))}{\partial \varepsilon}, \\ S_\gamma &= \int \frac{f(\gamma, \varepsilon) d\gamma}{\gamma}, \\ S_\varepsilon &= \int \frac{f(\gamma, \varepsilon) d\varepsilon}{\varepsilon}, \end{aligned} \quad (10)$$

$$J(h(\gamma, \varepsilon)) = f(\gamma, \varepsilon), Q_\alpha(h(\gamma, \varepsilon)) = \gamma^\alpha h(\gamma, \varepsilon).$$

## 2. Computational Results on Topological Indices for Indu-Bala Product of Two Paths $P_k$ and $P_j$ When $k > j$

Our fundamental objective of studying M-polynomial and all its related components is to establish a relationship between various affects of M-polynomials and its related things on the Indu-Bala graph, see Figure 1.

**2.1. Results.** We split vertices and edges degree of the Indu-Bala graph in Table 1. Similarly, we split the edge palpitations of points on the Indu-Bala graph in Table 2.

**Theorem 1.** Let  $G$  be a Indu-Bala graph  $P_k \blacktriangledown P_j$ , where  $j \geq 2, k \geq j + 2$ . We have

$$\begin{aligned} M(G; a, b) &= 4a^{j+1}b^{j+2} + 4ja^{j+1}b^{k+2} + 2(k-3)a^{j+1}b^{k+2} \\ &\quad + 2j(k-2)a^{j+2}b^{j+2} + 2ja^{k+2}b^{k+2}. \end{aligned} \quad (11)$$

*Proof.* As in Figure 1, now we will compute M-polynomial using the values of Tables 1 and 2:

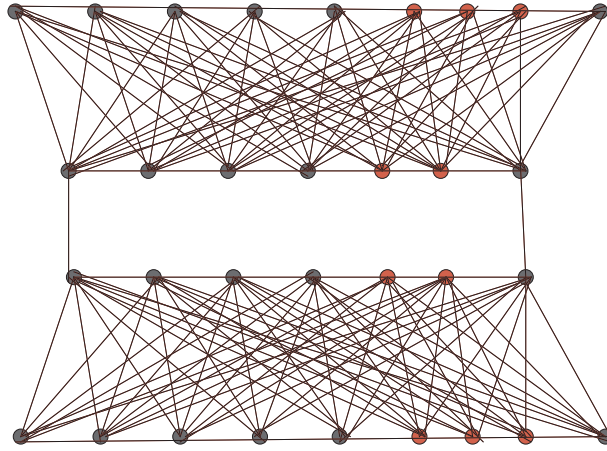


FIGURE 1: Indu-Bala graph  $P_9 \nabla P_7$ .

TABLE 1: Number of vertices of different degrees of Indu-Bala graph.

Vertices and edges	Total no. of $V(G)$ and $E(G)$
$V(G)$	$2(j+k)$
$E(G)$	$2jk + 2(j+k) - 2$

TABLE 2: Points of edge partitioning of  $P_k \nabla P_j$ .

Edges	Deg. of end nodes	Total no. of edges
$E_1$	$d(h) = j+1, d(i) = j+2$	4
$E_2$	$d(h) = j+1, d(i) = k+2$	$4j$
$E_3$	$d(h) = j+2, d(i) = j+2$	$2(k-3)$
$E_4$	$d(h) = j+2, d(i) = k+2$	$2j(k-2)$
$E_5$	$d(h) = k+2, d(i) = k+2$	$2j$

$$\begin{aligned}
 M(G; a, b) &= \sum_{i \leq j} m_{ij}(G; a^i b^j), \\
 &= \sum_{j+1 \leq j+2} m_{j+1, j+2}(G) a^{j+1} b^{j+2} + \sum_{j+1 \leq k+2} m_{j+1, k+2}(G) a^{j+1} b^{k+2} \\
 &\quad + \sum_{j+2 \leq j+2} m_{j+2, j+2}(G) a^{j+2} b^{j+2} + \sum_{j+2 \leq k+2} m_{j+2, k+2}(G) a^{j+2} b^{k+2} \\
 &\quad + \sum_{k+2 \leq k+2} m_{k+2, k+2}(G) a^{k+2} b^{k+2}, \\
 &= \sum_{uv \in E_{j+1, j+2}} m_{j+1, j+2}(G) a^{j+1} b^{j+2} + \sum_{uv \in E_{j+1, k+2}} m_{j+1, k+2}(G) a^{j+1} b^{k+2} \\
 &\quad + \sum_{uv \in E_{j+2, j+2}} m_{j+2, j+2}(G) a^{j+2} b^{j+2} + \sum_{uv \in E_{j+2, k+2}} m_{j+2, k+2}(G) a^{j+2} b^{k+2} \\
 &\quad + \sum_{uv \in E_{k+2, k+2}} m_{k+2, k+2}(G) a^{k+2} b^{k+2}, \\
 &= |E_{j+1, j+2}| a^{j+1} b^{j+2} + |E_{j+1, k+2}| a^{j+1} b^{k+2} + |E_{j+2, j+2}| a^{j+2} b^{j+2} \\
 &\quad + |E_{j+2, k+2}| a^{j+2} b^{k+2} + |E_{k+2, k+2}| a^{k+2} b^{k+2}, \\
 &= 4a^{j+1} b^{j+2} + 4ja^{j+1} b^{k+2} + 2(k-3)a^{j+1} b^{j+2} + 2j(k-2)a^{j+2} b^{k+2} + 2ja^{k+2} b^{k+2}.
 \end{aligned} \tag{12}$$

□

**Theorem 2.** In Indu-Bala graph  $P_k \blacktriangledown P_j$ ,  $j \geq 2$ ,  $k \geq j + 2$ . Proof. Then,

$$M_1(G) = 2jk(j+k+8) + 6(k-1). \quad (13)$$

---


$$M(G, a, b) = 4a^{j+1}b^{j+2} + 4ja^{j+1}b^{k+2} + 2(k-3)a^{j+2}b^{j+2} + 2j(k-2)a^{j+2}b^{k+2} + 2ja^{k+2}b^{k+2},$$

$$(G, a, b) = f(a, b); D_a f(a, b) = a \frac{\partial f}{\partial a},$$

$$\frac{\partial f}{\partial a} = \frac{\partial}{\partial a} \{4a^{j+1}b^{j+2} + 4ja^{j+1}b^{k+2} + 2(k-3)a^{j+2}b^{j+2} + 2j(k-2)a^{j+2}b^{k+2} + 2ja^{k+2}b^{k+2}\},$$

$$a \frac{\partial f}{\partial a} = 4(j+1)a^{j+1}b^{j+2} + 4j(j+1)a^{j+1}b^{k+2} + 2(j+2)(k-3)a^{j+2}b^{j+2}$$

$$+ 2j(j+2)(k-2)a^{j+2}b^{k+2} + 2j(k+2)a^{k+2}b^{k+2}; D_b f(a, b) = b \frac{\partial f}{\partial b}, \quad (14)$$

$$\frac{\partial f}{\partial b} = \frac{\partial}{\partial b} \{4a^{j+1}b^{j+2} + 4ja^{j+1}b^{k+2} + 2(k-3)a^{j+2}b^{j+2} + 2j(k-2)a^{j+2}b^{k+2} + 2ja^{k+2}b^{k+2}\},$$

$$b \frac{\partial f}{\partial b} = 4(j+2)a^{j+1}b^{j+2} + 4j(k+2)a^{j+1}b^{k+2} + 2(j+2)(k-3)a^{j+2}b^{j+2}$$

$$+ 2j(k+2)(k-2)a^{j+2}b^{k+2} + 2j(k+2)a^{k+2}b^{k+2},$$

$$M_1(G) = (D_a + D_b)(f(a, b))|_{(a=b=1)}$$


---

**Theorem 3.** In Indu-Bala graph  $P_k \blacktriangledown P_j$ ,  $j \geq 2$ ,  $k \geq j + 2$ ; Proof. Suppose then,

$$M_2(G) = 8(k-j) + j^2(2k^2 + 6k - 6) + 2jk(10 + 3k) - 16. \quad (15)$$


---

$$M(G, a, b) = 4a^{j+1}b^{j+2} + 4ja^{j+1}b^{k+2} + 2(k-3)a^{j+2}b^{j+2} + 2j(k-2)a^{j+2}b^{k+2} + 2ja^{k+2}b^{k+2},$$

$$D_a f(a, b) = 4(j+1)a^{j+1}b^{j+2} + 4j(j+1)a^{j+1}b^{k+2} + 2(j+2)(k-3)a^{j+2}b^{j+2}$$

$$+ 2j(j+2)(k-2)a^{j+2}b^{k+2} + 2j(k+2)a^{k+2}b^{k+2},$$

$$D_b D_a f(a, b) = 4(j+1)(j+2)a^{j+1}b^{j+2} + 4j(j+1)(k+2)a^{j+1}b^{k+2} + 2(j+2)^2(k-3)a^{j+2}b^{j+2}$$

$$+ 2j(j+2)(k+2)(k-2)a^{j+2}b^{k+2} + 2j(k+2)(k+2)a^{k+2}b^{k+2}, \quad (16)$$

$$M_2(G) = D_b D_a f(a, b)|_{(a=b=1)}$$

$$+ 2(j+2)^2(k-3) + 2j(j+2)(k^2 - 4) + 2j(k+2)^2,$$

$$M_2(G) = 8(k-j) + j^2(2k^2 + 6k - 6) + 2jk(10 + 3k) - 16.$$


---

**Theorem 4.** In Indu-Bala graph  $P_k \blacktriangledown P_j$ ,  $j \geq 2$ ,  $k \geq j + 2$ ; then (Figures 2 and 3),

$${}^m M_2(G) = \frac{2j^4 + j^3(2k^2 - 2k + 4) + j^2(2k^2 - 2k + 8) + j(2k^3 + 8k^2 - 8k + 6) + 4(k+1)^2}{j(j+1)^2(k+1)^2}. \quad (17)$$

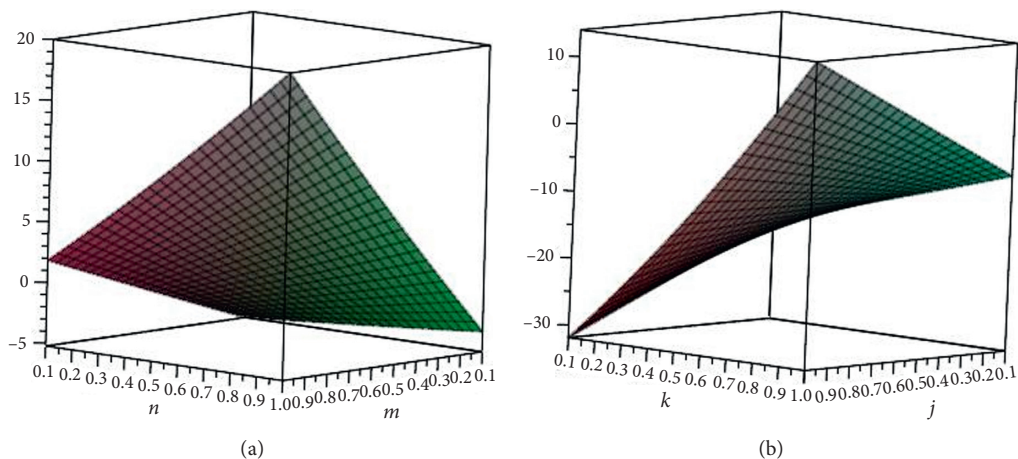


Figure 2: (a) First Zagreb index for  $j \leq k$ . (b) Second Zagreb index for  $j \leq k$ .

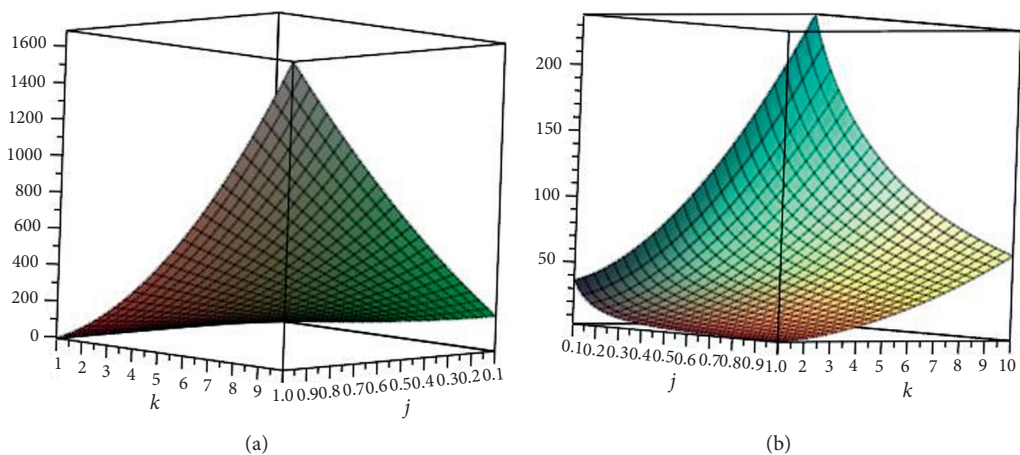


FIGURE 3: (a) Randić index for  $j \leq k$  and  $\alpha = 1$ . (b) Modified second Zagreb index for  $j \leq k$  and  $\alpha = 1$ .

*Proof.* Suppose

$$M(G; a, b) = 4a^{j+1}b^{j+2} + 4ja^{j+1}b^{k+2} + 2(k-3)a^{j+2}b^{j+2} + 2j(k-2)a^{j+2}b^{k+2} + 2ja^{k+2}b^{k+2},$$

$${}^m M_2(G) = S_a S_b f(a, b)|_{(a=b=1)},$$

$$S_a = \int_0^a \frac{f(u, b)}{u} du,$$

$$S_b = \int_0^b \frac{f(a, u)}{u} du,$$

$$\frac{f(u, b)}{u} = 4u^j b^{j+2} + 4uu^j b^{k+2} + 2(k-3)u^{j+1} b^{j+2} + 2u(k-2)u^{j+1} b^{k+2} + 2uu^{k+1} b^{k+2}, *$$

$$S_a = \frac{4}{j} a^{j+1} b^{j+2} + 4a^{j+1} b^{k+2} + \frac{2(k-3)}{j+1} a^{j+2} b^{j+2} + \frac{2j(k-2)}{j+1} a^{j+2} b^{k+2} + \frac{2j}{k+1} a^{k+2} b^{k+2},$$

$$\int_0^a \frac{f(a, u)}{u} dt = \frac{4}{j} a^{j+1} u^{j+1} + 4a^{j+1} u^{k+1} + \frac{2(k-3)}{j+1} a^{j+2} u^{j+1} + \frac{2j(k-2)}{j+1} a^{j+2} u^{k+1} + \frac{2j}{k+1} a^{k+2} u^{k+1},$$

$$S_b S_a f(a, b) = \int_0^b \frac{S_a f(a, u)}{u} du,$$

$$S_b S_a f(a, b) = \frac{4}{j(j+1)} a^{j+1} b^{j+2} + \frac{4}{k+1} a^{j+1} b^{k+2} + \frac{2(k-3)}{(j+1)^2} a^{j+2} b^{j+2}$$

$$+ \frac{2j(k-2)}{(j+1)(k+1)} a^{j+2} b^{k+2} + \frac{2j}{(k+1)^2} a^{k+2} b^{k+2}, \quad (18)$$

$${}^m M_2(G) = S_b S_a f(a, b)|_{(a=b=1)} = \frac{4}{j(j+1)} + \frac{4}{k+1} + \frac{2(k-3)}{(j+1)^2} + \frac{2j(k-2)}{(j+1)(k+1)} + \frac{2j}{(k+1)^2},$$

$$= \frac{2j^4 + j^3(2k^2 - 2k + 4) + j^2(2k^2 - 2k + 8) + j(2k^3 + 8k^2 - 8k + 6) + 4(k+1)^2}{j(j+1)^2(k+1)^2}.$$

**Theorem 5.** In Indu-Bala graph  $P_k \blacktriangledown P_j$ ,  $j \geq 2$ ,  $k \geq j + 2$ ; then,

$$R_\alpha(G) = 4(j+1)^\alpha \{ (j+2)^\alpha + j(k+2)^\alpha \} + 2(j+2)^\alpha \{ (k-3)(j+2)^\alpha + 2j(k-2)(k+2)^\alpha \} + 2j(k+2)^{2\alpha}. \quad (19)$$

*Proof.* Suppose

$$M(G; a; b) = 4a^{j+1}b^{j+2} + 4ja^{j+1}b^{k+2} + 2(k-3)a^{j+2}b^{j+2} + 2j(k-2)a^{j+2}b^{k+2} + 2ja^{k+2}b^{k+2},$$

$$R_\alpha(G) = D_a^\alpha D_b^\alpha f(a, b)|_{(a=b=1)},$$

$$D_b^\alpha f(a, b) = 4(2+j)^\alpha a^{j+1}b^{2+j} + 4j(2+k)^\alpha a^{j+1}b^{2+k} + 2(-3+k)(j+2)^\alpha a^{j+2}b^{j+2}$$

$$+ 2j(-2+k)(2+k)^\alpha a^{j+2}b^{2+k} + 2j(2+k)^\alpha a^{k+2}b^{2+k},$$

$$D_a^\alpha D_b^\alpha f(a, b) = 4(j+1)^\alpha (j+2)^\alpha a^{j+1}b^{j+2} + 4j(j+1)^\alpha (k+2)^\alpha a^{j+1}b^{k+2}$$

$$+ 2(k-3)(j+2)^{2\alpha} a^{j+2}b^{j+2} + 2j(-2+k)(2+j)^\alpha (2+k)^\alpha a^{j+2}b^{k+2}$$

$$+ 2j(k+2)^{2\alpha} a^{k+2}b^{k+2}, \quad (20)$$

$$R_\alpha(G) = D_a^\alpha D_b^\alpha f(a, b)|_{(a=b=1)} = 4(j+1)^\alpha (j+2)^\alpha + 4j(j+1)^\alpha (k+2)^\alpha$$

$$+ 2(-3+k)(2+j)^{2\alpha} + 2j(-2+k)(2+j)^\alpha (2+k)^\alpha + 2j(2+k)^{2\alpha},$$

$$R_\alpha(G) = 4(1+j)^\alpha \{ (2+j)^\alpha + j(2+k)^\alpha \} + 2(2+j)^\alpha \{ (-3+k)(2+j)^\alpha + 2j(-2+k)(k+2)^\alpha \} + 2j(2+k)^{2\alpha}.$$

**Theorem 6.** In Indu-Bala graph  $P_j \blacktriangledown P_k$ ,  $j \geq 2$ ,  $k \geq j + 2$ . Then,

$$RR_\alpha(G) = \frac{4}{(1+j)^\alpha} \left\{ \frac{1}{j^\alpha} + \frac{(k-3)}{2(j+1)^\alpha} + \frac{j(-2+k)}{2(1+k)^\alpha} \right\} + \frac{4}{(1+k)^\alpha} \left\{ \frac{j}{2(k+1)^\alpha} + 1 \right\}. \quad (21)$$

*Proof.* Suppose

$$\begin{aligned}
 M(G; a, b) &= 4a^{j+1}b^{j+2} + 4ja^{j+1}b^{k+2} + 2(k-3)a^{j+2}b^{j+2} + 2j(k-2)a^{j+2}b^{k+2} + 2ja^{k+2}b^{k+2}, \\
 RR_\alpha(G) &= S_a^\alpha S_b^\alpha f(a, b)|_{(a=b=1)}, \\
 S_b &= \frac{4}{j+1}a^{j+1}b^{j+2} + \frac{4j}{k+1}a^{j+1}b^{k+2} + \frac{2(k-3)}{j+1}a^{j+2}b^{j+2} + \frac{2j(k-2)}{k+1}a^{j+2}b^{k+2} \\
 &\quad + \frac{2j}{k+1}a^{k+2}b^{k+2}, \\
 S_b^\alpha &= \frac{4}{(j+1)^\alpha}a^{j+1}b^{j+2} + \frac{4j}{(k+1)^\alpha}a^{j+1}b^{k+2} + \frac{2(k-3)}{(j+1)^\alpha}a^{j+2}b^{j+2} \\
 &\quad + \frac{2j(k-2)}{(k+1)^\alpha}a^{j+2}b^{k+2} + \frac{2j}{(k+1)^\alpha}a^{k+2}b^{k+2}, \\
 S_a^\alpha S_b^\alpha f(a, b) &= \frac{4}{(j(j+1))^\alpha}a^{j+1}b^{j+2} + \frac{4}{(k+1)^\alpha}a^{j+1}b^{k+2} + \frac{2(k-3)}{(j+1)^{2\alpha}}a^{j+2}b^{j+2} \\
 &\quad + \frac{2j(k-2)}{((j+1)(k+1))^\alpha}a^{j+2}b^{k+2} + \frac{2j}{(k+1)^{2\alpha}}a^{k+2}b^{k+2}, \\
 S_a^\alpha S_b^\alpha f(a, b)|_{(a=b=1)} &= \frac{4}{(j(j+1))^\alpha} + \frac{4}{(1+k)^\alpha} + \frac{2(k-3)}{(1+j)^{2\alpha}} + \frac{2j(k-2)}{((1+j)(1+k))^\alpha} + \frac{2j}{(1+k)^{2\alpha}}, \\
 RR_\alpha(G) &= \frac{4}{(1+j)^\alpha} \left\{ \frac{1}{j^\alpha} + \frac{(-3+k)}{2(j+1)^\alpha} + \frac{j(-2+k)}{2(1+k)^\alpha} \right\} + \frac{4}{(1+k)^\alpha} \left\{ \frac{j}{2(1+k)^\alpha} + 1 \right\}.
 \end{aligned} \tag{22}$$

**Theorem 7.** In Indu-Bala graph  $P_k \blacktriangledown P_j$ ,  $j \geq 2$ ,  $k \geq j + 2$ ; then,

$$\text{SSD}(G) = \frac{j^4(k+2) + j^3(4k^2 + 3k + 2) + j^2(6k^2 + 3k - 2) + 4(k+1)(3jk + 2)}{j(j+1)(k+1)}. \tag{23}$$

*Proof.* Suppose

$$\begin{aligned}
 M(G; a, b) &= 4a^{j+1}b^{j+2} + 4ja^{j+1}b^{k+2} + 2(k-3)a^{j+2}b^{j+2} + 2j(k-2)a^{j+2}b^{k+2} \\
 &\quad + 2ja^{k+2}b^{k+2}, \\
 \text{SSD}(G) &= (S_b D_a + S_a D_b) f(a, b)|_{(a=b=1)}, \\
 S_b D_a f(a, b) &= 4a^{j+1}b^{j+2} + \frac{4j(j+1)}{k+1}a^{j+1}b^{k+2} + \frac{2(j+2)(k-3)}{j+1}a^{j+2}b^{j+2} \\
 &\quad + \frac{2j(j+2)(k-2)}{k+1}a^{j+2}b^{k+2} + \frac{2j(k+2)}{k+1}a^{k+2}b^{k+2},
 \end{aligned}$$

$$\begin{aligned}
S_a D_b f(a, b) &= \frac{4(j+2)}{j} a^{j+1} b^{j+2} + 4(k+2) a^{j+1} b^{k+2} + \frac{2(j+2)(k-3)}{j+1} a^{j+2} b^{j+2} \\
&\quad + \frac{2j(k+2)(k-2)}{j+1} a^{j+2} b^{k+2} + \frac{2j(k+2)}{k+1} a^{k+2} b^{k+2}; (S_b D_a + S_a D_b) f(a, b), \\
&= \left\{ 4 + \frac{4(j+2)}{j} \right\} a^{j+1} b^{j+2} + \left\{ \frac{4j(j+1)}{k+1} + 4(k+2) \right\} a^{j+1} b^{k+2} \\
&\quad + \left\{ \frac{2(j+2)(k-3)}{j+1} + \frac{2(j+2)(k-3)}{j+1} \right\} a^{j+2} b^{j+2} + \left\{ \frac{2j(j+2)(k-2)}{k+1} \right. \\
&\quad \left. + \frac{2j(k+2)(k-2)}{j+1} \right\} a^{j+2} b^{k+2} + \left\{ \frac{2j(k+2)}{k+1} + \frac{2j(k+2)}{k+1} \right\} a^{k+2} b^{k+2}, \\
SSD(G) &= (S_b D_a + S_a D_b) f(a, b)|_{(a=b=1)} = \frac{8(j+1)}{j} + \frac{4}{k+1} (j^2 + k^2 + j + 3k + 2) \\
&\quad + \frac{4(j+2)(k-3)}{j+1} + \frac{j(k-2)}{(j+1)(k+1)} (j^2 + k^2 + 3(j+k) + 4) + \frac{4j(k+2)}{k+1}, \\
SSD(G) &= \frac{4j^2 k - 4j^2 + 8jk - 8j + 8}{j(j+1)} + (4(j+1)(j^2 + k^2 + j + 3k + 2) \\
&\quad + j(k-2)(j^2 + k^2 + 3j + 3k + 4) + j(k+2)) \frac{1}{(j+1)(k+1)}, \\
&= \frac{4j^2 k - 4j^2 + 8jk - 8j + 8}{j(j+1)} \\
&\quad + \frac{j^3(k+2) + j^2(4k^2 + 3k + 2) + j(2k^2 + 3k + 2) + 4k(k+3) + 8}{(j+1)(k+1)}, \\
SSD(G) &= \frac{j^4(k+2) + j^3(4k^2 + 3k + 2) + j^2(6k^2 + 3k - 2) + 4(k+1)(3jk + 2)}{j(j+1)(k+1)}.
\end{aligned} \tag{24}$$

□

**Theorem 8.** In Indu-Bala graph  $P_k \blacktriangledown P_j$ ,  $j \geq 2$ ,  $k \geq j + 2$ ; *Proof.* Suppose then,

$$H(G) = \frac{2j^3 + 4j^2(k^2 + k) + j(4k^2 + 10k + 12) + 8(k+1)}{j(j+1)(k+1)}. \tag{25}$$

$$M(G; a, b) = 4a^{j+1} b^{j+2} + 4ja^{j+1} b^{k+2} + 2(k-3)a^{j+2} b^{j+2} + 2j(k-2)a^{j+2} b^{k+2} + 2ja^{k+2} b^{k+2},$$

$$H(G) = 2S_a j f(a, b)|_{a=1},$$

$$S_a f(a, b) = \frac{4}{j} a^{j+1} b^{j+2} + 4a^{j+1} b^{k+2} + \frac{2(k-3)}{j+1} a^{j+2} b^{j+2} + \frac{2j(k-2)}{j+1} a^{j+2} b^{k+2} + \frac{2j}{k+1} a^{k+2} b^{k+2},$$

$$2S_a j f(a, b) = \frac{8}{j} a^{2j+3} + 8a^{j+k+3} + \frac{4(k-3)}{j+1} a^{2j+4} + \frac{4j(k-2)}{j+1} a^{j+k+4} + \frac{4j}{k+1} a^{2k+4}, \tag{26}$$

$$2S_a j f(a, b)|_{a=1} = \frac{8}{j} + 8 + \frac{4(k-3)}{j+1} + \frac{4j(k-2)}{j+1} + \frac{4j}{k+1},$$

$$H(G) = \frac{2j^3 + 4j^2(k^2 + k) + j(4k^2 + 10k + 12) + 8(k+1)}{j(j+1)(k+1)}.$$

□

**Theorem 9.** In Indu-Bala graph  $P_k \blacktriangledown P_j$ ,  $j \geq 2$ ,  $k \geq j + 2$ ; then,

$$I(G) = \frac{4j^5 + 20j^4 + j^3(8k^2 + 40) + j^2(4k^3 + 14k^2 - 8k + 36) + j(16k^2 - 20k - 20) + 8(k + 1)}{j(j + 1)(k + 1)}. \quad (27)$$

*Proof.* Suppose

$$\begin{aligned} M(G; a, b) &= 4a^{j+1}b^{j+2} + 4ja^{j+1}b^{k+2} + 2(k-3)a^{j+2}b^{j+2} + 2j(k-2)a^{j+2}b^{k+2} + 2ja^{k+2}b^{k+2}, \\ I(G) &= S_a j D_a D_b f(a, b)|_{a=1}; D_a D_b f(a, b), \\ &= 4(j+1)(j+2)a^{j+1}b^{j+2} + 4j(j+1)(k+2)a^{j+1}b^{k+2} + 2(j+2)^2(k-3)a^{j+2}b^{j+2} \\ &\quad + 2j(j+2)(k+2)(k-2)a^{j+2}b^{k+2} + 2j(k+2)(k+2)a^{k+2}b^{k+2}; S_a j D_a D_b f(a, b), \\ &= \frac{4(j+1)(j+2)}{j} a^{2j+3} + 4(j+1)(k+2)a^{j+k+3} + \frac{2(j+2)^2(k-3)}{j+1} a^{2j+4} \\ &\quad + \frac{2j(j+2)(k+2)(k-2)}{j+1} a^{j+k+4} + \frac{2j(k+2)(k+2)}{k+1} a^{2k+4}; S_a j D_a D_b f(a, b)|_{a=1}, \\ &= \frac{4(j+1)(j+2)}{j} + 4(j+1)(k+2) + \frac{2(j+2)^2(k-3)}{j+1} \\ &\quad + \frac{2j(j+2)(k^2-4)}{j+1} + \frac{2j(k+2)(k+2)}{k+1}, \\ I(G) &= \frac{4j^5 + 20j^4 + j^3(8k^2 + 40) + j^2(4k^3 + 14k^2 - 8k + 36) + j(16k^2 - 20k - 20) + 8(k + 1)}{j(j + 1)(k + 1)}. \end{aligned} \quad (28)$$

**Theorem 10.** In Indu-Bala graph  $P_k \blacktriangledown P_j$ ,  $j \geq 2$ ,  $k \geq j + 2$ ; then,

$$I(G) = 2(j+2)^3 \left\{ \frac{2(j+1)^3}{(2j+1)^3} + \frac{(k-3)(j+2)^3}{(2j+2)^3} \right\} + \frac{2j(k+2)^3}{(j+k+1)^3} \{ 2(j+1)^3 + (k-2)(j+2)^3 \}. \quad (29)$$

*Proof.* Suppose

$$\begin{aligned} M(G; a, b) &= 4a^{j+1}b^{j+2} + 4ja^{j+1}b^{k+2} + 2(k-3)a^{j+2}b^{j+2} + 2j(k-2)a^{j+2}b^{k+2} + 2ja^{k+2}b^{k+2}, \\ A(G) &= S_a^3 Q_{-2} j D_a^3 D_b^3 f(a, b)|_{a=1}, \\ D_a^\alpha D_b^\alpha f(a, b) &= 4(j+1)^\alpha (j+2)^\alpha a^{j+1}b^{j+2} + 4j(j+1)^\alpha (k+2)^\alpha a^{j+1}b^{k+2} \\ &\quad + 2(k-3)(j+2)^{2\alpha} a^{j+2}b^{j+2} + 2j(k-2)(j+2)^\alpha (k+2)^\alpha a^{j+2}b^{k+2}, \end{aligned}$$

$$\begin{aligned}
D_a^3 D_b^3 f(a, b) &= 4(j+1)^3(j+2)^3 a^{j+1} b^{j+2} + 4j(j+1)^3(k+2)^3 a^{j+1} b^{k+2} \\
&\quad + 2(k-3)(j+2)^6 a^{j+2} b^{j+2} + 2j(k-2)(j+2)^3(k+2)^3 a^{j+2} b^{k+2}, \\
JD_a^3 D_b^3 f(a, b) &= 4(j+t1)^3(j+t2)^3 a^{2j+3} + 4j(j+t1)^3(k+t2)^3 a^{j+k+3} + 2(k-3)(j+t2)^6 a^{2j+4} \\
&\quad + 2j(k-2)(j+2)^3(k+2)^3 a^{j+k+4}; Q_{-2} j D_a^3 D_b^3 f(a, b), \\
&= 4(j+1)^3(j+2)^3 a^{2j+1} + 4j(j+1)^3(k+2)^3 a^{j+k+1} + 2(k-3)(j+2)^6 a^{2j+2} \\
&\quad + 2j(k-2)(j+2)^3(k+2)^3 a^{j+k+2}; S_a^3 Q_{-2} j D_a^3 D_b^3 f(a, b), \\
&= \frac{4(j+1)^3(j+2)^3}{(2j+1)^3} a^{2j+1} + \frac{4j(j+1)^3(k+2)^3}{(j+k+1)^3} a^{j+k+1} + \frac{2(k-3)(j+2)^6}{(2j+2)^3} a^{2j+2} \\
&\quad + \frac{2j(k-2)(j+2)^3(k+2)^3}{(j+k+1)^3} \left. \right\} a^{j+k+2}; S_a^3 Q_{-2} j D_a^3 D_b^3 f(a, b)|_{a=1} \\
&= \frac{4(j+1)^3(j+2)^3}{(2j+1)^3} + \frac{4j(j+1)^3(k+2)^3}{(j+k+1)^3} + \frac{2(k-3)(j+2)^6}{(2j+2)^3} \\
&\quad + \frac{2j(k-2)(j+2)^3(k+2)^3}{(j+k+1)^3}, \\
A(G) &= 2(j+2)^3 \left\{ \frac{2(j+1)^3}{(2j+1)^3} + \frac{(k-3)(j+2)^3}{(2j+2)^3} \right\} + \frac{2j(k+2)^3}{(j+k+1)^3} \{2(j+1)^3 + (k-2)(j+2)^3\}.
\end{aligned} \tag{30}$$

### 3. Computational Results on Topological Indices for Indu-Bala Product of Two Paths $P_j$ and $P_k$ When $j > k$

Our fundamental objective of studying M-polynomial and its related all components is to establish a relationship between various affects of M-polynomials and its related things on the Indu-Bala graph, see Figure 4.

**3.1. Results.** We split vertices and edge degree of the Indu-Bala graph in Table 3. Similarly, we split the edge palpitations of points on the Indu-Bala graph in Table 4.

**Theorem 11.** In Indu-Bala graph  $P_j \blacktriangledown P_k$ ,  $j \geq 2$ ,  $k \geq j+2$ ; then,

$$\begin{aligned}
M(G; a, b) &= 2ka^{j+2}b^{j+2} + 4ka^{j+2}b^{k+1} \\
&\quad + k(2j-4)a^{j+2}b^{k+2} \\
&\quad + 4a^{k+1}b^{k+2} + (2j-6)a^{k+2}b^{k+2}.
\end{aligned} \tag{31}$$

*Proof.* As in Figure 4, now we will compute M-polynomial using the values of Tables 3 and 4:

$$\begin{aligned}
M(G; a, b) &= \sum_{i \leq j} m_{ij}(G; a^i b^j), \\
&= \sum_{j+2 \leq j+2} j_{(j+2)(j+2)}(G) a^{j+2} b^{j+2} + \sum_{j+2 \leq k+1} j_{(j+2)(k+1)}(G) a^{j+2} b^{k+1} \\
&\quad + \sum_{j+2 \leq k+2} j_{(j+2)(k+2)}(G) a^{j+2} b^{k+2} + \sum_{k+1 \leq k+2} j_{(k+1)(k+2)}(G) a^{k+1} b^{k+2} \\
&\quad + \sum_{k+2 \leq k+2} j_{(k+2)(k+2)}(G) a^{k+2} b^{k+2}, \\
&= \sum_{uv \in E_{j+2, j+2}} j_{(j+2)(j+2)}(G) a^{j+2} b^{j+2} + \sum_{uv \in E_{j+2, k+1}} j_{(j+2)(k+1)}(G) a^{j+2} b^{k+1} \\
&\quad + \sum_{uv \in E_{j+2, k+2}} j_{(j+2)(k+2)}(G) a^{j+2} b^{k+2} + \sum_{uv \in E_{k+1, k+2}} j_{(k+1)(k+2)}(G) a^{k+1} b^{k+2} \\
&\quad + \sum_{uv \in E_{k+2, k+2}} j_{(k+2)(k+2)}(G) a^{k+2} b^{k+2}, \\
&= |E_{j+2, j+2}| a^{j+2} b^{j+2} + |E_{j+2, k+1}| a^{j+2} b^{k+1} + |E_{j+2, k+2}| a^{j+2} b^{k+2} \\
&\quad + |E_{k+1, k+2}| a^{k+1} b^{k+2} + |E_{k+2, k+2}| a^{k+2} b^{k+2}, \\
&= 2ka^{j+2}b^{j+2} + 4ka^{j+2}b^{k+1} + k(2j-4)a^{j+2}b^{k+2} + 4a^{k+1}b^{k+2} + (2j-6)a^{k+2}b^{k+2}.
\end{aligned} \tag{32}$$

□

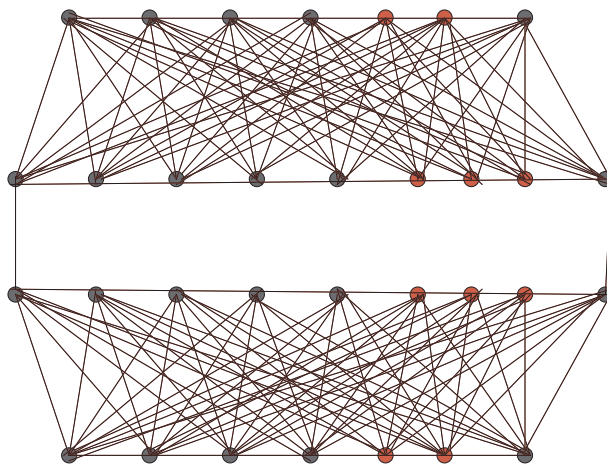


FIGURE 4: Indu-Bala graph  $P_7 \blacktriangledown P_9$ .

TABLE 3: Number of vertices of different degrees of the Indu-Bala graph.

Vertices	Total no. of $V(G)$ and $E(G)$
$V(G)$	$2(j+k)$
$E(G)$	$2jk + 2(j+k) - 2$

TABLE 4: Points of edge partitioning of  $P_j \blacktriangledown P_k$ .

Edges	Deg. of end nodes	Total no. of edges
$E_1$	$d(h) = j + 2, d(i) = j + 2$	$2k$
$E_2$	$d(h) = j + 2, d(i) = k + 1$	$4k$
$E_3$	$d(h) = j + 2, d(i) = k + 2$	$k(2j - 4)$
$E_4$	$d(h) = k + 1, d(i) = k + 2$	$4$
$E_5$	$d(h) = k + 2, d(i) = k + 2$	$2j - 6$

**Theorem 12.** In Indu-Bala graph  $P_j \blacktriangledown P_k$ ,  $j \geq 2$ ,  $k \geq j + 2$ ; Proof. then,

$$M_1(G) = j(2jk + 2k^2 + 16k + 8) - 12. \quad (33)$$

$$M(G, a, b) = 2ka^{j+2}b^{j+2} + 4ka^{j+2}b^{k+1} + k(2j - 4)a^{j+2}b^{k+2} + 4a^{k+1}b^{k+2} + (2j - 6)a^{k+2}b^{k+2},$$

$$(G, a, b) = f(a, b); D_a f(a, b) = a \frac{\partial f}{\partial a},$$

$$\frac{\partial f}{\partial a} = \frac{\partial}{\partial a} \{2ka^{j+2}b^{j+2} + 4ka^{j+2}b^{k+1} + k(2j - 4)a^{j+2}b^{k+2} + 4a^{k+1}b^{k+2} + (2j - 6)a^{k+2}b^{k+2}\},$$

$$a \frac{\partial f}{\partial a} = 2k(j + 2)a^{j+2}b^{j+2} + 4k(j + 2)a^{j+2}b^{k+1} + k(j + 2)(2j - 4)a^{j+2}b^{k+2}$$

$$+ 4(k + 1)a^{k+1}b^{k+2} + (k + 2)(2j - 6)a^{k+2}b^{k+2}; D_b f(a, b) = b \frac{\partial f}{\partial b},$$

$$\frac{\partial f}{\partial b} = \frac{\partial}{\partial b} \{2ka^{j+2}b^{j+2} + 4ka^{j+2}b^{k+1} + k(2j - 4)a^{j+2}b^{k+2} + 4a^{k+1}b^{k+2} + (2j - 6)a^{k+2}b^{k+2}\},$$

$$\begin{aligned}
b \frac{\partial f}{\partial b} &= 2k(j+2)a^{j+2}b^{j+2} + 4k(k+1)a^{j+2}b^{k+1} + k(k+2)(2j-4)a^{j+2}b^{k+2} + 4(k+2)a^{k+1}b^{k+2} \\
&\quad + (k+2)(2j-6)a^{k+2}b^{k+2}; M_1(G) = (D_a + D_b)(f(a, b))|_{(a=b=1)}, \\
&= 4k(j+2) + 4k(j+k+3) + k(2j-4)(j+k+4) + 4(2k+3) + 2(k+2)(2j-6), \\
M_1(G) &= j(2kj + 2k^2 + 16k + 8) - 12.
\end{aligned} \tag{34}$$

**Theorem 13.** In Indu-Bala graph  $P_j \blacktriangledown P_k$ ,  $j \geq 2$ ,  $k \geq j + 2$ ; *Proof.*  
then,

$$M_2(G) = j^2(2k^2 + 6k) + j(6k^2 + 20k + 8) - 2k^2 - 12k - 6. \tag{35}$$

$$\begin{aligned}
M(G, a, b) &= 2ka^{j+2}b^{j+2} + 4ka^{j+2}b^{k+1} + k(2j-4)a^{j+2}b^{k+2} + 4a^{k+1}b^{k+2} + (2j-6)a^{k+2}b^{k+2}, \\
D_a f(a, b) &= 2k(j+2)a^{j+2}b^{j+2} + 4k(j+2)a^{j+2}b^{k+1} + k(j+2)(2j-4)a^{j+2}b^{k+2} \\
&\quad + 4(k+1)a^{k+1}b^{k+2} + (k+2)(2j-6)a^{k+2}b^{k+2}, \\
D_b D_a f(a, b) &= 2k(j+2)^2 a^{j+2}b^{j+2} + 4k(j+2)(k+1)a^{j+2}b^{k+1} + k(j+2)(k+2)(2j-4)a^{j+2}b^{k+2} \\
&\quad + 4(k+1)(k+2)a^{k+1}b^{k+2} + (k+2)^2(2j-6)a^{k+2}b^{k+2}, \\
M_2(G) &= D_b D_a f(a, b)|_{(a=b=1)} = 2k(j+2)^2 + 4k(j+2)(k+1) + k(j+2)(k+2)(2j-4) \\
&\quad + 4(k+1)(k+2) + (k+2)^2(2j-6), \\
M_2(G) &= j^2(2k^2 + 6k) + j(6k^2 + 20k + 8) - 2k^2 - 12k - 6.
\end{aligned} \tag{36}$$

**Theorem 14.** In Indu-Bala graph  $P_j \blacktriangledown P_k$ ,  $j \geq 2$ ,  $k \geq j + 2$ ; *Proof.*  
then,

$${}^m M_2(G) = \frac{2k^4 + k^3(2j^2 - 6j) + k^2(6j^2 - 2j) + k(2j^3 + 2j^2 - 10j - 6) + 4j^2 + 8j + 4}{k(j+1)^2(k+1)^2}. \tag{37}$$

*Proof.*

$$\begin{aligned}
M(G, a, b) &= 2ka^{j+2}b^{j+2} + 4ka^{j+2}b^{k+1} + k(2j-4)a^{j+2}b^{k+2} + 4a^{k+1}b^{k+2} + (2j-6)a^{k+2}b^{k+2}, \\
{}^m M_2(G) &= S_a S_b f(a, b)|_{(a=b=1)}, \\
S_a &= \int_0^a \frac{f(x, b)}{x} dx; S_b = \int_0^b \frac{f(a, x)}{x} dx, \\
\frac{f(x, b)}{x} &= 2kx^{j+1}b^{j+2} + 4kx^{j+1}b^{k+1} + k(2j-4)x^{j+1}b^{k+2} + 4x^k b^{k+2} + (2j-6)x^{k+1}b^{k+2}, \\
S_a &= \frac{2k}{j+1}a^{j+2}b^{j+2} + \frac{4k}{j+1}a^{j+2}b^{k+1} + \frac{k(2j-4)}{j+1}a^{j+2}b^{k+2} + \frac{4}{k}a^{k+1}b^{k+2} + \frac{2j-6}{k+1}a^{k+2}b^{k+2},
\end{aligned}$$

$$\begin{aligned} \frac{S_a(a, x)}{x} &= \frac{2k}{j+1} a^{j+2} x^{j+1} + \frac{4k}{j+1} a^{j+2} x^{k+1} + \frac{k(2j-4)}{j+1} a^{j+2} x^{k+1} + \frac{4}{k} a^{k+1} x^{k+1} + \frac{2j-6}{k+1} a^{k+2} x^{k+1}, \\ S_b S_a f(a, b) &= \int_0^b \frac{S_a f(a, x)}{x} dx, \\ S_b S_a f(a, b) &= \frac{2k}{(j+1)^2} a^{j+2} b^{j+2} + \frac{4k}{(j+1)(k+1)} a^{j+2} b^{k+2} + \frac{k(2j-4)}{(j+1)(k+1)} a^{j+2} b^{k+2} \\ &\quad + \frac{4}{k(k+1)} a^{k+1} b^{k+2} + \frac{2j-6}{(k+1)^2} a^{k+2} b^{k+2}, \\ {}^m M_2(G) &= S_b S_a f(a, b)|_{(a=b=1)} = \frac{2k}{(j+1)^2} + \frac{4k}{(j+1)(k+1)} + \frac{k(2j-4)}{(j+1)(k+1)} + \frac{4}{k(k+1)} + \frac{2j-6}{(k+1)^2}, \\ &= \frac{2k^4 + k^3(2j^2 - 6j) + k^2(6j^2 - 2j) + k(2j^3 + 2j^2 - 10j - 6) + 4j^2 + 8j + 4}{k(j+1)^2(k+1)^2}. \end{aligned} \tag{38}$$

**Theorem 15.** In Indu-Bala graph  $P_j \blacktriangledown P_k$ ,  $j \geq 2$ ,  $k \geq j + 2$ ; then,

$$\begin{aligned} R_\alpha(G) &= 2k(j+1)^\alpha \{ (j+2)^\alpha + 2(k+1)^\alpha + k(j-2)(k+2)^\alpha \} \\ &\quad + 2(k+2)^\alpha \{ 2(k+1)^\alpha + j(k+2)^\alpha \}. \end{aligned} \tag{39}$$

*Proof.*

$$\begin{aligned} M(G, a, b) &= 2ka^{j+2}b^{j+2} + 4ka^{j+2}b^{k+1} + k(2j-4)a^{j+2}b^{k+2} + 4a^{k+1}b^{k+2} + (2j-6)a^{k+2}b^{k+2}, \\ R_\alpha(G) &= D_a^\alpha D_b^\alpha f(a, b)|_{(a=b=1)}, \\ D_b^\alpha f(a, b) &= 2k(j+2)^\alpha a^{j+2}b^{j+2} + 4k(k+1)^\alpha a^{j+2}b^{k+1} + k(2j-4)(k+2)^\alpha a^{j+2}b^{k+2} \\ &\quad + 4(k+2)^\alpha a^{k+1}b^{k+2} + (2j-6)(k+2)^\alpha a^{k+2}b^{k+2}, \\ D_a^\alpha D_b^\alpha f(a, b) &= 2k(j+2)^{2\alpha} a^{j+2}b^{j+2} + 4k(j+2)^\alpha(k+1)^\alpha a^{j+2}b^{k+1} + 4(k+1)^\alpha(k+2)^\alpha a^{k+1}b^{k+2} \\ &\quad + k(2j-4)(j+2)^\alpha(k+2)^\alpha a^{j+2}b^{k+2} + (2j-6)(k+2)^{2\alpha} a^{k+2}b^{k+2}, \\ R_\alpha(G) &= D_a^\alpha D_b^\alpha f(a, b)|_{(a=b=1)} = 2k(j+2)^{2\alpha} + 4k(j+2)^\alpha(k+1)^\alpha + k(2j-4)(j+2)^\alpha(k+2)^\alpha \\ &\quad + 4(k+1)^\alpha(k+2)^\alpha + (2j-6)(k+2)^{2\alpha}, \\ R_\alpha(G) &= 2k(j+1)^\alpha \{ (j+2)^\alpha + 2(k+1)^\alpha + k(j-2)(k+2)^\alpha \} \\ &\quad + 2(k+2)^\alpha \{ 2(k+1)^\alpha + j(k+2)^\alpha \}. \end{aligned} \tag{40}$$

**Theorem 16.** In Indu-Bala graph  $P_j \blacktriangledown P_k$ ,  $j \geq 2$ ,  $k \geq j + 2$ ; then,

$$\begin{aligned} RR_\alpha(G) &= \frac{2k}{((j+1)(k^2+k))^\alpha} \{ (kj+k)^\alpha + (2j+2)(k+1)^\alpha + (j-2)((k^2+k)(j+1))^\alpha \} \\ &\quad + \frac{2}{k^\alpha(k+1)^{2\alpha}} \{ 2(k+1)^\alpha + (j-3)k^\alpha \}. \end{aligned} \tag{41}$$

Proof.

$$M(G, a, b) = 2ka^{j+2}b^{j+2} + 4ka^{j+2}b^{k+1} + k(2j-4)a^{j+2}b^{k+2} + 4a^{k+1}b^{k+2} + (2j-6)a^{k+2}b^{k+2},$$

$$RR_\alpha(G) = S_a^\alpha S_b^\alpha f(a, b)|_{(a=b=1)},$$

$$S_b = \frac{2k}{j+1}a^{j+2}b^{j+2} + \frac{4k}{k}a^{j+2}b^{k+1} + \frac{k(2j-4)}{k+1}a^{j+2}b^{k+2} + \frac{4}{k+1}a^{k+1}b^{k+2} \\ + \frac{2j-6}{k+1}a^{k+2}b^{k+2},$$

$$S_b^\alpha = \frac{2k}{(j+1)^\alpha}a^{j+2}b^{j+2} + \frac{4k}{k^\alpha}a^{j+2}b^{k+1} + \frac{k(2j-4)}{(k+1)^\alpha}a^{j+2}b^{k+2} + \frac{4}{(k+1)^\alpha}a^{k+1}b^{k+2} \\ + \frac{2j-6}{(k+1)^\alpha}a^{k+2}b^{k+2},$$

$$S_a^\alpha S_b^\alpha f(a, b) = \frac{2k}{(j+1)^{2\alpha}}a^{j+2}b^{j+2} + \frac{4k}{(k(j+1))^\alpha}a^{j+2}b^{k+1} + \frac{k(2j-4)}{((j+1)(k+1))^\alpha}a^{j+2}b^{k+2} \\ + \frac{4}{(k(k+1))^\alpha}a^{k+1}b^{k+2} + \frac{2j-6}{(k+1)^{2\alpha}}a^{k+2}b^{k+2}, \quad (42)$$

$$S_a^\alpha S_b^\alpha f(a, b)|_{(a=b=1)} = \frac{2k}{(j+1)^{2\alpha}} + \frac{4k}{(k(j+1))^\alpha} + \frac{k(2j-4)}{((j+1)(k+1))^\alpha} + \frac{4}{(k(k+1))^\alpha} + \frac{2j-6}{(k+1)^{2\alpha}},$$

$$RR_\alpha(G) = \frac{2k}{(j+1)^\alpha} \left\{ \frac{1}{(j+1)^\alpha} + \frac{2}{k^\alpha} + \frac{(j-2)}{(j+1)^\alpha} \right\} + \frac{2}{(k+1)^\alpha} \left\{ \frac{2}{k^\alpha} + \frac{j-3}{(k+1)^\alpha} \right\},$$

$$RR_\alpha(G) = \frac{2k}{((j+1)(k^2+k))^\alpha} \{ (kj+k)^\alpha + (2j+2)(k+1)^\alpha + (j-2)((k^2+k)(j+1))^\alpha \} \\ + \frac{2}{k^\alpha(k+1)^{2\alpha}} \{ 2(k+1)^\alpha + (j-3)k^\alpha \}.$$

**Theorem 17.** In Indu-Bala graph  $P_j \blacktriangledown P_k$ ,  $j \geq 2$ ,  $k \geq j+2$ ; then,

$$SSD(G) = \frac{4}{j+1} (4j^2 + k^2 + jk + 3j + 3k + 2) + \frac{1}{k(j+1)(k+1)} (2k^2j^3 + j^2(6k^2 + 8k) \\ + j(2k^4 + 6k^3 - 28k^2 + 8k + 16) - 12k^3 - 28k^2 - 10k + 16). \quad (43)$$

Proof.

$$\begin{aligned}
 M(G, a, b) &= 2ka^{j+2}b^{j+2} + 4ka^{j+2}b^{k+1} + k(2j-4)a^{j+2}b^{k+2} + 4a^{k+1}b^{k+2} + (2j-6)a^{k+2}b^{k+2}, \\
 SSD(G) &= (S_b D_a + S_a D_b)f(a, b)|_{(a=b=1)}, \\
 S_b D_a f(a, b) &= \frac{2k(j+2)}{j+1}a^{j+2}b^{j+2} + \frac{4k(j+2)}{k}a^{j+2}b^{k+1} + \frac{k(2j-4)(j+2)}{k+1}a^{j+2}b^{k+2} \\
 &\quad + \frac{4(k+1)}{k+1}a^{k+1}b^{k+2} + \frac{(2j-6)(k+2)}{k+1}a^{k+2}b^{k+2}, \\
 S_a D_b f(a, b) &= \frac{2k(j+2)}{j+1}a^{j+2}b^{j+2} + \frac{4k(k+1)}{j+1}a^{j+2}b^{k+1} + \frac{k(k+2)(2j-4)}{j+1}a^{j+2}b^{k+2} \\
 &\quad + \frac{4(k+2)}{k}a^{k+1}b^{k+2} + \frac{(k+2)(2j-6)}{k+1}a^{k+2}b^{k+2}; (S_b D_a + S_a D_b)f(a, b), \\
 &= \frac{4k(j+2)}{j+1}a^{j+2}b^{j+2} + \frac{k(2j-4)(j^2+k^2+3j+3k+4)}{(j+1)(k+1)}a^{j+2}b^{k+2} \\
 &\quad + \frac{4(j^2+k^2+3j+k+2)}{j+1}a^{j+2}b^{j+1} + \frac{8(k+1)}{k}a^{k+1}b^{k+2} + \frac{4(j-3)(k+2)}{k+1}a^{k+2}b^{k+2}, \\
 SSD(G) &= (S_b D_a + S_a D_b)f(a, b)|_{(a=b=1)} = \frac{4k(j+2)}{j+1} + \frac{k(2j-4)(j^2+k^2+3j+3k+4)}{(j+1)(k+1)} \\
 &\quad + \frac{4(j^2+k^2+3j+k+2)}{j+1} + \frac{8(k+1)}{k} + \frac{4(j-3)(k+2)}{k+1}, \\
 SSD(G) &= \frac{4}{j+1}(4j^2+k^2+jk+3j+3k+2) + \frac{1}{k(j+1)(k+1)}(2k^2j^3+j^2(6k^2+8k) \\
 &\quad + j(2k^4+6k^3-28k^2+8k+16) - 12k^3 - 28k^2 - 10k + 16).
 \end{aligned} \tag{44}$$

**Theorem 18.** In Indu-Bala graph  $P_j \blacktriangledown P_k$ ,  $j \geq 2$ ,  $k \geq j + 2$ ; Proof.

then,

$$H(G) = \frac{4\{(j+7)(k^3+k^2) + k(j^2+2) - k+2\}}{k(j+1)(k+1)}. \tag{45}$$

$$M(G, a, b) = 2ka^{j+2}b^{j+2} + 4ka^{j+2}b^{k+1} + k(2j-4)a^{j+2}b^{k+2} + 4a^{k+1}b^{k+2} + (2j-6)a^{k+2}b^{k+2},$$

$$H(G) = 2S_a j f(a, b)|_{a=1},$$

$$\begin{aligned}
 S_a f(a, b) &= \frac{2k}{j+1}a^{j+2}b^{j+2} + \frac{4k}{j+1}a^{j+2}b^{k+1} + \frac{k(2j-4)}{j+1}a^{j+2}b^{k+2} + \frac{4}{k}a^{k+1}b^{k+2} \\
 &\quad + \frac{2j-6}{k+1}a^{k+2}b^{k+2},
 \end{aligned}$$

$$\begin{aligned}
2S_{ajf}(a, b) &= \frac{4k}{j+1}a^{2j+4} + \frac{8k}{j+1}a^{j+k+3} + \frac{k(4j-8)}{j+1}a^{j+k+4} + \frac{8}{k}a^{2k+3} + \frac{4j-12}{k+1}a^{2k+4} \\
2S_{ajf}(a, b)|_{a=1} &= \frac{4k}{j+1} + \frac{8k}{j+1} + \frac{k(4j-8)}{j+1} + \frac{8}{k} + \frac{4j-12}{k+1}, \\
H(G) &= \frac{4\{(j+7)(k^3+k^2) + k(j^2+2) - k+2\}}{k(j+1)(k+1)}.
\end{aligned} \tag{46}$$

**Theorem 19.** In Indu-Bala graph  $P_j \blacktriangledown P_k$ ,  $j \geq 2$ ,  $k \geq j+2$ ; then,

$$I(G) = \frac{j^2(2k^3 + 10k^2 + 18k + 16) + j(4k^3 + 16k^2 + 12k) - 2k^2 - 12k - 16}{(j+1)(k+1)}. \tag{47}$$

*Proof.*

$$\begin{aligned}
M(G, a, b) &= 2ka^{j+2}b^{j+2} + 4ka^{j+2}b^{k+1} + k(2j-4)a^{j+2}b^{k+2} + 4a^{k+1}b^{k+2} + (2j-6)a^{k+2}b^{k+2}, \\
I(G) &= S_{aj}D_aD_b f(a, b)|_{a=1}; D_aD_b f(a, b), \\
&= 2k(j+2)^2a^{j+2}b^{j+2} + 4k(j+2)(k+1)a^{j+2}b^{k+1} + k(j+2)(k+2)(2j-4)a^{j+2}b^{k+2} \\
&\quad + 4(k+1)(k+2)a^{k+1}b^{k+2} + (k+2)^2(2j-6)a^{k+2}b^{k+2}; S_{aj}D_aD_b f(a, b), \\
&= \frac{2k(j+2)^2}{j+1}a^{2j+4} + \frac{4k(j+2)(k+1)}{j+1}a^{j+k+3} + \frac{2k(k+2)(j+2)(j-2)}{j+1}a^{j+k+4} \\
&\quad + \frac{4(k+1)(k+2)}{k+1}a^{2k+3} + \frac{(2j-6)(k+2)^2}{k+1}a^{2k+4}; S_{aj}D_aD_b f(a, b)|_{a=1}, \\
&= \frac{2k(j+2)^2}{j+1} + \frac{4k(j+2)(k+1)}{j+1} + \frac{2k(k+2)(j+2)(j-2)}{j+1} \\
&\quad + \frac{4(k+1)(k+2)}{k+1} + \frac{(2j-6)(k+2)^2}{k+1}, \\
I(G) &= \frac{j^2(2k^3 + 10k^2 + 18k + 16) + j(4k^3 + 16k^2 + 12k) - 2k^2 - 12k - 16}{(j+1)(k+1)}.
\end{aligned} \tag{48}$$

**Theorem 20.** In Indu-Bala graph  $P_j \blacktriangledown P_k$ ,  $j \geq 2$ ,  $k \geq j+2$ ; then,

$$\begin{aligned}
A(G) &= 2k(j+2)^3 \left\{ \frac{(j+2)^3}{(2j+1)^3} + \frac{2(k+1)^3}{(j+k)^3} + \frac{(j-2)(k+2)^3}{(j+k+1)^3} \right\} \\
&\quad + 2(k+2)^3 \left\{ \frac{2(k+1)^3}{(2k)^3} + \frac{(j-3)(k+2)^3}{(2j+1)^3} \right\}.
\end{aligned} \tag{49}$$

Proof.

$$\begin{aligned}
 M(G, a, b) &= 2ka^{j+2}b^{j+2} + 4ka^{j+2}b^{k+1} + k(2j-4)a^{j+2}b^{k+2} + 4a^{k+1}b^{k+2} + (2j-6)a^{k+2}b^{k+2}, \\
 A(G) &= S_a^3 Q_{-2} j D_a^3 D_b^3 f(a, b)|_{a=1}, \\
 D_a^\alpha D_b^\alpha f(a, b) &= 2k(j+2)^{2\alpha} a^{j+2} b^{j+2} + 4k(j+2)^\alpha (k+1)^\alpha a^{j+2} b^{k+1} + 4(k+1)^\alpha (k+2)^\alpha a^{k+1} b^{k+2} \\
 &\quad + k(2j-4)(j+2)^\alpha (k+2)^\alpha a^{j+2} b^{k+2} + (2j-6)(k+2)^{2\alpha} a^{k+2} b^{k+2}, \\
 D_a^3 D_b^3 f(a, b) &= 2k(j+2)^6 a^{j+2} b^{j+2} + 4k(j+2)^3 (k+1)^3 a^{j+2} b^{k+1} + 4(k+1)^3 (k+2)^3 a^{k+1} b^{k+2} \\
 &\quad + k(2j-4)(j+2)^3 (k+2)^3 a^{j+2} b^{k+2} + (2j-6)(k+2)^6 a^{k+2} b^{k+2}, \\
 J D_a^3 D_b^3 f(a, b) &= 2k(j+2)^6 a^{2j+4} + 4k(j+2)^3 (k+1)^3 a^{j+k+3} + 4(k+1)^3 (k+2)^3 a^{2k+3} \\
 &\quad + k(2j-4)(j+2)^3 (k+2)^3 a^{j+k+4} + (2j-6)(k+2)^6 a^{2k+4}; Q_{-2} j D_a^3 D_b^3 f(a, b), \\
 &= 2k(j+2)^6 a^{2j+2} + 4k(j+2)^3 (k+1)^3 a^{j+k+1} + 4(k+1)^3 (k+2)^3 a^{2k+1} \\
 &\quad + k(2j-4)(j+2)^3 (k+2)^3 a^{j+k+2} + (2j-6)(k+2)^6 a^{2k+2}; S_a^3 Q_{-2} j D_a^3 D_b^3 f(a, b), \tag{50} \\
 &= \frac{2k(j+2)^6}{(2j+1)^3} a^{2j+2} + \frac{4k(j+2)^3 (k+1)^3}{(j+k)^3} a^{j+k+1} + \frac{4(k+1)^3 (k+2)^3}{(2k)^3} a^{2k+1} \\
 &\quad + \frac{k(2j-4)(j+2)^3 (k+2)^3}{(j+k+1)^3} a^{j+k+2} + \frac{(2j-6)(k+2)^6}{(2k+1)^3} a^{2k+2}; S_a^3 Q_{-2} j D_a^3 D_b^3 f(a, b)|_{a=1}, \\
 &= \frac{2k(j+2)^6}{(2j+1)^3} + \frac{4k(j+2)^3 (k+1)^3}{(j+k)^3} + \frac{4(k+1)^3 (k+2)^3}{(2k)^3} + \frac{(2j-6)(k+2)^6}{(2k+1)^3} \\
 &\quad + \frac{k(2j-4)(j+2)^3 (k+2)^3}{(j+k+1)^3}, \\
 A(G) &= 2k(j+2)^3 \left\{ \frac{(j+2)^3}{(2j+1)^3} + \frac{2(k+1)^3}{(j+k)^3} + \frac{(j-2)(k+2)^3}{(j+k+1)^3} \right\} \\
 &\quad + 2(k+2)^3 \left\{ \frac{2(k+1)^3}{(2k)^3} + \frac{(j-3)(k+2)^3}{(2j+1)^3} \right\}.
 \end{aligned}$$

□

#### 4. Graphical Results and Their Discussion

In this section, we present some graphical results which are related to M-polynomial and their degree-based indices for the Indu-Bala product of two paths when one path is greater than another path and vice versa. We have used different values of  $k$  and  $j$  and drawn their respective

graphs as shown in Figure 5(a) (inverse Randic index for  $j \geq k$  and  $\alpha = 1$ ) and Figure 5(b) (symmetric division index for  $j \geq k$  and  $\alpha = 1$ ). We have observed from Figure 6(a) (harmonic index for  $j \geq k$  and  $\alpha = 1$ ) and Figure 6(b) (inverse sum index for  $j \geq k$  and  $\alpha = 1$ ) that the overall structure of indices increase with the increase of the value of  $j$  and  $k$ .

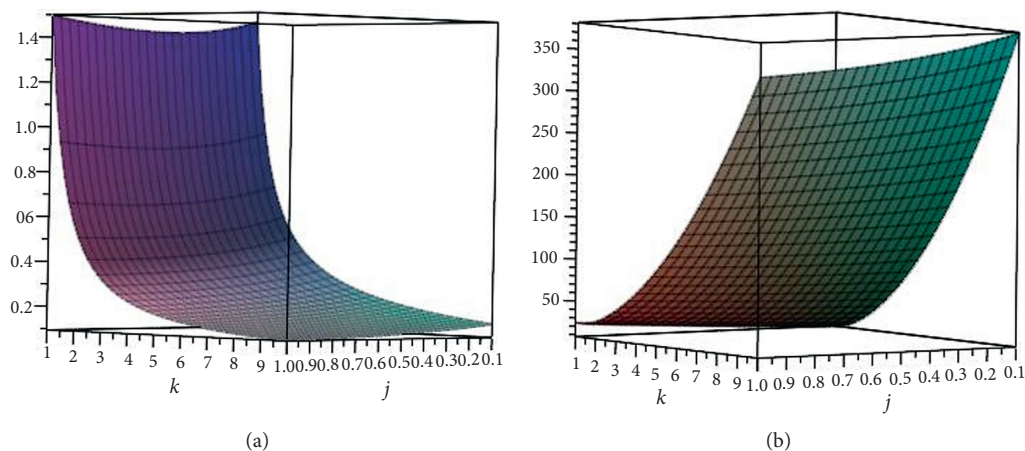


FIGURE 5: (a) Inverse Randic index for  $j \geq k$  and  $\alpha = 1$ . (b) Symmetric division index for  $j \geq k$  and  $\alpha = 1$ .

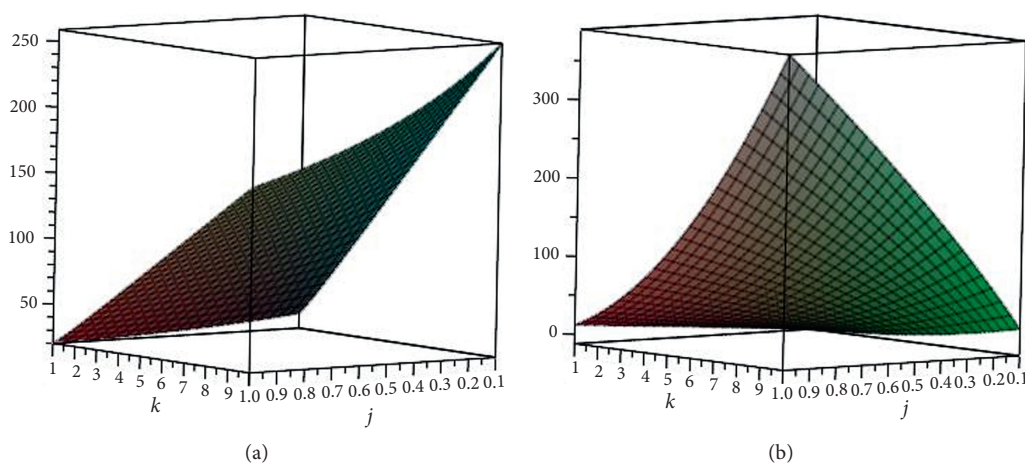


FIGURE 6: (a) Harmonic index for  $j \geq k$  and  $\alpha = 1$ . (b) Inverse sum index for  $j \geq k$  and  $\alpha = 1$ .

## 5. Conclusions

It is important to research the network through charts, and topological indicators are important for understanding its basic topology. This type of research finds global application in computer science, networks, and communication systems, which uses various indexes based on graph invariance to consider some stimulation summary. The Indu-Bala networks we studied in this paper are used to optimize (minimized) the operational cost of the network and find the shortest linkage between the connectors. In this article, we present some product for M-polynomial and nine different degree-based topological descriptors as discussed above for the Indu-Bala product of two paths.

## Data Availability

There are no data used in this research.

## Conflicts of Interest

The authors declare no conflicts of interest.

## References

- [1] P. Manuel, R. Bharati, I. Rajasingh, and C. Monica, "On minimum metric dimension of honeycomb networks," *Journal of Discrete Algorithms*, vol. 6, no. 1, pp. 20–27, 2008.
- [2] P. Manuel and I. Rajasingh, "Minimum metric dimension of silicate networks," *Ars Combinatoria*, vol. 98, pp. 501–510, 2011.
- [3] P. Manuel and I. Rajasingh, "Topological properties of silicate networks," in *Proceedings of the 2009 5th IEEEGCC Conference and Exhibition*, p. 15, Kuwait City, Kuwait, March 2009.
- [4] B. Rajan, A. William, C. Grigorious, and S. Stephen, "On certain topological indices of silicate, honeycomb and hexagonal networks," *Journal of Mathematical and Computational Science*, vol. 5, pp. 530–535, 2012.
- [5] S. Hayat and M. Imran, "Computation of topological indices of certain networks," *Applied Mathematics and Computation*, vol. 240, pp. 213–228, 2014.
- [6] S. Hayat, M. Imran, and M. Y. H. Maillk, "On topological indices of certain interconnection networks," *Applied Mathematics and Computation*, vol. 244, pp. 936–951, 2014.
- [7] M. Perc, J. Gómez-Gardeñes, A. Szolnoki, L. M. Floría, and Y. Moreno, "Evolutionary dynamics of group interactions on structured populations: a review," *Journal of The Royal Society Interface*, vol. 10, no. 80, Article ID 20120997, 2013.

- [8] M. Perc and A. Szolnoki, "Coevolutionary games-a mini review," *Biosystems*, vol. 99, no. 2, pp. 109–125, 2010.
- [9] A. Szolnoki, M. Perc, and G. Szabó, "Topology-independent impact of noise on cooperation in spatial public goods games," *Physical Review E, Statistical, Nonlinear, and Soft Matter Physics*, vol. 80, Article ID 056109, 2009.
- [10] Z. Wang, A. Szolnoki, and M. Perc, "If players are sparse social dilemmas are too: importance of percolation for evolution of cooperation," *Scientific Reports*, vol. 2, no. 1, p. 369, 2012.
- [11] H. Wiener, "Structural determination of paraffin boiling points," *Journal of the American Chemical Society*, vol. 69, no. 1, pp. 17–20, 1947.
- [12] A. A. Dobrynin, R. Entringer, and I. Gutman, "Wiener index of trees: theory and applications," *Acta Applicandae Mathematicae*, vol. 66, no. 3, pp. 211–249, 2001.
- [13] I. Gutman and O. E. Polansky, *Mathematical Concepts in Organic Chemistry*, Springer-Verlag, New York, NY, USA, 1986.
- [14] F. Torrens and G. Castellano, "Polarizability characterization of zeolitic bnpsted acidic sites," *Recent Progress in Computational Sciences and Engineering*, vol. 2, pp. 555–556, 2019.
- [15] Y. Li, F. Li, Z. Zhou, and Z. Chen, "SiC<sub>2</sub> silagraphene and its one-dimensional derivatives: where planar tetracoordinate silicon happens," *Journal of the American Chemical Society*, vol. 133, no. 4, pp. 900–908, 2010.
- [16] L.-J. Zhou, Y.-F. Zhang, and L.-M. Wu, "SiC<sub>2</sub> siligraphene and nanotubes: novel donor materials in excitonic solar cells," *Nano Letters*, vol. 13, no. 11, pp. 5431–5436, 2013.
- [17] T. F. W. Barth, "The structures of the minerals of the sodalite family," *Zeitschrift für Kristallographie-Crystalline Materials*, vol. 83, no. 1-6, pp. 405–414, 1932.
- [18] M. Arockiaraj, J. Clement, N. Tratnik, S. Mushtaq, and K. Balasubramanian, "Weighted mostar indices as measures of molecular peripheral shapes with applications to graphene, graphyne and graphdiyne nanoribbons," *SAR and QSAR in Environmental Research*, vol. 31, no. 3, pp. 187–208, 2020.
- [19] O. Ivanciuc, "QSAR comparative study of wiener descriptors for weighted molecular graphs," *Journal of Chemical Information and Computer Sciences*, vol. 40, no. 6, pp. 1412–1422, 2000.
- [20] O. Ivanciuc, "Chemical graphs, molecular matrices and topological indices in chemoinformatics and quantitative structure-activity relationships," *Current Computer-Aided Drug Design*, vol. 9, no. 2, pp. 153–163, 2013.
- [21] I. Gutman, "A formula for the Wiener number of trees and its extension to graphs containing cycles," *Graph Theory Notes NY*, vol. 27, no. 9, pp. 9–15, 1994.
- [22] I. Gutman, "Selected properties of the Schultz molecular topological index," *Journal of Chemical Information and Computer Sciences*, vol. 34, no. 5, pp. 1087–1089, 1994.
- [23] I. Gutman and A. Reza Ashrafi, "The edge version of the Szeged index," *Croatica Chemica Acta*, vol. 81, no. 2, pp. 263–266, 2008.
- [24] P. V. Khadikar, S. Karmarkar, and V. K. Agrawal, "A novel PI index and its applications to QSPR/QSAR studies," *Journal of Chemical Information and Computer Sciences*, vol. 41, no. 4, pp. 934–949, 2001.
- [25] M. H. Khalifeh, H. Yousefi-Azari, A. Reza Ashrafi, and I. Gutman, "The edge Szeged index of product graphs," *Croatica Chemica Acta*, vol. 81, no. 2, pp. 277–281, 2008.
- [26] M. H. Khalifeh, H. Yousefi-Azari, A. R. Ashrafi, and S. G. Wagner, "Some new results on distance-based graph invariants," *European Journal of Combinatorics*, vol. 30, no. 5, pp. 1149–1163, 2009.
- [27] D. J. Klein, I. Lukovits, and I. Gutman, "On the definition of the hyper-wiener index for cycle-containing structures," *Journal of Chemical Information and Computer Sciences*, vol. 35, no. 1, pp. 50–52, 1995.
- [28] H. P. Schultz, "Topological organic chemistry. 1. Graph theory and topological indices of alkanes," *Journal of Chemical Information and Modeling*, vol. 29, no. 3, pp. 227–228, 1989.
- [29] S. Hayat, S. Wang, and J.-B. Liu, "Valency-based topological descriptors of chemical networks and their applications," *Applied Mathematical Modelling*, vol. 60, pp. 164–178, 2018.
- [30] I. Gutman and N. Trinajstić, "Graph theory and molecular orbitals. Total  $\phi$ -electron energy of alternant hydrocarbons," *Chemical Physics Letters*, vol. 17, no. 4, pp. 535–538, 1972.
- [31] E. Estrada, L. Torres, L. Rodriguez, and I. Gutman, "An atom-bond connectivity index: modelling the enthalpy of formation of alkanes," *Indian Journal of Chemistry*, vol. 37A, 1998.
- [32] M. Randić, "Characterization of molecular branching," *Journal of the American Chemical Society*, vol. 97, no. 23, pp. 6609–6615, 1975.
- [33] S. Fajtlowicz, "On conjectures of Graffiti-II," *Congruent Number*, vol. 60, pp. 187–197, 1987.
- [34] B. Zhou and N. Trinajstić, "On a novel connectivity index," *Journal of Mathematical Chemistry*, vol. 46, no. 4, pp. 1252–1270, 2009.
- [35] W. Gao, M. K. Jamil, and M. R. Farahani, "The hyper-Zagreb index and some graph operations," *Journal of Applied Mathematics and Computing*, vol. 54, no. 1-2, pp. 263–275, 2017.
- [36] M. S. Alsharafi, M. M. Shubatah, and A. Q. Alameri, "The forgotten index of complement graph operations and its applications of molecular graph," *Open Journal of Discrete Applied Mathematics*, vol. 3, no. 3, pp. 53–61, 2020.
- [37] M. K. Jamil and I. Tomescu, "First reformulated Zagreb index and some graph operations," *Ars Combinatoria*, vol. 138, pp. 193–209, 2018.

## Research Article

# Computing the Hosoya Polynomial of $M$ -th Level Wheel and Its Subdivision Graph

Peng Xu <sup>1,2</sup>, Muhammad Numan,<sup>3</sup> Aamra Nawaz,<sup>3</sup> Saad Ihsan Butt <sup>4</sup>, Adnan Aslam <sup>5</sup>,  
and Asfand Fahad <sup>6</sup>

<sup>1</sup>Institute of Computational Science and Technology, Guangzhou University, Guangzhou, China

<sup>2</sup>School of Computer Science of Information Technology, Qiannan Normal University for Nationalities, Duyun 558000, China

<sup>3</sup>Department of Mathematics, COMSATS University Islamabad, Attock Campus, Islamabad, Pakistan

<sup>4</sup>Department of Mathematics, COMSATS University Islamabad, Lahore Campus, Islamabad, Pakistan

<sup>5</sup>Department of Natural Sciences and Humanities, University of Engineering and Technology, Lahore (RCET), Lahore, Pakistan

<sup>6</sup>Department of Mathematics, COMSATS University Islamabad, Vehari 61100, Pakistan

Correspondence should be addressed to Asfand Fahad; [asfandfahad1@yahoo.com](mailto:asfandfahad1@yahoo.com)

Received 3 June 2021; Accepted 23 October 2021; Published 27 November 2021

Academic Editor: Ajaya Kumar Singh

Copyright © 2021 Peng Xu et al. This is an open access article distributed under the Creative Commons Attribution License, which permits unrestricted use, distribution, and reproduction in any medium, provided the original work is properly cited.

The determination of Hosoya polynomial is the latest scheme, and it provides an excellent and superior role in finding the Wiener and hyper-Wiener index. The application of Wiener index ranges from the introduction of the concept of information theoretic analogues of topological indices to the use as major tool in crystal and polymer studies. In this paper, we will compute the Hosoya polynomial for multiwheel graph and uniform subdivision of multiwheel graph. Furthermore, we will derive two well-known topological indices for the abovementioned graphs, first Wiener index, and second hyper-Wiener index.

## 1. Introduction

Let  $G$  be a finite connected graph with vertex set  $V(G) = V$  and edge set  $E(G) = E$ . The distance  $d_{u,v}$  between  $u, v \in V(G)$  is the length of the shortest path joining  $u, v$ . The diameter  $d(G)$  of  $G$  is  $\max_{(u,v)} d_{u,v}$ . The terminologies not defined here can be seen in [1, 2]. The Wiener index  $W$  was first put forward in chemistry by Harold Wiener to compute the cardinality of the carbon-carbon bonds among all pairs of carbon atoms in alkane. For a molecular graph  $G$ , it is defined as

$$W(G) = \sum_{u,v \in V} d_{u,v}. \quad (1)$$

To read more about the chemical application of Wiener index, see [3–6], and for its mathematical properties, see [7, 8].

Milan Randić coined the term hyper-Wiener index  $WW(G)$  of  $G$  [9] as

$$WW(G) = \frac{1}{2} \sum_{u,v \in V} (d_{u,v} + d_{u,v}^2). \quad (2)$$

To read more the properties of hyper-Wiener index, see [9–12]. Hosoya polynomial was first introduced by Hosoya [13] and it received the attention of a lot of researchers. The same notion was independently put forward by Sagan et al. [14] as Wiener polynomial  $G$ . The Hosoya polynomial  $H(G, x)$  of  $G$  is defined as

$$H(G, x) = \sum_{u,v \in V} (x^{d_{u,v}}). \quad (3)$$

Let  $\alpha(G, k)$  be the number of ordered pair  $(u, v)$  in  $V$  with  $d_{u,v} = k$ . Then, the above definition of Hosoya polynomial can be expressed as

$$H(G, x) = \sum_{k=0}^{d(G)} (\alpha(G, k)x^k) \quad (4)$$

The Hosoya polynomial has been investigated on polycyclic aromatic hydrocarbons [15], benzenoid chains [16], Fibonacci and Lucas cubes [17], zigzag polyhexnanotorus [9], carbon nanotubes [18], Hanoi graphs [19], and circumcoronene series [20]. A significant importance of  $H(G, x)$  is that some distance-based topological indices (TIs) such as  $W(G)$  and  $WW(G)$  of  $G$  can be computed from the Hosoya polynomial as

$$W(G) = H'(G; 1), WW(G) = H'(G; 1) + \frac{1}{2}H''(G; 1). \quad (5)$$

The readers can see the following papers [21–25] for the results on distance-based TIs.

## 2. Hosoya Polynomial of $M$ -th Level Wheel Graph

For  $n \geq 2$ , the join  $K_1 \vee C_n$  is called a wheel graph denoted by  $W_{n+1}$ . The vertex that comes from the graph  $K_1$  is called the core and is denoted by  $c$ . It has order  $n + 1$  and size  $2n$ . A  $m$ -level wheel graph denoted by  $mW_n$  is the graph obtained by taking  $m$  copies of the cycle  $C_n$  and one copy of  $K_1$ , such that all the vertices of each copy of  $C_n$  are adjacent with the core vertex  $c$ . The graph of  $mW_n$  is depicted in Figure 1. Note that  $mW_n$  has  $mn + 1$  vertices and  $2mn$  edges. If we label the vertices of cycle at the  $m$ -th level by  $u_0^m, u_1^m, u_2^m, \dots, u_{n-1}^m$ , then the  $V(mW_n)$  and the  $E(mW_n)$  can be written as

$$\begin{aligned} V(mW_n) &= \{c, u_i^j, 0 \leq i \leq n-1, 1 \leq j \leq m\}, \\ E(mW_n) &= \{cu_i^j, 0 \leq i \leq n-1, 1 \leq j \leq m\} \cup \{u_i^j u_{i+1}^j, 0 \leq i \leq n-1, 1 \leq j \leq m\}. \end{aligned} \quad (6)$$

Next, the theorem gives the expression for the Hosoya polynomial of  $mW_n$ .

**Theorem 1.** Let  $m, n \geq 1$ , then  $H(mW_n; x)$  is of the form

$$\begin{aligned} H(mW_n; x) &= (mn + 1) + (2mn)x \\ &+ \left[ mn(n-3) + \frac{(n(m-1))^2(m)}{2} \right] x^2. \end{aligned} \quad (7)$$

*Proof.* It is easy to observe that the diameter of  $mW_n$  is 2. In order to derive the  $H(mW_n; x)$ , we compute the coefficients  $\alpha(mW_n, k)$  for  $k = 0, 1, 2$ . By definition, we have  $\alpha(mW_n, 0) = mn + 1$  and  $\alpha(mW_n, 1) = 2mn$ . To compute  $\alpha(mW_n, 2)$ , we use the following notation:

$$\alpha_A = \text{number of pair of vertices in set } A. \quad (8)$$

The cardinality of order pairs in  $V(mW_n)$  with distance 2 can be characterized by the following two sets:

$$\begin{aligned} A_1 &= \{(u_i^j, u_{i+1}^j), 1 \leq j \leq m, 0 \leq i \leq n-1, 2 \leq l \leq n-2\}, \\ A_2 &= \{(u_i^j, u_l^h), 0 \leq i \leq n-1, 0 \leq l \leq n-1, 1 \leq j \leq m-1, j+1 \leq h \leq m\}. \end{aligned} \quad (9)$$

The cardinality of the above sets is  $\alpha_{A_1} = mn(n-3)$  and  $\alpha_{A_2} = (n(m-1))^2(m)/2$  and hence the coefficient  $\alpha(mW_n, 2)$  is equal to  $\alpha(mW_n, 2) = \alpha_{A_1} + \alpha_{A_2} = mn(n-3) +$

$(n(m-1))^2(m)/2$ . Now, using the values of  $\alpha(mW_n, 0)$ ,  $\alpha(mW_n, 1)$ , and  $\alpha(mW_n, 2)$ , we get the desired result.  $\square$

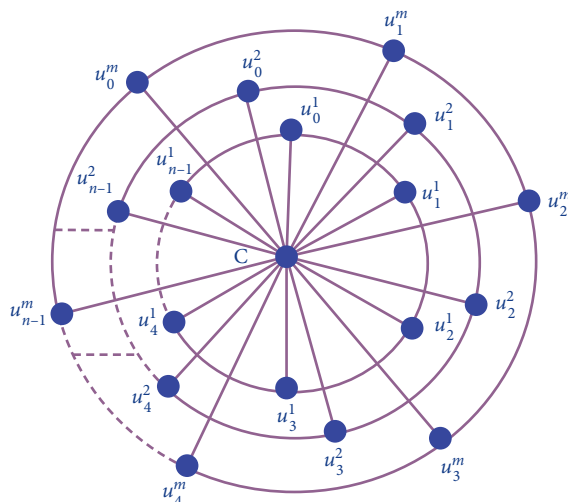


FIGURE 1: Multiwheel graph  $mW_n$ .

**Corollary 1.** Let  $m, n \geq 1$ , then  $W(mW_n)$  and  $WW(mW_n)$  are given as

$$\begin{aligned}
 W(mW_n) &= (2mn) + 2 \left[ mn(n-3) + \frac{(n(m-1))^2(m)}{2} \right], \\
 WW(mW_n) &= (2mn) + 3 \left[ mn(n-3) + \frac{(n(m-1))^2(m)}{2} \right].
 \end{aligned}
 \tag{10}$$

### 3. Hosoya Polynomial of Subdivision of M-th Level Wheel Graph

The subdivision graph  $S(mW_n)$  of  $mW_n$  is constructed from  $mW_n$  by adding a vertex into each edge of  $mW_n$ . In other words, we replace each edge of  $mW_n$  by a path of length 2. The graph of  $S(mW_n)$  is depicted in Figure 2. If we label the new vertices that we insert in the cycle at the  $j$ -th level by  $x_1^j, x_2^j, \dots, x_{n-1}^j$  for  $j = 1, 2, \dots, m$ , then the vertex set and edge set of  $S(mW_n)$  can be written as

$$\begin{aligned}
 V(S(mW_n)) &= \{c, u_i^j, v_i^j, x_i^j, \quad 0 \leq i \leq n-1, 1 \leq j \leq m\}, \\
 E(S(mW_n)) &= \{cv_i^j, v_i^j u_i^j, x_i^j u_i^j, u_i^j x_{i+1}^j, \quad 0 \leq i \leq n-1, 1 \leq j \leq m\} \cup \{u_i^j u_{i+1}^j, \quad 0 \leq i \leq n-1, 1 \leq j \leq m\}.
 \end{aligned}
 \tag{11}$$

It is easy to observe that order and size of are  $3mn + 1$  and  $4mn$ , respectively. In the next theorem, we give the analytic formula to derive the  $H(S(mW_n); x)$ .

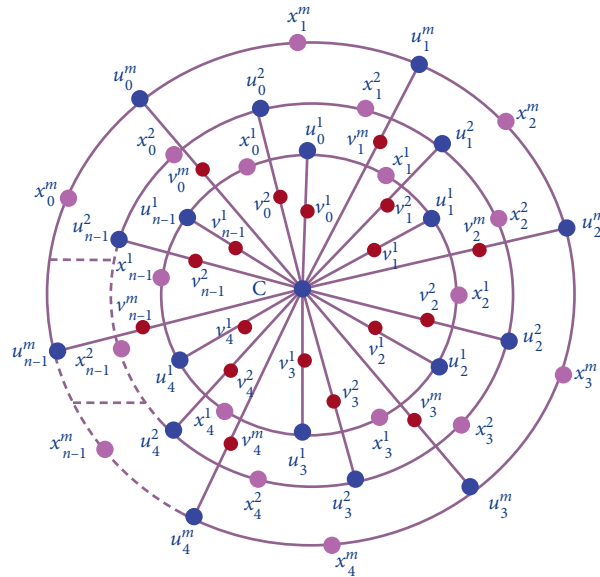
**Theorem 2.** Let  $m, n \geq 1$ , then the  $H(S(mW_n); x)$  is of the form

$$\begin{aligned}
 H(S(mW_n); x) &= (3mn + 1) + (4mn)x + [5mn + mn(n-1)]x^2 \\
 &+ \left[ \frac{(mn)^2(m-1)}{2} + 3mn + mn(n-1) \right] x^3 + [m((m-1)n)^2 + mn(2n-5) + mn] x^4 \\
 &+ \left[ mn(n-4) + \frac{m((m-1)n)^2}{2} \right] x^5 + \left[ mn(n-5) + \frac{m((m-1)n)^2}{2} \right] x^6.
 \end{aligned}
 \tag{12}$$

*Proof.* It is easy to observe that the diameter of  $mW_n$  is 6. In order to derive the  $H(S(mW_n); x)$ , we find the coefficients  $\alpha(S(mW_n), k)$  for  $k = 0, 1, 2, \dots, 6$ . By definition, we have  $\alpha(S(mW_n), 0) = 3mn + 1$  and  $\alpha(S(mW_n), 1) = 4mn$ . To

compute  $\alpha(S(mW_n), j)$  for  $j = 2, 3, 4, 5, 6$ , we use the following notation:

$$\alpha_A = \text{number of pair of vertices in set A.} \tag{13}$$

FIGURE 2: Uniform subdivision of multiwheel graph  $mS_n$ .

The cardinality of order pairs in  $V(S(mW_n))$  at distance 2 can be characterized by the following sets:

$$\begin{aligned}
 B_1 &= \{(c, u_i^j), \quad 1 \leq j \leq m, 0 \leq i \leq n-1\}, \\
 B_2 &= \{(v_i^j, v_{i+l}^j), \quad 1 \leq j \leq m, 0 \leq i \leq n-1, 1 \leq l \leq n-1\}, \\
 B_3 &= \{(v_i^j, x_{i+1}^j), \quad 1 \leq j \leq m, 0 \leq i \leq n-1\}, \\
 B_4 &= \{(v_i^j, x_i^j), \quad 0 \leq i \leq n-1, 1 \leq j \leq m\}, \\
 B_5 &= \{(u_i^j, u_{i+1}^j), \quad 1 \leq j \leq m, 0 \leq i \leq n-1\}, \\
 B_6 &= \{(x_i^j, x_{i+1}^j), \quad 1 \leq j \leq m, 0 \leq i \leq n-1\}.
 \end{aligned}
 \tag{14}$$

The cardinality of the above sets is  $\alpha_{B_1} = \alpha_{B_3} = \alpha_{B_4} = \alpha_{B_5} = \alpha_{B_6} = mn$ ,  $\alpha_{B_2} = mn(n-1)$ , and hence

$$\begin{aligned}
 \alpha(S(mW_n), 2) &= \alpha_{B_1} + \alpha_{B_2} + \alpha_{B_3} + \alpha_{B_4} + \alpha_{B_5} + \alpha_{B_6} \\
 &= 5mn + mn(n-1).
 \end{aligned}
 \tag{15}$$

The cardinality of order pairs in  $V(S(mW_n))$  at distance 3 can be characterized by the following sets:

$$\begin{aligned}
 C_1 &= \{(c, x_i^j), \quad 1 \leq j \leq m, 0 \leq i \leq n-1\}, \\
 C_2 &= \{(v_i^j, u_{i+l}^j), \quad 1 \leq j \leq m, 0 \leq i \leq n-1, 1 \leq l \leq n-1\}, \\
 C_3 &= \{(v_i^j, u_1^{j+k}), \quad 1 \leq j \leq m, 1 \leq k \leq m-j, 0 \leq i \leq n-1, 0 \leq l \leq n-1\}, \\
 C_4 &= \{(u_i^j, x_{i+2}^j), \quad 1 \leq j \leq m, 0 \leq i \leq n-1\}, \\
 C_5 &= \{(x_i^j, u_{i+1}^j), \quad 1 \leq j \leq m, 0 \leq i \leq n-1\}.
 \end{aligned}
 \tag{16}$$

The cardinality of the above sets is  $\alpha_{C_1} = \alpha_{C_4} = \alpha_{C_5} = mn$ ,  $\alpha_{C_2} = mn(n-1)$ ,  $\alpha_{C_3} = (mn)^2(m-1)/2$ , and hence

$$\begin{aligned}\alpha(S(mW_n), 3) &= \alpha_{C_1} + \alpha_{C_2} + \alpha_{C_3} + \alpha_{C_4} + \alpha_{C_5} \\ &= \frac{(mn)^2(m-1)}{2} + 3mn + mn(n-1).\end{aligned}\quad (17)$$

The cardinality of order pairs in  $V(S(mW_n))$  at distance 4 can be characterized by the following sets:

$$\begin{aligned}D_1 &= \{(v_i^j, x_{i+l}^j), \quad 1 \leq j \leq m, 0 \leq i \leq n-1, 2 \leq l \leq n-1\}, \\ D_2 &= \{(v_i^j, x_l^{j+k}), \quad 1 \leq j \leq m-1, 1 \leq k \leq m-j, 0 \leq i \leq n-1, 0 \leq l \leq n-1\}, \\ D_3 &= \{(u_i^j, u_{i+l}^j), \quad 1 \leq j \leq m, 0 \leq i \leq n-1, 2 \leq l \leq n-2\}, \\ D_4 &= \{(u_i^j, u_l^{j+k}), \quad 1 \leq j \leq m-1, 1 \leq k \leq m-j, 0 \leq i \leq n-1, 0 \leq l \leq n-1\}, \\ D_5 &= \{(x_i^j, x_{i+2}^j), \quad 1 \leq j \leq m, 0 \leq i \leq n-1\}.\end{aligned}\quad (18)$$

The cardinality of the above sets is  $\alpha_{D_1} = mn(n-2)$ ,  $\alpha_{D_2} = m((m-1)n)^2/2$ ,  $\alpha_{D_3} = mn(n-3)$ ,  $\alpha_{D_4} = m((m-1)n)^2/2$ ,  $\alpha_{D_5} = mn$ , and hence

$$\begin{aligned}\alpha(S(mW_n), 4) &= \alpha_{D_1} + \alpha_{D_2} + \alpha_{D_3} + \alpha_{D_4} + \alpha_{D_5} \\ &= m((m-1)n)^2 + mn(2n-4).\end{aligned}\quad (19)$$

The cardinality of order pairs in  $V(S(mW_n))$  at distance 5 can be characterized by the following sets:

$$\begin{aligned}E_1 &= \{(u_i^j, x_{i+l}^j), \quad 1 \leq j \leq m, 0 \leq i \leq n-1, 3 \leq l \leq n-2\}, \\ E_2 &= \{(u_i^j, x_l^{j+k}), \quad 1 \leq j \leq m-1, 1 \leq k \leq m-j, 0 \leq i \leq n-1, 0 \leq l \leq n-1\}.\end{aligned}\quad (20)$$

The cardinality of the above sets is  $\alpha_{E_1} = mn(n-4)$ ,  $\alpha_{E_2} = m((m-1)n)^2/2$ , and hence

$$\begin{aligned}\alpha(S(mW_n), 5) &= \alpha_{E_1} + \alpha_{E_2} \\ &= mn(n-4) + \frac{m((m-1)n)^2}{2}.\end{aligned}\quad (21)$$

The cardinality of order pairs in  $V(S(mW_n))$  at distance 6 can be characterized by the following sets:

$$\begin{aligned}F_1 &= \{(x_i^j, x_{i+l}^j), \quad 1 \leq j \leq m, 0 \leq i \leq n-1, 3 \leq l \leq n-3\}, \\ F_2 &= \{(x_i^j, x_l^{j+k}), \quad 1 \leq j \leq m-1, 1 \leq k \leq m-j, 0 \leq i \leq n-1, 0 \leq l \leq n-1\}.\end{aligned}\quad (22)$$

The cardinality of the above sets is  $\alpha_{F_1} = mn(n-5)$ ,  $\alpha_{F_2} = m((m-1)n)^2/2$ , and hence

$$\begin{aligned}\alpha(S(mW_n), 6) &= \alpha_{F_1} + \alpha_{F_2} \\ &= mn(n-5) + \frac{m((m-1)n)^2}{2}.\end{aligned}\quad (23)$$

Now, using the values of  $\alpha(S(mW_n), 0)$ ,  $\alpha(S(mW_n), 1)$ ,  $\alpha(S(mW_n), 2)$ ,  $\alpha(S(mW_n), 3)$ ,  $\alpha(S(mW_n), 4)$ ,  $\alpha(S(mW_n), 5)$ , and  $\alpha(S(mW_n), 6)$ , we get the desired result.  $\square$

**Corollary 2.** Let  $m, n \geq 1$ , then the  $W(mS_n)$  and  $WW(mS_n)$  are

$$\begin{aligned}
W(mS_n) &= (4mn) + 2[5mn + mn(n-1)] + 3\left[\frac{(mn)^2(m-1)}{2} + 3mn + mn(n-1)\right] \\
&\quad + 4\left[m((m-1)n)^2 + mn(2n-5) + mn\right] + 5\left[mn(n-4) + \frac{m((m-1)n)^2}{2}\right] \\
&\quad + 6\left[mn(n-5) + \frac{m((m-1)n)^2}{2}\right], \\
WW(mS_n) &= (4mn) + 3[5mn + mn(n-1)] + 6\left[\frac{(mn)^2(m-1)}{2} + 3mn + mn(n-1)\right] \\
&\quad + 10\left[m((m-1)n)^2 + mn(2n-5) + mn\right] + 15\left[mn(n-4) + \frac{m((m-1)n)^2}{2}\right] \\
&\quad + 21\left[mn(n-5) + \frac{m((m-1)n)^2}{2}\right].
\end{aligned} \tag{24}$$

#### 4. Conclusion

We examined the Hosoya polynomial and two vastly studied TIs  $W(G)$  and  $WW(G)$  for multiwheel graph  $mW_n$  and subdivision of multiwheel graph  $mS_n$ .

#### Data Availability

No data were used for this study.

#### Disclosure

Mathematics subject classification: 05C09, 05C92, 92E10.

#### Conflicts of Interest

The authors hereby declare that there are no conflicts of interest regarding the publication of this paper.

#### Acknowledgments

This work was supported by the National Natural Science Foundation of China, No. 62002079.

#### References

- [1] G. Chartrand, *Introduction to Graph Theory*, Tata McGraw-Hill Education, New York, NY, USA, 2006.
- [2] R. Diestel, *Graph Theory*, Springer-Verlag, Berlin, Germany, 1997.
- [3] Z. Mihalic and N. Trinajstic, "A graph theoretical approach to structure property relationships," *Journal of Chemical Education*, vol. 69, pp. 701–712, 1992.
- [4] I. Gutman, Y. N. Yeh, S. L. Lee, and Y. L. Luo, "Some recent results in the theory of the wiener number," *Indian Journal of Chemistry*, vol. 32A, pp. 651–661, 1993.
- [5] I. Gutman and J. H. Potgieter, "Wiener index and intermolecular forces," *Journal of the Serbian Chemical Society*, vol. 62, pp. 185–192, 1997.
- [6] D. H. Rouvray, "The rich legacy of half a century of the wiener index," in *Topology in Chemistry Discrete Mathematics of Molecules*, D. H. Rouvray and R. B. King, Eds., Horwood, Chichester, UK, pp. 16–37, 2002.
- [7] A. A. Dobrynin, R. Entringer, and I. Gutman, "Wiener index of trees: theory and applications," *Acta Applicandae Mathematica*, vol. 66, no. 3, pp. 211–249, 2001.
- [8] A. A. Dobrynin, I. Gutman, S. Klavžar, and P. Žigert, "Wiener index of hexagonal systems," *Acta Applicandae Mathematica*, vol. 72, no. 3, pp. 247–294, 2002.
- [9] M. Randic, "Novel molecular descriptor for structure property studies," *Chemical Physics Letters*, vol. 211, pp. 478–483, 1993.
- [10] D. J. Klein, I. Lukovits, and I. Gutman, "On the definition of the hyper-wiener index for cycle-containing structures," *Journal of Chemical Information and Computer Sciences*, vol. 35, no. 1, pp. 50–52, 1995.
- [11] I. Gutman, "Relation between hyper-wiener and wiener index," *Chemical Physics Letters*, vol. 364, no. 3–4, pp. 352–356, 2002.
- [12] I. Gutman and B. Furtula, "Hyper-wiener index vs. wiener index. two highly correlated structure-descriptors," *Monatshefte für Chemie—Chemical Monthly*, vol. 134, no. 7, pp. 975–981, 2003.
- [13] H. Hosoya, "On some counting polynomials in chemistry," *Discrete Applied Mathematics*, vol. 19, no. 1–3, pp. 239–257, 1988.
- [14] B. E. Sagan, Y.-N. Yeh, and P. Zhang, "The wiener polynomial of a graph," *International Journal of Quantum Chemistry*, vol. 60, no. 5, pp. 959–969, 1996.
- [15] S. Nikolic, N. Trinajstic, and Z. Mihalic, "The Wiener index: development and applications," *Croatica Chemica Acta*, vol. 68, pp. 105–129, 1995.
- [16] W. Gao, Y. Wang, B. Jamil, and M. Kamran, "Characteristics studies of molecular structures in drugs," *Saudi Pharmaceutical Journal*, vol. 25, no. 4, pp. 580–586, 2017.
- [17] N. PrabhakaraRao and A. LaxmiPrasanna, "On the Wiener index of pentachains," *Applied Mathematical Sciences*, vol. 2, pp. 2443–2457, 2008.
- [18] A. A. Ali and A. M. Ali, "Hosoya polynomials of pentachains," *MATCH Communications in Mathematical and in Computer Chemistry*, vol. 65, pp. 807–819, 2011.
- [19] I. Gutman, S. Klavžar, M. Petkovsek, and P. Žigert, "On Hosoya polynomials of benzenoid graphs," *MATCH Communications in Mathematical and in Computer Chemistry*, vol. 43, pp. 49–66, 2001.
- [20] M. Eliasi and B. Taeri, "Hosoya polynomial of zigzag polyhex nanotorus," *Journal of the Serbian Chemical Society*, vol. 73, no. 3, pp. 311–319, 2008.

- [21] M. Arockiaraj, S. R. J. Kavitha, K. Balasubramanian, and I. Gutman, "Hyper-Wiener and Wiener polarity indices of silicate and oxide frameworks," *Journal of Mathematical Chemistry*, vol. 56, no. 5, pp. 1493–1510, 2018.
- [22] W. Gao, Z. Iqbal, M. Ishaq, R. Sarfraz, M. Aamir, and A. Aslam, "On eccentricity-based topological indices study of a class of porphyrin-cored dendrimers," *Biomolecules*, vol. 8, no. 3, p. 71, 2018.
- [23] Z. Iqbal, M. Ishaq, A. Aslam, and W. Gao, "On eccentricity based topological descriptors of water soluble dendrimers," *Zeitschrift für Naturforschung C*, vol. 74, 2018.
- [24] W. Gao, Z. Iqbal, M. Ishaq, A. Aslam, and R. Sarfraz, "Topological aspects of dendrimers via distance based descriptors," *IEEE Access*, vol. 7, 2019.
- [25] Y. Rao, A. Aslam, M. U. Noor, A. Othman Almatroud, and Z. Shao, "Bond incident degree indices of catacondensed pentagonal systems," *Complexity*, vol. 2020, Article ID 4935760, 7 pages, 2020.

## Research Article

# The Second Hyper-Zagreb Coindex of Chemical Graphs and Some Applications

Ahmed Ayache <sup>1</sup>, Abdu Alameri <sup>2</sup>, Mohammed Alsharafi <sup>3</sup> and Hanan Ahmed <sup>4</sup>

<sup>1</sup>Department of Mathematics, Faculty of Science, University of Bahrain, Zallaq, Bahrain

<sup>2</sup>Department of Biomedical Engineering, Faculty of Engineering, University of Science and Technology, Taiz, Yemen

<sup>3</sup>Graduate School of Natural and Applied Sciences, Yildiz Technical University, Istanbul, Turkey

<sup>4</sup>Department of Mathematics, Yuvaraja's College, University of Mysore, Mysuru, India

Correspondence should be addressed to Abdu Alameri; a.alameri2222@gmail.com

Received 10 September 2021; Accepted 21 October 2021; Published 15 November 2021

Academic Editor: Syed Ahtsham Haq Bokhary

Copyright © 2021 Ahmed Ayache et al. This is an open access article distributed under the Creative Commons Attribution License, which permits unrestricted use, distribution, and reproduction in any medium, provided the original work is properly cited.

The second hyper-Zagreb coindex is an efficient topological index that enables us to describe a molecule from its molecular graph. In this current study, we shall evaluate the second hyper-Zagreb coindex of some chemical graphs. In this study, we compute the value of the second hyper-Zagreb coindex of some chemical graph structures such as sildenafil, aspirin, and nicotine. We also present explicit formulas of the second hyper-Zagreb coindex of any graph that results from some interesting graphical operations such as tensor product, Cartesian product, composition, and strong product, and apply them on a  $q$ -multiwalled nanotorus.

## 1. Introduction

A graph can be identified by a corresponding numerical value, a sequence of numbers, or a special polynomial or a matrix. Special attention is directed to chemical graphs which constitute a wonderful topic in graph theory because of the abundance of applications in chemistry or in medical science [1, 2]. Topological index and coindex are invariant under graph automorphism. The computation of these numerical quantities is useful and well-proven in medical information of new drugs without resorting to chemical experiments [3, 4]. All graphs in this study are finite and simple, let  $G$  be a finite simple graph on  $V(G) = n$ , vertices, and  $E(G) = m$ , edges, and the degree of a vertex  $v$  is the number of edges event to  $v$ , denoted by  $\delta_G(v)$ . The complement of  $G$ , denoted by  $\overline{G}$ , is a simple graph on the same set of vertices  $V(G)$ , in which two vertices  $u$  and  $v$  are adjacent by an edge  $uv$ , if and only if they are not adjacent in  $G$ . Hence,  $uv \in E(\overline{G})$  if and only if  $uv \notin E(G)$ . Obviously, we have  $E(G) \cup E(\overline{G}) = E(K_n)$ , so  $\overline{m} = E(\overline{G}) = \binom{n}{2} - m$ , and the degree of a vertex  $u$  in  $\overline{G}$  is given by

$$\delta_{\overline{G}}(u) = n - 1 - \delta_G(u). \quad (1)$$

Gutman and Trinajestić [5] introduced the first and second Zagreb indices as follows:

$$\begin{aligned} M_1(G) &= \sum_{v \in V(G)} \delta_G^2(v) = \sum_{uv \in E(G)} [\delta_G(u) + \delta_G(v)], \\ M_2(G) &= \sum_{uv \in E(G)} \delta_G(u)\delta_G(v). \end{aligned} \quad (2)$$

In 2008, Došlić defined Zagreb coindices [6], which are given as follows:

$$\begin{aligned} \overline{M}_1(G) &= \sum_{uv \notin E(G)} [\delta_G(u)\delta_G(v)], \\ \overline{M}_2(G) &= \sum_{uv \notin E(G)} [\delta_G(u)\delta_G(v)]. \end{aligned} \quad (3)$$

Later in 2010, Ashrafi et al. have established the following nice formulas for the precise relationship between the first and second Zagreb indices and their coindices [7]:

$$\begin{aligned}\overline{M}_1(G) &= 2m(n-1) - M_1(G), \\ \overline{M}_2(G) &= 2m^2 - \frac{1}{2}M_1(G) - M_2(G).\end{aligned}\quad (4)$$

In 2013, Shirdel et al. [8] introduced degree-based Zagreb indices named hyper-Zagreb index which is defined as

$$HM(G) = \sum_{uv \in E(G)} (\delta_G(u) + \delta_G(v))^2. \quad (5)$$

In 2013, Ranjini et al. introduced and defined the third Zagreb index of a graph as [9]

$$\text{ReZG}_3(G) = \sum_{uv \in E(G)} \delta_G(u)\delta_G(v)[\delta_G(u) + \delta_G(v)]. \quad (6)$$

Furtula and Gutman in 2015 introduced the forgotten index (F-index) [10], which is defined as

$$F(G) = \sum_{v \in V(G)} \delta_G^3(v) = \sum_{uv \in E(G)} [\delta_G^2(u) + \delta_G^2(v)]. \quad (7)$$

In 2016, De et al. introduced forgotten coindex as follows:

$$\begin{aligned}\overline{F}(G) &= \sum_{uv \notin E(G)} [\delta_G^2(u) + \delta_G^2(v)] \\ &= (n-1)M_1(G) - F(G).\end{aligned}\quad (8)$$

In 2016, Veylaki et al. [11] introduced hyper-Zagreb coindex as follows:

$$\overline{HM}(G) = \sum_{uv \notin E(G)} (\delta_G(u) + \delta_G(v))^2. \quad (9)$$

In 2016, Wei et al. [12] defined new version of Zagreb topological indices. It is called the hyper-Zagreb index that is defined as above. Then, the second hyper-Zagreb index of a graph  $G$  is defined as the sum of the weights  $(\delta_G(u)\delta_G(v))^2$  and is equal to

$$HM_2(G) = \sum_{uv \in E(G)} (\delta_G(u)\delta_G(v))^2. \quad (10)$$

In 2020, Alameri et al. [13, 14] defined a new degree-based of Zagreb indices named Y-index and Y-coindex as

$$\begin{aligned}Y(G) &= \sum_{uv \in E(G)} [\delta_G^3(u) + \delta_G^3(v)], \\ \overline{Y}(G) &= \sum_{uv \notin E(G)} [\delta_G^3(u) + \delta_G^3(v)],\end{aligned}\quad (11)$$

where

$$\overline{Y}(G) = (n-1)F(G) - Y(G). \quad (12)$$

Here, we define a new version of Zagreb topological indices, based on the hyper-Zagreb index that is defined as above. It is called the second hyper-Zagreb index of a graph  $G$  and defined as the sum of the weights  $(\delta_G(u)\delta_G(v))^2$ , such that  $uv \notin E(G)$  and is equal to

$$\overline{HM}_2(G) = \sum_{uv \notin E(G)} (\delta_G(u)\delta_G(v))^2. \quad (13)$$

Eventhough, there are several research reports contributing to the computation of topological indices of chemical graphs. However, the studies on the computation of topological coindices of octane isomers are very limited. This study focused on one of the important topological coindices named the second hyper-Zagreb coindex. Some chemical graphs were obtained by this parameter. Moreover, the second hyper-Zagreb coindex of graph operations was computed and gave some of their applications such as a  $q$ -multiwalled nanotorus.

## 2. Preliminaries

This section is devoted to some preparatory results that will play a prominent role in our study.

*Definition 2.1* (see [15, 16]). Suppose that  $G_1$  and  $G_2$  are two connected graphs, then

- (i) The tensor product  $G_1 \otimes G_2$  of  $G_1$  and  $G_2$  is the graph with  $V(G_1 \otimes G_2) = V(G_1) \times V(G_2)$ , and  $E(G_1 \otimes G_2) = \{(u_1, u_2)(v_1, v_2) \mid u_1v_1 \in E(G_1), u_2v_2 \in E(G_2)\}$ .
- (ii) The Cartesian product  $G_1 \times G_2$  of  $G_1$  and  $G_2$  has the vertex set  $V(G_1 \times G_2) = V(G_1) \times V(G_2)$ , and  $(a, x)(b, y)$  is an edge of  $G_1 \times G_2$  if  $a=b$  and  $xy \in E(G_2)$  or  $ab \in E(G_1)$  and  $x=y$ .
- (iii) The composition  $G_1[G_2]$  of  $G_1$  and  $G_2$  with disjoint vertex sets  $V(G_1)$  and  $V(G_2)$  and edge sets  $E(G_1)$  and  $E(G_2)$  is the graph with vertex set  $V(G_1) \times V(G_2)$  and any two vertices  $u = (u_1, v_1)$  is adjacent with  $v = (u_2, v_2)$  whenever  $(u_1$  is adjacent with  $u_2)$  or  $(u_1 = u_2$  and  $v_1$  is adjacent with  $v_2)$ .
- (iv) The strong product  $G_1 * G_2$  of  $G_1$  and  $G_2$  is a graph with  $V(G_1 * G_2) = V(G_1) \times V(G_2)$ , and any two vertices  $(u_1, v_1)$  and  $(u_2, v_2)$  are adjacent if and only if  $\{u_1 = u_2 \in V(G_1)$  and  $v_1v_2 \in E(G_2)\}$  or  $\{v_1 = v_2 \in V(G_2)$  and  $u_1u_2 \in E(G_1)\}$ .

**Lemma 2** (see [17, 18]). Let  $G_1$  and  $G_2$  be graphs with  $|V(G_1)| = n_1$ ,  $|V(G_2)| = n_2$ ,  $|E(G_1)| = m_1$ , and  $|E(G_2)| = m_2$ . Then,

- (i)  $|V(G_1 \otimes G_2)| = |V(G_1 \times G_2)| = |V(G_1[G_2])| = |V(G_1 * G_2)| = n_1n_2$
- (ii)  $|E(G_1 \otimes G_2)| = 2m_1m_2$
- (iii)  $|E(G_1 \times G_2)| = m_1n_2 + n_1m_2$
- (iv)  $|E(G_1[G_2])| = m_1n_2^2 + m_2n_1$
- (v)  $|E(G_1 * G_2)| = m_1n_2 + n_1m_2 + 2m_1m_2$
- (vi)  $\delta_{G_1 \otimes G_2}(u, v) = \delta_{G_1}(u)\delta_{G_2}(v)$ 
  - (a)  $\delta_{G_1 \times G_2}(u, v) = \delta_{G_1}(u) + \delta_{G_2}(v)$
  - (b)  $\delta_{G_1[G_2]}(u, v) = n_2\delta_{G_1}(u) + \delta_{G_2}(v)$
  - (c)  $\delta_{G_1 * G_2}(u, v) = \delta_{G_1}(u) + \delta_{G_2}(v) + \delta_{G_1}(u)\delta_{G_2}(v)$

**Lemma 2.3** (see [17, 18]). Let  $G_1, G_2$  be two graphs with  $n_1, n_2$  vertices and  $m_1, m_2$  edges, respectively, then.

- (i)  $M_1(G_1 \otimes G_2) = M_1(G_1)M_1(G_2)$
- (ii)  $M_1(G_1 \times G_2) = n_2M_1(G_1) + n_1M_1(G_2) + 8m_1m_2$
- (iii)  $M_1(G_1[G_2]) = n_2^3M_1(G_1) + n_1M_1(G_2) + 8n_2m_2m_1$
- (iv)  $M_1(G_1 * G_2) = (n_2 + 6m_2)M_1(G_1) + 8m_2m_1 + (6m_1 + n_1)M_1(G_2) + 2M_1(G_1)M_1(G_2)$

**Lemma 2.4** (see [17, 18]). Let  $G_1, G_2$  be two simple graphs with  $n_1, n_2$  vertices and  $m_1, m_2$  edges, respectively, then

- (i)  $Y(G_1 \otimes G_2) = Y(G_1)Y(G_2)$
- (ii)  $Y(G_1 \times G_2) = n_2Y(G_1) + n_1Y(G_2) + 8m_1F(G_2) + 8m_2F(G_1) + 6M_1(G_1)M_1(G_2)$
- (iii)  $Y(G_1[G_2]) = n_2^5Y(G_1) + n_1Y(G_2) + 8n_2^3m_2F(G_1) + 8n_2m_1F(G_2) + 6n_2^2M_1(G_1)M_1(G_2)$
- (iv)  $Y(G_1 * G_2) = Y(G_1)[4F(G_2) + 6M_1(G_2) + 8m_2 + n_2] + 4F(G_1)[3M_1(G_2) + 2m_2] + Y(G_2)[4F(G_1) + 6M_1(G_1) + 8m_1 + n_1] + 4F(G_2)[3M_1(G_1) + 2m_1] + Y(G_1)Y(G_2) + 12F(G_1)F(G_2) + 6M_1(G_1)M_1(G_2)$

**Lemma 2.5** (see [17, 18]). Let  $G_1, G_2$  be two simple graphs with  $n_1, n_2$  vertices and  $m_1, m_2$  edges, respectively, then

- (i)  $HM_2(G_1 \otimes G_2) = 2HM_2(G_1)HM_2(G_2)$
- (ii)  $HM_2(G_1 \times G_2) = n_2HM_2(G_1) + n_1HM_2(G_2) + 3F(G_1)M_1(G_2) + 3F(G_2)M_1(G_1) + m_1[Y(G_2) + 4ReZG_3(G_2)] + m_2[Y(G_1) + 4ReZG_3(G_1)] + 4M_1(G_1)M_2(G_2) + 4M_1(G_2)M_2(G_1)$
- (iii)  $HM_2(G_1[G_2]) = n_2^6HM_2(G_1) + n_1HM_2(G_2) + n_2^4m_2[Y(G_1) + 4ReZG_3(G_1)] + 4n_2m_1ReZG_3(G_2) + 3n_2^2F(G_1)M_1(G_2) + n_2^2M_1(G_1)$

$$[F(G_2) + 4M_2(G_2)] + m_1M_1^2(G_2) + 4n_2m_2[4n_2m_2M_2(G_1) + M_1(G_1)M_1(G_2)]$$

- (iv)  $HM_2(G_1 * G_2) = HM_2(G_2)[n_1 + 10m_1 + 10m_1(G_1) + 8m_2(G_1) + 6F(G_1) + 4ReZG_3(G_1) + Y(G_1)] + HM_2(G_2)[n_2 + 10m_2 + 10m_1(G_2) + 8m_2(G_2) + 6F(G_2) + 4ReZG_3(G_2) + Y(G_2)] + Y(G_2)[m_1 + 2M_1(G_1) + 4M_2(G_1) + F(G_1) + 2ReZG_3(G_1)]Y(G_1)[m_2 + 2M_1(G_2) + 4M_2(G_2) + F(G_2) + 2ReZG_3(G_2)] + 4ReZG_3(G_2)[m_1 + 2M_1(G_1) + 2M_2(G_1) + 2F(G_1)] + 4ReZG_3(G_1)[m_2 + 2M_1(G_2) + 2M_2(G_2) + 2F(G_2)] + F(G_2)[3M_1(G_1) + 8M_2(G_1)] + 4M_1(G_1)M_2(G_2) + 4M_1(G_2)M_2(G_1) + 2HM_2(G_1)HM_2(G_2) + 5F(G_1)F(G_2) + 6ReZG_3(G_1)ReZG_3(G_2)$

### 3. Main Results

In the following section, we study the second hyper-Zagreb coindex of some chemical graph structures, exactly sildenafil, aspirin, and nicotine.

**Proposition 3.1.** Let  $G$  be a graph with  $n$  vertices and  $m$  edges. Then,

$$\overline{HM}(G) = (n - 2)M_1(G) + 4m^2 - HM(G). \quad (14)$$

*Proof.* For the proof (Theorem 3.2), we refer to [10].  $\square$

**Proposition 3.2.** Let  $G$  be a graph with  $n$  vertices and  $m$  edges. Then,

$$\overline{HM}_2(G) = \frac{1}{2}M_1^2(G) - \frac{1}{2}Y(G) - HM_2(G). \quad (15)$$

*Proof.* By definition of the second hyper-Zagreb coindex and using a similar method, as above in Proposition 3.1, then

$$\begin{aligned} HM_2(G) + \overline{HM}_2(G) &= \left[ \sum_{uv \in E(G)} + \sum_{uv \notin E(G)} \right] [\delta_G(u)\delta_G(v)]^2 \\ &= \frac{1}{2} \left[ \sum_{u \in V(G)} \sum_{v \in V(G)} [\delta_G(u)\delta_G(v)]^2 - \sum_{v \in V(G)} [\delta_G(v)\delta_G(v)]^2 \right] \\ &= \frac{1}{2} [M_1^2(G) - Y(G)]. \end{aligned} \quad (16)$$

Sildenafil ( $C_{22}H_{30}N_6O_4S$ ) is a drug used for pulmonary arterial hypertension. It is taken by mouth or injection into a vein (Figure 1) [19].  $\square$

**Proposition 3.3.** The second hyper-Zagreb coindex of sildenafil.

From the graph structure of sildenafil (Figure 1), it is easy to obtain the dataset in Tables 1 and 2.

By Table 1 and definitions of the first Zagreb index and the Y-index, we have

$$M_1(\text{sildenafil}) = (7)(1) + (14)(4) + (11)(9) + (1)(16) = 178,$$

$$Y(\text{sildenafil}) = (7)(1) + (14)(16) + (11)(81) + (1)(256) = 1378.$$

$$(17)$$

Also, by Table 2 and definition of the second hyper-Zagreb index, we have

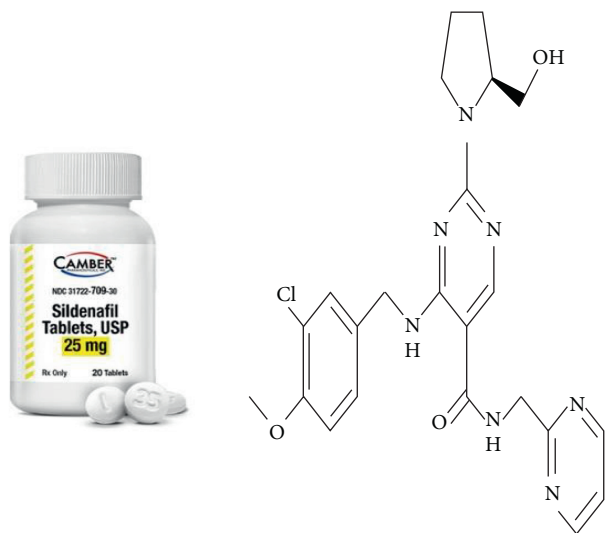


FIGURE 1: Graph structure of sildenafil.

TABLE 1: Atoms dataset of the graph structure of sildenafil.

No. of atoms	7	14	11	1
$\delta v$	1	2	3	4
$\delta^2 v$	1	4	9	16
$\delta^4 v$	1	16	81	256

TABLE 2: Links dataset of the graph structure of sildenafil.

No. of links	2	3	7	16	6	2
$\delta^2 u \delta^2 v$	4	9	16	36	81	144

$$HM_2(\text{sildenafil}) = (2)(4) + (3)(9) + (7)(16) + (16)(36) + (6)(81) + (2)(144) = 1497. \quad (18)$$

Using Proposition 3.2, we have

$$\overline{HM}_2(\text{sildenafil}) = 13656. \quad (19)$$

Aspirin ( $C_9H_8O_4$ ) is known as acetylsalicylic acid (ASA). Aspirin has many medicinal uses as it is a drug that is used to reduce fever or inflammation, also given after a heart attack to reduce the risk of death. Aspirin is also used as a nonsteroidal anti-inflammatory drug because it has an antiplatelet effect by inhibiting its normal functioning. Also, a lot of evidence indicates that aspirin is considered a chemical agent that may limit and reduce the incidence of general cancers (Figure 2) [20, 21].

**Proposition 3.4.** *The second hyper-Zagreb coindex of aspirin.*

From the graph structure of aspirin (Figure 2), it is easy to obtain the dataset in Tables 2 and 3.

Also, by Table 4 and definition of the second hyper-Zagreb index, we have

$$HM_2(\text{aspirin}) = (4)(9) + (3)(16) + (4)(36) + (2)(81) = 390. \quad (20)$$

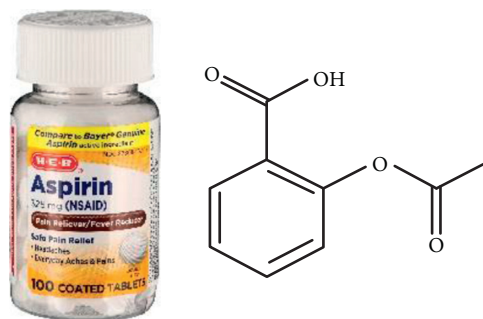


FIGURE 2: Graph structure of aspirin.

TABLE 3: Atoms dataset of the graph structure of aspirin.

No. of atoms	4	5	4
$\delta v$	1	2	3
$\delta^2 v$	1	4	9
$\delta^4 v$	1	16	81

TABLE 4: Links dataset of the graph structure of aspirin.

No. of links	4	3	4	2
$\delta^2 u \delta^2 v$	9	16	36	81

Using Proposition 3.2, we have

$$\overline{HM}_2(\text{aspirin}) = 1206. \quad (21)$$

Nicotine ( $C_{10}H_{14}N_2$ ) is an alkaloid that is widely used as an anxiolytic. Nicotine is used as a drug to quit smoking, and if it is not used well, it can lead to addiction. Many types of research conducted on animals indicate that some inhibitors found in tobacco smoke, such as monoamine oxidase, may enhance some of the addictive properties of nicotine (Figure 3) [21, 22]. Any unexplained terminology is standard, typically as in [22–24].

By Table 3 and definitions of the first Zagreb index and the Y-index, we have

$$M_1(\text{aspirin}) = (4)(1) + (5)(4) + (4)(9) = 60, \quad (22)$$

$$Y(\text{aspirin}) = (4)(1) + (5)(16) + (4)(81) = 408.$$

**Proposition 3.5.** *The second hyper-Zagreb coindex of nicotine.*

From the graph structure of nicotine (Figure 3), it is easy to obtain the dataset in Tables 5 and 6.

By Table 5 and definitions of the first Zagreb index and the Y-index, we have

$$M_1(\text{nicotine}) = (1)(1) + (8)(4) + (3)(9) = 60, \quad (23)$$

$$Y(\text{nicotine}) = (1)(1) + (8)(16) + (3)(81) = 372.$$

Also, by Table 6 and definition of the second hyper-Zagreb index, we have

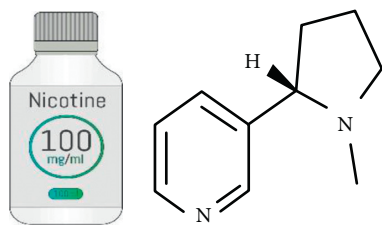


FIGURE 3: Graph structure of nicotine.

TABLE 5: Atoms dataset of the graph structure of nicotine.

No. of atoms	1	8	3
$\delta v$	1	2	3
$\delta^2 v$	1	4	9
$\delta^4 v$	1	16	81

TABLE 6: Links dataset of the graph structure of nicotine.

No. of links	1	6	4	2
$\delta^2 u \delta^2 v$	9	16	36	81

$$HM_2(\text{nicotine}) = (1)(9) + (6)(16) + (4)(36) + (2)(81) = 483. \quad (24)$$

Using Proposition 3.2, we have

$$\overline{HM}_2(\text{nicotine}) = 1131. \quad (25)$$

#### 4. Applications

In the following section, we provide the exact value of the second hyper-Zagreb coindex of graphs that are arisen from mathematical operations such as the tensor product  $G_1 \otimes G_2$ , the Cartesian product  $G_1 \times G_2$ , the composition

$G_1[G_2]$ , and the strong product  $G_1 * G_2$ . Also, we apply this coindex on a  $q$ -multiwalled nanotorus.

**Theorem 4.1.** *The second hyper-Zagreb coindex of  $G_1 \times G_2$  is given by*

$$\begin{aligned} \overline{HM}_2(G_1 \times G_2) &= \frac{1}{2} [n_2 M_1(G_1) + n_1 M_1(G_2) + 8m_1 m_2]^2 \\ &\quad - \frac{1}{2} [n_2 Y(G_1) + n_1 Y(G_2) + 8m_1 F(G_2) \\ &\quad + 8m_2 F(G_1) + 6M_1(G_1)M_1(G_2)] \\ &\quad - [n_2 HM_2(G_1) + n_1 HM_2(G_2) \\ &\quad + 3F(G_1)M_1(G_2) + 3F(G_2)M_1(G_1) \\ &\quad + m_1 [Y(G_2) + 4ReZG_3(G_2)] \\ &\quad + m_2 [Y(G_1) + 4ReZG_3(G_1)] + 4M_1 \\ &\quad \cdot (G_1)M_2(G_2) + 4M_1(G_2)M_2(G_1)]. \end{aligned} \quad (26)$$

*Proof.* We have  $\overline{HM}_2(G) = 1/2M_1^2(G) - 1/2Y(G) - HM_2(G)$ , given in Proposition 3.2, and by replacing each  $G$  by  $G_1 \times G_2$ , which yields  $\overline{HM}_2(G_1 \times G_2) = 1/2M_1^2(G_1 \times G_2) - 1/2Y(G_1 \times G_2) - HM_2(G_1 \times G_2)$ , and by using (Lemma 2.2–Lemma 2.4), we obtain the required.

All proofs in Theorems 4.2–4.4 are given as Theorem 4.1.  $\square$

**Theorem 4.2.** *The second hyper-Zagreb coindex of  $G_1 * G_2$  is given by*

$$\begin{aligned} \overline{HM}_2(G_1 * G_2) &= \frac{1}{2} [(n_2 + 6m_2)M_1(G_1) + 8m_2 m_1 (6m_1 + n_1)M_1(G_2) + 2M_1(G_1)M_1(G_2)]^2 \\ &\quad - \frac{1}{2} [Y(G_1)[4F(G_2) + 6M_1(G_2) + 8m_2 + n_2] + 4F(G_1)[3M_1(G_2) + 2m_2] \\ &\quad + Y(G_2)[4F(G_1) + 6M_1(G_1) + 8m_1 + n_1] + 4F(G_2)[3M_1(G_1) + 2m_1] \\ &\quad + Y(G_1)Y(G_2) + 12F(G_1)F(G_2) + 6M_1(G_1)M_1(G_2)] - HM_2(G_2) \\ &\quad \cdot [n_1 + 10m_1 + 10M_1(G_1) + 8M_2(G_1) + 6F(G_1) + 4ReZG_3(G_1) + Y(G_1)] \\ &\quad + HM_2(G_1)[n_2 + 10m_2 + 10M_1(G_2) + 8M_2(G_2) + 6F(G_2) + 4ReZG_3(G_2) + Y(G_2)] \\ &\quad + Y(G_2)[m_1 + 2M_1(G_1) + 4M_2(G_1) + F(G_1) + 2ReZG_3(G_1)] + Y(G_1)[m_2 + 2M_1(G_2) + 4M_2(G_2) \\ &\quad + F(G_2) + 2ReZG_3(G_2)] + 4ReZG_3(G_2)[m_1 + 2M_1(G_1) + 2M_2(G_1) + 2F(G_1)] \\ &\quad + 4ReZG_3(G_1)[m_2 + 2M_1(G_2) + 2M_2(G_2) + 2F(G_2)] + F(G_2)[3M_1(G_1) + 8M_2(G_1)] \\ &\quad + F(G_1)[3M_1(G_2) + 8M_2(G_2)]. \end{aligned} \quad (27)$$

**Theorem 4.3.** The second hyper-Zagreb coindex of  $G_1 \otimes G_2$  is given by

$$\begin{aligned} \overline{HM}_2(G_1 \otimes G_2) &= \frac{1}{2}[M_1(G_1)M_1(G_2)]^2 \\ &\quad - \frac{1}{2}[Y(G_1)Y(G_2)] \\ &\quad - [2HM_2(G_1)HM_2(G_2)]. \end{aligned} \quad (28)$$

**Theorem 4.4.** The second hyper-Zagreb coindex of  $G_1[G_2]$  is given by

*Proof.*  $\overline{HM}_2(G_1[G_2]) = 1/2[n_2^3M_1(G_1) + n_1M_1(G_2) + 8n_2m_2m_1Y(G_1[G_2]) + n_2^5Y(G_1) + n_1Y(G_2) + 8n_2^3m_2F(G_1) + 8n_2m_1F(G_2) + 6n_2^2M_1(G_1)M_1(G_2)]^2 + -1/2[n_2^5Y(G_1) + n_1Y(G_2) + 8n_2^3m_2F(G_1) + 8n_2m_1F(G_2) + 6n_2^2M_1(G_1)M_1(G_2)] - [n_2^6HM_2(G_1) + n_1HM_2(G_2) + n_2^4m_2[Y(G_1) + 4ReZG_3(G_1)] + 4n_2m_1ReZG_3(G_2) + 3n_2^2F(G_1)M_1(G_2) + n_2^2M_1(G_1)[F(G_2) + 4M_2(G_2)] + m_1M_1^2(G_2) + 4n_2m_2[4n_2m_2M_2(G_1) + M_1(G_1)M_1(G_2)]]$ .

In [19, 25–27], authors computed some topological indices of molecular graph of a nanotorus (Figure 4). In this section, we compute the second hyper-Zagreb coindex of a molecular graph of a nanotorus.  $\square$

**Corollary 4.5.** Let  $T = T[p; q]$  be the molecular graph of a nanotorus. Then, the first Zagreb index of a  $q$ -multiwalled nanotorus is  $M_1(P_n \times T) = pq(25n - 18)$ .

*Proof.* The proof of the above corollary is given by Gao et al. in [3]. Obviously,

$$\begin{aligned} |V(G_1)| &= |V(P_n)| = n, \\ |E(G_1)| &= |E(P_n)| = n - 1, \\ |V(G_2)| &= |V(T)| = pq, \\ |E(G_2)| &= |E(T)| = \left(\frac{3}{2}\right)pq, \\ |M_1(G_1)| &= |M_1(P_n)| = (4n - 6), \\ |M_1(G_2)| &= |M_1(T)| = 9pq. \end{aligned} \quad (29)$$

**Corollary 4.6.** Let  $T = T[p; q]$  be the molecular graph of a nanotorus. Then, the  $Y$ -index of a  $q$ -multiwalled nanotorus is

$$Y(P_n \times T) = pq(625n - 738). \quad (30)$$

*Proof.* We have by Lemma 4.2,

$$\begin{aligned} Y(G_1 \times G_2) &= n_2Y(G_1) + n_1Y(G_2) + 8m_1F(G_2) \\ &\quad + 8m_2F(G_1) + 6M_1(G_1)M_1(G_2). \end{aligned} \quad (31)$$

Then,

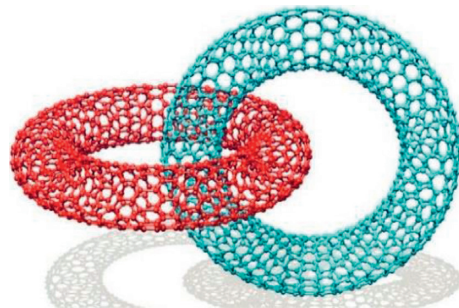


FIGURE 4: The molecular graph of a nanotorus.

$$\begin{aligned} Y(P_n \times T) &= (pq)Y(P_n) + nY(T) + 8(n - 1)F(T) \\ &\quad + 8\left(\frac{3}{2}\right)pqF(P_n) + 6M_1(P_n)M_1(T). \end{aligned} \quad (32)$$

Therefore,

$$\begin{aligned} Y(P_n \times T) &= (pq)(16n - 30) + n(81pq) + 8(n - 1)(27pq) \\ &\quad + 12pq(8n - 14) + 6(4n - 6)(9pq) \\ &= pq(625n - 738). \end{aligned} \quad (33)$$

**Corollary 4.7.** Let  $T = T[p; q]$  be the molecular graph of a nanotorus. Then, the second hyper-Zagreb index of a  $q$ -multiwalled nanotorus is

$$HM_2(P_n \times T) = \left(\frac{1}{2}\right)pq(2561n - 3632). \quad (34)$$

*Proof.* We have by Lemma 2.5,

$$\begin{aligned} HM_2(G_1 \times G_2) &= n_2HM_2(G_1) + n_1HM_2(G_2) \\ &\quad + 3F(G_1)M_1(G_2) + 3F(G_2)M_1(G_1) \\ &\quad + m_1[Y(G_2) + 4ReZG_3(G_2)] \\ &\quad + m_2[Y(G_1) + 4ReZG_3(G_1)] \\ &\quad + 4M_1(G_1)M_2(G_2) + 4M_1(G_2)M_2(G_1). \end{aligned} \quad (35)$$

As proof in Corollary 4.6, we have

$$HM_2(P_n \times T) = \left(\frac{1}{2}\right)pq(2561n - 3632), \quad (36)$$

where

$$|HM_2(P_n)| = (16n - 40), \quad |HM_2(T)| = \left(\frac{243}{2}\right)pq. \quad (37)$$

Now, we apply the second hyper-Zagreb coindex on a  $q$ -multiwalled nanotorus using Cartesian product operation.  $\square$

**Corollary 4.8.** Let  $T = T[p; q]$  be the molecular graph of a nanotorus. Then, the second hyper-Zagreb coindex of a  $q$ -multiwalled nanotorus is

$$\overline{HM}_2(P_n \times T) = \left(\frac{1}{2}\right) pq [pq(25n - 18)^2 - 3186n + 4370]. \quad (38)$$

*Proof.* We have by Proposition 3.2,

$$\overline{HM}_2(G) = \frac{1}{2} M_1^2(G) - \frac{1}{2} Y(G) - HM_2(G). \quad (39)$$

Then,

$$\overline{HM}_2(P_n \times T) = \frac{1}{2} M_1^2(P_n \times T) - \frac{1}{2} Y(G) - HM_2(P_n \times T). \quad (40)$$

By using Corollaries 4.5–4.7, we obtain

$$\overline{HM}_2(P_n \times T) = \left(\frac{1}{2}\right) pq [pq(25n - 18)^2 - 3186n + 4370]. \quad (41)$$

□

## 5. Conclusion

In this study, we obtained the value of the second hyper-Zagreb coindex of some chemical graphs, and we computed some explicit formulas for their numbers under several graph operations. Also, we applied the second hyper-Zagreb coindex on a  $q$ -multiwalled nanotorus. The results of this work may be used as a predictor, especially in the chemical graph theory. For example, in quantitative structure-activity relationships (QSAR) modelling, the predictors consist of theoretical molecular descriptors of chemicals.

## Data Availability

No data were used to support this study, except for the references that were mentioned.

## Conflicts of Interest

The authors declare that they have no conflicts of interest.

## References

- [1] H. Ahmed, A. Alwardi, M. R. Salestina, and D. S. Nandappa, "Domination,  $\gamma$ -domination, topological indices and  $\varphi_p$ -polynomial of some chemical structures applied for the treatment of COVID-19 patients," *Biointerface Research in Applied Chemistry*, pp. 13290–13302, 2021.
- [2] A. Ayache and A. Alameri, "Topological indices of the mk-graph," *Journal of the Association of Arab Universities for Basic and Applied Sciences*, vol. 24, no. 1, pp. 283–291, 2017.
- [3] W. Gao, M. K. Siddiqui, M. Imran, M. K. Jamil, and M. R. Farahani, "Forgotten topological index of chemical structure in drugs," *Saudi Pharmaceutical Journal*, vol. 24, no. 3, pp. 258–264, 2016.
- [4] A. Alameri, "Second hyper-zagreb index of titania nanotubes and their applications," *IEEE Access*, vol. 9, pp. 9567–9571, 2021.
- [5] I. Gutman and N. Trinajstić, "Graph theory and molecular orbitals. Total  $\varphi$ -electron energy of alternant hydrocarbons," *Chemical Physics Letters*, vol. 17, no. 4, pp. 535–538, 1972.
- [6] T. Došlić, "Vertex-weighted wiener polynomials for composite graphs," *Ars Mathematica Contemporanea*, vol. 1, pp. 66–80, 2008.
- [7] A. R. Ashrafi, T. Došlić, and A. Hamzeh, "The Zagreb coindices of graph operations," *Discrete Applied Mathematics*, vol. 158, no. 15, pp. 1571–1578, 2010.
- [8] G. H. Shirdel, H. Rezapour, and A. M. Sayadi, "The hyper-Zagreb index of graph operations," *Iranian Journal of Mathematical Chemistry*, vol. 4, no. 2, pp. 213–220, 2013.
- [9] P. S. Ranjini, V. Loksha, and A. Usha, "Relation between phenylene and hexagonal squeeze using harmonic index," *International Journal of Graph Theory*, vol. 1, no. 4, pp. 116–121, 2013.
- [10] B. Furtula and I. Gutman, "A forgotten topological index," *Journal of Mathematical Chemistry*, vol. 53, no. 4, pp. 1184–1190, 2015.
- [11] M. Veylaki, M. J. Nikmehr, and H. A. Tavallae, "The third and hyper-Zagreb coindices of some graph operations," *Journal of Applied Mathematics and Computing*, vol. 50, no. 1–2, pp. 315–325, 2016.
- [12] G. Wei, M. R. Farahani, and M. K. Siddiqui, "On the first and second Zagreb and first and second hyper-zagreb indices of carbon nanocones CN $\check{C}$ [n]," *Journal of Computational and Theoretical Nanoscience*, vol. 13, pp. 7475–7482, 2016.
- [13] A. Alameri, N. Al-Naggar, M. Al-Rumaima, and M. Alsharafi, "Y-index of some graph operations," *International Journal of Applied Engineering Research*, vol. 15, no. 2, p. 179, 2020.
- [14] A. Alameri, M. Al-Rumaima, and M. Almazah, "Y-coindex of graph operations and its applications of molecular descriptors," *Journal of Molecular Structure*, vol. 1221, Article ID 128754, 2020.
- [15] U. Knauer and K. Knauer, *Algebraic Graph Theory*, p. 1, de Gruyter, Berlin, Germany, 2019.
- [16] A. Alameri, A. Modabish, and A. Ayache, "New product operation on graphs and its properties," *International Mathematical Forum*, vol. 11, no. 8, pp. 357–368, 2016.
- [17] Ö. Ç. Havare, "On the inverse sum ind $\check{e}$ g index of some graph operations," *Journal of the Egyptian Mathematical Society*, vol. 28, no. 1, pp. 1–11, 2020.
- [18] A. Modabish, A. Alameri, M. S. Gumaan, and M. Alsharafi, "The second Hyper-Zagreb index of graph operations," *Journal of Mathematical and Computational Science*, vol. 11, no. 2, pp. 1455–1469, 2021.
- [19] I. Goldstein, A. L. Burnett, R. C. Rosen, P. W. Park, and V. J. Stecher, "The serendipitous story of sildenafil: an unexpected oral therapy for erectile dysfunction," *Sexual Medicine Reviews*, vol. 7, no. 1, pp. 115–128, 2019.
- [20] P. Patrignani and C. Patrono, "Aspirin and cancer," *Journal of the American College of Cardiology*, vol. 68, no. 9, pp. 967–976, 2016.
- [21] H. Ahmed, M. R. Farahani, A. Alwardi, and M. R. Salestina, "Domination topological properties of some chemical structures using  $\varphi_p$ -Polynomial approach," *Eurasian Chemical Communications*, vol. 3, no. 4, pp. 210–218, 2021.
- [22] R. K. Sajja, S. Rahman, and L. Cucullo, "Drugs of abuse and blood-brain barrier endothelial dysfunction: a focus on the role of oxidative stress," *Journal of Cerebral Blood Flow and Metabolism*, vol. 36, no. 3, pp. 539–554, 2016.
- [23] M. Ibraheem, M. M. Aljohani, M. Javaid, and A. M. Alanazi, "Forgotten coindex for the derived sum graphs under cartesian product," vol. 2021, Article ID 3235068, 13 pages, 2021.

- [24] M. Javaid, M. Ibraheem, U. Ahmad, and Q. Zhu, *Computing Bounds for Second Zagreb Coindex of Sum Graphs*, 2021.
- [25] M. H. Khalifeh, H. Yousefi-Azari, and A. R. Ashrafi, "The first and second Zagreb indices of some graph operations," *Discrete Applied Mathematics*, vol. 157, no. 4, pp. 804–811, 2009.
- [26] M. S. Alsharafi, M. M. Shubatah, and M. Q. Alameri, "On the Hyper-Zagreb coindex of some graphs," *Journal of Mathematical and Computational Science*, vol. 10, no. 5, pp. 1875–1890, 2020.
- [27] M. Alsharafi, M. Shubatah, and A. Alameri, "The hyper-Zagreb index of some complement graphs," *Advances in Mathematics: Scientific Journal*, vol. 9, no. 6, pp. 3631–3642, 2020.

## Review Article

# Vertex-Based Topological Indices of Double and Strong Double Graph of Dutch Windmill Graph

Muhammad Asad Ali,<sup>1</sup> Muhammad Shoaib Sardar ,<sup>1</sup> Imran Siddique ,<sup>2</sup>  
and Dalal Alrowaili <sup>3</sup>

<sup>1</sup>School of Mathematics, Minhaj University, Lahore, Pakistan

<sup>2</sup>Department of Mathematics, University of Management and Technology, Lahore 54770, Pakistan

<sup>3</sup>Mathematics Department, College of Science, Jouf University, P.O. Box, Sakaka 2014, Saudi Arabia

Correspondence should be addressed to Imran Siddique; [imransmsrazi@gmail.com](mailto:imransmsrazi@gmail.com)

Received 10 August 2021; Accepted 30 September 2021; Published 26 October 2021

Academic Editor: Muhammad Imran

Copyright © 2021 Muhammad Asad Ali et al. This is an open access article distributed under the Creative Commons Attribution License, which permits unrestricted use, distribution, and reproduction in any medium, provided the original work is properly cited.

A measurement of the molecular topology of graphs is known as a topological index, and several physical and chemical properties such as heat formation, boiling point, vaporization, enthalpy, and entropy are used to characterize them. Graph theory is useful in evaluating the relationship between various topological indices of some graphs derived by applying certain graph operations. Graph operations play an important role in many applications of graph theory because many big graphs can be obtained from small graphs. Here, we discuss two graph operations, i.e., double graph and strong double graph. In this article, we will compute the topological indices such as geometric arithmetic index (GA), atom bond connectivity index (ABC), forgotten index ( $F$ ), inverse sum indeg index (ISI), general inverse sum indeg index  $ISI_{(\alpha,\beta)}$ , first multiplicative-Zagreb index ( $PM_1$ ) and second multiplicative-Zagreb index ( $PM_2$ ), fifth geometric arithmetic index ( $GA_5$ ), fourth atom bond connectivity index ( $ABC_4$ ) of double graph, and strong double graph of Dutch Windmill graph  $D_3^p$ .

## 1. Introduction and Preliminaries

For undetermined notations and terminologies, we recommend Robin J. Wilson book [1].

Assume that  $G$  is a simple graph that has no multiple edges and loops.  $V(G)$  and  $E(G)$  are the vertex and edge sets of graph  $G$ , respectively. The number of elements in  $V(G)$  and  $E(G)$  represents the order and size of graph  $G$ . Vertex degree is the number of edges joining to a vertex in a graph  $G$ . A vertex degree is indicated by  $d_r$ ,  $\{r \in V(G)\}$  and  $S_r = \sum_{s \in N_G(r)} d_s$ , where  $N_G(r) = \{s \in V(G) \mid rs \in E(G)\}$ . The following lemma is useful for computing the total number of edges in a graph  $G$ .

**Lemma 1.** If  $G$  is a graph of size  $t$ , then

$$\sum_{r \in V(G)} \deg(r) = 2t. \quad (1)$$

This is also called the handshake lemma and was observed by Lenford Euler in 1736. This observation is often called the first theorem of graph theory [2].

The chemical graph theory connects graph theory and chemistry to solve organic chemistry problems. Structured-property (QSPR) and structured-activity (QSAR) relationships are among the most important topics in this field. QSPR/QSAR research relies heavily on topological indices. These topological indices analyse the structure of any finite graph and are based on mathematical equations. Several different kinds of topological indices exist, i.e., degree-based topological indices [3–5], distance-based topological indices [6], and counting-related topological indices [7, 8]. The topological index concept comes from the work of Wiener, who introduced the Wiener index, and thus, topological indexing history begins.

The Wiener index is defined in [9] as follows:

$$W(G) = \frac{1}{2} \sum_{(r,s)} d(r,s), \quad (2)$$

where  $(r, s)$  is the order pair of vertices in  $G$  and  $d(r, s)$  is the distance of vertex  $r$ - $s$  in  $G$ .

The geometric-arithmetic index (GA) [10] of graph  $G$  is defined as

$$GA(G) = \sum_{rs \in E(G)} \frac{2\sqrt{d_r d_s}}{d_r + d_s}. \quad (3)$$

The atomic bond connectivity index (ABC) of graph  $G$  is defined [11] as

$$ABC(G) = \sum_{rs \in E(G)} \sqrt{\frac{d_r + d_s - 2}{d_r d_s}}. \quad (4)$$

The forgotten index ( $F$ ) is defined [12] as

$$F(G) = \sum_{rs \in E(G)} (d_r^2 + d_s^2). \quad (5)$$

The inverse sum indeg index (ISI) is defined [13] as

$$ISI(G) = \sum_{rs \in E(G)} \frac{1}{1/d_r + 1/d_s}. \quad (6)$$

The general inverse sum indeg index ( $ISI_{(\alpha,\beta)}$ ) is defined [14] as

$$ISI_{(\alpha,\beta)}(G) = \sum_{rs \in E(G)} [d_r d_s]^\alpha [d_r + d_s]^\beta, \quad (7)$$

where  $\alpha$  and  $\beta$  are some real numbers.

The first multiplicative-Zagreb ( $PM_1$ ) and second multiplicative-Zagreb index ( $PM_2$ ) is defined [15] as

$$PM_1(G) = \prod_{rs \in E(G)} (d_r)^2, \quad (8)$$

$$PM_2(G) = \prod_{rs \in E(G)} (d_r \cdot d_s). \quad (9)$$

The first multiplicative-Zagreb index ( $PM_1$ ) can also be written in the sum of the edges [16] of  $G$ :

$$PM_1(G) = \prod_{rs \in E(G)} (d_r + d_s). \quad (10)$$

The  $GA_5(G)$  index is defined [17] as

$$GA_5(G) = \sum_{rs \in E(G)} \frac{2\sqrt{S_r \times S_s}}{S_r + S_s}, \quad (11)$$

where  $S_r$  is summation of degrees of all neighbor of vertex  $r$ , and the same for  $S_s$ .

The  $ABC_4(G)$  index is defined [18] as

$$ABC_4(G) = \sum_{rs \in E(G)} \sqrt{\frac{S_r + S_s - 2}{S_r \times S_s}}. \quad (12)$$

We suggest that readers read the following articles for more detailed information on topological indices and molecular graphs [19–22].

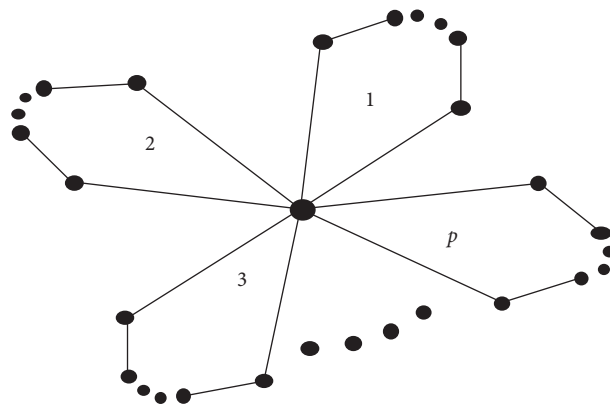


FIGURE 1: Dutch windmill graph  $D_n^p$ .

**Definition 1.** A Dutch Windmill graph [23] is the graph which is formed by taking the  $p$  copies of the cycle graph by taking one mutual vertex. It is denoted by  $D_n^p$ , where  $p \geq 1$  and  $n \geq 3$ . The order of Dutch Windmill graph is  $(n-1)p+1$  and size  $pn$ . Dutch Windmill graph  $D_n^p$  is depicted in Figure 1.

**Definition 2.** The double graph of graph  $G$  is represented by  $D[G]$ . Assume two copies of a graph, and join each vertex in one copy to its neighbor in the other copy in order to produce the double graph of the graph [24]. For example, the double graph of Dutch Windmill graph  $D_3^2$  is depicted in Figure 2.

**Definition 3.** The strong double graph  $SD[G]$  of the graph  $G$  is attained by taking two graphs and joining the closed neighbourhoods of each vertex in one graph to the adjacent vertex in the other graph [25]. For example, strong double graph of graph  $G$  is depicted in Figure 3. A new type of equienergetic and L-equienergetic graph has been found by using strong double graphs.

The following is the structure of this paper. Sections 2 and 3 will analyse some degree-based topological indices of double graphs and strong double graphs of Dutch Windmill graphs, respectively. In Section 4, we provide concluding remarks for the entire paper.

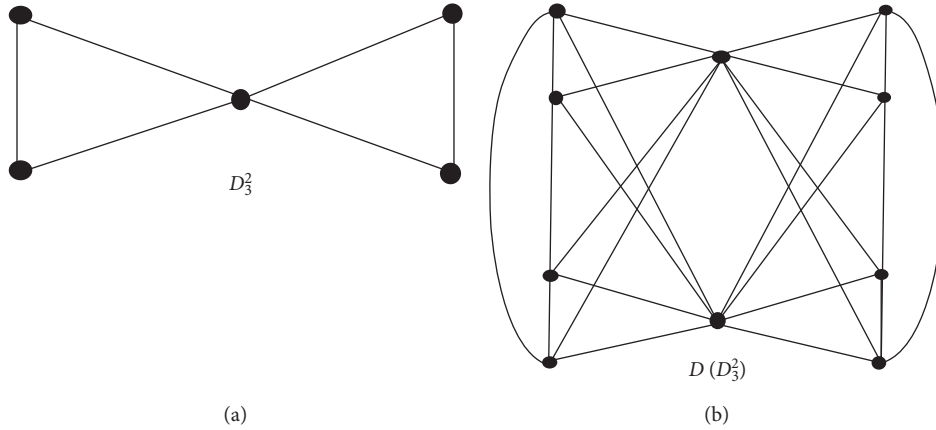
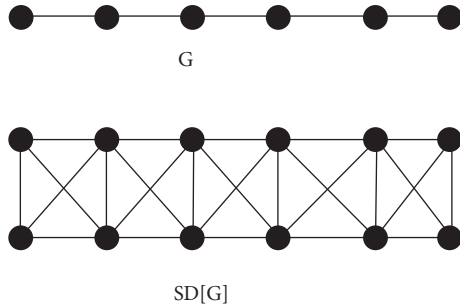
## 2. Degree-Based Topological Indices of Double Graph of Dutch Windmill Graph $D_3^p$

We will compute the vertex-based indices of the double graph of the Dutch Windmill graph  $D_3^p$  in this section.

**Theorem 4.** Let  $D(D_3^p)$  be the double graph of Dutch Windmill graph  $D_3^p$ . Then, the geometric arithmetic index of  $D(D_3^p)$  is

$$GA[D(D_3^p)] = 4p \left[ 1 + \frac{4\sqrt{p}}{1+p} \right]. \quad (13)$$

*Proof.* The total number of vertices and edges in the double graph of Dutch Windmill graph is  $2[2p+1]$  and  $12p$ , respectively. In  $[D(D_3^p)]$ , we have  $4p$  vertices of degree 4 and 2

FIGURE 2: (a). Dutch windmill graph  $D_3^2$ . (b). Double graph of Dutch windmill graph  $D_3^2$ .FIGURE 3: Strong double graph  $SD[G]$  of graph  $G$ .

vertices of degree  $8p$ . We split the edges of  $[D(D_3^p)]$  into those of the type  $E[d_r, d_s]$  in which  $r, s$  are edges.  $[D(D_3^p)]$  contains edges of type  $E_{(4,4)}$  and  $E_{(4,4p)}$ , and Table 1 presents the edges of these types.

By applying equation (3) and Table 1, we acquire the desired results, i.e.,

$$\begin{aligned} GA[G] &= \sum_{rs \in E(G)} \frac{2\sqrt{d_r d_s}}{d_r + d_s}, \\ GA[D(D_3^p)] &= |E_{(4,4)}| \sum_{rs \in E([D(D_3^p)])} \frac{2\sqrt{d_r d_s}}{d_r + d_s} \\ &\quad + |E_{(4,4p)}| \sum_{rs \in E([D(D_3^p)])} \frac{2\sqrt{d_r d_s}}{d_r + d_s}, \end{aligned} \quad (14)$$

$$GA[D(D_3^p)] = 4p \left[ \frac{2\sqrt{4(4)}}{4+4} \right] + 8p \left[ \frac{2\sqrt{4(4p)}}{4+4p} \right],$$

$$GA[D(D_3^p)] = 4p \left[ 1 + \frac{4\sqrt{p}}{1+p} \right]. \quad \square$$

**Theorem 5.** Let  $D(D_3^p)$  be the double graph of Dutch Windmill graph  $D_3^p$ . Then, the ABC index of  $D(D_3^p)$  is

TABLE 1: Partitioning of edges.

$E[d_r, d_s]$	$E_{(4,4)}$	$E_{(4,4p)}$
Number of edges	$4p$	$8p$

$$ABC[D(D_3^p)] = p\sqrt{6} + 2\sqrt{2p(1+2p)}. \quad (15)$$

*Proof.* By applying equation (4) and Table 1, we acquire the desired results, i.e.,

$$ABC(G) = \sum_{rs \in E(G)} \sqrt{\frac{d_r + d_s - 2}{d_r d_s}},$$

$$\begin{aligned} ABC[D(D_3^p)] &= |E_{(4,4)}| \sum_{rs \in E([D(D_3^p)])} \sqrt{\frac{d_r + d_s - 2}{d_r d_s}} \\ &\quad + |E_{(4,4p)}| \sum_{rs \in E([D(D_3^p)])} \sqrt{\frac{d_r + d_s - 2}{d_r d_s}}, \\ &= 4p \sqrt{\frac{4+4-2}{16}} + 8p \sqrt{\frac{4+4p-2}{(16p)}}, \\ &= 4p \sqrt{\frac{6}{16}} + 8p \sqrt{\frac{2+4p}{(16p)}}, \end{aligned}$$

$$ABC[D(D_3^p)] = p\sqrt{6} + 2\sqrt{2p(1+2p)}. \quad (16) \quad \square$$

**Theorem 6.** Let  $D(D_3^p)$  be the double graph of Dutch Windmill graph  $D_3^p$ . Then, the forgotten index of  $D(D_3^p)$  is

$$F[D(D_3^p)] = 128[p + (1+p^2)]. \quad (17)$$

*Proof.* By applying equation (5) and Table 1, we acquire the desired results, i.e.,

$$\begin{aligned}
F(G) &= \sum_{rs \in E(G)} (d_r^2 + d_s^2) \\
F[D(D_3^p)] &= |E_{(4,4)}| \sum_{rs \in E[D(D_3^p)]} (d_r^2 + d_s^2) \\
&\quad + |E_{(4,4p)}| \sum_{rs \in E[D(D_3^p)]} (d_r^2 + d_s^2) \quad (18) \\
&= 4p(4^2 + 4^2) + 8p(4^2 + (4p)^2) \\
F[D(D_3^p)] &= 128[p + (1 + p^2)]. \quad \square
\end{aligned}$$

**Theorem 7.** Let  $D(D_3^p)$  be the double graph of Dutch Windmill graph  $D_3^p$ . Then, the inverse sum indeg index of  $D(D_3^p)$  is

$$\text{ISI}[D(D_3^p)] = 8p \left[ 1 + \frac{4p}{(1+p)} \right]. \quad (19)$$

*Proof.* By applying equation (6) and Table 1, we acquire the desired results, i.e.,

$$\begin{aligned}
\text{ISI}[G] &= \sum_{rs \in E(G)} \frac{1}{1/d_r + 1/d_s} = \sum_{rs \in E(G)} \frac{(d_r d_s)}{(d_r + d_s)}, \\
\text{ISI}[D(D_3^p)] &= |E_{(4,4)}| \sum_{rs \in E[D(D_3^p)]} \frac{(d_r d_s)}{(d_r + d_s)} \\
&\quad + |E_{(4,4p)}| \sum_{rs \in E[D(D_3^p)]} \frac{(d_r d_s)}{(d_r + d_s)}, \\
\text{ISI}[D(D_3^p)] &= 4p \left[ \frac{(4)(4)}{(4+4)} \right] + 8p \left[ \frac{(4)(4p)}{(4+4p)} \right], \\
\text{ISI}[D(D_3^p)] &= 8p \left[ 1 + \frac{4p}{(1+p)} \right]. \quad (20)
\end{aligned}$$

**Theorem 8.** Let  $D(D_3^p)$  be the double graph of Dutch Windmill graph  $D_3^p$ . Then, the general inverse sum indeg index  $\text{ISI}_{(\alpha,\beta)}$  of  $D(D_3^p)$  is

$$\text{ISI}_{(\alpha,\beta)}[D(D_3^p)] = 4p[16]^\alpha [8]^\beta + 8p[16p]^\alpha [4(1+p)]^\beta. \quad (21)$$

*Proof.* By applying equation (7) and Table 1, we acquire the desired results, i.e.,

$$\begin{aligned}
\text{ISI}_{(\alpha,\beta)}(G) &= \sum_{rs \in E(G)} [d_u d_v]^\alpha [d_u + d_v]^\beta \\
&= |E_{(4,4)}| \sum_{rs \in E[D(D_3^p)]} [d_r d_s]^\alpha [d_r + d_s]^\beta \\
&\quad + |E_{(4,4p)}| \sum_{rs \in E[D(D_3^p)]} [d_r d_s]^\alpha [d_r + d_s]^\beta, \\
\text{ISI}_{(\alpha,\beta)}[D(D_2^p)] &= 4p[(4)(4)]^\alpha [4+4]^\beta \\
&\quad + 8p[(4)(4p)]^\alpha [4+4p]^\beta, \\
\text{ISI}_{(\alpha,\beta)}[D(D_2^p)] &= 4p[16]^\alpha [8]^\beta \\
&\quad + 8p[16p]^\alpha [4(1+p)]^\beta. \quad (22)
\end{aligned}$$

□

**Theorem 9.** Let  $D(D_3^p)$  be the double graph of Dutch Windmill graph  $D_3^p$ . Then, the first multiplicative-Zagreb index of  $D(D_3^p)$  is

$$\text{PM}_1[D(D_3^p)] = 1024p^2(1+p). \quad (23)$$

*Proof.* By applying equation (9) and Table 1, we acquire the desired results, i.e.,

$$\begin{aligned}
\text{PM}_1[G] &= \prod_{rs \in E(G)} (d_r + d_s), \\
\text{PM}_1[D(D_3^p)] &= |E_{(4,4)}| \prod_{rs \in E[D(D_3^p)]} (d_r + d_s) \\
&\quad \times |E_{(4,4p)}| \prod_{rs \in E[D(D_3^p)]} (d_r + d_s), \quad (24) \\
\text{PM}_1[D(D_3^p)] &= 4p(4+4) \times 8p(4+4p), \\
\text{PM}_1[D(D_3^p)] &= 1024p^2(1+p).
\end{aligned}$$

□

**Theorem 10.** Let  $D(D_3^p)$  be the double graph of Dutch Windmill graph  $D_3^p$ . Then, the second multiplicative-Zagreb index of  $D(D_3^p)$  is

$$\text{PM}_2[D(D_3^p)] = 8192p^3. \quad (25)$$

*Proof.* By applying equation (9) and Table 1, we acquire the desired results, i.e.,

$$\begin{aligned}
 \text{PM}_2[G] &= \prod_{rs \in E(G)} (d_r \cdot d_s), \\
 \text{PM}_2[D(D_3^p)] &= |E_{(4,4)}| \prod_{rs \in E[D(D_3^p)]} (d_r \cdot d_s) \\
 &\quad \times |E_{(4,4p)}| \prod_{rs \in E[D(D_3^p)]} (d_r \cdot d_s), \quad (26) \\
 \text{PM}_2[D(D_3^p)] &= 4p(4 \times 4) \times 8p(4 \times 4p), \\
 \text{PM}_2[D(D_3^p)] &= 8192p^3.
 \end{aligned}$$

**Theorem 11.** Let  $D(D_3^p)$  be the double graph of Dutch Windmill graph  $D_3^p$ . Then,  $\text{GA}_5(G)$  index of  $D(D_3^p)$  is

$$\text{GA}_5[D(D_3^p)] = 4p\sqrt{(p+1)} \left[ \frac{1}{(p+1)} + \frac{4p\sqrt{2}}{[3p+1]} \right]. \quad (27)$$

*Proof.* We split the edges of  $[D(D_3^p)]$  into those of the type  $E[S_r, S_s]$  in which “ $rs$ ” is an edge.  $[D(D_3^p)]$  contains edge of the type  $E_{[8(p+1), 8(p+1)]}$  and  $E_{[8(p+1), 16p]}$ , and Table 2 presents the edges of these types.

□ By applying equation (11) and Table 2, we acquire the desired results, i.e.,

$$\begin{aligned}
 \text{GA}_5(G) &= \sum_{rs \in E(G)} \frac{2\sqrt{S_r \times S_s}}{S_r + S_s} \\
 &= |E_{[8(p+1), 8(p+1)]}| \sum_{rs \in E[D(D_3^p)]} \frac{2\sqrt{S_r \times S_s}}{S_r + S_s} + |E_{[8(p+1), 16p]}| \sum_{rs \in E[D(D_3^p)]} \frac{2\sqrt{S_r \times S_s}}{S_r + S_s}, \quad (28)
 \end{aligned}$$

$$\text{GA}_5[D(D_3^p)] = 4p \left[ \frac{16\sqrt{(p+1)}}{2[8(p+1)]} \right] + 8p \left[ \frac{8\sqrt{8p(p+1)}}{8[3p+1]} \right]$$

$$\text{GA}_5[D(D_3^p)] = 4p\sqrt{(p+1)} \left[ \frac{1}{(p+1)} + \frac{4p\sqrt{2}}{[3p+1]} \right].$$

**Theorem 12.** Let  $D(D_3^p)$  be the double graph of Dutch Windmill graph  $D_3^p$ . Then, the fourth atom bond connectivity index of  $D(D_3^p)$  is

$$\text{ABC}_4[D(D_3^p)] = \frac{p}{2(p+1)} [\sqrt{16p-14}] + p \left[ \sqrt{\frac{3(4p-1)}{p(p+1)}} \right]. \quad (29)$$

□ *Proof.* By applying equation (12) and Table 2, we acquire the desired results, i.e.,

$$\begin{aligned}
 \text{ABC}_4(G) &= \sum_{rs \in E(G)} \sqrt{\frac{S_r + S_s - 2}{S_r \times S_s}} \\
 &= |E_{[8(p+1), 8(p+1)]}| \sum_{rs \in E[D(D_3^p)]} \sqrt{\frac{S_r + S_s - 2}{S_r \times S_s}} + |E_{[8(p+1), 16p]}| \sum_{rs \in E[D(D_3^p)]} \sqrt{\frac{S_r + S_s - 2}{S_r \times S_s}}, \quad (30)
 \end{aligned}$$

$$\text{ABC}_4[D(D_3^p)] = 4p \left[ \sqrt{\frac{16p-14}{[8(p+1)]^2}} \right] + 8p \left[ \sqrt{\frac{6(4p-1)}{128p(p+1)}} \right],$$

$$\text{ABC}_4[D(D_3^p)] = \frac{p}{2(p+1)} [\sqrt{16p-14}] + p \left[ \sqrt{\frac{3(4p-1)}{p(p+1)}} \right].$$

□

TABLE 2: Partitioning of edges.

$E[S_u, S_v]$	$E_{[8(p+1), 8(p+1)]}$	$E_{[8(p+1), 16p]}$
Number of edges	$4p$	$8p$

### 3. Degree-Based Topological Indices of Strong Double Graphs of Dutch Windmill Graph $D_3^p$

We will compute the vertex-based indices of the strong double graph of the Dutch Windmill graph  $D_3^p$  in this section. The strong double graph of  $D_3^p$  is depicted in Figure 4.

**Theorem 13.** Let  $SD(D_3^p)$  be the strong double graph of Dutch Windmill graph  $D_3^p$ . Then, the geometric arithmetic index of  $SD(D_3^p)$  is

$$\begin{aligned}
 GA[G] &= \sum_{rs \in E(G)} \frac{2\sqrt{d_r d_s}}{d_r + d_s} \\
 &= |E_{(5,5)}| \sum_{rs \in E([D(D_3^p)])} \frac{2\sqrt{d_r d_s}}{d_r + d_s} + |E_{(5,4p+1)}| \sum_{rs \in E([D(D_3^p)])} \frac{2\sqrt{d_r d_s}}{d_r + d_s} \\
 &\quad + |E_{(4p+1,4p+1)}| \sum_{rs \in E([D(D_3^p)])} \frac{2\sqrt{d_r d_s}}{d_r + d_s} \\
 &= (6p) \frac{\sqrt{25}}{5} + (8p) \frac{2\sqrt{5(4p+1)}}{5+(4p+1)} + (1) \frac{2\sqrt{(4p+1)(4p+1)}}{(4p+1)+(4p+1)}, \\
 GA[SD(D_3^p)] &= 1 + 6p + \frac{8p\sqrt{20p+5}}{(2p+3)}.
 \end{aligned} \tag{32}$$

**Theorem 14.** Let  $SD(D_3^p)$  be the strong double graph of Dutch Windmill graph  $D_3^p$ . Then, ABC index for

$$GA[SD(D_3^p)] = 1 + 6p + \frac{8p\sqrt{20p+5}}{(2p+3)}. \tag{31}$$

*Proof.* The total number of vertices and edges in  $[SD(D_3^p)]$  are  $2[2p+1]$  and  $14p+1$ , respectively. In  $[SD(D_3^p)]$ , we have  $4p$  vertices of degree 5 and 2 vertices of degree  $4p+1$ . We split the edges of  $[SD(D_3^p)]$  into those of the type  $E[d_r, d_s]$  in which “ $rs$ ” is an edge.  $[SD(D_3^p)]$  contains edges of the type  $E_{(5,5)}$ ,  $E_{(5,4p+1)}$ , and  $E_{(4p+1,4p+1)}$ , and Table 3 presents the edges of these types.

By applying Equation (3) and Table 3, we acquire the desired results, i.e.,

$SD(D_3^p)$  is □

$$ABC[SD(D_3^p)] = \frac{12p\sqrt{2}}{5} + 16p\sqrt{\frac{(p+1)}{(20p+5)} + \frac{2\sqrt{2p}}{(4p+1)}}. \tag{33}$$

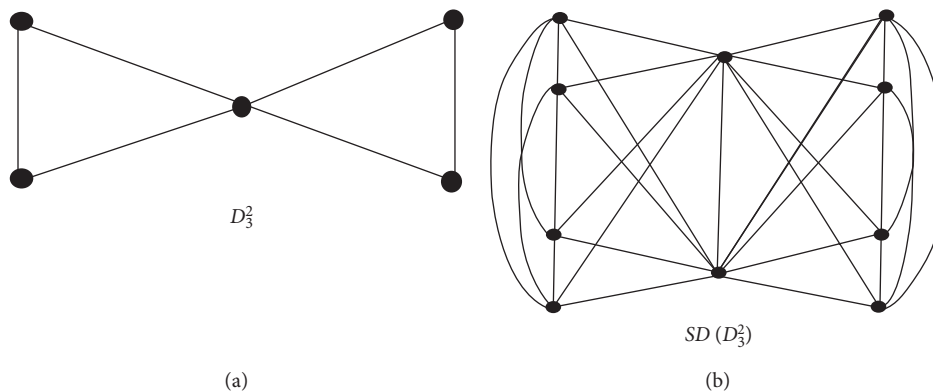
FIGURE 4: (a) Dutch Windmill graph  $D_3^2$ . (b). Strong double graph of Dutch Windmill graph  $D_3^p$ .

TABLE 3: Partitioning of edges.

$E[d_r, d_s]$	$E_{(5,5)}$	$E_{(5,4p+1)}$	$E_{(4p+1,4p+1)}$
Number of edges	$6p$	$8p$	$1$

*Proof.* By applying equation (4) and Table 3, we acquire the desired results, i.e.,

$$\begin{aligned}
 \text{ABC}[G] &= \sum_{rs \in E(G)} \sqrt{\frac{d_r + d_s - 2}{d_r d_s}}, \\
 \text{ABC}[\text{SD}(D_3^p)] &= |E_{(5,5)}| \sum_{rs \in E([D(D_3^p)])} \sqrt{\frac{d_r + d_s - 2}{d_r d_s}} \\
 &\quad + |E_{(5,4p+1)}| \sum_{rs \in E([D(D_3^p)])} \sqrt{\frac{d_r + d_s - 2}{d_r d_s}} \\
 &\quad + |E_{(4p+1,4p+1)}| \sum_{rs \in E([D(D_3^p)])} \sqrt{\frac{d_r + d_s - 2}{d_r d_s}}, \\
 \text{ABC}[\text{SD}(D_3^p)] &= 6p \sqrt{\frac{8}{25}} + 8p \sqrt{\frac{5 + (4p+1) - 2}{(5)(4p+1)}} + \sqrt{\frac{(8p+2) - 2}{(4p+1)^2}}, \\
 \text{ABC}[\text{SD}(D_3^p)] &= \frac{12p\sqrt{2}}{5} + 16p \sqrt{\frac{(p+1)}{(20p+5)}} + \frac{2\sqrt{2p}}{(4p+1)}.
 \end{aligned} \tag{34}$$

□

**Theorem 15.** Let  $SD(D_3^p)$  be the strong double graph of Dutch Windmill graph  $D_3^p$ . Then, the forgotten index of  $SD(D_3^p)$  is

$$F[SD(D_3^p)] = 128p^3 + 96p^2 + 524p + 2. \quad (35)$$

*Proof.* By applying equation (5) and Table 3, we acquire the desired results, i.e.,

$$\begin{aligned} F(G) &= \sum_{rs \in E(G)} (d_r^2 + d_s^2) \\ F[SD(D_3^p)] &= |E_{(5,5)}| \sum_{rs \in E[D(D_3^p)]} (d_r^2 + d_s^2) \\ &\quad + |E_{(5,4p+1)}| \sum_{rs \in E[D(D_3^p)]} (d_r^2 + d_s^2) \\ &\quad + |E_{(4p+1),(4p+1)}| \sum_{rs \in E[D(D_3^p)]} (d_r^2 + d_s^2) \\ &= 6p(50) + 8p(25 + 16p^2 + 8p + 1) \\ &\quad + 1[(16p^2 + 8p + 1) + (16p^2 + 8p + 1)], \\ F[SD(D_3^p)] &= 128p^3 + 96p^2 + 524p + 2. \end{aligned} \quad (36)$$

□

$$ISI[G] = \sum_{rs \in E(G)} \frac{1}{1/d_r + 1/d_s} = \sum_{rs \in E(G)} \frac{(d_r d_s)}{(d_r + d_s)},$$

$$ISI[SD(D_3^p)] = |E_{(5,5)}| \sum_{rs \in E[D(D_3^p)]} \frac{(d_r d_s)}{(d_r + d_s)} + |E_{(5,(4p+1))}| \sum_{rs \in E[D(D_3^p)]} \frac{(d_r d_s)}{(d_r + d_s)} + |E_{(4p+1),(4p+1)}| \sum_{rs \in E[D(D_3^p)]} \frac{(d_r d_s)}{(d_r + d_s)}, \quad (38)$$

$$ISI[SD(D_3^p)] = 6p \left[ \frac{25}{10} \right] + 8p \left[ \frac{(5)(4p+1)}{(5+4p+1)} \right] + \left[ \frac{(4p+1)(4p+1)}{(8p+2)} \right],$$

$$ISI[SD(D_3^p)] = 15p + 4p \left[ \frac{20p+5}{(2p+3)} \right] + \left[ \frac{(4p+1)^2}{2(4p+1)} \right].$$

**Theorem 17.** Let  $SD(D_3^p)$  be the strong double graph of Dutch Windmill graph  $D_3^p$ . Then, general inverse sum indeg index  $ISI_{(\alpha,\beta)}$  of  $SD(D_3^p)$  is

**Theorem 16.** Let  $SD(D_3^p)$  be the strong double graph of Dutch Windmill graph  $D_3^p$ . Then, the inverse sum indeg index of  $SD(D_3^p)$  is

$$ISI[SD(D_3^p)] = 15p + 4p \left[ \frac{20p+5}{(2p+3)} \right] + \left[ \frac{(4p+1)^2}{2(4p+1)} \right]. \quad (37)$$

*Proof.* By applying equation (6) and Table 3, we acquire the desired results, i.e.,

$$\begin{aligned} ISI_{(\alpha,\beta)}[SD(D_3^p)] &= 6p[25]^\alpha [10]^\beta \\ &\quad + 8p[20p+5]^\alpha [2(2p+3)]^\beta \\ &\quad + [(4p+1)^2]^\alpha [2(4p+1)]^\beta. \end{aligned} \quad (39)$$

□

*Proof.* By applying equation (7) and Table 3, we acquire the desired results, i.e.,

$$\begin{aligned}
 \text{ISI}_{(\alpha,\beta)}(G) &= \sum_{rs \in E(G)} [d_r d_s]^\alpha [d_r + d_s]^\beta \\
 &= |E_{(5,5)}| \sum_{rs \in E(G)} [d_r d_s]^\alpha [d_r + d_s]^\beta + |E_{(5,4p+1)}| \sum_{rs \in E(G)} [d_r d_s]^\alpha [d_r + d_s]^\beta + |E_{(4p+1),(4p+1)}| \sum_{rs \in E(G)} [d_r d_s]^\alpha [d_r + d_s]^\beta \\
 &= 6p[25]^\alpha [10]^\beta + 8p[(5)(4p+1)]^\alpha [4p+6]^\beta + [(4p+1)^2]^\alpha [(4p+1) + (4p+1)]^\beta \\
 \text{ISI}_{(\alpha,\beta)}[\text{SD}(D_3^p)] &= 6p[25]^\alpha [10]^\beta + 8p[20p+5]^\alpha [2(2p+3)]^\beta + [(4p+1)^2]^\alpha [2(4p+1)]^\beta.
 \end{aligned} \tag{40}$$

**Theorem 18.** Let  $\text{SD}(D_3^p)$  be the strong double graph of Dutch Windmill graph  $D_3^p$ . Then, the first multiplicative-Zagreb index of  $\text{SD}(D_3^p)$  is

$$\text{PM}_1[\text{SD}(D_3^p)] = 15360p^4 + 26880p^3 + 5760p^2. \tag{41}$$

*Proof.* By applying equation (10) and Table 3, we acquire the desired results, i.e.,

$$\begin{aligned}
 \text{PM}_1[G] &= \prod_{rs \in E(G)} (d_r + d_s), \\
 \text{PM}_1[\text{SD}(D_3^p)] &= |E_{(5,5)}| \prod_{rs \in E[D(D_3^p)]} (d_r + d_s) \\
 &\quad \times |E_{(5,4p+1)}| \prod_{rs \in E[D(D_3^p)]} (d_r + d_s) \\
 &\quad \times |E_{(4p+1,4p+1)}| \prod_{rs \in E[D(D_3^p)]} (d_r + d_s), \\
 \text{PM}_1[\text{SD}(D_3^p)] &= 6p(10) \times 16p(2p+3) \times (8p+2), \\
 \text{PM}_1[\text{SD}(D_3^p)] &= 15360p^4 + 26880p^3 + 5760p^2.
 \end{aligned} \tag{42}$$

**Theorem 19.** Let  $\text{SD}(D_3^p)$  be the strong double graph of Dutch Windmill graph  $D_3^p$ . Then, the second multiplicative-Zagreb index of  $\text{SD}(D_3^p)$  is

$$\text{PM}_2[\text{SD}(D_3^p)] = (4p+1)^2(24000p^3 + 6000p^2). \tag{43}$$

*Proof.* By applying equation (9) and Table 3, we acquire the desired results, i.e.,

$$\begin{aligned}
 \text{PM}_2[G] &= \prod_{rs \in E(G)} (d_r \cdot d_s), \\
 \text{PM}_2[\text{SD}(D_3^p)] &= |E_{(5,5)}| \prod_{rs \in E[D(D_3^p)]} (d_r \cdot d_s) \\
 &\quad \times |E_{(5,4p+1)}| \prod_{rs \in E[D(D_3^p)]} (d_r \cdot d_s) \\
 &\quad \times |E_{(4p+1),(4p+1)}| \prod_{rs \in E[D(D_3^p)]} (d_r \cdot d_s), \\
 \text{PM}_2[D(D_3^p)] &= 6p(25) \times 40p(4p+1) \times (4p+1)^2, \\
 \text{PM}_2[\text{SD}(D_3^p)] &= (4p+1)^2(24000p^3 + 6000p^2).
 \end{aligned} \tag{44}$$

**Theorem 20.** Let  $\text{SD}(D_3^p)$  be the strong double graph of Dutch Windmill graph  $D_3^p$ . Then, the  $\text{GA}_5$  index of  $\text{SD}(D_3^p)$  is

$$\text{GA}_5[\text{SD}(D_3^p)] = \frac{2p(48p+27+4\sqrt{8p(24p+52)+17})}{16p+9}. \tag{45}$$

*Proof.* We split the edges of  $[\text{SD}(D_3^p)]$  into those of the type  $E[S_r, S_s]$  in which “ $rs$ ” is an edge.  $[\text{SD}(D_3^p)]$  contains edges of the type  $E_{(8p+17,8+17)}$ ,  $E_{(8p+17,24p+1)}$ , and  $E_{(24p+1,24p+1)}$ , and Table 4 presents the edges of these types.

By applying equation (11) and Table 4, we acquire the desired results, i.e.,

$$\begin{aligned}
 GA_5(G) &= \sum_{rs \in E(G)} \frac{2\sqrt{S_r \times S_s}}{S_r + S_s}, \\
 GA_5[SD(D_3^p)] &= |E_{(8p+17, 8p+17)}| \sum_{rs \in E[D(D_3^p)]} \frac{2\sqrt{S_r \times S_s}}{S_r + S_s} \\
 &\quad + |E_{(8p+17, 24p+1)}| \sum_{rs \in E[D(D_3^p)]} \frac{2\sqrt{S_r \times S_s}}{S_r + S_s} + |E_{(24p+1, 24p+1)}| \sum_{rs \in E[D(D_3^p)]} \frac{2\sqrt{S_r \times S_s}}{S_r + S_s}, \quad (46) \\
 &= 6p \frac{2\sqrt{(8p+17)^2}}{16p+34} + 8p \frac{2\sqrt{(8p+17)(24p+1)}}{32p+18} + (1) \frac{2\sqrt{(24p+1)^2}}{48p+2} \\
 GA_5[SD(D_3^p)] &= \frac{2p(48p+27+4\sqrt{8p(24p+52)+17})}{16p+9}.
 \end{aligned}$$

**Theorem 21.** Let  $SD(D_3^p)$  be the strong double graph of Dutch Windmill graph  $D_3^p$ . Then, the fourth atom bond connectivity index of  $SD(D_3^p)$  is

$$\begin{aligned}
 ABC_4[SD(D_3^p)] &= \frac{12p\sqrt{4p+8}}{8p+17} + 32p \left[ \sqrt{\frac{2p+1}{8p(24p+52)+17}} \right] \\
 &\quad + \frac{4\sqrt{3p}}{24p+1}. \quad (47)
 \end{aligned}$$

*Proof.* By applying equation (11) and Table 4, we acquire the desired results, i.e., □

$$\begin{aligned}
 ABC_4(G) &= \sum_{rs \in E(G)} \sqrt{\frac{S_r + S_s - 2}{S_r \times S_s}} \\
 &= |E_{(8p+17, 8p+17)}| \sum_{rs \in E[D(D_3^p)]} \sqrt{\frac{S_r + S_s - 2}{S_r \times S_s}} \\
 &\quad + |E_{(8p+17, 24p+1)}| \sum_{rs \in E[D(D_3^p)]} \sqrt{\frac{S_r + S_s - 2}{S_r \times S_s}} + |E_{(24p+1, 24p+1)}| \sum_{rs \in E[D(D_3^p)]} \sqrt{\frac{S_r + S_s - 2}{S_r \times S_s}}, \quad (48) \\
 ABC_4[SD(D_3^p)] &= 6p \left[ \sqrt{\frac{16p+32}{(8p+17)^2}} \right] + 8p \left[ \sqrt{\frac{32p+16}{(8p+17)(24p+1)}} \right] + \left[ \sqrt{\frac{48p}{(24p+1)^2}} \right], \\
 ABC_4[SD(D_3^p)] &= \frac{12p\sqrt{4p+8}}{8p+17} + 32p \left[ \sqrt{\frac{2p+1}{8p(24p+52)+17}} \right] + \frac{4\sqrt{3p}}{24p+1}.
 \end{aligned}$$

□

TABLE 4: Partitioning of edges.

$E[S_r, S_s]$	$E_{(8p+17, 8p+17)}$	$E_{(8p+17, 24p+1)}$	$E_{(24p+1, 24p+1)}$
Number of edges	$6p$	$8p$	1

#### 4. Conclusion

The topological indices provide key information about a molecule's chemical structure and chemical activity, for example, in order to derive quantitative structure-activity relationships (QSARs). These models are derived by applying statistical measures of the molecular structure or properties with descriptors representative of the biological activity (including undesirable side effects) of chemicals (drugs, toxicants, and environmental pollutants). Drug discovery, lead optimization, and toxicity prediction are just a few of the areas in which QSAR is being used. Our purpose in this article was to construct two new graphs from the Dutch Windmill graph using two graph operations, namely, double graph and strong double graph. After that, we calculated some vertex-based topological indices of double graph and strong double graph of the Dutch Windmill graph. Many graph theory applications rely on graph operations. We recommend the readers to compute the topological indices for double and strong double graphs of some other classes of graphs or networks.

#### Data Availability

No data were used in this manuscript.

#### Conflicts of Interest

The authors declare that they have no conflicts of interest.

#### References

- [1] R. J. Wilson, *Introduction to Graph Theory*, John Wiley and Sons, New York, NY, USA, 1986.
- [2] G. Chartrand, L. Lesniak, and P. Zhang, *Graphs & Digraphs*, 640, 6th edition, Chapman and Hall/CRC, Boca Raton, FL, USA, 2015.
- [3] D. K. Ch, M. Marjan, M. Emina, and M. Igor, "Bonds for symmetric division deg index of graphs," *Faculty of Sciences and Mathematics*, vol. 33, no. 3, pp. 638–698, 2019.
- [4] M. Alaeiyan, M. S. Sardar, S. Zafar, Z. Zahid, and M. R. Farahani, "Computation of topological indices of line graph of Jahangir graph," *International Journal of Applied Mathematics and Machine Learning*, vol. 8, no. 2, pp. 91–107, 2018.
- [5] G. Hong, Z. Gu, M. Javaid, H. M. Awais, and M. K. Siddiqui, "Degree-based topological invariants of metal-organic networks," *IEEE access*, vol. 8, pp. 68288–68300, 2020.
- [6] M. Hu, H. Ali, M. A. Binyamin, B. Ali, and J.-B. Liu, "On distance-based topological descriptors of chemical interconnection networks," *Journal of Mathematics*, vol. 10, 2021.
- [7] A. Yousaf and M. Nadeem, "An efficient technique to construct certain counting polynomials and related topological indices for 2D-planar graphs," *Journal of the International Society for Polycyclic Aromatic Compounds*, vol. 14, 2021.
- [8] S. Hayat and M. Imran, "Computation of topological indices of certain networks," *Applied Mathematics and Computation*, vol. 240, pp. 213–228, 2014.
- [9] H. Wiener, "Structural determination of paraffin boiling points," *Journal of the American Chemical Society*, vol. 69, no. 1, pp. 17–20, 1947.
- [10] B. Furtula and D. Vukicevic, "Topological index based on the ratios of geometrical and arithmetical mean of end-vertex degrees of edge," *Journal of Mathematical Chemistry*, vol. 46, no. 4, pp. 1369–1376, 2009.
- [11] K. Das, I. Gutman, and B. Furtula, "On atom-bond connectivity index," *Filomat*, vol. 26, no. 4, pp. 733–738, 2012.
- [12] B. Furtula and I. Gutman, "A forgotten topological index," *Journal of Mathematical Chemistry*, vol. 53, no. 4, pp. 1184–1190, 2015.
- [13] K. Pattabiraman, "Inverse sum indeg index of graphs," *AKCE International Journal of Graphs and Combinatorics*, vol. 15, no. 2, pp. 155–167, 2018.
- [14] P. Ali, S. A. K. Kirmani, O. Al Rugaie, and F. Azam, "Degree-based topological indices and polynomials of hyaluronic acid-curcumin conjugates," *Saudi Pharmaceutical Journal*, vol. 28, no. 9, pp. 1093–1100, 2020.
- [15] R. Kazemi, "Note on the multiplicative Zagreb indices," *Discrete Applied Mathematics*, vol. 198, pp. 147–154, 2016.
- [16] M. Eliasi, A. Iranmanesh, and I. Gutman, "Multiplicative versions of first zagreb index," *MATCH Communications in Mathematical and in Computer Chemistry*, vol. 68, no. 1, pp. 217–230, 2012.
- [17] M. R. Farahani, "Computing GA\_5 index of armchair polyhex nonotube," *Le Matematiche*, vol. 2, pp. 69–76, 2014.
- [18] M. Ghorbani and M. A. Hosseinzadeh, "Computing ABC4 index of nanostar dendrimers," *Optoelectronics and Advanced Materials-Rapid Communications*, vol. 4, pp. 1419–1422, 2010.
- [19] Y. Kins, M. K. Kaabar, M. M. A. A. Shamiri, and R. C. Thivayarathi, "Radial radio number of hexagonal and its derived networks," *International journal of mathematics mathematical sciences*, vol. 2021, Article ID 5101021, 8 pages, 2021.
- [20] M. An and L. Xiong, "Some results on the inverse sum indeg index of a graph," *Information Processing Letters*, vol. 134, pp. 42–46, 2018.
- [21] M. K. Siddiqui, S. Manzoor, S. Ahmad, and M. K. Kaabar, "On computation and analysis of entropy measures for crystal structures," *Mathematical Problems in Engineering*, vol. 2021, Article ID 9936949, 16 pages, 2021.
- [22] K. Yenokey and M. K. Kaabar, "The bounds of the distance two labelling and radio labelling of nanostar tree dendrimer," *Telkomnika Telecommunication, Computing, Electronics And Control*, vol. 18, p. 8, 2020.
- [23] M. S. Sardar, S. Zafar, and Z. Zahid, "Certain topological indices of line graph of Dutch Windmill graphs," *Southeast Asian Bulletin of Mathematics*, vol. 44, no. 1, pp. 119–129, 2020.
- [24] E. Munarini, C. P. Cippo, A. Scagliola, and N. Z. Salvi, "Double graphs," *Discrete Mathematics*, vol. 308, no. 2-3, pp. 242–254, 2008.

- [25] T. A. Chishti, H. A. Ganie, and S. Pirzada, "Properties of strong double graphs," *Journal of Discrete Mathematical Sciences and Cryptography*, vol. 17, no. 4, pp. 311–319, 2014.

## Research Article

# Eccentricity-Based Topological Invariants of Dominating David-Derived Networks

Muhammad Imran <sup>1</sup>, Mian Muhammad Zobair <sup>2</sup>, and Hani Shaker <sup>3</sup>

<sup>1</sup>Department of Mathematical Sciences, United Arab Emirates University, Al Ain, UAE

<sup>2</sup>Department of Mathematics and Statistics, Riphah International University Islamabad, Rawalpindi, Pakistan

<sup>3</sup>Department of Mathematics, COMSATS University Islamabad, Lahore Campus, Lahore, Pakistan

Correspondence should be addressed to Muhammad Imran; [imrandhab@gmail.com](mailto:imrandhab@gmail.com)

Received 1 June 2021; Revised 29 September 2021; Accepted 30 September 2021; Published 22 October 2021

Academic Editor: Andrea Mastinu

Copyright © 2021 Muhammad Imran et al. This is an open access article distributed under the Creative Commons Attribution License, which permits unrestricted use, distribution, and reproduction in any medium, provided the original work is properly cited.

A topological index is a numerical descriptor of the molecular structure based on certain topological features of the corresponding molecular graph. Topological indices are scientific contemplations of a graph that outline its subatomic topology and are graph-invariant. In a QSAR/QSPR study, topological indices are utilized to anticipate the physico-concoction resources and bioactivity of compounds. In this paper, we study some distance-based topological indices such as eccentric connectivity index (ECI), total eccentricity index (TEI), and eccentricity-based Zagreb index for dominating David-derived networks (DD network) and provide exact formulae of the said indices. These outcomes are valuable to organize the science of hidden topologies of this network.

## 1. Introduction and Preliminary Results

Graph theory has given chemists a decent variety of helpful apparatuses in terms of topological indices. Atoms and molecular compounds are regularly displayed by a molecular graph. An atomic graph is a delineation of the basic equation of a synthetic compound as far as graph hypothesis whose vertices deliver a connection between the molecules of compound and edges relate to synthetic bonds. In the QSAR/QSPR contemplate, topological files are utilized to anticipate physico-concoction properties and bioactivity of the substance mixes. A topological index is a number related with a graph that portrays the topology of diagram; furthermore, it is invariant under graph automorphism. Distance-based topological records are of incredible significance and assume an essential part in concoction diagram hypothesis and especially in hypothetical science.

Let  $G$  be an  $n$ -vertex molecular graph with vertex set  $V(G) = \{v_1, v_2, \dots, v_n\}$  and edge set  $E(G)$ . The vertices of  $G$  correspond to atoms, and an edge between two vertices corresponds to the chemical bond between these atoms. For

a given vertex  $u \in V(G)$ , the eccentricity  $\varepsilon(u)$  is defined as the largest distance between  $u$  and any other vertex  $v$  in  $G$ .

The eccentric-connectivity index of graph  $G$  is denoted as  $\xi(G)$ . It is a distance-based topological index and is defined as

$$\xi(G) = \sum_{u \in V(G)} \deg(u)\varepsilon(u). \quad (1)$$

When the vertices' degrees are not taken into account, we obtain the total eccentricity index of graph  $G$  defined by

$$\zeta(G) = \sum_{u \in V(G)} (\varepsilon u). \quad (2)$$

A new version of Zagreb indices of a molecular graph  $G$  defined by Ghorbani and Hosseinzadeh [1] in terms of eccentricity are expressed as follows:

$$\begin{aligned} M_1^*(G) &= \sum_{v \in V(G)} (\varepsilon(v))^2, \\ M_2^*(G) &= \sum_{uv \in E(G)} (\varepsilon u)\varepsilon(v). \end{aligned} \quad (3)$$

This paper first contains a little insight of the graph and algorithm of dominating David-derived networks. Then, the labeling of critical vertices of dominating David-derived network is provided. Then, computation of eccentricities of vertices is given. In the last segment, we process and determine some distance-based topological indices, such as eccentric-connectivity index (ECI), total-eccentricity index (TEI), and eccentricity-based Zagreb index of dominating David-derived DDD[ $n$ ]. For some recent results, see [2, 3].

## 2. Algorithm and Insight into Dominating David-Derived Networks

Simonraj [4] gave a construction algorithm for the dominating David-derived networks, and DDD originated from the graph of star of David. The algorithm for constructing the DDD network (of dimension  $n$ ) is as follows.

Consider a honeycomb network HC[ $n$ ] of dimension  $n$ . Subdivide all edges of HC[ $n$ ] by inserting a new vertex in each edge. Then, connect every pair of vertices lying at distance four in each hexagon. After removing the original hexagonal network from the resulting graph, subdivide each horizontal edge into two edges to obtain the dominating David-derived network DDD[ $n$ ] of dimension  $n$ .

The graph DDD[1] is shown in Figure 1(a) is obtained from the star of David as described in [4]. The graphs DDD[3] and DDD[5] constructed from the same algorithm are shown in Figures 1(b) and 1(c).

By an easy calculation, one can find the order and size of DDD[ $n$ ], i.e.,  $|V(\text{DDD}[n])| = 15n^2 - 3n + 6$  and  $|E(\text{DDD}[n])| = 33n^2 - 19n + 11$ .

Imran et al. [5, 6] studied the general Randić index, ABC index, and GA index of DDD networks. Liu et al. [7] studied some degree-based indices of David-derived networks DD[ $n$ ], dominating David-derived networks DDD[ $n$ ], and regular triangulene silicate network RTSL[ $n$ ]. Farooq et al. [8, 9] studied some degree-based indices of some interconnection networks. Baig et al. [10] studied the Randić index, ABC index, and GA index of DDD networks. Dimitris [11] has also studied star of David which is a family of interwoven molecular inorganic knots, prepared by the employment of naphthalene-2,3-diol in 3  $d/4f$ -metal cluster chemistry. David-derived networks are being investigated for possible uses in information sciences and other fields. They have huge range of applications in nanoscience, biology, and chemistry. Bajaj et al. [12, 13] studied topological models for the prediction of anti-HIV activity of acylthiocarbamates. For more detailed study on the indices, see [14–18].

In this paper, we compute and derive closed analytical formulae for the distance-based topological indices such as ECI, TEI, and eccentricity-based Zagreb indices of some families of DD networks discussed in Section 4. The ECI gives the best forecast exactness rate with contrast to different indices used in different natural exercises, for example, anti-inflammatory activity, anticonvulsant

activity, and diuretic activity. Thus, these indices have the potential to be used in QSAR/QSPR studies. The obtained results are useful in to explore the certain physico-chemical properties of these chemical networks, for example, anti-inflammatory activity, anticonvulsant activity, and diuretic activity.

## 3. Main Results

**3.1. Labeling of Critical Vertices in Dominating David-Derived Networks.** Using the symmetry of the graphs of dominating David-derived networks DDD[ $n$ ], it is suffice to calculate the eccentricities of only one quadrant of DDD[ $n$ ]. The vertices of one quadrant of DDD[ $n$ ] are divided into six groups, namely,  $a, b, \dots, f$ . Each vertex of group  $x$ , where  $x$  is any of  $a, b, \dots, f$ , is represented by  $x_{i,j}$ , where  $i$  refers to the column and  $j$  refer to the position of vertex  $x$  in each column. Here, the index  $i$  increases towards the left and  $j$  increases downwards. For  $n = 3$ , one quadrant of DDD (2) is labeled in Figure 2.

There are some vertices in DDD[ $n$ ] which exhibit different patterns of eccentricities as compared to the eccentricities of other vertices. These vertices are referred to as critical vertices of the graph DDD[ $n$ ]. Thus, the vertices in one quadrant of DDD[ $n$ ] are further divided into three regions by the vertical axis represented by a dotted line in Figure 2. Regions I and II, respectively, contain the vertices lying above and below the critical vertices and region III contains the rest of the vertices. The critical vertices of the graph DDD[ $n$ ] are included in region I. For  $n = 3$  and 5, the edges incident with the critical vertices are represented by bold lines in Figure 2. The three regions are also labeled in the same figure.

**3.2. Eccentricities of Dominating David-Derived Network DDD[ $n$ ].** The grid vertices of DDD[ $n$ ] are the vertices of the underline grid represented by bold edges in Figure 3. Note that the grid vertices of DDD[ $n$ ] only belong to the groups  $a, c$ , and  $e$ . Let  $a_{i,k}$  (resp.,  $c_{i,k}$  and  $e_{i,k}$ ) denotes a grid vertex in the  $i^{\text{th}}$  column of group  $a$  (resp.,  $c$  and  $e$ ), where  $k$  denotes the position of grid vertex in column  $i$ . For  $n = 5$ , the grid vertices lying in region II of DDD[5] are also shown in Figure 2. The eccentricities of vertices of DDD[ $n$ ] lying in region II are calculated by the help of eccentricities of grid vertices. The eccentricities of vertices of DDD[ $n$ ] lying in region II are given by the following cases.

*Case 1.* When  $n \equiv 1 \pmod{4}$ . The eccentricities of grid vertices  $a_{i,k}$ 's are  $\varepsilon(a_{i,(3n/2)+(9i/2)+3k-7}) = 6n + 6i + 4k - 12$  for  $i \equiv 1 \pmod{2}$ ,  $\varepsilon(a_{i,(3n/2)+(9i/2)+3k-(13/2)}) = 6n + 6i + 4k - 12$  for  $i \equiv 0 \pmod{2}$ , where  $1 \leq i \leq (n-1)/4 + 1$ ,  $1 \leq k \leq n/2 - 2i + 5/2$ . The eccentricities of  $a_{i,k}$ 's above and below grid vertices of type  $a$  are given by  $\varepsilon(a_{i,(3n/2)+(9i/2)+3k-8}) = 6n + 6i + 4k - 13$ , where  $2 \leq k \leq (n/2) - 2i + (5/2)$  and  $1 \leq i \leq (n-1)/4$   $\varepsilon(a_{i,(3n/2)+(9i/2)+3k-6}) = 6n + 6i + 4k - 10$ , where  $1 \leq k \leq n/2 - 2i + 3/2$  and  $1 \leq i \leq (n-1)/4$

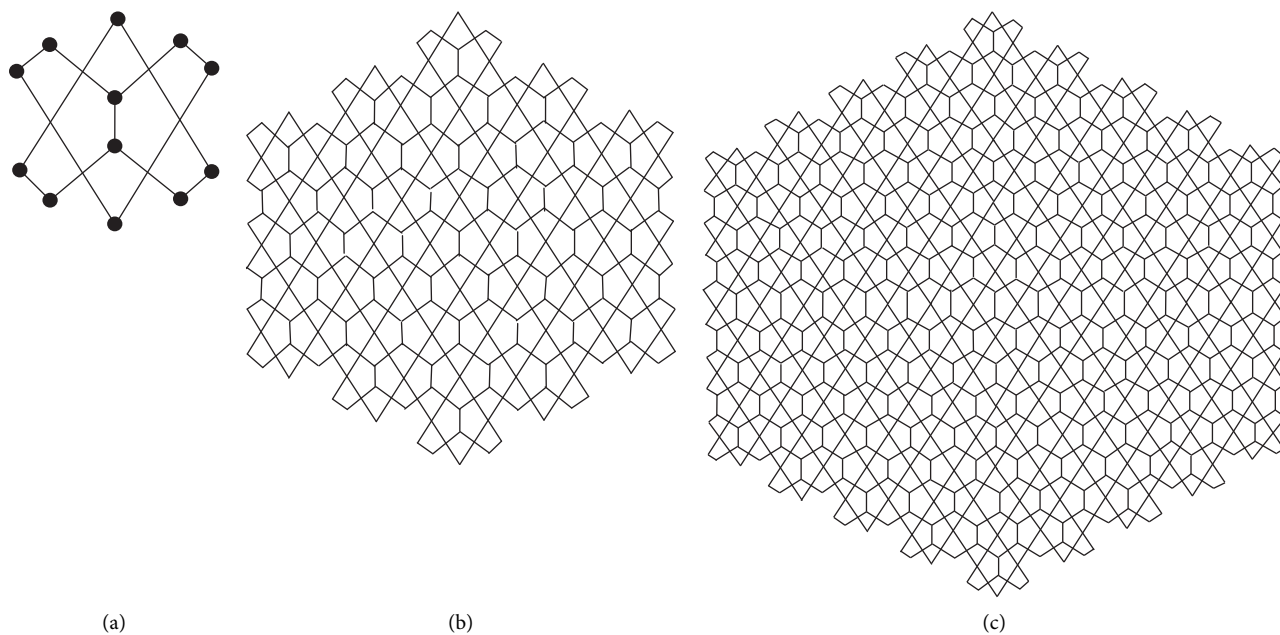


FIGURE 1: (a) DDD(1), (b) the graph DDD(3) of dominating David-derived networks for  $n = 3$ , (c) DDD(5).

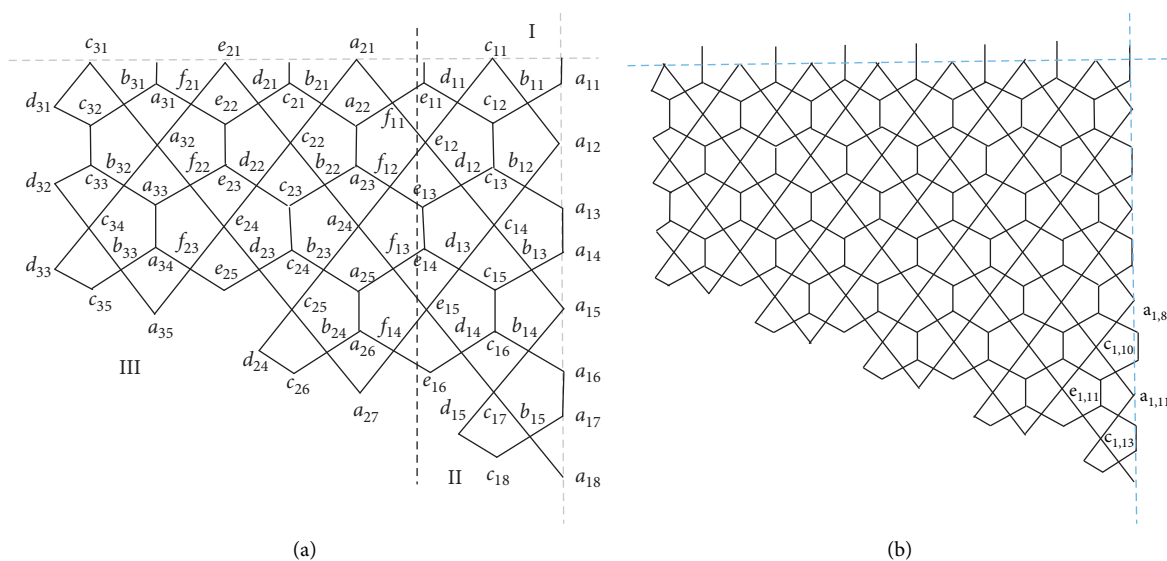


FIGURE 2: The vertex labeling of the dominating David-derived network DDD(3) (a) and grid representation of DDD(5) (b).

The eccentricities of grid vertices  $c_{i,k}$ 's are  $\varepsilon(c_{i,(3n/2)+(9i/2)+3k-5}) = 6n + 6i + 4k - 10$  for  $i \equiv 1 \pmod{2}$ ,  $\varepsilon(c_{i,(3n/2)+(9i/2)+3k-(13/2)}) = 6n + 6i + 4k - 10$  for  $i \equiv 0 \pmod{2}$ , where  $1 \leq i \leq (n-1)/4$ ,  $1 \leq k \leq n/2 - 2i + 3/2$ . The eccentricities of  $c_{i,k}$ 's above and below grid vertices of type  $c$  are given by  $\varepsilon(c_{i,(3n/2)+(9i/2)+3k-4}) = 6n + 6i + 4k - 8$ , where  $1 \leq k \leq n/2 - 2i + 3/2$  and  $1 \leq i \leq (n-1)/4$   $\varepsilon(c_{i,(3n/2)+(9i/2)+3k-6}) = 6n + 6i + 4k - 11$ , where  $2 \leq k \leq n/2 - 2i + 3/2$  and  $1 \leq i \leq (n-1)/4$ .

The eccentricities of grid vertices  $e_{i,k}$ 's are  $\varepsilon(e_{i,(3n/2)+(9i/2)+3k-4}) = 6n + 6i + 4k - 8$  for  $i \equiv 1 \pmod{2}$ ,  $\varepsilon(e_{i,(3n/2)+(9i/2)+3k-3}) = 6n + 6i + 4k - 8$  for  $i \equiv 0 \pmod{2}$ , where  $1 \leq i \leq (n-1)/4$ ,  $1 \leq k \leq n/2 - 2i + 1/2$ . The eccentricities of  $e_{i,k}$ 's above and below grid vertices of type  $e$  are given by  $\varepsilon(e_{i,(3n/2)+(9i/2)+3k-5}) = 6n + 6i + 4k - 9$ , where  $2 \leq k \leq n/2 - 2i + 1/2$  and  $1 \leq i \leq (n-1)/4$   $\varepsilon(e_{i,(3n/2)+(9i/2)+3k-3}) = 6n + 6i + 4k - 6$ , where  $1 \leq k \leq n/2 - 2i + 1/2$  and  $1 \leq i \leq (n-1)/4$ .

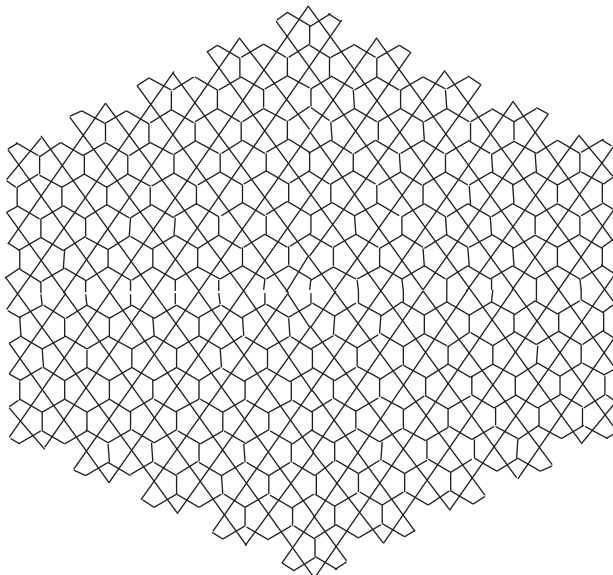


FIGURE 3: The grid vertex labeling of the dominating David-derived network DDD(5) along with critical line in bold.

Similarly, eccentricities of  $b_{i,k}$ ,  $d_{i,k}$ , and  $f_{i,k}$  in the  $i^{\text{th}}$  column are  $\varepsilon(b_{i,n+3i+k-3}) = 6n + 6i + 2k - 9$ , where  $1 \leq i \leq (n-1)/4$ ,  $1 \leq k \leq n - 4i + 3$ .  $\varepsilon(d_{i,n+3i+k-2}) = 6n + 6i + 2k - 7$ , where  $1 \leq i \leq (n-1)/4$ ,  $1 \leq k \leq n - 4i + 2$ .  $\varepsilon(f_{i,n+3i+k-1}) = 6n + 6i + 2k - 5$ , where  $1 \leq i \leq (n-1)/4$ ,  $1 \leq k \leq n - 4i$ .

Case 2. When  $n \equiv 3 \pmod{4}$ , the eccentricities of grid vertices  $a_{i,k}$ 's are given by  $\varepsilon(a_{i,(3n/2)+(9i/2)+3k-7}) = 6n + 6i + 4k - 12$  for  $i \equiv 1 \pmod{2}$ ,  $\varepsilon(a_{i,(3n/2)+(9i/2)+3k-(13/2)}) = 6n + 6i + 4k - 12$  for  $i \equiv 0 \pmod{2}$ , where  $1 \leq i \leq (n-3/4) + 1$ ,  $1 \leq k \leq (n/2) - 2i + (5/2)$ . The eccentricities of  $a_{i,k}$ 's above and below the grid vertices of type  $a$  are  $\varepsilon(a_{i,(3n/2)+(9i/2)+3k-8}) = 6n + 6i + 4k - 13$ , where  $2 \leq k \leq n/2 - 2i + (5/2)$  and  $1 \leq i \leq ((n-3)/4)$   $\varepsilon(a_{i,(3n/2)+(9i/2)+3k-6}) = 6n + 6i + 4k - 10$ , where  $1 \leq k \leq n/2 - 2i + 3/2$  and  $1 \leq i \leq (n-3)/4$ .

The eccentricities of grid vertices  $c_{i,k}$ 's are  $\varepsilon(c_{i,(3n/2)+(9i/2)+3k-5}) = 6n + 6i + 4k - 10$  for  $i \equiv 1 \pmod{2}$ ,  $\varepsilon(c_{i,(3n/2)+(9i/2)+3k-13/2}) = 6n + 6i + 4k - 10$  for  $i \equiv 0 \pmod{2}$ , where  $1 \leq i \leq (n-3)/4$ ,  $1 \leq k \leq n/2 - 2i + 3/2$ . The eccentricities of  $c_{i,k}$ 's above and below the grid vertices of type  $c$  are  $\varepsilon(c_{i,(3n/2)+(9i/2)+3k-4}) = 6n + 6i + 4k - 8$ , where  $1 \leq k \leq n/2 - 2i + 3/2$  and  $1 \leq i \leq (n-3)/4$   $\varepsilon(c_{i,(3n/2)+(9i/2)+3k-6}) = 6n + 6i + 4k - 11$ , where  $2 \leq k \leq (n/2) - 2i + (3/2)$  and  $1 \leq i \leq (n-3)/4$ .

The eccentricities of grid vertices  $e_{i,k}$ 's are  $\varepsilon(e_{i,(3n/2)+(9i/2)+3k-4}) = 6n + 6i + 4k - 8$  for  $i \equiv 1 \pmod{2}$ ,  $\varepsilon(e_{i,(3n/2)+(9i/2)+3k-3}) = 6n + 6i + 4k - 8$  for  $i \equiv 0 \pmod{2}$ , where  $1 \leq i \leq (n-3)/4$ ,  $1 \leq k \leq n/2 - 2i + 1/2$ . The eccentricities of  $e_{i,k}$ 's above and below the grid vertices are  $\varepsilon(e_{i,(3n/2)+(9i/2)+3k-5}) = 6n + 6i + 4k - 9$ , where  $2 \leq k \leq n/2 - 2i + 1/2$  and  $1 \leq i \leq (n-3)/4$   $\varepsilon(e_{i,(3n/2)+(9i/2)+3k-3})$

$= 6n + 6i + 4k - 6$ , where  $1 \leq k \leq n/2 - 2i + 1/2$  and  $1 \leq i \leq (n-3)/4$ .

Similarly, eccentricities of  $b_{i,k}$ ,  $d_{i,k}$ , and  $f_{i,k}$  in the  $i^{\text{th}}$  columns are  $\varepsilon(b_{i,n+3i+k-3}) = 6n + 6i + 2k - 9$ , where  $1 \leq i \leq (n-3)/4$ ,  $1 \leq k \leq n - 4i + 3$ ;  $\varepsilon(d_{i,n+3i+k-2}) = 6n + 6i + 2k - 7$ , where  $1 \leq i \leq (n-3)/4$ ,  $1 \leq k \leq n - 4i + 2$ ; and  $\varepsilon(f_{i,n+3i+k-1}) = 6n + 6i + 2k - 5$ , where  $1 \leq i \leq (n-3)/4$ ,  $1 \leq k \leq n - 4i$ .

### 3.3. Topological Invariants of DDD[n]

**Theorem 1.** The eccentric-connectivity index of David-derived networks DDD[n] for  $n \equiv 1 \pmod{4}$  and  $n \geq 1$  is given by

$$(-480n62 + 888n + 84) \left( \frac{1}{8}n + \frac{1}{2} \right). \quad (4)$$

*Proof.* Using symmetry of the network DDD[n], we use only one quadrant of DDD[n] as labeled in Figure 2. We take one representative from a set of vertices which has same degree and eccentricity. These representatives are labeled by  $a_i, b_i, c_i, d_i, e_i$ , and  $f_i$  for  $1 \leq i \leq n$  and shown in Table 1 with their eccentricities. Using Table 1, the ECI of DDD[n] for  $n \geq 1$  can be written as follows.

After simplification, we obtained the required result. This completes the proof.  $\square$

**Corollary 1.** The total-eccentricity index of DDD[n] David-derived networks for  $n \equiv 1 \pmod{4}$  is given by

$$\begin{aligned}
\xi(\text{DDD}[n]) = & \frac{755}{4} \left(\frac{1}{8}n + \frac{1}{2}\right)^3 + 504 \left(\frac{1}{4}n + \frac{3}{4}\right)^3 + \frac{112}{3} \left(\frac{1}{8}n + \frac{3}{8}\right)^3 + \frac{368}{3} \left(\frac{1}{8}n + \frac{7}{8}\right)^3 - 33n^2 - 48 \left(\frac{1}{2}n + \frac{1}{2}\right)^3 \\
& + \frac{1}{12} (3456n + 432) \left(\frac{1}{8}n\right)^2 + \frac{1}{12} (864n^2 + 432n - 696) \left(\frac{1}{8}n\right) \\
& \frac{1}{12} (864n - 432) \left(\frac{1}{2}n\right)^2 + \frac{1}{12} (1728n^2 - 1296n + 120) \left(\frac{1}{2}n\right) - \frac{2553}{2} + \\
& \frac{1}{12} (600n^2 - 3168n + 5464) \\
& \left(\frac{1}{8}n + \frac{7}{8}\right) + \frac{1}{12} (1488n - 5112) \left(\frac{1}{8}n + \frac{7}{8}\right)^2 \\
& + \frac{1}{12} (-1392n + 648) \left(\frac{1}{8}n + \frac{3}{8}\right)^2 + \frac{1}{12} (-192n^2 + 2160n - 176) \left(\frac{1}{8}n + \frac{3}{8}\right) + \frac{1}{12} (-864n - 1872) \left(\frac{1}{8}n + \frac{1}{2}\right)^2 \\
& + \frac{1}{12} (-1728n^2 + 3312n + 24) \left(\frac{1}{8}n + \frac{1}{2}\right) + \\
& \frac{1}{12} (3024n - 25236) \left(\frac{1}{4}n + \frac{3}{4}\right)^2 + \frac{1}{12} (-1512n^2 - 6228n + 33408) \left(\frac{1}{4}n + \frac{3}{4}\right) + \frac{1}{12} (432n + 648) \left(\frac{1}{2}n + \frac{1}{2}\right)^2 \\
& + \frac{1}{12} (864n^2 - 1728n + 408) \left(\frac{1}{2}n + \frac{1}{2}\right) \\
& - 96 \left(\frac{1}{2}n\right)^3 + 288 \left(\frac{1}{8}n\right)^3.
\end{aligned} \tag{5}$$

**Corollary 2.** *The first Zagreb-eccentricity index of DDD[n] David-derived networks for  $n \equiv 1 \pmod{4}$  is given by*

$$\begin{aligned}
M_1^*(\text{DDD}[n]) = & \frac{8224051}{16}n + \frac{8768419}{24}n^2 - \frac{4309975}{24}n^3 + \frac{1}{144} (2985984n^3 + 1244160n^2 - 1057536n \\
& - 138240) \left(\frac{1}{8}n\right)^3 + \frac{1}{144} (373248n^4 + 248832n^3 - 51840n^2 - 152064 + 260928) \left(\frac{1}{8}n\right)^2 \\
& \frac{1}{144} (11943936 + 995328) \left(\frac{1}{8}n\right)^5 + \frac{1}{144} (8957952n^2 + 1990656n - 1586304) \left(\frac{1}{8}n\right)^4 \\
& + \frac{1}{144} (1492992n^4 - 1492992n^3 - 109008n^2 1389312n - 85120) \left(\frac{1}{2}n\right)^2 + \frac{1}{144} (2985984n^4 \\
& - 74649604n^3 + 6220800n^2 - 2419200n + 313344) \left(\frac{1}{2}n\right) + \frac{1}{144} (-995328n - 995328) \left(\frac{1}{2}n\right)^5 \\
& + \frac{1}{144} (-1617408n^2 + 1244160n - 190080) \left(\frac{1}{2}n\right)^4 + \frac{1}{144} (1492992n^3 - 4976640n^2 + \\
& 5142528n - 1029888) \left(\frac{1}{2}n\right)^3 + \frac{1}{144} (-401472n^4 + 5172480n^3 - 25766016n^2 + 50038656n - 32767296) \left(\frac{1}{8}n + \frac{7}{8}\right) \\
& + \frac{1}{144} (200736n^4 - 4765248n^3 + 34604160n^2 - 90555840n \\
& + 76006112) \left(\frac{1}{8}n + \frac{7}{8}\right)^2 + \frac{1}{144} (1452672n^3 - 20433792n^2 + 80581632n - 92178048) \left(\frac{1}{8}n + \frac{7}{8}\right)^3 \\
& + \frac{1}{144} (6033408n - 21371904) \left(\frac{1}{8}n + \frac{7}{8}\right)^5 + \frac{1}{144} (-4464768n^2 35209728n \\
& + 61509056) \left(\frac{1}{8}n + \frac{7}{8}\right)^4 + \frac{1}{144} (-41472n + 131328) \left(\frac{1}{2}n\right)^2
\end{aligned}$$

$$\begin{aligned}
& + (-41472n^2 + 179712n - 153216)\left(\frac{1}{2}n\right) + (-2426112n^5 + 622080n^4 + 41615424n^3) \\
& - 107628480n^2 + 220515552n - 237895776\left(\frac{1}{4}n + \frac{3}{4}\right) + \frac{1}{144}\left(-41472\left(\frac{1}{2}n\right)^2 + -41472n\right) \\
& + 48384\left(\frac{1}{2}n\right) + 1446336n^4 - 31181760n^3 + 107639280n^2 - 319616928n + 435719808) \\
& \left(\frac{1}{4}n + \frac{3}{4}\right)^2 + \frac{1}{144}(7651584n^2 - 83420928n + 228655440)\left(\frac{1}{4}n + \frac{3}{4}\right)^4 + \frac{1}{144}(7216128n^3 - 47138112n^2 + 231435360n \\
& - 422601408)\left(\frac{1}{4}n + \frac{3}{4}\right)^3 + \frac{1}{144}(11943936n - 65380608)\left(\frac{1}{4}n + \frac{3}{4}\right)^5 + \frac{1}{144}((995328n^2 \\
& - 1990656n - 1078272)\left(\frac{1}{2}n\right)^3 + (-746496n^3 + 1866240n^2 + 20736n - 300672)\left(\frac{1}{2}n\right)^2 \\
& + (-1492992n^4 + 4478976n^3 - 2032128n^2 - 248832n + 622080)\left(\frac{1}{2}n\right) - 1605888n^4 \\
& + 4773888n^3 - 2711040n^2 - 905472n - 1027200)\left(\frac{1}{8}n + \frac{3}{8}\right) + \frac{1}{144}((497664n + 1741824)\left(\frac{1}{2}n\right)^3 \\
& + (-373248n^2 - 1119744n + 611712)\left(\frac{1}{2}n\right)^2 \\
& + (-746496n^3 - 1866240n^2 + 2260224n - 1067904)\left(\frac{1}{2}n\right) \\
& + 859392n^4 - 3377664n^3 - 354048n^2 + 4248576 + 3335296)\left(\frac{1}{8}n + \frac{3}{8}\right)^2 + \frac{1}{144}\left(-663552\left(\frac{1}{2}n\right)^3 + (497664n - 248832)\left(\frac{1}{2}n\right)^2 \right. \\
& \left. + (995328n^2 - 995328n + 414720)\left(\frac{1}{2}n\right) + 423936n^3 + 2784768n^2 - 5166336n - 5852544\right) \\
& \left(\frac{1}{8}n + \frac{3}{8}\right)^3 + \frac{1}{144}((995328n^2 - 1990656n - 193536)\left(\frac{1}{2}n\right)^3 + (-7464096n^3 + 2612736n^2 - 2135808n \\
& - 141696)\left(\frac{1}{2}n\right)^2 + (-1492992n^4 + 4478976n^3 - 3193344n^2 + 774144n - 50688)\left(\frac{1}{2}n\right) \\
& - 808704n^5 + 590976n^4 + 4677696n^3 - 6591456n^2 \\
& + 2104128n - 127008)\left(\frac{1}{8}n + \frac{1}{8}\right) + \frac{1}{144}(-6144n - 2921472)\left(\frac{1}{8}n + \frac{3}{8}\right)^5 + \frac{1}{144}(-922368n^2 + 1896192n + 5733184) \\
& \left(\frac{1}{8}n + \frac{3}{8}\right)^4 + \frac{1}{144}((497664n + 1244160)\left(\frac{1}{2}n\right)^3 + (-373248n^2 - 373248n + 1358208) \\
& \left(\frac{1}{2}n\right)^2 + (-746496n^3 - 1119744n^2 + 1596672n - 494208)\left(\frac{1}{2}n\right) \\
& + 1088640n^4 - 7091712n^3 + 6394464n^2 + 1924992n - 842400)\left(\frac{1}{8}n + \frac{1}{2}\right)^2 + \frac{1}{144}(-663552\left(\frac{1}{2}n\right)^3 \\
& + (497664n - 746496)\left(\frac{1}{2}n\right)^2 + (995328n^2 + 995328n + 304128) \\
& \left(\frac{1}{2}n\right) + 2032128n^3 + 684288n^2 - 7727616n + 815616)\left(\frac{1}{8}n + \frac{1}{2}\right)^3 + \frac{1}{144}(-995328n - 1990656)\left(\frac{1}{8}n + \frac{1}{2}\right)^5 \\
& + \frac{1}{144}(-1617408n^2 + 5474304n + 1330560)\left(\frac{1}{8}n + \frac{1}{2}\right)^4 + \frac{37120}{9} \\
& \left(\frac{1}{8}n + \frac{3}{8}\right)^6 + 4608\left(\frac{1}{2}n\right)^6 + 4608\left(\frac{1}{8}n + \frac{1}{2}\right)^6 + \frac{188672}{9}\left(\frac{1}{8}n + \frac{7}{8}\right)^6 + 41472\left(\frac{1}{8}n\right)^6 + 53568\left(\frac{1}{4}n + \frac{3}{4}\right)^6 \\
& + \frac{3337835}{8} + \frac{88453}{8}n^6 - \frac{289}{48}n^5 + \frac{265793}{24}n^4.
\end{aligned}$$

TABLE 1: Eccentricities of graph  $DDD[n]$  when  $n \equiv 1 \pmod{4}$ .

$\varepsilon(a_{ij}) = 6n + 6i - 9$	$1 \leq i \leq (n-1)/4 + 1$ $(n-1)/4 + 2 \leq i \leq n$	$1 \leq j \leq 3n/2 + 9i/2 - 5$ and $i$ odd, $1 \leq j \leq 3n/2 + 9i/2 - 9/2$ and $i$ even $1 \leq j \leq 3n - \frac{3i}{2} + \frac{1}{2}$ and $i$ odd, $1 \leq j \leq 3n - \frac{3i}{2} + 1$ and $i$ even
$\varepsilon(a_{ij}) = 6n + 6i - 8$	$1 \leq i \leq (n-1)/4 + 1$ $(n-1)/4 + 2 \leq i \leq n$	$1 \leq j \leq n + 3i - 3$ $1 \leq j \leq 2n - i$
$\varepsilon(a_{ij}) = 6n + 6i - 7$	$1 \leq i \leq \frac{n-1}{4} + 1$ $(n-1)/4 + 2 \leq i \leq n$	$1 \leq j \leq 3n/2 + 9i/2 - 3$ and $i$ odd, $1 \leq j \leq 3n/2 + 9i/2 - 9/2$ and $i$ even $1 \leq j \leq 3n - 3i/2 + 1/2$ and $i$ odd, $1 \leq j \leq 3n - 3i/2$ and $i$ even
$\varepsilon(a_{ij}) = 6n + 6i - 6$	$1 \leq i \leq (n-1)/4$ $(n-1)/4 + 1 \leq i \leq n$	$1 \leq j \leq n + 3i - 2$ $1 \leq j \leq 2n - i$
$\varepsilon(a_{ij}) = 6n + 6i - 5$	$1 \leq i \leq (n-1)/4$ $(n-1)/4 + 1 \leq i \leq n$	$1 \leq j \leq 3n/2 + 9i/2 - 2$ and $i$ odd, $1 \leq j \leq 3n/2 + 9i/2 - 3/2$ and $i$ even $1 \leq j \leq 3n - \frac{3i}{2} - \frac{3}{2}$ and $i$ odd, $1 \leq j \leq 3n - \frac{3i}{2} - 1$ and $i$ even
$\varepsilon(a_{ij}) = 6n + 6i - 4$	$1 \leq i \leq (n-1)/4$ $(n-1)/4 + 1 \leq i \leq n - 1$	$1 \leq j \leq n + 3i - 1$ $1 \leq j \leq 2n - i - 1$

**Theorem 2.** The eccentric-connectivity index of David-derived networks  $DDD[n]$  for  $n \equiv 3 \pmod{4}$  and  $n \geq 1$  is given by

$$\begin{aligned} \xi(DDD[n]) = & 1680\left(\frac{1}{4}n + \frac{1}{4}\right)^3 + \frac{1}{24}(20160n - 48240)\left(\frac{1}{4}n + \frac{1}{4}\right)^2 + \frac{1}{24}(-10080n^2 - 2160n + 6816) \\ & \left(\frac{1}{4}n + \frac{1}{4}\right) + \frac{3296}{3}\left(\frac{1}{8}n + \frac{1}{8}\right)^3 + \frac{1}{24}(24000n + 23616)\left(\frac{1}{8}n + \frac{1}{8}\right)^2 + \frac{1}{24}(11136n^2 \\ & + 13152n - 20368)\left(\frac{1}{8}n + \frac{1}{8}\right) + \frac{800}{3}\left(\frac{1}{8}n + \frac{5}{8}\right)^3 + \frac{1}{24}(-6960n - 6000)\left(\frac{1}{8}n + \frac{5}{8}\right)^2 + \frac{1}{24}(-10680n^2 \\ & + 30576n - 10792)\left(\frac{1}{8}n + \frac{5}{8}\right) - 320\left(\frac{1}{2}n\right)^3 + \frac{1}{24}(8640n - 6144)\left(\frac{1}{2}n\right)^2 + \frac{1}{24}(14400n^2 - 21024n + 8928)\left(\frac{1}{2}n\right) \\ & + \frac{12517}{12}n^3 - \frac{7421}{8}n^2 - \frac{3199}{3}n + \frac{6579}{8}. \end{aligned} \quad (7)$$

*Proof.* Using symmetry of the network  $DDD[n]$ , we use only one quadrant of  $DDD[n]$  as labeled in Figure 2. We take one representative from a set of vertices which has the same degree and eccentricity. These representatives are labeled by  $a_i, b_i, c_i, d_i, e_i,$  and  $f_i$  for  $1 \leq i \leq n$  and shown in Table 2 along

with their eccentricities and frequencies. The proof of the theorem is the analogue of Theorem 1.  $\square$

**Corollary 3.** The total eccentricity index of  $DDD[n]$  David-derived networks for  $n \equiv 3 \pmod{4}$  is given by

$$\begin{aligned} \xi(DDD[n]) = & 504\left(\frac{1}{4}n + \frac{1}{4}\right)^3 + \frac{1}{12}(3024n - 7380)\left(\frac{1}{4}n + \frac{1}{4}\right)^2 + \frac{1}{12}(-1512n^2 - 468n + 1320) + \left(\frac{1}{4}n + \frac{1}{4}\right)\frac{1184}{3}\left(\frac{1}{8}n + \frac{1}{8}\right)^3 \\ & + \frac{1}{12}(3792n + 2880)\left(\frac{1}{8}n + \frac{1}{8}\right)^2 + \frac{1}{12}(1104n^2 + 1800n \\ & - 2936)\left(\frac{1}{8}n + \frac{1}{8}\right) + \frac{244}{3}\left(\frac{1}{8}n + \frac{5}{8}\right)^3 + \frac{1}{12}(-1104n - 1584)\left(\frac{1}{8}n + \frac{5}{8}\right)^2 + \frac{1}{12}(-1560n^2 \\ & + 3816n + 208)\left(\frac{1}{8}n + \frac{5}{8}\right) - 96\left(\frac{1}{2}n\right)^3 + \frac{1}{12}(864n - 144)\left(\frac{1}{2}n\right)^2 + \frac{1}{12}(1728n^2 - 1008n \\ & + 72)\left(\frac{1}{2}n\right) + \frac{1295}{4}n^3 - \frac{435}{2}n^2 - \frac{1385}{4}n + 171. \end{aligned} \quad (8)$$

TABLE 2: Eccentricities of graph  $DDD[n]$  when  $n \equiv 3 \pmod{4}$ .

$\varepsilon(a_{ij}) = 6n + 6i - 9$	$\leq i \leq (n-3)/4 + 1$ $(n-3)/4 + 2 \leq i \leq n$	$1 \leq j \leq 3n/2 + 9i/2 - 5$ and $i$ odd, $1 \leq j \leq 3n/2 + 9i/2 - 9/2$ and $i$ even $1 \leq j \leq 3n - 3i/2 + 1/2$ and $i$ odd, $1 \leq j \leq 03n - 3i/2 + 1$ and $i$ even
$\varepsilon(a_{ij}) = 6n + 6i - 8$	$1 \leq i \leq (n-3)/4 + 1$ $(n-3)/4 + 2 \leq i \leq n$	$1 \leq j \leq n + 3i - 3$ $1 \leq j \leq 2n - i$ .
$\varepsilon(a_{ij}) = 6n + 6i - 7$	$1 \leq i \leq (n-3)/4 + 1$ $(n-3)/4 + 2 \leq i \leq n$	$1 \leq j \leq 3n/2 + 9i/2 - 3$ and $i$ odd, $1 \leq j \leq 3n/2 + 9i/2 - 5/2$ and $i$ even $1 \leq j \leq 3n - 3i/2 + 1/2$ and $i$ odd, $1 \leq j \leq 3n - 3i/2$ and $i$ even
$\varepsilon(a_{ij}) = 6n + 6i - 6$	$1 \leq i \leq (n-3)/4 + 1$ $(n-3)/4 + 2 \leq i \leq n$	$1 \leq j \leq n + 3i - 2$ $1 \leq j \leq 2n - i$ .
$\varepsilon(a_{ij}) = 6n + 6i - 5$	$1 \leq i \leq (n-3)/4 + 1$ $(n-3)/4 + 2 \leq i \leq n - 1$	$1 \leq j \leq 3n/2 + 9i/2 - 3$ and $i$ odd, $1 \leq j \leq 3n/2 + 9i/2 - 5/2$ and $i$ even $1 \leq j \leq 3n - 3i/2 + 3/2$ and $i$ odd, $1 \leq j \leq 3n - 3i/2 - 1$ and $i$ even
$\varepsilon(a_{ij}) = 6n + 6i - 4$	$1 \leq i \leq (n-3)/4$ $(n-3)/4 + 1 \leq i \leq n - 1$	$1 \leq j \leq n + 3i - 1$ $1 \leq j \leq 2n - i - 1$

**Corollary 4.** *The first Zagreb eccentricity index of  $DDD[n]$  David-derived networks for  $n \equiv 3 \pmod{4}$  is given by*

$$\begin{aligned}
M_1^*(DDD[n]) = & -\frac{693425}{48}n + (10368n^4 - 12096n^3 + 4464n^2 - 2880n + 1508) \left[ \left( \frac{1}{2}n \right) \right]^2 \\
& + (10368n^3 - 22464n^2 + 420160n - 3168) \left[ \left( \frac{1}{2}n \right) \right]^3 + \left( -\frac{19456}{3}n \right. \\
& \left. - 18816 \right) \left[ \left( \frac{1}{8}n + \frac{5}{8} \right) \right]^5 + \left( -\frac{33992}{3}n^2 + 38016n + \frac{249968}{9} \right) \left[ \left( \frac{1}{8}n + \frac{5}{8} \right) \right]^4 + ((3456n - 1728) \left[ \left( \frac{1}{2}n \right) \right]^2 \\
& + (6912n^2 - 6912n + 2880) \left[ \left( \frac{1}{2}n \right) \right] - 4608 \left[ \left( \frac{1}{2}n \right) \right]^3 + 13832n^3 \\
& + \frac{30488}{3}n^2 - \frac{184936}{3}n - \frac{65944}{3}) \left[ \left( \frac{1}{8}n + \frac{5}{8} \right) \right]^3 + ((-2592n^2 - 7776n + 3960) \left[ \left( \frac{1}{2}n \right) \right]^2 \\
& + ((-10368n^4 + 31104n^3 - 14400n^2 - 672n + 3352) \left[ \left( \frac{1}{2}n \right) \right]) \\
& + (6912n^2 - 13824n - 7488) \left[ \left( \frac{1}{2}n \right) \right]^3 + (6912n^2 - 13824n - 7488) \left[ \left( \frac{1}{2}n \right) \right]^3 - 5616n^5 + 3908n^4 \\
& + 31252^3 - \frac{101498}{3}n^2 - \frac{820}{3}n - \frac{17618}{3}) \left[ \left( \frac{1}{8}n + \frac{5}{8} \right) \right] \\
& + \left( \frac{373120}{3}n - 7040 \right) \left[ \left( \frac{1}{8}n + \frac{1}{8} \right) \right]^5 + \left( \frac{260720}{3}n^2 - 368n - \frac{38576}{9} \right) \left[ \left( \frac{1}{8}n + \frac{1}{8} \right) \right]^4 + ((3456n - 2880) \left[ \left( \frac{1}{2}n \right) \right]^2 \\
& + (6912n^2 - 4608n + 1728) \left[ \left( \frac{1}{2}n \right) \right] - 4608 \left[ \left( \frac{1}{2}n \right) \right]^3 + 3408n^3 \\
& + \frac{15248}{3}n^2 + \frac{10952}{3}n - \frac{69080}{3}) \left[ \left( \frac{1}{8}n + \frac{1}{8} \right) \right]^3 + \left( -2592 \left( n - \frac{5}{6} \right)^2 \left[ \left( \frac{1}{2}n \right) \right] \right) \\
& + (-5184n^3 + 7776n^2 - 4176n + 1080) \left[ \left( \frac{1}{2}n \right) \right] + (3456n \\
& - 2880) \left( \frac{1}{2}n \right)^3 + 9856n^4 - 2280n^3 + \frac{2020}{3}n^2 - 24592n + \frac{176812}{9} \left( \frac{1}{8}n + \frac{1}{8} \right)^2 + ((-5184n^3
\end{aligned}$$

$$\begin{aligned}
& + 7776n^2 - 4176n + 1080 \left( \left( \frac{1}{2}n \right)^2 - 10368 \left( n^2 - \frac{2}{3}n + \frac{1}{4} \right)^2 \left( \frac{1}{2}n \right) + (6912n^2 - 4608n + 1728) \left( \frac{1}{2}n \right)^3 - 784n^4 - 3136n^3 \right. \\
& + \left. \frac{4000}{3}n^2 + 9408n - \frac{18160}{3} \right) \left( \frac{1}{8}n + \frac{1}{8} \right) + \\
& \left( -288 \left( \frac{1}{2}n \right)^2 + (-288n + 336) \left( \frac{1}{2}n \right) + 10044n^4 - 67932n^3 + 90027n^2 - 48696n \right. \\
& + 12706) \left( \frac{1}{4}n + \frac{1}{4} \right)^2 + \left( (-288n + 336) \left( \frac{1}{2}n \right)^2 - 288 \left( n - \frac{7}{6} \right)^2 \left( \frac{1}{2}n \right) - 16848n^5 \right. \\
& + 24408n^4 + 6252n^3 - 21930n^2 + 11276n - 1798) \left( \frac{1}{4}n + \frac{1}{4} \right) + (82944n - 139536) \\
& \left( \frac{1}{4}n + \frac{1}{4} \right)^5 + (53136n^2 - 178416n + 134205) \left( \frac{1}{4}n + \frac{1}{4} \right)^4 \\
& \left( \begin{array}{c} 50112n^3 - 123444n^2 + 136662n \\ -58824 \end{array} \right) \left( \frac{1}{4}n + \frac{1}{4} \right)^3 + (-6912n + 4608) \left( \frac{1}{2}n \right)^5 \\
& + (-11232n62 + 8064n - 2952) \left( \frac{1}{2}n \right)^4 + \frac{8999}{2} - \frac{149865}{8}n^3 + \frac{623113}{24}n^2 \\
& + \frac{33403}{3}n^4 - \frac{733393}{48}n^5 + 53568 \left( \frac{1}{4}n + \frac{1}{4} \right)^6 + 4608 \left( \frac{1}{2}n \right)^6 + \frac{43520}{9} \left( \frac{1}{8}n + \frac{5}{8} \right)^6 \\
& + \frac{596992}{9} \left( \frac{1}{8}n + \frac{1}{8} \right)^6 \frac{88453}{8}n^6 + 10368 \left( n - \frac{3}{2} \right) \left( n^3 - n^2 + \frac{4}{9}n - \frac{1}{72} \right) \left( \frac{1}{2}n \right). \tag{9}
\end{aligned}$$

#### 4. Conclusion

Graph theory has been successfully employed through the translation of chemical structures into characteristic numerical descriptors in the chemical graph theory and computational chemistry. In the present study, the relationship of anti-inflammatory activity of David-derived networks with the eccentric connectivity index and the other eccentricity-based topological indices was investigated.

In this paper, we give formulae of the eccentric-connectivity index, total-eccentricity index, and an eccentricity-based Zagreb index of dominating David-derived network. Dominating David-derived networks being derived from honeycomb structures has an imperative impact in studying materials with minimal density and high compression properties in chemistry. These structures are also used in studying the tension in different materials which are used in aerospace structures. So, our subject study will be quite helpful in studying the interwoven molecular inorganic knots and metal cluster chemistry. It will also be attributable in slow relaxation of the magnetization and magnetocaloric properties, depending on the metal ion. Investigation of different indices for David-derived networks has the potential to provide the best forecast rate used in different natural exercises, as anti-inflammatory activity, anticonvulsant activity, and diuretic activity.

*Open Problem 1.* Researchers are invited for open problem to study the same network for the calculation of eccentric-connectivity index, total index, and Zagreb index of David-derived networks  $DDD[n]$  for  $n \equiv 0 \pmod{4}$  and  $n \equiv 2 \pmod{4}$  for  $n \geq 1$  which definitely will change the results and structure of the network.

#### Data Availability

The data used to support the findings of this study are included within the article.

#### Conflicts of Interest

The authors declare that there are no conflicts of interest.

#### Acknowledgments

This research was supported by the UPAR grant of United Arab Emirates University via grant no. G00003271.

#### References

- [1] M. Ghorbani and M. Hosseinzadeh, "A new version of Zagreb indices," *Filomat*, vol. 26, no. 1, pp. 93–100, 2012.
- [2] M. Javaid, M. Ibraheem, and A. A. Bhatti, "Connective eccentricity index of certain path-thorn graphs," *Journal of Prime Research in Mathematics*, vol. 14, pp. 87–99, 2018.
- [3] M. Javaid and J. Cao, "Computing topological indices of probabilistic neural network," *Neural Computing and Applications*, vol. 30, no. 12, pp. 3869–3876, 2018.
- [4] F. Simonraj, "Embedding of poly honeycomb networks and the metric dimension of star of David network," *International Journal on Applications of Graph Theory in wireless Ad Hoc Networks and Sensor Networks*, vol. 4, no. 4, pp. 11–28, 2012.
- [5] M. Imran, A. Q. Baig, and H. Ali, "On topological properties of dominating David derived networks," *Canadian Journal of Chemistry*, vol. 94, no. 2, pp. 137–148, 2016.
- [6] M. Imran, A. Q. Baig, H. Ali, and S. U. Rehman, "On topological properties of poly honeycomb networks," *Periodica Mathematica Hungarica*, vol. 73, no. 1, pp. 100–119, 2016.

- [7] J. B. Liu, S. Wang, C. Wang, and S. Hayat, "Further results on computation of topological indices of certain networks," *IET Control Theory & Applications*, vol. 11, no. 13, pp. 2065–2071, 2017.
- [8] R. Farooq, N. Nazir, M. A. Malik, and M. Arfan, "Eccentricity based topological indices of a hetrofunctional dendrimer," *Journal of Optoelectronics and Advanced Materials*, vol. 17, pp. 1799–1807, 2015.
- [9] M. Imran, S. Hayat, and M. Y. H. Maillk, "On topological indices of certain interconnection networks," *Applied Mathematics and Computation*, vol. 244, pp. 936–951, 2014.
- [10] A. Q. Baig, M. Imran, and H. Ali, "On topological indices of poly oxide, poly silicate, DOX, and DSL networks," *Canadian Journal of Chemistry*, vol. 93, no. 7, pp. 730–739, 2015.
- [11] I. Dimitris, "Alexandropoulos, dodecanuclear  $3d/4f$ -metal clusters with a "Star of David" topology: single-molecule magnetism and magnetocaloric properties," *Chemical Communications*, vol. 8, 2016.
- [12] S. Bajaj, S. S. Sambhi, and A. K. Madan, "Topological models for prediction of anti-HIV activity of acylthiocarbamates," *Bioorganic & Medicinal Chemistry*, vol. 13, no. 9, pp. 3263–3268, 2005.
- [13] S. Bajaj, S. S. Sambhi, S. Gupta, and A. K. Madan, "Model for prediction of anti-HIV activity of 2-pyridinone derivatives using novel topological descriptor," *QSAR & Combinatorial Science*, vol. 25, no. 10, pp. 813–823, 2006.
- [14] M. Baca, J. Horvathova, M. Mokrisova, and A. Suhanyiova, "On topological indices of fullerenes," *Applied Mathematics and Computation*, vol. 251, pp. 154–161, 2015.
- [15] M. Naeem, M. K. Siddiqui, J. L. G. Guirao, and W. Gao, "New and modified eccentric indices of octagonal grid  $Om_n$ ," *Applied Mathematics and Nonlinear Sciences*, vol. 3, no. 1, pp. 209–228, 2018.
- [16] X. Zhang, M. Siddiqui, M. Naeem, and A. Baig, "Computing eccentricity based topological indices of octagonal grid  $Omn$ ," *Mathematics*, vol. 6, no. 9, p. 153, 2018.
- [17] I. Gutman and N. Trinajstić, "Graph theory and molecular orbitals. total  $\phi$ -electron energy of alternant hydrocarbons," *Chemical Physics Letters*, vol. 17, no. 4, pp. 535–538, 1972.
- [18] H. Hosoya, "Topological index. a newly proposed quantity characterizing the topological nature of structural isomers of saturated hydrocarbons," *Bulletin of the Chemical Society of Japan*, vol. 44, pp. 2322–2329, 1971.

## Research Article

# Topological Descriptors on Some Families of Graphs

Iftikhar Ahmad <sup>1</sup>, Maqbool Ahmad Chaudhry,<sup>1</sup> Muhammad Hussain <sup>2</sup>,  
and Tariq Mahmood<sup>3</sup>

<sup>1</sup>Department of Mathematics, The University of Lahore, Lahore, Pakistan

<sup>2</sup>Department of Mathematics, COMSATS University Islamabad, Lahore Campus, Lahore, Pakistan

<sup>3</sup>Department of Mathematics, Government College Gujranwala, Gujranwala, Pakistan

Correspondence should be addressed to Iftikhar Ahmad; [iftikharahmadcheema072@gmail.com](mailto:iftikharahmadcheema072@gmail.com)

Received 1 August 2021; Revised 15 September 2021; Accepted 28 September 2021; Published 21 October 2021

Academic Editor: Muhammad Kamran Jamil

Copyright © 2021 Iftikhar Ahmad et al. This is an open access article distributed under the Creative Commons Attribution License, which permits unrestricted use, distribution, and reproduction in any medium, provided the original work is properly cited.

In view of the successful applications of graph theory, relationships between the biological activity and chemical structure have been developed. One of the popular topics in graph theory is problems relating to topological indices. Degree-based topological indices, distance-based topological indices, and counting-related topological indices are various types of topological indices. Physicochemical properties such as boiling point and stability of chemical compounds are correlated by these topological indices. A topological index of a graph is a numerical quantity obtained from the graph mathematically. A cactus graph is a connected graph in which no edge lies in more than one cycle. In this study, we have derived certain degree-based topological indices for some families of graphs consisting of graph obtained by the rooted product of paths and cycles and two types of cactus graph (paracactus and orthocactus) with the help of the generalized Zagreb index.

## 1. Introduction

Let  $G$  be a graph,  $V(G)$  be vertices of  $G$ , and  $E(G)$  be the edge of  $G$ ; then, the total number of vertices in  $G$  is called the order of  $G$ , and the total number of edges in  $G$  is called the size of  $G$ ; any edge having the same starting and ending vertex is called a loop. In a graph, if two or more edges have the same starting and ending vertex, then we call this multiple edge. A graph which does not contain a loop or multiple edge is called a simple graph, and a graph which contains a loop or multiple edge is called a multigraph. A graph  $G$  is a planar graph if we draw it into the plane without any edge intersection. If it is not possible, then we call it a nonplanar graph. In a graph  $G$ , from one vertex to another vertex, we give orientation or directions to each edge; then, this graph is called a directed graph; if we start moving from one vertex and, after travelling different edges, we reach back that vertex, then it forms a cycle. If a graph has no cycle, then we call it a tree. Spanning tree is a subgraph which has the

same vertex as the original graph. In this paper, we use undirected graphs. Graph theory was successfully employed through the translation of chemical structures into characteristic numerical descriptors by resorting to graph invariants. A graph invariant is any function on a graph that does not depend on labeling of its vertices. Such quantities are also called topological indices. Hundreds of different invariants have been employed to date in QSAR/QSPR studies. Among more useful of them appear two that are known under various name. Topological indices are numerical parameters of a graph which are invariant under graph isomorphism. Interest in the field of computational chemistry in topological indices has been on the rise for a considerable length of time. A graph can be recognized by a numerical number, a polynomial, an arrangement of numbers, and either a network or a matrix which represents the whole graph. A topological index is a numerical amount related to a graph, which describes the geography of the graph and is invariant under diagram automorphism [1–7].

There are some significant classes of topological indices, for example, distance-based topological indices, degree-based topological indices, and eccentricity-based and counting-related polynomials and indices of the graph. Among these classes, degree-based topological indices have overwhelming significance and perform a pivotal role in the preparation of graph hypothesis, especially in science. If it is made more precise, a topological list  $\text{Top}(G)$  of a graph is a number with the property that, for each graph  $H$  isomorphic to  $G$ ,  $\text{Top}(H) = \text{Top}(G)$ . The concept of topological indices came from Wiener when he was studying the boiling point of a member of the alkene family, called paraffins. He named this topological index the path number. When research in chemical graph theory progressed, the name Wiener index was given to the path number. Owing to its interesting theoretical properties and wide range of applications, the Wiener index is the most investigated molecular topological index in chemical graph theory [8, 9]. The first and the second Zagreb indices were introduced by Gutman and Trinajstić [10]. H. Wiener gave the concept of the topological index, namely, as the Wiener index [11] and is defined as

$$W(G) = \frac{1}{2} \sum_{pq \in E(G)} d(p, q). \quad (1)$$

The chemist Randić introduced a topological index under the name branching index:

$$R_\alpha(G) = \sum_{pq \in E(G)} [d(p)d(q)]^\alpha. \quad (2)$$

Vukicević and Furtula et al. introduced one of the well-known connectivity topological indices, namely, atom-bond connectivity (ABC) index [12], defined as

$$\text{ABC}(G) = \sum_{pq \in E(G)} \sqrt{\frac{d(p)d(q) - 2}{d(p)d(q)}}. \quad (3)$$

Nikolić et al. [13] introduced Zagreb indices defined as

$$\begin{aligned} M_1(G) &= \sum_{p \in V(G)} \delta(p)^2, \\ M_2(G) &= \sum_{p, q \in V(G)} \delta(p)\delta(q). \end{aligned} \quad (4)$$

Vukičević and Furtula [12] introduced another well-known connectivity topological descriptor, namely, geometric-arithmetic (GA) index:

$$\text{GA}(G) = \sum_{pq \in E(G)} \frac{2\sqrt{d(p)d(q)}}{d(p) + d(q)}. \quad (5)$$

Some more degree-based topological indices are discussed in [14–16]. Aslam et al. computed topological indices of line graphs of subdivision graphs of the  $i$ th vertex rooted product graphs [17]. Ahmad et al. computed polynomials of degree-based indices for swapped networks modeled by the optical transpose interconnection [1]. Ahmad computed

degree-based topological indices of the benzene ring in the  $p$ -type surface in the 2D network [3].

$$\begin{aligned} M_\alpha(G) &= (8mn + 4m + 4n)2^\alpha + (16mn - 4m - 4n)3^\alpha, \\ R_\alpha(G) &= (4m + 4n)2^{2\alpha} + (16mn - 6m - 6n)3^{2\alpha} + (16mn)6^\alpha. \end{aligned} \quad (6)$$

Vukicević and Furtula computed the topological index based on the ratios of geometrical and arithmetical means of the end vertex degree of edges. In this paper, they introduced a novel topological index based on the end vertex degree and its basic features. They named it as the geometric-arithmetic index [12].

Farahani computed Zagreb indices and Zagreb polynomials of polycyclic aromatic hydrocarbons. In this paper, he computed the first Zagreb index  $Z_{g_1}(G)$ , second Zagreb index  $Z_{g_2}(G)$ , and their polynomials  $Z_{g_1}(G, x)$  and  $Z_{g_2}(G, x)$  of the family of hydrocarbon structure polycyclic aromatic hydrocarbons [5]. Sarkar et al. computed the general Zagreb index of some carbon structures. They computed the general Zagreb index for three carbon allotropes theoretically [15]. Sarkar et al. computed the general Zagreb index of some dendrimer structures. Dendrimers are generally large, complex, and hyperbranched molecules synthesized by repeatable steps with nanometer-scale measurements. They computed the general Zagreb index of some regular dendrimers and hence obtained some vertex degree-based topological indices [16]. Mustapha Chellali computed bounds on the 2-domination number in cactus graphs. He proved that if  $G$  is a nontrivial connected cactus graph with  $K(G)$  even cycles, then  $\gamma_2(G) \geq \gamma_t(G) - K(G)$ , and if  $G$  is a graph of order  $n$  with at most one cycle, then  $\gamma_2(G) \geq (n + l - s)/2$  improving Fink and Jacobson's lower bound for trees with  $l > s$ , where  $\gamma_t$ ,  $l$ , and  $s$  are the total domination number. He also proved that if  $T$  is a tree of order  $n \geq 3$ , then  $\gamma_2 \leq \beta(T) + s - 1$  [8].

## 2. Main Results

We derive the topological indices of the rooted product graph  $C_n(P_m)$  of cycle and path graphs. In this work, the mathematical property of the general Zagreb index or  $(s, t)$ -Zagreb index of some general ortho- and paracactus chains is studied, and hence, their special cases such as triangular chain cactus  $T_n$ , orthochain square cactus  $O_n$ , and parachain square cactus  $Q_n$  are considered where  $n$  denotes the length of the chain, and then we derive some explicit expressions of the same for other degree-based topological indices such as Zagreb indices, forgotten index, redefined Zagreb index, general first Zagreb index, general Randić index, and symmetric division index for particular values of  $s$  and  $t$  of the general Zagreb index.

## 3. Topological Indices of the Rooted Product Graph $C_n(P_m)$ of the Cycle and Path Graphs

Let  $C_n$  and  $P_m$  be the cycle and path graphs on  $n$  and  $m$  vertices, respectively. Taking  $n$  copies of  $P_m$  and joining each vertex of  $C_n$  with one vertex of  $P_m$ , we get the rooted product

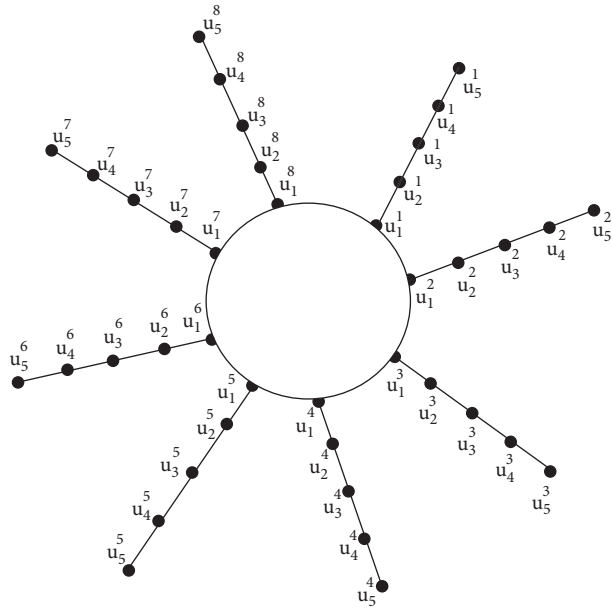


FIGURE 1: Example of the rooted product graph  $C_n(P_m)$  for  $n = 8$  and  $m = 5$ .

graph  $C_n(P_m)$  of the cycle and path graphs. The edge set of  $C_n(P_m)$  can be partitioned into the following subsets:

$$\begin{aligned}
 E_1(C_n(P_m)) &= \{e = pq; d(p) = d(q) = 3\}, \\
 E_2(C_n(P_m)) &= \{e = pq; d(p) = 3, d(q) = 2\}, \\
 E_3(C_n(P_m)) &= \{e = pq; d(p) = d(q) = 2\}, \\
 E_4(C_n(P_m)) &= \{e = pq; d(p) = 2, d(q) = 1\},
 \end{aligned}
 \tag{7}$$

such that  $|E_1(C_n(P_m))| = n$ ,  $|E_2(C_n(P_m))| = n$ ,  $|E_3(C_n(P_m))| = n(m - 3)$ , and  $|E_4(C_n(P_m))| = n$ . In Figure 1, the rooted product  $C_8(P_5)$  is explained.

**Theorem 1.** If  $C_n(P_m)$  is the rooted product graph of cycle and path graphs, then

- (1)  $M_1(C_n(P_m)) = M_{1,0}(C_n(P_m)) = 4nm + 2n$
- (2)  $M_2(C_n(P_m)) = 1/2M_{1,1}(C_n(P_m)) = 4nm + 5n$
- (3)  $F(C_n(P_m)) = M_{2,0}(C_n(P_m)) = 8nm + 12n$
- (4)  $R_e ZM(C_n(P_m)) = M_{2,1}(C_n(P_m)) = 16nm + 42n$
- (5)  $M^\alpha(C_n(P_m)) = M_{\alpha-1,0}(C_n(P_m)) = 3^\alpha \times n + 2^\alpha \times n \times (m - 2) + 1^\alpha \times n$

- (6)  $R_\alpha(C_n(P_m)) = 1/2M_{\alpha,\alpha}(C_n(P_m)) = n(9)^\alpha + n(6)^\alpha + n(m - 3)n(4)^\alpha + n(2)^\alpha$
- (7)  $SDD(C_n(P_m)) = M_{1,-1}(C_n(P_m)) = 2n + 13n/6 + n(m - 3)(2) + 5/2n$

*Proof*

- (1) We know that the corresponding  $(s, t)$ -Zagreb index of the first Zagreb index  $M_1(C_n(P_m))$  is  $M_{1,0}(C_n(P_m))$ .

$$\begin{aligned}
 M_1(C_n(P_m)) &= M_{1,0}(C_n(P_m)) = ? \\
 M_1(C_n(P_m)) &= \sum_{pq \in E(C_n(P_m))} \{d(p) + d(q)\} \\
 &= n(3 + 3) + n(3 + 2) + n(m - 3)(4) + n(3) \\
 &= 6n + 5n + 4nm - 12n + 3n \\
 M_1(C_n(P_m)) &= 4nm + 2n.
 \end{aligned}
 \tag{8}$$

The general Zagreb index of  $(C_{\setminus sn}(P_m))$  is given by

$$\begin{aligned}
 M_{s,t}(C_n(P_m)) &= \sum_{pq \in E(C_n(P_m))} \{d(p)^s d(q)^t + d(p)^t d(q)^s\} \\
 &= n(3^s 3^t + 3^t 3^s) + n(3^s 2^t + 3^t 2^s) + n(m - 3)(2^s 2^t + 2^t 2^s) + n(2^s 1^t + 2^t 1^s). \\
 M_{s,t}(C_n(P_m)) &= n(3^{s+t} + 3^{s+t}) + n(3^s 2^t + 3^t 2^s) \\
 &\quad + n(m - 3)(2^{s+t} + 2^{s+t}) + n(2^s 1^t + 2^t 1^s).
 \end{aligned}
 \tag{9}$$

Putting  $s = 1$  and  $t = 0$  in equation (1), we have

$$\begin{aligned}
M_{1,0}(C_n(P_m)) &= n(3+3) + n(3^1 2^0 + 3^0 2^1) \\
&\quad + n(m-3)(2^1 + 2^1) + n(2^1 1^0 + 2^0 1^1) \\
&= n(6) + n(3+2) + n(m-3)(4) + n(3) \\
&= 6n + 5n + 4nm - 12n + 3n \\
&= 4nm + 2n.
\end{aligned}
\tag{10}$$

(2) We know that the corresponding  $(s, t)$ -Zagreb index of the second Zagreb index  $M_2(C_n(P_m))$  is  $1/2M_{1,1}(C_n(P_m))$ .

---


$$\begin{aligned}
M_2(C_n(P_m)) &= \frac{1}{2}M_{1,1}(C_n(P_m)) = ? \\
M_2(C_n(P_m)) &= \sum_{pq \in E(C_n(P_m))} d(p)d(q) \\
M_2(C_n(P_m)) &= n(9) + n(6) + n(m-3)(4) + n(2) \\
&= 9n + 6n + 4nm - 12n + 2n \\
&= 4nm + 5n, \\
M_{1,1}(C_n(P_m)) &= n(3^1 \times 3^1 + 3^1 \times 3^1) + n(3^1 \times 2^1 + 2^1 \times 3^1) + n(m-3)(2^1 \times 2^1) \\
&= n(9+9) + n(6+6) + n(m-3)(4+4) + n(2+2) \\
&= 18n + 12n + n(m-3)(8) + 4n \\
&= 2[4nm + 5n], \\
\frac{1}{2}M_{1,1}(C_n(P_m)) &= M_2(C_n(P_m)) = 4nm + 5n.
\end{aligned}
\tag{11}$$

(3) We know that the corresponding  $(s, t)$ -Zagreb index of the forgotten topological index  $F(C_n(P_m))$  is  $M_{2,0}(C_n(P_m))$ .

Putting  $s = 2$  and  $t = 0$  in equation (1),

$$\begin{aligned}
F(C_n(P_m)) &= M_{2,0}(C_n(P_m)) = ? \\
F(C_n(P_m)) &= \sum_{pq \in E(C_n(P_m))} \{d(p)^2 + d(q)^2\} \\
&= n(3^2 + 3^2) + n(3^2 + 2^2) \\
&\quad + n(m-3)(2^2 + 2^2) + n(2^2 + 1^2) \\
&= 18n + 13n + n(m-3)(8) + 5n \\
&= 8mn + 12n.
\end{aligned}
\tag{12}$$

---


$$\begin{aligned}
M_{2,0}(C_n(P_m)) &= n(3^2 \times 3^0 + 3^0 \times 3^2) + n(3^2 \times 2^0 + 3^2 \times 2^0) + n(m-3)(2^2 \times 2^0 \\
&\quad + 2^0 \times 2^2) + n(2^2 \times 1^0 + 1^2 \times 2^0) \\
&= n(9+9) + n(9+4) + n(m-3)(4+4) + n(4+1) \\
&= 18n + 13n + 8mn - 24n + 5n \\
&= 8mn + 12n, \\
M_{2,0}(C_n(P_m)) &= F(C_n(P_m)) = 8mn + 12n.
\end{aligned}
\tag{13}$$

- (4) We know that the corresponding  $(s, t)$ -Zagreb index of the redefined Zagreb index  $ReZM(C_n(P_m))$  is  $M_{2,1}(C_n(P_m))$ .

$$\begin{aligned}
 ReZM(C_n(P_m)) &= M_{2,1}(C_n(P_m)) = ? \\
 ReZM(C_n(P_m)) &= \sum_{pq \in E(C_n(P_m))} d(p)d(q)\{d(p) + d(q)\} \\
 &= n(3)(3)(3+3) + n(3)(2)(3+2) + n(m-3)(2)(2)(2+2) \\
 &\quad + n(2)(1)(2+1) \\
 &= n(9)(6) + n(6)(5) + n(m-3)(4)(4) + n(2)(3) \\
 &= n(54) + n(30) + n(m-3)(16) + n(6) \\
 &= 54n + 30n + 16mn - 48n + 6n. \\
 ReZM(C_n(P_m)) &= 16mn + 42n.
 \end{aligned} \tag{14}$$

Putting  $s = 2$  and  $t = 1$  in equation (1),

$$\begin{aligned}
 M_{2,1}(C_n(P_m)) &= n(3^2 \times 3^1 + 3^1 \times 3^2) + n(3^2 \times 2^1 + 3^1 \times 2^2) + n(m-3)(2^2 \times 2^1 \\
 &\quad + 2^1 \times 2^2) + n(2^2 \times 1^1 + 1^1 \times 2^1) \\
 &= n(9 \times 3 + 3 \times 9) + n(9 \times 2 + 3 \times 4) + n(m-3)(4 \times 2 + 2 \times 4) \\
 &\quad + n(4 + 2) \\
 &= n(27 + 27) + n(18 + 12) + n(m-3)(8 + 8) + 6n, \\
 &= 54n + 30n + 16mn - 48n + 6n, \\
 M_{2,1}(C_n(P_m)) &= 16mn + 42n. \\
 M_{2,1}(C_n(P_m)) &= ReZM(C_n(P_m)) = 16mn + 42n.
 \end{aligned} \tag{15}$$

- (5) We know that the corresponding  $(s, t)$ -Zagreb index of the general Zagreb index  $M^\alpha(C_n(P_m))$  is  $M_{\alpha-1,0}(C_n(P_m))$ .

$$M^\alpha(C_n(P_m)) = M_{\alpha-1,0}(C_n(P_m)) = ?. \tag{16}$$

The general Zagreb index  $M^\alpha(C_n(P_m))$  is given by

$$\begin{aligned}
 M^\alpha(C_n(P_m)) &= \sum_{p \in V(C_n(P_m))} d(p)^\alpha. \\
 M^\alpha(C_n(P_m)) &= 3^\alpha \times n + 2^\alpha \times n \times (m-2) + 1^\alpha \times n.
 \end{aligned} \tag{17}$$

Putting  $s = \alpha - 1$  and  $t = 0$  in equation (1), we get

$$\begin{aligned}
M_{\alpha-1,0}(C_n(P_m)) &= n(3^{\alpha-1} \times 3^0 + 3^0 \times 3^{\alpha-1}) + n(3^{\alpha-1}) \times 2^0 + 3^0 \times 2^{\alpha-1} \\
&\quad + n(m-3)(2^{\alpha-1} \times 2^0 + 2^0 \times 2^{\alpha-1}) + n(2^{\alpha-1} \times 1^0 + 1^{\alpha-1} \times 2^0) \\
&= n(2 \times 3^{\alpha-1}) + n(3^{\alpha-1} + 2^{\alpha-1}) + n(m-3)(2 \times 2^{\alpha-1}) + n(2^{\alpha-1} \\
&\quad + 1^{\alpha-1} \times 2^0) \\
&= 2n \times 3^{\alpha-1} + n3^{\alpha-1} + n \times 2^{\alpha-1} + nm \times 2^\alpha - 3n \times 2^\alpha \\
&\quad + n(2^{\alpha-1} + 1^{\alpha-1} \times 1) \\
&= 3^{\alpha-1}[3n] + 2^{\alpha-1}[2n] + n \times 1^\alpha + mn.2^\alpha - 3n \times 2^\alpha \\
&= 3^\alpha \times n + 2^\alpha \times n + 2^\alpha \times n[m-3] + n \times 1^\alpha \\
&= 3^\alpha \times n + 2^\alpha \times n \times (m-3) + 1^\alpha \times n.
\end{aligned} \tag{18}$$

(6) We know that the corresponding  $(s, t)$ -Zagreb index of the general Randić index  $R_\alpha(C_n(P_m))$  is  $1/2M_{\alpha,\alpha}(C_n(P_m))$ .

$$R_\alpha(C_n(P_m)) = \frac{1}{2}M_{\alpha,\alpha}(C_n(P_m)) = ?. \tag{19}$$

The general Randić index  $R_\alpha(G)$  is given by

$$R_\alpha(C_n(P_m)) = \sum_{pq \in E(C_n(P_m))} \{d(p)d(q)\}^\alpha. \tag{20}$$

So,

$$R_\alpha(C_n(P_m)) = n(9)^\alpha + n(6)^\alpha + n(2)^\alpha + n(m-3)(4)^\alpha. \tag{21}$$

Using equation (1),

$$\begin{aligned}
M_{s,t}(C_n(P_m)) &= n(3^{s+t} + 3^{s+t}) + n(3^s 2^t + 3^t 2^s) \\
&\quad + n(m-3)(2^s 2^t + 2^t 2^s) \\
&\quad + n(2^s 1^t + 2^t 1^s).
\end{aligned} \tag{22}$$

Putting  $s = \alpha$  and  $t = \alpha$  in equation (1), we have

$$\begin{aligned}
M_{\alpha,\alpha}(C_n(P_m)) &= n(3^{2\alpha} + 3^{2\alpha}) + n(3^\alpha \times 2^\alpha + 3^\alpha \times 2^\alpha) + n(m-3)(2^{2\alpha} + 2^{2\alpha}) \\
&\quad + n(2^\alpha \times 1^\alpha + 2^\alpha \times 1^\alpha) \\
&= n(2 \times 3^{2\alpha}) + n(2 \times 2^\alpha 3^\alpha) + n(m-3)(2 \times 2^{2\alpha}) + n(2 \times 2^\alpha) \\
&= 2\{n(9)^\alpha + n(6)^\alpha + n(m-3)n(4)^\alpha + n(2)^\alpha\},
\end{aligned} \tag{23}$$

$$\frac{1}{2}M_{\alpha,\alpha}(C_n(P_m)) = n(9)^\alpha + n(6)^\alpha + n(m-3)n(4)^\alpha + n(2)^\alpha,$$

$$\frac{1}{2}M_{\alpha,\alpha}(C_n(P_m)) = R_\alpha(C_n(P_m)) = n(9)^\alpha + n(6)^\alpha + n(m-3)n(4)^\alpha + n(2)^\alpha.$$

(7) We know that the corresponding  $(s, t)$ -Zagreb index of the symmetric division deg index  $SDD(C_n(P_m))$  is  $M_{1,-1}(C_n(P_m))$ .

$$SDD(C_n(P_m)) = M_{1,-1}(C_n(P_m)) = ?. \tag{24}$$

Putting  $s = 1$  and  $t = -1$  in equation (1), we have

$$\begin{aligned}
M_{1,-1}(C_n(P_m)) &= n(3^{1-1} + 3^{1-1}) + n(3^1 \times 2^{-1} + 3^{-1} \times 2^1) + n(m-3)(2^{1-1} \\
&\quad + 2^{1-1}) + n(2^1 \times 1^{-1} + 1^1 \times 2^{-1}) \\
&= n(3^0 + 3^0) + n\left(\frac{3}{2} + \frac{2}{3}\right) + n(m-3)(2^0 + 2^0) + n\left(2 + \frac{1}{2}\right) \\
&= n(1+1) + n\left(\frac{9+4}{6}\right) + n(m-3)(1+1) + n\left(\frac{4+1}{2}\right), \\
M_{1,-1}(C_n(P_m)) &= 2n + \frac{13n}{6} + n(m-3)(2) + \frac{5n}{2}, \\
SDD(C_n(P_m)) &= \sum_{pq \in E(C_n(P_m))} \left\{ \frac{d(p)}{d(q)} + \frac{d(q)}{d(p)} \right\} \\
&= n\left(\frac{3}{3} + \frac{3}{3}\right) + n\left(\frac{3}{2} + \frac{2}{3}\right) + n(m-3)(2) + \frac{5n}{2} \\
&= 2n + \frac{13n}{6} + n(m-3)(2) + \frac{5n}{2}, \\
SDD(C_n(P_m)) &= M_{1,-1}(C_n(P_m)) = 2n + \frac{13n}{6} + n(m-3)(2) + \frac{5n}{2}.
\end{aligned} \tag{25}$$

#### 4. Topological Indices of Some General Cactus Chain Graphs

In this section, we find topological indices of two general cactus chain graphs, namely, paracactus chain graph and orthocactus chain graph of cycles. We first consider the paracactus chain graph in which the cut vertices are not adjacent. The paracactus chain graph of cycles is denoted by  $C_m^n$  where  $m$  is the number of vertices of each cycle and  $n$  is the length of the chain. The number of vertices of  $C_m^n$  is  $mn - n + 1$ , and the number of its edges is  $mn$ .

**Theorem 2.** Let  $C_m^n$  be the paracactus chain graphs of cycles for  $m \geq 3$  and  $n \geq 2$ ; then,

$$M_{(s,t)}(C_m^n) = 4(n-1)2^{s+t}(2^s + 2^t) + (mn - 4n + 4)2^{s+t+1}. \quad \square \tag{26}$$

*Proof.* The edge set of  $C_m^n$  can be partitioned into the following subsets:

$$\begin{aligned}
E_1(C_m^n) &= \{e = pq; d_{C_m^n}(p) = d_{C_m^n}(q) = 2\}, \\
E_2(C_m^n) &= \{e = pq; d_{C_m^n}(p) = 2, d_{C_m^n}(q) = 4\},
\end{aligned} \tag{27}$$

such that  $|E_1(C_m^n)| = 2(m-2) + (m-4)(n-2)$  and  $|E_2(C_m^n)| = 4(n-1)$ .

Then, for the general Zagreb index, we have

$$\begin{aligned}
M_{s,t}(C_m^n) &= \sum_{pq \in E(C_m^n)} \{d(p)^s d(q)^t + d(p)^t d(q)^s\} \\
&= \sum_{pq \in E_1(C_m^n)} (2^s 2^t + 2^t 2^s) + \sum_{pq \in E_2(C_m^n)} (2^s 4^t + 2^t 4^s) \\
&= |E_1(C_m^n)|(2^s 2^t + 2^t 2^s) + |E_2(C_m^n)|(2^s 4^t + 2^t 4^s) \\
&= \{2(m-2) + (m-4)(n-2)\} \times 2^{s+t+1} + 4(n-1) \times 2^{s+t}(2^s + 2^t) \\
&= 4(n-1)2^{s+t}(2^s + 2^t) + (mn - 4n + 4) \times 2^{(s+t+1)}.
\end{aligned} \tag{28}$$

**Corollary 1.** Let  $C_m^n$  be the paracactus chain graph of cycles for  $m \geq 3$  and  $n \geq 2$ ; then,

- (1)  $M_1(C_m^n) = 4mn + 8n - 8$
- (2)  $M_2(C_m^n) = 4mn + 16n - 16$

- (3)  $X(C_m^n) = 1/2\{mn - 4n(1 - (\sqrt{2}/3)) + 4(1 - (\sqrt{2}/3))\}$
- (4)  $ABC(C_m^n) = 1/\sqrt{2}mn - 2n(\sqrt{2} - \sqrt{3}) + 2(\sqrt{2} - \sqrt{3})$
- (5)  $S(C_m^n) = 1/8mn$
- (6)  $R_{(-1)}(C_m^n) = 1/2(mn - 2n + 2)$

$$(7) R_{(-1/2)}(C_m^n) = (1/2)\{mn - 2n(2 - \sqrt{2}) + 2(2 - \sqrt{2})\}$$

Proof

$$\begin{aligned} M_1(C_m^n) &= \sum_{pq \in E(C_m^n)} \{d(p) + d(q)\} \\ &= 2(m-2) + (m-4)(n-2)(2+2) + 4(n-1)(2+4) \\ &= (2m-4 + mn - 2m - 4n + 8)4 + (4n-4)6 \\ M_1(C_m^n) &= 4nm + 8n - 8. \end{aligned} \quad (29)$$

$$\begin{aligned} M_2(C_m^n) &= \sum_{pq \in E(C_m^n)} d(p)d(q) \\ &= (mn - 4n + 4)4 + (4n - 4)8 \\ &= 4mn - 16n + 16 + 32n - 32M_2(C_m^n) \\ &= 4nm + 16n - 16. \end{aligned} \quad (30)$$

(1) The sum-connectivity index of  $C_m^n$  is

$$\begin{aligned} X(C_m^n) &= \sum_{pq \in E(C_m^n)} \frac{1}{\sqrt{d(p) + d(q)}} \\ &= (mn - 4n + 4)\frac{1}{\sqrt{4}} + (4n - 4)\frac{1}{\sqrt{6}} \\ &= \frac{1}{2}(mn - 4n + 4) + \frac{1}{\sqrt{6}}(4n - 4) \\ &= \frac{1}{2}mn - 2n\left(1 - \frac{\sqrt{2}}{\sqrt{3}}\right) + 2\left(1 - \frac{\sqrt{2}}{\sqrt{3}}\right) \\ &= \frac{1}{2}\left\{mn - 4n\left(1 - \frac{\sqrt{2}}{\sqrt{3}}\right) + 4\left(1 - \frac{\sqrt{2}}{\sqrt{3}}\right)\right\}. \end{aligned} \quad (31)$$

(2) The atom-bond connectivity index is given by

$$\begin{aligned} ABC(C_m^n) &= \sum_{pq \in E(C_m^n)} \sqrt{\frac{d(p) \times d(q) - 2}{d(p) \times d(q)}} \\ &= (mn - 4n + 4)\sqrt{\frac{2 \times 2 - 2}{2 \times 2}} \\ &\quad + (4n - 4)\sqrt{\frac{2 \times 4 - 2}{2 \times 4}} \\ &= (mn - 4n + 4)\frac{1}{\sqrt{2}} + (4n - 4)\frac{\sqrt{3}}{2} \\ &= \frac{1}{\sqrt{2}}mn - 2n(\sqrt{2} - \sqrt{3}) + (\sqrt{2} - \sqrt{3}). \end{aligned} \quad (32)$$

(3) The Sanskruti index of  $C_m^n$  is given by

$$\begin{aligned} S(C_m^n) &= \sum_{pq \in E(C_m^n)} \left\{ \frac{d(p) + d(q) - 2}{d(p) \times d(q)} \right\}^3 \\ &= (mn - 4n + 4)\left(\frac{2+2-2}{2 \times 2}\right)^3 \\ &\quad + (4n - 4)\left(\frac{2+4-2}{2 \times 4}\right)^3 \\ &= \frac{1}{8}\{mn - 4n + 4 + 4n - 4\} \\ &= \frac{mn}{8}. \end{aligned} \quad (33)$$

$$\begin{aligned} R_{-1}(C_m^n) &= \sum_{pq \in E(C_m^n)} \frac{1}{d(p) \times d(q)} \\ &= (mn - 4n + 4)\frac{1}{2 \times 2} + (4n - 4)\frac{1}{2 \times 4} \\ &= \frac{1}{4}(mn - 4n + 4) + \frac{1}{8}(4n - 4) \\ &= \frac{1}{4}(mn - 4n + 4 + 2n - 2) \\ &= \frac{1}{4}(mn - 2n + 2). \end{aligned} \quad (34)$$

$$\begin{aligned} R_{(-1/2)}(C_m^n) &= \sum_{pq \in E(C_m^n)} \frac{1}{\sqrt{d(p) \times d(q)}} \\ &= (mn - 4n + 4)\left(\frac{1}{\sqrt{4}}\right) + (4n - 4)\left(\frac{1}{\sqrt{8}}\right) \\ &= \frac{1}{2}(mn - 4n + 4) + (4n - 4)\frac{1}{2\sqrt{2}} \\ &= \frac{1}{2}\{mn - 2n(2 - \sqrt{2}) + 2(2 - \sqrt{2})\}. \end{aligned} \quad (35)$$

□

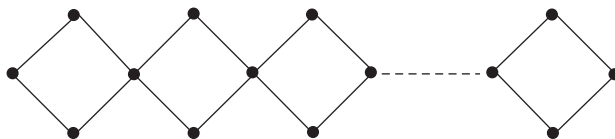
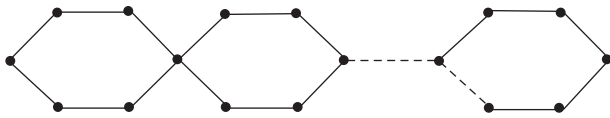
If  $m = 4$ , then we have the graph as shown in Figure 2.

If  $m = 6$ , then we have the graph as shown in Figure 3.

Putting  $m = 4$  and  $m = 6$  in equation (1), we get the desired results. Also, putting  $m = 4$  and  $m = 6$  in Corollary 1, we get results for the above graph.

Now, consider the orthochain cactus graph of cycles where its cut vertices are adjacent. Let this type of cactus chain graph be denoted by  $CO_m^n$  where  $m$  is the length of each cycle and  $n$  is the length of the chain. The number of vertices is  $mn - n + 1$ , and the number of edges is  $mn$ . We calculate the Zagreb index of  $CO_m^n$ .

**Theorem 3.** Let  $CO_m^n$  be the orthocactus chain graph of cycles for  $m \geq 3$  and  $n \geq 2$ ; then,

FIGURE 2: Example of the paracactus chain graph of cycles for  $m = 4$  and  $n = n$ .FIGURE 3: Example of the paracactus chain graph of cycles for  $m = 6$  and  $n = n$ .

$$M_{s,t}(CO_m^n) = 2(n-2)4^{(s+t)} + 2n \times 2^{(s+t)}(2^s + 2^t) + 2[2(m-2) + (m-3)(n-2)]2^{(s+t)}. \quad (36)$$

$$\begin{aligned} E_1(CO_m^n) &= \{e = pq; d(p) = d(q) = 4\}, \\ E_2(CO_m^n) &= \{e = pq; d(p) = 2, d(q) = 4\}, \\ E_3(CO_m^n) &= \{e = pq; d(p) = d(q) = 2\}, \end{aligned} \quad (37)$$

*Proof.* The edge set of  $CO_m^n$  can be partitioned into the following subsets:

such that  $|E_1(CO_m^n)| = (n-1)$ ,  $|E_2(CO_m^n)| = 2n$ , and  $|E_3(CO_m^n)| = 2(m-2) + (m-3)(n-2)$ . The general Zagreb index is

$$\begin{aligned} M_{s,t}(CO_m^n) &= \sum_{pq \in E(CO_m^n)} \{d(p)^s d(q)^t + d(p)^t d(q)^s\} \\ &= \sum_{pq \in E_1(CO_m^n)} (4^s 4^t + 4^t 4^s) + \sum_{pq \in E_2(CO_m^n)} (2^s 4^t + 2^t 4^s) + \sum_{pq \in E_3(CO_m^n)} (2^s 2^t + 2^t 2^s) \\ &= |E_1(CO_m^n)|(4^s 4^t + 4^t 4^s) + |E_2(CO_m^n)|(2^s 4^t + 2^t 4^s) + |E_3(CO_m^n)|(2^s 2^t + 2^t 2^s) \\ &= (n-1)(4^s 4^t + 4^t 4^s) + 2n(2^s 4^t + 2^t 4^s) + 2(m-2) + (m-3)(n-2)(2^s 2^t + 2^t 2^s) \\ &= 2(n-2)4^{s+t} + 2n \times 2^{s+t}(2^s + 2^t) + 2\{(m-2) + (m-3)(n-2)\}2^{s+t} \\ M_{s,t}(CO_m^n) &= 2(n-2)4^{s+t} + (mn - 3n + 4)2^{s+t+1} + 2n \times 2s + t + 1(2s + 2t). \end{aligned} \quad (38)$$

□

**Corollary 2.** Let  $CO_m^n$  be the orthocactus chain graph of cycles for  $m \geq 3$  and  $n \geq 2$ . Then,

- (1)  $M_1(CO_m^n) = 4mn + 8n - 8$
- (2)  $M_2(CO_m^n) = 4mn + 20n - 24$
- (3)  $GA(CO_m^n) = mn - 2n(1 - (2\sqrt{2}/3))$
- (4)  $X(CO_m^n) = 1/2mn + (n/4\sqrt{3})(\sqrt{6} + 4\sqrt{2} - 6\sqrt{3}) + (\sqrt{2} - 1/\sqrt{2})$

$$(5) ABC(CO_m^n) = 1/\sqrt{2}mn + n/4(4\sqrt{3} + \sqrt{14} + 6\sqrt{2}) + (4 - \sqrt{28}/2\sqrt{2})$$

$$(6) S(CO_m^n) = 1/8mn - 37/512n + 37/256$$

$$(7) R_{-1}(CO_m^n) = 1/16(4mn - 7n + 6)$$

$$(8) R_{-2}(CO_m^n) = 1/2mn + 1/4n(2\sqrt{2} - 5) + 1/2$$

*Proof*

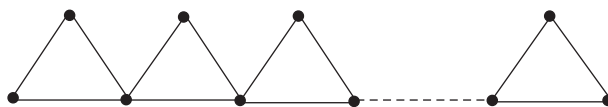
$$\begin{aligned}
M_1(CO_m^n) &= \sum_{pq \in E(CO_m^n)} \{d(p) + d(q)\} \\
&= (n-2)(4+4) + 2n(2+4) + [2(m-2) + (m-3)(n-2)](2+2) \\
&= 8n - 16 + 12n + (2m - 4 + mn - 2m - 3n + 6)4 \\
&= 8n - 16 + 12n + 4mn - 12n + 8 \\
&= 4mn + 8n - 8.
\end{aligned} \tag{39}$$

$$\begin{aligned}
M_2(CO_m^n) &= \sum_{pq \in E(CO_m^n)} \{d(p) \times d(q)\} \\
&= (n-2)(4 \times 4) + 2n(2 \times 4) + (mn - 3n + 2)(2 \times 2) \\
&= 16n - 32 + 16n + 4mn - 12n + 8 \\
&= 4mn + 20n - 24.
\end{aligned} \tag{40}$$

$$\begin{aligned}
GA(CO_m^n) &= \sum_{pq \in E(CO_m^n)} \frac{2\sqrt{d(p) \times d(q)}}{d(p) + d(q)} \\
&= (n-2) \frac{2\sqrt{4 \times 4}}{4+4} + 2n \frac{2\sqrt{2 \times 4}}{2+4} + (mn - 3n + 2) \times 2 \frac{\sqrt{2 \times 2}}{2+2} \\
&= (n-2) \frac{\sqrt{16}}{4} + 2n \frac{2\sqrt{8}}{6} + (mn - 3n + 2) \frac{\sqrt{4}}{2} \\
&= n - 2 + \frac{2}{3}n2\sqrt{2} + mn - 3n + 2 \\
&= mn - 2n \left(1 - \frac{2\sqrt{2}}{3}\right).
\end{aligned} \tag{41}$$

$$\begin{aligned}
X(CO_m^n) &= \sum_{pq \in E(CO_m^n)} \frac{1}{\sqrt{d(p) + d(q)}} \\
&= (n-2) \frac{1}{\sqrt{4+4}} + (2n) \frac{1}{\sqrt{2+4}} + (mn - 3n + 2) \frac{1}{\sqrt{2+2}} \\
&= (n-2) \frac{1}{\sqrt{8}} + (2n) \frac{1}{\sqrt{6}} + (mn - 3n + 2) \frac{1}{\sqrt{4}} \\
&= \frac{1}{2}mn + \frac{n}{2\sqrt{3}}(\sqrt{6} + 4\sqrt{2} - 6\sqrt{3}) + \frac{\sqrt{2}-1}{\sqrt{2}}.
\end{aligned} \tag{42}$$

$$\begin{aligned}
ABC(CO_m^n) &= \sum_{pq \in E(CO_m^n)} \sqrt{\frac{d(p) \times d(q) - 2}{d(p) \times d(q)}} \\
&= (n-2) \sqrt{\frac{4 \times 4 - 2}{4 \times 4}} + (2n) \sqrt{\frac{2 \times 4 - 2}{2 \times 4}} + (mn - 3n + 2) \sqrt{\frac{2 \times 2 - 2}{2 \times 2}} \\
&= (n-2) \sqrt{\frac{14}{16}} + (2n) \sqrt{\frac{3}{4}} + (mn - 3n + 2) \sqrt{\frac{2}{4}} \\
&= \frac{mn}{\sqrt{2}} - \frac{n}{4} \left( \sqrt{14} + \frac{4}{\sqrt{3}} - \frac{12}{\sqrt{2}} \right) + \left( \frac{4 - \sqrt{28}}{2\sqrt{2}} \right) \\
&= \frac{mn}{\sqrt{2}} - \frac{n}{4} (4\sqrt{3} + \sqrt{14} + 6\sqrt{2}) + \left( \frac{4 - \sqrt{28}}{2\sqrt{2}} \right).
\end{aligned} \tag{43}$$

FIGURE 4: Example of the orthocactus chain graph of cycles for  $m = 3$  and  $n = n$ .

$$\begin{aligned}
 S(CO_m^n) &= \sum_{pq \in E(CO_m^n)} \left( \frac{d(p) + d(q) - 2}{d(p) \times d(q)} \right)^3 \\
 &= (n-2) \left( \frac{4+4-2}{4 \times 4} \right)^3 + 2n \left( \frac{2+4-2}{2 \times 4} \right)^3 + (mn-3n+2) \left( \frac{2+2-2}{2 \times 2} \right)^3 \\
 &= (n-2) \left( \frac{6}{16} \right)^3 + 2n \left( \frac{4}{8} \right)^3 + (mn-3n+2) \left( \frac{2}{4} \right)^3 \\
 &= \frac{1}{8}mn - \frac{37}{512}n + \frac{37}{256}.
 \end{aligned} \tag{44}$$

$$\begin{aligned}
 R_{-1}(CO_m^n) &= \sum_{pq \in E(CO_m^n)} \frac{1}{d(p) \times d(q)} \\
 &= (n-2) \frac{1}{16} + \frac{2n}{8} + (mn-3n+2) \frac{1}{4} \\
 &= \frac{mn}{4} + \frac{n}{16} + \frac{2n}{8} - \frac{3n}{4} + \frac{2}{4} - \frac{2}{16} \\
 &= \frac{1}{16} (4mn - 7n + 6).
 \end{aligned} \tag{45}$$

$$R_{-2}(CO_m^n) = \frac{mn}{2} + \frac{1}{4}n(2\sqrt{2} - 5) + \frac{1}{2}. \tag{46}$$

**Corollary 3.** Let  $T_n$  be the triangular cactus chain for  $n \geq 2$ ; then,

$$M_{s,t}(T_n) = 2^{s+t+2} + n \times 2^{s+t+1} + 2 \times (n-2)4^{s+t}. \tag{47}$$

*Proof.* Putting  $m = 3$  in equation (1), we get the desired result.  $\square$

We have an orthocactus graph for  $m = 3$  and  $n = n$  as shown in Figure 4.

**Corollary 4.** Let  $T_n$  be the triangular cactus chain for  $n \geq 2$ ; then,

- (1)  $M_1(T_n) = 20n - 8$
- (2)  $M_2(T_n) = 32n - 24$
- (3)  $G(T_n) = 3n - 2n(2\sqrt{2}/3)$
- (4)  $X(T_n) = 3/2n + n/4\sqrt{3} \quad (\sqrt{6} + 4\sqrt{2} - 6\sqrt{3}) + ((\sqrt{2} - 1)/\sqrt{2})$
- (5)  $ABC(T_n) = 3/\sqrt{2}n + n/4 \quad (4/\sqrt{3} + \sqrt{14} + 6\sqrt{2}) + (4 - \sqrt{28}/2\sqrt{2})$
- (6)  $S(T_n) = 3/8n - 37/512n + 37/256$
- (7)  $R_{-1}(T_n) = 12/16n - 7/16n + 6/16$
- (8)  $(R_{-2}) = 3/2n + 1/4n(2\sqrt{2} - 5)$

*Proof.* Putting  $m = 3$  in the results of Corollary 2, we get the desired results.  $\square$

## 5. Conclusion

The topological indices such as the first Zagreb index, second Zagreb index, forgotten index, redefined Zagreb index, and general Randić index have been computed in this paper and have been compared with their corresponding  $(s, t)$ -Zagreb indices for the graph  $C_n(P_m)$ . In this study, some closed expressions of the general Zagreb index of some cactus chain graphs have also been obtained, leading to some other important degree-based topological indices for some particular values of  $s$  and  $t$ . Results given by these indices can be very much correlated with molecular structures so as to understand their physical and chemical properties. The general Zagreb index of some other graph structures can be computed for further studies.

## Data Availability

No data were used to support this study.

## Disclosure

This paper has not been published elsewhere, and it will not be submitted anywhere else for publication.

## Conflicts of Interest

The authors declare that they have no conflicts of interest.

## Authors' Contributions

All the authors contributed equally to this work.

## References

- [1] A. Ahmad, R. Hasni, K. Elahi, and M. A. Asim, "Polynomials of degree-based indices for swapped networks modelled by optical transpose interconnection system," *IEEE Access*, vol. 8, pp. 214293–214299, 2020.
- [2] N. Ali, A. Koam, A. Ahmad, and M. F. Nadeem, "Comparative study of valency-based topological descriptor for hexagon star network," *Computer Systems Science and Engineering*, vol. 36, no. 2, pp. 293–306, 2021.
- [3] A. Ahmad, "On the degree based topological indices of benzene ring embedded in the P-type-surface in 2D network," *Hacettepe Journal of Mathematics and Statistics*, vol. 47, no. 1, pp. 9–18, 2018.
- [4] J. Cao, U. Ali, M. Javaid, and C. Huang, "Zagreb connection indices of molecular graphs based on operations," *Complexity*, vol. 2020, Article ID 7385682, 15 pages, 2020.
- [5] M. .R. Farahani, "Zagreb indices and Zagreb polynomials of polycyclic aromatic hydro-carbons PAHs," *Journal of Chemica Acta*, vol. 2, pp. 70–72, 2013.
- [6] M. Javaid and J. Cao, "Computing topological indices of probabilistic neural networks," *Neural Computing and Applications*, vol. 30, no. 12, pp. 3869–3876, 2018.
- [7] H. Wang, M. Javaid, S. Akram, M. Jamal, and S. Wang, "Least eigenvalue of the connected graphs whose complements are cacti," *Open Mathematics*, vol. 17, no. 1, pp. 1319–1331, 2019.
- [8] M. Chellali, "Bounds on the 2-dimensional number in cactus graph," *Opuscula Mathematica*, vol. 2, pp. 5–12, 2006.
- [9] H. Wiener, "Structural determination of paraffin boiling points," *Journal of the American Chemical Society*, vol. 69, pp. 17–20, 1947.
- [10] I. Gutman and N. Trinajestić, "Graph theory and molecular orbitals total p-electron energy of alternant hydrocarbons," *Chemical Physics Letters*, vol. 17, pp. 535–538, 1972.
- [11] E. Estrada, L. Torres, L. Rodriguez, and I. Gutman, "An atom-bond connectivity index, modeling the enthalpy of formation of alkanes," *Indian Journal of Chemistry*, vol. 37A, pp. 849–855, 1998.
- [12] D. Vukicevic and B. Furtula, "Topological index based on the ratios of geometrical and arithmetic means of end-vertex degree of edges," *Journal of Mathematical Chemistry*, vol. 46, pp. 1369–1376, 2009.
- [13] S. Nikolić, G. Kovačević, A. Miličević, and N. Trinajstić, "The Zagreb indices 30 years after," *Croatica Chemica Acta*, vol. 76, pp. 113–124, 2003.
- [14] P. S. Ranjini, V. Loksha, and A. Usha, "Relation between phenylene and hexagonal squeeze using harmonic index," *International Journal of Graph Theory*, vol. 1, pp. 116–121, 2013.
- [15] P. Sarkar, N. De, and A. Pal, "The generalized Zagreb index of some carbon structures," *Acta Chemica Iasi*, vol. 26, no. 1, pp. 91–104, 2018.
- [16] P. Sarkar, N. De, and A. Pal, "Generalized Zagreb index of some dendrimer structures," *Universal Journal of Mathematics and Applications*, vol. 1, no. 3, pp. 160–165, 2018.
- [17] A. Aslam, M. Faisal Nadeem, Z. Zahid, S. Zafar, and W. Gao, "Computing certain topological indices of the line graphs of subdivision graphs of some rooted product graphs," *Mathematics*, vol. 7, p. 393, 2019.

## Research Article

# Topological Descriptors of M-Carbon $M[r, s, t]$

Hong Yang<sup>1</sup> and Muhammad Naeem<sup>2</sup>

<sup>1</sup>School of Information Science and Engineering, Chengdu University, Chengdu 610106, China

<sup>2</sup>Department of Mathematics and Statistics, Institute of Southern Punjab, Multan, Pakistan

Correspondence should be addressed to Muhammad Naeem; naempkn@gmail.com

Received 8 June 2021; Accepted 2 October 2021; Published 18 October 2021

Academic Editor: Muhammad Kamran Jamil

Copyright © 2021 Hong Yang and Muhammad Naeem. This is an open access article distributed under the Creative Commons Attribution License, which permits unrestricted use, distribution, and reproduction in any medium, provided the original work is properly cited.

We have studied topological indices of the one the hardest crystal structures in a given chemical system, namely, M-carbon. These structures are based and obtained by the famous algorithm USPEX. The computations and applications of topological indices in the study of chemical structures is growing exponentially. Our aim in this article is to compare and compute some well-known topological indices based on degree and sum of degrees, namely, general Randić indices, Zagreb indices, atom bond connectivity index, geometric arithmetic index, new Zagreb indices, fourth atom bond connectivity index, fifth geometric arithmetic index, and Sanskruti index of the M-carbon  $M(r, s, t)$ . Moreover, we have also computed closed formulas for these indices.

## 1. Introduction

One of the hardest structures of carbon is diamond. In 2011, Andriy and Artem searches 9500 structures of different system sizes, and they produced a large number of superhard allotropes; these allotropes being as hard as diamonds [1]. One of the superhard carbon allotropes that they studied was M-carbon (Figure 1). Scientists also believe that the synthesis and practical applications of some of these structures may be possible. Some studies also exist giving indications that these types of carbon allotropes such as M-carbon have been obtained by applying cold compression on graphite [2, 3].

In this study, we intend to study and compute the degree-based topological indices of M-carbon structures. One of the first and very old topological indices is the Wiener index [4], and this index is also known as the path number. After that, the scientists of various field started exploring this new technique to study chemical and physical properties of chemical structure, compounds, and molecules. A list of topological indices that we shall discuss in this study is given in Table 1, which includes Randić index, general Randić indices, Zagreb indices,

atom bond connectivity index, geometric arithmetic indices, new Zagreb indices, fourth atom bond connectivity index, fifth geometric arithmetic index, and Sanskruti index. For some literature study and results related to these indices, see [5–13].

In Table 1, the number  $S(o)$  represents the sum  $\sum_{o \in E(G)} d(o)$  and the number  $S(\ell)$  represents the sum  $\sum_{\ell \in E(G)} d(\ell)$ , where  $d_o$  is the degree of vertex  $o$  and  $d_\ell$  represents the degree of vertex  $\ell$ . In 2016, Gutman et al. [26] proved the following theorems for some of the indices in Table 1.

**Theorem 1** (See [26]). *Let  $G$  be a graph with  $|V(G)|$  vertices and  $|E(G)|$  edges. Then,*

$$\overline{M}_1(G) = 2|E(G)|(|V(G) - 1) - M_1(G). \quad (1)$$

**Theorem 2** (See [26]). *Let  $G$  be a graph with  $|V(G)|$  vertices and  $|E(G)|$  edges. Then,*

$$\overline{M}_2(G) = 2|E(G)|^2 - \frac{1}{2}M_1(G) - M_2(G). \quad (2)$$

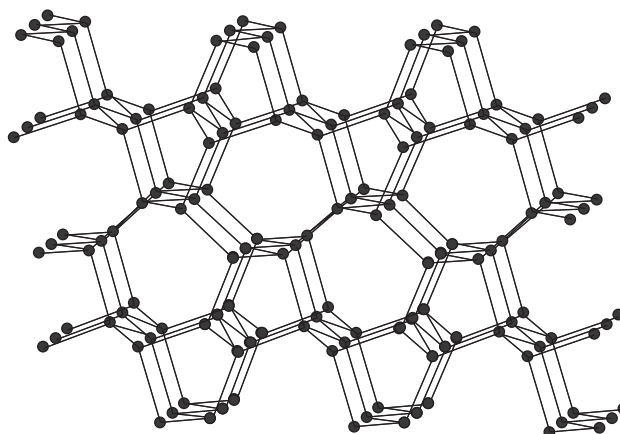
FIGURE 1: The M-carbon structure  $M[3,3,2]$ .

TABLE 1: Famous degree-based topological indices.

S. no.	Topological index	Notation	Formula	Authors
1	Randić index	$R_{-(1/2)}(G)$	$\sum_{o\ell \in E(G)} 1/\sqrt{d_o d_\ell}$	Randić [14] in 1975
2	General Randić index	$R_\alpha(G)$	$\sum_{o\ell \in E(G)} (d_o d_\ell)^\alpha$	Bollobás and Erdős [15] and Amic et al. [16] in 1988
3	Atom bond connectivity index	$ABC(G)$	$\sum_{o\ell \in E(G)} \sqrt{d_o + d_\ell - 2/d_o d_\ell}$	Estrada et al. [17]
4	Geometric arithmetic index	$GA(G)$	$\sum_{o\ell \in E(G)} 2\sqrt{d_o d_\ell / (d_o + d_\ell)}$	Vukićević and Furtula. [18]
5	First Zagreb	$M_1(G)$	$\sum_{o\ell \in E(G)} (d_o + d_\ell)$	Gutman and Trinajstić in 1972[19]
6	Second Zagreb	$M_2(G)$	$\sum_{o\ell \in E(G)} (d_o \times d_\ell)$	Gutman and Das in 2004 [20]
7	New degree-based Zagreb index	$HM(G)$	$\sum_{o\ell \in E(G)} (d_o + d_\ell)^2$	Shirdel et al. [21] in 2013
8	First Zagreb coindex	$\overline{M}_1(G)$	$\sum_{o\ell \notin E(G)} [d_o + d_\ell]$	In 2008, Došlić [22]
9	Second Zagreb coindex	$\overline{M}_2(G)$	$\sum_{o\ell \notin E(G)} d_o d_\ell$	Same as above
10	Fourth atom bond connectivity index	$ABC_4(G)$	$\sum_{o\ell \in E(G)} \sqrt{S(o) + S(\ell) - 2/S(o)S(\ell)}$	Ghorbani and Hosseinzadeh [23]
11	Fifth version of geometric arithmetic index	$GA_5$	$\sum_{o\ell \in E(G)} 2\sqrt{S(o)S(\ell)/S(o) + S(\ell)}$	Graovac et al. [24]
12	Sanskriti index	$S(G)$	$\sum_{o\ell \in E(G)} (S(o) \times S(\ell)/S(o) + S(\ell) - 2)^3$	In 2016, Hosamani [25]

## 2. Construction of $M[r, s, t]$ for Topological Study

In this section, we shall present our main results about the M-carbon structure denoted as  $M[r, s, t]$ . First, we need to give a brief explanation of the variables  $r, s, t$  in the notation  $M[r, s, t]$ . To find and compute the topological indices of the M-carbon structure, we have introduced a way of constructing its structure by the means of these three variables, where  $r$  represents the unit as shown in Figures 2(a) and 2(b) represents a chain containing three units, where the connection (bond) is shown in blue color. The variable  $s$  represents the number of connected chains with each having  $r$  numbers of units (Figure 3). The variable  $t$  represents the number of connected layers. There are two types of layers odd layer for  $t = 1, 3, 5, \dots$  and even layers for  $t = 2, 4, 6, \dots$ , both are generated by different unit cells. The one depicted in Figure 3 is the odd layer (that is for  $t = 1, 3, 5, \dots$ ) which was generated by the unit of Figure  $t = 2, 4, 6, \dots$ ). The unit cell of an even layer is shown in Figure 4(a), the chain in even

layer is shown in Figure 4(b), and Figure 4(c) depicts an even layer. Then, finally, the M-carbon structure  $M[r, s, t]$  is shown in Figure 5, which also depicts how two layers, an even and odd, are connecting. In Figure 5, these connections (bonds) between two layers are shown in red colour. So, in this way, we get structure of M-carbon (Figure 1). By our construction, the graph of M-carbon  $M[r, s, t], r \geq 2, s \geq 2, t \geq 2$  consists of  $8rst$  number vertices and  $16rst - 4rt - 5st - 2rs + t + s$  number of edges.

## 3. Main Results

The graph  $M[r, s, t]$  has  $2(s+1)t, 4r - 2 + 2(s-1)t, 2rst + 2rs + 6rt - st - 6r - s - 3t + 3$ , and  $6rst - 2rs - 6rt - 3st + 2r + s + 3t - 1$  vertices of degrees 1, 2, 3, and 4, respectively. The degree-based edge partition of  $M[r, s, t]$  is given in Table 2.

In all the theorems in the following, we used Maple for the computations of mathematical expression and graphical comparisons.

**Theorem 3.** Let  $G$  be the chemical structural graph of  $M$ -carbon  $M[r, s, t]$ , and the general Randić index of  $M[r, s, t]$  is given by

$$\begin{aligned}
 R_{\alpha}(M[r, s, t]) = & 2 \times 4^{\alpha} - 7 \times 16^{\alpha} + 2 \times 2^{\alpha}t + 8 \times 6^{\alpha}r + 2 \times 6^{\alpha}s + 2 \times 6^{\alpha}t - 4 \times 8^{\alpha}s - 6 \times 8^{\alpha}t \\
 & - 4 \times 9^{\alpha}r - 2 \times 9^{\alpha}s - 3 \times 9^{\alpha}t - 2 \times 12^{\alpha}s - 4 \times 12^{\alpha}t - 4 \times 16^{\alpha}r + 7 \times 16^{\alpha}s \\
 & + 10 \times 16^{\alpha}t - 8 \times 6^{\alpha} - 2 \times 3^{\alpha} + 2 \times 2^{\alpha} + 2 \times 3^{\alpha}st + 4 \times 8^{\alpha}st + 2 \times 9^{\alpha}rs \\
 & + 6 \times 9^{\alpha}rt + 4 \times 12^{\alpha}rs + 4 \times 12^{\alpha}rt - 8 \times 16^{\alpha}rs - 14 \times 16^{\alpha}rt - 11 \times 16^{\alpha}st \\
 & + 5 \times 9^{\alpha} + 16 \times 16^{\alpha}rst + 6 \times 8^{\alpha} + 2 \times 12^{\alpha}.
 \end{aligned} \tag{3}$$

*Proof.* Let  $G$  be the chemical structural graph of  $M$ -carbon  $M[r, s, t]$ ; then, by using serial number 2 of Table 1 and edge

partition given in Table 2, the general Randić index  $R_{\alpha}(G)$  of  $M[r, s, t]$  is computed as follows:

$$\begin{aligned}
 R_{\alpha}(M[r, s, t]) = & \sum_{o \in E(G)} (d_o \times d_{\ell})^{\alpha} \\
 = & (2t + 2)(1 \times 2)^{\alpha} + (2s - 2)(1 \times 3)^{\alpha} + (2)(2 \times 2)^{\alpha} + (8r + 2s + 2t - 8)(2 \times 3)^{\alpha} \\
 & + (4st - 4s - 6t + 6)(2 \times 4)^{\alpha} + (6rt + 2rs - 4r - 2s - 3t + 5)(3 \times 3)^{\alpha} + (4rs + 4rt - 2s - 4t + 2)(3 \times 4)^{\alpha} \\
 & + (16rst - 8rs - 14rt - 11st - 4r + 7s + 10t - 7)(4 \times 4)^{\alpha}.
 \end{aligned} \tag{4}$$

The result follows after some simple computations from this equation.

It is very simple and clear to see that from the above Theorem 3, the following Corollary is true.  $\square$

#### Corollary 1

$$R_{\alpha}(M[r, s, t]) = \left\{ \begin{array}{ll} 256rst - 62rs - 122rt - 138st - 52r + 50s + 53t - 37 & \text{if } \alpha = 1 \\ \frac{23r}{36} - \frac{17s}{144} + \frac{23st}{48} + \frac{13t}{24} + \frac{rt}{8} + \frac{rs}{18} + rst + \frac{77}{144} & \text{if } \alpha = -1 \\ 2\sqrt{3}st + 4\sqrt{8}st + 2\sqrt{9}rs + 16\sqrt{16}rst - 2\sqrt{3} & \text{if } \alpha = \frac{1}{2} \\ +2\sqrt{2} + 2\sqrt{2}t + 8\sqrt{6}r + 2\sqrt{6}s + 2\sqrt{6}t - 4\sqrt{8}s & \\ -6\sqrt{8}t - 4\sqrt{9}r - 2\sqrt{9}s - 3\sqrt{9}t - 2\sqrt{12}s & \\ -4\sqrt{12}t - 4\sqrt{16}r + 7\sqrt{16}s + 10\sqrt{16}t + 2\sqrt{4} & \\ -8\sqrt{6} + 6\sqrt{8} + 5\sqrt{9} + 2\sqrt{12} - 7\sqrt{16} + 6\sqrt{9}rt & \\ +4\sqrt{12}rs + 4\sqrt{12}rt - 11\sqrt{16}st - 14\sqrt{16}rt - 8\sqrt{16}rs & \\ \frac{2\sqrt{3}st}{3} + \frac{\sqrt{8}st}{2} + \frac{2\sqrt{9}rs}{9} + \sqrt{16}rst - \frac{2\sqrt{3}}{3} + \sqrt{2} & \text{if } \alpha = \frac{-1}{2} \\ +\sqrt{2}t + \frac{4\sqrt{6}r}{3} + \frac{\sqrt{6}s}{3} + \frac{\sqrt{6}t}{3} - \frac{\sqrt{8}s}{2} - \frac{3\sqrt{8}t}{4} - \frac{4\sqrt{9}r}{9} & \\ \frac{2\sqrt{9}s}{9} - \frac{\sqrt{9}t}{3} - \frac{\sqrt{12}s}{6} - \frac{\sqrt{12}t}{3} - \frac{\sqrt{16}r}{4} + \frac{7\sqrt{16}s}{16} + \frac{5\sqrt{16}t}{8} & \\ +\frac{\sqrt{4}}{2} - \frac{4\sqrt{6}}{3} + \frac{3\sqrt{8}}{4} + \frac{5\sqrt{9}}{9} + \frac{\sqrt{12}}{6} - \frac{7\sqrt{16}}{16} + \frac{2\sqrt{9}rt}{3} & \\ +\frac{\sqrt{12}rs}{3} + \frac{\sqrt{12}rt}{3} - \frac{11\sqrt{16}st}{16} - \frac{7\sqrt{16}rt}{8} - \frac{\sqrt{16}rs}{2} & \end{array} \right. \tag{5}$$

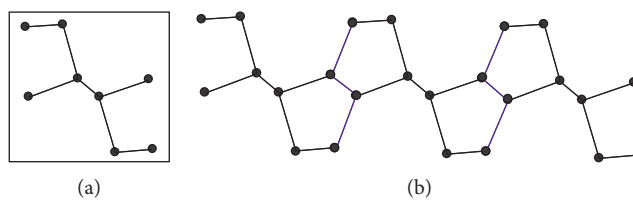


FIGURE 2: (a) The M-carbon unit cell. (b) Chain of three units and units connected by blue edges.

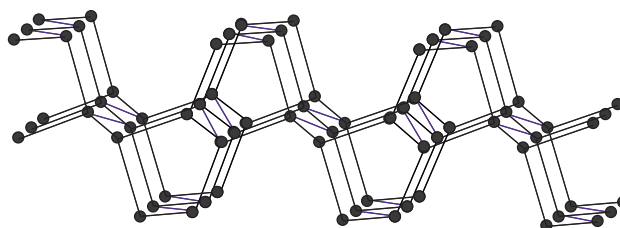


FIGURE 3: The odd layer (for  $t = 1$ ) of three chains and bonding of chains is shown by blue edges.

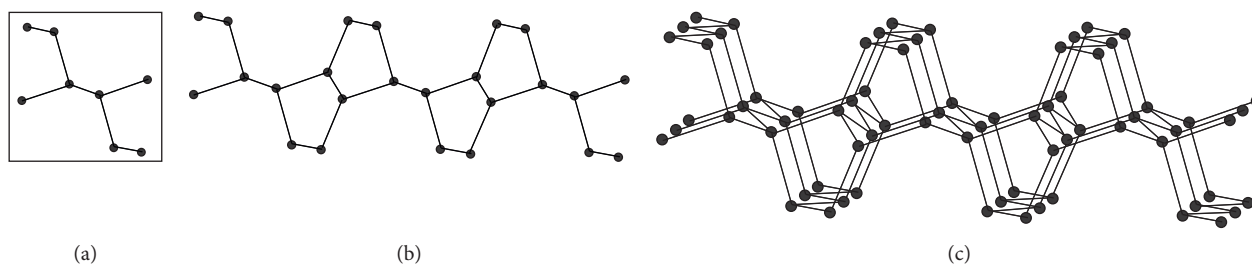


FIGURE 4: Even layer construction. (a) The unit cell. (b) Chain of three units. (c) The layer of three chains.

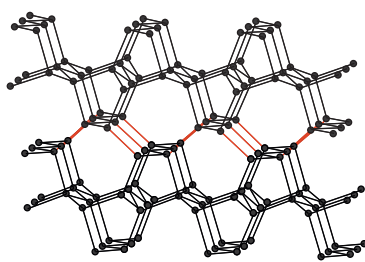


FIGURE 5: The structure  $M[3,3,2]$ . The connection of two layers. Bonding is shown in red color.

**Corollary 2.** The second Zagreb index  $M_2(M[r, s, t])$  is the same as  $R_\alpha(M[r, s, t])$  for  $\alpha = 1$ , so  $M_2([M[r, s, t]])$  can be obtained from Corollary 1.

**Theorem 4.** The first Zagreb index  $M_1(M[r, s, t])$  of M-carbon structure is given by

TABLE 2: Degree-based edge partition of  $M[r, s, t]$  for  $r, s, t \geq 2$ .

$(d_u, d_v)$	Frequency
(1, 2)	$2t + 2$
(1, 3)	$2st - 2$
(2, 2)	2
(2, 3)	$8r + 2s + 2t - 8$
(2, 4)	$4st - 4s - 6t + 6$
(3, 3)	$6rt + 2sr - 4r - 2s - 3t + 5$
(3, 4)	$4rs + 4rt - 2s - 4t + 2$
(4, 4)	$16rst - 8rs - 14rt - 11st - 4r + 7s + 10t - 7$

$$M_1(M[r, s, t]) = 128rst - 24rs - 48rt - 56st - 16r + 16s + 14t - 10. \quad (6)$$

*Proof.* Let  $G$  be the chemical structural graph of M-carbon  $M[r, s, t]$ ; then, by using serial number 5 of Table 1 and edge partition given in Table 2, the first Zagreb index  $R_\alpha(G)$  of  $M[r, s, t]$  is computed as follows:

TABLE 3: Sum degree-based edge partition of  $M[r, s, t]$  for  $r, s, t \geq 3$ .

$(S(o), S(\ell))$	Frequency	$(S(o), S(\ell))$	Frequency
(3, 7)	4	(3, 8)	2
(4, 11)	$2t$	(4, 12)	$2st-2s-4t+6$
(4, 13)	$2st-2s-4t+4$	(5, 5)	2
(5, 7)	2	(5, 8)	2
(6, 7)	2	(6, 8)	$4s-10$
(6, 9)	$8r-8$	(7, 8)	$2t-2$
(7, 11)	2	(7, 12)	$2t-2$
(7, 15)	2	(8, 8)	$2t-2$
(8, 10)	$2t-2$	(8, 11)	$2t-2$
(8, 12)	$4st-10t+6$	(8, 14)	2
(8, 15)	$2t-4$	(9, 10)	$8r-8$
(9, 12)	2	(9, 14)	$2r-2$
(9, 15)	$4r-6$	(10, 10)	$4rs+6rt-16r-4s-8t+18$
(10, 11)	2	(10, 14)	$4r-6$
(10, 15)	$4rs+4rt-12r-4s-4t+12$	(11, 12)	$2t-2$
(11, 15)	$2t-2$	(11, 16)	2
(12, 13)	$2st-2s-4t+4$	(12, 15)	$2t$
(12, 16)	$2st+2s-4t-6$	(13, 14)	$2t-2$
(13, 15)	$4st-4s-10t+10$	(14, 15)	$4r-4$
(14, 16)	$4r-6$	(15, 15)	$6rt-2r-7t+1$
(15, 16)	$10rs-28r-10s+4rt-4t+30$	(16, 16)	$16rst-24rt-20rs-21st+38t+23s+24r-40$

TABLE 4: Numerical comparison of indices of  $M[r, s, t]$  for some initial values of  $r, s, t \geq 2$ .

$(r, s, t)$	$R_1$	$R_{-1}$	$R_{1/2}$	$R_{-1/2}$	$M_1$	$\overline{M}_1$	$\overline{M}_2$	HM
(2, 2, 2)	825	13.3	260.9	32.4	530	10558	14398	3376
(3, 3, 3)	4130	36.7	1157.6	106.2	2336	143 434	2245544	16724
(4, 4, 4)	11399	79	1157.6	250	6190	868642	1450978	45992
(5, 5, 5)	24168	147.3	6397.8	489.6	12860	3453670	5989852	97324
(6, 6, 6)	43973	246.6	11510	847	23114	10587574	18818838	176864
(7, 7, 7)	72350	383	18796	1339	1347	37720	$2.72 \times 10^7$	290756
(8, 8, 8)	110835	563	28636	2013	57446	$6.14 \times 10^7$	$1.1 \times 10^8$	445144
(9, 9, 9)	160964	792	41418	2871	83060	$1.2 \times 10^8$	$2.3 \times 10^8$	646172
(10, 10, 10)	224273	1077	57525	3943	115330	$2.3 \times 10^8$	$4.4 \times 10^8$	899984

TABLE 5: Numerical comparison of indices of  $M[r, s, t]$  for some initial values of  $r, s, t \geq 2$ .

$(r, s, t)$	ABC	GA	$ABC_4$	$GA_5$	S
(2, 2, 2)	59.3	86.2	—	—	—
(3, 3, 3)	220	334.6	138.8	334.7	114310
(4, 4, 4)	546.8	847.8	330.6	843.3	347250
(5, 5, 5)	1098	1721	651.8	1712.2	775750
(6, 6, 6)	1933	3052	1135	3037	$1.4595 \times 10^6$
(7, 7, 7)	3110	4936	1813	4914	$2.46 \times 10^6$
(8, 8, 8)	4688	7469	2720	7440	$3.8 \times 10^6$
(9, 9, 9)	6725	10747	3887	10711	$5.6 \times 10^6$
(10, 10, 10)	9282	14865	5348	14820	$7.9 \times 10^6$

$$\begin{aligned}
 M_1(M[r, s, t]) &= \sum_{o\ell \in E(G)} (d_o + d_\ell) \\
 &= (2t + 2)(1 + 2) + (2st - 2)(1 + 3) + (2)(2 + 2) + (8r + 2s + 2t - 8)(2 + 3) \\
 &\quad + (4st - 4s - 6t + 6)(2 + 4) + (6rt + 2rs - 4r - 2s - 3t + 5)(3 + 3) + (4rs + 4rt - 2s - 4t + 2)(3 + 4) \\
 &\quad + (16rst - 8rs - 14rt - 11st - 4r + 7s + 10t - 7)(4 + 4).
 \end{aligned} \tag{7}$$

Thus, the result follows by simple calculations.

The next theorem gives us the new degree-based Zagreb index as defined in [21].  $\square$

**Theorem 5.** *The new degree-based Zagreb index  $HM(M[r, s, t])$  of  $M$ -carbon structure is given by*

$$\begin{aligned}
 HM(M[r, s, t]) &= 1024rst - 244rs - 484rt - 528st \\
 &\quad - 200r + 184s + 188t - 136.
 \end{aligned} \tag{8}$$

*Proof.* Let  $G$  be the chemical structural graph of  $M$ -carbon  $M[r, s, t]$ ; then, by using serial number 7 of Table 1 and edge partition given in Table 2, the new degree-based Zagreb index  $HM$  of  $M[r, s, t]$  is computed as follows:

$$\begin{aligned}
 HM(M[r, s, t]) &= \sum_{o\ell \in E(G)} (d_o + d_\ell)^2 \\
 &= (2t + 2)(1 + 2)^2 + (2st - 2)(1 + 3)^2 + (2)(2 + 2)^2 + (8r + 2s + 2t - 8)(2 + 3)^2 \\
 &\quad + (4st - 4s - 6t + 6)(2 + 4)^2 + (6rt + 2rs - 4r - 2s - 3t + 5)(3 + 3)^2 + (4rs + 4rt - 2s - 4t + 2)(3 + 4)^2 \\
 &\quad + (16rst - 8rs - 14rt - 11st - 4r + 7s + 10t - 7)(4 + 4)^2.
 \end{aligned} \tag{9}$$

Thus, the result follows by simple calculations.

In the next two theorems, we shall compute the newly defined Zagreb coindex indices which are defined in the form of nonedges of a chemical graph.  $\square$

**Theorem 6.** *The first Zagreb coindex index  $\overline{M}_1(M[r, s, t])$  of  $M$ -carbon structure is given by*

$$\begin{aligned}
 \overline{M}_1(M[r, s, t]) &= 256r^2s^2t^2 - 32r^2s^2t - 64r^2st^2 - 80s^2t^2r + 16s^2rt + 16t^2rs - 160rst + 28rs \\
 &\quad + 56rt + 66st + 16r - 18s - 16t + 10.
 \end{aligned} \tag{10}$$

*Proof.* The first Zagreb coindex index of chemical structural graph of  $M$ -carbon  $M[r, s, t]$  can be computed by using both

serial number 8 of Table 1 and Theorem 1. It is explained and calculated as follows:

$$\begin{aligned}
 \overline{M}_1(M[r, s, t]) &= 2|E(M[r, s, t])|(|V(M[r, s, t]) - 1) - M_1(M[r, s, t]) \\
 &= 2(16rst - 4rt - 5st - 2rs + t + s)(8rst - 1) - 128rst - 24rs - 48rt - 56st \\
 &\quad - 16r + 16s + 14t - 10.
 \end{aligned} \tag{11}$$

Thus, the result follows by simple calculations.  $\square$

**Theorem 7.** The second Zagreb coindex index  $\overline{M}_2(M[r, s, t])$  of M-carbon structure is given by

$$\begin{aligned} \overline{M}_2(M[r, s, t]) &= 512r^2s^2t^2 - 128r^2s^2t - 256r^2st^2 - 320s^2t^2r + 8r^2s^2 + 32r^2st + 32r^2t^2 \\ &\quad + 104s^2rt + 144t^2rs + 50s^2t^2 - 8s^2r - 344rst - 16rt^2 - 20s^2t - 20st^2 + 74rs \\ &\quad + 146rt + 2s^2 + 170st + 2t^2 + 60r - 58s - 60t + 42. \end{aligned} \quad (12)$$

*Proof.* The second Zagreb coindex index of chemical structural graph of M-carbon  $M[r, s, t]$  can be computed by

using both serial number 9 of Table 1 and Theorem 2. It is explained and calculated as follows:

$$\begin{aligned} \overline{M}_2(M[r, s, t]) &= 2|E(M[r, s, t])|^2 - \frac{1}{2}M_1(M[r, s, t]) - M_2(M[r, s, t]) \\ &= 2(16rst - 4rt - 5st - 2rs + t + s)^2 - (1/2)(128rst - 24rs - 48rt - 56st - 16r + 16s + 14t - 10) \\ &\quad - (256rst - 62rs - 122rt - 138st - 52r + 50s + 53t - 37). \end{aligned} \quad (13)$$

Thus, the result follows by simple calculations.

In the coming two theorems, we shall find closed formulas for the ABC and GA indices of  $M[r, s, t]$  M-carbon structure.  $\square$

**Theorem 8.** Consider the graph  $G \cong M[r, s, t]$  of M-carbon with  $r \geq 2, s \geq 2, t \geq 2$ ; then, its ABC index is equal to

$$\begin{aligned} ABC(M[r, s, t]) &= +\frac{2rs\sqrt{15}}{3} + \frac{2rt\sqrt{15}}{3} - 2rs\sqrt{6} - \frac{7rt\sqrt{6}}{2} - \frac{25st\sqrt{6}}{12} + 4rt + \frac{4rs}{3} - \frac{s\sqrt{15}}{3} \\ &\quad - \frac{2t\sqrt{15}}{3} + 4rst\sqrt{6} - \frac{29\sqrt{6}}{12} - \sqrt{2}t - \sqrt{2}s + \frac{10}{3} + \frac{\sqrt{15}}{3} + 2\sqrt{2}st - \sqrt{6}r \\ &\quad + \frac{7\sqrt{6}s}{4} + \frac{5\sqrt{6}t}{2} + \sqrt{2} + 4\sqrt{2}r - \frac{8r}{3} - \frac{4s}{3} - 2t. \end{aligned} \quad (14)$$

*Proof.* Let  $G$  be the chemical structural graph of M-carbon  $M[r, s, t]$ ; then, by using serial number 3 of Table 1 and edge

partition given in Table 2, the ABC index of  $M[r, s, t]$  is computed as follows:

$$\begin{aligned} ABC(M[r, s, t]) &= \sum_{o\ell \in E(G)} \sqrt{\frac{d_o + d_\ell - 2}{d_o d_\ell}} \\ &= (2t + 2) \left( \sqrt{\frac{1+2-2}{1 \times 2}} \right) + (2st - 2) \left( \sqrt{\frac{1+3-2}{1 \times 3}} \right) + (2) \left( \sqrt{\frac{2+2-2}{2 \times 2}} \right) + (8r + 2s + 2t - 8) \\ &\quad + \left( \sqrt{\frac{2+3-2}{2 \times 3}} \right) + (4st - 4s - 6t + 6) \left( \sqrt{\frac{2+4-2}{2 \times 4}} \right) + (6rt + 2rs - 4r - 2s - 3t + 5) \\ &\quad \cdot \left( \sqrt{\frac{3+3-2}{3 \times 3}} \right) + (4rs + 4rt - 2s - 4t + 2) \left( \sqrt{\frac{3+4-2}{3 \times 4}} \right) \\ &\quad + (16rst - 8rs - 14rt - 11st - 4r + 7s + 10t - 7) \left( \sqrt{\frac{4+4-2}{4 \times 4}} \right). \end{aligned} \quad (15)$$

The results now follow after some simple computations of above expression.  $\square$

**Theorem 9.** Consider the graph  $G \cong M[r, s, t]$  of  $M$ -carbon with  $r \geq 2, s \geq 2, t \geq 2$ ; then, its  $GA$  index is equal to

$$GA(M[r, s, t]) = 16rst - 11st - \frac{8\sqrt{2}t}{3} + \frac{16\sqrt{2}}{3} + \sqrt{3}st + \frac{\sqrt{3}}{7} + \frac{16\sqrt{6}r}{5} + \frac{4\sqrt{6}s}{5} + \frac{4\sqrt{6}t}{5} - \frac{16\sqrt{6}}{5} + \frac{8\sqrt{2}st}{3} - \frac{8\sqrt{2}s}{3} - 6rs - 8rt - 8r + 5s + 7t + \frac{16\sqrt{3}rs}{7} + \frac{16\sqrt{3}rt}{7} - \frac{8\sqrt{3}s}{7} - \frac{16\sqrt{3}t}{7}. \quad (16)$$

*Proof.* Let  $G$  be the chemical structural graph of  $M$ -carbon  $M[r, s, t]$ ; then, by using serial number 4 of Table 1 and edge

partition given in Table 2, the  $GA$  index of  $M[r, s, t]$  is computed as follows:

$$GA(M[r, s, t]) = \sum_{ol \in E(G)} \frac{2\sqrt{d_o \times d_l}}{d_o + d_l},$$

$$\cdot (2t + 2) \left( \frac{2\sqrt{1 \times 2}}{1 + 2} \right) + (2st - 2) \left( \frac{2\sqrt{1 \times 3}}{1 + 3} \right) + (2) \left( \frac{2\sqrt{2 \times 2}}{2 + 2} \right) + (8r + 2s + 2t - 8) \left( \frac{2\sqrt{2 \times 3}}{2 + 3} \right)$$

$$+ (4st - 4s - 6t + 6) \left( \frac{2\sqrt{2 \times 4}}{2 + 4} \right) + (6rt + 2rs - 4r - 2s - 3t + 5) \left( \frac{2\sqrt{3 \times 3}}{3 + 3} \right) \quad (17)$$

$$+ (4rs + 4rt - 2s - 4t + 2) \left( \frac{2\sqrt{3 \times 4}}{3 + 4} \right)$$

$$+ (16rst - 8rs - 14rt - 11st - 4r + 7s + 10t - 7) \left( \frac{2\sqrt{4 \times 4}}{4 + 4} \right).$$

The results now follow after some simple computations of the above expression.

Table 3 provides the edge partition of the  $M$ -carbon structure  $M[r, s, t]$  on the bases of sum of the degrees in the open neighbourhood of the end vertices of each an edge for each edge of  $M[r, s, t]$ . The first of such type of indices were introduced by Ghorbani and Hosseinzadeh [23], and then,

another one was introduced by Hosamani [25]. These are defined in Table 1.

In the following three theorems, we gave closed formula for the three indices, namely, fourth atom bond connectivity index  $ABC_4(G)$ , fifth version of geometric arithmetic index  $GA_5(G)$ , and Sanskruti index  $S(G)$  for the graph of  $G \cong M[r, s, t]$ .  $\square$

**Theorem 10.** The  $ABC_4$  index of the graph  $G \cong M[r, s, t]$  of  $M$ -carbon with  $r \geq 3, s \geq 3, t \geq 3$  is given by

$$\begin{aligned}
 ABC_4(G) = & 3 + \sqrt{3}st + \frac{\sqrt{462}}{21} + \frac{11t\sqrt{5}}{15} + \frac{t\sqrt{143}}{11} - \frac{3\sqrt{770}}{35} + \frac{\sqrt{2090}}{55} - \frac{2\sqrt{5}}{5} + \frac{3\sqrt{3}}{2} + \frac{47\sqrt{2}}{10} \\
 & - \frac{6\sqrt{2}s}{5} - \frac{5\sqrt{3}t}{2} + \frac{\sqrt{57}}{18} - \frac{\sqrt{357}}{21} + \frac{5\sqrt{11}}{22} + \frac{\sqrt{14}}{28} - \frac{12\sqrt{2}t}{5} + \frac{\sqrt{6}r}{3} + \frac{t\sqrt{14}}{4} + \frac{t\sqrt{77}}{11} \\
 & + \frac{4r\sqrt{330}}{45} - \frac{4\sqrt{7}r}{15} - \frac{14\sqrt{7}t}{15} + \frac{2r\sqrt{770}}{35} + \frac{6r\sqrt{70}}{35} + \frac{t\sqrt{70}}{10} - \frac{s\sqrt{42}}{6} - \frac{t\sqrt{42}}{3} \\
 & + \frac{23t\sqrt{182}}{182} + \frac{3r\sqrt{30}}{2} + \frac{281s\sqrt{30}}{240} + \frac{41t\sqrt{30}}{24} + \frac{4t\sqrt{110}}{55} + \frac{4r\sqrt{170}}{15} - \frac{2r\sqrt{138}}{5} \\
 & - \frac{2s\sqrt{138}}{15} - \frac{2t\sqrt{138}}{15} + \frac{4r\sqrt{78}}{9} + \frac{s\sqrt{78}}{12} - \frac{t\sqrt{78}}{6} + \frac{t\sqrt{374}}{22} + \frac{t\sqrt{357}}{21} - \frac{7r\sqrt{435}}{15} \\
 & - \frac{s\sqrt{435}}{6} - \frac{t\sqrt{435}}{15} \\
 & - \frac{s\sqrt{195}}{13} - \frac{2t\sqrt{195}}{13} - \frac{s\sqrt{897}}{39} - \frac{2t\sqrt{897}}{39} - \frac{5rs\sqrt{30}}{4} - \frac{3rt\sqrt{30}}{2} - \frac{251st\sqrt{30}}{240} \\
 & + \frac{2rs\sqrt{138}}{15} + \frac{2rt\sqrt{138}}{15} + \frac{st\sqrt{78}}{12} + \frac{\sqrt{6}}{6} + rst\sqrt{30} + \frac{37\sqrt{42}}{42} - \frac{\sqrt{374}}{22} \\
 & + \frac{rs\sqrt{435}}{6} + \frac{rt\sqrt{435}}{15} + \frac{st\sqrt{195}}{13} + \frac{st\sqrt{897}}{39} + \frac{st\sqrt{42}}{6} + \frac{6\sqrt{2}rs}{5} + \frac{9\sqrt{2}rt}{5} \\
 & + \frac{4\sqrt{7}rt}{5} - \frac{4\sqrt{170}}{15} + \frac{4\sqrt{21}}{21} + \frac{2\sqrt{195}}{13} + \frac{2\sqrt{138}}{5} + \frac{\sqrt{77}}{77} + \frac{3\sqrt{110}}{110} - \frac{11\sqrt{30}}{6} + \frac{\sqrt{35}}{7} \\
 & + \frac{\sqrt{435}}{2} + \frac{2\sqrt{7}}{15} - \frac{13\sqrt{70}}{35} - \frac{23\sqrt{182}}{182} - \frac{25\sqrt{78}}{36} + \frac{2\sqrt{897}}{39} - \frac{19\sqrt{2}r}{5} - \frac{2\sqrt{330}}{15}.
 \end{aligned} \tag{18}$$

*Proof.* Let  $G$  be the chemical structural graph of  $M$ -carbon  $M[r, s, t]$ ; then, by using serial number 10 of Table 1 and

edge partition given in Table 3, the  $ABC$  index of  $M[r, s, t]$  is computed as follows:

$$\begin{aligned}
 ABC_4(M[r, s, t]) &= \sum_{o\ell \in E(G)} \sqrt{\frac{S(o) + S(\ell) - 2}{S(o)S(\ell)}} \\
 &= (4) \left( \sqrt{\frac{3+7-2}{3 \times 7}} \right) + (2) \left( \sqrt{\frac{3+8-2}{3 \times 8}} \right) + (2t) \left( \sqrt{\frac{4+11-2}{4 \times 11}} \right) + (2st - 2s - 4t + 6) \\
 &\quad \cdot \left( \sqrt{\frac{4+12-2}{4 \times 12}} \right) + (2st - 2s - 4t + 4) \left( \sqrt{\frac{4+13-2}{4 \times 13}} \right) \\
 &\quad + (2) \left( \sqrt{\frac{5+5-2}{5 \times 5}} \right) + (2) \left( \sqrt{\frac{5+7-2}{5 \times 7}} \right) + (2) \left( \sqrt{\frac{5+8-2}{5 \times 8}} \right) + (2) \left( \sqrt{\frac{6+7-2}{6 \times 7}} \right) + (2) \left( \sqrt{\frac{6+8-2}{6 \times 8}} \right) \\
 &\quad + (8r - 8) \left( \sqrt{\frac{6+9-2}{6 \times 9}} \right) + (2t - 2) \left( \sqrt{\frac{7+8-2}{7 \times 8}} \right) + (2) \left( \sqrt{\frac{7+11-2}{7 \times 11}} \right) + (2t - 2) \left( \sqrt{\frac{7+12-2}{7 \times 12}} \right)
 \end{aligned}$$

$$\begin{aligned}
& + (2) \left( \sqrt{\frac{7+15-2}{7 \times 15}} \right) + (2t-2) \left( \sqrt{\frac{8+8-2}{8 \times 8}} \right) + (2t-2) \left( \sqrt{\frac{8+10-2}{8 \times 10}} \right) + (2t-2) \left( \sqrt{\frac{8+11-2}{8 \times 11}} \right) \\
& + (4st-10t+6) \left( \sqrt{\frac{8+12-2}{8 \times 12}} \right) + (2) \left( \sqrt{\frac{8+14-2}{8 \times 14}} \right) + (2t-4) \left( \sqrt{\frac{8+15-2}{8 \times 15}} \right) + (8r-8) \left( \sqrt{\frac{9+10-2}{9 \times 10}} \right) \\
& + (2) \left( \sqrt{\frac{9+12-2}{9 \times 12}} \right) + (2r-2) \left( \sqrt{\frac{9+14-2}{9 \times 14}} \right) + (4r-6) \left( \sqrt{\frac{9+15-2}{9 \times 15}} \right) \\
& + (4rs+6rt-16r-4s-8t+18) \left( \sqrt{\frac{10+10-2}{10 \times 10}} \right) + (2) \left( \sqrt{\frac{10+11-2}{10 \times 11}} \right) + (4r-6) \left( \sqrt{\frac{10+14-2}{10 \times 14}} \right) \\
& + (4rs+4rt-12r-4s-4t+12) \left( \sqrt{\frac{10+15-2}{10 \times 15}} \right) + (2t-2) \left( \sqrt{\frac{11+12-2}{11 \times 12}} \right) + (2t-2) \left( \sqrt{\frac{11+15-2}{11 \times 15}} \right) \\
& + (2) \left( \sqrt{\frac{11+16-2}{11 \times 16}} \right) + (2st-2s-4t+4) \left( \sqrt{\frac{12+13-2}{12 \times 13}} \right) + (2t) \left( \sqrt{\frac{12+15-2}{12 \times 15}} \right) + (2st+2s-4t-6) \\
& \cdot \left( \sqrt{\frac{12+16-2}{12 \times 16}} \right) + (2t-2) \left( \sqrt{\frac{13+14-2}{13 \times 14}} \right) + (4st-4s-10t+10) \times \left( \sqrt{\frac{13+15-2}{13 \times 15}} \right) \\
& + (4r-4) \left( \sqrt{\frac{14+15-2}{14 \times 15}} \right) + (4r-6) \left( \sqrt{\frac{14+16-2}{14 \times 16}} \right) + (6rt-2r-7t+1) \left( \sqrt{\frac{15+15-2}{15 \times 15}} \right) \\
& + (10rs-28r-10s+4rt-4t+30) \left( \sqrt{\frac{15+16-2}{15 \times 16}} \right) + (16rst-24rt-20rs-21st+38t+23s+24r-40) \\
& \cdot \left( \sqrt{\frac{16+16-2}{16 \times 16}} \right).
\end{aligned} \tag{19}$$

The results now follow after some simple computation of the above expression.  $\square$

**Theorem 11.** Consider the graph  $G \cong M[r, s, t]$  of  $M$ -carbon with  $r, s, t \geq 3$ ; then, its  $GA_5$  index is given by

$$\begin{aligned}
GA_5(G) = & -21 + 6r + 19s + \frac{15\sqrt{3}st}{7} + \frac{16t\sqrt{5}}{9} - 21st - \frac{8\sqrt{5}}{9} + \frac{13\sqrt{3}}{7} + 25t + \frac{4\sqrt{19}}{5} \\
& + \frac{16\sqrt{13}}{17} + \frac{\sqrt{3}s}{7} - \frac{30\sqrt{3}t}{7} + \frac{16\sqrt{11}}{27} - \frac{916\sqrt{14}}{345} + \frac{548r\sqrt{14}}{345} + \frac{2r\sqrt{35}}{3} + \frac{8t\sqrt{21}}{19} + \frac{48r\sqrt{10}}{19} \\
& + \frac{8t\sqrt{22}}{19} - \frac{80s\sqrt{15}}{31} - \frac{32t\sqrt{15}}{31} - \frac{8\sqrt{6}r}{5} - \frac{8\sqrt{6}s}{5} - \frac{28\sqrt{6}t}{5} - 12rt - 16rs + \frac{8t\sqrt{14}}{15} - \frac{8\sqrt{210}}{29} \\
& - \frac{2\sqrt{165}}{13} + \frac{4t\sqrt{182}}{27} + \frac{8t\sqrt{30}}{23} - \frac{2s\sqrt{195}}{7} - \frac{5t\sqrt{195}}{7} + \frac{52\sqrt{6}}{11} + \frac{8st\sqrt{39}}{25} \\
& + \frac{8\sqrt{13}st}{17} + \frac{4\sqrt{42}}{13} + \frac{2st\sqrt{195}}{7} + 16rst + \frac{2\sqrt{105}}{11} + \frac{8t\sqrt{11}}{15} + \frac{2t\sqrt{165}}{13} - \frac{8\sqrt{21}}{19} + \frac{5\sqrt{195}}{7} \\
& - \frac{8\sqrt{13}s}{17} - \frac{16\sqrt{13}t}{17} + \frac{387\sqrt{15}}{62} - \frac{8\sqrt{22}}{19} - \frac{472\sqrt{10}}{247} + \frac{2\sqrt{77}}{9} + \frac{4\sqrt{110}}{21} \\
& - \frac{16\sqrt{30}}{23} - \frac{2\sqrt{35}}{3} + \frac{8\sqrt{7}}{11} - \frac{4\sqrt{182}}{27} + \frac{8r\sqrt{210}}{29} + \frac{16\sqrt{39}}{25} - \frac{8\sqrt{33}}{23} + \frac{8t\sqrt{33}}{23} \\
& - \frac{8s\sqrt{39}}{25} - \frac{16t\sqrt{39}}{25} - \frac{193r\sqrt{15}}{31} + \frac{80rs\sqrt{15}}{31} + \frac{32rt\sqrt{15}}{31} + \frac{8rs\sqrt{6}}{5} + \frac{8rt\sqrt{6}}{5} + \frac{8st\sqrt{6}}{5}.
\end{aligned} \tag{20}$$

*Proof.* Let  $G$  be the chemical structural graph of  $M$ -carbon  $M[r, s, t]$ ; then, by using serial number 11 of Table 1 and

edge partition given in Table 3, the  $GA$  index of  $M[r, s, t]$  is computed as follows:

$$\begin{aligned}
 GA_5(M[r, s, t]) &= \sum_{o\ell \in E(G)} \frac{2\sqrt{S(o) \times S(\ell)}}{S(o) + S(\ell)} \\
 &= (4)\left(\frac{2\sqrt{3 \times 7}}{3 + 7}\right) + (2)\left(\frac{2\sqrt{3 \times 8}}{3 + 8}\right) + (2t)\left(\frac{2\sqrt{4 \times 11}}{4 + 11}\right) + (2st - 2s - 4t + 6) \\
 &\quad \cdot \left(\frac{2\sqrt{4 \times 12}}{4 + 12}\right) + (2st - 2s - 4t + 4)\left(\frac{2\sqrt{4 \times 13}}{4 + 13}\right) + (2)\left(\frac{2\sqrt{5 \times 5}}{5 + 5}\right) \\
 &\quad + (2)\left(\frac{2\sqrt{5 \times 7}}{5 + 7}\right) + (2)\left(\frac{2\sqrt{5 \times 8}}{5 + 8}\right) + (2)\left(\frac{2\sqrt{6 \times 7}}{6 + 7}\right) + (2)\left(\frac{2\sqrt{6 \times 8}}{6 + 8}\right) \\
 &\quad + (8r - 8)\left(\frac{2\sqrt{6 \times 9}}{6 + 9}\right) + (2t - 2)\left(\frac{2\sqrt{7 \times 8}}{7 + 8}\right) + (2)\left(\frac{2\sqrt{7 \times 11}}{7 + 11}\right) + (2t - 2) \\
 &\quad \cdot \left(\frac{2\sqrt{7 \times 12}}{7 + 12}\right) + (2)\left(\frac{2\sqrt{7 \times 15}}{7 + 15}\right) + (2t - 2)\left(\frac{2\sqrt{8 \times 8}}{8 + 8}\right) + (2t - 2) \\
 &\quad \cdot \left(\frac{2\sqrt{8 \times 10}}{8 + 10}\right) + (2t - 2)\left(\frac{2\sqrt{8 \times 11}}{8 + 11}\right) + (4st - 10t + 6)\left(\frac{2\sqrt{8 \times 12}}{8 + 12}\right) \\
 &\quad + (2)\left(\frac{2\sqrt{8 \times 14}}{8 + 14}\right) + (2t - 4)\left(\frac{2\sqrt{8 \times 15}}{8 + 15}\right) + (8r - 8)\left(\frac{2\sqrt{9 \times 10}}{9 + 10}\right) \\
 &\quad + (2)\left(\frac{2\sqrt{9 \times 12}}{9 + 12}\right) + (2r - 2)\left(\frac{2\sqrt{9 \times 14}}{9 + 14}\right) + (4r - 6)\left(\frac{2\sqrt{9 \times 15}}{9 + 15}\right) \\
 &\quad + (4rs + 6rt - 16r - 4s - 8t + 18)\left(\frac{2\sqrt{10 \times 10}}{10 + 10}\right) + (2)\left(\frac{2\sqrt{10 \times 11}}{10 + 11}\right) + (4r - 6) \\
 &\quad \cdot \left(\frac{2\sqrt{10 \times 14}}{10 + 14}\right) + (4rs + 4rt - 12r - 4s - 4t + 12)\left(\frac{2\sqrt{10 \times 15}}{10 + 15}\right) + (2t - 2) \\
 &\quad \cdot \left(\frac{2\sqrt{11 \times 12}}{11 + 12}\right) + (2t - 2)\left(\frac{2\sqrt{11 \times 15}}{11 + 15}\right) + (2)\left(\frac{2\sqrt{11 \times 16}}{11 + 16}\right) + (2st - 2s - 4t + 4) \\
 &\quad \cdot \left(\frac{2\sqrt{12 \times 13}}{12 + 13}\right) + (2t)\left(\frac{2\sqrt{12 \times 15}}{12 + 15}\right) + (2st + 2s - 4t - 6) \\
 &\quad \cdot \left(\frac{2\sqrt{12 \times 16}}{12 + 16}\right) + (2t - 2)\left(\frac{2\sqrt{13 \times 14}}{13 + 14}\right) + (4st - 4s - 10t + 10) \\
 &\quad \times \left(\frac{2\sqrt{13 \times 15}}{13 + 15}\right) + (4r - 4)\left(\frac{2\sqrt{14 \times 15}}{14 + 15}\right) + (4r - 6)\left(\frac{2\sqrt{14 \times 16}}{14 + 16}\right) + (6rt - 2r - 7t + 1) \\
 &\quad \cdot \left(\frac{2\sqrt{15 \times 15}}{15 + 15}\right) + (10rs - 28r - 10s + 4rt - 4t + 30)\left(\frac{2\sqrt{15 \times 16}}{15 + 16}\right) \\
 &\quad + (16rst - 24rt - 20rs - 21st + 38t + 23s + 24r - 40)\left(\frac{2\sqrt{16 \times 16}}{16 + 16}\right).
 \end{aligned} \tag{21}$$

The results now follow after some simple computation of the above expression.  $\square$

**Theorem 12.** Consider the graph  $G \cong M[r, s, t]$  of  $M$ -carbon with  $r, s, t \geq 3$ ; then, its Sanskruti index  $S(G)$  is given by

$$S(G) = c_1 r + c_2 s - c_0 - c_4 st + c_2 t - c_5 rt - c_6 rs + c_7 rst, \quad (22)$$

where  $c_0 = (177434147265976313012358335881357 \ 65065 \ 63/ \ 233972495845970544399543494688000000)$ ,  $c_1 = (384 \ 10 \ 15904100770126879995213/ \ 3876335270 \ 2814242 \ 799$

$6964000)$ ,  $c_2 = (42042269311169825975177/81507807551 \ 42420850)$ ,  $c_3 = (33779105325980576848378857231211/ \ 3203582868001177090884000000)$ ,  $c_4 = (56697 \ 7749527 \ 70 \ 1739/61888713909750)$ ,  $c_5 = (731518633569104009441/98 \ 93 \ 2250100348000)$ ,  $c_6 = (26845875203 \ 03660 \ 8/5408 \ 104050675)$  and,  $c_7 = (33554432/3375)$ .

*Proof.* Let  $G$  be the chemical structural graph of  $M$ -carbon  $M[r, s, t]$ ; then, by using serial number 12 of Table 1 and edge partition given in Table 3, the Sanskruti index  $S(M[r, s, t])$  of  $M[r, s, t]$  is computed as follows:

$$\begin{aligned} GA_5(M[r, s, t]) &= \sum_{o\ell \in E(G)} \left( \frac{S(o) \times S(\ell)}{S(o) + S(\ell) - 2} \right)^3 \\ &= (4) \left( \frac{3 \times 7}{3+7-2} \right)^3 + (2) \left( \frac{3 \times 8}{3+8-2} \right)^3 + (2t) \left( \frac{4 \times 11}{4+11-2} \right)^3 + (2st - 2s - 4t + 6) \\ &\quad \cdot \left( \frac{4 \times 12}{4+12-2} \right)^3 + (2st - 2s - 4t + 4) \left( \frac{4 \times 13}{4+13-2} \right)^3 + (2) \left( \frac{5 \times 5}{5+5-2} \right)^3 \\ &\quad + (2) \left( \frac{5 \times 7}{5+7-2} \right)^3 + (2) \left( \frac{5 \times 8}{5+8-2} \right)^3 + (2) \left( \frac{6 \times 7}{6+7-2} \right)^3 + (2) \left( \frac{6 \times 8}{6+8-2} \right)^3 \\ &\quad + (8r - 8) \left( \frac{6 \times 9}{6+9-2} \right)^3 + (2t - 2) \left( \frac{7 \times 8}{7+8-2} \right)^3 + (2) \left( \frac{7 \times 11}{7+11-2} \right)^3 + (2t - 2) \\ &\quad \cdot \left( \frac{7 \times 12}{7+12-2} \right)^3 + (2) \left( \frac{\times 15}{7+15-2} \right)^3 + (2t - 2) \left( \frac{8 \times 8}{8+8-2} \right)^3 + (2t - 2) \\ &\quad \cdot \left( \frac{8 \times 10}{8+10-2} \right)^3 + (2t - 2) \left( \frac{8 \times 11}{8+11-2} \right)^3 + (4st - 10t + 6) \left( \frac{8 \times 12}{8+12-2} \right)^3 \\ &\quad + (2) \left( \frac{8 \times 14}{8+14-2} \right)^3 + (2t - 4) \left( \frac{8 \times 15}{8+15-2} \right)^3 + (8r - 8) \left( \frac{9 \times 10}{9+10-2} \right)^3 \\ &\quad + (2) \left( \frac{9 \times 12}{9+12-2} \right)^3 + (2r - 2) \left( \frac{9 \times 14}{9+14-2} \right)^3 + (4r - 6) \left( \frac{9 \times 15}{9+15-2} \right)^3 \\ &\quad + (4rs + 6rt - 16r - 4s - 8t + 18) \left( \frac{10 \times 10}{10+10-2} \right)^3 + (2) \left( \frac{10 \times 11}{10+11-2} \right)^3 + (4r - 6) \\ &\quad \cdot \left( \frac{10 \times 14}{10+14-2} \right)^3 + (4rs + 4rt - 12r - 4s - 4t + 12) \left( \frac{10 \times 15}{10+15-2} \right)^3 + (2t - 2) \\ &\quad \cdot \left( \frac{11 \times 12}{11+12-2} \right)^3 + (2t - 2) \left( \frac{11 \times 15}{11+15-2} \right)^3 + (2) \left( \frac{11 \times 16}{11+16-2} \right)^3 + (2st - 2s - 4t + 4) \\ &\quad \cdot \left( \frac{12 \times 13}{12+13-2} \right)^3 + (2t) \left( \frac{12 \times 15}{12+15-2} \right)^3 + (2st + 2s - 4t - 6) \\ &\quad \cdot \left( \frac{12 \times 16}{12+16-2} \right)^3 + (2t - 2) \left( \frac{13 \times 14}{13+14-2} \right)^3 + (4st - 4s - 10t + 10) \\ &\quad \times \left( \frac{13 \times 15}{13+15-2} \right)^3 + (4r - 4) \left( \frac{14 \times 15}{14+15-2} \right)^3 + (4r - 6) \left( \frac{14 \times 16}{14+16-2} \right)^3 + (6rt - 2r - 7t + 1) \\ &\quad \cdot \left( \frac{15 \times 15}{15+15-2} \right)^3 + (10rs - 28r - 10s + 4rt - 4t + 30) \left( \frac{15 \times 16}{15+16-2} \right)^3 \\ &\quad + (16rst - 24rt - 20rs - 21st + 38t + 23s + 24r - 40) \left( \frac{16 \times 16}{16+16} \right)^3. \end{aligned} \quad (23)$$

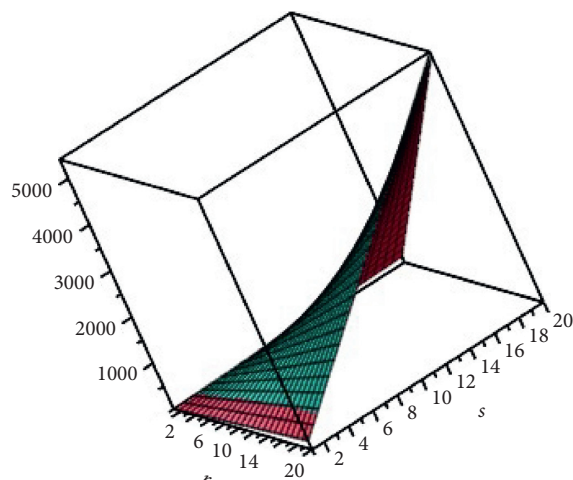


FIGURE 6: Comparison of  $GA$  index and  $GA_5$  index of  $M[r, s, t]$  for fix  $t = 1$ . Red color represents  $GA$ , and green color represents  $GA_5$ .

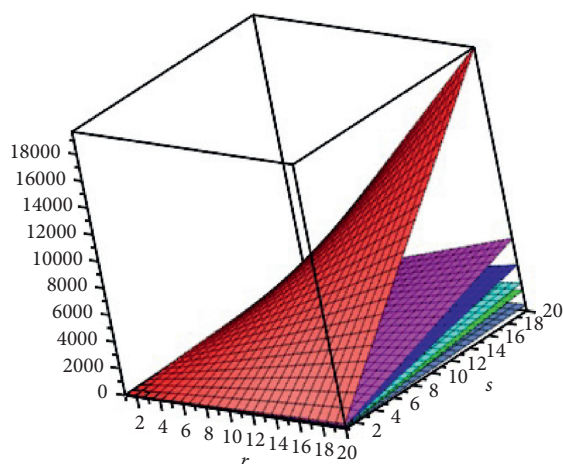


FIGURE 7: Comparison of  $R_{-1}$ ,  $R_{-1/2}$ ,  $ABC_4$ ,  $R_{1/2}$ ,  $ABC$ , and  $GA$  indices of  $M[r, s, t]$  for fix  $t = 1$ . Niagara azure, green, cyan, blue, purple, and red represents  $R_{-1}$ ,  $R_{-1/2}$ ,  $ABC_4$ ,  $R_{1/2}$ ,  $ABC$ , and  $GA$  indices, respectively.

The results now follow after some simple calculations.  $\square$

#### 4. Comparison and Discussion

In this section, we shall discuss and compare all the computed indices (degree based and sum degree based) from Theorems 3–12 both graphically and numerically (by a tables).

Tables 4 and 5 provide us a numerical comparison. From these two tables and computations, we can analyse that which type of indices are closed related and can be used to study the same type of chemical, biochemical, physical, and biophysical properties of the structure of  $M[r, s, t]$ . We can see that the values of  $GA$  and  $GA_5$  are very close and almost similar, so we can purpose that any one of them can be used in place of each other for the study of chemical structure  $M[r, s, t]$ . They also show the same kind of behaviour in graphical analysis (Figure 6). On the same pattern, we can also see the closely

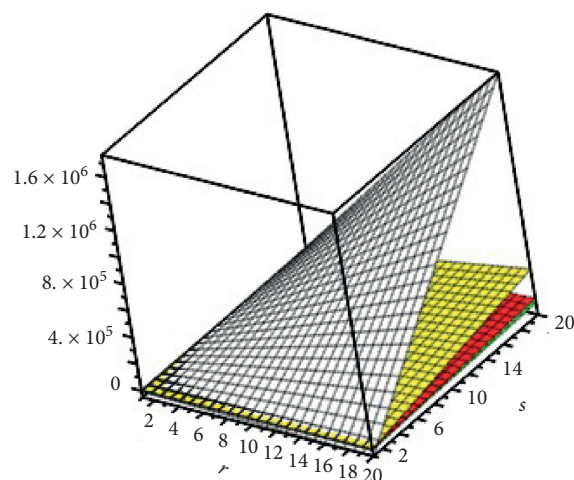


FIGURE 8: Comparison of first Zagreb coindex index  $\overline{M}_1$  and second Zagreb coindex  $\overline{M}_2$  of  $M[r, s, t]$ . Purple and blue represents  $\overline{M}_1$  and  $\overline{M}_2$ , respectively.

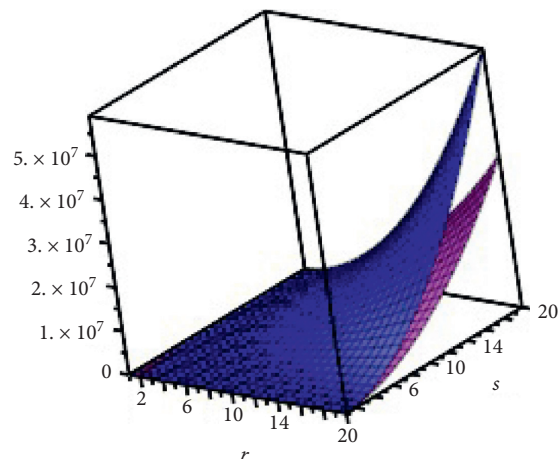


FIGURE 9: Comparison of  $\overline{M}_1$  and  $\overline{M}_2$  indices of  $M[r, s, t]$ , where purple color represents  $\overline{M}_1$  and blue color represents  $\overline{M}_2$ .

related values of  $R_{-1}$ ,  $R_{-1/2}$ ,  $ABC_4$ ,  $R_{1/2}$ ,  $ABC$ ,  $GA$ , and  $GA_5$ , and these values are also produced in an increasing order, respectively. So, we can purpose to use those indices which give smaller values for the study of respective properties of structure  $M[r, s, t]$  giving smaller values after the experimental study and the graphical comparison in Figure 7 which also shows the same type of patterns. Similarly, the indices  $M_1$ ,  $R_1$ ,  $HM$ ,  $S$ ,  $\overline{M}_1$ , and  $\overline{M}_2$  give us larger values even for such small initial inputs of  $r, s, t$ . Such behaviour shows that (and we purpose that) they cannot be used as closely related to the previous mentioned indices to study the same type of properties of  $M[r, s, t]$ . We can also see the behaviour of these indices in Figures 8 and 9. It is purposed to use these indices in the study of such properties of  $M[r, s, t]$  which gives higher experimental values.

#### 5. Conclusion

In this article, we have studied the structure  $M[r, s, t]$  of M-carbon in the form of its degree and sum degree-based

indices. The indices that we computed and discussed in the article are  $R_{-1}$ ,  $R_{-1/2}$ ,  $ABC_4$ ,  $R_{1/2}$ ,  $ABC$ ,  $GA$ ,  $GA_5M_1$ ,  $R_1$ ,  $HM$ ,  $S$ ,  $M_1$ , and  $M_2$ . We also compared these indices numerically and graphically to show which type of indices behaved in different and same patterns (or values). We have found exact formulas for these indices for the structure of  $M[r, s, t]$  of M-carbon.

## Data Availability

The data used to support the findings of this study are included within the article.

## Conflicts of Interest

The authors declare that they have no conflicts of interest.

## Acknowledgments

The authors wish to thank the referees for their careful reading of the manuscript and valuable suggestions. This work was supported by the National Key Research and Development Program (2018YFB0904205), Sichuan Science and Technology Program (21GJHZ0012), Chengdu Science and Technology Bureau Program (2020-YF09-00005-SN), and the Key Laboratory of Pattern Recognition and Intelligent Information Processing and Institutions of Higher Education of Sichuan Province (MSSB-2020-12).

## References

- [1] A. O. Lyakhov and A. R. Oganov, "Evolutionary search for superhard materials: methodology and applications to forms of carbon and  $TiO_2$ ," *Physical Review B*, vol. 84, Article ID 092103, 2011.
- [2] Q. Li, Y. Ma, A. R. Oganov et al., "Superhard monoclinic polymorph of carbon," *Physical Review Letters*, vol. 102, no. 17, Article ID 175506, 2009.
- [3] K. Umamoto, R. M. Wentzcovitch, S. Saito, and T. Miyake, "Body-centered TetragonalC4: a Viable sp<sup>3</sup> Carbon allotrope," *Physical Review Letters*, vol. 104, no. 12, p. 125504, 2010.
- [4] H. Wiener, "Structural determination of paraffin boiling points," *Journal of the American Chemical Society*, vol. 69, no. 1, pp. 17–20, 1947.
- [5] A. Q. Baig, M. Imran, W. Khalid, and M. Naeem, "Molecular description of carbon graphite and crystal cubic carbon structures," *Canadian Journal of Chemistry*, vol. 95, no. 6, pp. 674–686, 2017.
- [6] W. Gao, M. Siddiqui, M. Naeem, and N. Rehman, "Topological characterization of carbon graphite and crystal cubic carbon structures," *Molecules*, vol. 22, no. 9, p. 1496, 2017.
- [7] M. Imran, M. Naeem, A. Q. Baig, M. K. Siddiqui, M. A. Zahid, and W. Gao, "Modified eccentric descriptors of crystal cubic carbon," *Journal of Discrete Mathematical Sciences and Cryptography*, vol. 22, no. 7, pp. 1215–1228, 2019.
- [8] H. Yang and X. Zhou, "Some properties of double roman domination," *Discrete Dynamics in Nature and Society*, vol. 2020, Article ID 6481092, 5 pages, 2020.
- [9] H. Yang, M. Kamran Siddiqui, M. Naeem, and N. Abdul Rehman, "Molecular properties of carbon crystal cubic structures," *Open Chemistry*, vol. 18, no. 1, pp. 339–346, 2020.
- [10] H. Yang, A. Q. Baig, W. Khalid, M. R. Farahani, and X. Zhang, "M-polynomial and topological indices of benzene ring embedded in P-type surface network," *Journal of Chemistry*, vol. 2019, Article ID 7297253, 9 pages, 2019.
- [11] H. Yang, M. A. Rashid, S. Ahmad, S. S. Khan, and M. K. Siddiqui, "On molecular descriptors of face-centered cubic lattice," *Processes*, vol. 7, no. 5, pp. 1–15, 2019.
- [12] H. Yang, P. Wu, S. Nazari-Moghaddam et al., "Bounds for signed double Roman k-domination in trees," *RAIRO-Operations Research*, vol. 53, no. 2, pp. 627–643, 2019.
- [13] M. A. Zahid, M. Naeem, A. Q. Baig, and W. Gao, "General fifth M-Zagreb indices and fifth M-Zagreb polynomials of crystal cubic carbon," *Utilitas Mathematica*, vol. 109, pp. 263–270, 2018.
- [14] M. Randić, "Characterization of molecular branching," *Journal of the American Chemical Society*, vol. 97, no. 23, pp. 6609–6615, 1975.
- [15] B. Bollobás and P. Erdős, "Graphs of extremal weights," *Ars Combinatoria*, vol. 50, pp. 225–233, 1998.
- [16] D. Amic, D. Beslo, B. Lucic, S. Nikolic, and N. Trinajstić, "The vertex-connectivity index revisited," *Journal of Chemical Information and Computer Sciences*, vol. 38, pp. 819–822, 1998.
- [17] E. Estrada, L. Torres, L. Rodríguez, and I. Gutman, "An atom-bond connectivity index: modelling the enthalpy of formation of alkanes," *Indian Journal of Chemistry*, vol. 37A, pp. 849–855, 1998.
- [18] D. Vukičević and B. Furtula, "Topological index based on the ratios of geometric and arithmetic means of end-vertex degrees of edges," *Journal of Mathematical Chemistry*, vol. 46, pp. 1369–1376, 2009.
- [19] I. Gutman and N. Trinajstić, "Graph theory and molecular orbitals. Total  $\pi$ -electron energy of alternant hydrocarbons," *Chemical Physics Letters*, vol. 17, no. 4, pp. 535–538, 1972.
- [20] I. Gutman and K. C. Das, "The first Zagreb index 30 years after," *MATCH Communications in Mathematical and in Computer Chemistry*, vol. 50, pp. 83–92, 2004.
- [21] G. H. Shirdeh, H. R. Pour, and A. M. Sayadi, "The hyper-zagreb index of graph operations," *Iranian Journal of Mathematical Chemistry*, vol. 4, no. 2, pp. 213–220, 2013.
- [22] T. Doslic, "Vertex-weighted Wiener polynomials for composite graphs," *Ars Mathematica Contemporanea*, vol. 1, pp. 66–80, 2008.
- [23] A. Ghorbani and M. A. Hosseinzadeh, "Computing  $ABC_4$  index of nanostar dendrimers," *Optoelectronics and Advanced Materials-Rapid Communications*, vol. 4, pp. 1419–1422, 2010.
- [24] A. Graovac, M. Ghorbani, and M. A. Hosseinzadeh, "Computing fifth geometric-arithmetic index for nanostar dendrimers," *Journal of Mathematical Nanoscience*, vol. 1, pp. 33–42, 2011.
- [25] S. M. Hosamani, "Computing sanskruti index of certain nanostructures," *Journal of Applied Mathematics and Computing*, vol. 54, 2016.
- [26] I. Gutman, B. Furtula, Ž. K. Vukičević, and G. Popivoda, "On zagreb indices and coindices," *MATCH Communications in Mathematical and in Computer Chemistry*, vol. 74, pp. 5–16, 2015.

## Research Article

# Comparing Zinc Oxide- and Zinc Silicate-Related Metal-Organic Networks via Connection-Based Zagreb Indices

Muhammad Tanveer Hussain,<sup>1</sup> Muhammad Javaid ,<sup>1</sup> Usman Ali,<sup>1</sup> Ali Raza,<sup>1</sup> and Md Nur Alam <sup>2</sup>

<sup>1</sup>Department of Mathematics, School of Science, University of Management and Technology, Lahore 54770, Pakistan

<sup>2</sup>Department of Mathematics, Pabna University of Science and Technology, Pabna 6600, Bangladesh

Correspondence should be addressed to Md Nur Alam; nuralam23@pust.ac.bd

Received 13 August 2021; Revised 29 September 2021; Accepted 4 October 2021; Published 18 October 2021

Academic Editor: Ajaya Kumar Singh

Copyright © 2021 Muhammad Tanveer Hussain et al. This is an open access article distributed under the Creative Commons Attribution License, which permits unrestricted use, distribution, and reproduction in any medium, provided the original work is properly cited.

Metal-organic networks (MONs) are among the unique complex and porous chemical compounds. So, these chemical compounds consist of metal ions (vertices) and organic ligands (edges between vertices). These networks represent large pore volume, extreme surface area, morphology, excellent chemical stability, highly porous and crystalline materials, and octahedral clusters. MONs are mostly used in assessment of chemicals, gas and energy storage devices, sensing, separation and purification of different gases, heterogeneous catalysis, environmental hazard, toxicology, adsorption analysis, biomedical applications, and biocompatibility. Recently, drug delivery, cancer imaging, and biosensing have been investigated by biomedical applications of zinc-related MONs. The versatile applications of these MONs make them helpful tools in many fields of science in recent decade. In this paper, we discuss the two different zinc oxide and zinc silicate related MONs according to the number of increasing layers of metal and organic ligands together. We also compute the connection-based Zagreb indices such as first Zagreb connection index (ZCI), second ZCI, modified first ZCI, modified second ZCI, modified third ZCI, and modified fourth ZCI. Moreover, a comparison is also included between the zinc-related MONs by using numerical values of connection-based Zagreb indices. Finally, we conclude that zinc silicate-related MON is better than zinc oxide-related MON for all values of  $n$ .

## 1. Introduction

There are so many chemical compounds in the field of chemistry. One of the most popular recent chemical compounds is metal-organic network (MON) which consists of metal ions and organic ligands. A new MON with zinc as the metal ion and benzene-1,3-dicarboxylic acid as the organic ligand (linker) has been synthesized with the help of hydrothermal method. This MON is also used as a selective nano-adsorbent for the preconcentration and extraction of trace amounts of cadmium with the help of solid-phase extraction method. A category of crystalline and porous materials is porous coordination polymers which are newly known as MONs [1]. One of the most important aspects which can be considered in the matter of MONs in bioapplications is their surface modification and

control of their particle size distribution [2]. Zn-related MONs as chemical sensors could be converted into devices for luminescent characteristics [3]. The electron-rich T-conjugated fluorescent ligands are friendly to make Zn-MONs with nucleophilic properties in efficient luminescent sensors [4].

The low toxicity of zinc ions as the desirable character is considered to introduce Zn-related MONs into bio-application domains, especially drug carriers. The anti-bacterial activity has been validated by combining different antibiotic drugs and metals [5]. In reality,  $Zn^{2+}$  is an endogenous low-toxic transition metal cation which is widely used in dermatology as a cicatrizing agent and skin moisturizer with astringent, antidandruff, antibacterial, and anti-inflammatory agents [6]. In nonlinear optically active MONs,  $Zn^{2+}$  is commonly used as a connecting point

to prevail undesired d-d transitions in the visible region. Moreover, the toxicology, biomedical applications, and their biocompatibility are recently reported production procedures of zinc-related MONs. For more details, refer to [7].

Eddaoudi et al. [8] synchronized the isorecticular series (IRMOF-1 to IRMOF-16) of 16 highly crystalline materials. The free and fixed diameter of pores from IRMOF-1 to IRMOF-16 varies in the range of 3.8–19.1 and 12.8–28.8, respectively. The design of an IRMOF-10 series based on MON-5 was initiated by determining the reaction conditions necessary to produce the octahedral cluster with a ditopic linear carboxylate. Therefore, many IRMOF structures can be developed by using zinc oxide octahedral clusters ( $Zn_4O(CO)_2$ ) as the metal corners linked via diverse organic dicarboxylate linkers and different three-dimensional cubic networks are formed. For more information, see [9]. All the IRMOFs have the expected topology of  $CaB_6(13)$  and happened through the prototype IRMOF-1 in which an oxide-centered  $Zn_4O$  tetrahedron is edge bridged. Some IRMOFs such as IRMOF-8, IRMOF-10, IRMOF-12, and IRMOF-16 have been seen in noncrystalline porous systems for  $SiO_2$  xerogels and aerogels (16). For further investigation, see [7, 10–12].

MONs also predict the physicochemical properties such as grafting active groups [13], impregnating suitable active material [14], ion exchange [15], preparing composites with different substances [11], changing organic ligands and postsynthetic ligands [16], and biosensors enhancing sensitivity, response time, and selectivity [17]. Yap et al. [18] and Lin et al. [19] presented the recent progress in precursors on the preparation of several nanostructures and MON-related applications such as sensing, photocatalysis, electrocatalysis, supercapacitors, catalyst for production of fine chemicals, and lithium ion batteries. Graph theory provides useful tools in the field of modern chemistry which represent the chemical and physical properties of chemical compounds such as heat of formation, heat of evaporation, flash point, melting point, boiling point, temperature, pressure, density, retention in chromatography, and tension and partition coefficient [20–22]. First, distance-based topological index (TI) was discovered by Wiener to study the different properties of chemical compounds (boiling point of paraffin) in 1947 [23]. The very well-reputed first-degree-based TI was discovered by Gutman and Trinajstić to check the chemical physibility on the total  $\pi$ -electron energy of the chemical compounds (alternant hydrocarbons) in 1972 [24].

Recently, Zhao et al. [25] introduced two connection number (number of vertices at distance two) based TIs to compute the general results for modified Zagreb connection indices of subdivision and semitotal point operations on graphs. Nowadays, these degree and connection number-based TIs are abundantly used in the topological properties of four-layered neural networks and MONs [26, 27]. Ali et al. [28] computed connection-based indices and coindices for the product of molecular networks. Gutman and Furtula

discussed various topological properties of different molecular structures; see [29–31]. Ali and Trinajstić [32] and Javaid et al. [33] computed different connection-based TIs of graphs under different operations. Moreover, a variety of networks has been defined with the help of connection number-based TIs [34–37].

In this paper, we compute the connection-based Zagreb indices of two different zinc-related MONs such as zinc oxide ( $ZNOX(n) = IRMOF-10$ ) and zinc silicate ( $ZNCL(n) = IRMOF-14$ ) networks with respect to the increasing layers,  $n \geq 3$ , taking both metal nodes and linkers together. The rest of the paper is organized as follows. Section 2 provides the preliminaries, definitions, and some important results which can be used in the main results. Sections 3 and 4 provides the main results for zinc oxide and zinc silicate networks, and Section 5 provides comparisons and conclusions.

## 2. Preliminaries

The vertex and edge sets are  $V(G)$  and  $E(G)$  for a simple and connected network  $G$ .  $|V(G)|$  and  $|E(G)|$  are the cardinalities of vertex set and edge set which are equal to  $u$  and  $e$ , respectively. In a connected network, there is a path between two vertices. The distance between two vertices  $p$  and  $q$  is the shortest path between them. It is denoted by  $d_G(p, q)$ . In general [37],  $N_G(q/m) = \{p \in V(G); d(p, q) = m\}$  is the open  $m$ -neighborhood set of  $q$ , where  $m$  represents a positive integer and  $|N_G(q/m)| = d_G(q/m)$  is called  $m$ -distance degree of a vertex  $q$ . In particular,

- (i) If  $m = 1$ ,  $d_G(q/1) = |N_G(q/1)| = d_G(q) = \text{degree of } q$  (number of vertices at distance one from  $q$ )
- (ii) If  $m = 2$ ,  $d_G(q/2) = |N_G(q/2)| = \tau_G(q) = \text{connection number of } q$  (number of vertices at distance two from  $q$ )

For more terminologies and notations, see [36] and references therein.

*Definition 1.* For a (molecular) network  $G$ , the first Zagreb index ( $M_1(G)$ ), second Zagreb index ( $M_2(G)$ ), and third Zagreb index ( $M_3(G)$ ) are defined as follows:

- (a)  $M_1(G) = \sum_{q \in V(G)} [d_G(q)]^2 = \sum_{pq \in E(G)} [d_G(p) + d_G(q)]$
- (b)  $M_2(G) = \sum_{pq \in E(G)} [d_G(p) \times d_G(q)]$
- (c)  $M_3(G) = \sum_{q \in V(G)} [d_G(q)]^3 = \sum_{pq \in E(G)} [d_G^2(p) + d_G^2(q)]$

These degree-based TIs are defined by Gutman and Trinajstić [24]. These are abundantly used to predict better findings in molecular networks such as ZE isomerism, absolute value of correlation coefficient, entropy, acentric factor, and heat capacity.

*Definition 2.* For a (molecular) network  $G$ , the first ZCI ( $ZC_1(G)$ ), second ZCI ( $ZC_2(G)$ ), and modified first ZCI ( $ZC_1^+(G)$ ) are defined as follows:

- (a)  $ZC_1(G) = \sum_{q \in V(G)} [\tau_G(q)]^2$   
 (b)  $ZC_2(G) = \sum_{pq \in E(G)} [\tau_G(p) \times \tau_G(q)]$   
 (c)  $ZC_1^*(G) = \sum_{(pq \in E(G))} = [\tau_G(p) + \tau_G(q)]$

These connection-based TIs are defined by Ali and Trinajstić [32] (2018). They also reported that the modified first Zagreb connection index has better correlation coefficient value for the thirteen physicochemical properties of octane isomers than classical Zagreb indices.

**Definition 3.** For a (molecular) network  $G$ , the modified second Zagreb connection index ( $ZC_2^*(G)$ ) and modified third Zagreb connection index ( $ZC_3^*(G)$ ) are defined as follows:

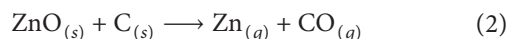
- (a)  $ZC_2^*(G) = \sum_{pq \in E(G)} [d_G(p)\tau_G(q) + d_G(q)\tau_G(p)]$   
 (b)  $ZC_3^*(G) = \sum_{pq \in E(G)} [d_G(p)\tau_G(p) + d_G(q)\tau_G(q)]$

**Definition 4.** For a (molecular) network  $G$ , the modified fourth Zagreb connection index ( $ZC_4^*(G)$ ) is defined as follows:

$$ZC_4^*(G) = \sum_{pq \in E(G)} [d_G(p)\tau_G(p) \times d_G(q)\tau_G(q)]. \quad (1)$$

These connection-based TIs are defined by Javaid et al. [35] to compute the exact solutions of several wheel-related graphs.

**Definition 5.** Zinc oxide network (ZNOX ( $n$ )): a chemical compound zinc oxide (ZnO) is insoluble in water which is an inorganic compound of white powder shape with  $5.61 \text{ g/cm}^3$  density. The zinc oxide is heated with carbon (coke) that reduces to the metal vapor to condense the liquid from which the solid metal freezes.



Zinc is a reactive metal to produce zinc ion ( $\text{Zn}^{2+}$ ) and hydrogen gas. It also reduces those metal ions whose reduction potentials are higher than  $\text{Zn}^{2+}$ . Zinc oxide is mostly used in making rubber, enamels, glazes, pigment in white paint, photoconductive surfaces, and protective coating for other metals. Zinc oxide-related MON is  $\text{Zn}_4\text{O}(\text{BPDC})_3$ , which is also known as IRMOF-10. IRMOF-9 is a catenated version of IRMOF-10. IRMOF-10 is three-dimensional cubic structures with a pore size diameter of  $16.7/20.2 \text{ \AA}^0$ . In Figure 1, the zinc oxide-related MON of dimension 3 is presented. In general, the vertices and edges in ZNOX ( $n$ ) of dimension  $n$  are  $70n + 46$  and  $85n + 55$ , respectively. For more understanding, see Figure 1.

**Definition 6.** Zinc silicate network (ZNSL ( $n$ )): silicate ( $\text{SiO}_4$ ) is the most charming class of minerals. Silicate is the

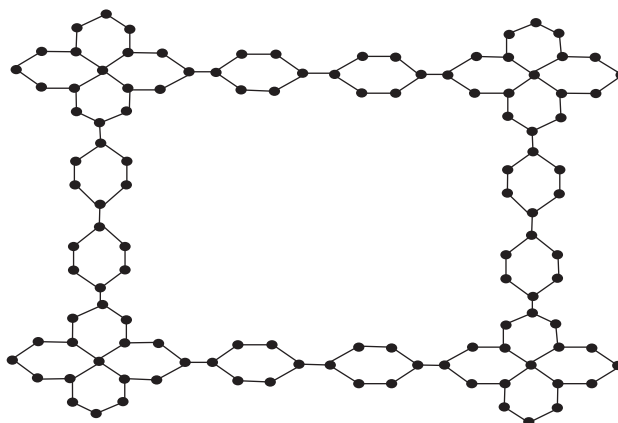


FIGURE 1: Zinc oxide network ( $ZNOX(n) \cong H$ ) for  $n=3$ .

chemical mixture of metal oxide or metal carbonate with sand. The basic unit of silicate is tetrahedron. So, all silicates gain  $\text{SiO}_4$  tetrahedron. In chemistry, oxygen ions and silicon ions are represented by the corner vertices and centre vertices of  $\text{SiO}_4$ , respectively. In graph theory, we represent corner vertices and centre vertices of  $\text{SiO}_4$  with oxygen nodes and silicon nodes. If we require a variety of silicate networks, it is easy to change the arrangement of the tetrahedron silicate. Zinc silicate-related MON is  $\text{Zn}_4\text{O}(\text{PDC})_3$ , which is also known as IRMOF-14. IRMOF-14 is three-dimensional cubic structures with a pore size diameter of  $14.7/20.1 \text{ \AA}^0$ . In Figure 2, the zinc silicate-related MON of dimension 3 is presented. In general, the vertices and edges in ZNSL ( $n$ ) of dimension  $n$  are  $82n + 50$  and  $103n + 61$ , respectively. For more understanding, see Figure 2.

Now, we present some important results which are used in the main results.

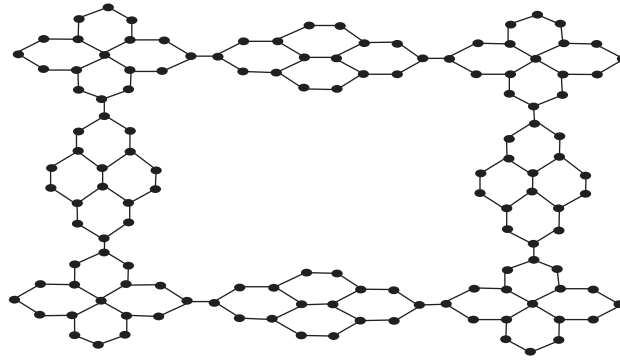
**Lemma 1.** Let  $G$  be a connected network with  $u$  vertices and  $e$  edges. Then,  $\tau_G(p) + d_G(p) \leq \sum_{q \in N_G(p)} d_G(q)$ , where equality holds if and only if  $G$  is a  $\{C_3, C_4\}$ -free network.

**Lemma 2** (see [35]). Let  $G$  be a connected and  $\{C_3, C_4\}$ -free network with  $u$  vertices and  $e$  edges. Then,

- (i)  $\sum_{q \in V(G)} d_G(q) = 2e$   
 (ii)  $\sum_{q \in V(G)} \tau_G(q) = M_1(G) - 2e$

**Lemma 3** (see [25]). Let  $G$  be a connected and  $\{C_3, C_4\}$ -free network with  $u$  vertices and  $e$  edges. Also,  $G \cong P_u$ . Then

- (i)  $ZC_2^*(G) = 8u - 22$  if  $u \geq 4$   
 (ii)  $ZC_3^*(G) = 8u - 22$  if  $u \geq 3$

FIGURE 2: Zinc silicate network (ZNSL( $n$ )  $\cong$   $K$ ) for  $n = 3$ .

### 3. Main Results Based on Zinc Oxide Network (ZNOX ( $n$ ))

In this section, we compute the main results for first Zagreb connection index (ZCI), second ZCI, modified first ZCI, modified second ZCI, modified third ZCI, and modified fourth ZCI of zinc oxide-related MON (ZNOX ( $n$ )). Let  $H \cong$  ZNOX( $n$ ) be the zinc oxide network of dimension  $n$  in the plane, see Figure 1. The partitions of  $H$  with respect to the vertex set and edge set are  $V(H)$  and  $E(H)$ . We can easily see each vertex of degrees 2, 3, and 4. We have  $V_1 = \{v \in V(H) | d_v = 2\}$ ,  $V_2 = \{v \in V(H) | d_v = 3\}$ , and  $V_3 = \{v \in V(H) | d_v = 4\}$ , where  $|V_1| = 42n + 30$ ,  $|V_2| = 26n + 14$ , and  $|V_3| = 2n + 2$ . So,  $|V(H)| = v = |V_1| + |V_2| + |V_3| = 70n + 46$ . Now, the partitions of vertices according to connection number are  $V_1 = \{v \in V(H) | \tau_v = 2\}$ ,  $V_2 = \{v \in V(H) | \tau_v = 3\}$ ,  $V_3 = \{v \in V(H) | \tau_v = 4\}$ ,  $V_4 = \{v \in V(H) | \tau_v = 5\}$ , and  $V_5 = \{v \in V(H) | \tau_v = 8\}$ , where  $|V_1| = 2n + 6$ ,  $|V_2| = 28n + 20$ ,  $|V_3| = 30n + 10$ ,  $|V_4| = 8n + 8$ , and  $|V_5| = 2n + 2$ . So,  $|V(H)| = v = |V_1| + |V_2| + |V_3| + |V_4| + |V_5| = 70n + 46$ . These vertex partitions are shown in Tables 1 and 2.

There are four types of partitions of edge sets of  $H$  according to the degree as  $|E(H)| = |E_{2,2}^d| + |E_{2,3}^d| + |E_{3,3}^d| + |E_{3,4}^d| = 85n + 55$ , and there are seven types of partitions of edge sets of  $H$  according to the connection number of vertices as  $|E(H)| = |E_{2,3}^c| + |E_{3,3}^c| + |E_{3,4}^c| + |E_{3,5}^c| + |E_{4,4}^c| + |E_{4,5}^c| + |E_{5,8}^c| = 85n + 55$ . These edge partitions are shown in Tables 3 and 4.

TABLE 1: Partitions of  $H$ 's vertices according to the degree.

$d_v$	2	3	4
$ d_v $	$42n + 30$	$26n + 14$	$2n + 2$

TABLE 2: Partitions of  $H$ 's vertices according to the connection number.

$\tau_v$	2	3	4	5	8
$ \tau_v $	$2n + 6$	$28n + 20$	$30n + 10$	$8n + 8$	$2n + 2$

TABLE 3: Partitions of  $H$ 's edges according to the degree.

$E_{d(p),d(q)}^d$	$E_{2,2}^d$	$E_{2,3}^d$	$E_{3,3}^d$	$E_{3,4}^d$
$ E_{d(p),d(q)}^d $	$6n + 16$	$52n + 28$	$9n + 3$	$8n + 8$

**Theorem 1.** Let  $H \cong$  ZNOX( $n$ ) be a zinc oxide network of dimensions  $n \geq 3$ . Then, the first Zagreb connection index is

$$ZC_1(H) = 1068n + 692. \quad (3)$$

*Proof.* By definition,

$$\begin{aligned} ZC_1(G) &= \sum_{q \in V(G)} [\tau_G(q)]^2 \\ &= (2n + 6)(2)^2 + (28n + 20)(3)^2 + (30n + 10)(4)^2 + (8n + 8)(5)^2 + (2n + 2)(4)^2 \\ &= 8n + 24 + 252n + 180 + 480n + 160 + 200n + 200 + 128n + 128 \\ &= 1068n + 692. \end{aligned} \quad (4)$$

**Theorem 2.** Let  $H \cong$  ZNOX( $n$ ) be a zinc oxide network of dimensions  $n \geq 3$ . Then, the second Zagreb connection index is

$$ZC_2(H) = 1376n + 896. \quad (5)$$

□

TABLE 4: Partition of  $H$ 's edges according to the connection number.

$E_{\tau(p),\tau(q)}^c$	$E_{2,3}^c$	$E_{3,3}^c$	$E_{3,4}^c$	$E_{3,5}^c$	$E_{4,4}^c$	$E_{4,5}^c$	$E_{5,8}^c$
$ E_{\tau(p),\tau(q)}^c $	$4n + 12$	$4n + 12$	$24n + 12$	$4n + 12$	$21n + 7$	$12n + 4$	$8n + 8$

*Proof.* By definition,

$$\begin{aligned}
ZC_2(G) &= \sum_{pq \in E(G)} [\tau_G(p) \times \tau_G(q)] \\
&= \sum_{pq \in E_{2,3}^c} [\tau_H(p) \times \tau_H(q)] + \sum_{pq \in E_{3,3}^c} [\tau_H(p) \times \tau_H(q)] + \sum_{pq \in E_{3,5}^c} [\tau_H(p) \times \tau_H(q)] \\
&\quad + \sum_{pq \in E_{4,5}^c} [\tau_H(p) \times \tau_H(q)] + \sum_{pq \in E_{4,4}^c} [\tau_H(p) \times \tau_H(q)] + \sum_{pq \in E_{3,4}^c} [\tau_H(p) \times \tau_H(q)] \\
&\quad + \sum_{pq \in E_{4,4}^c} [\tau_H(p) \times \tau_H(q)] + \sum_{pq \in E_{5,8}^c} [\tau_H(p) \times \tau_H(q)] \\
&= |E_{(2,3)(H)}| (2 \times 3) + |E_{(3,3)(H)}| (3 \times 3) + |E_{(3,5)(H)}| (3 \times 5) + |E_{(4,5)(H)}| (4 \times 5) \\
&\quad + |E_{(4,4)(H)}| (4 \times 4) + |E_{(3,4)(H)}| (3 \times 4) + |E_{(4,4)(H)}| (4 \times 4) + |E_{(5,8)(H)}| (5 \times 8) \\
&= (4n + 12)(2 \times 3) + (12n + 4)(3 \times 3) + (4n + 12)(3 \times 5) + (12n + 4)(4 \times 5) \\
&\quad + (12n + 4)(4 \times 4) + (24n + 8)(3 \times 4) + (9n + 3)(4 \times 4) + (8n + 8)(5 \times 8) \\
&= 24n + 72 + 108n + 36 + 60n + 180 + 240n + 80 + 192n + 64 \\
&\quad + 288n + 96 + 144n + 48 + 320n + 320 \\
&= 1376n + 896.
\end{aligned} \tag{6}$$

$$ZC_1^*(H) = 672n + 432. \tag{7}$$

**Theorem 3.** Let  $H \cong ZNOX(n)$  be a zinc oxide network of dimensions  $n \geq 3$ . Then, the modified first Zagreb connection index is

*Proof.* By definition,

$$\begin{aligned}
ZC_1^*(G) &= \sum_{pq \in E(G)} [\tau_G(p) + \tau_G(q)] \\
&= \sum_{pq \in E_{2,3}^c} [\tau_H(p) + \tau_H(q)] + \sum_{pq \in E_{3,3}^c} [\tau_H(p) + \tau_H(q)] + \sum_{pq \in E_{3,5}^c} [\tau_H(p) + \tau_H(q)] \\
&\quad + \sum_{pq \in E_{4,5}^c} [\tau_H(p) + \tau_H(q)] + \sum_{pq \in E_{4,4}^c} [\tau_H(p) + \tau_H(q)] + \sum_{pq \in E_{3,4}^c} [\tau_H(p) + \tau_H(q)] \\
&\quad + \sum_{pq \in E_{4,4}^c} [\tau_H(p) + \tau_H(q)] + \sum_{pq \in E_{5,8}^c} [\tau_H(p) + \tau_H(q)] \\
&= |E_{(2,3)(H)}| (2 + 3) + |E_{(3,3)(H)}| (3 + 3) + |E_{(3,5)(H)}| (3 + 5) + |E_{(4,5)(H)}| (4 + 5) \\
&\quad + |E_{(4,4)(H)}| (4 + 4) + |E_{(3,4)(H)}| (3 + 4) + |E_{(4,4)(H)}| (4 + 4) + |E_{(5,8)(H)}| (5 + 8) \\
&= (4n + 12)(5) + (12n + 4)(6) + (4n + 12)(8) + (12n + 4)(9) + (12n + 4)(8) \\
&\quad + (24n + 8)(7) + (9n + 3)(8) + (8n + 8)(13) \\
&= 20n + 60 + 72n + 24 + 32n + 96 + 108n + 36 + 96n + 32 + 168n + 56 \\
&\quad + 72n + 24 + 104n + 104 \\
&= 672n + 432.
\end{aligned} \tag{8}$$

**Theorem 4.** Let  $H \cong ZNOX(n)$  be a zinc oxide network of dimensions  $n \geq 3$ . Then, the modified second Zagreb connection index is

$$ZC_2^*(H) = 1740n + 1124. \quad (9)$$

*Proof.* By definition,

$$\begin{aligned} ZC_2^*(G) &= \sum_{pq \in E(G)} [d_G(p)\tau_G(q) + d_G(q)\tau_G(p)] \\ &= \sum_{pq \in E_{2,3}^c} [d_H(p)\tau_H(q) + d_H(q)\tau_H(p)] + \sum_{pq \in E_{3,3}^c} [d_H(p)\tau_H(q) + d_H(q)\tau_H(p)] \\ &\quad + \sum_{pq \in E_{3,5}^c} [d_H(p)\tau_H(q) + d_H(q)\tau_H(p)] + \sum_{pq \in E_{4,5}^c} [d_H(p)\tau_H(q) + d_H(q)\tau_H(p)] \\ &\quad + \sum_{pq \in E_{3,4}^c} [d_H(p)\tau_H(q) + d_H(q)\tau_H(p)] + \sum_{pq \in E_{3,4}^c} [d_H(p)\tau_H(q) + d_H(q)\tau_H(p)] \\ &\quad + \sum_{pq \in E_{4,4}^c} [d_H(p)\tau_H(q) + d_H(q)\tau_H(p)] + \sum_{pq \in E_{5,8}^c} [d_H(p)\tau_H(q) + d_H(q)\tau_H(p)] \\ &= |E_{2,3}^c| (2 \times 3 + 2 \times 2) + |E_{3,3}^c| (2 \times 3 + 2 \times 3) + |E_{3,5}^c| (2 \times 5 + 3 \times 3) + |E_{4,5}^c| (2 \times 5 + 3 \times 4) \\ &\quad + |E_{4,4}^c| (2 \times 4 + 3 \times 4) + |E_{3,4}^c| (2 \times 4 + 3 \times 3) + |E_{4,4}^c| (3 \times 4 + 3 \times 4) + |E_{5,8}^c| (3 \times 8 + 4 \times 5) \\ &= (4n + 12)(10) + (12n + 4)(12) + (4n + 12)(19) + (12n + 4)(22) + (12n + 4)(20) \\ &\quad + (24n + 8)(17) + (9n + 3)(24) + (8n + 8)(44) \\ &= 40n + 120 + 144n + 48 + 76n + 228 + 264n + 88 + 240n + 80 \\ &\quad + 408n + 136 + 216n + 72 + 352n + 352 \\ &= 1740n + 1124. \end{aligned} \quad (10)$$

□

**Theorem 5.** Let  $H \cong ZNOX(n)$  be a zinc oxide network of dimensions  $n \geq 3$ . Then, the modified third Zagreb connection index is

$$ZC_3^*(H) = 1808n + 1184. \quad (11)$$

*Proof.* By definition,

$$\begin{aligned} ZC_3^*(G) &= \sum_{pq \in E(G)} [d_G(p)\tau_G(p) + d_G(q)\tau_G(q)] \\ &= \sum_{pq \in E_{2,3}^c} [d_H(p)\tau_H(p) + d_H(q)\tau_H(q)] + \sum_{pq \in E_{3,3}^c} [d_H(p)\tau_H(p) + d_H(q)\tau_H(q)] \\ &\quad + \sum_{pq \in E_{3,5}^c} [d_H(p)\tau_H(p) + d_H(q)\tau_H(q)] + \sum_{pq \in E_{4,5}^c} [d_H(p)\tau_H(p) + d_H(q)\tau_H(q)] \\ &\quad + \sum_{pq \in E_{3,4}^c} [d_H(p)\tau_H(p) + d_H(q)\tau_H(q)] + \sum_{pq \in E_{3,4}^c} [d_H(p)\tau_H(p) + d_H(q)\tau_H(q)] \\ &\quad + \sum_{pq \in E_{4,4}^c} [d_H(p)\tau_H(p) + d_H(q)\tau_H(q)] + \sum_{pq \in E_{5,8}^c} [d_H(p)\tau_H(p) + d_H(q)\tau_H(q)] \\ &= |E_{2,3}^c| (2 \times 2 + 2 \times 3) + |E_{3,3}^c| (2 \times 3 + 2 \times 3) + |E_{3,5}^c| (2 \times 3 + 3 \times 5) + |E_{4,5}^c| (2 \times 4 + 3 \times 5) \\ &\quad + |E_{4,4}^c| (2 \times 4 + 3 \times 4) + |E_{3,4}^c| (2 \times 3 + 3 \times 4) + |E_{4,4}^c| (3 \times 4 + 3 \times 4) + |E_{5,8}^c| (3 \times 5 + 4 \times 8) \\ &= (4n + 12)(10) + (12n + 4)(12) + (4n + 12)(21) + (12n + 4)(23) + (12n + 4)(20) \\ &\quad + (24n + 8)(18) + (9n + 3)(24) + (8n + 8)(47) \\ &= 40n + 120 + 144n + 48 + 84n + 252 + 276n + 92 + 240n + 80 \\ &\quad + 432n + 144 + 216n + 72 + 376n + 376 \\ &= 1808n + 1184. \end{aligned} \quad (12)$$

□

**Theorem 6.** Let  $H \cong ZNOX(n)$  be a zinc oxide network of dimensions  $n \geq 3$ . Then, the modified fourth Zagreb connection index is

$$ZC_4^*(H) = 10344n + 7224. \quad (13)$$

*Proof.* By definition,

$$\begin{aligned} ZC_4^*(G) &= \sum_{pq \in E(G)} [d_G(p)\tau_G(q) \times d_G(q)\tau_G(p)] \\ &= \sum_{pq \in E_{2,3}^c} [d_H(p)\tau_H(q) \times d_H(q)\tau_H(p)] + \sum_{pq \in E_{3,3}^c} [d_H(p)\tau_H(q) \times d_H(q)\tau_H(p)] \\ &\quad + \sum_{pq \in E_{3,5}^c} [d_H(p)\tau_H(q) \times d_H(q)\tau_H(p)] + \sum_{pq \in E_{4,5}^c} [d_H(p)\tau_H(q) \times d_H(q)\tau_H(p)] \\ &\quad + \sum_{pq \in E_{3,4}^c} [d_H(p)\tau_H(q) \times d_H(q)\tau_H(p)] + \sum_{pq \in E_{3,4}^c} [d_H(p)\tau_H(q) \times d_H(q)\tau_H(p)] \\ &\quad + \sum_{pq \in E_{4,4}^c} [d_H(p)\tau_H(q) \times d_H(q)\tau_H(p)] + \sum_{pq \in E_{5,8}^c} [d_H(p)\tau_H(q) \times d_H(q)\tau_H(p)] \\ &= |E_{2,3}^c| (2 \times 3 \times 2 \times 2) + |E_{3,3}^c| (2 \times 3 \times 2 \times 3) + |E_{3,5}^c| (2 \times 5 \times 3 \times 3) + |E_{4,5}^c| (2 \times 5 \times 3 \times 4) \\ &\quad + |E_{4,4}^c| (2 \times 4 \times 3 \times 4) + |E_{3,4}^c| (2 \times 4 \times 3 \times 3) + |E_{4,4}^{C*}| (3 \times 4 \times 3 \times 4) + |E_{5,8}^c| (3 \times 8 \times 4 \times 5) \\ &= (4n + 12)(24) + (12n + 4)(36) + (4n + 12)(90) + (12n + 4)(120) + (12n + 4)(96) \\ &\quad + (24n + 8)(72) + (9n + 3)(144) + (8n + 8)(480) \\ &= 96n + 288 + 432n + 144 + 360n + 1080 + 1440n + 480 + 1152n + 384 \\ &\quad + 1728n + 576 + 1296n + 432 + 3840n + 3840 \\ &= 10344n + 7224. \end{aligned} \quad (14)$$

#### 4. Main Results Based on Zinc Silicate Network (ZNSL ( $n$ ))

In this section, we compute the main results for first Zagreb connection index (ZCI), second ZCI, modified first ZCI, modified second ZCI, modified third ZCI, and modified fourth ZCI of zinc silicate-related MON (ZNSL ( $n$ )). Let  $K \cong ZNSL(n)$  be the zinc silicate network of dimension  $n$  in the plane, see Figure 2. The partitions of  $K$  with respect to the vertex set and edge set are  $V(K)$  and  $E(K)$ . We can easily see each vertex of degrees 2, 3, and 4. We have  $V_1 = \{v \in V(K) | d_v = 2\}$ ,  $V_2 = \{v \in V(K) | d_v = 3\}$ , and  $V_3 = \{v \in V(K) | d_v = 4\}$ , where  $|V_1| = 42n + 30$ ,  $|V_2| = 38n + 18$ , and  $|V_3| = 2n + 2$ . So,  $|V(K)| = v = |V_1| + |V_2| + |V_3| = 82n + 50$ . Now, the partitions of vertices according to connection number are  $V_1 = \{v \in V(K) | \tau_v = 2\}$ ,  $V_2 = \{v \in V(K) | \tau_v = 3\}$ ,  $V_3 = \{v \in V(K) | \tau_v = 4\}$ ,  $V_4 = \{v \in V(K) | \tau_v = 5\}$ ,  $V_5 = \{v \in V(K) | \tau_v = 6\}$ , and  $V_6 = \{v \in V(K) | \tau_v = 8\}$ , where  $|V_1| = 2n + 6$ ,  $|V_2| = 16n + 16$ ,

$|V_3| = 48n + 16$ ,  $|V_4| = 8n + 8$ ,  $|V_5| = 6n + 2$ , and  $|V_6| = 2n + 2$ . So,  $|V(K)| = v = |V_1| + |V_2| + |V_3| + |V_4| + |V_5| = 82n + 50$ . These vertex partitions are shown in Tables 5 and 6.

There are four types of partitions of edge sets of  $K$  according to the degree as  $|E(K)| = |E_{2,2}^d| + |E_{2,3}^d| + |E_{3,3}^d| + |E_{3,4}^d| = 103n + 61$ , and there are seven types of partitions of edge sets of  $K$  according to the connection number of vertices as  $|E(K)| = |E_{2,3}^c| + |E_{3,3}^c| + |E_{3,4}^c| + |E_{3,5}^c| + |E_{4,4}^c| + |E_{4,5}^c| + |E_{4,6}^c| + |E_{5,8}^c| + |E_{6,6}^c| = 103n + 61$ . These edge partitions are shown in Tables 7 and 8.

**Theorem 7.** Let  $K \cong ZNSL(n)$  be a zinc silicate network of dimensions  $n \geq 3$ . Then, the first Zagreb connection index is

$$ZC_1(K) = 1464n + 824. \quad (15)$$

*Proof.* By definition,

$$\begin{aligned} ZC_1(G) &= \sum_{q \in V(G)} [\tau_G(q)]^2 \\ &= (2n + 6)(2)^2 + (16n + 16)(3)^2 + (48n + 16)(4)^2 + (8n + 8)(5)^2 + (6n + 2)(6)^2 + (2n + 2)(8)^2 \\ &= 8n + 24 + 144n + 144 + 768n + 256 + 200n + 200 + 216n + 72 + 128n + 128 \\ &= 1464n + 824. \end{aligned} \quad (16)$$

□

TABLE 5: Partitions of  $K$ 's vertices according to the degree.

$d_v$	2	3	4
$ d_v $	$42n + 30$	$38n + 18$	$2n + 2$

TABLE 6: Partitions of  $K$ 's vertices according to the connection number.

$\tau_v$	2	3	4	5	6	8
$ \tau_v $	$2n + 6$	$16n + 16$	$48n + 16$	$8n + 8$	$6n + 2$	$2n + 2$

TABLE 7: Partitions of  $K$ 's edges according to the degree.

$E_{d(p),d(q)}^d$	$E_{2,2}^d$	$E_{2,3}^d$	$E_{3,3}^d$	$E_{3,4}^d$
$ E_{d(p),d(q)}^d $	$10n + 14$	$64n + 32$	$21n + 7$	$8n + 8$

TABLE 8: Partition of  $K$ 's edges according to the connection number.

$E_{\tau(p),\tau(q)}^c$	$E_{2,3}^c$	$E_{3,3}^c$	$E_{3,4}^c$	$E_{3,5}^c$	$E_{4,4}^c$	$E_{4,5}^c$	$E_{4,6}^c$	$E_{5,8}^c$	$E_{6,6}^c$
$ E_{\tau(p),\tau(q)}^c $	$4n + 12$	$6n + 2$	$12n + 4$	$4n + 12$	$42n + 14$	$12n + 4$	$12n + 4$	$8n + 8$	$3n + 1$

**Theorem 8.** Let  $K \cong \text{ZNSL}(n)$  be a zinc silicate network of dimensions  $n \geq 3$ . Then, the second Zagreb connection index is

$$ZC_2(K) = 1910n + 1074. \quad (17)$$

*Proof.* By definition,

$$\begin{aligned}
 ZC_2(G) &= \sum_{pq \in E(G)} [\tau_G(p) \times \tau_G(q)] \\
 &= \sum_{pq \in E_{2,3}^c} [\tau_K(p) \times \tau_K(q)] + \sum_{pq \in E_{3,3}^c} [\tau_K(p) \times \tau_K(q)] + \sum_{pq \in E_{3,5}^c} [\tau_K(p) \times \tau_K(q)] \\
 &\quad + \sum_{pq \in E_{4,5}^c} [\tau_K(p) \times \tau_K(q)] + \sum_{pq \in E_{4,4}^c} [\tau_K(p) \times \tau_K(q)] + \sum_{pq \in E_{3,4}^c} [\tau_K(p) \times \tau_K(q)] \\
 &\quad + \sum_{pq \in E_{4,4}^c} [\tau_K(p) \times \tau_K(q)] + \sum_{pq \in E_{3,6}^c} [\tau_K(p) \times \tau_K(q)] + \sum_{pq \in E_{6,6}^c} [\tau_K(p) \times \tau_K(q)] \\
 &\quad + \sum_{pq \in E_{5,8}^c} [\tau_K(p) \times \tau_K(q)] \\
 &= |E_{(2,3)(K)}| (2 \times 3) + |E_{(3,3)(K)}| (3 \times 3) + |E_{(3,5)(K)}| (3 \times 5) + |E_{(4,5)(K)}| (4 \times 5) \\
 &\quad + |E_{(4,4)(K)}| (4 \times 4) + |E_{(3,4)(K)}| (3 \times 4) + |E_{(4,4)(K)}| (4 \times 4) + |E_{(4,6)(K)}| (4 \times 6) \\
 &\quad + |E_{(6,6)(K)}| (6 \times 6) + |E_{(5,8)(K)}| (5 \times 8) \\
 &= (4n + 12)(2 \times 3) + (6n + 2)(3 \times 3) + (4n + 12)(3 \times 5) + (12n + 4)(4 \times 5) \\
 &\quad + (36n + 12)(4 \times 4) + (12n + 4)(3 \times 4) + (6n + 2)(4 \times 4) + (12n + 4)(4 \times 6) \\
 &\quad + (3n + 1)(6 \times 6) + (8n + 8)(5 \times 8) \\
 &= 24n + 72 + 54n + 18 + 60n + 180 + 240n + 80 + 576n + 192 \\
 &\quad + 144n + 48 + 96n + 32 + 288n + 96 + 108n + 36 + 320n + 320 \\
 &= 1910n + 1074.
 \end{aligned} \quad (18)$$

□

**Theorem 9.** Let  $K \cong \text{ZNSL}(n)$  be a zinc silicate network of dimensions  $n \geq 3$ . Then, the modified first Zagreb connection index is

$$ZC_1^*(K) = 876n + 500. \quad (19)$$

*Proof.* By definition,

$$\begin{aligned} ZC_1^*(G) &= \sum_{pq \in E(G)} [\tau_G(p) + \tau_G(q)] \\ &= \sum_{pq \in E_{2,3}^c} [\tau_K(p) + \tau_K(q)] + \sum_{pq \in E_{3,3}^c} [\tau_K(p) + \tau_K(q)] + \sum_{pq \in E_{3,5}^c} [\tau_K(p) + \tau_K(q)] \\ &\quad + \sum_{pq \in E_{4,5}^c} [\tau_K(p) + \tau_K(q)] + \sum_{pq \in E_{4,4}^c} [\tau_K(p) + \tau_K(q)] + \sum_{pq \in E_{3,4}^c} [\tau_K(p) + \tau_K(q)] \\ &\quad + \sum_{pq \in E_{4,4}^c} [\tau_K(p) + \tau_K(q)] + \sum_{pq \in E_{4,6}^c} [\tau_K(p) + \tau_K(q)] + \sum_{pq \in E_{6,6}^c} [\tau_K(p) + \tau_K(q)] \\ &\quad + \sum_{pq \in E_{5,8}^c} [\tau_K(p) + \tau_K(q)] \\ &= |E_{(2,3)(K)}|(2+3) + |E_{(3,3)(K)}|(3+3) + |E_{(3,5)(K)}|(3+5) + |E_{(4,5)(K)}|(4+5) \\ &\quad + |E_{(4,4)(K)}|(4+4) + |E_{(3,4)(K)}|(3+4) + |E_{(4,4)(K)}|(4+4) + |E_{(4,6)(K)}|(4+6) \\ &\quad + |E_{(6,6)(K)}|(6+6) + |E_{(5,8)(K)}|(5+8) \\ &= (4n+12)(2+3) + (6n+2)(3+3) + (4n+12)(3+5) + (12n+4)(4+5) \\ &\quad + (36n+12)(4+4) + (12n+4)(3+4) + (6n+2)(4+4) + (12n+4)(4+6) \\ &\quad + (3n+1)(6+6) + (8n+8)(5+8) \\ &= 20n+60+36n+12+32n+96+108n+36+288n+96+84n+28+48n+16 \\ &\quad + 120n+40+36n+12+104n+104 \\ &= 876n+500. \end{aligned} \quad (20)$$

**Theorem 10.** Let  $K \cong \text{ZNSL}(n)$  be a zinc silicate network of dimensions  $n \geq 3$ . Then, the modified second Zagreb connection index is

$$ZC_2^*(K) = 2340n + 1324. \quad (21)$$

*Proof.* By definition,

$$\begin{aligned}
ZC_2^*(G) &= \sum_{pq \in E(G)} [d_G(p)\tau_G(q) + d_G(q)\tau_G(p)] \\
&= \sum_{pq \in E_{2,3}^c} [d_K(p)\tau_K(q) + d_K(q)\tau_K(p)] + \sum_{pq \in E_{3,3}^c} [d_K(p)\tau_K(q) + d_K(q)\tau_K(p)] \\
&\quad + \sum_{pq \in E_{3,5}^c} [d_K(p)\tau_K(q) + d_K(q)\tau_K(p)] + \sum_{pq \in E_{4,5}^c} [d_K(p)\tau_K(q) + d_K(q)\tau_K(p)] \\
&\quad + \sum_{pq \in E_{4,4}^c} [d_K(p)\tau_K(q) + d_K(q)\tau_K(p)] + \sum_{pq \in E_{3,4}^c} [d_K(p)\tau_K(q) + d_K(q)\tau_K(p)] \\
&\quad + \sum_{pq \in E_{4,4}^{c*}} [d_K(p)\tau_K(q) + d_K(q)\tau_K(p)] + \sum_{pq \in E_{4,6}^c} [d_K(p)\tau_K(q) + d_K(q)\tau_K(p)] \\
&\quad + \sum_{pq \in E_{6,6}^c} [d_K(p)\tau_K(q) + d_K(q)\tau_K(p)] + \sum_{pq \in E_{5,8}^c} [d_K(p)\tau_K(q) + d_K(q)\tau_K(p)] \\
&= |E_{2,3}^c| (2 \times 3 + 2 \times 2) + |E_{3,3}^c| (2 \times 3 + 2 \times 3) + |E_{3,5}^c| (2 \times 5 + 3 \times 3) + |E_{4,5}^c| (2 \times 5 + 3 \times 4) + |E_{4,4}^c| (2 \times 4 + 3 \times 4) \\
&\quad + |E_{3,4}^c| (2 \times 4 + 3 \times 3) + |E_{4,4}^{c*}| (3 \times 4 + 3 \times 4) + |E_{4,6}^c| (3 \times 6 + 3 \times 4) + |E_{6,6}^c| (3 \times 6 + 3 \times 6) + |E_{5,8}^c| (3 \times 8 + 4 \times 5) \\
&= (4n + 12)(10) + (6n + 2)(12) + (4n + 12)(19) + (12n + 4)(22) + (36n + 12)(20) + (12n + 4)(17) \\
&\quad + (6n + 2)(24) + (12n + 4)(30) + (3n + 1)(36) + (8n + 8)(44) \\
&= 40n + 120 + 72n + 24 + 76n + 228 + 264n + 88 + 720n + 240 + 204n + 68 + 144n + 48 + 360n + 120 \\
&\quad + 108n + 36 + 352n + 352 \\
&= 2340n + 1324.
\end{aligned}$$

(22)

$$ZC_3^*(K) = 2396n + 1380. \quad (23)$$

**Theorem 11.** Let  $K \cong ZNSL(n)$  be a zinc silicate network of dimensions  $n \geq 3$ . Then, the modified third Zagreb connection index is

*Proof.* By definition,

$$\begin{aligned}
ZC_3^*(G) &= \sum_{pq \in E(G)} [d_G(p)\tau_G(p) + d_G(q)\tau_G(q)] \\
&= \sum_{pq \in E_{2,3}^c} [d_K(p)\tau_K(p) + d_K(q)\tau_K(q)] + \sum_{pq \in E_{3,3}^c} [d_K(p)\tau_K(p) + d_K(q)\tau_K(q)] \\
&\quad + \sum_{pq \in E_{3,5}^c} [d_K(p)\tau_K(p) + d_K(q)\tau_K(q)] + \sum_{pq \in E_{4,5}^c} [d_K(p)\tau_K(p) + d_K(q)\tau_K(q)] \\
&\quad + \sum_{pq \in E_{4,4}^c} [d_K(p)\tau_K(p) + d_K(q)\tau_K(q)] + \sum_{pq \in E_{3,4}^c} [d_K(p)\tau_K(p) + d_K(q)\tau_K(q)] \\
&\quad + \sum_{pq \in E_{4,4}^{c*}} [d_K(p)\tau_K(p) + d_K(q)\tau_K(q)] + \sum_{pq \in E_{4,6}^c} [d_K(p)\tau_K(p) + d_K(q)\tau_K(q)] \\
&\quad + \sum_{pq \in E_{6,6}^c} [d_K(p)\tau_K(p) + d_K(q)\tau_K(q)] + \sum_{pq \in E_{5,8}^c} [d_K(p)\tau_K(p) + d_K(q)\tau_K(q)] \\
&= |E_{2,3}^c| (2 \times 2 + 2 \times 3) + |E_{3,3}^c| (2 \times 3 + 2 \times 3) + |E_{3,5}^c| (2 \times 3 + 3 \times 5) + |E_{4,5}^c| (2 \times 4 + 3 \times 5) + |E_{4,4}^c| (2 \times 4 + 3 \times 4) \\
&\quad + |E_{3,4}^c| (2 \times 3 + 3 \times 4) + |E_{4,4}^{c*}| (3 \times 4 + 3 \times 4) + |E_{4,6}^c| (3 \times 4 + 3 \times 6) + |E_{6,6}^c| (3 \times 6 + 3 \times 6) + |E_{5,8}^c| (3 \times 5 + 4 \times 8) \\
&= (4n + 12)(10) + (6n + 2)(12) + (4n + 12)(21) + (12n + 4)(23) + (36n + 12)(20) + (12n + 4)(18) \\
&\quad + (6n + 2)(24) + (12n + 4)(30) + (3n + 1)(36) + (8n + 8)(47) \\
&= 40n + 120 + 72n + 24 + 84n + 252 + 276n + 92 + 720n + 240 + 216n + 72 + 144n + 48 + 360n \\
&\quad + 120 + 108n + 36 + 376n + 376 \\
&= 2396n + 1380.
\end{aligned}$$

(24)

□

**Theorem 12.** Let  $K \cong ZNSL(n)$  be a zinc silicate network of dimensions  $n \geq 3$ . Then, the modified fourth Zagreb connection index is

$$ZC_4^*(K) = 14700n + 8676. \quad (25)$$

*Proof.* By definition,

$$\begin{aligned} ZC_4^*(G) &= \sum_{pq \in E(G)} [d_G(p)\tau_G(q) \times d_G(q)\tau_G(p)] \\ &= \sum_{pq \in E_{2,3}^c} [d_K(p)\tau_K(q) \times d_K(q)\tau_K(p)] + \sum_{pq \in E_{3,3}^c} [d_K(p)\tau_K(q) \times d_K(q)\tau_K(p)] \\ &\quad + \sum_{pq \in E_{3,5}^c} [d_K(p)\tau_K(q) \times d_K(q)\tau_K(p)] + \sum_{pq \in E_{4,5}^c} [d_K(p)\tau_K(q) \times d_K(q)\tau_K(p)] \\ &\quad + \sum_{pq \in E_{4,4}^c} [d_K(p)\tau_K(q) \times d_K(q)\tau_K(p)] + \sum_{pq \in E_{3,4}^c} [d_K(p)\tau_K(q) \times d_K(q)\tau_K(p)] \\ &\quad + \sum_{pq \in E_{4,4}^{c*}} [d_K(p)\tau_K(q) \times d_K(q)\tau_K(p)] + \sum_{pq \in E_{4,6}^c} [d_K(p)\tau_K(q) \times d_K(q)\tau_K(p)] \\ &\quad + \sum_{pq \in E_{6,6}^c} [d_K(p)\tau_K(q) \times d_K(q)\tau_K(p)] + \sum_{pq \in E_{5,8}^c} [d_K(p)\tau_K(q) \times d_K(q)\tau_K(p)] \\ &= |E_{2,3}^c| (2 \times 3 \times 2 \times 2) + |E_{3,3}^c| (2 \times 3 \times 2 \times 3) + |E_{3,5}^c| (2 \times 5 \times 3 \times 3) + |E_{4,5}^c| (2 \times 5 \times 3 \times 4) + |E_{4,4}^c| (2 \times 4 \times 3 \times 4) \\ &\quad + |E_{3,4}^c| (2 \times 4 \times 3 \times 3) + |E_{4,4}^{c*}| (3 \times 4 \times 3 \times 4) + |E_{4,6}^c| (3 \times 6 \times 3 \times 4) + |E_{6,6}^c| (3 \times 6 \times 3 \times 6) + |E_{5,8}^c| (3 \times 8 \times 4 \times 5) \\ &= (4n + 12)(24) + (6n + 2)(36) + (4n + 12)(90) + (12n + 4)(120) + (36n + 12)(96) + (12n + 4)(72) \\ &\quad + (6n + 2)(144) + (12n + 4)(216) + (3n + 1)(324) + (8n + 8)(480) \\ &= 96n + 288 + 216n + 72 + 360n + 1080 + 1440n + 480 + 3456n + 1152 \\ &\quad + 864n + 288 + 864n + 288 + 2592n + 864 + 972n + 324 + 3840n + 3840 \\ &= 14700n + 8676. \end{aligned} \quad (26)$$

## 5. Comparisons and Conclusions

In this section, we compare zinc oxide (H) and zinc silicate (K) related MONs via some Zagreb connection indices (ZCIs) such as first ZCI, second ZCI, modified first ZCI, modified second ZCI, modified third ZCI, and modified fourth ZCI with the help of Tables 9–14 that have been constructed by using numerical values of the aforementioned ZCIs. The graphical presentations for ZCIs of MONs are presented in Figures 3–10.

The comparative study of zinc-related MONs is highlighted by the following conclusions:

- (i) From Tables 9–14 and Figures 3–8, we see that the behaviors for all the ZCIs of zinc silicate MONs have more values and upper lines than zinc oxide MONs with the following order:

$$ZC_1(K) \geq ZC_1(H), ZC_2(K) \geq ZC_2(H), ZC_1^*(K) \geq ZC_1^*(H), ZC_2^*(K) \geq ZC_2^*(H), ZC_3^*(K) \geq ZC_3^*(H), \text{ and } ZC_4^*(K) \geq ZC_4^*(H).$$

- (ii) From Tables 15 and 16 and Figures 9 and 10, we see that modified fourth ZCI ( $ZC_4^*$ ) attains more values

and upper lines than other ZCIs for both zinc-related MONs. □

- (iii) The modified first Zagreb connection index ( $ZC_1^*$ ) attained better values of correlation coefficient for the thirteen physicochemical properties of octane isomers than other classical Zagreb indices. In this paper, novel connection-based Zagreb index  $ZC_4^*$  attains better values of correlation coefficient for increasing order in both the cases of zinc-related MONs.
- (iv) Table 17 shows that zinc silicate-related MON of dimension  $n$  for the aforesaid ZCIs has attained upward position than zinc oxide-related MON.
- (v) Moreover, these general relations (Tables 15–17) indicate that the chemical capability of zinc silicate-related MON is better than zinc oxide-related MON for all values of  $n$ .

Now, the problem is still open for prism, product, subdivision, and their compliment networks with the help of connection-based Zagreb indices.

TABLE 9: Numerical values of  $ZC_1$  for  $H$  and  $K$  networks on dimensions  $3 \leq n \leq 10$ .

ZCIs	3	4	5	6	7	8	9	10
$ZC_1(H)$	3896	4964	6032	7100	8168	9236	10304	11372
$ZC_1(K)$	5216	6680	8144	9608	11072	12536	14000	15464

TABLE 10: Numerical values of  $ZC_2$  for  $H$  and  $K$  networks on dimensions  $3 \leq n \leq 10$ .

ZCIs	3	4	5	6	7	8	9	10
$ZC_2(H)$	5024	6400	7776	9152	10528	11904	13280	14656
$ZC_2(K)$	6804	8714	10624	12534	14444	16354	18264	20174

TABLE 11: Numerical values of  $ZC_1^*$  for  $H$  and  $K$  networks on dimensions  $3 \leq n \leq 10$ .

ZCIs	3	4	5	6	7	8	9	10
$ZC_1^*(H)$	2448	3120	3792	4464	5136	5808	6480	7152
$ZC_1^*(K)$	3128	4004	4880	5756	6632	7508	8384	9260

TABLE 12: Numerical values of  $ZC_2^*$  for  $H$  and  $K$  networks on dimensions  $3 \leq n \leq 10$ .

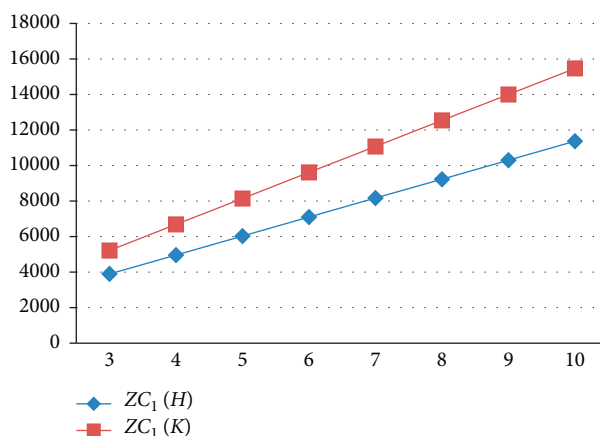
ZCIs	3	4	5	6	7	8	9	10
$ZC_2^*(H)$	6344	8084	9824	11564	13304	15044	16784	18524
$ZC_2^*(K)$	8344	10684	13024	15364	17704	20044	22384	24724

TABLE 13: Numerical values of  $ZC_3^*$  for  $H$  and  $K$  networks on dimensions  $3 \leq n \leq 10$ .

ZCIs	3	4	5	6	7	8	9	10
$ZC_3^*(H)$	6608	8416	10224	12032	13840	15648	17456	19264
$ZC_3^*(K)$	8568	10964	13360	15756	18152	20548	22944	25340

TABLE 14: Numerical values of  $ZC_4^*$  for  $H$  and  $K$  networks on dimensions  $3 \leq n \leq 10$ .

ZCIs	3	4	5	6	7	8	9	10
$ZC_4^*(H)$	38256	48600	58944	69288	79632	89976	100320	110664
$ZC_4^*(K)$	52776	67476	82176	96876	111576	126276	140976	155676

FIGURE 3: Comparison of  $ZC_1$  index for  $H$  and  $K$  networks on dimensions  $3 \leq n \leq 10$ .

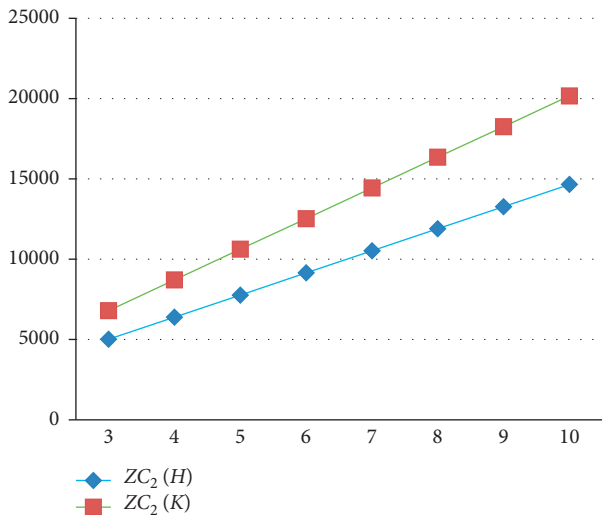


FIGURE 4: Comparison of  $ZC_2$  index for  $H$  and  $K$  networks on dimensions  $3 \leq n \leq 10$ .

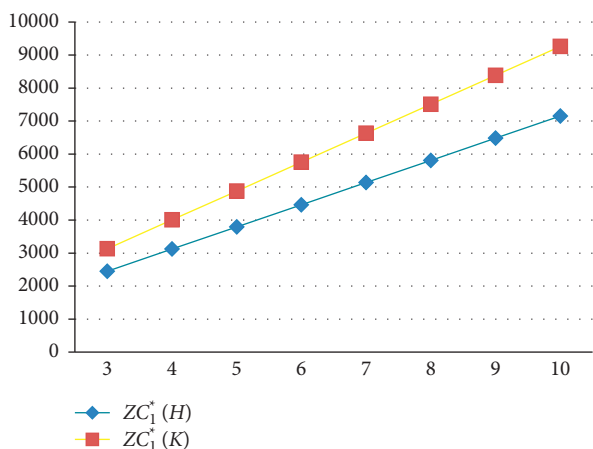


FIGURE 5: Comparison of  $ZC_1^*$  index for  $H$  and  $K$  networks on dimensions  $3 \leq n \leq 10$ .

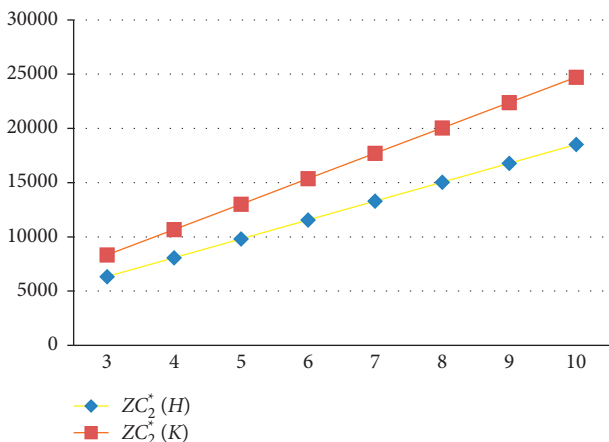


FIGURE 6: Comparison of  $ZC_2^*$  index for  $H$  and  $K$  networks on dimensions  $3 \leq n \leq 10$ .

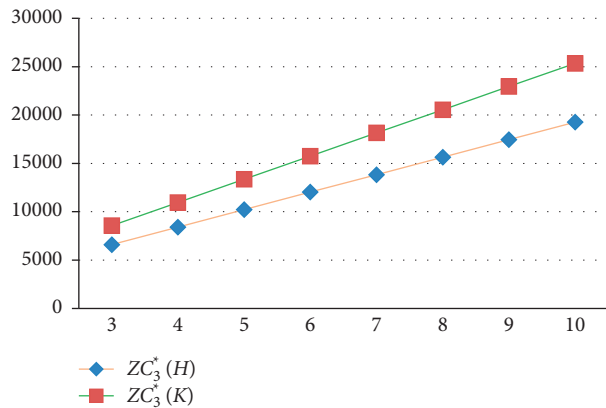


FIGURE 7: Comparison of  $ZC_3^*$  index for  $H$  and  $K$  networks on dimensions  $3 \leq n \leq 10$ .

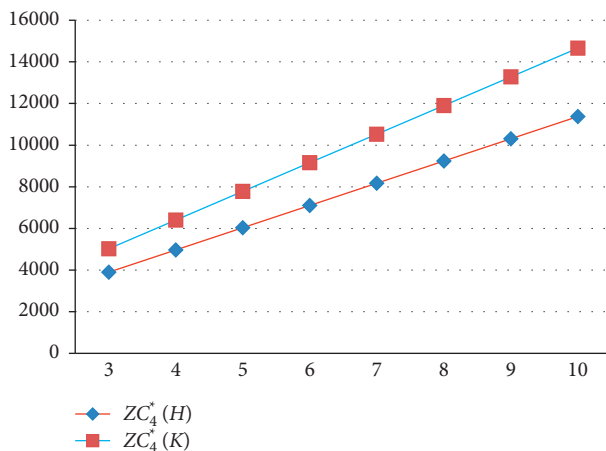


FIGURE 8: Comparison of  $ZC_4^*$  index for  $H$  and  $K$  networks on dimensions  $3 \leq n \leq 10$ .

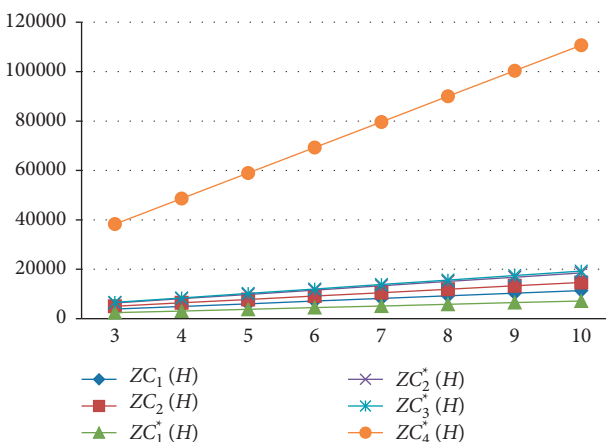
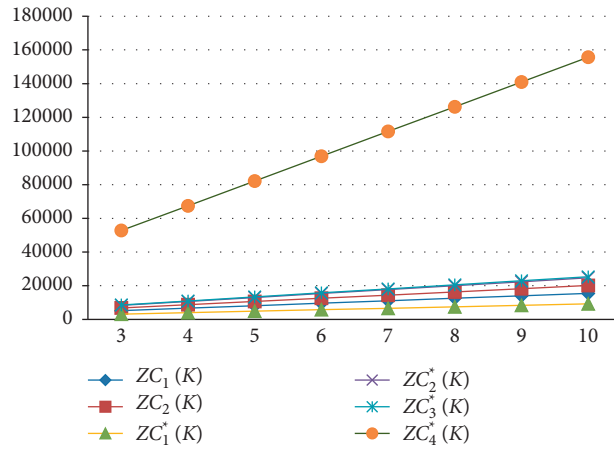


FIGURE 9: Comparison of ZCIs of network  $H$  on dimensions  $3 \leq n \leq 10$ .

FIGURE 10: Comparison of ZCIs of network  $K$  on dimensions  $3 \leq n \leq 10$ .TABLE 15: Numerical table for indicated ZCIs of network  $H$  on dimensions  $3 \leq n \leq 10$ .

ZCIs	$ZC_1(H)$	$ZC_2(H)$	$ZC_1^*(H)$	$ZC_2^*(H)$	$ZC_3^*(H)$	$ZC_4^*(H)$
3	3896	5024	2448	6344	6608	38256
4	4964	6400	3120	8084	8416	48600
5	6032	7776	3792	9824	10224	58944
6	7100	9152	4464	11564	12032	69288
7	8168	10528	5136	13304	13840	79632
8	9236	11904	5808	15044	15648	89976
9	10304	13280	6480	16784	17456	100320
10	11372	14656	7152	18524	19264	110664

TABLE 16: Numerical table for indicated ZCIs of network  $K$  on dimensions  $3 \leq n \leq 10$ .

ZCIs	$ZC_1(K)$	$ZC_2(K)$	$ZC_1^*(K)$	$ZC_2^*(K)$	$ZC_3^*(K)$	$ZC_4^*(K)$
3	5216	6804	3128	8344	8568	52776
4	6680	8714	4004	10684	10964	67476
5	8144	10624	4880	13024	13360	82176
6	9608	12534	5756	15364	15756	96876
7	11072	14444	6632	17704	18152	111576
8	12536	16354	7508	20044	20548	126276
9	14000	18264	8384	22384	22944	140976
10	15464	20174	9260	24724	25340	155676

TABLE 17: Comparison of indicated ZCIs for all  $n$ .

ZCIs	$K - H = \text{ZNSL}(n) - \text{ZNOX}(n)$	Results
First ZCI	$396n + 132$	$K > H$
Second ZCI	$534n + 178$	$K > H$
Modified first ZCI	$204n + 68$	$K > H$
Modified second ZCI	$600n + 200$	$K > H$
Modified third ZCI	$588n + 196$	$K > H$
Modified fourth ZCI	$4356n + 1452$	$K > H$

## Data Availability

All data are included within this article. However, the reader may contact the corresponding author for more details of the data.

## Conflicts of Interest

The authors declare that they have no conflicts of interest.

## References

- [1] T. B. Celic, M. Mazaj, N. Guillou, V. Kaucic, and N. Z. Logar, "New zinc-based metal organic framework material," in *Proceedings of the 3rd Croatian-Slovenian Symposium on Zeolites*, Trogir, Croatia, September 2010.
- [2] P. Horcajada, R. Gref, T. Baati et al., "Metal-organic frameworks in biomedicine," *Chemical Reviews*, vol. 112, no. 2, pp. 1232–1268, 2012.
- [3] Y. Cui, H. Xu, Y. Yue et al., "A luminescent mixed-lanthanide metal-organic framework thermometer," *Journal of the American Chemical Society*, vol. 134, no. 9, pp. 3979–3982, 2012.
- [4] C. Wang, L. Tian, W. Zhu et al., "Dye@bio-MOF-1 composite as a dual-emitting platform for enhanced detection of a wide range of explosive molecules," *ACS Applied Materials & Interfaces*, vol. 9, no. 23, pp. 20076–20085, 2017.
- [5] H. Lu, J. Sun, H. Zhang, S. Lu, and W. C. H. Choy, "Room-temperature solution-processed and metal oxide-free nanocomposite for the flexible transparent bottom electrode of perovskite solar cells," *Nanoscale*, vol. 8, no. 11, pp. 5946–5953, 2016.
- [6] A. S. Prasad, "Zinc in human health: effect of zinc on immune cells," *Molecular Medicine*, vol. 14, no. 5–6, pp. 353–357, 2008.
- [7] S. Bahrani, S. A. Hashemi, S. M. Mousavi, and R. Azhdari, "Zinc-based metal-organic frameworks as nontoxic and biodegradable platforms for biomedical applications: review study," *Drug Metabolism Reviews*, vol. 51, no. 3, pp. 356–377, 2019.
- [8] M. Eddaoudi, J. Kim, N. Rosi et al., "Systematic design of pore size and functionality in isoreticular MOFs and their application in methane storage," *Science*, vol. 295, no. 5554, pp. 469–472, 2002.
- [9] J. Feng, Z. Yang, D. Yang et al., "E-beam evaporated Nb<sub>2</sub>O<sub>5</sub> as an effective electron transport layer for large flexible perovskite solar cells," *Nanomaterials and Energy*, vol. 36, pp. 1–8, 2017.
- [10] S. Keskin and D. S. Sholl, "Efficient methods for screening of metal organic framework membranes for gas separations using atomically detailed models," *Langmuir*, vol. 25, no. 19, pp. 11786–11795, 2009.
- [11] I. Ahmad and S. H. Jung, "Composites of metal-organic frameworks: preparation and application in adsorption," *Materials Today*, vol. 17, no. 3, pp. 136–146, 2014.
- [12] H. Li, L. Li, R.-B. Lin et al., *Porous Metal-Organic Frameworks for Gas Storage and Separation: Status and Challenges*, Elsevier, Amsterdam, Netherlands, 2019.
- [13] Y. K. Hwang, D.-Y. Hong, J.-S. Chang et al., "Amine grafting on coordinatively unsaturated metal centers of MOFs: consequences for catalysis and metal encapsulation," *Angewandte Chemie International Edition*, vol. 47, no. 22, pp. 4144–4148, 2008.
- [14] A. W. Thornton, K. M. Nairn, J. M. Hill, A. J. Hill, and M. R. Hill, "Metal-Organic frameworks impregnated with magnesium-decorated fullerenes for methane and hydrogen storage," *Journal of the American Chemical Society*, vol. 131, no. 30, pp. 10662–10669, 2009.
- [15] M. Kim, J. F. Cahill, H. Fei, K. A. Prather, and S. M. Cohen, "Postsynthetic ligand and cation exchange in robust metal-organic frameworks," *Journal of the American Chemical Society*, vol. 134, no. 43, pp. 18082–18088, 2012.
- [16] Z. Yin, Y.-L. Zhou, M.-H. Zeng, and M. Kurmoo, "The concept of mixed organic ligands in metal-organic frameworks: design, tuning and functions," *Dalton Transactions*, vol. 44, no. 12, pp. 5258–5275, 2015.
- [17] G. Ding, J. Yuan, F. Jin et al., "High-performance all-polymer nonfullerene solar cells by employing an efficient polymer-small molecule acceptor alloy strategy," *Nanomaterials and Energy*, vol. 36, pp. 356–365, 2017.
- [18] M. H. Yap, K. L. Fow, and G. Z. Chen, "Synthesis and applications of MOF-derived porous nanostructures," *Green Energy & Environment*, vol. 2, no. 3, pp. 218–245, 2017.
- [19] R.-B. Lin, S. Xiang, H. Xing, W. Zhou, and B. Chen, "Exploration of porous metal-organic frameworks for gas separation and purification," *Coordination Chemistry Reviews*, vol. 378, pp. 87–103, 2019.
- [20] S. Klavzar and I. Gutman, "Selected properties of the Schultz molecular topological index," *Journal of Chemical Information and Computer Sciences*, vol. 36, pp. 1001–1003, 1996.
- [21] G. Rücker and C. Rücker, "On topological indices, boiling points, and cycloalkanes," *Journal of Chemical Information and Computer Sciences*, vol. 39, no. 5, pp. 788–802, 1999.
- [22] H. Gonzalez-Diaz, S. Vilar, L. Santana, and E. Uriarte, "Medicinal chemistry and bioinformatics - current trends in drugs discovery with networks topological indices," *Current Topics in Medicinal Chemistry*, vol. 7, no. 10, pp. 1015–1029, 2007.
- [23] H. Weiner, "Prediction of isomeric difference in paraffin properties," *Journal of the American Chemical Society*, vol. 69, pp. 17–20, 1947.
- [24] I. Gutman and N. Trinajstić, "Graph theory and molecular orbitals. Total  $\phi$ -electron energy of alternant hydrocarbons," *Chemical Physics Letters*, vol. 17, no. 4, pp. 535–538, 1972.
- [25] D. Zhao, Y.-M. Chu, M. K. Siddiqui et al., "On reverse degree based topological indices of polycyclic metal organic network," *Polycyclic Aromatic Compounds*, pp. 1–18, 2021.
- [26] J.-H. Tang, U. Ali, M. Javaid, and K. Shabbir, "Zagreb connection indices of subdivision and semi-total point operations on graphs," *Journal of Chemistry*, vol. 2020, Article ID 9846913, 14 pages, 2020.
- [27] J. Cao, U. Ali, M. Javaid, and C. Huang, "Zagreb connection indices of molecular graphs based on operations," *Complexity*, vol. 2020, Article ID 7385682, 15 pages, 2020.
- [28] U. Ali, M. Javaid, and A. M. Alanazi, "Computing analysis of connection-based indices and coincides for product of molecular networks," *Symmetry*, vol. 12, no. 8, Article ID 1320, 2020.
- [29] I. Gutman, B. Ruscic, N. Trinajstić, and C. F. Wilson, "Graph theory and molecular orbitals. XII. Acyclic polyenes," *The Journal of Chemical Physics*, vol. 62, no. 9, pp. 3399–3405, 1975.
- [30] B. Furtula and I. Gutman, "A forgotten topological index," *Journal of Mathematical Chemistry*, vol. 53, no. 4, pp. 1184–1190, 2015.
- [31] I. Gutman and O. Polansky, *Mathematical Concepts in Organic Chemistry*, Springer-Verlag, Berlin, Germany, 1986.
- [32] A. Ali and N. Trinajstić, "A novel/old modification of the first Zagreb index," *Mol. Inform.* vol. 37, pp. 1–7, 2018.

- [33] M. Javaid, U. Ali, and J.-B. Liu, "Computing first Zagreb connection index and coindex of resultant graphs," *Mathematical Problems in Engineering*, vol. 2021, Article ID 6019517, 19 pages, 2021.
- [34] R. Todeschini and V. Consonni, *Handbook of Molecular Descriptors*, Wiley VCH, Weinheim, Germany, 2002.
- [35] M. Javaid, U. Ali, and K. Siddiqui, "Novel connection based Zagreb indices of several wheel-related graphs," *Comp. J. Combin. Math.* vol. 1, pp. 1–28, 2021.
- [36] S. Keskin and D. S. Sholl, "Screening Metal–Organic framework materials for membrane-based methane/carbon dioxide separations," *Journal of Physical Chemistry C*, vol. 111, no. 38, pp. 14055–14059, 2007.
- [37] S. Yamaguchi, "Estimating the Zagreb indices and the spectral radius of triangle-and-quadrangle-free connected graphs," *Chemical Physics Letters*, vol. 458, no. 4, pp. 396–398, 2008.

## Research Article

# Forgotten Coindex for the Derived Sum Graphs under Cartesian Product

Muhammad Ibraheem,<sup>1</sup> Meshari M. Aljohani,<sup>2</sup> Muhammad Javaid <sup>1</sup>  
and Abdulaziz Mohammed Alanazi <sup>3</sup>

<sup>1</sup>Department of Mathematics, School of Science, University of Management and Technology, Lahore 54770, Pakistan

<sup>2</sup>Department of Chemistry, University of Tabuk, Tabuk, Saudi Arabia

<sup>3</sup>Department of Mathematics, University of Tabuk, Tabuk, Saudi Arabia

Correspondence should be addressed to Muhammad Javaid; javaidmath@gmail.com

Received 29 July 2021; Accepted 18 September 2021; Published 4 October 2021

Academic Editor: Syed Ahtsham Haq Bokhary

Copyright © 2021 Muhammad Ibraheem et al. This is an open access article distributed under the Creative Commons Attribution License, which permits unrestricted use, distribution, and reproduction in any medium, provided the original work is properly cited.

A topological index (TI) is a molecular descriptor that is applied on a chemical structure to compute the associated numerical value which measures volume, density, boiling point, melting point, surface tension, or solubility of this structure. It is an efficient mathematical method in avoiding laboratory experiments and time-consuming. The forgotten coindex of a structure or (molecular) graph  $H$  is defined as the sum of the degrees of all the possible pairs of nonadjacent vertices in  $H$ . For  $D \in \{S, R, Q, T\}$  and the connected graph  $H$ , the derived graphs  $D(H)$  are obtained by applying the operations  $S$  (subdivided),  $R$  (triangle parallel),  $Q$  (line superposition), and  $T$  (total graph), respectively. Moreover, a derived sum graph ( $D$ -sum graph) is obtained by the Cartesian product of the graph  $H_2$  with the graph  $D(H_1)$ . In this study, we compute forgotten coindex of the  $D$ -sum graphs  $H_{1+S}H_2$  ( $S$ -sum),  $H_{1+R}H_2$  ( $R$ -sum),  $H_{1+Q}H_2$  ( $Q$ -sum), and  $H_{1+T}H_2$  ( $T$ -sum) in the form of various indices and coindices of the factor graphs  $H_1$  and  $H_2$ . At the end, we have analyzed our results using numerical tables and graphical behaviour for some particular  $D$ -sum graphs.

## 1. Introduction

Chemical graph theory being the combination of graph theory and chemistry is a branch of mathematical chemistry in which we study the various physical and chemical properties of a chemical structure or network using different graph theoretical techniques. A topological index is one of the most used graph theoretical technique that studies the different properties of the molecular structure such as volume, density, freezing point, vaporization point, boiling point, melting point, surface tension or solubility, heat of formation, and heat of evaporation numerically [1, 2].

TIs are categorized in three types such as degree, distance, and polynomial based, but according the latest survey [3], the degree-based TIs are more studied than others. Wiener was the first scientist who calculated the boiling point of paraffin by using a distance-based TI [4]. Gutman and Trinajsti [5] introduced degree-based TIs known as

Zagreb indices to calculate total  $\pi$ -electron energy of hydrocarbons. Rouvray [6] and Balaban [7, 8] discussed the structure-activity correlations of different chemical phenomenon using TIs. Klein et al. introduced a molecular topological index and drive a close relation with the Wiener index [9, 10]. Mendiratta et al. and Cornwell used Wiener's TI to study structure-activity study on antiviral 5-vinyl-pyrimidine nucleoside analogs [11]. Gutman and Estrada calculated the TIs based on the line graph of the molecular graph [12]. Biye et al. wrote a novel on TI for QSPR/QSAR study of organic compounds [13]. Qinghua et al. calculated the TI for octane number of acyclic alkane by autocorrelation [14]. Baig et al. computed the TIs for polyoxide and silicate DSL and DOX-like networks [15].

In 2015, Furtula and Gutman redefined a TI with the name forgotten index ( $F$ -index) as the sum of cubes of vertex degrees of a molecular graph [16]. Gutman et al. listed the graphs having smallest forgotten index [17]. Zhongyuan and

Zhibo computed bounds of the  $F$ -index using Cauchy-Schwarz inequality, Jensen's inequality, and Chebyshev's sum inequality [18]. Gao and Liu calculated  $F$ -index of different chemical structures [19, 20]. Ahmad et al. worked online graph of benzene ring in the 2D network and calculated the degree-based TIs for these graphs [21]. Javaid et al. calculated bound on  $F$ -index for unicyclic graphs with fixed number of pendent vertices [22]. Imran et al. [23] investigated the family of unicyclic graphs with extreme  $F$ -coindex.

Ashrafi et al. introduced the concept of coindex of graph and investigated Zagreb coindices of composite graph operations such as union, disjunction, and various product of graphs [24]. Havare et al. computed the  $F$ -index and  $F$ -coindex for carbon base nanomaterial [25]. Basavanagoud and Desai calculated the  $F$ -index and hyper-Zagreb index of generalized transformation graphs [26]. Gao et al. calculated electron energy of molecular structures  $F$ -index [27]. Yasir et al. computed  $F$ -index of dendrimers-like structure [28]. Basavanagoud and Timmanaiakar calculated first Zagreb and  $F$ -index of some dominating transformation graphs [29]. Sana et al. characterized the extremal graphs and proved the ordering among the different subfamilies of graphs with respect to  $F$ -index [30].

Various operations on a graph play the important role in the development of different new classes of graphs. Yan et al. listed five graphs line graph  $L(H)$ , subdivided graph  $S(H)$ , line superposition graph  $Q(H)$ , triangle parallel  $R(H)$ , and total  $T(H)$  by performing different operations on  $H$  and computed Wiener indices of these five graphs [31]. Eliasi and Taeri defined the derived sum graphs ( $H_{1+D}H_2$ ) and computed their Wiener indices, where  $D \in \{S, R, Q, T\}$  [32]. Later on, for these derived sum graphs, Deng et al. [33] computed first two Zagreb indices, and Akhtar and Imran calculated the  $F$ -index [34, 35]. Javaid et al. (2021) investigated the first Zagreb connection index and coindex [36], and Javaid et al. investigated forgotten index of these graphs [37]. Moreover, Pattabiraman and Peng computed  $F$ -indices and their coindices of some classes of graphs [38, 39]. Ali et al. forgotten coindex of some nontoxic dendrimers structure used in targeted drug delivery [40].

In this study, we compute forgotten coindices of  $D$ -sum graphs  $H_{1+D}H_2$ , where  $D \in \{S, R, Q, T\}$  in the form of forgotten index, first Zagreb indices, and coindices of their basic graphs  $H_1$  and  $H_2$ . At the end, the obtained results are also illustrated with the assistance of the examples for some particular  $D$ -sum graphs. In Section 2, the definitions and notations are presented, Section 3 includes the main results of our work, and Section 4 presents particular examples related to the main results.

## 2. Preliminaries

Let  $H = (V(H), E(H))$  be a connected graph, where  $V(H)$  and  $E(H)$  be the set of vertices and edges of  $H$ , respectively. For any vertex  $x \in V(H)$ , its degree is denoted by  $d(x)$  and defined as the number of edges connecting it. The joining of two vertices  $x, y \in V(H)$  formed an edge denoted by  $xy \in E(H)$ . Gutman and Trinajstic [5] introduced Zagreb

indices  $M_1(H)$  and  $M_2(H)$  to calculate total  $\pi$  electron energy of hydrocarbons. The Zagreb indices  $M_1(H)$  and  $M_2(H)$  are defined as

$$M_1(H) = \sum_{r_1 r_2 \in E(H)} [d_H(r_1) + d_H(r_2)],$$

$$M_2(H) = \sum_{r_1 r_2 \in E(H)} [d_H(r_1)d_H(r_2)].$$
(1)

Ashrafi et al. [24] defined Zagreb coindices such as  $\overline{M}_1(H)$  and  $\overline{M}_2(H)$  of the Zagreb indices. The Zagreb coindices are defined as

$$\overline{M}_1(H) = \sum_{r_1 r_2 \notin E(H)} [d_H(r_1) + d_H(r_2)],$$

$$\overline{M}_2(H) = \sum_{r_1 r_2 \notin E(H)} [d_H(r_1)d_H(r_2)].$$
(2)

Furtula and Gutman [16] defined forgotten index ( $F$ -index), and its mathematical form is given by

$$F(H) = \sum_{r_1 r_2 \in E(H)} [d_H(r_1)^2 + d_H(r_2)^2].$$
(3)

Nilanjan et al. [41] introduced the forgotten coindex ( $F$ -coindex) for  $F$ -index with mathematical formulation as

$$\overline{F}(H) = \sum_{r_1 r_2 \notin E(H)} [d_H(r_1)^2 + d_H(r_2)^2].$$
(4)

Let  $H$  be a simple connected graph; then, its derived graphs are defined as follows.

- (i)  $S(H)$  is a graph formed by inserting a new vertex in each edge of  $H$
- (ii)  $R(H)$  is a graph obtained from  $S(H)$  by adding an edge between the adjacent vertices of  $H$
- (iii)  $Q(H)$  is a graph formed from  $S(H)$  by adding an edge between the pairs of new vertices which are on the adjacent edges of  $H$
- (iv)  $T(H)$  is formed by performing both operations of  $R(H)$  and  $Q(H)$  on  $S(H)$

Suppose that  $H_1$  and  $H_2$  are two connected graphs; then, their derived sum graph ( $D$ -sum graphs) is denoted by  $H_{1+D}H_2$  and defined with vertex set  $V(H_{1+D}H_2) = V(H_1) \cup E(H_1) \times V(H_2)$ , and edge set is defined as the vertices  $(r_1, r_2)$  and  $(s_1, s_2)$  of  $H_{1+D}H_2$ , where  $D \in \{S, R, Q, T\}$  are joined iff.

- (i)  $r_1 = s_1 \in V(H_1)$  and  $r_2 \sim s_2 \in H_2$
- (ii)  $r_2 = s_2 \in V(H_2)$  and  $r_1 \sim s_1 \in D(H_1)$

Where  $r \sim s \in H_2$  presents the  $xy$  is an edge in  $H_2$  [26]. For the  $D$ -sum graphs, refer Figures 1 and 2.

## 3. Main Results

In this section, we discuss main results related to  $F$ -coindex for  $D$ -sum graphs. Let  $H_1$  be a graph of its order, and the size is denoted by  $n_1$  and  $e_1$ , respectively. Let  $\overline{H}_1$  be the complement of  $H_1$ , and the edge set for  $\overline{H}_1$  is given by

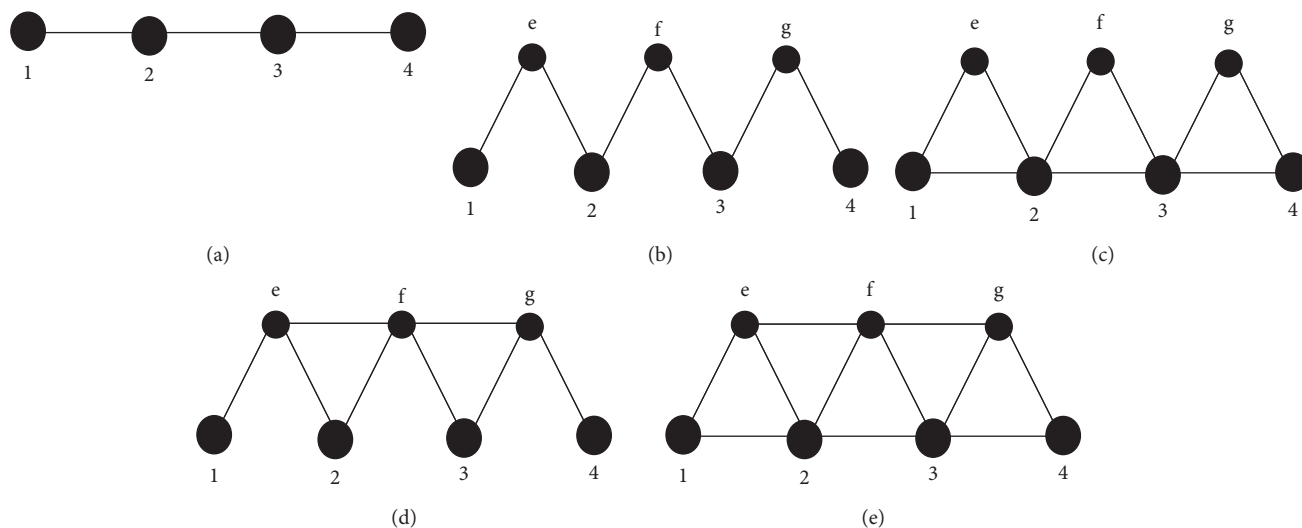


FIGURE 1: (a)  $G \cong P_4$ , (b)  $S(G) \cong S(P_4)$ , (c)  $R(G) \cong R(P_4)$ , (d)  $Q(G) \cong Q(P_4)$ , and (e)  $T(G) \cong T(P_4)$ .

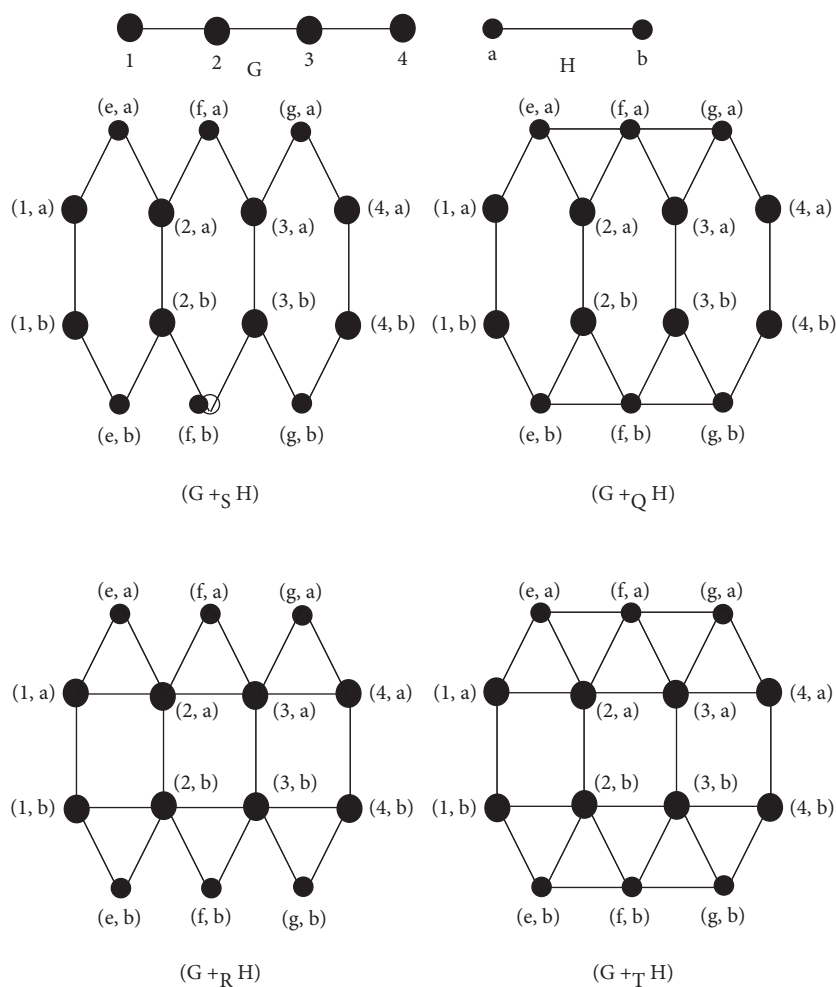


FIGURE 2:  $G \cong P_4$ ,  $H \cong P_2$ , and  $G_{+D}H \cong P_{4+D}P_2$ .

$\binom{n_1}{2} - e_1$ . Further assumed some sums by  $\alpha, \alpha_1, \alpha_2, \alpha_3$ , and  $\alpha_4$  are given as follows.

$$\begin{aligned} \text{(i)} \quad \alpha &= (n_2(n_2 - 1) + \bar{e}_2(\bar{n}_2 - 1)) \\ \text{(ii)} \quad \alpha_1 &= \sum_{\substack{r_1 r_2 \notin E(D(H_1)) \\ r_1 \in V(H_1) \\ r_2 \in V(D(H_1)-V(H_1))}} [d_{H_1}(r_1)^2 + d_{D(H_1)}(r_2)^2] \\ \text{(iii)} \quad \alpha_2 &= \sum_{\substack{r_1 r_2 \notin E(D(H_1)) \\ r_1 \in V(H_1) \\ r_2 \in V(D(H_1)-V(H_1))}} [d_{H_1}(r_1)^2 + d_{D(H_1)}(r_2)^2] \end{aligned}$$

$$\begin{aligned} \text{(iv)} \quad \alpha_3 &= \sum_{\substack{r_1 r_2 \notin E(D(H_1)) \\ r_1 \in V(H_1) \\ r_2 \in V(D(H_1)-V(H_1))}} d_{H_1}(r_1) \\ \text{(v)} \quad \alpha_4 &= \sum_{\substack{r_1 r_2 \notin E(D(H_1)) \\ r_1 \in V(H_1) \\ r_2 \in V(D(H_1)-V(H_1))}} d_{H_1}(r_1) \end{aligned}$$

**Theorem 1.** Let  $H_{1+S}H_2$  be a  $S$ -sum graph; then, its  $F$ -coindex is

$$\begin{aligned} \bar{F}(H_{1+S}H_2) &= 4(n_2^2 e_1^2 - n_2 e_1) + 2\bar{e}_2 M_1(H_1) + 4e_1 \bar{M}_1(H_2) + n_1 \bar{F}(H_2) + n_2 (F(H_1) + \bar{F}(H_1)) \\ &\quad + 2(e_1 + \bar{e}_1) + (e_1(n_1 - 2))M_1(H_2) + 4e_2(M_1(H_1) + \bar{M}_1(H_1)) + 2[(e_2 + \bar{e}_2)(F(H_1) \\ &\quad + \bar{F}(H_1)) + (e_1 + \bar{e}_1)(F(H_2) + \bar{F}(H_2)) + (M_1(H_2) + \bar{M}_1(H_2))(M_1(H_1) + \bar{M}_1(H_1))] \\ &\quad + n_2 \alpha_1 + \alpha(\alpha_1 + \alpha_2) + e_1 n_1 (M_1(H_2) + \bar{M}_1(H_2)) + 4(e_2 + \bar{e}_2)(2\alpha_3 + \alpha_4). \end{aligned} \quad (5)$$

*Proof.* Using equation (4), we have

$$\begin{aligned} \bar{F}(H_{1+S}H_2) &= \sum_{(r_1, r_2) \in (S_1, S_2) \notin E(H_{1+S}H_2)} [d(r_1, s_1)^2 + d(r_2, s_2)^2], \\ \bar{F}(H_{1+S}H_2) &= \left[ \sum_{r_1, r_2 \in (V(SH_1)-V(H_1))} + \sum_{r_1, r_2 \in V_{H_1}} + \sum_{\substack{r_1, r_2 \in V(S(H_1)) \\ r_1 \in V(H_1) \\ r_2 \in V(S(H_1)-V(H_1))}} \right] \sum_{s_1, s_2 \in V_{H_2}} [d(r_1, s_1)^2 + d(r_2, s_2)^2], \\ &= \sum A + \sum B + \sum C, \end{aligned} \quad (6)$$

$$\sum A = \sum_{r_1, r_2 \in (S(H_1)-V(H_1))} \sum_{s_1, s_2 \in V_{H_2}} [d_{S(H_1)}(r_1) + d_{S(H_1)}(r_2)] = \sum_{r_1, r_2 \in (S(H_1)-V(H_1))} \sum_{s_1, s_2 \in V_{H_2}} (2^2 + 2^2), \quad (7)$$

$$\sum A = 4(n_2^2 e_1^2 - n_2 e_1),$$

$$\sum B = \sum B_1 + \sum B_2 + \sum B_3,$$

$$\begin{aligned} \sum B_1 &= \sum_{r \in V_{H_1}} \sum_{s_1, s_2 \notin E_{H_2}} [d(r, s_1)^2 + d(r, s_2)^2] = \sum_{r \in V_{H_1}} \sum_{s_1, s_2 \notin E_{H_2}} [(d(r) + d(s_1))^2 + (d(r) + d(s_2))^2] \\ &= \sum_{r \in V_{H_1}} \sum_{s_1, s_2 \notin E_{H_2}} [(d(r)^2 + d(s_1)^2 + 2d(r)d(s_1)) + (d(r)^2 + d(s_2)^2 + 2d(r)d(s_2))] \\ &= \sum_{r \in V_{H_1}} \sum_{s_1, s_2 \notin E_{H_2}} [2d(r)^2 + (d(s_1)^2 + d(s_2)^2) + 2d(r)(d(s_1) + d(s_2))] \\ &= 2\bar{e}_2 M_1(H_1) + 4e_1 \bar{M}_1(H_2) + n_1 \bar{F}(H_2), \\ &\quad \sum B_2 \sum_{s \in V_{H_2}} \sum_{r_1, r_2 \in V_{H_1}} [(d(r_1) + d(s))^2 + (d(r_2) + d(s))^2] \\ &= \sum_{s \in V_{H_2}} \left( \sum_{r_1, r_2 \in E_{H_1}} + \sum_{r_1, r_2 \notin E_{H_1}} \right) [(d(r_1)^2 + d(s)^2 + 2d(r_1)d(s)) + (d(r_2)^2 + d(s)^2 + 2d(r_2)d(s))] \\ &= \sum_{s \in V_{H_2}} \left( \sum_{r_1, r_2 \in E_{H_1}} + \sum_{r_1, r_2 \notin E_{H_1}} \right) [(d(r_1)^2 + d(r_2)^2) + 2d(s)^2 + 2d(s)(d(r_1) + d(r_2))] \end{aligned}$$

$$\begin{aligned}
&= n_2(F(H_1) + \bar{F}(H_1)) + 2M_1(H_2)(e_1 + \bar{e}_1) + 4e_2(M_1(H_1) + \bar{M}_1(H_1)), \\
\sum B_3 &= \left[ \left( \sum_{r_1 r_2 \in E_{H_1}} + \sum_{r_1 r_2 \notin E_{H_1}} \right) \left( \sum_{s_1 s_2 \in E_{H_2}} + \sum_{s_1 s_2 \notin E_{H_2}} \right) \right] [d(r_1, s_1)^2 + d(r_2, s_2)^2] \\
&= \left[ \left( \sum_{r_1 r_2 \in E_{H_1}} + \sum_{r_1 r_2 \notin E_{H_1}} \right) \left( \sum_{s_1 s_2 \in E_{H_2}} + \sum_{s_1 s_2 \notin E_{H_2}} \right) \right] [(d(r_1)^2 + d(r_2)^2) + 2(d(r_1)d(s_1) + d(r_2)d(s_2)) + (d(s_1)^2 + d(s_2)^2)] \\
&= 2[(e_2 + \bar{e}_2)(F(H_1) + \bar{F}(H_1)) + (e_1 + \bar{e}_1)(F(H_2) + \bar{F}(H_2)) + (M_1(H_2) + \bar{M}_1(H_2))(M_1(H_1) + \bar{M}_1(H_1))], \\
\sum B &= 2\bar{e}_2 M_1(H_1) + 4e_1 \bar{M}_1(H_2) + n_1 \bar{F}(H_2) + n_2(F(H_1) + \bar{F}(H_1) + 2M_1(H_2)(e_1 + \bar{e}_1) \\
&\quad + 4e_2(M_1(H_1) + \bar{M}_1(H_1)) + 2[(e_2 + \bar{e}_2)(F(H_1) + \bar{F}(H_1)) + (e_1 + \bar{e}_1)(F(H_2) + \bar{F}(H_2))], \\
\sum C &= \sum C_1 + \sum C_2 + \sum C_3, \\
\sum C_1 &= \sum_{\substack{r_1 r_2 \notin E(S(H_1)) \\ r_1 \in V(H_1) \\ r_2 \in V(S(H_1)-V(H_1))}} \sum_{s \in V_{H_2}} [d(r_1, s)^2 + d(r_2, s)^2] \\
&= \sum_{\substack{r_1 r_2 \notin E(S(H_1)) \\ r_1 \in V(H_1) \\ r_2 \in V(S(H_1)-V(H_1))}} \sum_{s \in V_{H_2}} [(d(r_1)^2 + d(s)^2 + 2d(r_1)d(s)) + (d_{S(H_1)}(r_2)^2)] \\
&= n_2 \alpha_1 + e_1(n_1 - 2)M_1(H_2) + 4e_2 \alpha_3, \\
\sum C_2 &= \sum_{\substack{r_1 r_2 \notin E(S(H_1)) \\ r_1 \in V(H_1) \\ r_2 \in V(S(H_1)-V(H_1))}} \sum_{s_1, s_2 \in V_{H_2}} [d(r_1, s_1)^2 + d(r_2, s_2)^2] \\
&= \sum_{\substack{r_1 r_2 \notin E(S(H_1)) \\ r_1 \in V(H_1) \\ r_2 \in V(S(H_1)-V(H_1))}} \left( \sum_{s_1, s_2 \in V_{H_2}} + \sum_{s_1, s_2 \notin V_{H_2}} \right) [(d(r_1)^2 + d(s_1)^2 + 2d(r_1)d(s_1)) + (d_{S(H_1)}(r_2)^2)] \\
&= \alpha \alpha_1 + e_1(n_1 - 2)(M_1(H_2) + \bar{M}_1(H_2)) + 4(e_2 + \bar{e}_2) \alpha_3, \\
\sum C_3 &= \sum_{\substack{r_1 r_2 \in E(S(H_1)) \\ r_1 \in V(H_1) \\ r_2 \in V(S(H_1)-V(H_1))}} \sum_{s_1, s_2 \in V_{H_2}} [d(r_1, s_1)^2 + d(r_2, s_2)^2] \\
&= \sum_{\substack{r_1 r_2 \in E(S(H_1)) \\ r_1 \in V(H_1) \\ r_2 \in V(S(H_1)-V(H_1))}} \left( \sum_{s_1, s_2 \in V_{H_2}} + \sum_{s_1, s_2 \notin V_{H_2}} \right) [(d(r_1)^2 + d(s_1)^2 + 2d(r_1)d(s_1)) + (d_{S(H_1)}(r_2)^2)] \\
&= \alpha \alpha_2 + 2e_1(M_1(H_2) + \bar{M}_1(H_2)) + 4(e_2 + \bar{e}_2) \alpha_4.
\end{aligned}$$

By substituting the values in equation (6), we get the required result.  $\square$

**Theorem 2.** Let  $H_{1+R}H_2$  be a  $R$ -sum graph; then, its  $F$ -coindex is

$$\begin{aligned} \overline{F}(H_{1+R}H_2) &= 4(n_2^2e_1^2 - n_2e_1) + 8\overline{e}_2M_1(H_1) + 8e_1\overline{M}_1(H_2) + n_1\overline{F}(H_2) \\ &\quad + 4n_2(\overline{F}(H_1) + (2\overline{e}_1 + (e_1(n_1 - 2))))M_1(H_2) + 8e_2\overline{M}_1(H_1) \\ &\quad + 24(e_2 + \overline{e}_2)(F(H_1) + \overline{F}(H_1)) + (e_1 + \overline{e}_1)(F(H_2) + \overline{F}(H_2)) \\ &\quad + 2(M_1(H_2) + \overline{M}_1(H_2))(M_1(H_1) + \overline{M}_1(H_1)) \\ &\quad + n_2\alpha_1 + \alpha(\alpha_1 + \alpha_2) + e_1n_1(M_1(H_2) + \overline{M}_1(H_2)) + 4(e_2 + \overline{e}_2)(2\alpha_3 + \alpha_4). \end{aligned} \quad (9)$$

*Proof.* Using equation (4), we have

$$\begin{aligned} \overline{F}(H_{1+R}H_2) &= \sum_{(t_1, t_2) (x_1, x_2) \notin E(H_{1+R}H_2)} [d(t_1, x_1)^2 + d(t_2, x_2)^2], \\ \overline{F}(H_{1+R}H_2) &= \left[ \sum_{r_1, r_2 \in (V(R(H_1)) - V(H_1))} + \sum_{r_1, r_2 \in V_{H_1}} + \sum_{\substack{r_1, r_2 \in V(R(H_1)) \\ r_1 \in V(H_1) \\ r_2 \in V(R(H_1)) - V(H_1)}} \right] \sum_{s_1, s_2 \in V_{H_2}} [d(r_1, s_1)^2 + d(r_2, s_2)^2] \\ &= \sum A + \sum B + \sum C. \end{aligned} \quad (10)$$

Using equation (7),

$$\begin{aligned} \sum A &= 4(n_2^2e_1^2 - n_2e_1), \\ \sum B &= \sum B_1 + \sum B_2 + \sum B_3 \\ \sum B_1 &= \sum_{r \in V_{H_1}} \sum_{s_1, s_2 \notin E_{H_2}} [d(r, s_1)^2 + d(r, s_2)^2] = \sum_{r \in V_{H_1}} \sum_{s_1, s_2 \notin E_{H_2}} [(d(r) + d(s_1))^2 + (d(r) + d(s_2))^2] \\ &= \sum_{r \in V_{H_1}} \sum_{s_1, s_2 \notin E_{H_2}} [8d(r)^2 + (d(s_1)^2 + d(s_2)^2) + 4d(r)(d(s_1) + d(s_2))] \\ &= 8\overline{e}_2M_1(H_1) + 8e_1\overline{M}_1(H_2) + n_1\overline{F}(H_2), \\ \sum B_2 &= \sum_{s \in V_{H_2}} \sum_{r_1, r_2 \in V_{H_1}} [(d(r_1) + d(s))^2 + (d(r_2) + d(s))^2] \\ &= \sum_{s \in V_{H_2}} \left( \sum_{r_1, r_2 \in E_{H_1}} + \sum_{r_1, r_2 \notin E_{H_1}} \right) [4(d(r_1)^2 + d(r_2)^2) + 2d(s)^2 + 4d(s)(d(r_1) + d(r_2))] \\ &= 4n_2(\overline{F}(H_1) + 2\overline{e}_1M_1(H_2) + 8e_2\overline{M}_1(H_1)), \\ \sum B_3 &= \left[ \left( \sum_{r_1, r_2 \in E_{H_1}} + \sum_{r_1, r_2 \notin E_{H_1}} \right) \left( \sum_{s_1, s_2 \in E_{H_2}} + \sum_{s_1, s_2 \notin E_{H_2}} \right) \right] [d(r_1, s_1)^2 + d(r_2, s_2)^2] \end{aligned}$$

$$\begin{aligned}
&= \left[ \left( \sum_{r_1 r_2 \in E_{H_1}} + \sum_{r_1 r_2 \notin E_{H_1}} \right) \left( \sum_{s_1 s_2 \in E_{H_2}} + \sum_{s_1 s_2 \notin E_{H_2}} \right) \right] \left[ (d(r_1)^2 + d(r_2)^2) + (d(s_1)^2 + d(s_2)^2) + 2(d(r_1)d(s_1) + d(r_2)d(s_2)) \right] \\
&= \left[ \left( \sum_{r_1 r_2 \in E_{H_1}} + \sum_{r_1 r_2 \notin E_{H_1}} \right) \left( \sum_{s_1 s_2 \in E_{H_2}} + \sum_{s_1 s_2 \notin E_{H_2}} \right) \right] \left[ 2^2(d(r_1)^2 + d(r_2)^2) + (d(s_1)^2 + d(s_2)^2) + 4(d(r_1)d(s_1) + d(r_2)d(s_2)) \right] \\
&= 2[4(e_2 + \bar{e}_2)(F(H_1) + \bar{F}(H_1)) + (e_1 + \bar{e}_1)(F(H_2) + \bar{F}(H_2)) + 2(M_1(H_2) + \bar{M}_1(H_2))(M_1(H_1) + \bar{M}_1(H_1))] \\
\sum B &= 8\bar{e}_2 M_1(H_1) + 8e_1 \bar{M}_1(H_2) + n_1 \bar{F}(H_2) + 4n_2 (\bar{F}(H_1) + 2\bar{e}_1 M_1(H_2) + 8e_2 \bar{M}_1(H_1)) \\
&\quad + 2[4(e_2 + \bar{e}_2)(F(H_1) + \bar{F}(H_1)) + (e_1 + \bar{e}_1)(F(H_2) + \bar{F}(H_2)) \\
&\quad + 2(M_1(H_2) + \bar{M}_1(H_2))(M_1(H_1) + \bar{M}_1(H_1))], \\
\sum C &= \sum C_1 + \sum C_2 + \sum C_3, \\
\sum C_1 &= \sum_{\substack{r_1 r_2 \notin E(R(H_1)) \\ r_1 \in V(H_1) \\ r_2 \in V(R(H_1)-V(H_1))}} \sum_{s \in V_{H_2}} [d(r_1, s)^2 + d(r_2, s)^2] \\
&= \sum_{\substack{r_1 r_2 \notin E(R(H_1)) \\ r_1 \in V(H_1) \\ r_2 \in V(R(H_1)-V(H_1))}} \sum_{s \in V_{H_2}} \left[ 2^2(d(r_1)^2 + d(s)^2 + 4d(r_1)d(s)) + (d_{S(H_1)}(r_2))^2 \right] \\
&= n_2 \alpha_1 + e_1 (n_1 - 2) M_1(H_2) + 4e_2 \alpha_3, \\
\sum C_2 &= \sum_{\substack{r_1 r_2 \notin E(R(H_1)) \\ r_1 \in V(H_1) \\ r_2 \in V(R(H_1)-V(H_1))}} \left( \sum_{s_1, s_2 \in V_{H_2}} + \sum_{s_1, s_2 \notin V_{H_2}} \right) \left[ (d(r_1)^2 + d(s_1)^2 + 2d(r_1)d(s_1)) + (d_{S(H_1)}(r_2))^2 \right] \\
&= \alpha \alpha_1 + e_1 (n_1 - 2) (M_1(H_2) + \bar{M}_1(H_2)) + 4(e_2 + \bar{e}_2) \alpha_3, \\
\sum C_3 &= \sum_{\substack{r_1 r_2 \in E(R(H_1)) \\ r_1 \in V(H_1) \\ r_2 \in V(R(H_1)-V(H_1))}} \left( \sum_{s_1, s_2 \in V_{H_2}} + \sum_{s_1, s_2 \notin V_{H_2}} \right) \left[ (d(r_1)^2 + d(s_1)^2 + 2d(r_1)d(s_1)) + (d_{S(H_1)}(r_2))^2 \right] \\
&= \alpha \alpha_2 + 2e_1 (M_1(H_2) + \bar{M}_1(H_2)) + 4(e_2 + \bar{e}_2) \alpha_4.
\end{aligned} \tag{11}$$

By substituting the values in equation (10), we get the required result.  $\square$

**Theorem 3.** Let  $H_{1+Q}H_2$  be a Q-sum graph; then, F-coindex is

$$\begin{aligned} \overline{F}(H_{1+Q}H_2) &= n_2 \overline{F}(Q'(G_1)) + 2(\overline{e}_2 + (n_2 - 1)) \left( M_1(Q'H_1) + 1 \right) F(Q'(G_1)) \\ &\quad + \overline{F}(Q'(G_1)) + 2\overline{e}_2 M_1(H_1) + 4e_1 \overline{M}_1(H_2) + n_1 \overline{F}(H_2) + n_2 (F(H_1) + \overline{F}(H_1)) \\ &\quad + 2M_1(H_2)(e_1 + \overline{e}_1) + 4e_2 (M_1(H_1) + \overline{M}_1(H_1)) + 2[(e_2 + \overline{e}_2)(F(H_1) + \overline{F}(H_1)) \\ &\quad + (e_1 + \overline{e}_1)(F(H_2) + \overline{F}(H_2))] + n_2 \overline{F}(Q(H_1')) + e_1(n_1 - 2)M_1(H_2) \\ &\quad + \alpha(\alpha_1 + \alpha_2) + e_1 n_1 (M_1(H_2) + \overline{M}_1(H_2)) + 4(e_2 + \overline{e}_2)(2\alpha_3 + \alpha_4). \end{aligned} \quad (12)$$

*Proof.* Using equation (4), we have

$$\begin{aligned} \overline{F}(H_{1+Q}H_2) &= \sum_{(t_1, t_2)(x_1, x_2) \notin E(H_{1+Q}H_2)} [d(t_1, x_1)^2 + d(t_2, x_2)^2], \\ \overline{F}(H_{1+Q}H_2) &= \left[ \sum_{r_1, r_2 \in (V(Q(H_1)) - V(H_1))} \sum_{s_1, s_2 \in V_{H_2}} + \sum_{r_1, r_2 \in V_{H_1}} + \sum_{\substack{r_1, r_2 \in V(Q(H_1)) \\ r_1 \in V(H_1) \\ r_2 \in V(Q(H_1)) - V(H_1)}} \right] \\ &\quad \cdot \sum_{s_1, s_2 \in V_{H_2}} [d(r_1, s_1)^2 + d(r_2, s_2)^2] \\ &= \sum A + \sum B + \sum C, \\ \sum A &= \sum A_1 + \sum A_2 + \sum A_3 + \sum A_4, \\ \sum A_1 &= \sum_{\substack{r_1, r_2 \notin E(Q(H_1)) \\ r_1, r_2 \in V(Q(H_1)) - H_1}} \sum_{s \in V_{H_2}} [d_{Q(H_1)}(r_1)^2 + d_{Q(H_1)}(r_2)^2] = n_2, \\ &\quad \cdot \sum_{\substack{r_1, r_2 \notin E(Q(H_1)) \\ r_1, r_2 \in V(Q(H_1)) - H_1}} [d_{Q(H_1)}(r_1)^2 + d_{Q(H_1)}(r_2)^2] \end{aligned}$$

if  $\sum_{\substack{r_1, r_2 \notin E(Q(H_1)) \\ r_1, r_2 \in V(Q(H_1)) - H_1}} [d_{Q(H_1)}(r_1)^2 + d_{Q(H_1)}(r_2)^2] = \overline{F}(Q'(H_1))$ , then  $\sum A_1 = n_2 \overline{F}(Q'(H_1))$ ,

$$\begin{aligned} \sum A_2 &= \sum_{r \in (V(Q(H_1)) - (H_1))} \sum_{s_1, s_2 \in E_{H_2}} [d_{Q(H_1)}(r_1)^2 + d_{Q(H_1)}(r_2)^2] \\ &= \sum_{r \in (V(Q(H_1)) - V(H_1))} \left( \sum_{s_1, s_2 \notin E_{H_2}} + \sum_{s_1, s_2 \in E_{H_2}} \right) [d_{Q(H_1)}(r_1)^2 + d_{Q(H_1)}(r_2)^2] \\ &= 2(\overline{e}_2 + (n_2 - 1)) \sum_{r \in (V(Q(H_1)) - V(H_1))} [d_{Q(H_1)}(r)^2] \end{aligned}$$

$$\begin{aligned}
& \text{if } \sum_{r \in V(Q(H_1) - (H_1))} \left[ d_{Q(H_1)}(r)^2 \right] = M_1(Q(H_1)), \text{ then } = 2(\bar{e}_2 + (n_2 - 1))M_1(Q(H_1)), \\
& \sum A_3 = \sum_{\substack{r_1 r_2 \notin E(Q(H_1)) \\ r_1, r_2 \in V(Q(H_1) - (H_1))}} \sum_{s_1, s_2 \in V(H_2)} \left[ d_{Q(H_1)}(r_1)^2 + d_{Q(H_1)}(r_2)^2 \right] \\
& = \sum_{\substack{r_1 r_2 \notin E(Q(H_1)) \\ r_1, r_2 \in V(Q(H_1) - V(H_1))}} \left[ \sum_{s_1, s_2 \in E(H_2)} \left( d_{Q(H_1)}(r_1)^2 + d_{Q(H_1)}(r_2)^2 \right) \right. \\
& \quad \left. + \sum_{s_1, s_2 \notin E(H_2)} \left( d_{Q(H_1)}(r_1)^2 + d_{Q(H_1)}(r_2)^2 \right) \right] \\
& = 2(\bar{e}_2 + (n_2 - 1)) \sum_{\substack{r_1 r_2 \notin E(Q(H_1)) \\ r_1, r_2 \in V(Q(H_1) - V(H_1))}} \left[ d_{Q(H_1)}(r_1)^2 + d_{Q(H_1)}(r_2)^2 \right]
\end{aligned}$$

$$\text{if } \sum_{\substack{r_1 r_2 \notin E(Q(H_1)) \\ r_1, r_2 \in V(Q(H_1) - V(H_1))}} \left[ d_{Q(H_1)}(r_1)^2 + d_{Q(H_1)}(r_2)^2 \right] = F(Q(H_1)) = 2(\bar{e}_2 + (n_2 - 1))F(Q(H_1)),$$

$$\begin{aligned}
& \sum A_4 = \sum_{\substack{r_1 r_2 \notin E(Q(H_1)) \\ r_1, r_2 \in V(Q(H_1) - V(H_1))}} \sum_{s_1, s_2 \in V(H_2)} \left[ d_{Q(H_1)}(r_1)^2 + d_{Q(H_1)}(r_2)^2 \right] \\
& = \sum_{\substack{r_1 r_2 \notin E(Q(H_1)) \\ r_1, r_2 \in V(Q(H_1) - V(H_1))}} \left[ \sum_{s_1, s_2 \in E(H_2)} \left( d_{Q(H_1)}(r_1)^2 + d_{Q(H_1)}(r_2)^2 \right) \right. \\
& \quad \left. + \sum_{s_1, s_2 \notin E(H_2)} \left( d_{Q(H_1)}(r_1)^2 + d_{Q(H_1)}(r_2)^2 \right) \right] \\
& = 2(\bar{e}_2 + (n_2 - 1)) \sum_{\substack{r_1 r_2 \notin E(Q(H_1)) \\ r_1, r_2 \in V(Q(H_1) - V(H_1))}} \left[ d_{Q(H_1)}(r_1)^2 + d_{Q(H_1)}(r_2)^2 \right].
\end{aligned}$$

$$\text{Take } \sum_{\substack{r_1 r_2 \notin E(Q(H_1)) \\ r_1, r_2 \in V(Q(H_1) - V(H_1))}} \left[ d_{Q(H_1)}(r_1)^2 + d_{Q(H_1)}(r_2)^2 \right] = \bar{F}(Q(H_1)), \text{ then } = 2(\bar{e}_2 + (n_2 - 1))\bar{F}(Q(H_1)).$$

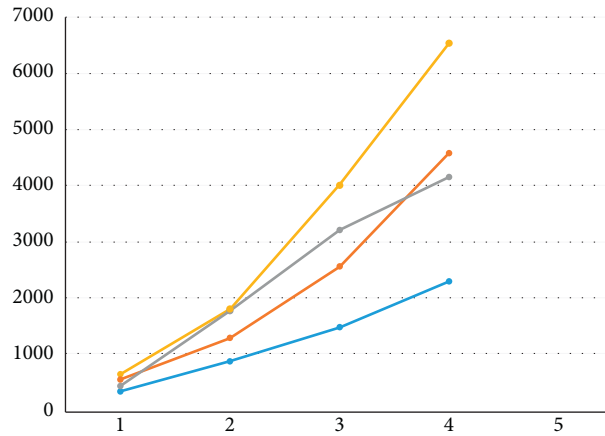
(13)

Consequently,

$$\sum A = n_2 \bar{F}(Q(G_1)) + 2(\bar{e}_2 + (n_2 - 1))M_1(Q(H_1)) + 2(\bar{e}_2 + (n_2 - 1))F(Q(G_1)) + \bar{F}(Q(G_1)). \quad (14)$$

TABLE 1: For two graphs,  $H_1 \cong P_n$  and  $H_2 \cong P_m$  values of forgotten coindex for their  $D$ -sum graphs by taking different values for  $n$  and  $m$ .

$n, m$	$\overline{F}(P_{n+S}P_m)$	$\overline{F}(P_{n+R}P_m)$	$\overline{F}(P_{n+Q}P_m)$	$\overline{F}(P_{n+T}P_m)$
3,2	332	528	410	632
4,2	840	1268	1760	1820
5,2	1476	2552	3214	4002
6,2	2276	4585	4160	6552
7,2	3332	6448	7034	9830
8,2	4840	9512	9514	14362

FIGURE 3: Graphical presentations of  $F$ -coincides for  $P_{n+D}P_m$  graphs such as  $H_{1+S}H_2$ ,  $H_{1+R}H_2$ ,  $H_{1+Q}H_2$ , and  $H_{1+T}H_2$  are represented by blue, orange, gray, and yellow, respectively.

Using equation (8), we directly have

$$\begin{aligned}
 \sum B &= 2\overline{e}_2M_1(H_1) + 4e_1\overline{M}_1(H_2) + n_1\overline{F}(H_2) + n_2(F(H_1) + \overline{F}(H_1) + 2M_1(H_2)(e_1 + \overline{e}_1) \\
 &\quad + 4e_2(M_1(H_1) + \overline{M}_1(H_1)) + 2[(e_2 + \overline{e}_2)(F(H_1) + \overline{F}(H_1)) + (e_1 + \overline{e}_1)(F(H_2) + \overline{F}(H_2))], \\
 \sum C &= \sum C_1 + \sum C_2 + \sum C_3, \\
 \sum C_1 &= \sum_{\substack{r_1 r_2 \notin E(S(H_1)) \\ r_1 \in V(H_1) r_2 \in V(Q(H_1)-V(H_1))}} \sum_{s \in V_{H_2}} [d(r_1, s)^2 + d(r_2, s)^2] \\
 &= \sum_{\substack{r_1 r_2 \notin E(Q(H_1)) \\ r_1 \in V(H_1) \\ r_2 \in V(S(H_1)-V(H_1))}} \sum_{s \in V_{H_2}} [(d(r_1)^2 + d(r_2)^2) + d(s)^2 + 2d(r_1)d(s)] = n_2\alpha_1 + e_1(n_1 - 2)M_1(H_2) + 4e_2\alpha_3, \\
 \sum C_2 &= \sum_{\substack{r_1 r_2 \notin E(Q(H_1)) \\ r_1 \in V(H_1) \\ r_2 \in V(S(H_1)-V(H_1))}} \left( \sum_{s_1, s_2 \in V_{H_2}} + \sum_{s_1, s_2 \notin E_{H_2}} \right) [(d(r_1, s_1)^2 + d(r_2, s_2)^2)] \\
 &= \alpha\alpha_1 + e_1(n_1 - 2)(M_1(H_2) + \overline{M}_1(H_2)) + 4(e_2 + \overline{e}_2)\alpha_3, \\
 \sum C_3 &= \sum_{\substack{r_1 r_2 \in E(Q(H_1)) \\ r_1 \in V(H_1) r_2 \in V(S(H_1)-V(H_1))}} \left( \sum_{s_1, s_2 \in V_{H_2}} + \sum_{s_1, s_2 \notin V_{H_2}} \right) [(d(r_1, s_1)^2 + d(r_2, s_2)^2)] \\
 &= \alpha\alpha_2 + 2e_1(M_1(H_2) + \overline{M}_1(H_2)) + 4(e_2 + \overline{e}_2)\alpha_4.
 \end{aligned} \tag{15}$$

By substituting the values in equation (13), we get the required result.  $\square$

**Theorem 4.** Let  $H_{1+T}H_2$  be a  $T$ -sum graph; then, its  $F$ -coindex is

$$\begin{aligned} \overline{F}(H_{1+T}H_2) &= n_2 \overline{F}(Q'(G_1)) + 2(\overline{e}_2 + (n_2 - 1)) \left( M_1(Q'H_1) + 1 \right) F(Q'(G_1)) \\ &\quad + 2(\overline{e}_2 + (n_2 - 1)) \overline{F}(Q'(G_1)) + \overline{e}_2 M_1(H_1) + 8e_1 \overline{M}_1(H_2) + n_1 \overline{F}(H_2) \\ &\quad + 4n_2 (\overline{F}(H_1) + 2\overline{e}_1 M_1(H_2) + 8e_2 \overline{M}_1(H_1) + 2[4(e_2 + \overline{e}_2)(F(H_1) \\ &\quad + \overline{F}(H_1)) + (e_1 + \overline{e}_1)(F(H_2) + \overline{F}(H_2)) + 2(M_1(H_2) + \overline{M}_1(H_2))(M_1(H_1) \\ &\quad + \overline{M}_1(H_1))] + n_2 \overline{F}(T(H_1)) + e_1(n_1 - 2)M_1(H_2) + \alpha(\alpha_1 + \alpha_2) \\ &\quad + e_1 n_1 (M_1(H_2) + \overline{M}_1(H_2)) + 4(e_2 + \overline{e}_2)(2\alpha_3 + \alpha_4). \end{aligned} \quad (16)$$

*Proof.* It follows from Theorems 2 and 3.  $\square$

#### 4. Conclusion

In this study, we have computed forgotten coindex of  $D$ -sum graphs such as  $\overline{F}(H_{1+S}H_2)$ ,  $\overline{F}(H_{1+R}H_2)$ ,  $\overline{F}(H_{1+Q}H_2)$ , and  $\overline{F}(H_{1+T}H_2)$  in their general forms. If  $H_1 = P_n$  and  $H_2 = P_m$  of order  $n, m \geq 2$ , then

- (i) In this study, we computed the exact values of forgotten coindex of  $D$ -sum graphs such as  $(H_{1+D}H_2)$ , where  $D \in \{S, R, Q, T\}$  in the form of

forgotten index, first Zagreb indices, and coincides their basic graphs  $H_1$  and  $H_2$ .

- (ii) We illustrated Theorems 1–4 with the help of some particular path graphs such as  $P_{n+S}P_m$ ,  $P_{n+R}P_m$ ,  $P_{n+Q}P_m$ , and  $P_{n+T}P_m$  for  $n, m \geq 2$ . Forgotten coindex of  $D$ -sum graphs from the paths is also computed as applications of the obtained results.
- (iii) Table 1 and Figure 3 present that forgotten coindex of  $(P_{n+T}P_m)$  is dominant than forgotten coindex of  $P_{n+S}P_m$ ,  $P_{n+R}P_m$ , and  $P_{n+Q}P_m$ .

$$\begin{aligned} \overline{F}(P_{m+S}P_n) &= 4m(n-1)(m(n-1)-1) + (m-1)(m-2)M(P_n) + 4(n-1)\overline{M}P_m + n\overline{F}(P_m) \\ &\quad + m(F(P_n) + \overline{F}(P_n)) + n(n-1)M_1(P_m) + 4(m-1)(M_1(P_n) + \overline{M}_1(P_n)) \\ &\quad + m(m-1)(F(P_n) + \overline{F}(P_n)) + n(n-1)(F(P_m) + \overline{F}(P_m)) + 2(M_1(P_m) + \overline{M}_1(P_m))(M_1(P_n) \\ &\quad + \overline{M}_1(P_n)) + m\overline{F}(S(P'_n)) + (n-1)(n-2)M_1(P_m) + 4(m-1)\overline{\beta}(S(P'_n)) + \alpha\overline{F}(S(P'_n)) \\ &\quad + (n-1)(n-2)(M_1(P_m) + \overline{M}_1(P_m)) + 2m(m-1)\overline{\beta}(S(P'_n)) + \alpha F(S(P'_n)) \\ &\quad + 2(n-1)(M_1(P_m) + \overline{M}_1(P_m)) + 2m(m-1)\beta(S(P'_n)), \end{aligned}$$

$$\begin{aligned} \overline{F}(P_{m+R}P_n) &= 4m(n-1)(m(n-1)-1) + 4(m-1)(m-2)M(P_n) + 8(n-1)\overline{M}P_m + n\overline{F}(P_m) \\ &\quad + 4m\overline{F}(P_n) + n(n-1)M_1(P_m) + 8(m-1)\overline{M}_1(P_n) + 4m(m-1)(F(P_n) + \overline{F}(P_n)) + n(n-1)(F(P_m) \\ &\quad + \overline{F}(P_m)) + 4(M_1(P_m) + \overline{M}_1(P_m))(M_1(P_n) + \overline{M}_1(P_n)) + m\overline{F}(R(P'_n)) + (n-1)(n-2)M_1(P_m) \\ &\quad + 4(m-1)\overline{\beta}(R(P'_n)) + \alpha\overline{F}(R(P'_n)) + (n-1)(n-2)(M_1(P_m) + \overline{M}_1(P_m)) + 2m(m-1)\overline{\beta}(R(P'_n)) \\ &\quad + \alpha F(R(P'_n)) + 2(n-1)(M_1(P_m) + \overline{M}_1(P_m)) + 2m(m-1)\beta(R(P'_n)), \end{aligned}$$

$$\begin{aligned} \overline{F}(P_{m+Q}P_n) &= n\overline{F}(Q'P_n) + 2(m+n-2) \left( M_1(Q'H_1) + \overline{F}(Q'P_n) + F(Q'P_n) \right) \\ &\quad + (m-1)(m-2)M_{P_n} + 4(n-1)\overline{M}_{P_m} + n\overline{F}(P_m) + m(F(P_n) + \overline{F}(P_n)) + n(n-1)M_1(P_m) \\ &\quad + 4(m-1)(M_1(P_n) + \overline{M}_1(P_n)) + m(m-1)(F(P_n) + \overline{F}(P_n)) + n(n-1)(F(P_m) + \overline{F}(P_m)) \end{aligned}$$

$$\begin{aligned}
& + 2(M_1(P_m) + \overline{M}_1(P_m))(M_1(P_n) + \overline{M}_1(P_n)) + m\overline{F}(Q(P'_n)) + (n-1)(n-2)M_1(P_m) \\
& + 4(m-1)\overline{\beta}(S(P'_n)) + \alpha\overline{F}(S(Q'_n)) + 2m(m-1)\overline{\beta}(S(Q'_n)) \\
& + (n-1)(n-2)(M_1(P_m) + \overline{M}_1(P_m)) + \alpha F(Q(P'_n)) + 2(n-1)(M_1(P_m) + \overline{M}_1(P_m)) \\
& + 2m(m-1)\beta(Q(P'_n)), \\
\overline{F}(P_{m+T}P_n) = & n\overline{F}(Q'P_n) + 2(m+n-2)(M_1(Q'H_1) + \overline{F}(Q'P_n) + F(Q'P_n)) \\
& + 4(m-1)(m-2)M_{P_n} + 8(n-1)\overline{M}_{P_m} + n\overline{F}(P_m) + 4m\overline{F}(P_n + n(n-1)M_1(P_m) + 8(m-1)\overline{M}_1(P_n)) \\
& + 4m(m-1)(F(P_n) + \overline{F}(P_n)) + n(n-1)(F(P_m) + \overline{F}(P_m)) + 4(M_1(P_m) + \overline{M}_1(P_m))(M_1(P_n) \\
& + \overline{M}_1(P_n)) + m\overline{F}(T(P'_n)) + (n-1)(n-2)M_1(P_m) + 4(m-1)\overline{\beta}(\beta(P'_n)) + \alpha\overline{F}(T(P'_n)) \\
& + 2m(m-1)\beta(S(P'_n)) + (n-1)(n-2)(M_1(P_m) + \overline{M}_1(P_m)) + 2m(m-1)\overline{\beta}(T(P'_n)) \\
& + \alpha F(T(P'_n)) + 2(n-1)(M_1(P_m) + \overline{M}_1(P_m)).
\end{aligned} \tag{17}$$

*Open problem 1.* Investigate the existence of the distance-based coindices for the  $D$ -sum graphs.

### Data Availability

The data used to support the findings of this study are included within the article and are available from the corresponding author upon request.

### Conflicts of Interest

The authors declare that they have no conflicts of interest.

### Acknowledgments

The authors are very thankful for the referees' comments, which helped them to improve the results and presentation of the manuscript to a great extent. This study was partially supported by University of Tabuk, Tabuk, Saudi Arabia.

### References

- [1] A. R. Matamala and E. Estrada, "Generalised topological indices: optimisation methodology and physico-chemical interpretation," *Chemical Physics Letters*, vol. 410, pp. 343–347, 2005.
- [2] G. Rücker and C. Rücker, "On topological indices, boiling points, and cycloalkanes," *Journal of Information and Computer Sciences*, vol. 39, pp. 788–802, 1999.
- [3] I. Gutman, "Degree-based topological indices," *Croatica Chemica Acta*, vol. 4, pp. 351–361, 2013.
- [4] H. Wiener, "Structural determination of paraffin boiling points," *Journal of the American Chemical Society*, vol. 69, no. 1, pp. 17–20, 1947.
- [5] I. Gutman and N. Trinajstić, "Graph theory and molecular orbitals. Total energy of alternant hydrocarbons," *Chemical Physics Letters*, vol. 4, pp. 535–538, 1972.
- [6] D. H. Rouvray, "The modeling of chemical phenomena using topological indices," *Journal of Computational Chemistry*, vol. 8, no. 4, pp. 470–480, 1987.
- [7] A. T. Balaban, "Topological indices based on topological distances in molecular graphs," *Pure and Applied Chemistry*, vol. 55, no. 2, pp. 199–206, 1983.
- [8] A. T. Balaban, I. Motoc, D. Bonchev, and O. Mekenyan, "Topological indices for structure-activity correlations," *Steric effects in drug design*, pp. 21–55, Springer, Berlin, Germany, 1983.
- [9] E. Cornwell, "New idea for the topological index evaluation and treatise multiple regression with three independent variables. Saturated Hydrocarbons used like a model," *Journal of the Chilean Chemical Society*, vol. 1, no. 1, pp. 765–768, 2006.
- [10] D. J. Klein, Z. Mihalic, D. Plavsic, and N. Trinajstić, "Molecular topological index: a relation with the Wiener index," *Journal of Chemical Information and Computer Sciences*, vol. 32, no. 4, pp. 304–305, 1992.
- [11] S. Mendiratta and A. K. Madan, "Structure-activity study on antiviral 5-vinylpyrimidine nucleoside analogs using Wiener's topological index," *Journal of Chemical Information and Computer Sciences*, vol. 34, no. 4, pp. 867–871, 1994.
- [12] I. Gutman and E. Estrada, "Topological indices based on the line graph of the molecular graph," *Journal of Chemical Information and Computer Sciences*, vol. 36, no. 3, pp. 541–543, 1996.
- [13] R. Biye, X. You, and C. Guobin, "A novel topological index for QSPR/QSAR study of organic compounds," *Acta Chimica Sinica*, vol. 57, no. 6, pp. 563–571, 1999.
- [14] W. Qinghua, F. Xinlu, Y. Guanhan, Y. Xiaodong, and T. Chengling, "Study on a prediction method for Octane number of acyclic alkane by autocorrelation topological index," *Journal of Petrochemical Universities*, vol. 13, no. 3, pp. 50–53, 2000.
- [15] A. Q. Baig, M. Imran, and H. Ali, "On topological indices of poly oxide, poly silicate, DOX, and DSL networks," *Canadian Journal of Chemistry*, vol. 93, no. 7, pp. 730–739, 2015.
- [16] B. Furtula and I. Gutman, "A forgotten topological index," *Journal of Mathematical Chemistry*, vol. 53, no. 4, pp. 1184–1190, 2015.
- [17] I. Gutman, A. Ghalavand, T. Dehghan-Zadeh, and A. R. Ashrafi, "Graphs with smallest forgotten index," *Iranian*

- Journal of Mathematical Chemistry*, vol. 8, no. 3, pp. 259–273, 2017.
- [18] Z. Che and Z. Chen, “Lower and upper bounds of the forgotten topological index,” *MATCH Communications in Mathematical and in Computer Chemistry*, vol. 76, no. 3, pp. 635–648, 2016.
- [19] W. Gao, M. K. Siddiqui, M. Imran, M. K. Jamil, and M. R. Farahani, “Forgotten topological index of chemical structure in drugs,” *Saudi Pharmaceutical Journal*, vol. 24, no. 3, pp. 258–264, 2016.
- [20] J. B. Liu, M. M. Matejic, E. I. Milovanovic, and I. Z. Milovanovic, “Some new inequalities for the forgotten topological index and coindex of graphs,” *MATCH Communications in Mathematical and in Computer Chemistry*, vol. 84, no. 3, pp. 719–738, 2020.
- [21] A. Ahmad, K. Elahi, R. Hasni, and M. F. Nadeem, “Computing the degree based topological indices of line graph of benzene ring embedded in P-type-surface in 2D network,” *Journal of Information and Optimization Sciences*, vol. 40, no. 7, pp. 1511–1528, 2019.
- [22] M. Javaid, M. Ahmad, M. Hussain, and W. C. Teh, “Bounds of F-index for unicyclic graphs with fixed pendent vertices,” *Journal of Prime Research in Mathematics*, vol. 14, pp. 51–61, 2018.
- [23] M. Imran, Y. Ali, Z. Bibi, and M. S. Ghafar, “Characterization of Extremal Unicyclic Graphs Using F-Coindex,” *Complexity*, vol. 2021, Article ID 8480971, 9 pages, 2021.
- [24] A. R. Ashrafi, T. Došlić, and A. Hamzeh, “The Zagreb coindices of graph operations,” *Discrete Applied Mathematics*, vol. 158, no. 15, pp. 1571–1578, 2010.
- [25] O. C. Havare and A. K. Havare, “Computation of the forgotten topological index and coindex for carbon base nanomaterial,” *Polycyclic Aromatic Compounds*, vol. 2020, pp. 1–13, 2020.
- [26] B. Basavanagoud and V. R. Desai, “Forgotten topological index and hyper-Zagreb index of generalized transformation graphs,” *Bulletin of Mathematical Sciences and Applications*, vol. 14, pp. 1–6, 2016.
- [27] W. Gao, W. Wang, M. K. Jamil, and M. R. Farahani, “Electron energy studying of molecular structures via forgotten topological index computation,” *Journal of Chemistry*, vol. 2016, Article ID 1053183, 7 pages, 2016.
- [28] Y. Bashir, A. Aslam, M. Kamran et al., “Forgotten topological indices of some dendrimers structure,” *Molecules*, vol. 22, no. 6, p. 867, 2017.
- [29] B. Basavanagoud and S. Timmanaikar, “Computing first Zagreb and forgotten indices of certain dominating transformation graphs of Kragujevac trees,” *Journal of Computer and Mathematical Sciences*, vol. 8, no. 3, pp. 50–61, 2017.
- [30] S. Akram, M. Javaid, and M. Jamal, “Bounds on F-index of tricyclic graphs with fixed pendant vertices,” *Open Mathematics*, vol. 18, no. 1, pp. 150–161, 2020.
- [31] W. Yan, B. Y. Yang, and Y. N. Yeh, “The behavior of Wiener indices and polynomials of graphs under five graph decorations,” *Applied Mathematics Letters*, vol. 20, pp. 290–295, 2007.
- [32] M. Eliasi and B. Taeri, “Four new sums of graphs and their Wiener indices,” *Discrete Applied Mathematics*, vol. 157, pp. 794–803, 2009.
- [33] H. Deng, D. Sarala, S. K. Ayyaswamy, and S. Balachandran, “The Zagreb indices of four operations on graphs,” *Applied Mathematics and Computation*, vol. 275, pp. 422–431, 2016.
- [34] S. Akhter and M. Imran, “The sharp bounds on general sum-connectivity index of four operations on graphs,” *Journal of Inequalities and Applications*, vol. 1, pp. 1–10, 2016.
- [35] S. Akhter and M. Imran, “Computing the forgotten topological index of four operations on graphs,” *AKCE International Journal of Graphs and Combinatorics*, vol. 14, no. 1, pp. 70–79, 2017.
- [36] M. Javaid, U. Ali, and J. B. Liu, “Computing analysis for first Zagreb connection index and coindex of resultant graphs,” *Mathematical Problems in Engineering*, vol. 2021, Article ID 6019517, 2021.
- [37] M. Javaid, S. Javed, S. Q. Memon, and A. M. Alanazi, “Forgotten index of generalized operations on graphs,” *Journal of Chemistry*, vol. 2021, Article ID 9971277, , 2021.
- [38] K. Pattabiraman, “F-indices and its coindices of some classes of graphs,” *Creative Mathematics and Informatics*, vol. 26, no. 2, pp. 203–212, 2017.
- [39] Z. B. Peng, S. Javed, M. Javaid, and J. B. Liu, “Computing FGZ index of sum graphs under strong product,” *Journal of Mathematics*, vol. 2021, Article ID 6654228, 2021.
- [40] Y. Ali, Z. Bibi, and Q. Kiran, “Forgotten coindex of some non-toxic dendrimers structure used in targeted drug delivery,” *Main Group Metal Chemistry*, vol. 44, no. 1, pp. 22–31, 2020.
- [41] N. De, S. M. A. Nayeem, and A. Pal, “The F-coindex of some graph operations,” *SpringerPlus*, vol. 5, no. 1, pp. 1–13, 2016.

## Research Article

# Novel Degree-Based Topological Descriptors of Carbon Nanotubes

M. C. Shanmukha,<sup>1</sup> A. Usha,<sup>2</sup> M. K. Siddiqui,<sup>3</sup> K. C. Shilpa,<sup>4</sup> and A. Asare-Tuah <sup>5</sup>

<sup>1</sup>Department of Mathematics, Jain Institute of Technology, Davanagere-577003, Karnataka, India

<sup>2</sup>Department of Mathematics, Alliance School of Applied Mathematics, Alliance University, Bangalore-562106, Karnataka, India

<sup>3</sup>Department of Mathematics, Comsats University Islamabad, Lahore Campus, Lahore, Pakistan

<sup>4</sup>Department of Computer Science and Engineering, Bapuji Institute of Engineering and Technology, Davanagere-577004, Karnataka, India

<sup>5</sup>Department of Mathematics, University of Ghana, Legon, Ghana

Correspondence should be addressed to A. Asare-Tuah; [aasare-tuah@ug.edu.gh](mailto:aasare-tuah@ug.edu.gh)

Received 27 July 2021; Accepted 27 August 2021; Published 8 September 2021

Academic Editor: Ajaya Kumar Singh

Copyright © 2021 M. C. Shanmukha et al. This is an open access article distributed under the Creative Commons Attribution License, which permits unrestricted use, distribution, and reproduction in any medium, provided the original work is properly cited.

The most significant tool of mathematical chemistry is the numerical descriptor called topological index. Topological indices are extensively used in modelling of chemical compounds to analyse the studies on quantitative structure activity/property/toxicity relationships and combinatorial library virtual screening. In this work, an attempt is made in defining three novel descriptors, namely, neighborhood geometric-harmonic, harmonic-geometric, and neighborhood harmonic-geometric indices. Also, the aforementioned three indices along with the geometric-harmonic index are tested for physicochemical properties of octane isomers using linear regression models and computed for some carbon nanotubes.

## 1. Introduction

The applications of graph theory are diversified in every field, but chemistry is the major area of the implementation of graph theory. In chemical graph theory, topological index plays a vital role which facilitates the chemists with a treasure of data that correlate with the structure of the chemical compound. The topological index is a numerical descriptor, defines the graph topology of the molecule, and predicts an extensive range of molecular properties [5–6].

From the last two decades, topological indices (TIs) are identified and used in pharmacological medicine, bio-inorganic chemistry, toxicity, and theoretical chemistry and are also used for correlation analysis [7–11].

Topological descriptors are frequently used in the discovery of drugs as they have rich datasets that give high predictive values. These descriptors give the information depending on the arrangement of atoms and their bonds of a chemical compound. They are studied for chemical

compounds where, generally, the hydrogen atoms are suppressed. The originality of QSAR/QSPR models depends on physicochemical properties for chemical compounds with high degree of precision. These models depend on various factors such as selecting the suitable compounds, suitable descriptors, and suitable algorithms or tools used in model development [12]. The QSAR/QSPR analysis is based on the data obtained by the numerical descriptors. These data are used to verify whether the compound under the study is suitable for drug making as the TIs provide computational data about the compound. Considering the information of the compound, QSAR/QSPR/QSTR analyses are carried out.

The TIs have increasing popularity in the field of research as they involve only computation without performing any physical experiment. Recent years have proved considerable attention in TIs as the effects of an atomic type and group efforts are considered in QSAR/QSPR modelling [13–15]. Distance-based TIs are used in QSAR analysis,

while chirality descriptors are introduced based on molecular graphs [16].

Alkanes are acyclic saturated hydrocarbons in which carbons and hydrogens are arranged in a tree-like structure. The main use of alkanes is found in crude oil such as petroleum, cooking gas, pesticides, and drug synthesis. The compounds that contain absolutely the same number of atoms but their arrangement differs are termed as isomers. A study is carried out for eighteen octane isomers (refer Figure 1).

A structure whose size is between the microscopic and molecular structure is referred to as a nanostructure. There are different types of nanostructures, namely, nanocages, nanocomposites, nanoparticles, nanofabrics, etc. In the recent years, nanostructures have attracted a lot of researchers in the areas of biology, chemistry, and medicines. Topological indices of nanostructures can be studied from [17–24]. The nanostructures made of carbons with cylindrical shape are carbon nanotubes (CNTs). They have a similar structure to that of a fullerene and graphene except their cylindrical shape. The shape of fullerene is as that of a football or basketball design where hexagons are connected.

In 1991, Iijima [25] used carbon nanotubes that have attracted many researchers in nanoscience and nanotechnology worldwide. As they have exotic properties, they are widely used in both research and applications. Nanotubes have a distinctive structure with remarkable mechanical and electrical properties. In case of carbon nanotubes, the hexagons are surrounded by squares, and each of these patterns is linearly arranged. Carbon nanotubes reveal exceptional electrical conductivity and possess wonderful tensile strength and thermal conductivity as they have nanostructures in which the carbon atoms are strongly connected.

Carbon nanotubes have applications in orthopaedic implants, especially in total hip replacement and other treatments pertaining to bone-related ailments. They are used as a grouting agent placed between the prosthesis and the bone as a part of their therapeutic use. The CNTs are used in biomedical fields because of their structural stiffness and effective optical absorption from UV to IR. Also, they can be altered chemically which are expected to be useful in many fields of technology such as electronics, composited materials, and carbon fibres. They have incredible applications in the field of materials science [26]. When the hexagonal lattice is rolled in different directions, it looks like single-wall carbon nanotubes have spiral shape and translational symmetry along the tube axis. It has rotational symmetry along its own axis. Even though nanotubes have favourable applications in a variety of fields, their large-scale production has been restricted. The main constraint that obstructs their use lies in difficulty in controlling their structure, impurities, and poor process ability. To enhance their usage, they have grabbed the attention especially in the formation of composites with polymers.

There are two types of configurations in the arrangement of nanotubes, namely, zigzag and armchair. In the zigzag configuration, the hexagons are placed one below the other linearly, whereas in the armchair configuration, they are

placed next to each other. This gives two different types of configurations with different terminologies discussed now. To explain the structure of a nanotube that is infinitely long, we imagine it to be cut open by a parallel axis and placed on a plane. Then, the atoms and bonds coincide with an imaginary graphene sheet. The length of the two atoms on opposite edges of the strip corresponds to circumference of the cylindrical graphene sheet [27–29].

The main objectives of this work are as follows:

To define novel indices

To discuss the physical and chemical applicability of octane isomers using regression models

To compute defined indices for carbon nanotubes such as  $C_4C_8(S)$ ,  $C_4C_8(R)$ , and H-naphthalenic nanosheets

Let  $G = (V, E)$  be a graph with a vertex set  $V(G)$  and an edge set  $E(G)$  such that  $|V(G)| = n$  and  $|E(G)| = m$ . For standard graph terminologies and notations, refer to [30, 31]. where  $(u, v)$  is an element of  $E(G)$ ,  $d_u$  represents the degree of the vertex  $u$ , and  $S_u$  represents the neighborhood degree of the vertex  $u$ .

*Definition 1.* Recently, Usha et al. [32] defined the geometric-harmonic (GH) index, inspired by Vukicevic and Furtula [33] in designing the GA index:

$$GH(G) = \sum \frac{(d_u + d_v)\sqrt{d_u \cdot d_v}}{2} \quad (1)$$

Motivated by the above work, in this paper, an attempt is made to define three novel indices based on degree and neighborhood degree, namely, harmonic-geometric (HG), neighborhood geometric-harmonic (NGH), and neighborhood harmonic-geometric (NHG) indices. They are defined as follows:

$$\begin{aligned} HG(G) &= \sum \frac{2}{(d_u + d_v)\sqrt{d_u \cdot d_v}} \\ NGH(G) &= \sum \frac{(S_u + S_v)\sqrt{S_u \cdot S_v}}{2} \\ NHG(G) &= \sum \frac{2}{(S_u + S_v)\sqrt{S_u \cdot S_v}} \end{aligned} \quad (2)$$

*1.1. Chemical Applicability of GH, NGH, HG, and NHG Indices.* In this section, a linear regression model of four physical properties is presented for GH, NGH, HG, and NHG indices. The physical properties such as entropy (S), acentric factor (AF), enthalpy of vaporization (HVAP), and standard enthalpy of vaporization (DHVAP) of octane isomers have shown good correlation with the indices considered in the study. The GH, HG, NGH, and NHG indices are tested for the octane isomers' database available at <https://www.molecularDescriptors.eu/dataset.htm>. The GH, HG, NGH, and NHG indices are computed and tabulated in columns 6, 7, 8, and 9 of Table 1.

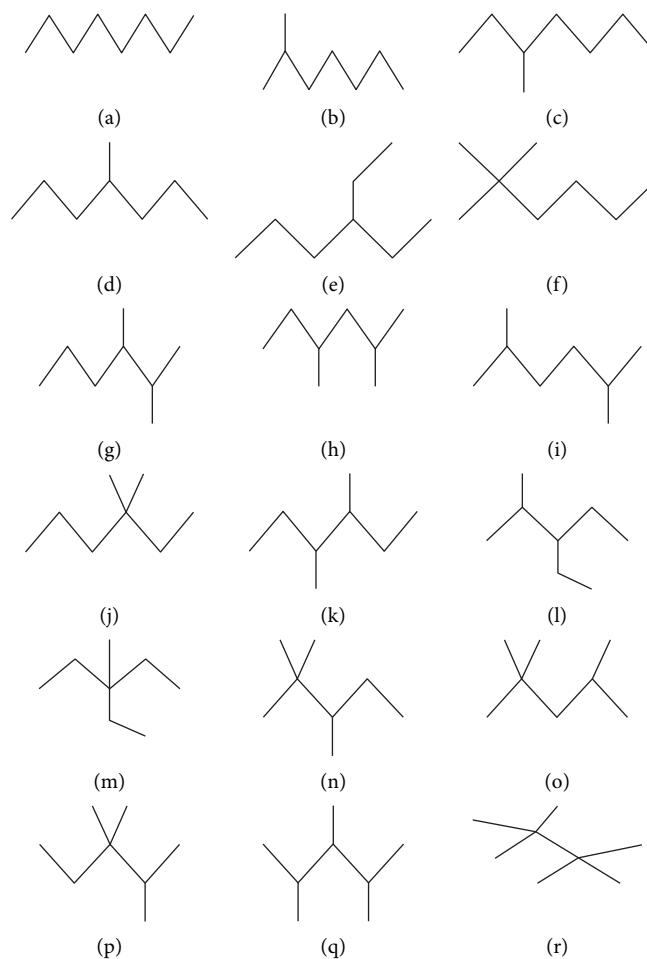


FIGURE 1: (a) *n*-Octane, (b) 2-methylheptane, (c) 3-methylheptane, (d) 4-methylheptane, (e) 3-ethylhexane, (f) 2,2-dimethylhexane, (g) 2,3-dimethylhexane, (h) 2,4-dimethylhexane, (i) 2,5-dimethylhexane, (j) 3,3-dimethylhexane, (k) 3,4-dimethylhexane, (l) 3-ethyl-2-methylpentane, (m) 3-ethyl-3-methylpentane, (n) 2,2,3-trimethylpentane, (o) 2,2,4-trimethylpentane, (p) 2,3,3-trimethylpentane, (q) 2,3,4-trimethylpentane, and (r) 2,2,3,3-trimethylbutane.

TABLE 1: Experimental values of *S*, *AF*, *HVAP*, and *DHVAP* and the corresponding values of the *GH* index, *HG* index, *NGH* index, and *NHG* index of octane isomers.

Alkane	<i>S</i>	<i>AF</i>	<i>HVAP</i>	<i>DHVAP</i>	<i>GH</i>	<i>NGH</i>	<i>HG</i>	<i>NHG</i>
<i>n</i> -Octane	111.700	0.398	73.190	9.915	24.423	84.496	2.193	0.679
2-Methylheptane	109.800	0.378	70.300	9.484	27.173	98.746	1.962	0.573
3-Methylheptane	111.300	0.371	71.300	9.521	27.954	107.475	2.058	0.568
4-Methylheptane	109.300	0.372	70.910	9.483	27.954	113.356	2.058	0.600
3-Ethylhexane	109.400	0.362	71.700	9.476	28.735	131.941	2.154	0.476
2,2-Dimethylhexane	103.400	0.339	67.700	8.915	33.607	122.970	1.689	0.471
2,3-Dimethylhexane	108.000	0.348	70.200	9.272	31.637	110.622	1.862	0.498
2,4-Dimethylhexane	107.000	0.344	68.500	9.029	30.885	123.236	1.827	0.474
2,5-Dimethylhexane	105.700	0.357	68.600	9.051	32.248	133.242	1.731	0.469
3,3-Dimethylhexane	104.700	0.323	68.500	8.973	35.213	151.398	1.829	0.449
3,4-Dimethylhexane	106.600	0.340	70.200	9.316	32.418	117.701	1.958	0.578
2-Methyl-3-ethylpentane	106.100	0.332	69.700	9.209	32.418	176.111	1.958	0.342
3-Methyl-3-ethylpentane	101.500	0.307	69.300	9.081	36.820	149.222	1.968	0.377
2,2,3-Trimethylpentane	101.300	0.301	67.300	8.826	38.834	164.366	1.606	0.338
2,2,4-Trimethylpentane	104.100	0.305	64.870	8.402	36.537	155.874	1.459	0.358
2,3,3-Trimethylpentane	102.100	0.293	68.100	8.897	39.659	141.657	1.649	0.462
2,3,4-Trimethylpentane	102.400	0.317	68.370	9.014	35.321	168.797	1.666	0.390
2,2,3,3-Trimethylbutane	93.060	0.255	66.200	8.410	46.000	223.620	1.263	0.227

Using the method of least squares, the linear regression models for S, AF, HVAP, and DHVAP are fitted using the data of Table 1.

The fitted models for the GH index are

$$S = 133.078 (\pm 1.82) - 0.833 (\pm 0.054)GH, \quad (3)$$

$$\text{acentric factor} = 0.557 (\pm 0.009) - 0.007 (\pm 0.000)GH, \quad (4)$$

$$HVAP = 79.613 (\pm 1.878) - 0.315 (\pm 0.056)GH, \quad (5)$$

$$DHVAP = 11.273 (\pm 0.285) - 0.065 (\pm 0.008)GH. \quad (6)$$

The fitted models for the HG index are

$$S = 76.608 (\pm 4.486) + 15.766 (\pm 2.435)HG, \quad (7)$$

$$\text{acentric factor} = 0.114 (\pm 0.037) + 0.121 (\pm 0.020)HG, \quad (8)$$

$$HVAP = 54.960 (\pm 1.356) + 7.773 (\pm 0.736)HG, \quad (9)$$

$$DHVAP = 6.428 (\pm 0.249) + 1.477 (\pm 0.135)HG. \quad (10)$$

The fitted models for the NGH index are

$$S = 121.77 (\pm 2.35) - 0.119 (\pm 0.017)NGH, \quad (11)$$

$$\text{acentric factor} = 0.465 (\pm 0.018) - 0.001 (\pm 0.000)NGH, \quad (12)$$

$$HVAP = 75.007 (\pm 1.552) - 0.043 (\pm 0.011)NGH, \quad (13)$$

$$DHVAP = 10.363 (\pm 0.257) - 0.009 (\pm 0.002)NGH. \quad (14)$$

The fitted models for the NHG index are

$$S = 89.524 (\pm 2.505) + 34.35 (\pm 5.271)NHG, \quad (15)$$

$$\text{acentric factor} = 0.207 (\pm 0.018) + 0.277 (\pm 0.038)NHG, \quad (16)$$

$$HVAP = 62.667 (\pm 1.352) + 14.044 (\pm 2.846)NHG, \quad (17)$$

$$DHVAP = 7.793 (\pm 0.219) + 2.882 (\pm 0.460)NHG. \quad (18)$$

Note: in equations (3)–(18), the errors of the regression coefficients are represented within brackets.

Tables 2–5 and Figures 2–5 show the correlation coefficient and residual standard error for the regression models of four physical properties with GH, HG, NGH, and NHG indices.

From Table 2 and Figure 2, it is obvious that the GH index highly correlates with the acentric factor and the correlation coefficient  $|r| = 0.987$ . Also, the GH index has good correlation coefficient  $|r| = 0.968$  with entropy,  $|r| = 0.815$  with HVAP, and  $|r| = 0.885$  with DHVAP.

From Table 3 and Figure 3, it is noticed that the HG index highly correlates with DHVAP and the correlation coefficient  $r = 0.939$ . Also, the HG index has good correlation coefficient  $r = 0.85$  with entropy,  $r = 0.833$  with the acentric factor, and  $r = 0.935$  with HVAP.

From Table 4 and Figure 4, it is clear that the NGH index highly correlates with the acentric factor and the correlation coefficient  $|r| = 0.877$ . Also, the NGH index has good correlation coefficient  $|r| = 0.873$  with entropy,  $|r| = 0.695$  with HVAP, and  $|r| = 0.778$  with DHVAP.

From Table 5 and Figure 5, it is clear that the NHG index highly correlates with the acentric factor and the correlation coefficient  $r = 0.877$ . Also, the NHG index has good correlation coefficient  $r = 0.852$  with entropy,  $r = 0.777$  with HVAP, and  $r = 0.843$  with DHVAP.

## 2. GH, NGH, HG, and NHG Indices of $C_4C_8(S)$ , $C_4C_8(R)$ , and H-Naphthalenic Nanosheets

*2.1. Results for the  $C_4C_8(S)$  Nanosheet.* The alternating pattern of 4 carbon atoms forming squares and 8 carbon atoms forming octagons constitutes the  $TUC_4C_8(S)[a, b]$  nanosheet.

In this section, GH, HG, NGH, and NHG indices of the  $C_4C_8(S)$  nanosheet are computed. The pattern of carbon atoms gives rise to two types of nanosheets, namely,  $T^1[a, b]$  and  $T^2[a, b]$ . The 2-dimensional nanosheet is represented by  $T^1[a, b]$ , where  $a$  and  $b$  are parameters (Figure 6). In  $T^1[a, b]$ ,  $C_4$  acts as a square, while  $C_8$  is an octagon in which  $a$  and  $b$  represent the column and row, respectively. Figure 7 depicts the type 1- $C_4C_8(S)$  nanosheet. The number of vertices of the  $C_4C_8(S)$  nanosheet is  $8ab$ , and the number of edges is  $12ab - 2a - 2b$ .

The edge partition of the  $T^1[a, b]$  nanosheet based on the degree of vertices is detailed in Table 6.

**Theorem 1.** Let  $T^1[a, b]$  be an  $(a, b)$ -dimensional nanosheet; then, GH and HG indices are equal to

$$GH(T^1[a, b]) = 108ab - \frac{4938}{125}a - \frac{4938}{125}b + \frac{376}{125}, \quad (19)$$

$$HG(T^1[a, b]) = \frac{4}{3}ab + \frac{33}{125}a + \frac{33}{125}b + \frac{69}{500}.$$

*Proof.* Using Table 6, the definitions of GH and HG indices are as follows:

TABLE 2: Parameters of regression models for the GH index.

Physical properties	Value of the correlation coefficient	Residual standard error
Entropy	-0.968	1.17
Acentric factor	-0.987	0.0059
HVAP	-0.815	1.21
DHVAP	-0.885	0.184

TABLE 3: Parameters of regression models for the HG index.

Physical properties	Value of the correlation coefficient	Residual standard error
Entropy	0.85	2.448
Acentric factor	0.833	0.020
HVAP	0.935	0.74
DHVAP	0.939	0.136

TABLE 4: Parameters of regression models for the NGH index.

Physical properties	Value of the correlation coefficient	Residual standard error
Entropy	-0.873	2.274
Acentric factor	-0.877	0.0176
HVAP	-0.695	1.502
DHVAP	-0.778	0.248

TABLE 5: Parameters of regression models for the NHG index.

Physical properties	Value of the correlation coefficient	Residual standard error
Entropy	0.852	2.436
Acentric factor	0.877	0.018
HVAP	0.777	1.315
DHVAP	0.843	0.213

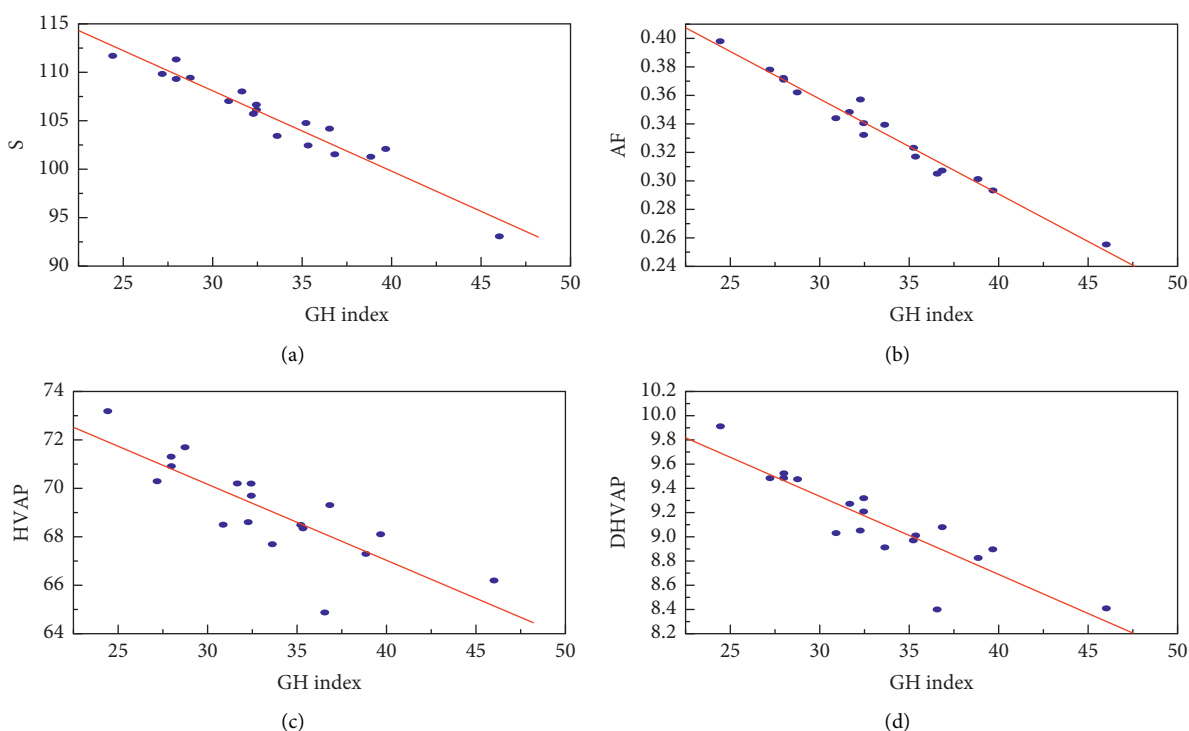


FIGURE 2: Scatter diagram of physical properties S, AF, HVAP, and DHVAP with the GH index.

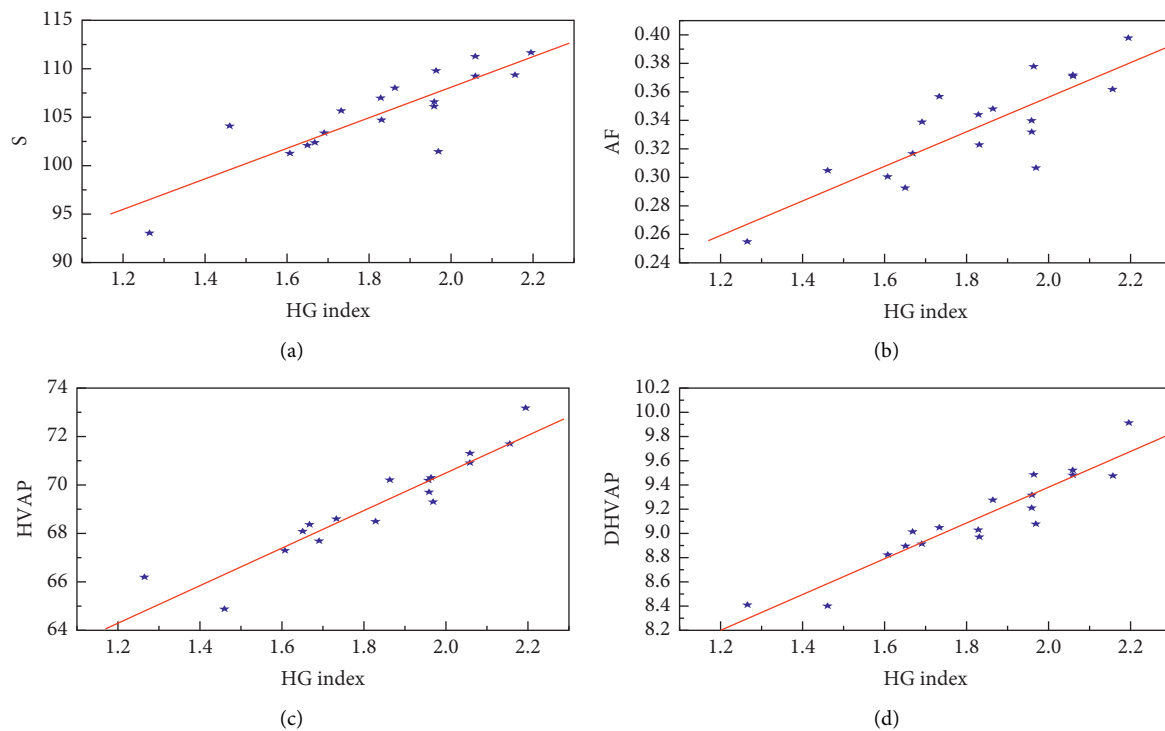


FIGURE 3: Scatter diagram of physical properties S, AF, HVAP, and DHVAP with the HG index.

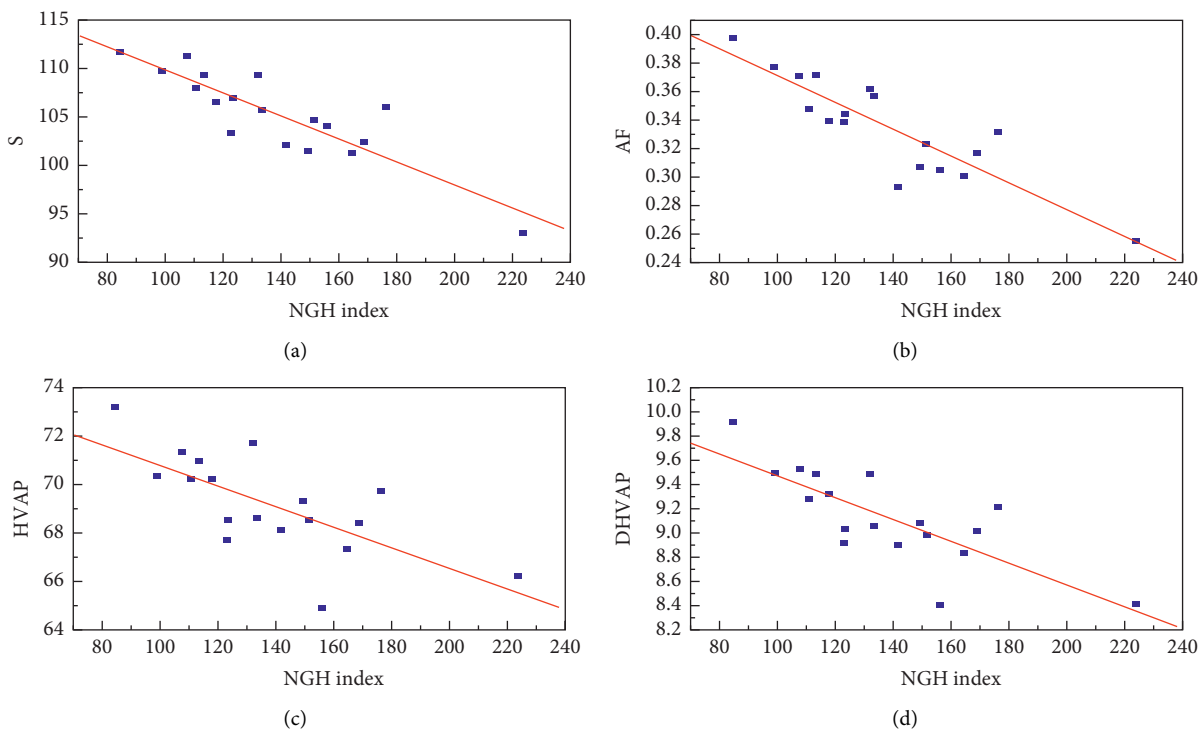


FIGURE 4: Scatter diagram of physical properties S, AF, HVAP, and DHVAP with the NGH index.

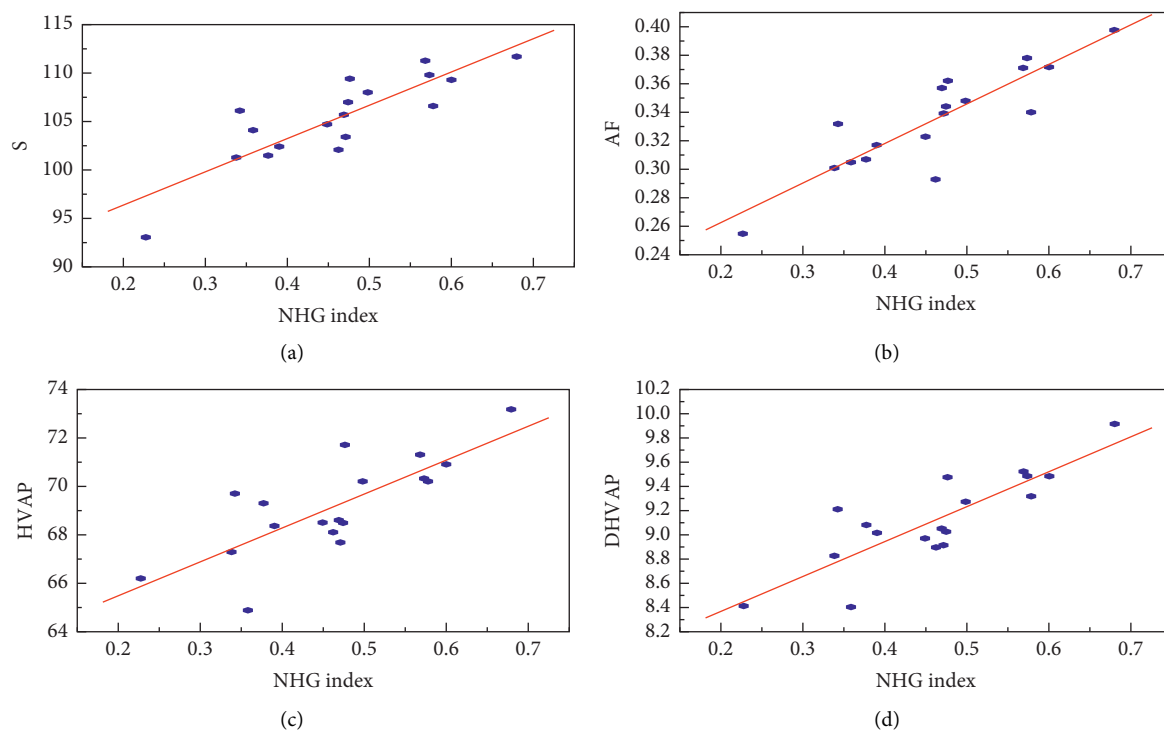


FIGURE 5: Scatter diagram of physical properties  $S$ ,  $AF$ ,  $HVAP$ , and  $DHVAP$  with the NHG index.

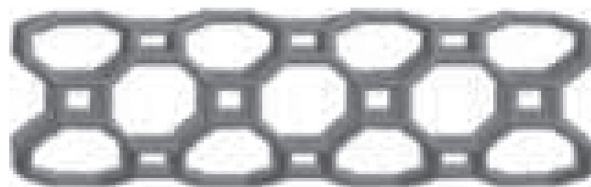


FIGURE 6: A  $TUC_4C_8(S)[a, b]$  nanotube.

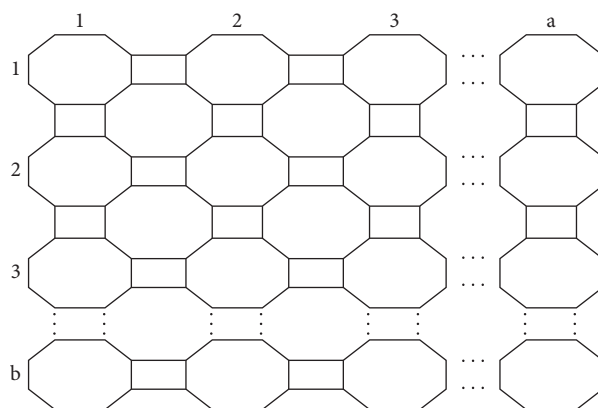


FIGURE 7: Type I- $C_4C_8(S)$  nanosheet  $T^1[a, b]$ .

TABLE 6: The edge partition of  $T^1[a, b]$ .

$(d_u, d_v)$ with $uv \in E(G)$	Number of edges
(2, 2)	$2(a + b + 2)$
(2, 3)	$4a + 4b - 8$
(3, 3)	$12ab - 8a - 8b + 4$

$$\begin{aligned}
\text{GH}(T^1[a, b]) &= \sum_{uv \in E(G)} \frac{(d_u + d_v)\sqrt{d_u \times d_v}}{2} \\
&= (2a + 2b + 4) \left\{ \frac{(2+2)(\sqrt{2 \times 2})}{2} \right\} + (4a + 4b - 8) \left\{ \frac{(2+3)(\sqrt{2 \times 3})}{2} \right\} \\
&\quad + (12ab - 8a - 8b + 4) \left\{ \frac{(2+3)(\sqrt{2 \times 3})}{2} \right\} \\
\text{GH}(T^1[a, b]) &= 108ab - \frac{4938}{125}a - \frac{4938}{125}b + \frac{376}{125}, \\
\text{HG}(T^1[a, b]) &= \sum_{uv \in E(G)} \frac{2}{(d_u + d_v)\sqrt{d_u \times d_v}} \\
&= (2a + 2b + 4) \left\{ \frac{2}{(2+2)(\sqrt{2 \times 2})} \right\} + (4a + 4b - 8) \left\{ \frac{2}{(2+3)(\sqrt{2 \times 3})} \right\} \\
&\quad + (12ab - 8a - 8b + 4) \left\{ \frac{2}{(2+3)(\sqrt{2 \times 3})} \right\} \\
\text{HG}(T^1[a, b]) &= \frac{4}{3}ab + \frac{33}{125}a + \frac{33}{125}b + \frac{69}{500}.
\end{aligned} \tag{20}$$

□

The edge partition of the  $T^1[a, b]$  nanosheet based on the neighborhood degree of vertices is detailed in Table 7.

**Theorem 2.** Let  $T^1[a, b]$  be an  $(a, b)$ -dimensional nanosheet; then, NGH and NHG indices are equal to

$$\begin{aligned}
\text{NGH}(T^1[a, b]) &= 972ab - \frac{251531}{500}a - \frac{251531}{500}b + \frac{159121}{1000}, \\
\text{NHG}(T^1[a, b]) &= \frac{37}{250}ab + \frac{91}{1000}a + \frac{91}{1000}b + \frac{157}{1000}.
\end{aligned} \tag{21}$$

*Proof.* Using Table 7, the definitions of NGH and NHG indices are as follows:

TABLE 7: Edge partition of  $T^1[a, b]$  for neighborhood degree-based vertices.

$(S_u, S_v)$ with $uv \in E(G)$	Number of edges
(4, 4)	4
(4, 5)	8
(5, 5)	$2a + 2b - 8$
(5, 8)	$4a + 4b - 8$
(8, 8)	$2a + 2b - 4$
(8, 9)	$4a + 4b - 8$
(9, 9)	$12ab - 14a - 14b + 16$

$$\begin{aligned} \text{NGH}(T^1[a, b]) &= \sum_{uv \in E(G)} \frac{(S_u + S_v)\sqrt{S_u \times S_v}}{2} \\ &= 4 \left\{ \frac{(4+4)(\sqrt{4 \times 4})}{2} \right\} + 8 \left\{ \frac{(4+5)(\sqrt{4 \times 5})}{2} \right\} + (2a+2b-8) \left\{ \frac{(5+5)(\sqrt{5 \times 5})}{2} \right\} + (4a+4b-8) \\ &\quad \cdot \left\{ \frac{(5+8)(\sqrt{5 \times 8})}{2} \right\} + (2a+2b-4) \left\{ \frac{(8+8)(\sqrt{8 \times 8})}{2} \right\} + (4a+4b-8) \left\{ \frac{(8+9)(\sqrt{8 \times 9})}{2} \right\} \\ &\quad + (12ab - 14a - 14b + 16) \left\{ \frac{(9+9)(\sqrt{9 \times 9})}{2} \right\} \end{aligned}$$

$$\text{NGH}(T^1[a, b]) = 972ab - \frac{251531}{500}a - \frac{251531}{500}b + \frac{159121}{1000},$$

(22)

$$\begin{aligned} \text{NHG}(T^1[a, b]) &= \sum_{uv \in E(G)} \frac{(S_u + S_v)\sqrt{S_u \times S_v}}{2} \\ &= 4 \left\{ \frac{2}{(4+4)(\sqrt{4 \times 4})} \right\} + 8 \left\{ \frac{2}{(4+5)(\sqrt{4 \times 5})} \right\} + (2a+2b-8) \left\{ \frac{2}{(5+5)(\sqrt{5 \times 5})} \right\} + (4a+4b-8) \\ &\quad \cdot \left\{ \frac{2}{(5+8)(\sqrt{5 \times 8})} \right\} + (2a+2b-4) \left\{ \frac{2}{(8+8)(\sqrt{8 \times 8})} \right\} + (4a+4b-8) \left\{ \frac{2}{(8+9)(\sqrt{8 \times 9})} \right\} \\ &\quad + (12ab - 14a - 14b + 16) \left\{ \frac{2}{(9+9)(\sqrt{9 \times 9})} \right\} \end{aligned}$$

$$\text{NHG}(T^1[a, b]) = \frac{37}{250}ab + \frac{91}{1000}a + \frac{91}{1000}b + \frac{157}{1000}.$$

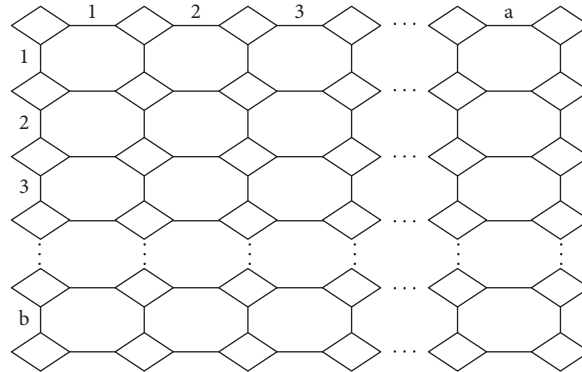
□

2.2. *Results for the  $C_4C_8(R)$  Nanosheet.* This structure is formed by 4 carbon atoms forming a rhombus that are linearly bridged by edges whose sequence looks like 4 rhombuses connected by 4 edges row and column wise resulting in an alternating pattern of rhombuses and octagons and is represented as  $T^2[a, b]$ . The 2-dimensional lattice of the  $TUC_4C_8(R)[a, b]$  nanosheet, where  $a$  and  $b$  are parameters, is shown in Figure 8. Figure 9 shows the type 2 -  $C_4C_8(R)$  nanosheet. In the following theorem, GH, HG, NGH, and NHG indices of this nanosheet are computed. The number of vertices of the type-2 structure is  $4ab + 4(a + b) + 4$ , and the number of edges is  $6ab + 5a + 5b + 4$ .

The edge partition of the  $T^2[a, b]$  nanosheet for degree-based vertices is detailed in Table 8.

**Theorem 3.** Let  $T^2[a, b]$  be an  $(a, b)$ -dimensional nanosheet; then, GH and HG indices are equal to

$$\begin{aligned} \text{GH}(T^2[a, b]) &= 54ab + \frac{669}{20}a + \frac{669}{20}b + 16, \\ \text{HG}(T^2[a, b]) &= \frac{2}{3}ab + \frac{191}{250}a + \frac{191}{250}b + 1. \end{aligned} \quad (23)$$

FIGURE 8: A  $TUC_4C_8(R)[a, b]$  nanotube.FIGURE 9: Type II- $C_4C_8(R)$  nanosheet  $T^2[a, b]$ .TABLE 8: Edge partition of  $T^2[a, b]$ .

$(d_u, d_v)$ with $uv \in E(G)$	Number of edges
(2, 2)	4
(2, 3)	$4(a + b)$
(3, 3)	$6ab + a + b$

*Proof.* Using Table 8, the definitions of GH and HG indices are as follows:

$$\begin{aligned}
 GH(T^2[a, b]) &= \sum_{uv \in E(G)} \frac{(d_u + d_v)\sqrt{d_u \times d_v}}{2} \\
 &= 4 \left\{ \frac{(2+2)(\sqrt{2 \times 2})}{2} \right\} + (4a + 4b) \left\{ \frac{(2+3)(\sqrt{2 \times 3})}{2} \right\} + (6ab + a + b) \left\{ \frac{(3+3)(\sqrt{3 \times 3})}{2} \right\} \\
 GH(T^2[a, b]) &= 54ab + \frac{669}{20}a + \frac{669}{20}b + 16, \\
 HG(T^2[a, b]) &= \sum_{uv \in E(G)} \frac{2}{(d_u + d_v)\sqrt{d_u \times d_v}} \\
 &= 2 \left\{ \frac{2}{(2+2)(\sqrt{2 \times 2})} \right\} + (4a + 4b) \left\{ \frac{2}{(2+3)(\sqrt{2 \times 3})} \right\} + (6ab + a + b) \left\{ \frac{2}{(3+3)(\sqrt{3 \times 3})} \right\} \\
 HG(T^2[a, b]) &= \frac{2}{3}ab + \frac{191}{250}a + \frac{191}{250}b + 1.
 \end{aligned} \tag{24}$$

□

The edge partition of the  $T^2[a, b]$  nanosheet based on the neighborhood degree of vertices is detailed in Table 9.

**Theorem 4.** Let  $T^2[a, b]$  be an  $(a, b)$ -dimensional nanosheet; then, NGH and NHG indices are equal to

$$\begin{aligned} \text{NGH}(T^2[a, b]) &= 486ab + \frac{20549}{100}a + \frac{20549}{100}b + \frac{21549}{500}, \\ \text{NHG}(T^2[a, b]) &= \frac{37}{500}ab + \frac{107}{1000}a + \frac{107}{1000}b + \frac{19}{100}. \end{aligned} \quad (25)$$

TABLE 9: Edge partition of  $T^2[a, b]$ .

$(S_u, S_v)$ with $uv \in E(G)$	Number of edges
(5, 5)	4
(5, 8)	8
(6, 8)	$4a + 4b - 8$
(8, 8)	$2a + 2b + 4$
(8, 9)	$4a + 4b - 8$
(9, 9)	$6ab - 5a - 5b + 4$

*Proof.* Using Table 9, the definitions of NGH and NHG indices are as follows:

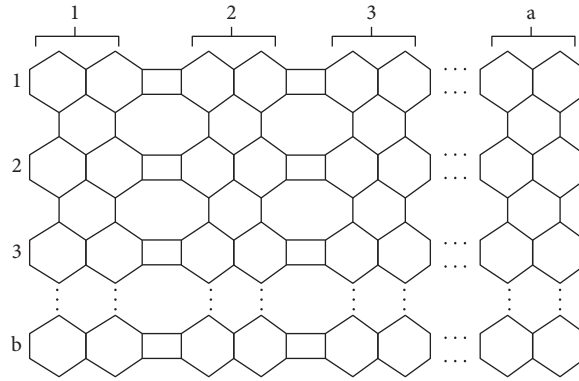
$$\begin{aligned} \text{NGH}(T^2[a, b]) &= \sum_{uv \in E(G)} \frac{(S_u + S_v)\sqrt{S_u \times S_v}}{2} \\ &= 4 \left\{ \frac{(5+5)(\sqrt{5 \times 5})}{2} \right\} + 8 \left\{ \frac{(5+8)(\sqrt{5 \times 8})}{2} \right\} + (4a+4b-8) \left\{ \frac{(6+8)(\sqrt{6 \times 8})}{2} \right\} + (2a+2b+4) \\ &\quad \cdot \left\{ \frac{(8+8)(\sqrt{8 \times 8})}{2} \right\} + (4a+4b-8) \left\{ \frac{(8+9)(\sqrt{8 \times 9})}{2} \right\} + (6ab-5a-5b+4) \left\{ \frac{(9+9)(\sqrt{9 \times 9})}{2} \right\} \\ \text{NGH}(T^2[a, b]) &= 486ab + \frac{20549}{100}a + \frac{20549}{100}b + \frac{21549}{500}, \\ \text{NHG}(T^2[a, b]) &= \sum_{uv \in E(G)} \frac{2}{(S_u + S_v)\sqrt{S_u \times S_v}} \\ &= 4 \left\{ \frac{2}{(5+5)(\sqrt{5 \times 5})} \right\} + 8 \left\{ \frac{2}{(5+8)(\sqrt{5 \times 8})} \right\} + (4a+4b-8) \left\{ \frac{2}{(6+8)(\sqrt{6 \times 8})} \right\} + (2a+2b+4) \\ &\quad \cdot \left\{ \frac{2}{(8+8)(\sqrt{8 \times 8})} \right\} + (4a+4b-8) \left\{ \frac{2}{(8+9)(\sqrt{8 \times 9})} \right\} + (6ab-5a-5b+4) \left\{ \frac{2}{(9+9)(\sqrt{9 \times 9})} \right\} \\ \text{NHG}(T^2[a, b]) &= \frac{37}{500}ab + \frac{107}{1000}a + \frac{107}{1000}b + \frac{19}{100}. \end{aligned} \quad (26)$$

**2.3. Results for the H-Naphthalenic Nanosheet.** Carbon atoms bonded in the form of a hexagonal structure constitute carbon nanotubes. They are peri-condensed benzenoids which mean three or more rings share the same atoms. H-Naphthalenic nanosheet is constituted by the alternating sequence of squares  $C_4$ , hexagons  $C_6$ , and octagons  $C_8$  and is represented as  $T^3[a, b]$ , where  $a$  and  $b$  are the parameters. The number of vertices of the H-naphthalenic nanosheet is  $10ab$ , and the edges are  $15ab - 2a - 2b$ . The GH, HG, NGH, and NHG indices of this nanosheet are computed; see Figure 10.

The edge partition of the  $T^3[a, b]$  nanosheet based on the degree of vertices is detailed in Table 10.

**Theorem 5.** Let  $T^3[a, b]$  be an  $(a, b)$ -dimensional nanosheet; then, GH and HG indices are equal to

$$\begin{aligned} \text{GH}(T^3[a, b]) &= 135ab - \frac{4101}{100}a - \frac{7901}{200}b + \frac{301}{100}, \\ \text{HG}(T^3[a, b]) &= \frac{1667}{1000}ab + \frac{39}{200}a + \frac{33}{125}b + \frac{69}{1500}. \end{aligned} \quad (27)$$

FIGURE 10: An H-naphthalenic nanosheet  $T^3[a, b]$ .TABLE 10: The details of edges and types of the  $T^3[a, b]$  nanosheet based on the degree of vertices.

$(d_u, d_v)$ with $uv \in E(G)$	Number of edges
(2, 2)	$2a + 4$
(2, 3)	$8a + 4b - 8$
(3, 3)	$15ab - 10a - 8b + 4$

*Proof.* Using Table 10, the definitions of GH and HG indices are as follows:

$$\begin{aligned}
 \text{GH}(T^3[a, b]) &= \sum_{uv \in E(G)} \frac{(d_u + d_v)\sqrt{d_u \times d_v}}{2} \\
 &= (2b + 4) \left\{ \frac{(2 + 2)(\sqrt{2 \times 2})}{2} \right\} + (8a + 8b - 8) \left\{ \frac{(2 + 3)(\sqrt{2 \times 3})}{2} \right\} \\
 &\quad + (15ab - 10a - 8b + 4) \left\{ \frac{(3 + 3)(\sqrt{3 \times 3})}{2} \right\} \\
 \text{GH}(T^3[a, b]) &= 135ab - \frac{4101}{100}a - \frac{7901}{200}b + \frac{301}{100}. \tag{28} \\
 \text{HG}(T^3[a, b]) &= \sum_{uv \in E(G)} \frac{2}{(d_u + d_v)\sqrt{d_u \times d_v}} \\
 &= (2b + 4) \left\{ \frac{2}{(2 + 2)(\sqrt{2 \times 2})} \right\} + (8a + 8b - 8) \left\{ \frac{2}{(2 + 3)(\sqrt{2 \times 3})} \right\} \\
 &\quad + (15ab - 10a - 8b + 4) \left\{ \frac{2}{(3 + 3)(\sqrt{3 \times 3})} \right\} \\
 \text{HG}(T^3[a, b]) &= \frac{1667}{1000}ab + \frac{39}{200}a + \frac{33}{125}b + \frac{69}{1500}.
 \end{aligned}$$

□

TABLE 11: Edge partition of  $T^3[a, b]$ .

$(S_u, S_v)$ with $uv \in E(G)$	Number of edges
(4, 5)	8
(5, 5)	$2b - 4$
(5, 7)	4
(5, 8)	$4b - 4$
(6, 7)	$4a - 4$
(6, 8)	$4a - 4$
(7, 9)	$2a$
(8, 8)	$2a + 2b - 4$
(8, 9)	$4a + 4b - 8$
(9, 9)	$15ab - 18a - 14b + 16$

The edge partition of the  $T^3[a, b]$  nanosheet based on the neighborhood degree of vertices is detailed in Table 11.

*Proof.* Using Table 11, the definitions of NGH and NHG indices are as follows:

**Theorem 6.** Let  $T^3[a, b]$  be an  $(a, b)$ -dimensional nanosheet; then, NGH and NHG indices are equal to

$$\text{NGH}(T^3[a, b]) = 1215ab - \frac{11199}{20}a - \frac{251531}{500}b + \frac{17382}{125},$$

$$\text{NHG}(T^3[a, b]) = \frac{37}{200}ab + \frac{15}{200}a + \frac{91}{1000}b + \frac{249}{2500}. \quad (29)$$

$$\begin{aligned} \text{NGH}(T^3[a, b]) &= \sum_{uv \in E(G)} \frac{(S_u + S_v)\sqrt{S_u \times S_v}}{2} \\ &= 8 \left\{ \frac{(4+5)(\sqrt{4 \times 5})}{2} \right\} + (2b-4) \left\{ \frac{(5+5)(\sqrt{5 \times 5})}{2} \right\} + 4 \left\{ \frac{(5+7)(\sqrt{7 \times 7})}{2} \right\} + (4b-4) \\ &\quad \cdot \left\{ \frac{(5+8)(\sqrt{5 \times 8})}{2} \right\} + (4a-4) \left\{ \frac{(6+7)(\sqrt{6 \times 7})}{2} \right\} + (4a-4) \left\{ \frac{(6+8)(\sqrt{6 \times 8})}{2} \right\} \\ &\quad + 2a \left\{ \frac{(7+9)(\sqrt{7 \times 9})}{2} \right\} + (2a+2b-4) \left\{ \frac{(8+8)(\sqrt{8 \times 8})}{2} \right\} + (4a+4b-8) \\ &\quad \cdot \left\{ \frac{(8+9)(\sqrt{8 \times 9})}{2} \right\} + (15ab-18a-14b+16) \left\{ \frac{(9+9)(\sqrt{9 \times 9})}{2} \right\} \\ \text{NGH}(T^3[a, b]) &= 1215ab - \frac{11199}{20}a - \frac{251531}{500}b + \frac{17382}{125}, \\ \text{NHG}(T^3[a, b]) &= \sum_{uv \in E(G)} \frac{(S_u + S_v)\sqrt{S_u \times S_v}}{2} \\ &= 8 \left\{ \frac{2}{(4+5)(\sqrt{4 \times 5})} \right\} + (2b-4) \left\{ \frac{2}{(5+5)(\sqrt{5 \times 5})} \right\} + 4 \left\{ \frac{2}{(5+7)(\sqrt{7 \times 7})} \right\} + (4b-4) \\ &\quad \cdot \left\{ \frac{2}{(5+8)(\sqrt{5 \times 8})} \right\} + (4a-4) \left\{ \frac{2}{(6+7)(\sqrt{6 \times 7})} \right\} + (4a-4) \left\{ \frac{2}{(6+8)(\sqrt{6 \times 8})} \right\} \\ &\quad + 2a \left\{ \frac{2}{(7+9)(\sqrt{7 \times 9})} \right\} + (2a+2b-4) \left\{ \frac{2}{(8+8)(\sqrt{8 \times 8})} \right\} + (4a+4b-8) \\ &\quad \cdot \left\{ \frac{2}{(8+9)(\sqrt{8 \times 9})} \right\} + (15ab-18a-14b+16) \left\{ \frac{2}{(9+9)(\sqrt{9 \times 9})} \right\} \\ \text{NHG}(T^3[a, b]) &= \frac{37}{200}ab + \frac{15}{200}a + \frac{91}{1000}b + \frac{249}{2500}. \end{aligned} \quad (30)$$

□

### 3. Conclusion

This paper is devoted to defining NGH, HG, and NHG indices, and the chemical applicability is studied for some physical and chemical properties of octane isomers using regression models including the recently introduced GH index. The GH index has a high negative correlation with acentric factor having  $r = 0.987$  with a residual standard error of 0.0059. The HG index has a high positive correlation with DHVAP having  $r = 0.939$  with a residual standard error of 0.136. The NGH index has a high negative correlation with acentric factor having  $r = 0.877$  with a residual standard error of 0.0176. The NHG index has a high positive correlation with acentric factor having  $r = 0.877$  with a residual standard error of 0.018. The applications of carbon nanotubes have considerably increased because of their excellent mechanical, thermal, and electrical properties. The novel indices introduced in this paper would be of great help to understand the physicochemical and biological properties of various compounds in addition to the existing degree-based indices.

### Data Availability

The data used to support the findings of this study are cited at relevant places within the text as references.

### Conflicts of Interest

The authors declare that they have no conflicts of interest.

### Authors' Contributions

All authors contributed equally to this work.

### References

- [1] D. Bonchev, *Information Theoretic Indices for Characterization of Chemical Structures*, Research Studies Press, 1983.
- [2] B. Furtula and I. Gutman, "A forgotten topological index," *Journal of Mathematical Chemistry*, vol. 53, no. 4, pp. 1184–1190, 2015.
- [3] I. Gutman and O. E. Polansky, *Mathematical Concepts in Organic Chemistry*, Springer, Berlin, Germany, 2012.
- [4] I. Gutman and N. Trinajstić, "Graph theory and molecular orbitals. Total  $\phi$ -electron energy of alternant hydrocarbons," *Chemical Physics Letters*, vol. 17, no. 4, pp. 535–538, 1972.
- [5] R. Todeschini and V. Consonni, *Handbook of Molecular Descriptors*, Wiley VCH, Weinheim, Germany, 2000.
- [6] N. Trinajstić, *Chemical Graph Theory*, CRC Press, Boca Raton, FL, USA, 1992.
- [7] S. Hayat, M. Imran, and J. B. Liu, "Correlation between the Esrada index and  $\pi$ -electron energies for benzenoid hydrocarbons with applications to boron nanotubes," *International Journal of Quantum Chemistry*, vol. 119, pp. 1–13, 2019.
- [8] M. Randić, "Quantitative structure-property relationship. Boiling points of planar benzenoids," *New Journal of Chemistry*, vol. 20, pp. 1001–1009, 1996.
- [9] M. C. Shanmukha, A. Usha, N. S. Basavarajappa, and K. C. Shilpa, "Novel Neighbourhood redefined First and Second Zagreb indices on Carborundum Structures," *Journal of Applied Mathematics and Computing*, vol. 66, pp. 1–14, 2020.
- [10] M. C. Shanmukha, N. S. Basavarajappa, K. C. Shilpa, and A. Usha, "Degree-based topological indices on anticancer drugs with QSPR analysis," *Heliyon*, vol. 6, Article ID e04235, 2020.
- [11] S. A. K. Kirmani, P. Ali, F. Azam, and P. A. Alvi, "Topological indices and QSPR/QSAR analysis of some antiviral drugs being investigated for the treatment of COVID-19 patients," *International Journal of Quantum Chemistry*, vol. 121, pp. 1–22, 2021.
- [12] K. Roy, "Topological descriptors in drug design and modeling studies," *Molecular Diversity*, vol. 8, no. 4, pp. 321–323, 2004.
- [13] A. T. Balaban and J. Devillers, *Topological Indices and Related Descriptors in QSAR and QSPR*, CRC Press, London, UK, 2014.
- [14] J. C. Dearden, *Advances in QSAR Modeling*, Springer, Cham, Switzerland, pp. 57–88, 2017.
- [15] E. Estrada, L. Torres, L. Roriguez, and I. Gutman, "An atom-bond connectivity index: modelling the enthalpy of formation of alkanes," *Indian Journal of Chemistry*, vol. 37, pp. 849–855, 1998.
- [16] H. Wiener, "Structural determination of parafin boiling points," *Journal of the American Chemical Society*, vol. 69, no. 1, pp. 17–20, 1947.
- [17] B. Basavangouda and S. Policepatil, "Chemical applicability of Gourava and hyper-Gourava indices," *Nanosystems: Physics, Chemistry, Mathematics*, vol. 12, pp. 142–150, 2021.
- [18] P. S. R. Harisha and V. Loksha, "M-Polynomial of valency-based topological indices of operators on titania nanotubes  $\text{TiO}_2[m, n]$  networks," *Advances and Applications in Mathematical Sciences*, vol. 20, pp. 1493–1508, 2021.
- [19] P. S. Hemavathi, V. Loksha, M. Manjunath, P. S. KReddy, and R. Shruti, "Topological aspects boron triangular nanotube and boron- $\alpha$  nanotube," *Vladikavkaz Mathematical Journal*, vol. 22, pp. 66–77, 2020.
- [20] V. Loksha, T. Deepika, P. S. Ranjini, and I. N. Cangul, "Operations of nanostructures via SDD, ABC 4 and GA 5 indices," *Applied Mathematics and Nonlinear Sciences*, vol. 2, no. 1, pp. 173–180, 2017.
- [21] V. Loksha, R. Shruti, P. S. Ranjini, and S. Cevik, "On certain topological indices of nanostructures using  $Q(G)$  and  $R(G)$  perators," *Communications*, vol. 67, pp. 178–187, 2018.
- [22] S. Mondal, A. Bhosale, N. De, and A. Pal, "Topological properties of some nanostructures," *Nanosystems: Physics, Chemistry, Mathematics*, vol. 11, no. 1, pp. 14–24, 2020.
- [23] M. F. Nadeem, S. Zafar, and Z. Zahid, "On topological properties of the line graphs of subdivision graphs of certain nanostructures," *Applied Mathematics and Computation*, vol. 273, pp. 125–130, 2016.
- [24] Y. Shanthakumari, P. Siva Kota Reddy, V. Loksha, and P. S. Hemavathi, "Topological aspects boron triangular nanotube and boron- $\alpha$  nanotube-II, south east asian," *Journal of Mathematics and Mathematical Sciences (SEAJMMS)*, vol. 16, pp. 145–156, 2020.
- [25] S. Iijima, "Synthesis of Carbon Nanotubes," *Nature*, vol. 354, pp. 56–58, 1991.
- [26] S. Hayat, M. K. Shafiq, A. Khan et al., "On topological properties of 2-dimensional lattices of carbon nanotubes," *Journal of Computational and Theoretical Nanoscience*, vol. 13, no. 10, pp. 6606–6615, 2016.
- [27] A. Ali, W. Nazeer, M. Munir, and M. K. Shin, "M-polynomials and topological indices of zigzag and rhombic benzenoid systems," *Open Chemistry*, vol. 16, pp. 73–78, 2017.

- [28] A. Q. Baig, M. Imran, and H. Ali, "Computing omega, sadhana and PI polynomials of benzenoid carbon nanotubes," *Optoelectronics and advanced materials-rapid communications*, vol. 9, pp. 248–255, 2015.
- [29] M. Nadeem, A. Yousaf, and A. Razaq, "Certain polynomials and related topological indices for the series of benzenoid graphs," *Scientific Reports*, vol. 9, pp. 1–6, 2019.
- [30] F. Harary, *Graph Theory*, Addison-Wesely, Reading Mass, Boston, MA, USA, 1969.
- [31] V. R. Kulli, *College Graph Theory*, Vishwa International Publications, Gulbarga, India, 2012.
- [32] A. Usha, M. C. Shanmukha, K. N. Anil Kumar, and K. C. Shilpa, "Comparision of novel index with geometric-arithmetic and sum-connectivity indices," *Journal of Mathematical and Computational Science*, vol. 11, pp. 5344–5360, 2021.
- [33] D. Vukicevic and B. Furtula, "Topological index based on the ratios of geometric and arithmetical means of end-vertex degrees of edges," *Journal of Mathematical Chemistry*, vol. 46, pp. 1369–1376, 2009.

## Research Article

# On Analysis of Topological Properties for Terbium IV Oxide via Enthalpy and Entropy Measurements

Muhammad Kamran Siddiqui <sup>1</sup>, Sana Javed,<sup>1</sup> Lubna Sherin,<sup>2</sup> Sadia Khalid,<sup>1</sup>  
Muhammad Mathar Bashir,<sup>2</sup> Amir Hassan,<sup>1</sup> and Mlamuli Dhlamini <sup>3</sup>

<sup>1</sup>Department of Mathematics, COMSATS University Islamabad, Lahore Campus, Lahore 54000, Pakistan

<sup>2</sup>Department of Chemistry, COMSATS University Islamabad, Lahore Campus, Lahore 54000, Pakistan

<sup>3</sup>Department of Applied Mathematics, National University of Science and Technology, Islamabad, Zimbabwe

Correspondence should be addressed to Mlamuli Dhlamini; [mlamuli.dhlamini@nust.ac.zw](mailto:mlamuli.dhlamini@nust.ac.zw)

Received 9 June 2021; Accepted 14 August 2021; Published 24 August 2021

Academic Editor: Teodorico C. Ramalho

Copyright © 2021 Muhammad Kamran Siddiqui et al. This is an open access article distributed under the Creative Commons Attribution License, which permits unrestricted use, distribution, and reproduction in any medium, provided the original work is properly cited.

A relation between topological indices and thermodynamics properties of terbium IV oxide has been established by using a rational method as it was found the most efficient method based on mean squared error (MSE). Terbium IV oxide has huge application as an insulator in modern technologies such as microelectronics, gas detectors, and luminiferous owing to mechanical and thermal stability, high dielectric constant, radiation resistance, and variable electrical conductivity. The chemical graph and topological indices have attracted the research community due to their potential application in discrete mathematics, biology, and chemistry. Our commitment is to investigate topological indices and thermodynamic properties of terbium IV oxide that depend on an innovative data utilitarian. Moreover, a relationship between topological indices and curve fitting has been established as an application point of view. All curve fittings have been found using MATLAB software.

## 1. Introduction

Terbium, a rare earth metal, is a member of the 4f series of the periodic table called lanthanides and has electronic configuration  $[\text{Xe}] 4f^9 6s^2$ . It is found between the  $(n-1)d$  and ns block elements and has properties identical to d-block elements. Due to unfilled f orbital, electrons are added to the  $(n-2)$  level's 'f' suborbitals. It is silvery white soft metal with a silvery appearance whose melting point ranges from 1000 to 1200 degrees Celsius and is an excellent heat and electricity conductor. Except for promethium, lanthanides are nonradioactive in nature [1, 2]. The synthesis of terbium IV oxide conventionally uses the precipitation approach, but newly designed self-propagation high-temperature synthesis (SHS) provides the high yield of weakly agglomerated nanosized powder of terbium IV oxide. The flow sheet of this process is given in Figures 1 and 2 [3].

Terbium IV oxide films have huge application as an insulator in microelectronics, gas detectors, and

luminophores due to unique properties such as radiation resistance and very small leakage current density besides variable electrical conductivity in different gaseous fluids [4, 5]. It is found that various oxidation states cause changes in the stoichiometry of terbium IV oxide that predetermines variations in its optical properties, thus making it useful for the aforementioned applications as well as in Fresnel lenses, pigments, antireflection layers, and photoelastic films [6, 7]. Terbium compounds are brightly fluorescent, and most terbium supplies are used to produce green phosphorous worldwide that allow trichromatic lighting [8]. It is also often used as a dopant for fuel-cell materials and crystalline solid-state devices. The large surface basicity, rapid oxygen ion mobility, and interesting catalytic characteristics of earth oxides are well known. These are the qualities which make them a good chemical sensor [9].

The bulk structure of  $\text{TbO}_2$  is crystallized as a  $\text{Tb}_4\text{O}_8$ . In a crystal of terbium oxide, oxygen atoms are located in the cubic closed packed terbium atoms (Figure 1) [10].

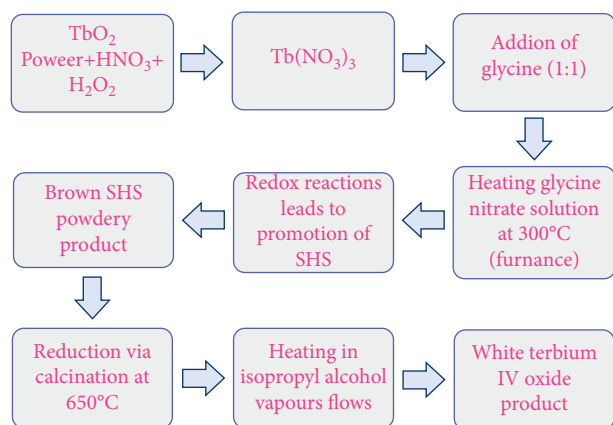


FIGURE 1: Schematic illustration of terbium IV oxide synthesis of by SHS.

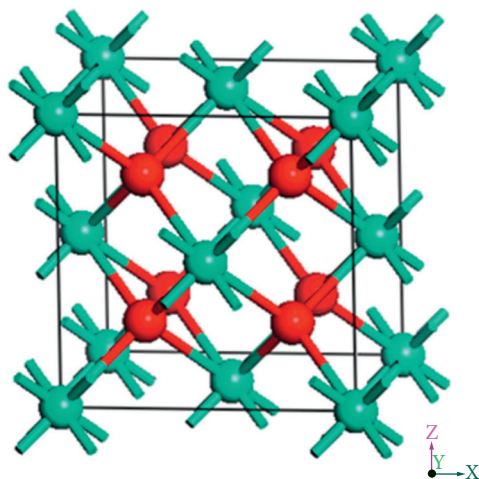
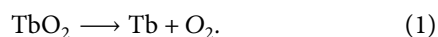


FIGURE 2: Unit cell structure of terbium oxide [4].

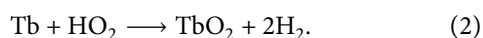
Metal oxide redox reactions are currently regarded being one of the most favorable long-term methods for producing renewable  $H_2$  for immediate use in fuel cells. Terbium IV oxide is a promising candidate for thermochemical production of hydrogen through solar thermochemical water splitting (Tb-WS) cycle. The first step of the cycle includes the thermal reduction of  $TbO_2$  into Tb and  $O_2$ , while the second step involves oxidation of Tb through a water splitting reaction to produce  $H_2$ . The unit cell structure of terbium oxide is depicted in Figure 2.

Step 1. Step 1:



Equation (1) is the endothermic reduction.

Step 2.



Equation (2) is the endothermic reduction.

## 2. Degree-Based Topological Indices

Let  $G = (V, E)$  be a graph where  $V$  is the vertex set and  $E$  is the edge set of  $G$ . The degree  $\tilde{I}(a)$  of a vertex  $a$  is the number of edges of  $G$  incident with  $a$ .

In 2013, Shirdel et al. [11] introduced the ‘‘Hyper-Zagreb index’’:

$$HM = HM(G) = \sum_{ab \in E(G)} [\tilde{I}(a) + \tilde{I}(b)]^2. \quad (3)$$

In 2012, Ghorbani and Azimi [12] defined multiple Zagreb indices as

$$PM_1(G) = \prod_{ab \in E(G)} [\tilde{I}(a) + \tilde{I}(b)],$$

$$PM_2(G) = \prod_{ab \in E(G)} [\tilde{I}(a) + \tilde{I}(b)]. \quad (4)$$

For more details about these indices, see [13, 14].

In 1972, Furtula and Gutman [15, 16] presented the forgotten topological index which was characterized as

$$F(G) = \sum_{ab \in E(G)} (\tilde{I}(a)^2 + \tilde{I}(b)^2). \quad (5)$$

Furtula et al. [17] introduced the ‘‘augmented Zagreb index’’:

$$AZI(G) = \sum_{ab \in E(G)} \left( \frac{\tilde{I}(a) \times \tilde{I}(b)}{\tilde{I}(a) + \tilde{I}(b) - 2} \right)^3. \quad (6)$$

The Balaban index [18, 19] is a topological index based on order  $n$  and size  $m$  of graph  $G$ :

$$J(G) = \frac{m}{m - n + 2} \sum_{ab \in E(G)} \frac{1}{\sqrt{\tilde{I}(a) \times \tilde{I}(b)}}, \quad (7)$$

where  $\tilde{I}(a), \tilde{I}(b)$  are the degrees of the vertices  $a, b \in V(G)$ .

For more details about these indices, see [20–22].

The redefined version of the Zagreb indices was defined by Ranjini et al. [23].

$$ReZG_1(G) = \sum_{ab \in E(G)} \frac{\tilde{I}(a) + \tilde{I}(b)}{\tilde{I}(a) \times \tilde{I}(b)},$$

$$ReZG_2(G) = \sum_{ab \in E(G)} \frac{\tilde{I}(a) \times \tilde{I}(b)}{\tilde{I}(a) + \tilde{I}(b)}, \quad (8)$$

$$ReZG_3(G) = \sum_{ab \in E(G)} \tilde{I}(a) \times \tilde{I}(b) (\tilde{I}(a) + \tilde{I}(b)).$$

For more details about these indices, see [24–31].

## 3. Results for Terbium Oxide ( $TbO_2$ )

The number of vertices and edges of the structure of terbium oxide denoted by  $(TbO_2)$  are 22 mn and 32 mn, respectively. There are three type of vertices in  $TbO_2$ , namely, the vertices of degree 1, 2, and 4, respectively. The vertex partition of the

vertex set  $TbO_2$  is presented in Table 1. Also, the edge partition of  $TbO_2$  based on degrees of end vertices of each edge is depicted in Table 2.

(i) The Hyper-Zagreb index:

$$\begin{aligned}
 HM(G) &= \sum_{ab \in E(G)} (\tilde{I}(a) + \tilde{I}(b))^2, \\
 &= \sum_{ab \in E_1(G)} (\tilde{I}(a) + \tilde{I}(b))^2 + \sum_{ab \in E_2(G)} (\tilde{I}(a) + \tilde{I}(b))^2 + \sum_{ab \in E_3(G)} (\tilde{I}(a) + \tilde{I}(b))^2, \\
 &= HM(G) = (12mn - 2n - 2m)(1 + 4)^2 + (4mn - 2m - 2n)(2 + 4)^2 \\
 &\quad + (16mn + 4m + 4n)(4 + 4)^2, \\
 &= HM(G) = 4540mn + 902m + 902n.
 \end{aligned} \tag{9}$$

(ii) The first and second multiplicative Zagreb index:

The first multiplicative Zagreb index is computed as

$$\begin{aligned}
 PM_1(G) &= (1 + 4)^{(12mn - 2n - 2m)} \cdot (2 + 4)^{(4mn - 2m - 2n)} \cdot (4 + 4)^{(16mn + 4m + 4n)}, \\
 PM_1(G) &= 5^{(12mn - 2n - 2m)} \cdot 6^{(4mn - 2m - 2n)} \cdot 8^{(16mn + 4m + 4n)}, \\
 PM_1(G) &= \prod_{ab \in E(G)} (\tilde{I}(a) + \tilde{I}(b)) = \prod_{ab \in E_1(G)} (\tilde{I}(a) + \tilde{I}(b)) + \prod_{ab \in E_2(G)} (\tilde{I}(a) + \tilde{I}(b)) + \prod_{ab \in E_3(G)} (\tilde{I}(a) + \tilde{I}(b)).
 \end{aligned} \tag{10}$$

The second multiplicative Zagreb index is computed as

$$\begin{aligned}
 PM_2(G) &= \prod_{ab \in E(G)} ((\tilde{I}(a) + \tilde{I}(b))) = \prod_{ab \in E_1(G)} (\tilde{I}(a) + \tilde{I}(b)) + \prod_{ab \in E_2(G)} (\tilde{I}(a) + \tilde{I}(b)) + \prod_{ab \in E_3(G)} (\tilde{I}(a) + \tilde{I}(b)), \\
 PM_2(G) &= (1 + 4)^{(12mn - 2n - 2m)} \cdot (2 + 4)^{(4mn - 2m - 2n)} \cdot (4 + 4)^{(16mn + 4m + 4n)}, \\
 PM_2(G) &= 4^{(12mn - 2n - 2m)} \cdot 8^{(4mn - 2m - 2n)} \cdot 16^{(16mn + 4m + 4n)}.
 \end{aligned} \tag{11}$$

(iii) The first and second multiplicative Zagreb index:  
The numerical representation of the above computed results is presented in Table 3.

(iv) The forgotten index:

The forgotten index is computed as

$$\begin{aligned}
 F(G) &= \sum_{ab \in E(G)} (\tilde{I}(a)^2 + \tilde{I}(b)^2), \\
 &= F(G) = \sum_{ab \in E_1(G)} [\tilde{I}(a)^2 + \tilde{I}(b)^2] + \sum_{ab \in E_2(G)} [\tilde{I}(a)^2 + \tilde{I}(b)^2] + \sum_{ab \in E_3(G)} [\tilde{I}(a)^2 + \tilde{I}(b)^2], \\
 &= (12mn - 2n - 2m)((1)^2 + (4)^2) + (4mn - 2m - 2n)((2)^2 + (4)^2) + (16mn + 4m + 4n)((4)^2 + (4)^2), \\
 &= (12mn - 2n - 2m)(17) + (4mn - 2m - 2n)(20) + (16mn + 4m + 4n)(32) \\
 &\quad \cdot 796mn + 54m + 54n.
 \end{aligned} \tag{12}$$

TABLE 1: Vertex partition of  $TbO_2$  based on the degree of vertex.

$\tilde{I}(a)$	Frequency	Set of vertices
1	$4mn + 4$	$V_1$
2	$2n + 2m - 4$	$V_2$
4	$18mn - 2m - 2n$	$V_3$

TABLE 2: Edge partition of  $TbO_2$ .

$(\tilde{I}(a), \tilde{I}(b))$	Frequency	Set of edges
(1, 4)	$12mn - 2n - 2m$	$E_1$
(2, 4)	$4mn - 2m - 2n$	$E_2$
(4, 4)	$16mn + 4m + 4n$	$E_3$

TABLE 3: Comparison of indices  $HM(G)$ ,  $PM_1(G)$ ,  $PM_2(G)$ .

$[m, n]$	$HM(G)$	$PM_1(G)$	$PM_2(G)$
[1, 1]	6344	$1.844 \times 10^{27}$	$5.192296859 \times 10^{33}$
[2, 2]	21768	$2.699 \times 10^{106}$	$4.332296397 \times 10^{127}$
[3, 3]	46272	$3.132 \times 10^{237}$	$5.808659799 \times 10^{281}$
[4, 4]	79856	$2.883 \times 10^{420}$	$1.251505764 \times 10^{496}$
[5, 5]	122520	$2.105 \times 10^{655}$	$4.333002103 \times 10^{770}$
[6, 6]	174264	$1.219 \times 10^{942}$	$2.410705053 \times 10^{1105}$
[7, 7]	235088	$5.600 \times 10^{1280}$	$2.155253650 \times 10^{1500}$

The Augmented Zagreb index is computed as follows:

(v) The Augmented Zagreb index:

$$\begin{aligned}
 AZI(G) &= \sum_{ab \in E(G)} \left( \frac{\tilde{I}(a) \times \tilde{I}(b)}{\tilde{I}(a) + \tilde{I}(b) - 2} \right)^3, \\
 AZI(G) &= \sum_{ab \in E_1} \left( \frac{\tilde{I}(a) \times \tilde{I}(b)}{\tilde{I}(a) + \tilde{I}(b) - 2} \right)^3 + \sum_{ab \in E_2} \left( \frac{\tilde{I}(a) \times \tilde{I}(b)}{\tilde{I}(a) + \tilde{I}(b) - 2} \right)^3 + \sum_{ab \in E_3} \left( \frac{\tilde{I}(a) \times \tilde{I}(b)}{\tilde{I}(a) + \tilde{I}(b) - 2} \right)^3, \\
 &= \sum_{ab \in E_1} \left( \frac{1 \times 4}{1 + 4 - 2} \right)^3 + \sum_{ab \in E_2} \left( \frac{2 \times 4}{2 + 4 - 2} \right)^3 + \sum_{ab \in E_3} \left( \frac{4 \times 4}{4 + 4 - 2} \right)^3, \\
 &= \frac{64}{27} (12mn - 2n - 2m) + 8(4mn - 2m - 2n) + \frac{512}{27} (16mn + 4m + 4n), \\
 &= \frac{9824mn}{27} + \frac{496m}{9} + \frac{496n}{9}.
 \end{aligned} \tag{13}$$

(vi) The Balaban index:

The Balaban index is computed as

$$\begin{aligned}
 J(G) &= \frac{q}{q-p+2} \sum_{ab \in E(G)} \frac{1}{\sqrt{\tilde{I}(a) \times \tilde{I}(b)}}, \\
 J(G) &= \frac{q}{q-p+2} \left[ \sum_{ab \in E_1} \frac{1}{\sqrt{\tilde{I}(a) \times \tilde{I}(b)}} + \sum_{ab \in E_2} \frac{1}{\sqrt{\tilde{I}(a) \times \tilde{I}(b)}} + \sum_{ab \in E_3} \frac{1}{\sqrt{\tilde{I}(a) \times \tilde{I}(b)}} \right], \\
 &= \frac{q}{q-p+2} \left[ \sum_{ab \in E_1} \frac{1}{\sqrt{1 \times 4}} + \sum_{ab \in E_2} \frac{1}{\sqrt{2 \times 4}} + \sum_{ab \in E_3} \frac{1}{\sqrt{4 \times 4}} \right], \\
 &= \frac{22mn}{10mn-2} \times \left[ \frac{1}{2} (12mn - 2n - 2m) + \frac{1}{2\sqrt{2}} (4mn - 2m - 2n) + \frac{1}{4} (16mn + 4m + 4n) \right].
 \end{aligned} \tag{14}$$

The numerical representation of the above-computed results is presented in Table 4.

(vii) The redefined Zagreb indices:

The redefined Zagreb indices are computed as

$$\begin{aligned}
 \text{ReG}_1(G) &= \sum_{ab \in E(G)} \frac{\tilde{I}(a) + \tilde{I}(b)}{\tilde{I}(a) \times \tilde{I}(b)}, \\
 \text{ReG}_1(G) &= \sum_{ab \in E_1} \frac{\tilde{I}(a) + \tilde{I}(b)}{\tilde{I}(a) \times \tilde{I}(b)} + \sum_{ab \in E_2} \frac{\tilde{I}(a) + \tilde{I}(b)}{\tilde{I}(a) \times \tilde{I}(b)} + \sum_{ab \in E_3} \frac{\tilde{I}(a) + \tilde{I}(b)}{\tilde{I}(a) \times \tilde{I}(b)} \\
 &= \sum_{ab \in E_1} \frac{1+4}{1 \times 4} + \sum_{ab \in E_2} \frac{2+4}{2 \times 4} + \sum_{ab \in E_3} \frac{4+4}{4 \times 4}, \\
 &= \frac{5}{4}(12mn - 2n - 2m) + \frac{3}{4}(4mn - 2m - 2n) + \frac{1}{2}(16mn + 4m + 4n), \\
 \text{ReG}_2(G) &= \sum_{ab \in E(G)} \frac{\tilde{I}(a) + \tilde{I}(b)}{\tilde{I}(a) \times \tilde{I}(b)}, \\
 \text{ReG}_2(G) &= \sum_{ab \in E_1} \frac{\tilde{I}(a) + \tilde{I}(b)}{\tilde{I}(a) \times \tilde{I}(b)} + \sum_{ab \in E_2} \frac{\tilde{I}(a) + \tilde{I}(b)}{\tilde{I}(a) \times \tilde{I}(b)} + \sum_{ab \in E_3} \frac{\tilde{I}(a) + \tilde{I}(b)}{\tilde{I}(a) \times \tilde{I}(b)} \\
 &= \sum_{ab \in E_1} \frac{1 \times 4}{1+4} + \sum_{ab \in E_2} \frac{2 \times 4}{2+4} + \sum_{ab \in E_3} \frac{4 \times 4}{4+4}, \\
 &= \frac{4}{5}(12mn - 2n - 2m) + \frac{4}{3}(4mn - 2m - 2n) + (2)(16mn + 4m + 4n), \\
 \text{ReG}_3(G) &= \sum_{ab \in E(G)} [\tilde{I}(a)\tilde{I}(b)(\tilde{I}(a) + \tilde{I}(b))], \\
 \text{ReG}_3(G) &= \sum_{ab \in E_1} [\tilde{I}(a)\tilde{I}(b)(\tilde{I}(a) + \tilde{I}(b))] \\
 &\quad + \sum_{ab \in E_2} [\tilde{I}(a)\tilde{I}(b)(\tilde{I}(a) + \tilde{I}(b))] + \sum_{ab \in E_3} [\tilde{I}(a)\tilde{I}(b)(\tilde{I}(a) + \tilde{I}(b))], \\
 &= 20(12mn - 2n - 2m) + 48(4mn - 2m - 2n) + 128(16mn + 4m + 4n), \\
 &= 2480mn + 376m + 376n.
 \end{aligned} \tag{15}$$

The numerical representation of the above computed results is presented in Table 5.

#### 4. Heat of Formation and Entropy of Terbium IV Oxide

The topological indices  $HM(G)$ ,  $PM(G)$ ,  $PM2(G)$ ,  $F(G)$ ,  $AZI(G)$ ,  $J(G)$ ,  $ReG1(G)$ ,  $ReG2(G)$ , and  $ReG3(G)$  were calculated for various numbers of unit cells of terbium IV oxide. The thermodynamic properties of terbium IV oxide, such as heat of formation or enthalpy and entropy, are related to these indices  $HM(G)$ ,  $PM(G)$ ,  $PM2(G)$ ,  $F(G)$ ,  $AZI(G)$ ,  $J(G)$ ,  $ReG1(G)$ ,  $ReG2(G)$ , and  $ReG3(G)$ . Terbium

IV oxide has a standard molar enthalpy of  $-972.2 \text{ kJmol}^{-1}$ , and the standard molar enthalpy for one formula unit was calculated by dividing it by Avogadro's number. The enthalpy of a cell was determined by multiplying the acquired value by the number of formula units within the cell. The enthalpy of terbium IV oxide is directly proportional to its crystal size and increases as the number of unit cells increases, according to these findings. The entropy of terbium IV oxide was calculated using the same process. The molar standard entropy of terbium IV oxide is  $86.9 \text{ Jmol}^{-1}\text{K}^{-1}$ . The result was then determined by multiplying the number of formula units in a single unit cell. If the number of cells gets exponential, the entropy value decreases. The downward

TABLE 4: Comparison of indices for  $F(G)$ ,  $AZI(G)$ ,  $J(G)$   $TbO_2$ .

$[m, n]$	$F(G)$	$AZI(G)$	$J(G)$
[1, 1]	904	474.07	27.5
[2, 2]	3400	1675.85	99.18
[3, 3]	7488	3605.33	221.59
[4, 4]	13168	6262.52	394.26
[5, 5]	20440	9647.41	617.16
[6, 6]	29304	13760	890.28
[7, 7]	39760	18600.3	1213.63

TABLE 5: Comparison of  $ReG_1(G)$ ,  $ReG_2(G)$ ,  $ReG_3(G)$  indices for  $TbO_2$ .

$[m, n]$	$ReG_1(G)$	$ReG_2(G)$	$ReG_3(G)$
[1, 1]	22	54.4	3232
[2, 2]	96	202.67	11424
[3, 3]	222	444.8	24576
[4, 4]	400	780.8	42688
[5, 5]	630	1210.67	65760
[6, 6]	912	1734.4	93792
[7, 7]	1246	2352	126784

trend is the complete opposite of the heat of formation. The graphical representation is depicted in Figures 3–5.

The values for entropy and heat of formation of terbium oxide ( $TbO_2$ ) for  $1 \leq m \leq 7$  and  $1 \leq n \leq 7$  corresponding to different formula units are computed in Table 6.

## 5. A Mathematical Description of Heat of Formation and Entropy of Terbium Oxide in Terms of Topological Indices

Computational approaches integrated with other disciplines of science provide a coherent way to understand a scientific problem more intensely. Usually, it is not apprehending to understand a problem based on just one science discipline, so adding some computational approaches to the study might provide a clear picture which helps to investigate the underlying phenomenon more deeply and clearly. Developing a mathematical model to describe the dynamics of objects or components involved in a study provides a very convenient mode to tackle and analyze the matter of concern. At present, software technology is playing a vital role in conducting such studies, as they provide more efficient programs to convert an experimental study into a mathematical problem and analyze it.

In this section, we have developed mathematical models to represent the thermodynamic properties, namely, heat of formation and entropy, in the form of topological indices of terbium oxide. This might provide us an efficient way to understand the molecular structure of terbium oxide based on its chemical graph structure properties. We have used the software of MATLAB to estimate such models. There are several built-in methods to fit curves between two variables. We tried all of them and found the rational method as the most efficient one as it was providing the least residuals

between empirical and fitted values. Tables 7 and 8 contain root mean squared error (RMSE), sum of squared error (SSE), and  $R^2$ , where  $ratij$  represents rational fit with numerator degree  $i$  and denominator degree  $j$ .

*5.1. General Models for Indices vs. Heat of Formation.* In this section, a mathematical framework has been developed between each topological index and heat of formation (HoF) of terbium oxide. All the fitted curves are shown in Figures 6–12, whereas the estimated parametric values are provided in Tables 9–15.

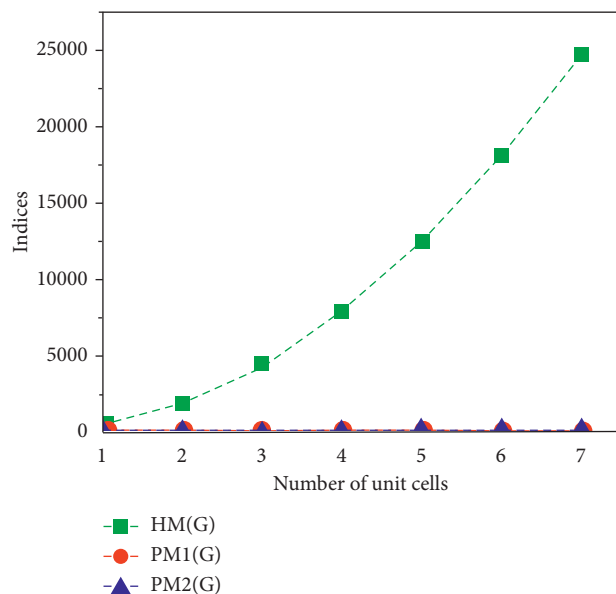
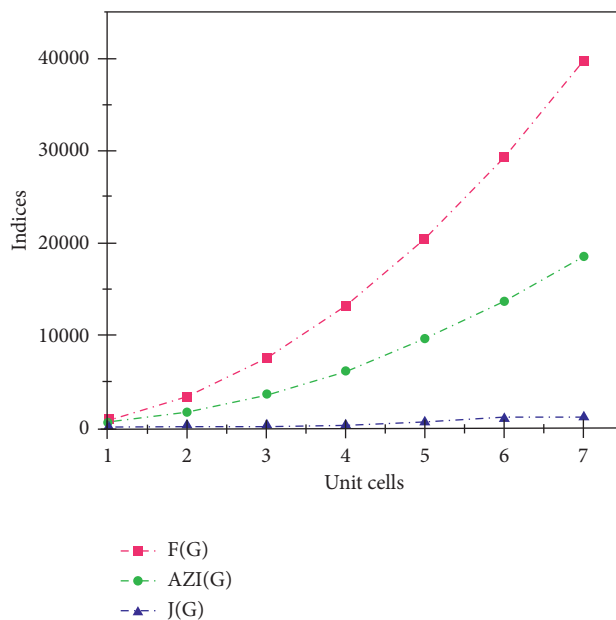
$$\text{HoF}(\text{HM}) = \frac{p_1}{(\text{HM})^3 + q_1 \times (\text{HM})^2 + q_2 \times \text{HM} + q_3} \quad (16)$$

$$\text{HoF}(F) = \frac{p_1 \times F^2 + p_2 \times F + p_3}{F^3 + q_1 \times F^2 + q_2 \times F + q_3} \quad (17)$$

$$\text{HoF}(\text{AZI}) = \frac{p_1 \times (\text{AZI})^2 + p_2 \times \text{AZI} + p_3}{(\text{AZI})^3 + q_1 \times (\text{AZI})^2 + q_2 \times \text{AZI} + q_3} \quad (18)$$

$$\text{HoF}(J) = \frac{p_1 \times J^2 + p_2 \times J + p_3}{J^3 + q_1 \times J^2 + q_2 \times J + q_3} \quad (19)$$

$$\text{HoF}(\text{Re}G_1) = \frac{p_1 \times \text{Re}G_1 + p_2}{(\text{Re}G_1)^3 + q_1 \times (\text{Re}G_1)^2 + q_2 \times \text{Re}G_1 + q_3} \quad (20)$$

FIGURE 3: HM(G),  $PM_1(G)$ ,  $PM_2(G)$  indices vs. unit cell.FIGURE 4: Comparison of indices F(G), AZI(G), and J(G) for  $TbO_2$ .

$$\text{HoF}(\text{ReG}_2) = \frac{p_1}{(\text{ReG}_2)^3 + q_1 \times (\text{ReG}_2)^2 + q_2 \times \text{ReG}_2 + q_3} \quad (21)$$

$$\text{HoF}(\text{ReG}_3) = \frac{p_1}{(\text{ReG}_3)^3 + q_1 \times (\text{ReG}_3)^2 + q_2 \times \text{ReG}_3 + q_3} \quad (22)$$

Coefficients (with 95% confidence interval (CI)) are given in Table 9.

Coefficients (with 95% confidence bounds) are given in Table 10.

Coefficients (with 95% confidence bounds) are given in Table 11.

Coefficients (with 95% confidence bounds) are given in Table 12.

Coefficients (with 95% confidence bounds) are given in Table 13.

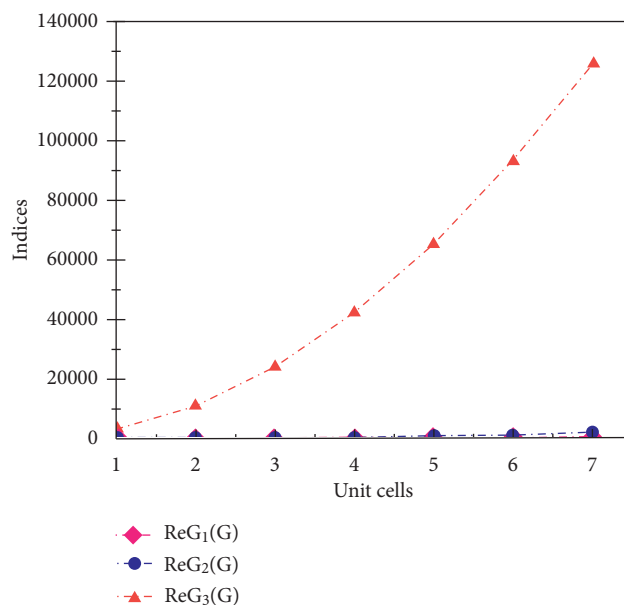


FIGURE 5: Comparison of  $\text{ReG}_1(G)$ ,  $\text{ReG}_2(G)$ , and  $\text{ReG}_3(G)$  indices for  $\text{TbO}_2$ .

TABLE 6: Values of heat of formation and entropy for different formula units of  $\text{TbO}_2$ .

$[m, n]$	Formula units	Heat of formation $\times 10^{-21}$ kJ	Entropy $\times 10^{-22}$ kJ
[1, 1]	4	-6.456	5.768
[2, 2]	16	-0.258	0.2307
[3, 3]	32	-0.516	0.5191
[4, 4]	64	-0.0103	0.9228
[5, 5]	100	-0.0614	0.0144
[6, 6]	144	-0.0232	0.0207
[7, 7]	196	-0.0316	0.0286

TABLE 7: Goodness of fit for heat of formation vs. indices for  $\text{TbO}_2$ .

Index	Fit type	SSE	$R^2$	RMSE
HM(G)	rat03	0.0121	0.9996	0.0635
F(G)	rat23	0.003584	0.9999	0.05987
AZI(G)	rat23	0.0001696	1.000	0.01302
J(G)	rat23	0.001481	1.000	0.03849
$\text{ReG}_1(G)$	rat13	0.003094	0.9999	0.03933
$\text{ReG}_2(G)$	rat03	0.005014	0.9999	0.04088
$\text{ReG}_3(G)$	rat03	0.01194	0.9997	0.06308

TABLE 8: Goodness of fit for entropy vs. indices for  $\text{TbO}_2$ .

Index	Fit type	SSE	$R^2$	RMSE
HM(G)	rat13	0.001071	1.000	0.02314
F(G)	rat13	0.001065	1.000	0.02307
AZI(G)	rat03	0.001078	1.000	0.01895
J(G)	rat05	0.001031	1.000	0.0321
$\text{ReG}_1(G)$	rat14	0.001118	1.000	0.03344
$\text{ReG}_2(G)$	rat05	0.0004906	1.000	0.02215
$\text{ReG}_3(G)$	rat13	0.001069	1.000	0.02312

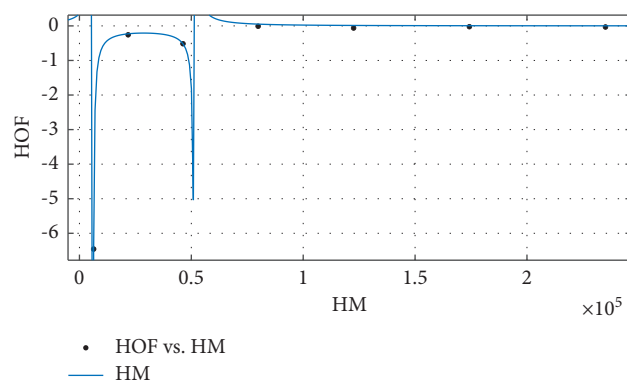


FIGURE 6: HoF(HM).

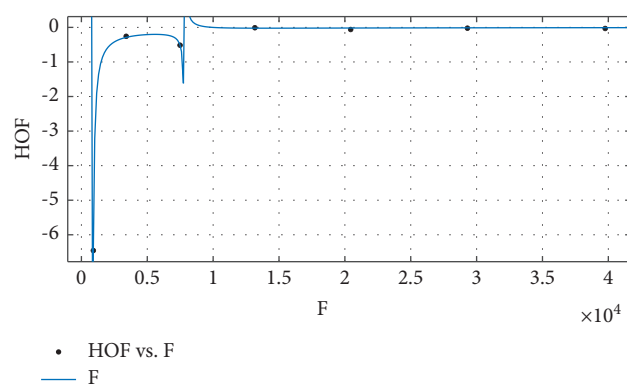


FIGURE 7: HoF(F).

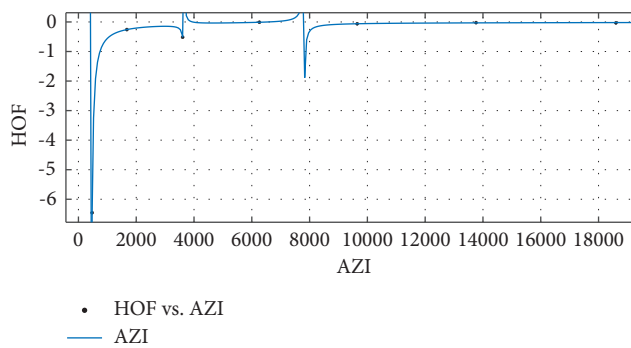


FIGURE 8: HoF(AZI).

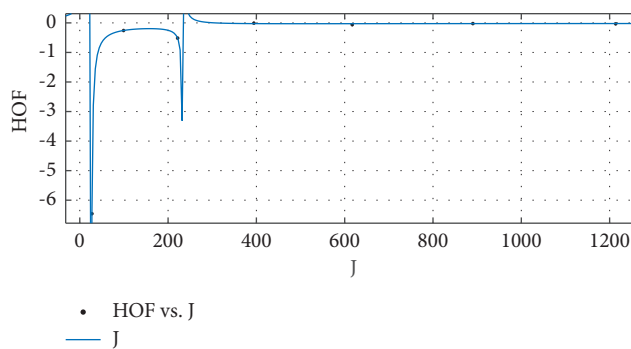
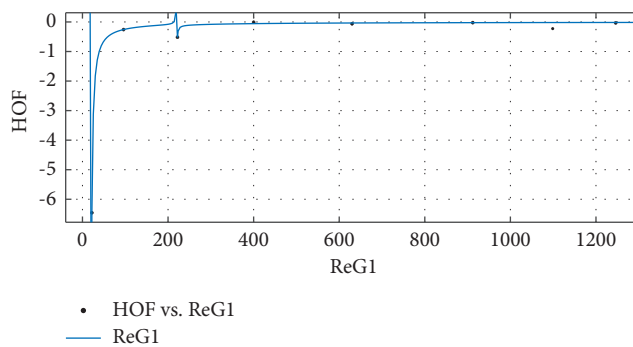
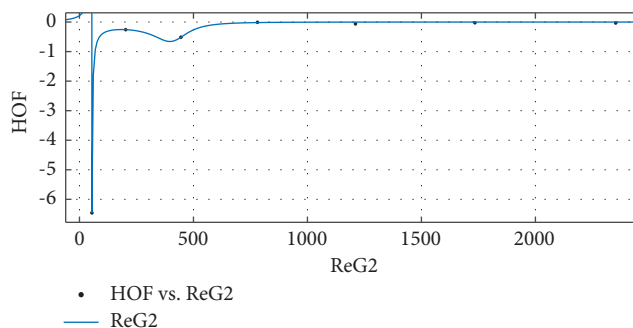
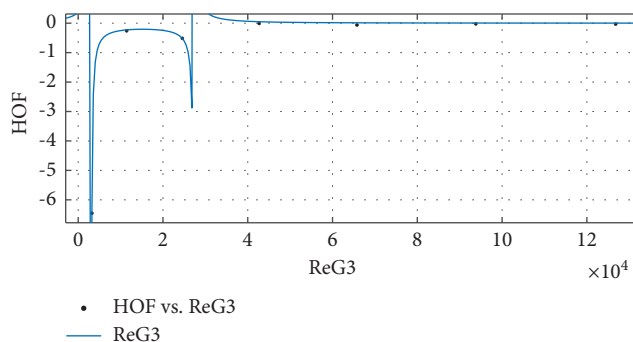


FIGURE 9: HoF(J).

FIGURE 10: HoF(ReG<sub>1</sub>).FIGURE 11: HoF(ReG<sub>2</sub>).FIGURE 12: HoF(ReG<sub>3</sub>).

Coefficients (with 95% confidence bounds) are given in Table 15.

5.2. *General Models for Indices vs. Entropy.* This section establishes a mathematical framework between each

topological index and entropy of terbium oxide. All the fitted curves are shown in Figures 13–19 while the estimated parametric values are given in Tables 16–22.

$$\text{Entropy}(\text{HM}) = \frac{p_1 \times \text{HM} + p_2}{(\text{HM})^3 + q_1 \times (\text{HM})^2 + q_2 \times \text{HM} + q_3} \quad (23)$$

$$\text{Entropy}(F) = \frac{p_1 \times F + p_2}{F^3 + q_1 \times F^2 + q_2 \times F + q_3} \quad (24)$$

TABLE 9: HoF vs. HM.

	$p_i$	CI	$q_i$	CI
$i = 1$	178.2	(-9.679 e + 06, 9.679 e + 06)	1.176 e + 04	(-6.386 e + 08, 6.386 e + 08)
$i = 2$	—	—	1.94 e + 04	(-1.053 e + 09, 1.053 e + 09)
$i = 3$	—	—	7138	(-3.876 e + 08, 3.876 e + 08)

TABLE 10: HoF vs. F.

	$p_i$	CI	$q_i$	CI
$i = 1$	2.805	(-6.115 e + 05, 6.115 e + 05)	688.5	(-1.482 e + 08, 1.482 e + 08)
$i = 2$	-20.61	(-4.445 e + 06, 4.445 e + 06)	1156	(-2.493 e + 08, 2.493 e + 08)
$i = 3$	-9.782	(-2.11 e + 06, 2.11 e + 06)	444.4	(-9.587 e + 07, 9.587 e + 07)

TABLE 11: HoF vs. AZI.

	$p_i$	CI	$q_i$	CI
$i = 1$	-0.05294	(-0.3091, 0.2032)	1.691	(-1.61, 4.992)
$i = 2$	-0.03912	(-0.4201, 0.3419)	0.6454	(-4.759, 6.05)
$i = 3$	-0.005199	(-0.08769, 0.07729)	-0.008204	(-1.979, 1.962)

TABLE 12: HoF vs. J.

	$p_i$	CI	$q_i$	CI
$i = 1$	-190.1	(-1.44 e + 08, 1.44 e + 08)	1.333 e + 04	(-1.009 e + 10, 1.009 e + 10)
$i = 2$	-630	(-4.771 e + 08, 4.771 e + 08)	2.228 e + 04	(-1.687 e + 10, 1.687 e + 10)
$i = 3$	-236.6	(-1.792 e + 08, 1.792 e + 08)	8555	(-6.479 e + 09, 6.479 e + 09)

TABLE 13: HoF vs.  $ReG_1$ .

	$p_i$	CI	$q_i$	CI
$i = 1$	-175.5	(-2.397 e + 06, 2.396 e + 06)	3781	(-5.159 e + 07, 5.16 e + 07)
$i = 2$	-112.8	(-1.541 e + 06, 1.54 e + 06)	6438	(-8.788 e + 07, 8.79 e + 07)
$i = 3$	—	—	2553	(-3.485 e + 07, 3.486 e + 07)

TABLE 14: HoF vs.  $ReG_2$ .

	$p_i$	CI	$q_i$	CI
$i = 1$	-0.003307	(-0.02053, 0.01391)	2.406	(1.359, 3.452)
$i = 2$	—	—	1.881	(0.1678, 3.595)
$i = 3$	—	—	0.4865	(-0.1403, 1.113)

TABLE 15: HoF vs.  $ReG_3$ .

	$p_i$	CI	$q_i$	CI
$i = 1$	172.1	(-9.52 e + 06, 9.52 e + 06)	1.171 e + 04	(-6.476 e + 08, 6.476 e + 08)
$i = 2$	—	—	1.93 e + 04	(-1.067 e + 09, 1.067 e + 09)
$i = 3$	—	—	7118	(-3.937 e + 08, 3.937 e + 08)

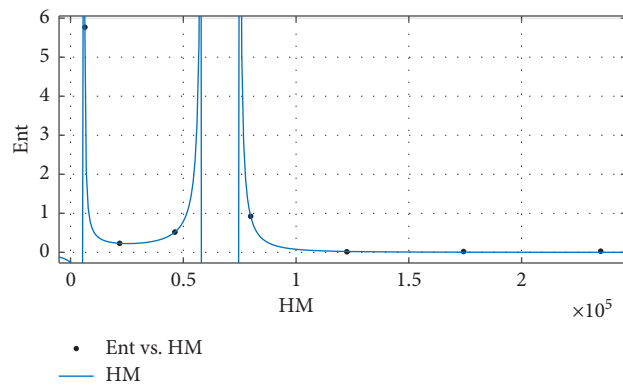


FIGURE 13: Entropy (HM).

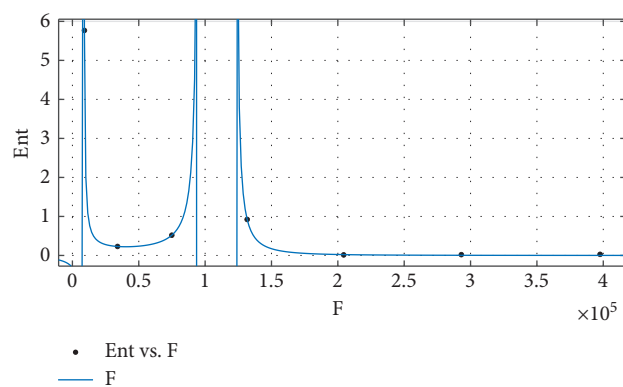
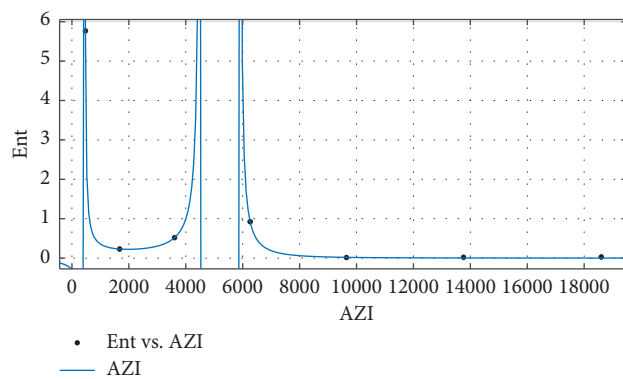
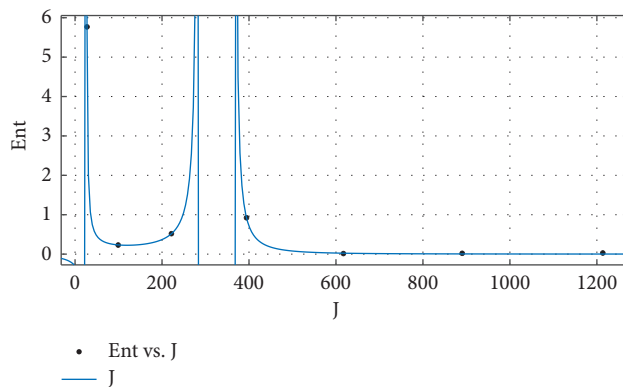
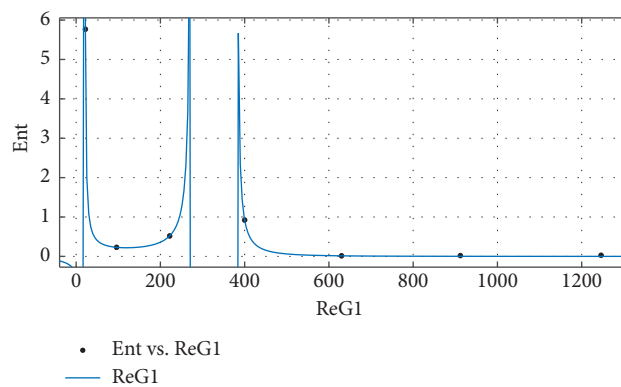
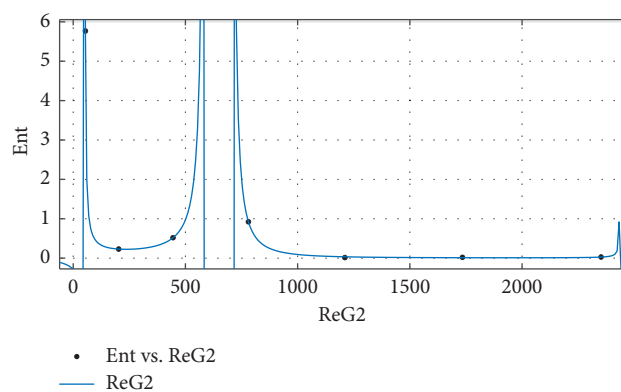
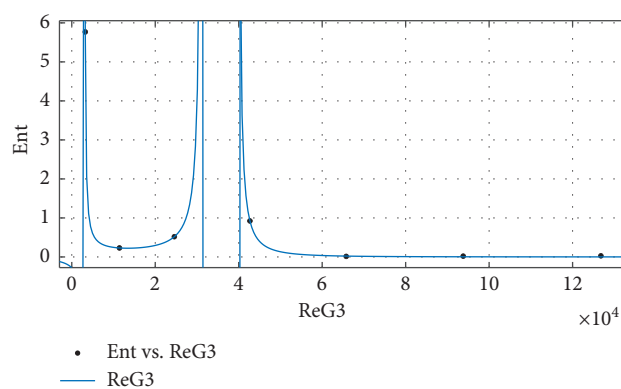
FIGURE 14: Entropy ( $F$ ).

FIGURE 15: Entropy (AZI).

FIGURE 16: Entropy ( $J$ ).

FIGURE 17: Entropy (ReG<sub>1</sub>).FIGURE 18: Entropy ReG<sub>2</sub>.FIGURE 19: Entropy ReG<sub>3</sub>.

$$\text{Entropy (AZI)} = \frac{p_1}{(AZI)^3 + q_1 \times (AZI)^2 + q_2 \times AZI + q_3}, \quad (25)$$

$$\text{Entropy (J)} = \frac{p_1}{J^5 + q_1 \times J^4 + q_2 \times J^3 + q_3 \times J^2 + q_4 \times J + q_5}. \quad (26)$$

TABLE 16: Entropy vs. HM.

	$P_i$	CI	$q_i$	CI
$i = 1$	0.001132	(-0.04439, 0.04666)	1.842	(1.762, 1.922)
$i = 2$	0.01288	(-0.03159, 0.05736)	0.9484	(0.8749, 1.022)
$i = 3$	—	—	0.1427	(0.1092, 0.1761)

TABLE 17: Entropy vs.  $F$ .

	$P_i$	CI	$q_i$	CI
$i = 1$	0.001791	(-0.04354, 0.04713)	1.845	(1.766, 1.925)
$i = 2$	0.01254	(-0.03159, 0.05667)	0.9604	(0.8889, 1.032)
$i = 3$	—	—	0.1465	(0.1139, 0.1792)

TABLE 18: Entropy vs. AZI.

	$P_i$	CI	$q_i$	CI
$i = 1$	0.01144	(0.007304, 0.01558)	1.845	(1.812, 1.877)
$i = 2$	—	—	0.9537	(0.9148, 0.9925)
$i = 3$	—	—	0.1431	(0.1392, 0.147)

TABLE 19: Entropy vs.  $J$ .

	$P_i$	CI	$q_i$	CI
$i = 1$	-110.9	(-2.497 e + 07, 2.497 e + 07)	2563	(-5.765 e + 08, 5.765 e + 08)
$i = 2$	—	—	-3952	(-8.901 e + 08, 8.901 e + 08)
$i = 3$	—	—	-1.355 e + 04	(-3.052 e + 09, 3.052 e + 09)
$i = 4$	—	—	-8056	(-1.814 e + 09, 1.814 e + 09)
$i = 5$	—	—	-1311	(-2.951 e + 08, 2.951 e + 08)

TABLE 20: Entropy vs.  $ReG_1$ .

	$P_i$	CI	$q_i$	CI
$i = 1$	1.041	(-1.206 e + 06, 1.206 e + 06)	-1145	(-1.341 e + 09, 1.341 e + 09)
$i = 2$	-10.05	(-1.175 e + 07, 1.175 e + 07)	-2126	(-2.487 e + 09, 2.487 e + 09)
$i = 3$	—	—	-1121	(-1.311 e + 09, 1.311 e + 09)
$i = 4$	—	—	-170.7	(-1.996 e + 08, 1.996 e + 08)

TABLE 21: Entropy vs.  $ReG_2$ .

	$P_i$	CI	$q_i$	CI
$i = 1$	103.9	(-2.399 e + 06, 2.399 e + 06)	-3508	(-8.104 e + 07, 8.103 e + 07)
$i = 2$	—	—	-384.3	(-8.831 e + 06, 8.83 e + 06)
$i = 3$	—	—	7836	(-1.81 e + 08, 1.81 e + 08)
$i = 4$	—	—	5312	(-1.227 e + 08, 1.227 e + 08)
$i = 5$	—	—	909.8	(-2.101 e + 07, 2.101 e + 07)

TABLE 22: Entropy vs.  $ReG_3$ .

	$P_i$	CI	$q_i$	CI
$i = 1$	0.001368	(-0.04409, 0.04682)	1.843	(1.763, 1.923)
$i = 2$	0.01276	(-0.0316, 0.05712)	0.9527	(0.8799, 1.025)
$i = 3$	—	—	0.144	(0.1109, 0.1772)

$$\text{Entropy}(\text{ReG}_1) = \frac{p_1 \times \text{ReG}_1 + p_2}{(\text{ReG}_1)^4 + q_1 \times (\text{ReG}_1)^3 + q_2 \times (\text{ReG}_1)^2 + q_3 \times \text{ReG}_1 + q_4}. \quad (27)$$

$$\text{Entropy}(\text{ReG}_2) = \frac{p_1}{(\text{ReG}_2)^5 + q_1 \times (\text{ReG}_2)^4 + q_2 \times (\text{ReG}_2)^3 + q_3 \times (\text{ReG}_2)^2 + q_4 \times \text{ReG}_2 + q_5}. \quad (28)$$

$$\text{Entropy}(\text{ReG}_3) = \frac{p_1 \times \text{ReG}_3 + p_2}{(\text{ReG}_3)^3 + q_1 \times (\text{ReG}_3)^2 + q_2 \times \text{ReG}_3 + q_3}. \quad (29)$$

Coefficients (with 95% confidence bounds) are given in Table 16.

Coefficients (with 95% confidence bounds) are given in Table 17.

Coefficients (with 95% confidence bounds) are given in Table 18.

Coefficients (with 95% confidence bounds) are given in Table 19.

Coefficients (with 95% confidence bounds) are given in Table 20.

Coefficients (with 95% confidence bounds) are given in Table 21.

Coefficients (with 95% confidence bounds) are given in Table 22.

## 6. Conclusions

A connection between topological indices and thermodynamic properties of terbium IV oxide has been developed. This study helps to understand the chemical structure of terbium IV oxide based on the graphical properties of its underlying graph more deeply as this was economical and more efficient. Curve fitting techniques have been utilized to establish such a relation among indices and heat of formation and entropy. The rational fitting approach was selected based on its efficacy. This direct connection might help to explore the dynamical properties of this terbium IV oxide.

## Data Availability

The data used to support the findings of this study are cited at relevant places within the text as references.

## Conflicts of Interest

The authors declare no conflicts of interest.

## Authors' Contributions

All authors contributed equally to this work.

## References

- [1] S. P. Sinha, "Systematics and the properties of the lanthanides," *Springer Science and Business Media*, vol. 109, pp. 33–43, 2012.
- [2] V. G. Minkina, "Initial compounds for obtaining high-temperature superconducting films by the CVD-method," *Russian Chemical Bulletin*, vol. 42, no. 9, pp. 1460–1466, 1993.
- [3] S. Abanades, "Metal oxides applied to thermochemical water-splitting for hydrogen production using concentrated solar energy," *ChemEngineering*, vol. 3, no. 3, pp. 63–83, 2019.
- [4] S. Yang, S. Huang, M. Schnee, Q. T. Zhao, J. Schubert, and K. J. Chen, "Enhancement-mode LaLuO<sub>3</sub>-AlGaIn/GaN metal-insulator-semiconductor high-electron-mobility transistors using fluorine plasma ion implantation," *Japanese Journal of Applied Physics*, vol. 52, no. 8S, pp. 88–98, 2013.
- [5] S. Pavunny, J. Scott, and R. Katiyar, "Lanthanum gadolinium oxide: a new electronic device material for CMOS logic and memory devices," *Materials*, vol. 7, no. 4, pp. 2669–2696, 2014.
- [6] P. R. Armstrong, M. L. Mah, S. S. Kim, and J. J. Talghader, "Thermoluminescence of Y<sub>2</sub>O<sub>3</sub>:Tb<sup>3+</sup> thin films deposited by electron beam evaporation," *Journal of Luminescence*, vol. 148, pp. 225–229, 2014.
- [7] S. Shu Yang, S. Sen Huang, H. Hongwei Chen, C. Chunhua Zhou, Q. Qi Zhou, M. Schnee et al., "AlGaIn/GaN MISHEMTs with high-κLaLuO<sub>3</sub> gate dielectric," *IEEE Electron Device Letters*, vol. 33, no. 7, pp. 979–981, 2012.
- [8] A. Ziani, C. Davesne, C. Labbé et al., "Annealing effects on the photoluminescence of terbium doped zinc oxide films," *Thin Solid Films*, vol. 553, pp. 52–57, 2014.
- [9] S. Singh, A. Singh, B. C. Yadav, and P. K. Dwivedi, "Fabrication of nanobeads structured perovskite type neodymium iron oxide film: its structural, optical, electrical and LPG sensing investigations," *Sensors and Actuators B: Chemical*, vol. 177, pp. 730–739, 2013.
- [10] H. A. Miran, M. Altarawneh, Z. N. Jaf, B. Z. Dlugogorski, and Z. T. Jiang, "Structural, electronic and thermodynamic properties of bulk and surfaces of terbium oxide (TbO<sub>2</sub>)," *Materials Research Express*, vol. 5, no. 8, pp. 85–90, 2018.
- [11] G. H. Shirdel, H. Rezapour, and A. M. Sayadi, "The hyper-Zagreb index of graph operations," *Iranian Journal of Mathematical Chemistry*, vol. 4, no. 2, pp. 213–220, 2013.
- [12] M. Ghorbani and N. Azimi, "Note on multiple Zagreb indices," *Iranian Journal of Mathematical Chemistry*, vol. 3, no. 2, pp. 137–143, 2012.

- [13] M. K. Siddiqui, M. Imran, and A. Ahmad, "On Zagreb indices, Zagreb polynomials of some nanostar dendrimers," *Applied Mathematics and Computation*, vol. 280, pp. 132–139, 2016.
- [14] M. K. Siddiqui, M. Naeem, N. A. Rahman, and M. Imran, "Computing topological indices of certain networks," *Journal of Optoelectronics and Advanced Materials*, vol. 18, pp. 884–892, 2016.
- [15] I. Gutman and N. Trinajstić, "Graph theory and molecular orbitals. Total  $\pi$ -electron energy of alternant hydrocarbons," *Chemical Physics Letters*, vol. 17, no. 4, pp. 535–538, 1972.
- [16] B. Furtula and I. Gutman, "A forgotten topological index," *Journal of Mathematical Chemistry*, vol. 53, no. 4, pp. 1184–1190, 2015.
- [17] B. Furtula, A. Graovac, and D. Vukićević, "Augmented Zagreb index," *Journal of Mathematical Chemistry*, vol. 48, no. 2, pp. 370–380, 2010.
- [18] A. T. Balaban, "Highly discriminating distance-based topological index," *Chemical Physics Letters*, vol. 89, no. 5, pp. 399–404, 1982.
- [19] A. T. Balaban and L. V. Quintas, "The smallest graphs, trees, and 4-trees with degenerate topological index," *Journal of Mathematical Chemistry*, vol. 14, pp. 213–233, 1983.
- [20] H. Yang, M. Imran, S. Akhter, Z. Iqbal, and M. K. Siddiqui, "On distance-based topological descriptors of subdivision vertex-edge join of three graphs," *IEEE ACCESS*, vol. 7, no. 1, pp. 143381–143391, 2019.
- [21] S. M. Kang, M. K. Siddiqui, N. A. Rehman, M. Naeem, and M. H. Muhammad, "Topological properties of 2-dimensional silicon-carbons," *IEEE Access*, vol. 6, pp. 59362–59373, 2018.
- [22] M. Imran, M. K. Siddiqui, M. Naeem, and M. A. Iqbal, "On topological properties of symmetric chemical structures," *Symmetry*, vol. 10, no. 5, pp. 173–183, 2018.
- [23] P. S. Ranjini, V. Loksha, and A. Usha, "Relation between phenylene and hexagonal squeeze using harmonic index," *International Journal of Applied Graph Theory*, vol. 1, no. 4, pp. 116–121, 2013.
- [24] M. Imran, M. K. Siddiqui, A. Q. Baig, W. Khalid, and H. Shaker, "Topological properties of cellular neural networks," *Journal of Intelligent and Fuzzy Systems*, vol. 37, no. 3, pp. 3605–3614, 2019.
- [25] W. Gao, H. Wu, M. K. Siddiqui, and A. Q. Baig, "Study of biological networks using graph theory," *Saudi Journal of Biological Sciences*, vol. 25, no. 6, pp. 1212–1219, 2018.
- [26] S. A. Nadeem, M. K. Siddiqui, and M. Naeem, "Topological descriptor of 2-dimensional silicon carbons and their applications," *Open Chemistry*, vol. 17, no. 1, pp. 1473–1482, 2019.
- [27] J. B. Liu, C. Wang, S. Wang, and B. Wei, "Zagreb indices and multiplicative Zagreb indices of eulerian graphs," *Bulletin of the Malaysian Mathematical Sciences Society*, vol. 42, no. 1, pp. 67–78, 2019.
- [28] Z. Shao, P. Wu, X. Zhang, D. Dimitrov, and J. B. Liu, "On the maximum ABC index of graphs with prescribed size and without pendent vertices," *IEEE Access*, vol. 6, pp. 27604–27616, 2018.
- [29] Z. Raza, "The expected values of arithmetic bond connectivity and geometric indices in random phenylene chains," *Heliyon*, vol. 6, no. 7, pp. 44–59, 2020.
- [30] B. Assaye, M. Alamneh, L. N. Mishra, and Y. Mebrat, "Dual skew Heyting almost distributive lattices," *Applied Mathematics and Nonlinear Sciences*, vol. 4, no. 1, pp. 151–162, 2019.
- [31] D. Zhao, M. K. Siddiqui, S. Javed, L. Sherin, and F. Kausar, "Molecular topological indices-based analysis of thermodynamic properties of graphitic carbon nitride," *The European Physical Journal Plus*, vol. 135, no. 12, pp. 1–19, 2020.

## Research Article

# Molecular Descriptor Analysis of Certain Isomeric Natural Polymers

Maqsood Ahmad,<sup>1</sup> Muhammad Saeed ,<sup>2</sup> Muhammad Javaid ,<sup>2</sup> and Ebenezer Bonyah <sup>3</sup>

<sup>1</sup>Department of Mathematics, COMSATS University Islamabad, Lahore Campus, Lahore 54000, Pakistan

<sup>2</sup>Department of Mathematics, School of Science, University of Management and Technology, Lahore 54000, Pakistan

<sup>3</sup>Department of Mathematics Education, Akenten Appiah-Menka University of Skills Training and Entrepreneurial Development, Kumasi 00233, Ghana

Correspondence should be addressed to Ebenezer Bonyah; ebbonyah@gmail.com

Received 1 July 2021; Accepted 7 August 2021; Published 24 August 2021

Academic Editor: Ajaya Kumar Singh

Copyright © 2021 Maqsood Ahmad et al. This is an open access article distributed under the Creative Commons Attribution License, which permits unrestricted use, distribution, and reproduction in any medium, provided the original work is properly cited.

Polymers, drugs, and almost all chemical or biochemical compounds are frequently modeled as diverse  $\omega$ -cyclic, acyclic, bipartite, and polygonal shapes and regular graphs. Molecular descriptors (topological indices) are the numerical quantities and computed from the molecular graph  $\Gamma$  (2D lattice). These descriptors are highly significant in quantitative structure-property or activity relationship (QSPR and QSAR) modeling that provides the theoretical and the optimal basis to expensive experimental drug design. In this paper, we study three isomeric natural polymers of glucose (polysaccharides), namely, cellulose, glycogen, and amylopectin (starch), having promising pharmaceutical applications, exceptional properties, and fascinating molecular structures. We intend to investigate and compute various closed-form formulas such as ABC, GA, sum-connectivity  $\chi_{(-1/2)}$ ,  $ABC_4$ ,  $GA_5$ , and Sanskruti indices for the aforementioned macromolecules. Also, we present the closed-form formulas for the first, second, modified, and augmented Zagreb indices, inverse and general Randić indices, and symmetric division deg, harmonic, and inverse sum indices. Furthermore, we provide a comparative analysis using 3D graphs for these families of macromolecules to clarify their nature.

## 1. Introduction

Cheminformatics is a comparatively new area of information technology that comprises chemistry, mathematics, and other informational sciences that concentrate on gathering, storage, treatment, and examination of chemical data. A molecular descriptor (MD) distinguishes the topology of a molecular graph and is invariant under isomorphism. Some of these descriptors take part in QSAR/QSPR analysis [1, 2] which infer about the bioactivities and physicochemical properties of biochemical materials. Various types of distance-based, degree-based, spectral, and polynomial-related descriptors of graphs are well established and extensively studied in the literature. Out of these classes, vertex degree-based descriptors turn out to be the most important and play a phenomenal role in chemical graph theory (CGT). These descriptors are used, in combination, to infer physicochemical, biological, and pharmacological properties such as the stability, chirality, melting

point, boiling point, similarity, connectivity, entropy, enthalpy of formation, surface tension, density, critical temperature, and toxicity of chemical compounds in CGT; see [3, 4].

Throughout, in this work,  $\Gamma$  denotes a simple, finite, and connected graph, whereas  $E(\Gamma)$  and  $V(\Gamma)$  represent the edge and vertex set of  $\Gamma$ , respectively. For a vertex  $v \in V(\Gamma)$ , degree of vertex  $v$  is denoted by  $d_v$ , and the sum of the degree of vertices at unit distance from  $v$  is represented by  $S_v$ , i.e.,  $S_v = \sum_{w \in N_\Gamma(v)} d_w$ , where  $N_\Gamma(v) = \{w \in V(\Gamma) | vw \in E(\Gamma)\}$ . Here, we specify few distinct, significant, and well-studied bond-additive invariants of our concern.

In [5], Gutman and Trinajstić proposed two degree-based invariants known as the first Zagreb index (FZI)  $M_1$  and the second Zagreb index (SZI)  $M_2$ . These indices initially appeared in the expression of the total  $\pi$ -electron of the molecular graph and were later applied to study molecular complexity and ZE isomerism. The formulas of  $M_1$ ,  $M_2$ , and the modified Zagreb index (MSZI) are given as

$$\begin{aligned}
 M_1(\Gamma) &= \sum_{uv \in E(\Gamma)} (d_u + d_v), \\
 M_2(\Gamma) &= \sum_{uv \in E(\Gamma)} (d_u \times d_v), \\
 {}^m M_2(\Gamma) &= \sum_{uv \in E(\Gamma)} \frac{1}{(d_u d_v)}.
 \end{aligned} \tag{1}$$

In [6], Randić offered a very influential invariant which is considered to be a prototype of degree-based invariants and is called Randić index. It is the oldest and extensively studied invariant that measures the amount of branching in the carbon atom skeleton of saturated hydrocarbons [7, 8]. For a molecular graph  $\Gamma$ , Randić index is defined as

$$R(\Gamma) = \sum_{uv \in E(\Gamma)} \frac{1}{\sqrt{d_u d_v}}. \tag{2}$$

In [9], Bollobás and Erdős initiated the concept of the general Randić index (GRI), and it is given as

$$R_\alpha(\Gamma) = \sum_{uv \in E(\Gamma)} (d_u d_v)^\alpha, \quad \alpha \in \mathbb{R}. \tag{3}$$

Moreover, the inverse Randić index (IRI) is defined by the following formula:

$$RR_\alpha(\Gamma) = \sum_{uv \in E(\Gamma)} (d_u d_v)^\alpha. \tag{4}$$

In [10], Zhou and Trinajstić instigated the concept of the generalized sum-connectivity index (GSCI) that is defined as follows:

$$\chi_\alpha(\Gamma) = \sum_{uv \in E(\Gamma)} (d_u + d_v)^\alpha, \quad \alpha \in \mathbb{R}. \tag{5}$$

For  $\alpha = (-1/2)$  and  $\alpha = 2$ , we have sum-connectivity index  $\chi_{(-1/2)}$  (SCI) and “hyper-Zagreb index” (HZI) [11], respectively.

In [12], Li and Zheng introduced the first general Zagreb index (FGZI), and it is defined by the following formula:

$$M_1^\alpha = \sum_{v \in V(\Gamma)} (d_v)^\alpha = \sum_{uv \in E(\Gamma)} (d_u^{\alpha-1} + d_v^{\alpha-1}). \tag{6}$$

For  $\alpha = 3$ , we obtain the forgotten index (FI). In [13], Azari and Iranmanesh initiated the idea of the generalized Zagreb index (GZI) that is given as

$$Z_{r,s}(\Gamma) = \sum_{uv \in E(\Gamma)} (d_u^r d_v^s + d_u^s d_v^r), \tag{7}$$

where  $r, s \in \mathbb{Z}^+ \cup \{0, -1\}$ .

In [14], Estrada et al. introduced a significant invariant called atom-bond connectivity index  $ABC(\Gamma)$  that proved to be a good predictor for the stability of alkanes and strain energy of cycloalkanes [15, 16]. In [17], Vukičević and Furtula suggested another prominent invariant known as geometric-arithmetic index  $GA(\Gamma)$ . These indices are defined as follows:

$$ABC(\Gamma) = \sum_{uv \in E(\Gamma)} \sqrt{\frac{d_u + d_v - 2}{d_u d_v}}, \tag{8}$$

$$GA(\Gamma) = \sum_{uv \in E(\Gamma)} \frac{2\sqrt{d_u d_v}}{d_u + d_v}. \tag{9}$$

An interested reader may refer to the surveys [18, 19] regarding Randić and GA indices of graphs, respectively. In [20, 21], Ghorbani and Hosseinzadeh and Graovac et al. proposed the fourth version of ABC and the fifth version of GA that are denoted by  $ABC_4$  and  $GA_5$ , respectively. Likewise, Hosamani introduced the Sanskruti index denoted by SI [22]. These invariants are based on the sum of neighbor's degrees of end vertices and are defined as

$$ABC_4(\Gamma) = \sum_{uv \in E(\Gamma)} \sqrt{\frac{S_u + S_v - 2}{S_u S_v}}, \tag{10}$$

$$GA_5(\Gamma) = \sum_{uv \in E(\Gamma)} \frac{2\sqrt{S_u S_v}}{S_u + S_v}, \tag{11}$$

$$SI(\Gamma) = \sum_{uv \in E(\Gamma)} \left( \frac{S_u S_v}{S_u + S_v - 2} \right)^3. \tag{12}$$

For a molecular graph ( $\Gamma$ ), some other invariants of key importance and related to our concern are SDD (symmetric division deg), HI (harmonic index), ISI (inverse sum index), and AZI (augmented Zagreb index). These indices are defined as follows:

$$\begin{aligned}
 SDD(\Gamma) &= \sum_{uv \in E(\Gamma)} \left( \frac{d_u^2 + d_v^2}{d_u d_v} \right), \\
 HI(\Gamma) &= \sum_{uv \in E(\Gamma)} \left( \frac{2}{d_u + d_v} \right), \\
 ISI(\Gamma) &= \sum_{uv \in E(\Gamma)} \left( \frac{d_u d_v}{d_u + d_v} \right), \\
 AZI(\Gamma) &= \sum_{uv \in E(\Gamma)} \left( \frac{d_u d_v}{d_u + d_v - 2} \right)^3.
 \end{aligned} \tag{13}$$

In [23], Ranjini et al. proposed the idea of first, second, and third redefined Zagreb invariants that are given by the following formulas:

$$\begin{aligned}
 ReZM_1(\Gamma) &= \sum_{uv \in E(\Gamma)} \left( \frac{d_u + d_v}{d_u d_v} \right), \\
 ReZM_2(\Gamma) &= \sum_{uv \in E(\Gamma)} \left( \frac{d_u d_v}{d_u + d_v} \right), \\
 ReZM_3(\Gamma) &= \sum_{uv \in E(\Gamma)} (d_u d_v)(d_u + d_v).
 \end{aligned} \tag{14}$$

It is evident that  $\text{ReZM}_1 = n$  and violates the criteria to be a topological index. Furthermore,  $\text{ReZM}_2$  is the same as the already defined topological index called the inverse sum index. Consequently, the only novel invariant is  $\text{ReZM}_3(\Gamma)$  known as redefined Zagreb index (ReZI) and is denoted by  $\text{ReZM}(\Gamma)$ .

In [24], Deutsch and Klavžar initiated the idea of  $M$ -polynomial for graph  $\Gamma = (V(\Gamma), E(\Gamma))$ , and it is mathematically given as

$$M(\Gamma; x, y) = f(x, y) = \sum_{i \leq j} m_{ij}(\Gamma) x^i y^j, \quad (15)$$

where  $m_{ij}(\Gamma)$  denotes the number of edges  $uv \in E(\Gamma)$ , where  $\{d_u, d_v\} = \{i, j\}$ .

Table 1 depicts the relationship between some essential topological indices and the  $M$ -polynomial, where  $D_x M = x(\partial M/\partial x)$ ,  $D_y M = y(\partial M/\partial y)$ ,  $J(M(x, y)) = M(x, x)$ ,  $S_x M = \int_0^x (M(t, y)/t) dt$ ,  $S_y M = \int_0^y (M(x, t)/t) dt$ , and  $Q_\alpha M = x^\alpha M$ .

Note: all formulas depicted in Table 1 will be calculated at  $x = y = 1$ .

We summarize the relationship of GZI with certain important invariants in Table 2.

Harry Wiener, an American theoretical chemist, observed that invariants estimated from the molecular graph of a chemical compound carry information and properties of that chemical compound. Camarda and Maranas [25] employed the connectivity indices to invent and create the polymers correlated with a certain optimal characteristic. Dendrimers are acknowledged to be the ‘‘polymers of the 21st century’’ due to their increased popularity, which is evident through research articles and patents registered. In [26], Wang et al. provided the closed-form formula for the  $k$ -connectivity invariant in the class of nanostars and dendrimers. In [27], Ali et al. derived general formulas of certain invariants for some specific polymers such as polyphenylenes, nanostars, and dendrimers. In [28], Shao et al. worked out for the maximum value of the ABC index and provided its characterization in the class of chemically oriented graphs. In [29], Gao et al. figured out the enthalpy and entropy for copper oxide I and copper oxide II. Kang et al. [30], Liu et al. [31], and Gao et al. [32] studied various topological aspects of 2D silicon-carbons, nanotubes, and dendrimers, respectively.

Liu et al. [33] investigated and identified proteins having nucleotide-binding activity using star graph TIs. Ali et al. [34, 35] and Du et al. [36] studied and applied some degree-based TIs such as the first Zagreb connection index, ordinary generalized geometric-arithmetic index, general Platt index, and general sum-connectivity index to establish extremal results for alkanes. Hayat et al. [37] performed comparative testing of certain chemical structures (carbon nanotubes, carbon nanocones, and tetrahedral diamond) using various degree-based TIs. Arockiaraj et al. [38] computed variants of Wiener indices for the molecular graphs of coronoid systems, carbon nanocones, and  $\text{SiO}_2$  nanostructures. In [39], Ahmad et al. computed and compared several invariants of synthetic polymers such as bakelite, vulcanized rubber, and

TABLE 1: Formulas to derive some promising invariants from the  $M$ -polynomial.

Topological indices	Formulas derived from the $M$ -polynomial
FZI $M_1$	$(D_x + D_y)M(x, y)$
SZI $M_2$	$(D_x \cdot D_y)M(x, y)$
MSZI ${}^m M_2$	$(S_x \cdot S_y)M(x, y)$
GRI $R_\alpha$	$D_x^\alpha \cdot D_y^\alpha M(x, y)$
IRI $RR_\alpha$	$S_x^\alpha \cdot S_y^\alpha M(x, y)$
SDD	$(D_x S_y + S_x D_y)M(x, y)$
HI	$2S_x J M(x, y)$
ISI	$S_x J D_x D_y M(x, y)$
AZI	$S_x^3 Q_{-2} J D_x^3 D_y^3 M(x, y)$

TABLE 2: Few particular cases of GZI.

Topological index	Corresponding $(r, s)$ -Zagreb index
FZI $M_1(\Gamma)$	$Z_{1,0}$
SZI $M_2(\Gamma)$	$(1/2)Z_{1,1}$
FI $F(\Gamma)$	$Z_{2,0}$
ReZI $\text{ReZM}(\Gamma)$	$Z_{2,1}$
GFZI $M^\alpha(\Gamma)$	$Z_{\alpha-1,0}$
GRI $R_\alpha(\Gamma)$	$(1/2)Z_{\alpha,\alpha}$
SDD index $\text{SDD}(\Gamma)$	$Z_{1,-1}$

acrylic (polymethyl methacrylate) to ascertain a relationship between their physicochemical properties. From their monomers, we develop the polymeric graphs of three closely related natural polymers (isomeric), broadly known as cellulose, glycogen, and amylopectin, to compute certain invariants to anticipate their physicochemical properties. Numerous theoretical, mathematical, and chemical properties of diverse chemical structures based on various invariants obtained from their molecular graphs have been investigated in [40–43].

Polymers pervade every aspect of our daily life, and it is hard to imagine a society without natural as well as synthetic polymers, and they are characterized into four major types based on their molecular chains; see Figure 1.

Typically, almost all food items comprise macromolecules which are some sort of polymers. Most of the food items primarily include naturally occurring polymers (polysaccharides) such as starch and cellulose. The main biological functions of these polysaccharides are nutritional, e.g., energy storage for metabolism (starch and glycogen), and building material (cellulose). Like graphite and diamonds, glycogen, starch, and cellulose are also composed of the same substance but with different structures. We know glycogen, starch, and cellulose are all natural polymers of glucose (carbohydrate) having the same chemical formula  $(\text{C}_6\text{H}_{10}\text{O}_5)_n$ . The entire class of natural polymers is made up of smaller segments called monomers (monosaccharides), and glucose is the basic building block for cellulose, glycogen, and starch. They differ from each other based on the glucose type present and the nature of the bond which links the glucose monomers together. Glucose is a type of sugar comprising carbon, hydrogen, and oxygen. These elements bind together to create a hexagonal structure having six carbon atoms (numbered  $\text{C}_1$  to  $\text{C}_6$ ) with one of the carbons

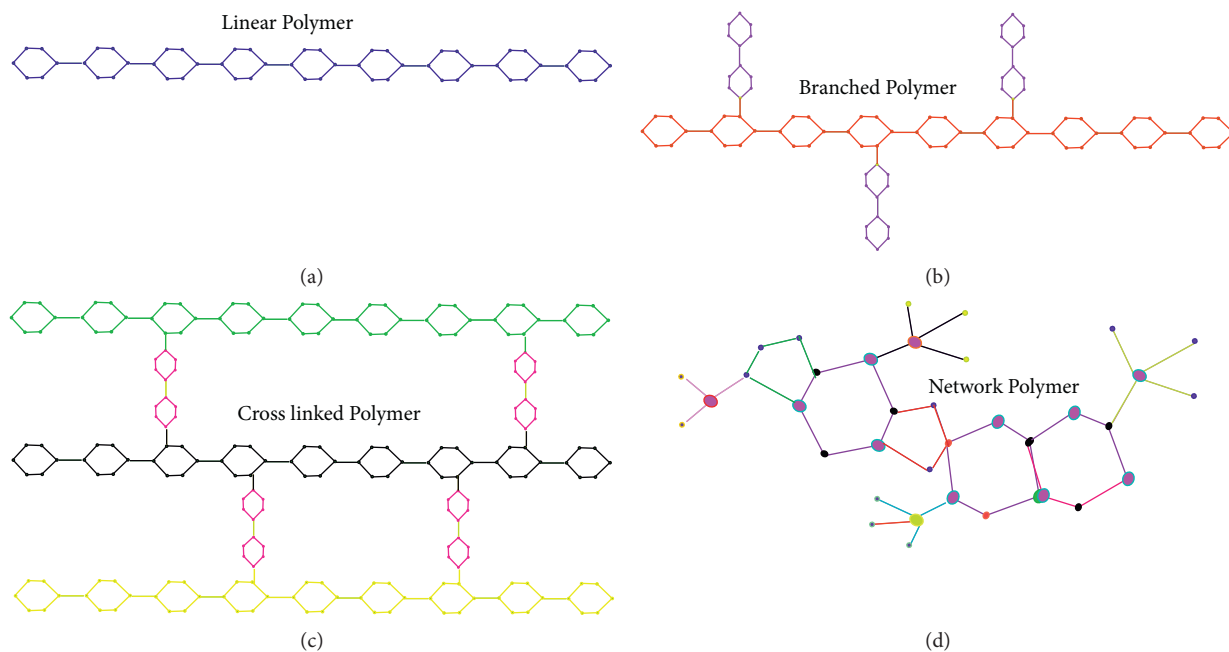


FIGURE 1: Polymer characterization with regard to structural chains.

sticking off the end. Distinct glucose rings can be attached at different carbons to produce different types of structures. Some segments of the ring are flipped, causing two different forms of glucose, known as  $\alpha$ -glucose (alcohol OH attached to  $C_1$  is down) and  $\beta$ -glucose (alcohol OH attached to  $C_1$  is up); see Figure 2. There are two types of bonding, namely,  $\alpha(C_1 - C_4)$  and  $\alpha(C_1 - C_6)$  glycosidic bonding in amylopectin and glycogen; see Figure 2. Natural polymers, particularly of carbohydrate origin, have been found very promising pharmaceutical applications in different forms [44–46].

## 2. Discussion and Construction of the Planar Graph of Cellulose Network $CL_m^n$

Cellulose is among the most abundant, renewable, and biodegradable organic compounds found in nature. Anselme Payen (1838), a French chemist, recognized the existence of cellulose in green plants [47]. It is the main component of tough cell walls that surround plant cells, thus making plant stems, leaves, and branches strong as well as rigid. The rigid structure of cellulose allows plants to stand upright, difficult to digest, and hard to break down. Recently, the government, as well as industry, is highly interested in products from sustainable and renewable energy resources that produce low human health and environmental risks [48]. Cellulose-based materials (cellulosics) are used as key excipients in compounding pharmaceutical objectives and gained immense attraction due to various intriguing features such as low cost, biocompatibility, reproducibility, and recyclability (green technology).

First, we explain the chemical structure of cellulose, in general, and then convert it into a mathematical object called a molecular graph to investigate its properties using tools

from graph theory. It comprises over 3,000 D-glucose units that are linked by  $\beta(C_1 - C_4)$  glycosidic bonding (see Figure 3) and have general formula  $(C_6H_{10}O_5)_n$ . Cellulose is a linear unbranched polymer: unlike glycogen and starch, no coiling occurs. Multiple hydroxyl groups on the glucose ring from one chain create hydrogen-oxygen bonding on the same or a neighboring linear chain (highly cross-linked polymer) that results in the formation of microfibrils having high tensile strength.

Now, we provide the construction, from scratch, for the molecular graph of  $CL_m^n$ . The basic building unit of the cellulose network is  $(C_6H_{10}O_5)_2$ , depicted in Figure 3, consisting of three hexagons and one octagon with three pendant edges. Out of these pendants, one is fixed carbon, and the remaining two pendants are OH (hydroxyl group), one at the upper side and one at the lower side for further bonding. Here,  $n$  represents the number of hexagons in basic units, and when we add one monomer to the basic unit, we get 7 hexagons. Similarly, every single addition of the monomer resulted in an increment of four hexagons.

Assume  $n$  to be the number of hexagons in one hexagonal chain with  $l$  isomeric units and  $m$  to be the number of hexagonal chains in cellulose network  $CL_m^n$ . Clearly, the number of hexagons in each chain is odd, and the relation between hexagons in one chain with isomeric units  $l$  is given as  $n = 4l + 3$ ,  $l = 0, 1, 2, 3, \dots$  Figure 4 elaborates a three-dimensional network of cellulose  $CL_4^7$  along with its planar network. We recognize three types of the polygon in the molecular graph of cellulose, namely, hexagons, octagons, and decagons.

**2.1. Results for Cellulose Network  $CL_m^n$ .** Using simple counting techniques, we observe that the total number of vertices in

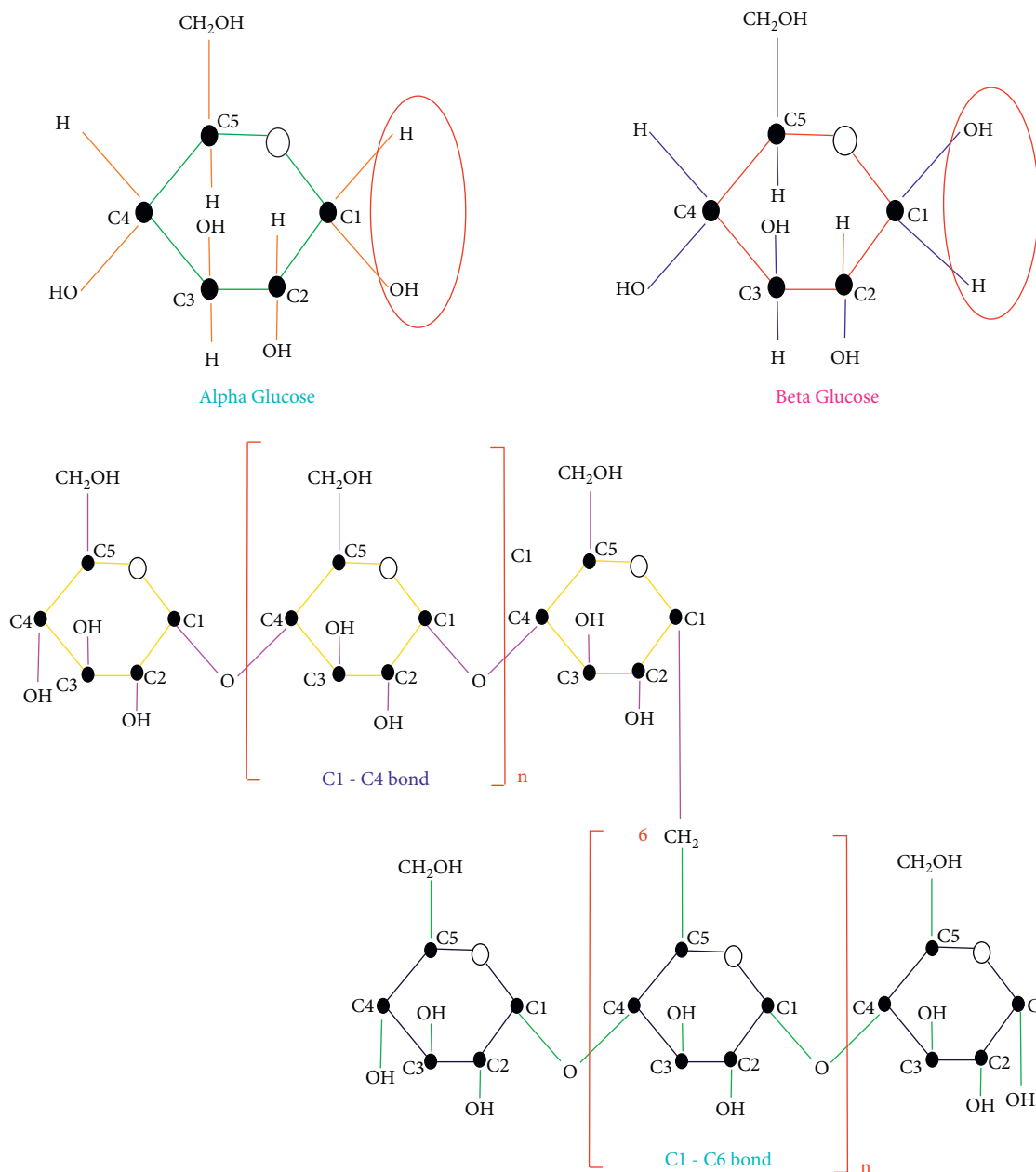


FIGURE 2: Basic units,  $\alpha$ - and  $\beta$ -glucose, and their linkages.

$CL_m^n$ ,  $n = 4l + 3$ , is  $22ml + 20m - 2$ , and the number of edges is  $30ml + 25m - 2l - 4$ . To compute our results, we require edge partition of edge set  $E(CL_m^n)$ . There is one and only edge having degrees 1 and 3 of end vertices, i.e.,  $|E_{13}(CL_m^n)| = 1$ . The number of edges with end vertices, each of degree 2, is  $|E_{22}(CL_m^n)| = 4m + 4l + 1$ . We detect total edges with degrees 2 and 3 of end vertices as  $|E_{23}(CL_m^n)| = 12ml + 12m - 2$ . Finally, we identified the number of edges with end vertices, each of degree 3, as  $|E_{33}(CL_m^n)| = 18ml + 9m - 6l - 4$ . An

edge partition of the cellulose network comprising different parameters is presented in [49]. For the sake of computational ease, we summarized the edge partition of the cellulose network in Table 3.

**Theorem 1.** Let  $CL_m^n$  be a cellulose network having  $m$  hexagonal chains and  $n = 4l + 3$  hexagons in each chain. The formula for  $GZI Z_{r,s}(CL_m^n)$  is given as

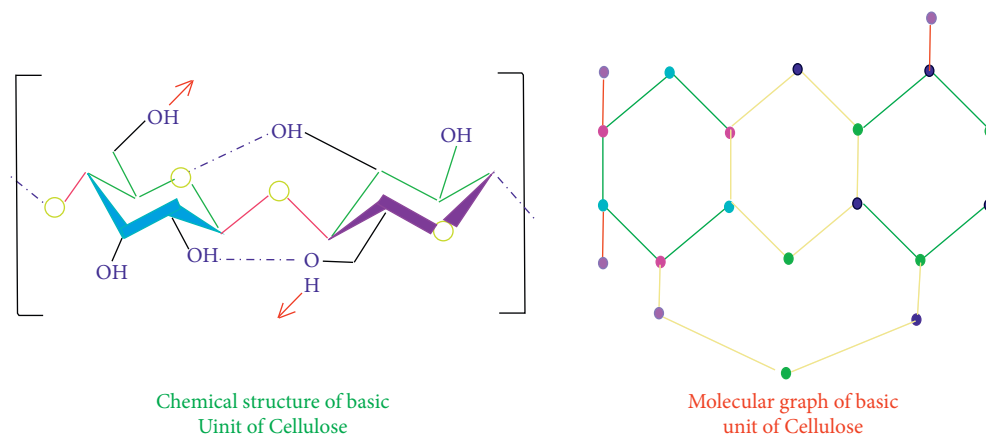
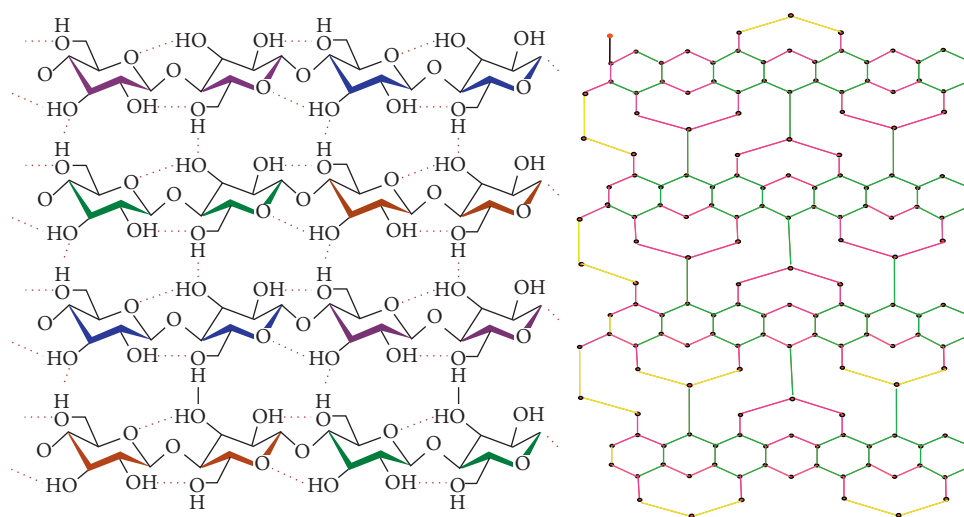


FIGURE 3: 2D skeleton of basic units of cellulose.

FIGURE 4: Chemical structure and equivalent molecular graph of cellulose  $CL_4^7$ .TABLE 3: Partitioning of the edge set with respect to degrees of end vertices for  $CL_m^n$ .

$(d_v, d_w): vw \in E(CL_m^n)$	(1, 3)	(2, 2)	(2, 3)	(3, 3)
Number of edges = $ E_{(i,j)} $	1	$4m + 4l + 1$	$12ml + 12m - 2$	$18ml + 9m - 6l - 4$

$$\begin{aligned}
 Z_{r,s}(CL_m^n) &= (4 \times 3^{r+s+2} + 2^{r+2} \times 3^{s+1} + 2^{s+2} \times 3^{r+1})ml \\
 &\quad + (2^{r+s+3} + 2^{r+2} \times 3^{s+1} + 2^{s+2} \times 3^{r+1} + 2 \times 3^{r+s+2})m + (2^{r+s+3} - 4 \times 3^{r+s+1})l \\
 &\quad + (3^r + 3^s + 2^{r+s+1} - 2^{r+1} \times 3^s - 2^{s+1} \times 3^r - 8 \times 3^{r+s}).
 \end{aligned} \tag{16}$$

*Proof.* Employing equation (7) and using Table 3, we obtain the desired result as follows:

$$\begin{aligned}
 Z_{r,s}(CL_m^n) &= \sum_{vw \in E(CL_m^n)} (d_v^r d_w^s + d_w^r d_v^s) = \sum_{vw \in E_{13}} (d_v^r d_w^s + d_w^r d_v^s) + \sum_{vw \in E_{22}} (d_v^r d_w^s + d_w^r d_v^s) \\
 &+ \sum_{vw \in E_{23}} (d_v^r d_w^s + d_w^r d_v^s) + \sum_{vw \in E_{33}} (d_v^r d_w^s + d_w^r d_v^s) \\
 &= (3^s + 3^r) + (4m + 4l + 1)(2^r 2^s + 2^r 2^s) + (12ml + 12m - 2)(2^r 3^s + 3^r 2^s) \\
 &+ (18ml + 9m - 6l - 4)(3^r 3^s + 3^r 3^s) \\
 &= (12(2^r 3^s + 2^s 3^r) + 36 \times 3^{r+s})ml + (12(2^r 3^s + 2^s 3^r) + 2 \times 3^{r+s+2} + 2^{r+s+3})m \\
 &= (2^{r+s+3} - 4 \times 3^{r+s+1})l + (3^r + 3^s - 2(2^r 3^s + 2^s 3^r) + 2^{r+s+1} - 8 \times 3^{r+s}) \\
 &= (4 \times 3^{r+s+2} + 2^{r+2} \times 3^{s+1} + 2^{s+2} \times 3^{r+1})ml \\
 &+ (2^{r+s+3} + 2^{r+2} \times 3^{s+1} + 2^{s+2} \times 3^{r+1} + 2 \times 3^{r+s+2})m + (2^{r+s+3} - 4 \times 3^{r+s+1})l \\
 &+ (3^r + 3^s + 2^{r+s+1} - 2^{r+1} \times 3^s - 2^{s+1} \times 3^r - 8 \times 3^{r+s}).
 \end{aligned} \tag{17}$$

**Corollary 1.** Using formulas outlined in Table 2 in equation (17), we derived the following results of different TIs:

- (1)  $M_1(CL_m^n) = Z_{1,0}(CL_m^n) = 168ml + 130m - 20l - 26$
- (2)  $M_2(CL_m^n) = (1/2)Z_{1,1}(CL_m^n) = 468ml + 338m - 76l - 82$
- (3)  $F(CL_m^n) = Z_{2,0}(CL_m^n) = 480ml + 350m - 76l - 80$
- (4)  $ReZM(CL_m^n) = Z_{2,1}(CL_m^n) = 1332ml + 910m - 260l - 248$
- (5)  $M^\alpha(CL_m^n) = Z_{\alpha-1,0}(CL_m^n) = (16 \times 3^\alpha + 3 \times 2^{\alpha+1})ml + 5(2^{\alpha+1} + 2 \times 3^\alpha)m + 4(2^\alpha - 3^\alpha)r + (1 - 3^{\alpha+1})$
- (6)  $R_\alpha(CL_m^n) = (1/2)Z_{\alpha,\alpha}(CL_m^n) = (6^{\alpha+1} + 9^{\alpha+1})ml + (2^{2\alpha+1} + 6^{\alpha+1} + (9^{\alpha+1}/2))m + (2^{2\alpha+1} - 3^{2\alpha+2})l - ((3^\alpha/2) + 2^{2\alpha-1} - 6^\alpha - 2 \times 3^{2\alpha})$
- (7)  $SDD(CL_m^n) = Z_{1,-1}(CL_m^n) = 62ml + 52m - 4l - 7$

**Theorem 2.** Let  $CL_m^n$  be a cellulose network having  $n$  hexagonal chains and  $n = 4l + 3$  hexagons in each chain. Then,

- (1)  $ABC(CL_m^n) = (12 + 6\sqrt{2})ml + (6 + 8\sqrt{2})m + (2\sqrt{2} - 4)l + (1/6)(2\sqrt{6} - 3\sqrt{2} - 16)$
- (2)  $GA(CL_m^n) = (90 + 24\sqrt{6})(ml/5) + (65 + 24\sqrt{6})(m/5) - 2l - (1/10)(5\sqrt{3} - 8\sqrt{6} - 30)$
- (3)  $SCI(CL_m^n) = \chi_{(-1/2)}(CL_m^n) = ((12/\sqrt{5}) + 3\sqrt{6})ml + (2 + (12/\sqrt{5}) + (9/\sqrt{6}))m + (2 - \sqrt{6})l + (1 - (2/\sqrt{5}) - (4/\sqrt{6}))$

*Proof.* We determine the required results with the help of Table 3 along with equations (8), (9), and (5), respectively.

$$\begin{aligned}
 1 \text{ } ABC(CL_m^n) &= \sum_{uv \in E(CL_m^n)} \sqrt{\frac{d_u + d_v - 2}{d_u d_v}} = \sum_{uv \in E_{13}(CL_m^n)} \sqrt{\frac{d_u + d_v - 2}{d_u d_v}} \\
 &+ \sum_{uv \in E_{22}(CL_m^n)} \sqrt{\frac{d_u + d_v - 2}{d_u d_v}} + \sum_{uv \in E_{23}(CL_m^n)} \sqrt{\frac{d_u + d_v - 2}{d_u d_v}} \\
 &+ \sum_{uv \in E_{33}(CL_m^n)} \sqrt{\frac{d_u + d_v - 2}{d_u d_v}} \\
 &= \sqrt{\frac{2}{3}} + (4m + 4l + 1)\sqrt{\frac{2}{4}} + (12ml + 12m - 2)\sqrt{\frac{3}{6}} + (18ml + 9m - 6l - 4)\sqrt{\frac{4}{9}} \\
 &= (12 + 6\sqrt{2})ml + (6 + 8\sqrt{2})m + (2\sqrt{2} - 4)l + \frac{1}{6}(2\sqrt{6} - 3\sqrt{2} - 16),
 \end{aligned}$$

$$\begin{aligned}
2 \text{GA}(\text{CL}_m^n) &= \sum_{uv \in E(\text{CL}_m^n)} \frac{2\sqrt{d_u d_v}}{d_u + d_v} = \sum_{uv \in E_{13}(\text{CL}_m^n)} \frac{2\sqrt{d_u d_v}}{d_u + d_v} + \sum_{uv \in E_{22}(\text{CL}_m^n)} \frac{2\sqrt{d_u d_v}}{d_u + d_v} \\
&\quad + \sum_{uv \in E_{23}(\text{CL}_m^n)} \frac{2\sqrt{d_u d_v}}{d_u + d_v} + \sum_{uv \in E_{33}(\text{CL}_m^n)} \frac{2\sqrt{d_u d_v}}{d_u + d_v} \\
&= \left(\frac{2\sqrt{3}}{4}\right) + (4m + 4l + 1)\left(\frac{2\sqrt{4}}{4}\right) + (12ml + 12m - 2)\left(\frac{2\sqrt{6}}{5}\right) + (18ml + 9m - 6l - 4)\left(\frac{2\sqrt{9}}{6}\right) \\
&= (90 + 24\sqrt{6})\frac{ml}{5} + (65 + 24\sqrt{6})\frac{m}{5} - 2l - \frac{1}{10}(5\sqrt{3} - 8\sqrt{6} - 30), \\
3\chi_{-1/2}(\text{CL}_m^n) &= \sum_{uv \in E(\text{CL}_m^n)} \frac{1}{\sqrt{d_u + d_v}} = \sum_{uv \in E_{13}(\text{CL}_m^n)} \frac{1}{\sqrt{d_u + d_v}} + \sum_{uv \in E_{22}(\text{CL}_m^n)} \frac{1}{\sqrt{d_u + d_v}} \\
&\quad + \sum_{uv \in E_{23}(\text{CL}_m^n)} \frac{1}{\sqrt{d_u + d_v}} + \sum_{uv \in E_{33}(\text{CL}_m^n)} \frac{1}{\sqrt{d_u + d_v}} \\
&= \frac{1}{\sqrt{4}} + \frac{1}{\sqrt{4}}(4m + 4l + 1) + \frac{1}{\sqrt{5}}(12ml + 12m - 2) + \frac{1}{\sqrt{6}}(18ml + 9m - 6l - 4) \\
&= \left(\frac{12}{\sqrt{5}} + 3\sqrt{6}\right)ml + \left(2 + \frac{12}{\sqrt{5}} + \frac{9}{\sqrt{6}}\right)m + (2 - \sqrt{6})l + \left(1 - \frac{2}{\sqrt{5}} - \frac{4}{\sqrt{6}}\right).
\end{aligned} \tag{18}$$

□

**Theorem 3.** Let  $\text{CL}_m^n$  be a cellulose network having  $m$  hexagonal chains and  $n = 4l + 3$  hexagons in each chain; then, the  $M$ -polynomial of  $\text{CL}_m^n$  is

$$M(\text{CL}_m^n; x, y) = xy^3 + (4m + 4l + 1)x^2y^2 + (12ml + 12m - 2)x^2y^3 + (18ml + 9m - 6l - 4)x^3y^3. \tag{19}$$

*Proof.* To calculate the  $M$ -polynomial of  $\text{CL}_m^n$ , we apply equation (15) as follows:

$$\begin{aligned}
M(\text{CL}_m^n; x, y) &= \sum_{\delta \leq i \leq j \leq \Delta} M_{ij} x^i y^j = \sum_{1 \leq 3} M_{13} x y^3 \\
&\quad + \sum_{2 \leq 2} M_{22} x^2 y^2 + \sum_{2 \leq 3} M_{23} x^2 y^3 + \sum_{3 \leq 3} M_{33} x^3 y^3 \\
&= |E_{13}(\text{CL}_m^n)| x y^3 + |E_{22}(\text{CL}_m^n)| x^2 y^2 + |E_{23}(\text{CL}_m^n)| x^2 y^3 + |E_{33}(\text{CL}_m^n)| x^3 y^3 \\
&= x y^3 + (4m + 4l + 1)x^2 y^2 + (12ml + 12m - 2)x^2 y^3 \\
&\quad + (18ml + 9m - 6l - 4)x^3 y^3.
\end{aligned} \tag{20}$$

□

**Proposition 1.** For cellulose network  $CL_m^n$ , the formulas for the modified second Zagreb, inverse Randić, harmonic, inverse sum, and augmented Zagreb indices are

$$(1) {}^m Z_2(CL_m^n) = 4ml + 4m + (l/3) - (7/36)$$

$$(2) RR_\alpha(CL_m^n) = 2(6^{1-\alpha} + 9^{1-\alpha})ml + (4^{1-\alpha} + 2 \times 6^{1-\alpha} + 9^{1-\alpha})m + (4^{1-\alpha} - 6 \times 9^{-\alpha})l + (3^{-\alpha} + 4^{-\alpha} - 2 \times 6^{-\alpha} - 4 \times 9^{-\alpha})$$

$$(3) HI(CL_m^n) = (54/5)ml + (49/5)m - (17/15)$$

$$(4) ISI(CL_m^n) = (207/5)ml + (319/10)m - 5l - (133/20)$$

$$(5) AZI(CL_m^n) = (9633/32)ml + (14753/64)m - (1163/32)l - (803/16)$$

*Proof.* Consider the  $M$ -polynomial derived in Theorem 3:

$$M(CL_m^n; x, y) = xy^3 + (4m + 4l + 1)x^2y^2 + (12ml + 12m - 2)x^2y^3 + (18ml + 9m - 6l - 4)x^3y^3. \quad (21)$$

First, we apply the combination of operators given in derivation Table 1 on the above polynomial as follows:

$$(S_x S_y)M(x, y) = \frac{1}{3}xy^3 + \frac{1}{4}(4m + 4l + 1)x^2y^2 + \frac{1}{6}(12ml + 12m - 2)x^2y^3 + \frac{1}{9}(18ml + 9m - 6l - 4)x^3y^3,$$

$$S_x^\alpha S_y^\alpha M(x, y) = \frac{1}{3^\alpha}xy^3 + \frac{1}{4^\alpha}(4m + 4l + 1)x^2y^2 + \frac{1}{6^\alpha}(12ml + 12m - 2)x^2y^3 + \frac{1}{9^\alpha}(18ml + 9m - 6l - 4)x^3y^3,$$

$$S_x J M(x, y) = \frac{1}{2}(2m + 2l + 1)x^4 + \frac{2}{5}(6ml + 6m - 1)x^5 + \frac{1}{6}(18ml + 9m - 6l - 4)x^6, \quad (22)$$

$$S_x J D_x D_y M(x, y) = \left(4m + 4l + \frac{7}{4}\right)x^4 + \frac{6}{5}(12ml + 12m - 2)x^5 + \frac{3}{2}(18ml + 9m - 6l - 4)x^6,$$

$$S_x^3 Q_{-2} J D_x^3 D_y^3 M(x, y) = \left(32m + 32l + \frac{91}{8}\right)x^2 + \frac{216}{27}(12ml + 12m - 2)x^3 + \frac{729}{64}(18ml + 9m - 6l - 4)x^4.$$

- (1) Modified second Zagreb index =  $(S_x S_y)M|_{x=y=1} = 4ml + 4m + (l/3) - (7/36)$
- (2) Inverse Randić index =  $(S_x^\alpha \cdot S_y^\alpha)M|_{x=y=1} = 2(6^{1-\alpha} + 9^{1-\alpha})ml + (4^{1-\alpha} + 2 \times 6^{1-\alpha} + 9^{1-\alpha})m + (4^{1-\alpha} - 6 \times 9^{-\alpha})l + (3^{-\alpha} + 4^{-\alpha} - 2 \times 6^{-\alpha} - 4 \times 9^{-\alpha})$
- (3) Harmonic index =  $2S_x J M(x)|_{x=1} = (54/5)ml + (49/5)m - (17/15)$
- (4) Inverse sum index =  $S_x J D_x D_y M|_{x=1} = (207/5)ml + (319/10)m - 5l - (133/20)$
- (5) Augmented Zagreb index =  $S_x^3 Q_{-2} J D_x^3 D_y^3 M|_{x=1} = (9633/32)ml + (14753/64)m - (1163/32)l - (803/16)$

To compute  $ABC_4(CL_m^n)$ ,  $GA_5(CL_m^n)$ , and  $SI(CL_m^n)$ , we need the partitioning of edge set  $E(CL_m^n)$  with respect to neighbor's degree sum of end vertices for cellulose network  $CL_m^n$ . We observe and identify eight different kinds of edges in  $CL_m^n$ . Now, the partition of the edge set of  $CL_m^n$  with respect to the degree-sum of the neighbors of the end vertices of each edge is summarized in Table 4.  $\square$

**Theorem 4.** Let  $CL_m^n$  be a cellulose network having  $m$  hexagonal chains and  $n = 4l + 3$  hexagons in each chain; then,  $ABC_4$ ,  $GA_5$ , and  $SI$  of  $CL_m^n$  are given as follows:

(1)

$$ABC_4(CL_m^n) = \frac{1}{126}(12\sqrt{462} + 84\sqrt{2} + 63\sqrt{14} + 84\sqrt{30} + 728)ml$$

$$+ \frac{1}{1260}(504\sqrt{35} + 855\sqrt{14} + 63\sqrt{110} + 150\sqrt{462} + 90\sqrt{182} + 840\sqrt{2} + 210\sqrt{30} + 4130)m$$

$$+ \frac{1}{315}(126\sqrt{35} + 450\sqrt{14} + 63\sqrt{110} - 30\sqrt{462} - 210\sqrt{2} - 210\sqrt{3} - 560)l$$

$$+ \frac{1}{2520}(1185\sqrt{14} - 672\sqrt{2} - 126\sqrt{110} + 420\sqrt{10} - 300\sqrt{462} - 90\sqrt{182} - 420\sqrt{30} - 980).$$

TABLE 4: Partitioning of the edge set with respect to neighbor's degree sum of end vertices for  $CL_m^n$ .

$(s_v, s_w): vw \in E(CL_m^n)$	Number of edges
(3, 6)	1
(4, 5)	$4(m + l)$
(5, 5)	1
(5, 7)	$3(m + 1)$
(5, 8)	$m + 4l - 1$
(6, 6)	1
(6, 7)	$4ml + 5m - 4l - 5$
(6, 8)	$8ml + 3m + 1$
(7, 8)	$2m + 1$
(7, 9)	$2ml + 2m - 2l - 2$
(8, 8)	$4ml + 2m + 8l - 1$
(8, 9)	$8ml + 2m - 8l - 2$
(9, 9)	$4ml + m - 4l - 1$
Total edges	$30ml + 25m - 2l - 4$

(2)

$$\begin{aligned}
 GA_5(CL_m^n) = & \frac{1}{6188} (3808\sqrt{42} + 28288\sqrt{3} + 4641\sqrt{7} + 34944\sqrt{2} + 49504)ml \\
 & + \frac{1}{278460} (495040\sqrt{5} + 139230\sqrt{35} + 85680\sqrt{10} + 214200\sqrt{42} \\
 & + 477360\sqrt{3} + 148512\sqrt{14} + 208845\sqrt{7} + 393120\sqrt{2} + 835380)m \\
 & + \frac{1}{7956} (14144\sqrt{5} + 9792\sqrt{10} - 4896\sqrt{42} - 5967\sqrt{7} - 44928\sqrt{2} + 31824)l \\
 & + \frac{1}{92820} (53040\sqrt{3} - 69160\sqrt{2} + 46410\sqrt{35} - 28560\sqrt{10} - 71400\sqrt{42} + 24752\sqrt{14} - 69615\sqrt{7} - 92820).
 \end{aligned} \tag{24}$$

(3)

$$\begin{aligned}
 SI(CL_m^n) = & \left( \frac{157939036549489}{58436224000} \right) ml + \left( \frac{821225692630075333}{513537536512000} \right) m - \left( \frac{45814497669489}{58436224000} \right) l \\
 & - \left( \frac{26341741253143399}{36681252608000} \right).
 \end{aligned} \tag{25}$$

*Proof.* Using equation (10) and edge partition presented in Table 5, we proceed as follows:

$$\begin{aligned}
 1 ABC_4(CL_m^n) = & \sum_{vw \in E(CL_m^n)} \sqrt{\frac{s_v + s_w - 2}{s_v s_w}} = |E_{36}| \sqrt{\frac{7}{18}} \\
 & + |E_{45}| \sqrt{\frac{7}{20}} + |E_{55}| \sqrt{\frac{8}{25}} + |E_{57}| \sqrt{\frac{10}{35}} + |E_{58}| \sqrt{\frac{11}{40}} \\
 & + |E_{66}| \sqrt{\frac{10}{36}} + |E_{67}| \sqrt{\frac{11}{42}} + |E_{68}| \sqrt{\frac{12}{48}} + |E_{78}| \sqrt{\frac{13}{56}} \\
 & + |E_{79}| \sqrt{\frac{14}{63}} + |E_{88}| \sqrt{\frac{14}{64}} + |E_{89}| \sqrt{\frac{15}{72}} + |E_{99}| \sqrt{\frac{16}{81}} \\
 = & \sqrt{\frac{7}{18}} + \sqrt{\frac{7}{20}}(4m + 4l) + \frac{2\sqrt{2}}{5} + \sqrt{\frac{2}{7}}(3m + 3) + \sqrt{\frac{11}{40}}(m + 4l - 1) \\
 & + \sqrt{\frac{11}{42}}(4ml + 5m - 4l - 5) + \frac{1}{2}(8ml + 3m + 1) + \sqrt{\frac{13}{56}}(2m - 1)
 \end{aligned}$$

TABLE 5: Partitioning of the edge set with respect to neighbor's degree sum of end vertices for  $GL_m^l$ .

$(s_v, s_w): vw \in E(GL_m^l)$	Number of edges
(3, 5)	$m + 1$
(3, 6)	$8m + ml - l - 1$
(4, 5)	$2m + 2$
(5, 5)	$11m + ml - l - 1$
(5, 6)	$12m + ml - l$
(5, 7)	$10m + ml - l - 2$
(6, 6)	$28m + 3ml - 3l - 4$
(6, 7)	$17m + 2ml - 2l + 1$
(7, 7)	$m - 1$
Total edges	$9m(l + 10) - 9l - 5$

$$\begin{aligned}
& + \sqrt{\frac{5}{18}} + \sqrt{\frac{14}{63}}(2ml + 2m - 2l - 2) + \sqrt{\frac{7}{32}}(4ml + 2m + 8l - 1) \\
& + \sqrt{\frac{15}{72}}(8ml + 2m - 8l - 2) + \frac{4}{9}(4ml + m - 4l - 2) \\
= & \frac{1}{126}(12\sqrt{462} + 84\sqrt{2} + 63\sqrt{14} + 84\sqrt{30} + 728)ml + \frac{1}{1260}(504\sqrt{35} \\
& + 855\sqrt{14} + 63\sqrt{110} + 150\sqrt{462} + 90\sqrt{182} + 840\sqrt{2} + 210\sqrt{30} + 4130)m \\
& + \frac{1}{315}(126\sqrt{35} + 450\sqrt{14} + 63\sqrt{110} - 30\sqrt{462} - 210\sqrt{2} - 210\sqrt{3} - 560)l \\
& + \frac{1}{2520}(1185\sqrt{14} - 672\sqrt{2} - 126\sqrt{110} + 420\sqrt{10} - 300\sqrt{462} - 90\sqrt{182} - 420\sqrt{30} - 980).
\end{aligned} \tag{26}$$

Employing equation (11) and edge partition presented in Table 5, we compute the result in the following manner:

$$\begin{aligned}
2GA_5(CL_m^n) &= \sum_{vw \in E(CL_m^n)} \frac{2\sqrt{s_v s_w}}{s_v + s_w} = |E_{36}| \left( \frac{2\sqrt{18}}{9} \right) \\
& + |E_{45}| \left( \frac{2\sqrt{20}}{9} \right) + |E_{55}| \left( \frac{2\sqrt{25}}{10} \right) + |E_{57}| \left( \frac{2\sqrt{35}}{12} \right) + |E_{58}| \left( \frac{2\sqrt{40}}{13} \right) \\
& + |E_{66}| \left( \frac{2\sqrt{36}}{12} \right) + |E_{67}| \left( \frac{2\sqrt{42}}{13} \right) + |E_{68}| \left( \frac{2\sqrt{48}}{14} \right) + |E_{78}| \left( \frac{2\sqrt{56}}{15} \right) \\
& + |E_{79}| \left( \frac{2\sqrt{63}}{16} \right) + |E_{88}| \left( \frac{2\sqrt{64}}{16} \right) + |E_{89}| \left( \frac{2\sqrt{72}}{17} \right) + |E_{99}| \left( \frac{2\sqrt{81}}{18} \right) \\
= & \left( \frac{2\sqrt{2}}{3} \right) + \left( \frac{4\sqrt{5}}{9} \right) (4m + 4l) + 1 + \left( \frac{\sqrt{35}}{6} \right) (3m + 3) + \left( \frac{4\sqrt{10}}{13} \right) (m + 4l - 1) \\
& + 1 + \left( \frac{2\sqrt{42}}{13} \right) (4ml - 5m - 4l - 5) + \left( \frac{4\sqrt{3}}{7} \right) (8ml + 3m + 1) \\
& + \left( \frac{4\sqrt{14}}{15} \right) (2m + 1) + \left( \frac{\sqrt{63}}{8} \right) (2ml + 2m - 2l - 2) + (4ml + 2m + 8l - 1) \\
& + \left( \frac{12\sqrt{2}}{17} \right) (8ml + 2m - 8l - 2) + (4ml + m - 4l - 2)
\end{aligned}$$

$$\begin{aligned}
&= \frac{1}{6188} (3808\sqrt{42} + 28288\sqrt{3} + 4641\sqrt{7} + 34944\sqrt{2} + 49504)ml \\
&+ \frac{1}{278460} (495040\sqrt{5} + 139230\sqrt{35} + 85680\sqrt{10} + 214200\sqrt{42} + 477360\sqrt{3} \\
&+ 148512\sqrt{14} + 208845\sqrt{7} + 393120\sqrt{2} + 835380)m \\
&+ \frac{1}{7956} (14144\sqrt{5} + 9792\sqrt{10} - 4896\sqrt{42} - 5967\sqrt{7} - 44928\sqrt{2} + 31824)l \\
&+ \frac{1}{92820} (53040\sqrt{3} - 69160\sqrt{2} + 46410\sqrt{35} - 28560\sqrt{10} - 71400\sqrt{42} + 24752\sqrt{14} - 69615\sqrt{7} - 92820).
\end{aligned} \tag{27}$$

The Sanskruti index  $SI(CL_m^n)$  can be calculated as

$$\begin{aligned}
3 SI(CL_m^n) &= \sum_{vw \in E(CL_m^n)} \left( \frac{s_v s_w}{s_v + s_w - 2} \right)^3 = |E_{36}| \left( \frac{18}{7} \right)^3 \\
&+ |E_{45}| \left( \frac{20}{7} \right)^3 + |E_{55}| \left( \frac{25}{8} \right)^3 + |E_{57}| \left( \frac{35}{10} \right)^3 + |E_{58}| \left( \frac{40}{11} \right)^3 \\
&+ |E_{66}| \left( \frac{36}{10} \right)^3 + |E_{67}| \left( \frac{42}{11} \right)^3 + |E_{68}| \left( \frac{48}{12} \right)^3 + |E_{78}| \left( \frac{56}{13} \right)^3 \\
&+ |E_{79}| \left( \frac{63}{14} \right)^3 + |E_{88}| \left( \frac{64}{14} \right)^3 + |E_{89}| \left( \frac{72}{15} \right)^3 + |E_{99}| \left( \frac{81}{16} \right)^3 \\
&= \left( \frac{18}{7} \right)^3 + \left( \frac{20}{7} \right)^3 (4m + 4l) + \left( \frac{25}{8} \right)^3 + \left( \frac{7}{2} \right)^3 (3m + 3) + \left( \frac{40}{11} \right)^3 (m + 4l - 1) \\
&+ \left( \frac{18}{5} \right)^3 + \left( \frac{42}{11} \right)^3 (4ml + 5m - 4l - 5) + 64(8ml + 3m + 1) + \left( \frac{56}{13} \right)^3 (2m + 1) \\
&+ \left( \frac{63}{14} \right)^3 (2ml + 2m - 2l - 2) + \left( \frac{32}{7} \right)^3 (4ml + 2m + 8l - 1) \\
&+ \left( \frac{24}{5} \right)^3 (8ml + 2m - 8l - 2) + \left( \frac{81}{16} \right)^3 (4ml + m - 4l - 2) \\
&= \left( \frac{157939036549489}{58436224000} \right) ml + \left( \frac{821225692630075333}{513537536512000} \right) m \\
&- \left( \frac{45814497669489}{58436224000} \right) l - \left( \frac{26341741253143399}{36681252608000} \right).
\end{aligned} \tag{28}$$

### 3. Discussion and Construction of the Planar Graph of Glycogen $GL_m^l$ and Amylopectin $AM_m^l$ Networks

In the 19th century, Claude Bernard, a prominent French physiologist, discovered glycogen that mainly resides in the liver and muscles. Natural polymers such as cellulose, chitin, proteins, carbohydrates, and glycogen are a great source of

energy as they are the key component for life to keep going. Glycogen  $(C_6H_{10}O_5)_n$  is a giant, complex, and highly branched polymer consisting of about 30,000 monomers of glucose. It comprises chains of glucose molecules linearly linked via  $\alpha(C_1 - C_4)$  glycosidic linkages, and after every ten to twelve residues, a chain of glucose branches off via  $\alpha(C_1 - C_6)$  glycosidic linkages. This latter kind of bonding creates branching and winding patterns in glycogen. On the contrary, cellulose (a close ally) has  $\beta(C_1 - C_4)$  glycosidic linkages that produce a

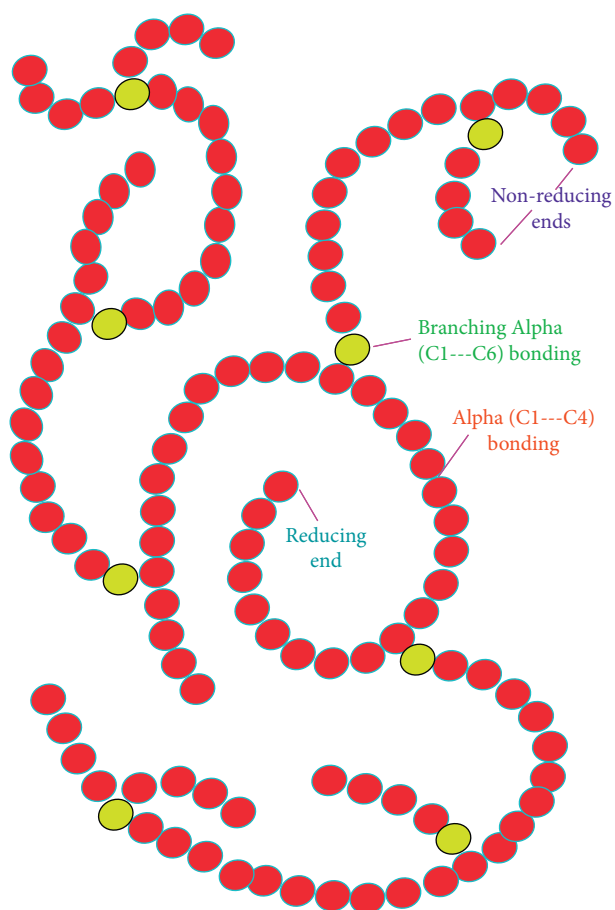


FIGURE 5: Abstract molecular structure of glycogen.

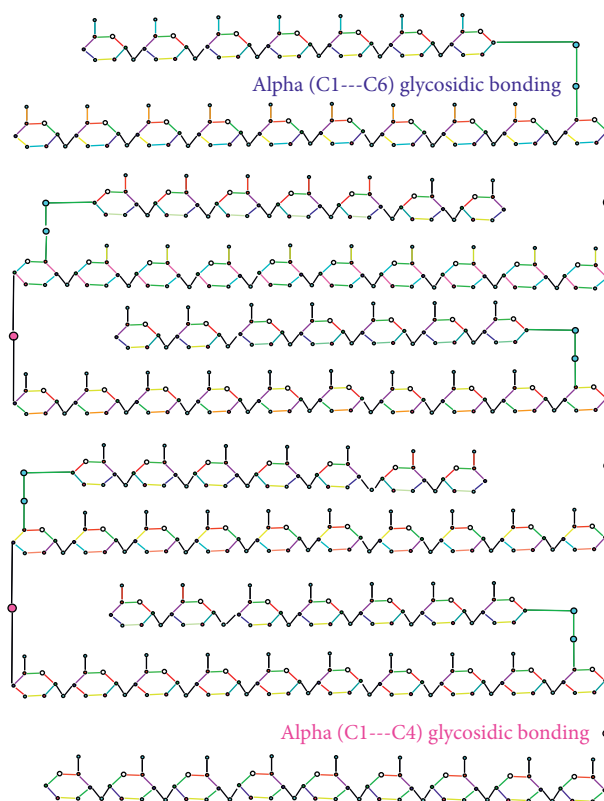


FIGURE 6: Hydrogen-depleted molecular graph of glycogen network  $GL_6^7$ .

more rigid linear chain and hence cannot be broken down in our stomach. Glycogen has only one reducing end, whereas it has plenty of nonreducing ends; see Figure 5. Glycogen molecules contain glucose as the principal storage reservoir in human and animal cells, and when desired, glycogen is readily processed to release glucose. This self-regulating process maintains the amount of glucose in blood at a constant level even though the supply is uneven. The interaction between glycogen and glucose is at the heart of what is commonly interpreted as the Cori cycle (muscle glycogen  $\rightarrow$  blood lactic acid  $\rightarrow$  liver glycogen  $\rightarrow$  blood glucose  $\rightarrow$  muscle glycogen). Although sufficient investigation has been performed about the regulation of glycogen metabolism by hormones such as insulin, glucagon, and adrenaline [50–52], however, still it is the subject of extensive investigation. In glycogen, approximately after every 10 glucose residues,  $\alpha(C_1 - C_6)$  glycosidic bonding occurs which creates the branch. The network of our interest  $GL_m^l$  is constructed from the glycogen molecule in such a way that it has  $m - 1$  branches of length  $1 < l < 10$ ; see Figure 6.

Amylopectin is an analog of glycogen that has fewer branches and is less compact as compared to glycogen. The helical branching structure gives an open structure to these molecules; as a result, they are easily accessible by enzymes, and so, they can be broken down or assembled quickly. In amylopectin, approximately after every 20 glucose residues,  $\alpha(C_1 - C_6)$  glycosidic bonding occurs which creates the branch. The network of our interest  $AM_m^l$  is constructed from the amylopectin molecule in such a way that it has  $m - 1$  branches of length  $1 < l < 20$ .

**3.1. Results for Glycogen Network  $GL_m^l$  and Amylopectin Network  $AM_m^l$ .** The following lemmas manifest some basic structural properties of the glycogen and amylopectin networks and are essential for upcoming results.

**Lemma 1.** *Let  $GL_m^l$  be the glycogen network shown in Figure 6, with  $m - 1$  branches each of length  $l$ ; then, the total*

*number of vertices and edges is  $8m(l + 10) - 8l - 9$  and  $9m(l + 10) - 9l - 11$ , respectively.*

*Proof.* Suppose  $V_{\text{deg}}(GL_m^l)$  and  $E_{xy}(GL_m^l)$  denote the vertex set and edge set partition and are defined as  $V_d = \{u \in V(GL_m^l) | d_u = \text{deg}\}$  and  $E_{xy}(GL_m^l) = \{uv \in E(GL_m^l) | (d_u, d_v) = (x, y)\}$ , respectively. In the molecular graph of glycogen network  $GL_m^l$ , we recognize three kinds of vertices with degrees 1, 2, and 3, i.e.,  $\delta(GL_m^l) = 1$  and  $\Delta(GL_m^l) = 3$ . By applying the basic counting principle, we acquire the partition of the vertex set, and it is presented as  $|V_1| = m(9 + l) - l$ ,  $|V_2| = 42m + 4ml - 4l - 2$ , and  $|V_3| = 29m + 3ml - 3l - 2$ . Subsequently, the total number of vertices  $|V(GL_m^l)|$  of the glycogen network is  $8m(l + 10) - 8l - 4$ . Similarly, we identify four types of edges in  $GL_m^l$  with respect to degrees of end vertices of each edge. Again, employing the basic counting principle, we get the partition of the edge set, and it is given as  $|E_{13}| = 9m + ml - l$ ,  $|E_{22}| = 12m + ml - l$ ,  $|E_{23}| = 60m + 6ml - 6l - 4$ , and  $|E_{33}| = 9m + ml - l - 1$ . Therefore, the total number of edges  $|E(GL_m^l)|$  is  $9m(l + 10) - 9l - 5$ .

Lemma 2 reveals some basic properties of the amylopectin network that are of utmost importance for promising results. Note that we skip the proofs of results for the amylopectin network as they would have been attained by working on the same lines as for the glycogen network.  $\square$

**Lemma 2.** *Let  $AM_m^l$  be the amylopectin network with  $m - 1$  branches each of length  $l$ ; then, the total number of vertices and edges is  $8m(l + 10) - 8l - 4$  and  $9m(l + 10) - 9l - 5$ , respectively.*

Without loss of generality and further use, the vertex set and edge set partition of  $GL_m^l$  and  $AM_m^l$  are illustrated in Tables 6 and 7, respectively.

**Theorem 5.** *Let  $GL_m^l$  be a glycogen network having  $(m - 1)$  branches of length  $l$ , where  $1 < l < 10$ . The formula for  $GZI_{r,s}(GL_m^l)$  is given as*

$$\begin{aligned} Z_{r,s}(GL_m^l) &= (3^{s+1}(3 + 5 \times 2^{r+2}) + 3^{r+1}(3 + 5 \times 2^{s+2}) + 3 \times 2^{r+s+3})m \\ &\quad + (3^r(1 + 3^s) + 3^s(1 + 53^r) + 2^{r+1} \times 2^{s+1})(m - 1) \\ &\quad + (2^{r+2} \times 3^s - 2^{s+2} \times 3^r - 2 \times 3^{r+s}). \end{aligned} \quad (29)$$

*Proof.* Employing equation (7) and using Table 6, we obtain the desired result as follows:

$$\begin{aligned} Z_{r,s}(GL_m^l) &= \sum_{vw \in E(GL_m^l)} (d_v^r d_w^s + d_w^r d_v^s) = \sum_{vw \in E_{13}} (d_v^r d_w^s + d_w^r d_v^s) + \sum_{vw \in E_{22}} (d_v^r d_w^s + d_w^r d_v^s) \\ &\quad + \sum_{vw \in E_{23}} (d_v^r d_w^s + d_w^r d_v^s) + \sum_{vw \in E_{33}} (d_v^r d_w^s + d_w^r d_v^s) \end{aligned}$$

TABLE 6: Degree-based partitioning of the vertex set and edge set for  $GL_m^l$ .

$d_v: v \in V(GL_m^l)$	Number of vertices	$(d_v, d_w): vw \in E(GL_m^l)$	Number of edges
1	$m(9+l) - l$	(1, 3)	$9m + ml - l$
2	$42m + 4ml - 4l - 2$	(2, 2)	$12m + ml - l$
3	$29m + 3ml - 3l - 2$	(2, 3)	$60m + 6ml - 6l - 4$
		(3, 3)	$9m + ml - l - 1$
Total vertices	$8m(l+10) - 8l - 4$	Total edges	$9m(l+10) - 9l - 5$

TABLE 7: Partitioning of the edge set with respect to the degree of end vertices for  $AM_m^l$ .

$d_v: v \in V(AM_m^l)$	Number of vertices	$(d_v, d_w): vw \in E(AM_m^l)$	Number of edges
1	$19m + ml - l$	(1, 3)	$19m + ml - l$
2	$82m + 4ml - 4l - 2$	(2, 2)	$22m + ml - l$
3	$59m + 3ml - 3l - 2$	(2, 3)	$120m + 6ml - 6l - 4$
		(3, 3)	$19m + ml - l - 1$
Total vertices	$160m + 8ml - 8l - 4$	Total edges	$180m + 9ml - 9l - 5$

$$\begin{aligned}
&= (9m + ml - l)(3^s + 3^r) + (12m + ml - l)(2^r 2^s + 2^r 2^s) \\
&\quad + (60m + 6ml - 6l - 4)(2^r 3^s + 3^r 2^s) + (9m + ml - l - 1)(3^r 3^s + 3^r 3^s) \\
&= (3^{r+2} + 3^{s+2} + 3 \times 2^{r+s+3} + 60(2^r 3^s + 3^r 2^s) + 2 \times 3^{r+s+2})m \\
&\quad + (3^r + 3^s + 2^{r+s+1} + 6(2^r 3^s + 3^r 2^s) + 2 \times 3^{r+s})(ml - l) \\
&\quad + (2^{r+2} \times 3^s - 2^{s+2} \times 3^r - 3^{r+s+1}) \\
&= (3^{s+1}(3 + 5 \times 2^{r+2}) + 3^{r+1}(3 + 5 \times 2^{s+2}) + 3 \times 2^{r+s+3})m \\
&\quad + (3^r(1 + 3^s) + 3^s(1 + 5 \times 3^r) + 2^{r+1} \times 2^{s+1})(m - 1)l \\
&\quad + (2^{r+2} \times 3^s - 2^{s+2} \times 3^r - 2 \times 3^{r+s}).
\end{aligned}$$

(30)

□

**Corollary 2.** From equation (30) of the GZI, we derived the following results of different TIs presented in Table 2:

- (1)  $M_1(GL_m^l) = Z_{1,0}(GL_m^l) = 438m + 44l(m - 1) - 26$
- (2)  $M_2(GL_m^l) = (1/2)Z_{1,1}(GL_m^l) = 516m + 52l(m - 1) - 33$
- (3)  $F(GL_m^l) = Z_{2,0}(GL_m^l) = 1128m + 114l(m - 1) - 70$
- (4)  $ReZM(GL_m^l) = Z_{2,1}(GL_m^l) = 2586m + 262l(m - 1) - 174$
- (5)  $M^\alpha(GL_m^l) = Z_{\alpha-1,0}(GL_m^l) = (42 \times 2^\alpha + 29 \times 3^\alpha + 9)m + (2^{\alpha+2} + 3^{\alpha+1} + 1)(m - 1)l - (2^{\alpha+1} + 2 \times 3^{\alpha+1})$

- (6)  $R_\alpha(GL_m^l) = (1/2)Z_{\alpha,\alpha}(GL_m^l) = (3 \times 2^{2\alpha+2} + 3^{\alpha+2}(1 + 3^\alpha) + 10 \times 6^{\alpha+1})m + (2^{2\alpha} + 3^\alpha(1 + 3^\alpha) + 6^{\alpha+1})(m - 1)l - (2^{\alpha+3} \times 3^\alpha + 2 \times 3^{2\alpha})$
- (7)  $SDD(GL_m^l) = Z_{1,-1}(GL_m^l) = 202m + (61/3)(m - 1)l - (32/3)$

**Theorem 6.** Let  $AM_m^l$  be an amylopectin network having  $(m - 1)$  branches of length  $l$ , where  $1 < l < 10$ . The formula for GZI  $Z_{r,s}(AM_m^l)$  is given as

$$\begin{aligned}
Z_{r,s}(AM_m^l) &= (19(3^r + 3^s) + 11 \times 2^{r+s+2} + 5(2^{r+3}3^{s+1} + 3^{r+1}2^{s+3}) + 2 \times 3^{r+s+2})m \\
&\quad + (3^r(1 + 3 \times 2^{s+1}) + 3^s(1 + 3 \times 2^{r+1}) \\
&\quad + 2(2^{r+s} + 3^{r+s}))(m - 1)l - 2 \times 3^r(2^{s+1} + 3^s(2^{r+1} + 1)).
\end{aligned}$$

(31)

**Corollary 3.** From equation (31) of the generalized Zagreb index, we derived the following results of different TIs:

- (1)  $M_1(AM_m^l) = Z_{1,0}(AM_m^l) = 878m + 44l(m-1) - 26$
- (2)  $M_2(AM_m^l) = (1/2)Z_{1,1}(AM_m^l) = 1036m + 52l(m-1) - 33$
- (3)  $F(AM_m^l) = Z_{2,0}(AM_m^l) = 2268m + 114l(m-1) - 70$
- (4)  $ReZM(AM_m^l) = Z_{2,1}(AM_m^l) = 5206m + 262l(m-1) - 174$
- (5)  $M^\alpha(AM_m^l) = Z_{\alpha-1,0}(AM_m^l) = (41 \times 2^{\alpha+1} + 177 \times 3^{\alpha-1} + 19)m + (2^{\alpha+2} + 3^{\alpha+1} + 1)(m-1)l - (2^{\alpha+1} + 2 \times 3^\alpha)$
- (6)  $R_\alpha(AM_m^l) = (1/2)Z_{\alpha,\alpha}(AM_m^l) = (38 \times 3^\alpha(1 + 3^\alpha) + 2^{\alpha+2}(11 \times 2^\alpha + 20 \times 3^{\alpha+1}))m + (2^{2\alpha+1} + 2 \times 3^\alpha(1 + 3^\alpha + 3 \times 2^{\alpha+1}))(m-1)l - 2 \times 3^\alpha(2^{\alpha+2} + 3^\alpha)$
- (7)  $SDD(AM_m^l) = Z_{1,-1}(AM_m^l) = (1216/3)m + (61/3)(m-1)l - (32/3)$

**Theorem 7.** Let  $GL_m^l$  be a glycogen network having  $(m-1)$  branches of length  $l$ , where  $1 < l < 10$ ; then,

- (1)  $ABC(GL_m^l) = 3(12\sqrt{2} + \sqrt{6} + 2)m + (1/6)(21\sqrt{2} + 2\sqrt{6} + 4)(m-1)l - ((6\sqrt{2} + 2)/3)$
- (2)  $GA(GL_m^l) = ((9\sqrt{3}/2) + 24\sqrt{6} + 21)m + ((12\sqrt{6}/5) + (\sqrt{3}/2 + 2)(m-1)l - ((8\sqrt{6} - 5)/5))$
- (3)  $SCI(GL_m^l) = \chi_{(-1/2)}(GL_m^l) = ((21/2) + 3\sqrt{(3/2)} + 12\sqrt{5})m + ((6/\sqrt{5}) + (1/\sqrt{6}) + 1)(m-1)l + ((5\sqrt{6} - 24\sqrt{5})/30)$

*Proof.* Using Table 6 and equations (8), (9), and (5), respectively, we compute the desired result as given in the following:

$$\begin{aligned}
 (1) \text{ABC}(GL_m^l) &= \sum_{uv \in E(GL_m^l)} \sqrt{\frac{d_u + d_v - 2}{d_u d_v}} = \sum_{uv \in E_{13}(GL_m^l)} \sqrt{\frac{d_u + d_v - 2}{d_u d_v}} \\
 &+ \sum_{uv \in E_{22}(GL_m^l)} \sqrt{\frac{d_u + d_v - 2}{d_u d_v}} + \sum_{uv \in E_{23}(GL_m^l)} \sqrt{\frac{d_u + d_v - 2}{d_u d_v}} \\
 &+ \sum_{uv \in E_{33}(GL_m^l)} \sqrt{\frac{d_u + d_v - 2}{d_u d_v}} \\
 &= (9m + ml - l)\sqrt{\frac{2}{3}} + (12m + ml - l)\sqrt{\frac{2}{4}} + (60m + 6ml - 6l - 4)\sqrt{\frac{3}{6}} \\
 &+ (9m + ml - l - 1)\sqrt{\frac{4}{9}} \\
 &= 3(12\sqrt{2} + \sqrt{6} + 2)m + \frac{1}{6}(21\sqrt{2} + 2\sqrt{6} + 4)(m-1)l - \left(\frac{6\sqrt{2} + 2}{3}\right), \\
 (2) \text{GA}(GL_m^l) &= \sum_{uv \in E(GL_m^l)} \frac{2\sqrt{d_u d_v}}{d_u + d_v} = \sum_{uv \in E_{13}(GL_m^l)} \frac{2\sqrt{d_u d_v}}{d_u + d_v} + \sum_{uv \in E_{22}(GL_m^l)} \frac{2\sqrt{d_u d_v}}{d_u + d_v} \\
 &+ \sum_{uv \in E_{23}(GL_m^l)} \frac{2\sqrt{d_u d_v}}{d_u + d_v} + \sum_{uv \in E_{33}(GL_m^l)} \frac{2\sqrt{d_u d_v}}{d_u + d_v} \\
 &= \left(\frac{2\sqrt{3}}{4}\right)(9m + ml - l) + (12m + ml - l)\left(\frac{2\sqrt{4}}{4}\right) + (60m + 6ml - 6l - 4)\left(\frac{2\sqrt{6}}{5}\right) \\
 &+ (9m + ml - l - 1)\left(\frac{2\sqrt{9}}{6}\right) \\
 &= \left(\frac{9\sqrt{3}}{2} + 24\sqrt{6} + 21\right)m + \left(\frac{12\sqrt{6}}{5} + \frac{\sqrt{3}}{2} + 2\right)(m-1)l - \left(\frac{8\sqrt{6} - 5}{5}\right),
 \end{aligned}$$

$$\begin{aligned}
(3) \chi_{(-1/2)}(GL_m^l) &= \sum_{uv \in E(GL_m^l)} \frac{1}{\sqrt{d_u + d_v}} = \sum_{uv \in E_{13}(GL_m^l)} \frac{1}{\sqrt{d_u + d_v}} + \sum_{uv \in E_{22}(GL_m^l)} \frac{1}{\sqrt{d_u + d_v}} \\
&+ \sum_{uv \in E_{23}(GL_m^l)} \frac{1}{\sqrt{d_u + d_v}} + \sum_{uv \in E_{33}(GL_m^l)} \frac{1}{\sqrt{d_u + d_v}} \\
&= \frac{1}{\sqrt{4}} (9m + ml - l) + \frac{1}{\sqrt{4}} (12m + ml - l) + \frac{1}{\sqrt{5}} (60m + 6ml - 6l - 4) \\
&+ \frac{1}{\sqrt{6}} (9m + ml - l - 1) \\
&= \left( \frac{21}{2} + 3\sqrt{\frac{3}{2}} + 12\sqrt{5} \right) m + \left( \frac{6}{\sqrt{5}} + \frac{1}{\sqrt{6}} + 1 \right) (m - 1)l + \left( \frac{5\sqrt{6} - 24\sqrt{5}}{30} \right).
\end{aligned} \tag{32}$$

□

**Theorem 8.** Let  $AM_m^l$  be an amylopectin network having  $(m - 1)$  branches of length  $l$ , where  $1 < l < 10$ ; then,

- (1)  $ABC(AM_m^l) = (38 + 213\sqrt{2} + 19\sqrt{6})(m/3) + (4 + 21\sqrt{2} + 2\sqrt{6})((m - 1)l/6) + (3\sqrt{2} + 1)(2/3)$
- (2)  $GA(AM_m^l) = (19\sqrt{3} + 96\sqrt{6} + 82)(m/2) + (5\sqrt{3} + 24\sqrt{6} + 20)((m - 1)l/10) - ((8\sqrt{6} + 5)/5)$
- (3)  $SCI(AM_m^l) = \chi_{-1/2}(AM_m^l) = (144\sqrt{5} + 19\sqrt{6} + 123)(m/6) + (30\sqrt{5} + 5\sqrt{6} + 30)((m - 1)l/30) + ((24\sqrt{5} + 5\sqrt{6})/30)$

In the next theorem, we compute the  $M$ -polynomial of glycogen network  $GL_m^l$ , which will eventually be used to formulate closed-form formulas of certain TIs of our interest.

**Theorem 9.** Let  $GL_m^l$  be the glycogen network consisting of  $(m - 1)$  branches where each branch has length  $l$ ; then,  $M$ -polynomial of  $GL_m^l$  is

$$M(GL_m^l; x, y) = (9m + ml - l)xy^3 + (12m + ml - l)x^2y^2 + (60m + 6ml - 6l - 4)x^2y^3 + (9m + ml - l - 1)x^3y^3. \tag{33}$$

*Proof.* To calculate the  $M$ -polynomial of  $GL_m^l$ , we apply equation (15):

$$\begin{aligned}
M(GL_m^l; x, y) &= \sum_{\delta \leq i \leq j \leq \Delta} M_{ij} x^i y^j = \sum_{1 \leq 3} M_{13} x y^3 + \sum_{2 \leq 2} M_{22} x^2 y^2 + \sum_{2 \leq 3} M_{23} x^2 y^3 + \sum_{3 \leq 3} M_{33} x^3 y^3 \\
&= |E_{13}(GL_m^l)| x y^3 + |E_{22}(GL_m^l)| x^2 y^2 + |E_{23}(GL_m^l)| x^2 y^3 + |E_{33}(GL_m^l)| x^3 y^3 \\
&= (9m + ml - l)xy^3 + (12m + ml - l)x^2y^2 + (60m + 6ml - 6l - 4)x^2y^3 + (9m + ml - l - 1)x^3y^3.
\end{aligned} \tag{34}$$

□

**Proposition 2.** For glycogen network  $GL_m^l$ , formulas for the modified second Zagreb index, inverse Randić index, symmetric division degree index, harmonic index, inverse sum index, and augmented Zagreb index are as follows:

- (1)  ${}^m Z_2(GL_m^l) = 17m + (61/36)(m - 1)l - (7/9)$
- (2)  $RR_\alpha(GL_m^l) = (3^{2-\alpha} + 3 \times 4^{1-\alpha} + 10 \times 6^{1-\alpha} + 9^{1-\alpha})m + (6^{1-\alpha} + 9^{1-\alpha} + (1/3^\alpha) + (1/4^\alpha))(m - 1)l - ((4/6^\alpha) + (1/9^\alpha))$

$$(3) HI(GL_m^l) = (75/2)m + (56/15)(m - 1)l - (29/15)$$

$$(4) ISI(GL_m^l) = (417/4)m + (209/20)(m - 1)l - (63/10)$$

$$(5) AZI(GL_m^l) = (45369/64)m + (4529/64)(m - 1)l - (2777/64)$$

*Proof.* Consider the  $M$ -polynomial derived in Theorem 9:

$$M(GL_m^l; x, y) = (9m + ml - l)xy^3 + (12m + ml - l)x^2y^2 + (60m + 6ml - 6l - 4)x^2y^3 + (9m + ml - l - 1)x^3y^3. \tag{35}$$

We apply the combination of operators given in derivation Table 1 on the above polynomial as follows:

$$\begin{aligned}
 (S_x S_y)M(x, y) &= \frac{1}{3} (9m + ml - l)xy^3 + \frac{1}{4} (12m + ml - l)x^2 y^2 \\
 &\quad + \frac{1}{6} (60m + 6ml - 6l - 4)x^2 y^3 + \frac{1}{9} (9m + ml - l - 1)x^3 y^3, \\
 S_x^\alpha S_y^\alpha M(x, y) &= \frac{1}{3^\alpha} (9m + ml - l)xy^3 + \frac{1}{4^\alpha} (12m + ml - l)x^2 y^2 \\
 &\quad + \frac{1}{6^\alpha} (60m + 6ml - 6l - 4)x^2 y^3 + \frac{1}{9^\alpha} (9m + ml - l - 1)x^3 y^3, \\
 2S_x J M(x, y) &= \frac{1}{2} (21m + 2ml - 2l)x^4 + \frac{2}{5} (60m + 6ml - 6l - 4)x^5 + \frac{1}{3} (9m + ml - l - 1)x^6, \\
 S_x J D_x D_y M(x, y) &= \frac{1}{4} (75m + 7ml - 7l)x^4 + \frac{6}{5} (60m + 6ml - 6l - 4)x^5 + \frac{3}{2} (9m + ml - l - 1)x^6, \\
 S_x^3 Q_{-2} J D_x^3 D_y^3 M(x, y) &= \frac{27}{8} (9m + ml - l)x^2 + 8(12m + ml - l)x^2 \\
 &\quad + 8(60m + 6ml - 6l - 4)x^3 + \frac{729}{64} (9m + ml - l - 1)x^4.
 \end{aligned} \tag{36}$$

- (1) Modified second Zagreb index =  $(S_x S_y)M|_{x=y=1} = 17m - (61/36)(m - 1)l - (7/9)$   
 (2) Inverse Randić index =  $(S_x^\alpha \cdot S_y^\alpha)M|_{x=y=1} = (3^{2-\alpha} + 3 \times 4^{1-\alpha} + 10 \times 6^{1-\alpha} + 9^{1-\alpha})m + (6^{1-\alpha} + 9^{1-\alpha} + (1/3^\alpha) + (1/4^\alpha))(m - 1)l - ((4/6^\alpha) + (1/9^\alpha))$   
 (3) Harmonic index =  $2S_x J M(x)|_{x=1} = (75/2)m + (56/15)(m - 1)l - (29/15)$

- (4) Inverse sum index =  $S_x J D_x D_y M|_{x=1} = (417/4)m + (209/20)(m - 1)l - (63/10)$   
 (5) Augmented Zagreb index =  $S_x^3 Q_{-2} J D_x^3 D_y^3 M|_{x=1} = (45369/64)m + (4529/64)(m - 1)l - (2777/64)$  □

**Theorem 10.** Let  $AM_m^l$  be the amylopectin network consisting of  $(m - 1)$  branches where each branch has length  $l$ ; then,  $M$ -polynomial of  $AM_m^l$  is

$$M(AM_m^l; x, y) = (19m + ml - l)xy^3 + (22m + ml - l)x^2 y^2 + (120m + 6ml - 6l - 4)x^2 y^3 + (19m + ml - l - 1)x^3 y^3. \tag{37}$$

**Proposition 3.** For amylopectin network  $AM_m^l$ , formulas for the modified second Zagreb index, inverse Randić index, symmetric division degree index, harmonic index, inverse sum index, and augmented Zagreb index are as follows:

- (1)  ${}^m Z_2(AM_m^l) = (611/18)m - (61/36)(m - 1)l - (7/9)$   
 (2)  $RR_\alpha(AM_m^l) = (19 \times 3^{-\alpha} (1 + 3^{-\alpha}) + 11 \times 2^{1-\alpha} + 20 \times 6^{1-\alpha})m + (3^{-\alpha} (1 + 3^{-\alpha}) + 2^{-2\alpha} + 6^{1-\alpha})(m - 1)l - (4 \times 6^{-\alpha} + 3^{-2\alpha})$   
 (3)  $HI(AM_m^l) = (449/6)m + (56/15)(m - 1)l - (29/15)$   
 (4)  $ISI(AM_m^l) = (835/4)m + (209/20)(m - 1)l - (63/10)$

- (5)  $AZI(AM_m^l) = (90659/64)m + (4529/64)(m - 1)l - (2777/64)$

Again, to calculate  $ABC_4(CL_m^n)$ ,  $GA_5(CL_m^n)$ , and  $SI(CL_m^n)$ , we require the partitioning of edge set  $E(GL_m^l)$  with respect to neighbor's degree sum of end vertices for glycogen network  $GL_m^l$ . We observe and identify eight different types of edges in  $GL_m^l$ . Now, the partition of the edge set of  $GL_m^l$  with respect to the degree-sum of the neighbors of the end vertices of each edge is summarized in Table 5.

TABLE 8: Partitioning of the edge set with respect to neighbor's degree sum of end vertices for  $AM_m^l$ .

$(s_v, s_w): vw \in E(AM_m^l)$	Number of edges
(3, 5)	$m + 1$
(3, 6)	$18m + ml - l - 1$
(4, 5)	$2m + 2$
(5, 5)	$21m + ml - l - 1$
(5, 6)	$22m + ml - l$
(5, 7)	$20m + ml - l - 2$
(6, 6)	$58m + 3ml - 3l - 4$
(6, 7)	$37m + 2ml - 2l + 1$
(7, 7)	$m - 1$
Total edges	$180m + 9ml - 9l - 5$

Similarly, the neighbor's degree sum edge partition for amylopectin is depicted in Table 8.

**Theorem 11.** Let  $GL_m^l$  be the glycogen network consisting of  $(m - 1)$  branches where each branch has length  $l$ ; then,  $ABC_4$ ,  $GA_5$ , and  $SI$  of  $GL_m^l$  are given as follows:

(1)

$$\begin{aligned}
 ABC_4(GL_m^l) &= \frac{1}{210} (1022\sqrt{10} + 580\sqrt{14} + 42\sqrt{35} + 924\sqrt{2} + 252\sqrt{30} + 85\sqrt{462} + 60\sqrt{3})m \\
 &+ \frac{1}{210} (65\sqrt{14} + 84\sqrt{2} + 105\sqrt{10} + 10\sqrt{462} + 21\sqrt{30})(m - 1)l \\
 &+ \frac{1}{210} (42\sqrt{35} - 98\sqrt{10} - 95\sqrt{14} - 168\sqrt{2} + 5\sqrt{462} - 60\sqrt{3}).
 \end{aligned} \tag{38}$$

(2)

$$\begin{aligned}
 GA_5(GL_m^l) &= \frac{1}{5148} (1287\sqrt{15} + 27456\sqrt{2} + 4576\sqrt{5} + 936\sqrt{30} + 8580\sqrt{35} + 13464\sqrt{42} + 205920)m \\
 &+ \frac{1}{858} (572\sqrt{2} - 156\sqrt{30} + 143\sqrt{35} + 264\sqrt{42} + 3432)(m - 1)l \\
 &+ \frac{1}{468} (117\sqrt{15} - 312\sqrt{2} + 416\sqrt{5} - 156\sqrt{35} + 72\sqrt{42} - 2808).
 \end{aligned} \tag{39}$$

(3)

$$SI(GL_m^l) = \left(\frac{2940909850294457}{788889024000}\right)m + \left(\frac{298773851517107}{788889024000}\right)(m - 1)l - \left(\frac{216711945260101}{788889024000}\right). \tag{40}$$

*Proof.* Using equation (10) and edge partition presented in Table 5, we proceed as follows:

$$\begin{aligned}
 (1) ABC_4(GL_m^l) &= \sum_{vw \in E(GL_m^l)} \sqrt{\frac{s_v + s_w - 2}{s_v s_w}} = |E_{35}| \sqrt{\frac{6}{15}} \\
 &+ |E_{36}| \sqrt{\frac{7}{18}} + |E_{45}| \sqrt{\frac{7}{20}} + |E_{55}| \sqrt{\frac{8}{25}} + |E_{56}| \sqrt{\frac{9}{30}}
 \end{aligned}$$

$$\begin{aligned}
& + |E_{57}| \sqrt{\frac{10}{35}} + |E_{66}| \sqrt{\frac{10}{36}} + |E_{67}| \sqrt{\frac{11}{42}} + |E_{77}| \sqrt{\frac{12}{49}} \\
& = \sqrt{\frac{2}{5}}(m+1) + \sqrt{\frac{7}{18}}(8m+ml-l-1) + \sqrt{\frac{7}{20}}(2m+2) \\
& + \sqrt{\frac{8}{5}}(11m+ml-l-2) + \sqrt{\frac{3}{10}}(12m+ml-l) + \sqrt{\frac{2}{7}}(10m+ml-l-2) \\
& + \frac{5}{18}(28m+3ml-3l-4) + \sqrt{\frac{11}{42}}(17m+2ml-2l+1) + \frac{\sqrt{12}}{7}(m-1) \\
& = \frac{1}{210}(1022\sqrt{10} + 580\sqrt{14} + 42\sqrt{35} + 924\sqrt{2} + 252\sqrt{30} + 85\sqrt{462} + 60\sqrt{3})m \\
& + \frac{1}{210}(65\sqrt{14} + 84\sqrt{2} + 105\sqrt{10} + 10\sqrt{462} + 21\sqrt{30})(m-1)l \\
& + \frac{1}{210}(42\sqrt{35} - 98\sqrt{10} - 95\sqrt{14} - 168\sqrt{2} + 5\sqrt{462} - 60\sqrt{3}).
\end{aligned} \tag{41}$$

Employing equation (11) and edge partition presented in Table 5, we compute the result in the following manner:

$$\begin{aligned}
(2) \text{GA}_5(\text{GL}_m^l) &= \sum_{vw \in E(\text{GL}_m^l)} \frac{2\sqrt{s_v s_w}}{s_v + s_w} = |E_{35}| \left( \frac{2\sqrt{15}}{8} \right) \\
& + |E_{36}| \left( \frac{2\sqrt{18}}{9} \right) + |E_{45}| \left( \frac{2\sqrt{20}}{9} \right) + |E_{55}| \left( \frac{2\sqrt{25}}{10} \right) + |E_{56}| \left( \frac{2\sqrt{30}}{11} \right) \\
& + |E_{57}| \left( \frac{2\sqrt{35}}{12} \right) + |E_{66}| \left( \frac{2\sqrt{36}}{12} \right) + |E_{67}| \left( \frac{2\sqrt{42}}{13} \right) + |E_{77}| \left( \frac{2\sqrt{49}}{14} \right) \\
& = \left( \frac{\sqrt{15}}{4} \right)(m+1) + \left( \frac{2\sqrt{2}}{3} \right)(8m+ml-l-1) + \left( \frac{4\sqrt{5}}{9} \right)(2m+2) \\
& + (11m+ml-l-1) + \left( \frac{2\sqrt{30}}{11} \right)(12m+ml-l) + \left( \frac{\sqrt{35}}{6} \right)(10m+ml-l-2) \\
& + (28m+3ml-3l-4) + \left( \frac{2\sqrt{42}}{13} \right)(17m+2ml-2l+1) + (m-1), \\
\text{GA}_5(\text{GL}_m^l) &= \frac{1}{5148}(1287\sqrt{15} + 27456\sqrt{2} + 4576\sqrt{5} + 936\sqrt{30} + 8580\sqrt{35} + 13464\sqrt{42} + 205920)m \\
& + \frac{1}{858}(572\sqrt{2} - 156\sqrt{30} + 143\sqrt{35} + 264\sqrt{42} + 3432)(m-1)l \\
& + \frac{1}{468}(117\sqrt{15} - 312\sqrt{2} + 416\sqrt{5} - 156\sqrt{35} + 72\sqrt{42} - 2808).
\end{aligned} \tag{42}$$

The Sanskruti index  $SI(\text{GL}_m^l)$  can be calculated by using equation (12) as follows:

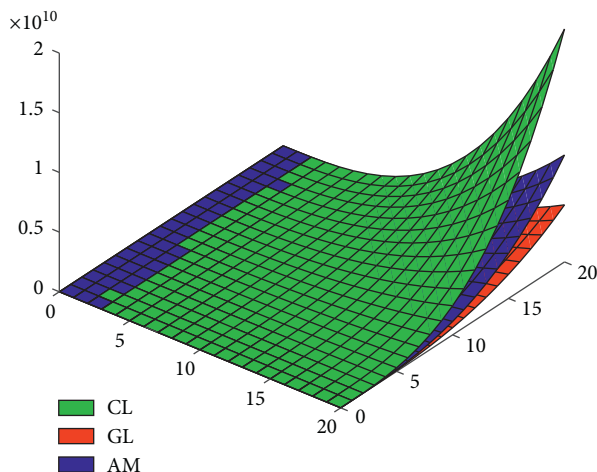


FIGURE 7: 3D graph of the  $M$ -polynomial of  $CL_5^{15}$ ,  $GL_6^3$ , and  $AM_3^5$ .

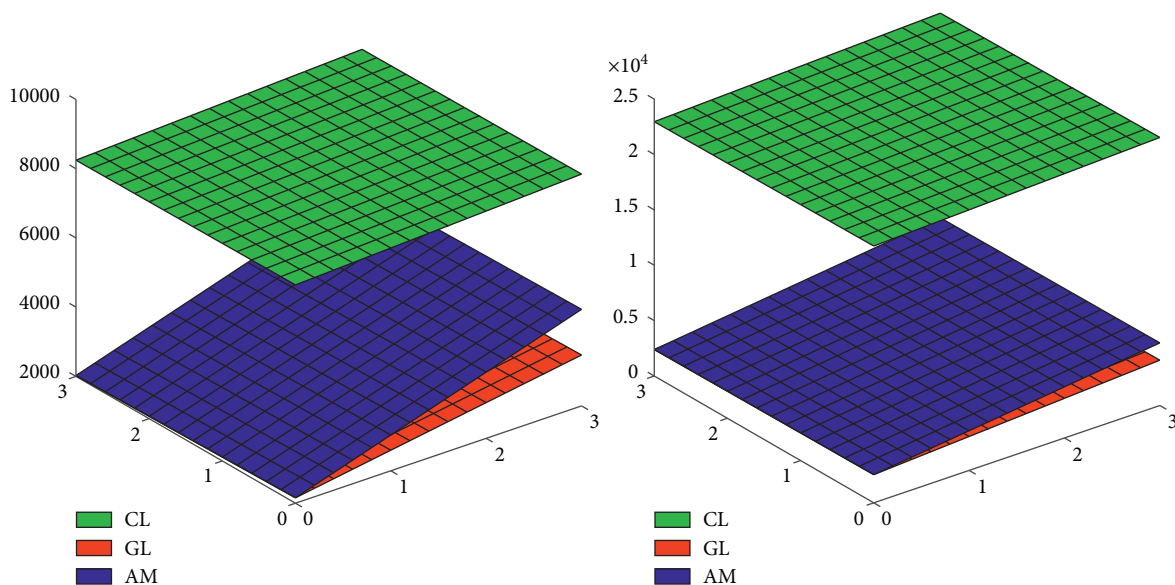


FIGURE 8: Comparison of  $CL_m^l$ ,  $GL_m^l$ , and  $AM_m^l$  using  $M_1$  and  $M_2$ . (a) 3D graphs of the first Zagreb index. (b) 3D graphs of the second Zagreb index.

$$\begin{aligned}
 (3) \text{SI}(GL_m^l) &= \sum_{vw \in E(GL_m^l)} \left( \frac{s_v s_w}{s_v + s_w - 2} \right)^3 = |E_{35}| \left( \frac{15}{6} \right)^3 \\
 &+ |E_{36}| \left( \frac{18}{7} \right)^3 + |E_{45}| \left( \frac{20}{7} \right)^3 + |E_{55}| \left( \frac{25}{8} \right)^3 + |E_{56}| \left( \frac{30}{9} \right)^3 \\
 &+ |E_{57}| \left( \frac{35}{10} \right)^3 + |E_{66}| \left( \frac{36}{10} \right)^3 + |E_{67}| \left( \frac{42}{11} \right)^3 + |E_{77}| \left( \frac{49}{12} \right)^3 \\
 &= \left( \frac{125}{8} \right) (m + 1) + \left( \frac{5832}{343} \right) (8m + ml - l - 1) + \left( \frac{8000}{343} \right) (2m + 2)
 \end{aligned}$$

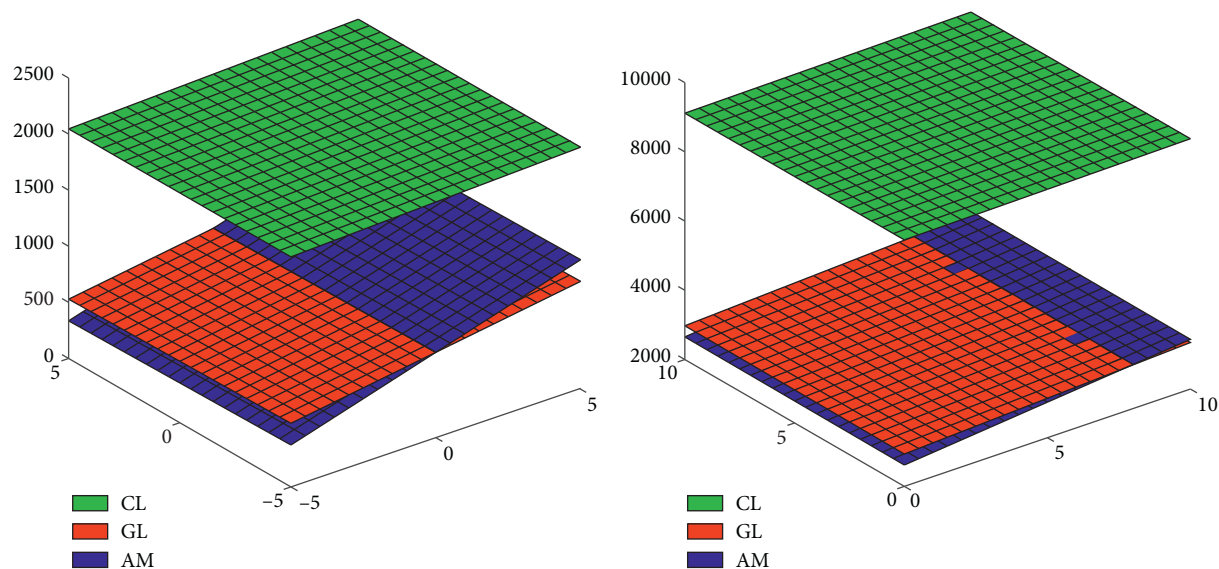


FIGURE 9: Comparison of  $CL_m^l$ ,  $GL_m^l$ , and  $AM_m^l$  using  $R_{(-1/2)}$  and  $\chi_{(-1/2)}$ . (a) 3D graphs of the Randić index. (b) 3D graphs of the sum-connectivity index.

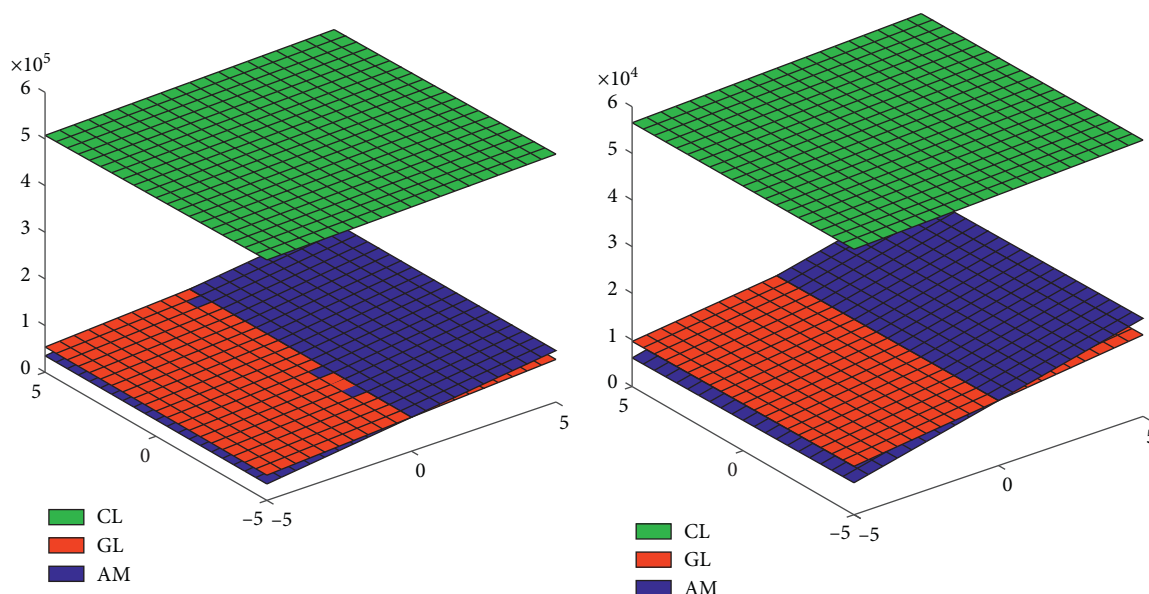


FIGURE 10: Comparison of  $CL_m^l$ ,  $GL_m^l$ , and  $AM_m^l$  using Sanskruti and augmented Zagreb indices. (a) 3D graphs of the first SI. (b) 3D graphs of the AZI.

$$\begin{aligned}
 & + \left(\frac{15625}{512}\right)(11m + ml - l - 1) + \left(\frac{1000}{27}\right)(12m + ml - l) + \\
 & + \left(\frac{343}{8}\right)(10m + ml - l - 2) + \left(\frac{5832}{125}\right)(28m + 3ml - 3l - 4) \\
 & + \left(\frac{74088}{1331}\right)(17m + 2ml - 2l + 1) + \left(\frac{117649}{1728}\right)(m - 1) \\
 & = \left(\frac{2940909850294457}{788889024000}\right)m + \left(\frac{298773851517107}{788889024000}\right)(m - 1)l - \left(\frac{216711945260101}{788889024000}\right).
 \end{aligned} \tag{43}$$

□

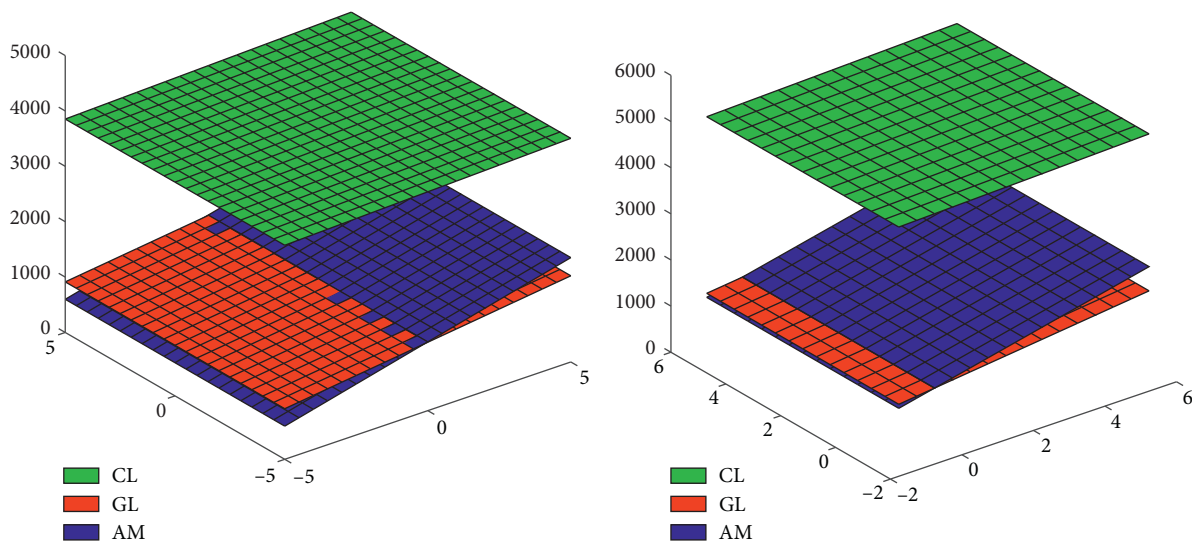


FIGURE 11: Comparison of  $CL_m^l$ ,  $GL_m^l$ , and  $AM_m^l$  using ABC and GA. (a) 3D graphs of the ABC index. (b) 3D graphs of the GA index.

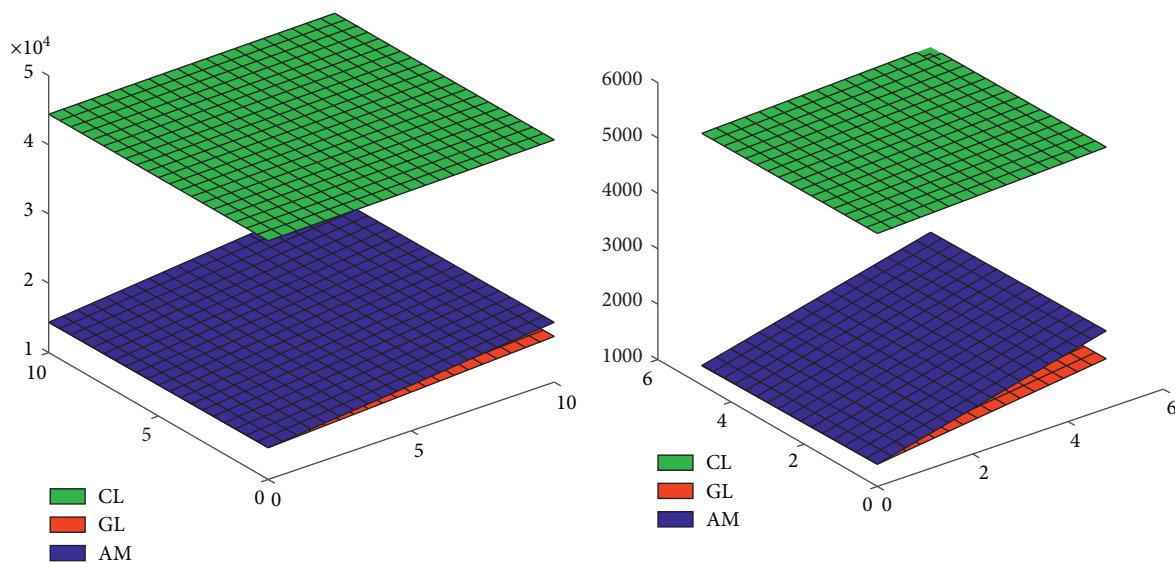


FIGURE 12: Comparison of  $CL_m^l$ ,  $GL_m^l$ , and  $AM_m^l$  using SDD and ISI. (a) 3D graphs of the SDD index. (b) 3D graphs of the ISI.

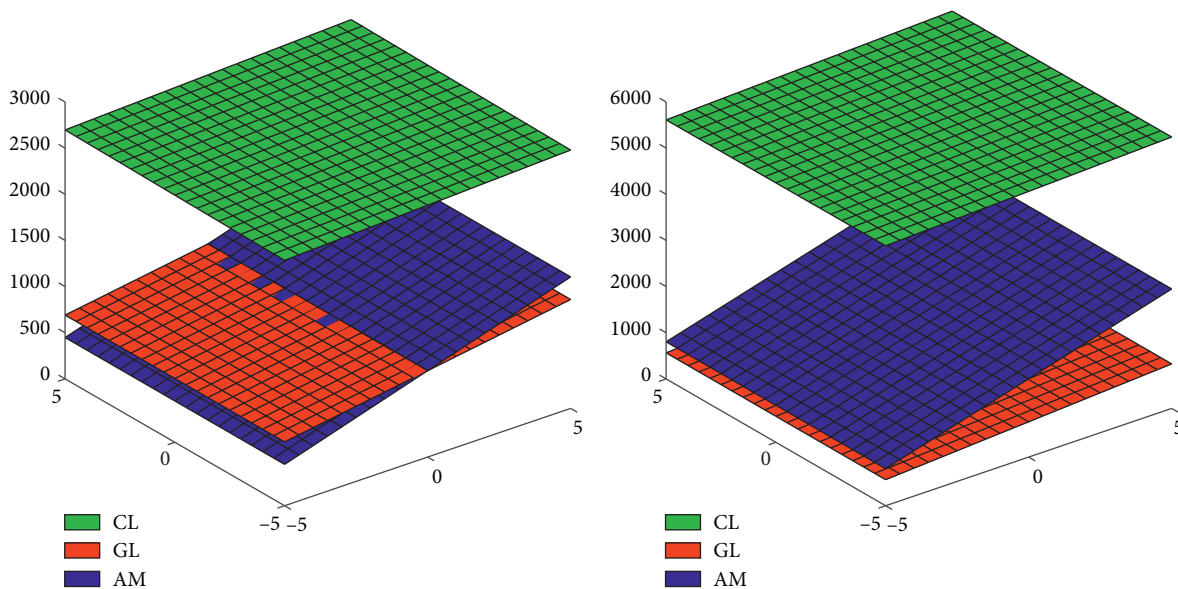


FIGURE 13: Comparison of  $CL_m^l$ ,  $GL_m^l$ , and  $AM_m^l$  using  $ABC_4$  and  $GA_5$ . (a) 3D graphs of the  $ABC_4$  index. (b) 3D graphs of the  $GA_5$  index.

**Theorem 12.** Let  $AM_m^l$  be the amylopectin network consisting of  $(m - 1)$  branches where each branch has length  $l$ ; then,  $ABC_4$ ,  $GA_5$ , and  $SI$  of  $AM_m^l$  are given as follows:

(1)

$$\begin{aligned} ABC_4(AM_m^l) &= \frac{1}{210} (2072\sqrt{10} + 1230\sqrt{14} + 42\sqrt{35} + 1764\sqrt{2} + 462\sqrt{30} + 185\sqrt{462} + 60\sqrt{3})m \\ &+ \frac{1}{210} (65\sqrt{14} + 84\sqrt{2} + 105\sqrt{10} + 10\sqrt{462} + 21\sqrt{30})(m - 1)l \\ &+ \frac{1}{210} (42\sqrt{35} - 98\sqrt{10} - 95\sqrt{14} - 84\sqrt{2} + 5\sqrt{462} - 60\sqrt{3}). \end{aligned} \quad (44)$$

(2)

$$\begin{aligned} GA_5(AM_m^l) &= \frac{1}{468} (117\sqrt{15} + 5616\sqrt{2} + 416\sqrt{5} + 1872\sqrt{30} + 1560\sqrt{35} + 2664\sqrt{42} + 37440)m \\ &+ \frac{1}{858} (572\sqrt{2} + 143\sqrt{35} + 156\sqrt{30} + 264\sqrt{42} + 3432)(m - 1)l \\ &+ \frac{1}{468} (117\sqrt{15} - 312\sqrt{2} + 416\sqrt{5} + 156\sqrt{35} + 72\sqrt{42} - 12168). \end{aligned} \quad (45)$$

(3)

$$\begin{aligned} SI(AM_m^l) &= \left( \frac{5928648365465527}{788889024000} \right) m \\ &+ \left( \frac{298773851517107}{788889024000} \right) (m - 1)l \\ &- \left( \frac{213033772785851}{788889024000} \right). \end{aligned} \quad (46)$$

#### 4. Concluding Remarks: A Comparative Analysis of Cellulose, Glycogen, and Amylopectin Networks

Figure 7 demonstrates a comparison between 3D graphs of the  $M$ -polynomial of cellulose, glycogen, and amylopectin networks (all having the same number of monomers, i.e., 75 hexagons).

Figures 8–13 provide a visual comparison among various TIs of cellulose, glycogen, and amylopectin networks.

Although both natural and synthetic polymers are appropriate for the drug delivery and, in general, for the pharmaceutical industry, however, natural polymers are more suitable as they are nontoxic, biocompatible, without side effects, and economical. As pointed out earlier,  $M_1$ ,  $M_2$ ,  $R_{(-1/2)}$ , and Randić-type indices ( $\chi_{(-1/2)}$ ,  $ABC$ , and  $AZI$ ) assess the intensity of branching and connectivity in the molecular graph. Figures 8–11 pronounce the subsequent order between the indices for the same number of monomers (i.e., same values of  $m$  and  $l$  in each polymer). Hence,

$TI(GL_m^l) \leq TI(AM_m^l) \leq TI(CL_m^l)$  where  $TI \in \{M_1, M_2, R_{(-1/2)}, \chi_{(-1/2)}, ABC, AZI\}$ . This ordering is convincing due to the fact that there exists extensive cross-linking in cellulose, while glycogen (frequent branching) and amylopectin (less branching) are branched polymers. In [53], properties of the SDD index and ISI are investigated, and it turned out that the ISI and SDD index are reasonable predictors of total surface area for octane isomers and polychlorobiphenyls, respectively. We conjecture, relying on the comparison presented in Figure 12, the relationship between surface areas (SAs) of cellulose, glycogen, and amylopectin which could have been organised as  $SA(AM_m^l) \leq SA(GL_m^l) \leq SA(CL_m^l)$ , for the same number of monomers.

We observe, from Figures 8–11 and Figure 13, that all the graphs of TIs for cellulose behave like an outlier as compared to glycogen and amylopectin. We anticipate that the eccentric behavior of cellulose is due to its nature of being used as a building material (forms the plant cell wall) as well as its physical properties such as the presence of monomer  $\beta$ -glucose, insoluble, indigestible, and considerable tensile strength. Moreover, all the graphs of TIs for glycogen and amylopectin go alongside, which might be due to the presence of monomer  $\alpha$ -glucose, solubility, digestibility, and their nature of being used as energy storage (bonds break easily) in animal organs and plants, respectively. Also, the results obtained in this section could further be applicable in QSPR/QSAR analysis to predict the biological properties of the natural polymers under discussion.

For future research, the study of polysaccharides can be further enhanced to molecular graphs of other natural polymers. Develop molecular graphs for some new natural

polymers such as proteins and nucleotides (RNA and DNA), and give a mathematical formulation of degree-based indices studied in this article. Finally, compare their physico-chemical properties, theoretically and mathematically, using these indices.

## Data Availability

All the data used to support the findings of this study are included within this article. However, the reader may contact the corresponding author for more details of the data.

## Conflicts of Interest

The authors declare no conflicts of interest.

## References

- [1] S. C. Basak, G. J. Niemi, and G. D. Veith, "Predicting properties of molecules using graph invariants," *Journal of Mathematical Chemistry*, vol. 7, no. 1, pp. 243–272, 1991.
- [2] S. C. Basak and G. D. Grunwald, "Molecular similarity and estimation of molecular Properties," *Journal of Chemical Information and Computer Sciences*, vol. 35, no. 3, pp. 366–372, 1995.
- [3] M. V. Diudea, *QSPR/QSAR Studies by Molecular Descriptors*, NOVA, New York, NY, USA, 2001.
- [4] R. Todeschini and V. Consonni, *Handbook of Molecular Descriptors for Chemoinformatics*, Wiley VCH, Weinheim, Germany, 2009.
- [5] I. Gutman and N. Trinajstić, "Graph theory and molecular orbitals. Total  $\phi$ -electron energy of alternant hydrocarbons  $\pi$ -electron energy of alternant hydrocarbons," *Chemical Physics Letters*, vol. 17, no. 4, pp. 535–538, 1972.
- [6] M. Randić, "Characterization of molecular branching," *Journal of the American Chemical Society*, vol. 97, no. 23, pp. 6609–6615, 1975.
- [7] M. Cavers, S. Fallat, and S. Kirkland, "On the normalized Laplacian energy and general Randić index  $R_{-1}$  of graphs," *Linear Algebra and Its Applications*, vol. 433, no. 1, pp. 172–190, 2010.
- [8] I. Gutman, B. Furtula, and Ş. B. Bozkurt, "On Randić energy," *Linear Algebra and Its Applications*, vol. 442, pp. 50–57, 2014.
- [9] B. Böllöbás and P. Erdős, "Graphs of extremal weights," *Ars Combinatoria*, vol. 50, pp. 225–233, 1998.
- [10] B. Zhou and N. Trinajstić, "On general sum-connectivity index," *Journal of Mathematical Chemistry*, vol. 47, no. 1, pp. 210–218, 2010.
- [11] G. Shirdel, H. Rezapour, and A. Sayadi, "The hyper-Zagreb index of graph operations," *Iranian Journal of Mathematical Chemistry*, vol. 4, pp. 213–220, 2013.
- [12] X. Li and J. Zheng, "A unified approach to the extremal trees for different indices," *MATCH Communications in Mathematical and in Computer Chemistry*, vol. 54, pp. 195–208, 2005.
- [13] M. Azari and A. Iranmanesh, "Generalized zagreb index of graphs," *Studia Universitatis Babeş Bolyai*, vol. 56, pp. 59–70, 2011.
- [14] E. Estrada, L. Torres, L. Rodriguez, and I. Gutman, "An atom-bond connectivity index: modelling the enthalpy of formation of alkanes," *Indian Journal of Chemistry*, vol. 37, pp. 849–855, 1998.
- [15] E. Estrada, "Atom-bond connectivity and the energetic of branched alkanes," *Chemical Physics Letters*, vol. 463, no. 4–6, pp. 422–425, 2008.
- [16] I. Gutman, J. Tošović, S. Radenković, and S. Marković, "On atom bond connectivity index and its chemical applicability," *Indian Journal of Chemistry*, vol. 51, pp. 690–694, 2012.
- [17] D. Vukičević and B. Furtula, "Topological index based on the ratios of geometrical and arithmetical means of end-vertex degrees of edges," *Journal of Mathematical Chemistry*, vol. 46, pp. 1369–1376, 2009.
- [18] X. Li and Y. Shi, "A survey on the Randić index," *MATCH Commun. Math. Comput. Chem.* vol. 59, pp. 127–156, 2008.
- [19] K. C. Das, I. Gutman, and B. Furtula, "Survey on geometric-arithmetic indices of graphs," *MATCH Communications in Mathematical and in Computer Chemistry*, vol. 65, pp. 595–644, 2011.
- [20] M. Ghorbani and M. Hosseinzadeh, "Computing ABC4 index of nanostar dendrimers," *Optoelectronics and Advanced Materials–Rapid Communications*, vol. 4, pp. 1419–1422, 2010.
- [21] A. Graovac, M. Ghorbani, and M. A. Hosseinzadeh, "Computing fifth geometric-arithmetic index for nanostar dendrimers," *Journal of Mathematical NanoScience*, vol. 1, pp. 33–42, 2011.
- [22] S. M. Hosamani, "Computing Sanskruti index of certain nanostructures," *International Journal of Applied Mathematics and Computer Science*, vol. 54, no. 1-2, pp. 425–433, 2017.
- [23] P. S. Ranjini, V. Loksha, and A. Usha, "Relation between phenylene and hexagonal squeeze using harmonic index," *International Journal of Graph Theory*, vol. 1, pp. 116–121, 2013.
- [24] E. Deutsch and S. Klavžar, "M-Polynomial and degree-based topological indices," *Iranian Journal of Mathematical Chemistry*, vol. 6, pp. 93–102, 2015.
- [25] K. V. Camarda and C. D. Maranas, "Optimization in polymer design using connectivity indices," *Industrial & Engineering Chemistry Research*, vol. 38, no. 5, pp. 1884–1892, 1999.
- [26] W. Wang, X. Hou, and W. Ning, "The k-connectivity index of an infinite class of dendrimer nanostars," *Digest Journal of Nanomaterials and Biostructures*, vol. 6, pp. 1199–1205, 2011.
- [27] A. Ali, A. A. Bhatti, and Z. Raza, "Topological study of tree-like polyphenylene systems, spiro hexagonal systems and polyphenylene dendrimer nanostars," *Quantum Matter*, vol. 5, no. 4, pp. 534–538, 2016.
- [28] Z. Shao, P. Wu, X. Zhang, D. Dimitrov, and J.-B. Liu, "On the maximum ABC index of graphs with prescribed size and without pendent vertices," *IEEE Access*, vol. 6, pp. 27604–27616, 2018.
- [29] W. Gao, M. Imran, M. K. Siddiqui, M. Naeem, and F. Jamil, "Molecular description of copper (I) oxide and copper (II) oxide," *Quimica Nova*, vol. 41, pp. 874–879, 2018.
- [30] S. M. Kang, M. K. Siddiqui, N. A. Rehman, M. Naeem, and M. H. Muhammad, "Topological properties of 2-dimensional silicon-carbons," *IEEE Access*, vol. 6, pp. 59362–59373, 2018.
- [31] J.-B. Liu, M. Younas, M. Habib, M. Yousaf, and W. Nazeer, "M-Polynomials and Degree-Based Topological Indices of VC5C7[p,q] and HC5C7[p,q] Nanotubes," *IEEE Access*, vol. 7, pp. 41125–41132, 2019.
- [32] W. Gao, Z. Iqbal, M. Ishaq, A. Aslam, and R. Sarfraz, "Topological aspects of dendrimers via distance based descriptors," *IEEE Access*, vol. 7, pp. 35619–35630, 2019.
- [33] Y. Liu, C. R. Munteanu, E. Fernández Blanco, Z. Tan, A. Santos del Riego, and A. Pazos, "Prediction of nucleotide

- binding peptides using star graph topological indices," *Molecular Informatics*, vol. 34, no. 11-12, pp. 736–741, 2015.
- [34] A. Ali and N. Trinajstić, "A novel/old modification of the first Zagreb index," *Molecular informatics*, vol. 37, pp. 6-7, 2018.
- [35] A. Ali, Z. Du, and K. Shehzadi, "Estimating some general molecular descriptors of saturated hydrocarbons," *Molecular Informatics*, vol. 38, Article ID e1900007, 2019.
- [36] Z. Du, A. Ali, and N. Trinajstić, "Alkanes with the first three maximal/minimal modified first Zagreb connection indices," *Molecular Informatics*, vol. 38, no. 4, Article ID 1800116, 2019.
- [37] S. Hayat, S. Wang, and J.-B. Liu, "Valency-based topological descriptors of chemical networks and their applications," *Applied Mathematical Modelling*, vol. 60, pp. 164–178, 2018.
- [38] M. Arockiaraj, S. Klavžar, J. Clement, S. Mushtaq, and K. Balasubramanian, "Edge distance-based topological indices of strength-weighted graphs and their application to coronoid systems, carbon nanocones and SiO<sub>2</sub> nanostructures," *Molecular Informatics*, vol. 38, Article ID 1900039, 2019.
- [39] M. Ahmad, M. Saeed, and M. Javaid, "Comparative study of certain synthetic polymers via bond-additive invariants," *IEEE Access*, vol. 9, pp. 15388–15403, 2021.
- [40] B. Borovicani, "On the extremal Zagreb indices of trees with given number of segments or given number of branching vertices," *MATCH Communications in Mathematical and in Computer Chemistry*, vol. 74, pp. 57–79, 2015.
- [41] M. Eliasi, A. Iranmanesh, and I. Gutman, "Multiplicative versions of first Zagreb index," *MATCH Communications in Mathematical and in Computer Chemistry*, vol. 68, pp. 217–230, 2012.
- [42] I. Gutman, B. Furtula, Z. K. Vukičević, and G. Popivoda, "On Zagreb indices and coindices," *MATCH Communications in Mathematical and in Computer Chemistry*, vol. 74, pp. 5–16, 2015.
- [43] Y. Shi, "Note on two generalizations of the Randić index," *Applied Mathematics and Computation*, vol. 265, pp. 1019–1025, 2015.
- [44] T. R. Hoare and D. S. Kohane, "Hydrogels in drug delivery: progress and challenges," *Polymer*, vol. 49, no. 8, pp. 1993–2007, 2008.
- [45] V. D. Prajapati, G. K. Jani, N. G. Moradiya, and N. P. Randeria, "Pharmaceutical applications of various natural gums, mucilages and their modified forms," *Carbohydrate Polymers*, vol. 92, no. 2, pp. 1685–1699, 2013.
- [46] N. Ngwuluka, N. Ochekepe, and O. Aruoma, "Naturapolyceutics: the science of utilizing natural polymers for drug delivery," *Polymers*, vol. 6, no. 5, pp. 1312–1332, 2014.
- [47] D. Klemm, B. Heublein, H.-P. Fink, and A. Bohn, "Cellulose: fascinating biopolymer and sustainable raw material," *Angewandte Chemie International Edition*, vol. 44, no. 22, pp. 3358–3393, 2005.
- [48] R. J. Moon, A. Martini, J. Nairn, J. Simonsen, and J. Youngblood, "Cellulose nanomaterials review: structure, properties and nanocomposites," *Chemical Society Reviews*, vol. 40, no. 7, pp. 3941–3994, 2011.
- [49] S. Imran, M. K. Siddiqui, M. Imran, and M. Hussain, "Computing the upper bounds for the metric dimension of cellulose network," *Applied Mathematics E-Notes*, vol. 19, pp. 585–605, 2019.
- [50] J. Jensen, P. I. Rustad, A. J. Kolnes, and Y.-C. Lai, "The role of skeletal muscle glycogen breakdown for regulation of insulin sensitivity by exercise," *Frontiers in Physiology*, vol. 2, p. 112, 2011.
- [51] P. J. Roach, A. A. Depaoli-Roach, T. D. Hurley, and V. S. Tagliabracchi, "Glycogen and its metabolism: some new developments and old themes," *Biochemical Journal*, vol. 441, no. 3, pp. 763–787, 2012.
- [52] M. M. Adeva-Andany, M. González-Lucán, C. Donapetry-García, C. Fernández-Fernández, and E. Ameneiros-Rodríguez, "Glycogen metabolism in humans," *BBA Clinical*, vol. 5, pp. 85–100, 2016.
- [53] D. Vukičević and M. Gašperov, "Bond additive modeling 1. Adriatic indices," *Croatica Chemica Acta*, vol. 83, no. 3, pp. 243–260, 2010.

## Research Article

# Study of Generalized Hourglass Section in Carbon Nanocone via Connection Number

Muhammad Mubashar <sup>1</sup>, Muhammad Hussain <sup>1</sup>, Fatimah Abdulrahman Alrawajeh <sup>2</sup>,  
and Sultan Almotairi <sup>3</sup>

<sup>1</sup>Department of Mathematics, COMSATS University Islamabad, Lahore Campus, Islamabad 54000, Pakistan

<sup>2</sup>Department of Mathematics, Faculty of Science College, Imam Abdulrahman Bin Faisal University (IAU), Dammam 31441, Saudi Arabia

<sup>3</sup>Department of Natural and Applied Sciences, Faculty of Community College, Majmaah University, Majmaah 11952, Saudi Arabia

Correspondence should be addressed to Fatimah Abdulrahman Alrawajeh; falrawjih@iau.edu.sa

Received 3 July 2021; Accepted 25 July 2021; Published 3 August 2021

Academic Editor: Muhammad Imran

Copyright © 2021 Muhammad Mubashar et al. This is an open access article distributed under the Creative Commons Attribution License, which permits unrestricted use, distribution, and reproduction in any medium, provided the original work is properly cited.

In 1972, Gutman and Trinajstić showed that total  $\pi$ -energy of a molecule depends upon a numeric quantity which is often called as Zagreb index. In the same report, they also discussed another numeric quantity depending on the number of atoms at a distance two from a particular atom and proved influencing results on  $\pi$ -energy of a molecule. In modern literature, this quantity is named as connection number. In this article, we will describe some Zagreb connection numbers for hourglass section in carbon nanocone network with different lengths of cycle in the central core.

## 1. Introduction

In the theoretical branch of chemistry, molecular quantities are important for modeling structural information of different molecules. The purpose for getting this information is to capture physical and chemical properties of the molecules. To attain this, a chemical structure of a molecule is presented as graphs, and the molecular quantities obtained from a particular chemical structure are graph invariants under graph isomorphism. In the mathematical branch of chemistry, this study is termed as quantitative structural activity relationship (QSAR). Predicting electron energy and melting (boiling) point for a structure are primary applications of these studies [1].

In discrete branch of mathematics, studying mathematical structures by modeling pairwise relations between sets of objects results in graphs. Simply, a graph consists of some vertices, which are joined by edges. Commonly, the set of vertices in a graph  $G$  is described by  $V$ , whereas the set of edges is represented by  $E$ . Chemical graph theory is a branch

of mathematics which combines graph theory and chemistry. Graph theory is used to mathematically model molecules in order to gain insight into the physical properties of these chemical compounds. In this branch, a chemical structure for a compound is visualized as a unique form of a graph by showing its atoms as vertices and bonds between atoms as edges. This is a simple transformation of a structure into a graph which helps chemists to study physical and chemical structural properties for a particular network [2]. Very recently, a new two-dimensional bilayered naturally existing network of germanium phosphide is topologically explained in [3]. Some degree-based topological indices for p-type benzene ring for a two-dimensional network are given in [4]. A computer paradigm cellular neural network is explained by a new kind of dominating topological invariants by Ejaz et al. [5].

In 1972, Ivan Gutman and Nenad Trinajstić [6] very firstly defined a numeric quantity while studying the electron energy of a molecule. Later on, this quantity will have been called as the Zagreb index. It depends on the number of

bonds (edges) connected to an atom. Particularly, the number of bonds attached to an atom is called degree, and Zagreb index is purely based on degrees of all atoms in a structure. After this, these same mathematicians defined another quantity while studying molecular branching of orbitals which is called the second Zagreb index. With the passage of time, the abovementioned quantities would be termed as the first and second Zagreb indices by many graph theorists and chemists. More than hundreds of researchers did work on it and published their work in highly reputed journals [7].

In [1, 8], these two quantities are modified and redefined as novel quantities on the basis of connection numbers, and this experiment shows very effective results in different aspects. As we know that the number of edges (bonds) is the degree of an atom (vertex), similarly, the second degree is the number of edges from a particular vertex to a vertex at a distance two. In other words, for a vertex  $u$  in a graph, the number of vertices at a distance two is called the connection number for  $u$  and represented as  $\tau_u$ . In the following, we will define these modified versions of Zagreb indices and are termed as the first Zagreb connection number ( $ZC_1$ ), second Zagreb connection number ( $ZC_2$ ), and more modified type of first Zagreb as first modified connection number ( $ZC_1^*$ ).

$$ZC_1 = \sum_{u \in V} \tau_u^2, \quad (1)$$

$$ZC_2 = \sum_{uv \in E} (\tau_u \cdot \tau_v), \quad (2)$$

$$ZC_1^* = \sum_{uv \in E} (\tau_u + \tau_v). \quad (3)$$

## 2. Carbon Nanocone

Round about in 1968, the first appearance of a carbon nanocone comes under observation by naturally existing graphite surface. The attraction of these structures is its applications in biosensors, energy and gas storage, nano-electric devices, and many more. These nanocones are carbon-consisting networks which are infinite undirected planar structures in theory of graphs [9].

Carbon nanomaterials have drawn focusable attention and attraction during the last two decades because of its effective physical applications in nanotechnology as emerging materials of splendid practical application. But carbon nanocones (CNCs) have drawn full attention after the discovery of free-standing structures or canonical topology as cap on one end of nanotubes (CNTs) [10–12]. CNCs are admired as alternatives of (CNTs) because of the absence of potentially poisonous metal catalyst in synthesis and mass production at room temperature [13]. In general, during the declamation of CNTs, strong acids are used in order to close out metal catalysts. In this process, deficiency introduced with the hindrance of destructing the graphite structure. On the other hand, the useful applications and attractive properties of CNCs are easy to approach. The application of CNCs as drug delivery capsules [14] and gas

storage devices increased their significance in modern era. Throughout the years, this subject has been developing unique scientific obsession with planar, curved, and wrapped nanoscale structures, such as graphene, fullerenes, and nanotubes [15]. It has a strong technological interest just as their innovative structural, noticeable electronic and mechanical properties. Curved carbon structures are used to investigate growth and nucleation. Especially, pentagon presence in CNCs plays vital role [16]. The 60 declination defect was detected when the pentagon inserted in a graphite sheet. This is the key of CNCs formation with pentagon as tip apex which leads us to the existence of nanotubes with tip topology [17]. This type of defects in graphite networks were theoretically considered for the study of electronic states [18]. CNCs have free-standing structures with sharp edges as these properties have applications in technology and electronics [19, 20]. The basic cell unit of carbon nanocone-consisting benzene ring is shown in Figure 1(a), and two benzene rings having a common edge in naphthalene is shown in Figure 1(b).

A graphical representation of these cones shows conical shape with a cycle of specific length at its core with hexagonal layers around the core. We are interested particularly in a structure with some different structural forms with  $n$  layers of hexagons around the centre. In Section 3, we will explain the novel structural form derived from CNC very similar to the bow-tie shape. Javaid et al. discussed some important results related to rhombus-type silicate and oxide networks and calculated indices to study the chemical behaviour [21]. Chemical properties and chemical bonding networking in the neural network were studied significantly by using indices [22, 23]. These gave a wider range to study the connection numbers and other indices on different chemical networks for observing the chemical behaviour and connectivity among the chemical bonds. Calculation of Zagreb connection numbers is based upon the specific distance. Formulas for many topological indices look like similar to one another. Degree-based, distance-based, and specific-restricted domain topological indices can differentiate among all of them. Leap Zagreb indices, dominating topological indices, and zagreb connection indices are close to each other by formulas but different by chemical structural properties of chemical structural-based compound [24].

## 3. Hourglass Section in Carbon Nanocone

Carbon nanocones have nice and interesting geometrical properties. These structures are connected, with infinite chains of concatenated hexagons having the property of two adjacent connected hexagons with a common edge. The construction property defines a definite rule for carbon nanostructure and it provides building block structure. That is why, it gives a planar simple connected graph obtained by connected regular hexagons [25].

Observing this geometrical property of the CNC here, we will describe its structure as similar to the hourglass. In this system, the core is centred with a cycle of specific length, whereas the layers of hexagons are around it. Moreover, this structure is similar to the doubled cone having a common

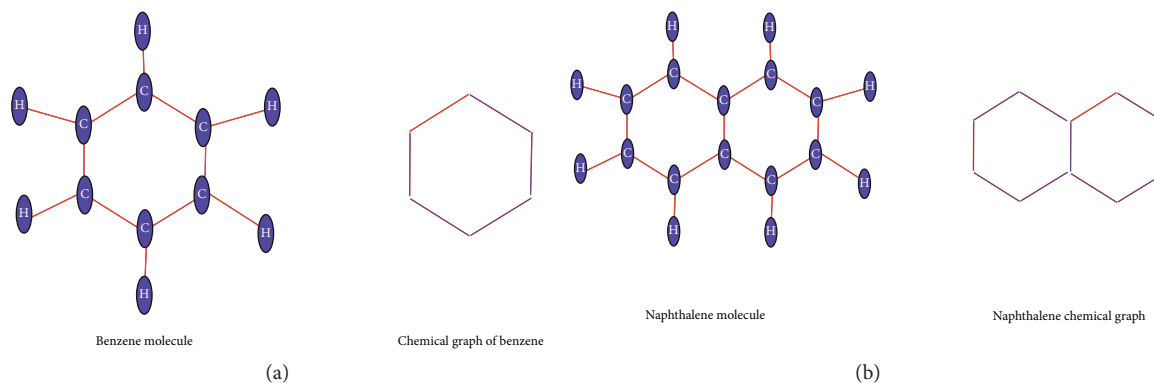


FIGURE 1: Some hydrocarbons with associated chemical graphs. (a) Benzene with chemical graph. (b) Naphthalene with chemical graph.

cycle core at the centre. We will term this unique noval system as “hourglass system carbon nanocone” (HGSCNC), whereas we will express the  $n$ -dimensional system as  $HGSCNC(n, k)$ , where  $n$  is the dimension of the system which is the number of hexagon layers around the core and  $k$  represent the length of cycle at the core. We will discuss two cases for  $k$ : (1) when  $k$  is odd and (2) when  $k$  is even.

**3.1. When Length of Cycle  $m$  Is Odd in  $n$ -Dimensional HGSCNC.** In this case, we are presenting the HGSCNC with a cycle of odd length  $m$  up to  $n$ -dimension. We will observe sharpness and scattered pattern in  $n$ -dimensional hexagonal layers with odd length cycle. By observing the structural property of this particular case, we have found that this structure has  $2n^2 + 12n + m$  total number of vertices with  $n \geq 2$  and  $m \geq 7$ , whereas the edge set has total  $3n^2 + 15n + m$  edges with  $n \geq 2$  and  $m \geq 9$ . Here,  $n$  represents the number of hexagon layers and  $m \in O$  is the length of the cycle. A simple connected graph for this particular case is shown in Figure 2 and mathematically expressed as  $HGSCNC(n, m)$ . A graphical display for HGSCNC for  $n = 4$  with cycle of odd length for  $m = 7$  is shown in Figure 3.

By working on some structural properties and behaviour of  $HGSCNC(n, m)$  upto  $n$  dimensions, we found it very interesting and rapid growing network. Here, we will state a lemma about its structural behaviour given as follows.

**Lemma 1.** For  $n \geq 2$  and  $m = 7$  HGSCNC, we have the first Zagreb connection number  $ZC_1$  which is as follows:

$$ZC_1(HGSCNC(n, 7)) = 72n^2 + 192n + 58. \quad (4)$$

**Lemma 2.** For  $n \geq 2$  and  $m = 9$  HGSCNC, we have first Zagreb connection number  $ZC_1$ , second Zagreb connection number  $ZC_2$ , and first modified Zagreb connection number  $ZC_1^*$  which are as follows:

$$\begin{aligned} ZC_2(HGSCNC(n, 9)) &= 108n^2 + 228n + 84, \\ ZC_1^*(HGSCNC(n, 9)) &= 36n^2 + 120n + 46. \end{aligned} \quad (5)$$

**3.1.1. Main Results.** In this section, we will state our main results about connection numbers with the help of the abovementioned lemma and its consequences. These results are related to Zagreb connection numbers  $HGSCNC(n, m)$ .

**Theorem 1.** Hourglass carbon nanocone system holds closed expression for first Zagreb connection number  $ZC_1$ , second Zagreb connection number  $ZC_2$ , and first modified Zagreb connection number  $ZC_1^*$  which are as follows:

$$\begin{aligned} ZC_1(HGSCNC(n, m)) &= 72n^2 + 192n + 4m + 30 \forall n \geq 2 \text{ and } m \geq 7, \\ ZC_2(HGSCNC(n, m)) &= 108n^2 + 228n + 4m + 40 \forall n \geq 2 \text{ and } m \geq 9, \\ ZC_1^*(HGSCNC(n, m)) &= 36n^2 + 120n + 4m + 70 \forall n \geq 2 \text{ and } m \geq 9. \end{aligned} \quad (6)$$

*Proof.* Working on Lemma 1, we have found some properties of the vertex set in Table 1 and edge set properties in Table 2 concluded as a result of 2 for  $HGSCNC(n, m)$

depending on the connection number of carbon atoms in the  $n$ -dimensional network. By using equation (1), we have

$$\begin{aligned} ZC_1(HGSCNC(n, m)) &= 4(m - 3) + 9(10) + 16(12n - 10) + 25(2) + 36(2n^2 - 1) + 49(2) \\ \Rightarrow ZC_1(HGSCNC(n, m)) &= 72n^2 + 192n + 4m + 30. \end{aligned} \quad (7)$$

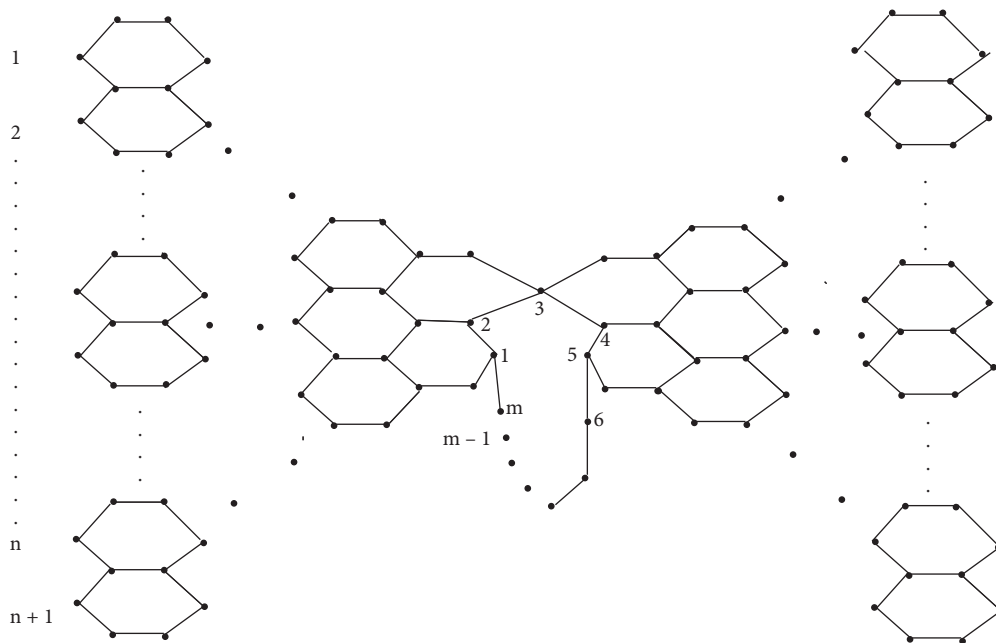


FIGURE 2: Generalized hourglass carbon nanocone  $HGSCNC(n, m)$ .

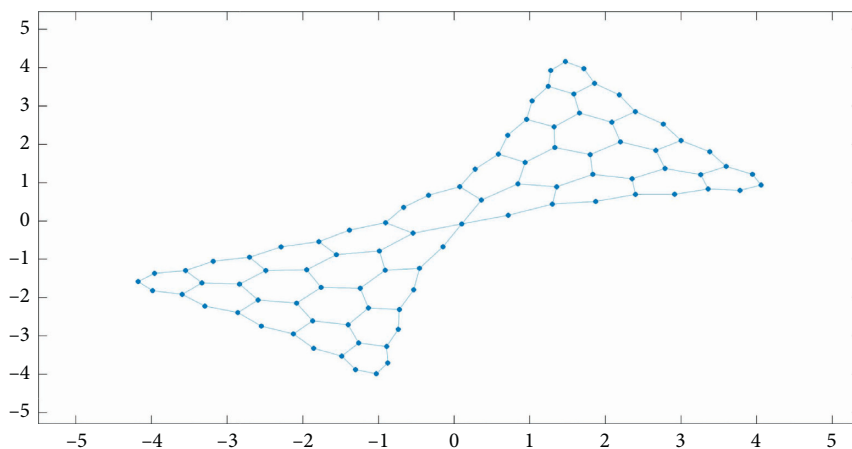


FIGURE 3: Hourglass carbon nanocone  $HGSCNC(4, 7)$ .

TABLE 1: Vertex partition of  $HGSCNC(n, m) \forall n \geq 2$  and  $m \geq 7$  with respect to connection number  $\tau$ .

$\tau_u$	2	3	4	5	6	7
Number of vertices	$m - 3$	10	$12n - 10$	2	$2n^2 - 1$	2

TABLE 2: Edge partition of  $HGSCNC(n, m) \forall n \geq 2$  and  $m \geq 9$ .

$(\tau_u, \tau_v)$	(2, 3)	(4, 3)	(4, 4)	(4, 5)	(6, 6)	(4, 6)	(5, 6)	(6, 7)	(4, 7)	(2, 2)
Number of edges	10	10	$12n - 16$	2	$3n^2 - 3n - 2$	$6n - 4$	2	4	2	$m - 8$

From equation (2) and by using the abovementioned connection numbers for different edges, we have

$$\begin{aligned} ZC_2(\text{HGSCNC}(n, m)) &= 6(10) + 12(10) + 16(12n - 16) + 20(2) \\ &\quad + 36(3n^2 - 3n - 2) + 24(6n - 4) + 30(2) + 42(4) + 28(2) + 4(m - 8) \\ \Rightarrow ZC_2(\text{CNC}_5(n)) &= 108n^2 + 228n + 4m + 40. \end{aligned} \quad (8)$$

From equation (3) and by using the abovementioned connection numbers for different edges, we have

$$\begin{aligned} ZC_1^*(\text{HGSCNC}(n, m)) &= 5(10) + 7(10) + 8(12n - 16) + 9(2) \\ &\quad + 12(3n^2 - 3n - 2) + 10(6n - 4) + 11(2) + 13(4) + 11(2) + 4(m - 8) \\ \Rightarrow ZC_1^*(\text{HGSCNC}(n, m)) &= 36n^2 + 120n + 4m + 70. \end{aligned} \quad (9)$$

**3.2. When the Length of Cycle  $p$  Is Even in  $n$ -Dimensional HGSCNC.** In this case, we are presenting the HGSCNC with even length  $p \in E$  cycle up to  $n$  dimensions. We will observe sharpness and scattered pattern in  $n$ -dimensional hexagonal layers with even length cycle. On observing the structural property of this particular case, we have found that this structure has  $2n^2 + 8n + p + 8$  total number of vertices with  $n \geq 2$  and  $p \geq 10$ , whereas the edge set has total  $3n^2 + 15n + p$  edges with  $n \geq 2$  and  $p \geq 14$ . Here,  $n$  is representing the number of hexagonal layers and  $p \in E$  is the length of cycle. A simple connected graph for this particular case is shown in Figure 4 and mathematically expressed as  $\text{HGSCNC}(n, p)$ . A graphical display for HGSCNC for  $n = 3$  with a cycle of odd length for  $p = 10$  is shown in Figure 5.

On working some structural properties and behaviour of  $\text{HGSCNC}(n, m)$  up to  $n$  dimensions, we found it very interesting and rapid growing network. Here, we will state some lemmas about particular cases for connection numbers when the length of the cycle is fixed.

**Lemma 3.** For  $n \geq 2$  and  $p = 10$  HGSCNC, we have first Zagreb connection number  $ZC_1$  which is as follows:

$$ZC_1(\text{HGSCNC}(n, 10)) = 72n^2 + 128n + 156. \quad (10)$$

**Lemma 4.** For  $n \geq 2$  and  $p = 14$  HGSCNC, we have first Zagreb connection number  $ZC_1$ , second Zagreb connection number  $ZC_2$ , and first modified Zagreb connection number  $ZC_1^*$  which are as follows:

$$\begin{aligned} ZC_2(\text{HGSCNC}(n, 14)) &= 108n^2 + 228n + 32, \\ ZC_1^*(\text{HGSCNC}(n, 14)) &= 36n^2 + 120n + 56. \end{aligned} \quad (11) \quad \square$$

**3.2.1. Main Results.** In this section, we will state our main results about connection numbers with the help of the abovementioned lemma and its consequences. These results are related to Zagreb connection numbers for  $\text{HGSCNC}(n, p)$ .

**Theorem 2.** Hourglass carbon nanocone system holds closed expression for first Zagreb connection number  $ZC_1$ , second Zagreb connection number  $ZC_2$ , and first modified Zagreb connection number  $ZC_1^*$  which are as follows:

$$ZC_1(\text{HGSCNC}(n, p)) = 72n^2 + 128n + 4p + 116, \quad (12)$$

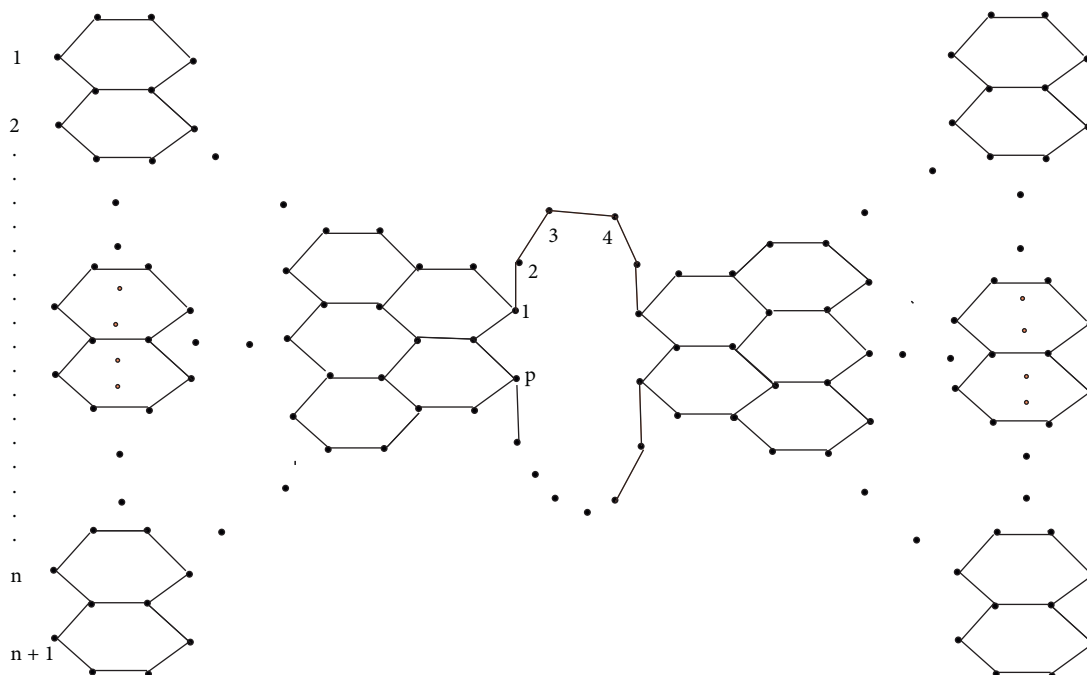
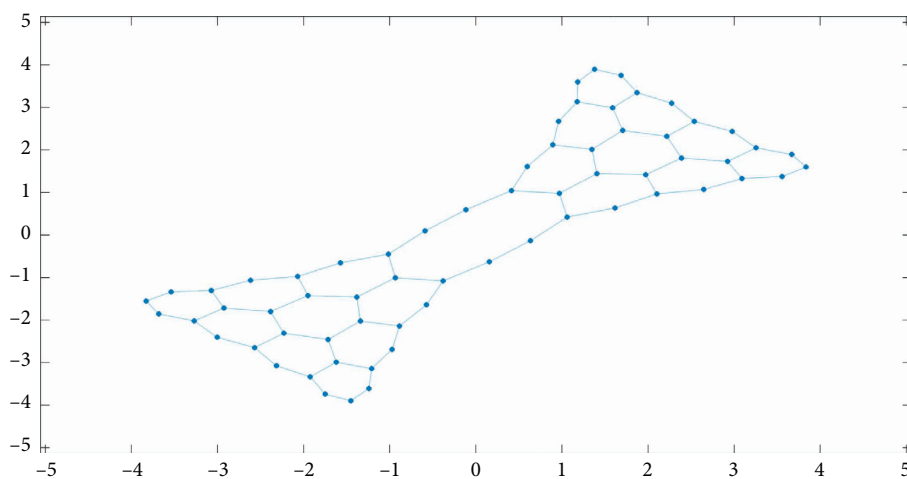
$\forall n \geq 2$  and  $p \geq 10$

$$ZC_2(\text{HGSCNC}(n, p)) = 108n^2 + 228n + 4p - 24, \quad (13)$$

$\forall n \geq 2$  and  $p \geq 14$

$$ZC_1^*(\text{HGSCNC}(n, p)) = 36n^2 + 120n + 4p \quad \forall n \geq 2 \text{ and } p \geq 14. \quad (14)$$

*Proof.* Working on the lemma, we have found some properties of the vertex set in Table 3 and edge set in Table 4 of  $\text{HGSCNC}(n, p)$  depending on the connection number of carbon atoms in the  $n$ -dimensional network. By using equation (1), we have

FIGURE 4: Generalized hourglass carbon nanocone  $\text{HGSCNC}(n, p)$ .FIGURE 5: Hourglass carbon nanocone  $\text{HGSCNC}(3, 10)$ .

$$\begin{aligned} ZC_1(\text{HGSCNC}(n, p)) &= 4(p - 6) + 9(12) + 16(8n + 2) + 36(2n^2) \\ \Rightarrow ZC_1(\text{HGSCNC}(n, p)) &= 72n^2 + 128n + 4p + 116. \end{aligned} \quad (15)$$

From equation (2) and by using the abovementioned connection numbers for different edges, we have

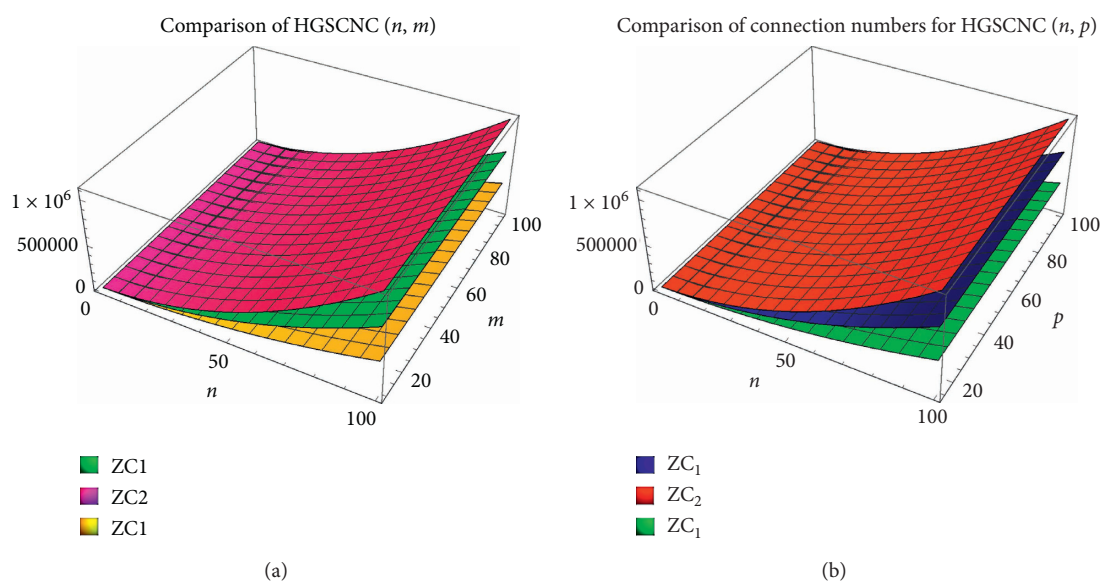
$$\begin{aligned} ZC_2(\text{HGSCNC}(n, p)) &= 6(12) + 12(12) + 16(12n - 12) + 36(3n^2 - 3n) + 24(6n) + 4(p - 12) \\ \Rightarrow ZC_2(\text{HGSCNC}(n, p)) &= 108n^2 + 228n + 4p - 24. \end{aligned} \quad (16)$$

TABLE 3: Vertex partition of HGSCNC( $n, p$ ) $\forall n \geq 2$  and  $p \geq 10$ .

$\tau_u$	2	3	4	6
Number of vertices	$p - 6$	12	$8n + 2$	$2n^2$

TABLE 4: Edge partition of HGSCNC( $n, m$ ) $\forall n \geq 2$  and  $p \geq 14$ .

$(\tau_u, \tau_v)$	(2, 3)	(4, 3)	(4, 4)	(6, 6)	(4, 6)	(2, 2)
Number of edges	12	12	$12n - 12$	$3n^2 - 3n$	$6n$	$p - 12$

FIGURE 6: Comparison of connection number for HGSCNC. (a) Comparison of  $ZC_1$ ,  $ZC_2$ , and  $ZC_1^*$  for HGSCNC( $n, m$ ). (b) Comparison of  $ZC_1$ ,  $ZC_2$ , and  $ZC_1^*$  for HGSCNC( $n, p$ ).

From equation (3) and by using the abovementioned connection numbers for different edges, we have

$$\begin{aligned} ZC_1^*(\text{HGSCNC}(n, p)) &= 5(12) + 7(12) + 8(12n - 12) + 12(3n^2 - 3n) + 10(6n) + 4(p - 12) \\ &\Rightarrow ZC_1^*(\text{HGSCNC}(n, p)) = 36n^2 + 120n + 4p. \end{aligned} \quad (17)$$

#### 4. Graphical Comparison

In this section, we will compare our results via graphical view. Firstly, we have compared our output results among  $ZC_1$ ,  $ZC_2$ , and  $ZC_1^*$  for HGSCNC( $n, m$ ), and results are shown in Figure 6(a). Similarly, we have compared our output results among  $ZC_1$ ,  $ZC_2$ , and  $ZC_1^*$  for HGSCNC( $n, p$ ), and results are shown in Figure 6(b).

#### 5. Conclusion

In this article, we have computed closed results for the family of Zagreb connection number in the hourglass system

carbon nanocone (HGSCNC) and with its core of even length and its core of odd length. For the first time, we have evaluated the Zagreb connection numbers for HGSCNC( $n, m$ ) and HGSCNC( $n, p$ ). The results are very interesting, and we concluded that HGSCNC( $n, m$ ) is the fast predicting network as compared to HGSCNC( $n, p$ ). Furthermore, we have concluded that  $ZC_2$  has better prediction for both HGSCNC( $n, m$ ) as well as for HGSCNC( $n, p$ ). Predicting ability of a topological index encourages the theoretical study of the chemical structure. We computed Zagreb connection indices  $ZC_1$ ,  $ZC_2$ , and  $ZC_1^*$  for HGSCNC upto  $n$  dimensions for different lengths of central core. These results will facilitate the understanding of

topological properties of the noval structure of HGSCNC. Our results will motivate to investigate new structure of different chemical structures and their line graphs and studying their topological and physical properties.

### Data Availability

No data were used to support this study.

### Disclosure

The paper has not been published elsewhere, and it will not be submitted anywhere else for publication.

### Conflicts of Interest

The authors declare no conflicts of interest.

### Authors' Contributions

All authors contributed equally to this work.

### Acknowledgments

The authors extend their appreciation to the deputyship for Research and Innovation, Ministry of Education, Saudi Arabia, for funding this research work through the project number IFP-2020-17.

### References

- [1] R. Zahid, "Zagreb connection indices for some benzenoid systems," *Polycyclic Aromatic Compounds*, vol. 40, pp. 1–14, 2020.
- [2] L. Yan, Y. Li, S. Hayat et al., "On degree-based and frustration related topological indices of single-walled titania nanotubes," *Journal of Computational and Theoretical Nanoscience*, vol. 13, no. 11, pp. 9027–9032, 2016.
- [3] F. Ejaz, M. Hussain, and R. Hasni, "On topological aspects of bilayer Germanium Phosphide," *Journal of Mathematics and Computer Science*, vol. 22, no. 4, pp. 347–362, 2021.
- [4] A. Ahmad, "On the degree based topological indices of benzene ring embedded in P-type-surface in 2D network," *Hacetatepe Journal of Mathematics and Statistics*, vol. 47, no. 1, 2018.
- [5] F. Ejaz, M. Hussain, H. Almohamedh, K. M. Alhamed, R. Alabdian, and S. Almotairi, "Dominating topological analysis and Comparison of the cellular neural network," *Mathematical Problems in Engineering*, vol. 2021, Article ID 6613433, 9 pages, 2021.
- [6] I. Gutman and N. Trinajstić, "Graph theory and molecular orbitals. Total  $\varphi$ -electron energy of alternant hydrocarbons," *Chemical Physics Letters*, vol. 17, no. 4, pp. 535–538, 1972.
- [7] D. Maji and G. Ghorai, "Computing F-index, coindex and Zagreb polynomials of the kth generalized transformation graphs," *Heliyon*, vol. 6, no. 12, Article ID e05781, 2020.
- [8] A. Ali and N. Trinajstić, "A novel/old modification of the first Zagreb index," *Molecular Informatics*, vol. 37, no. 6-7, Article ID 1800008, 2018.
- [9] N. Tagmatarchis, *Advances in Carbon Nanomaterials: Science and Applications*, CRC Press, Boca Raton, FL, USA, 2012.
- [10] T. Ichihashi and Y. Ando, "Pentagons, heptagons and negative curvature in graphite microtubule growth," *Nature*, vol. 356, pp. 776–778, 1992.
- [11] S. Iijima, P. M. Ajayan, and T. Ichihashi, "Growth model for carbon nanotubes," *Physical Review Letters*, vol. 69, no. 21, pp. 3100–3103, 1992.
- [12] S. Iijima, "Helical microtubules of graphitic carbon," *Nature*, vol. 354, no. 6348, pp. 56–58, 1991.
- [13] M. Nadolska, M. Przeźniak-Welenc, M. Łapiński, and K. Sadowska, "Synthesis of phosphonated carbon nanotubes: new insight into carbon nanotubes functionalization," *Materials*, vol. 14, no. 11, p. 2726, 2021.
- [14] B. A. Ardeshtana, U. B. Jani, A. M. Patel, and A. Y. Joshi, "Characterizing the vibration behavior of double walled carbon nano cones for sensing applications," *Materials Technology*, vol. 33, no. 7, pp. 451–466, 2018.
- [15] M. Ge and K. Sattler, "Observation of fullerene cones," *Chemical Physics Letters*, vol. 220, no. 3-5, pp. 192–196, 1994.
- [16] B. Bumbacila, O. Ori, F. Cataldo, and M. V. Putz, "Topological modeling of carbon nano-lattices," *Current Organic Chemistry*, vol. 21, no. 27, pp. 2705–2718, 2017.
- [17] V. R. Kulli, "General reduced second Zagreb index of certain networks," *International Journal of Current Research in Life Sciences*, vol. 7, no. 11, pp. 2827–2833, 2018.
- [18] Z. Hussain, M. Munir, A. Ahmad, and M. Chaudhary, J. Alam Khan and I. Ahmed, "Metric basis and metric dimension of 1-pentagonal carbon nanocone networks," *Scientific Reports*, vol. 10, no. 1, p. 19687, 2020.
- [19] M. Asif, M. Hussain, H. Almohamedh et al., "Study of carbon nanocones via connection Zagreb indices," *Mathematical Problems in Engineering*, vol. 2021, Article ID 5539904, 13 pages, 2021.
- [20] W. Gao and M. R. Farahani, "Computing the reverse eccentric connectivity index for certain family of nanocone and fullerene structures," *Journal of Nanotechnology*, vol. 2016, Article ID 3129561, 6 pages, 2016.
- [21] M. Javaid, M. U. Rehman, and J. Cao, "Topological indices of rhombus type silicate and oxide networks," *Canadian Journal of Chemistry*, vol. 95, no. 2, pp. 134–143, 2017.
- [22] J.-B. Liu, J. Zhao, S. Wang, M. Javaid, and J. Cao, "On the topological properties of the certain neural networks," *Journal of Artificial Intelligence and Soft Computing Research*, vol. 8, no. 4, pp. 257–268, 2018.
- [23] M. Javaid and J. Cao, "Computing topological indices of probabilistic neural network," *Neural Computing and Applications*, vol. 30, no. 12, pp. 3869–3876, 2018.
- [24] I. Gutman, Z. Shao, Z. Li, S. Wang, and P. Wu, "Leap Zagreb indices of trees and unicyclic graphs," *Communications in Combinatorics and Optimization*, vol. 3, no. 2, pp. 179–194, 2018.
- [25] Y. C. Kwun, A. Ali, W. Nazeer, M. A. Chaudhary, and S. M. Kang, "M-polynomials and degree-based topological indices of triangular, hourglass, and jagged-rectangle benzenoid systems," *Journal of Chemistry*, vol. 2018, Article ID 8213950, 8 pages, 2018.

## Research Article

# On Degree-Based Topological Indices for Strong Double Graphs

Muhammad Rafiullah <sup>1</sup>, Hafiz Muhammad Afzal Siddiqui <sup>1</sup>,  
Muhammad Kamran Siddiqui,<sup>1</sup> and Mlamuli Dhlamini <sup>2</sup>

<sup>1</sup>Department of Mathematics, COMSATS University Islamabad Lahore Campus, Lahore 54000, Pakistan

<sup>2</sup>Department of Applied Mathematics, National University of Science and Technology, Bulawayo, Zimbabwe

Correspondence should be addressed to Mlamuli Dhlamini; mlamuli.dhlamini@nust.ac.zw

Received 10 June 2021; Accepted 21 July 2021; Published 2 August 2021

Academic Editor: Syed Ahtsham Haq Bokhary

Copyright © 2021 Muhammad Rafiullah et al. This is an open access article distributed under the Creative Commons Attribution License, which permits unrestricted use, distribution, and reproduction in any medium, provided the original work is properly cited.

A topological index is a characteristic value which represents some structural properties of a chemical graph. We study strong double graphs and their generalization to compute Zagreb indices and Zagreb coindices. We provide their explicit computing formulas along with an algorithm to generate and verify the results. We also find the relation between these indices. A 3D graphical representation and graphs are also presented to understand the dynamics of the aforementioned topological indices.

## 1. Introduction

Chemical graph theory is an important topological field of mathematical chemistry that deals with mathematical modelling of chemical compound structures. A molecular structure of a compound consists of many atoms. Specially, hydrocarbons are chemical compounds which consist of carbon and hydrogen atoms. A graph consisting of hydrocarbons is known as a molecular graph which represents the carbon structure of a molecule [1].

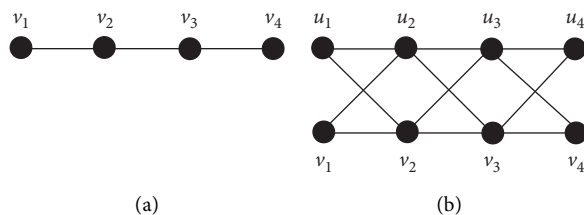
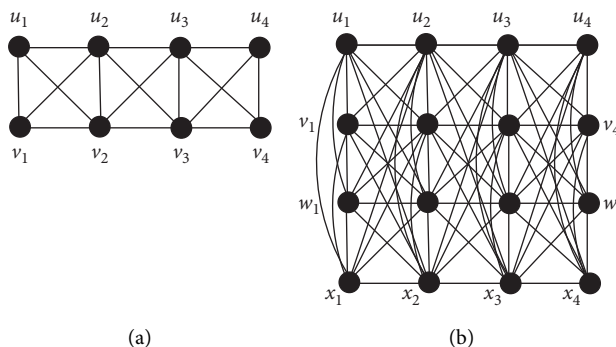
We consider a simple molecular graph, say  $G$ , which consists of nonhydrogen atoms and covalent bonds. In graph theory, the nonhydrogen atoms are represented by a set of vertices  $V = V(G)$  and the covalent bonds with the set of edges  $E = E(G)$ . The number of atoms and bonds in a structure is represented by  $n = |V|$  and  $m = |E|$ , respectively. The valency of an atom is represented by  $\mathfrak{R}_G(v)$ , and it is known as the degree of vertex  $v \in V(G)$ , which also represents the number of adjacent (or neighboring) vertices of  $V$ . A set consisting of neighboring vertices of  $v$  is known as open neighborhood and denoted as  $N(v) = \{w \in V(G) : vw \in E(G)\}$ . If the vertex  $v$  is included in open neighborhood, then the set of vertices is called closed neighborhood, and it is denoted as  $N[v] = N(v) \cup \{v\}$ .

A double graph  $D(G)$  is generated by taking two copies of a graph  $G$  and connecting every vertex  $v_i$  in one copy with the opened neighborhood  $N(v_i)$  of the corresponding vertex

with its second copy. For details, see Figure 1 in which a path graph  $P_4$  and its double graph are presented. A strong double graph  $SD(G)$  is generated by taking two copies of a graph  $G$  and connecting every vertex  $v_i$  in one copy with closed neighborhood  $N[v_i] = N(v_i) \cup \{v_i\}$  of the corresponding vertex with its second copy. For details, see Figure 2 in which a strong double graph of  $P_4$  and its  $k$ -iterated strong double graph are presented.

A complement  $\bar{G}$  of a graph  $G$  consists of the same set of vertices, where two vertices  $v$  and  $w$  are adjacent by an edge  $vw$  if and only if they are not adjacent in  $G$ . Hence,  $vw \in E(\bar{G}) \Leftrightarrow vw \notin E(G)$ . A complement of a graph consists of a number of edges and the degree of vertex  $v$  which are represented as  $\bar{m} = \binom{n}{2} - m$  and  $d_{\bar{G}}(v) = n - 1 - \mathfrak{R}_G(v)$ , respectively.

A molecular descriptor is known as the topological index provides specific information about the structure of molecules. In graph theory, the molecular structure is considered as a graph  $G$ . The topological index is also known as the connectivity index [2, 3]. Topological indices are largely applied in chemistry to develop the quantitative structure-activity relationship (QSAR) in which the characteristics of molecules can be correlated with their chemical structures [4]. The physicochemical properties of a molecule can also be explained through topological indices. The first index of a

FIGURE 1: The graph  $P_4$  and its double graph. (a)  $P_4$ . (b)  $D(P_4)$ .FIGURE 2: The strong double graph of  $P_4$  and its generalization. (a)  $SD^{*1}(P_4)$ . (b)  $SD^{*2}(P_4)$ .

chemical graph was introduced by Harold Wiener [5] in 1947 as an aid to determining the boiling point of the paraffin compound. This index is known as the Wiener index and defined as  $W(G) = \sum_{\{u,v\} \subseteq V(G)} d(u, v)$ , where the notation  $d(u, v)$  represents the distance between  $u$  and  $v$ .

A topological index is defined as a function  $T: \psi \rightarrow \mathbb{R}$ , where  $\psi$  is the set of finite simple graphs and  $\mathbb{R}$  is a set of real numbers which satisfy the relation  $T(G) = T(H)$  if  $G$  is isomorphic to  $H$ . Recently published work [6, 7] motivated us to further investigate the Zagreb indices and coindices of strong double graphs.

The first Zagreb index  $M_1(G)$  and second Zagreb index  $M_2(G)$  were introduced by Gutman and Trinajstić in 1972 [8] and elaborated by Nikolić et al. after 30 years in 2003 [9].  $M_1(G)$  and  $M_2(G)$  are defined as

$$\begin{aligned} M_1(G) &= \sum_{uv \in E(G)} [\mathfrak{R}_G(u) + \mathfrak{R}_G(v)], \\ M_2(G) &= \sum_{uv \in E(G)} [\mathfrak{R}_G(u)\mathfrak{R}_G(v)]. \end{aligned} \quad (1)$$

The first Zagreb index is also written as  $\sum_{v \in V(G)} [\mathfrak{R}_G(v)]^2$ .

Recently, some useful versions of Zagreb indices have been discovered, such as multiplicative Zagreb indices [3, 7, 10], multiplicative sum Zagreb indices [11, 12], Zagreb coindices [6], and multiplicative Zagreb coindices [13].

The important variants of the Zagreb index are the first and second Zagreb coindices, which are defined as follows, respectively:

$$\begin{aligned} \overline{M}_1(G) &= \sum_{u \neq v; uv \notin E(G)} [\mathfrak{R}_G(u) + \mathfrak{R}_G(v)], \\ \overline{M}_2(G) &= \sum_{u \neq v; uv \notin E(G)} [\mathfrak{R}_G(u)\mathfrak{R}_G(v)]. \end{aligned} \quad (2)$$

Doslic [14] introduced  $\overline{M}_1(G)$  and  $\overline{M}_2(G)$  in 2008. In 2009, Ashrafi et al. [15] determined the extremal values of these new invariants for some special graphs. They [6] also explored their fundamental properties and provided some explicit formulas for these versions under different graph operations.

## 2. Main Results

In this section, we study Zagreb indices and Zagreb coindices of strong double graphs. We also study these indices for generalized  $k$ -iterated strong double graphs. We use the concept of edge partition to reduce computation complexity and obtain computing formulas for these indices.

For the sake of simplicity, we consider  $SD(G) = G^{1*} = G^*$  and  $G^{k*} = (G^{(k-1)*})^*$  for  $k \geq 2$ . Assume that  $G^{0*} = G$  for the sake of consistency.

In the following theorem, we study the first and second Zagreb indices of the strong double graph.

**Theorem 1.** *Let  $G$  be a simple connected graph of order  $n$  and size  $m$ ; then,*

$$\begin{aligned} (i) \quad M_1(G^*) &= 8M_1(G) + 16m + 2n \\ (ii) \quad M_2(G^*) &= 16M_2(G) + 12M_1(G) + 12m + n \end{aligned}$$

*Proof.* For the sake of convenience, we label all vertices in  $G$  as  $\{v_1, v_2, \dots, v_n\}$ . Suppose that  $x_i$  and  $y_i$  are the corresponding clone vertices, in strong double graph  $G^*$ , of  $v_i$  for each  $i = 1, \dots, n$ .

For any given vertex  $v_i$  in  $G$  and its clone vertices  $x_i$  and  $y_i$ , there exists  $d_{G^*}(x_i) = d_{G^*}(y_i) = 2\mathfrak{R}_G(v_i) + 1$  by the definition of the strong double graph.

For  $v_i, v_j \in V(G)$ , if  $v_i v_j \in E(G)$ , then  $x_i x_j \in E(G^*)$ ,  $y_i y_j \in E(G^*)$ ,  $x_i y_j \in E(G^*)$ , and  $y_i x_j \in E(G^*)$ .

So, we only need to consider the total contribution of the following three types of adjacent vertex pairs both to  $M_1(G^*)$  and to  $M_2(G^*)$ .

Type 1: the adjacent vertex pairs  $\{x_i, x_j\}$  and  $\{y_i, y_j\}$ , where  $v_i v_j \in E(G)$

Type 2: the adjacent vertex pairs  $\{x_i, y_i\}$  for each  $i = 1, \dots, n$

Type 3: the adjacent vertex pairs  $\{x_i, y_j\}$  and  $\{y_i, x_j\}$ , where  $v_i v_j \in E(G)$

The total contribution of adjacent vertex pairs of type 1 in  $M_1(G^*)$  is given by

$$\begin{aligned} \sum_{x_i x_j \in E(G^*)} [d_{G^*}(x_i) + d_{G^*}(x_j)] &= \sum_{y_i y_j \in E(G^*)} [d_{G^*}(y_i) + d_{G^*}(y_j)] \\ &= \sum_{v_i v_j \in E(G)} [(2\mathfrak{R}_G(v_i) + 1) + (2\mathfrak{R}_G(v_j) + 1)] \\ &= 2 \sum_{v_i v_j \in E(G)} [\mathfrak{R}_G(v_i) + \mathfrak{R}_G(v_j)] + 2|E(G)|_{v_i v_j \in E(G)} \\ &= 2M_1 + 2m, \end{aligned} \quad (3)$$

and  $M_2(G^*)$  is given by

$$\begin{aligned} \sum_{x_i x_j \in E(G^*)} [d_{G^*}(x_i) \cdot d_{G^*}(x_j)] &= \sum_{y_i y_j \in E(G^*)} [d_{G^*}(y_i) \cdot d_{G^*}(y_j)] \\ &= \sum_{v_i v_j \in E(G)} [(2\mathfrak{R}_G(v_i) + 1) \cdot (2\mathfrak{R}_G(v_j) + 1)] \\ &= 4 \sum_{v_i v_j \in E(G)} [\mathfrak{R}_G(v_i) \cdot \mathfrak{R}_G(v_j)] + 2 \sum_{v_i v_j \in E(G)} [\mathfrak{R}_G(v_i) + \mathfrak{R}_G(v_j)] + |E(G)|_{v_i v_j \in E(G)} \\ &= 4M_2 + 2M_1 + m. \end{aligned} \quad (4)$$

The total contribution of adjacent vertex pairs of type 2 in  $M_1(G^*)$  is given by

$$\begin{aligned} \sum_{x_i y_i \in E(G^*)} [d_{G^*}(x_i) + d_{G^*}(y_i)] &= \sum_{v_i \in V(G)} [(2\mathfrak{R}_G(v_i) + 1) + (2\mathfrak{R}_G(v_i) + 1)] \\ &= 4 \sum_{v_i \in V(G)} \mathfrak{R}_G(v_i) + 2|V(G)|_{v_i \in V(G)} \\ &= 8m + 2n, \end{aligned} \quad (5)$$

and  $M_2(G^*)$  is given by

$$\begin{aligned} \sum_{x_i y_i \in E(G^*)} [d_{G^*}(x_i) + d_{G^*}(y_i)] &= \sum_{v_i \in V(G)} [(2\mathfrak{R}_G(v_i) + 1) \cdot (2\mathfrak{R}_G(v_i) + 1)] \\ &= 4 \sum_{v_i \in V(G)} [\mathfrak{R}_G(v_i)]^2 + 4 \sum_{v_i \in V(G)} \mathfrak{R}_G(v_i) + |V(G)|_{v_i \in V(G)} \\ &= 4M_1(G) + 8m + n. \end{aligned} \quad (6)$$

The total contribution of adjacent vertex pairs of type 3 in  $M_1(G^*)$  is given by

$$\begin{aligned} \sum_{x_i y_i \in E(G^*)} [d_{G^*}(x_i) + d_{G^*}(y_i)] &= \sum_{y_i x_j \in E(G^*)} [d_{G^*}(y_i) + d_{G^*}(x_j)] \\ &= \sum_{v_i v_j \in E(G)} [(2\mathfrak{R}_G(v_i) + 1) + (2\mathfrak{R}_G(v_j) + 1)] \\ &= 2 \sum_{v_i v_j \in E(G)} [\mathfrak{R}_G(v_i) + \mathfrak{R}_G(v_j)] + |E(G)|_{v_i v_j \in E(G)} \\ &= 2M_1(G) + 2m, \end{aligned} \quad (7)$$

and  $M_2(G^*)$  is given by

$$\begin{aligned}
 \sum_{x_i, y_j \in E(G^*)} [d_{G^*}(x_i) \cdot d_{G^*}(y_j)] &= \sum_{y_i, x_j \in E(G^*)} [d_{G^*}(y_i) \cdot d_{G^*}(x_j)] \\
 &= \sum_{v_i, v_j \in E(G)} [(2\mathfrak{R}_G(v_i) + 1) \cdot (2\mathfrak{R}_G(v_j) + 1)] \\
 &= 4 \sum_{v_i, v_j \in E(G)} [\mathfrak{R}_G(v_i) \cdot \mathfrak{R}_G(v_j)] + 2 \sum_{v_i, v_j \in E(G)} [\mathfrak{R}_G(v_i) + \mathfrak{R}_G(v_j)] + |E(G)|_{v_i, v_j \in E(G)} \\
 &= 4M_2(G) + 2M_1(G) + m.
 \end{aligned} \tag{8}$$

Therefore, by using equations (3), (5) and (7), we have

$$\begin{aligned}
 M_1(G^*) &= \sum_{x_i, x_j \in E(G^*)} [d_{G^*}(x_i) + d_{G^*}(x_j)] + \sum_{y_i, y_j \in E(G^*)} [d_{G^*}(y_i) + d_{G^*}(y_j)] \\
 &\quad + \sum_{x_i, y_i \in E(G^*)} [d_{G^*}(x_i) + d_{G^*}(y_i)] + \sum_{x_i, y_j \in E(G^*)} [d_{G^*}(x_i) + d_{G^*}(y_j)] + \sum_{y_i, x_j \in E(G^*)} [d_{G^*}(y_i) + d_{G^*}(x_j)] \\
 &= (2M_1(G) + 2m) + (2M_1(G) + 2m) + (8m + 2n) + (2M_1(G) + 2m) + (2M_1(G) + 2m) \\
 &= 8M_1(G) + 16m + 2n.
 \end{aligned} \tag{9}$$

By using (4), (6) and (8), we also have

$$\begin{aligned}
 M_2(G^*) &= \sum_{x_i, x_j \in E(G^*)} [d_{G^*}(x_i) \cdot d_{G^*}(x_j)] + \sum_{y_i, y_j \in E(G^*)} [d_{G^*}(y_i) \cdot d_{G^*}(y_j)] \\
 &\quad + \sum_{x_i, y_i \in E(G^*)} [d_{G^*}(x_i) \cdot d_{G^*}(y_i)] + \sum_{x_i, y_j \in E(G^*)} [d_{G^*}(x_i) \cdot d_{G^*}(y_j)] + \sum_{y_i, x_j \in E(G^*)} [d_{G^*}(y_i) \cdot d_{G^*}(x_j)] \\
 &= (4M_2(G) + 2M_1(G) + m) + (4M_2(G) + 2M_1(G) + m) \\
 &\quad + (4M_1(G) + 8m + n) + (4M_2(G) + 2M_1(G) + m) + (4M_2(G) + 2M_1(G) + m) \\
 &= 16M_2(G) + 12M_1(G) + 12m + n.
 \end{aligned} \tag{10}$$

In this theorem, we study the first and second Zagreb coindices of the strong double graph.  $\square$

**Theorem 2.** Let  $G$  be a simple connected graph of order  $n$  and size  $m$ ; then,

- (i)  $\overline{M}_1(G^*) = 8\overline{M}_1(G) + 4n^2 - 4n - 8m$
- (ii)  $\overline{M}_2(G^*) = 16\overline{M}_2(G) + 8\overline{M}_1(G) + 2n^2 - 2n - 4m$

*Proof.* For the sake of convenience, we label all vertices in  $G$  as  $\{v_1, v_2, \dots, v_n\}$ . Suppose that  $x_i$  and  $y_i$  are the corresponding clone vertices, in strong double graph  $G^*$ , of  $v_i$  for each  $i = 1, \dots, n$ .

For any given vertex  $v_i$  in  $G$  and its clone vertices  $x_i$  and  $y_i$ , there exists  $d_{G^*}(x_i) = d_{G^*}(y_i) = 2\mathfrak{R}_G(v_i) + 1$  by the definition of the strong double graph.

For  $v_i, v_j \in V(G)$ , if  $v_i v_j \notin E(G)$ , then  $x_i x_j \notin E(G)$ ,  $y_i y_j \notin E(G)$ ,  $x_i y_j \notin E(G)$ , and  $y_i x_j \notin E(G)$ .

So, we only need to consider the total contribution of the following two types of nonadjacent vertex pairs both to  $\overline{M}_1(G^*)$  and to  $\overline{M}_2(G^*)$ .

Type 1: the nonadjacent vertex pairs  $\{x_i, x_j\}$  and  $\{y_i, y_j\}$ , where  $v_i v_j \notin E(G)$

Type 2: the nonadjacent vertex pairs  $\{x_i, y_j\}$  and  $\{y_i, x_j\}$ , where  $v_i v_j \notin E(G)$

The total contribution of nonadjacent vertex pairs of type 1 in  $\overline{M}_1(G^*)$  is given by

$$\begin{aligned}
\sum_{x_i, x_j \notin E(G^*)} [d_{G^*}(x_i) + d_{G^*}(x_j)] &= \sum_{y_i, y_j \notin E(G^*)} [d_{G^*}(y_i) + d_{G^*}(y_j)] \\
&= \sum_{v_i, v_j \notin E(G)} [(2\mathfrak{R}_G(v_i) + 1) + (2\mathfrak{R}_G(v_j) + 1)] \\
&= 2 \sum_{v_i, v_j \notin E(G)} [\mathfrak{R}_G(v_i) + \mathfrak{R}_G(v_j)] + 2|E(\overline{G})| \\
&= 2M_1(G) - 2m + n^2 - n,
\end{aligned} \tag{11}$$

and  $\overline{M}_2(G^*)$  is given by

$$\begin{aligned}
\sum_{x_i, x_j \notin E(G^*)} [d_{G^*}(x_i) \cdot d_{G^*}(x_j)] &= \sum_{y_i, y_j \notin E(G^*)} [d_{G^*}(y_i) \cdot d_{G^*}(y_j)] \\
&= \sum_{v_i, v_j \notin E(G)} [(2\mathfrak{R}_G(v_i) + 1) \cdot (2\mathfrak{R}_G(v_j) + 1)] \\
&= 4 \sum_{v_i, v_j \notin E(G)} [\mathfrak{R}_G(v_i) \cdot \mathfrak{R}_G(v_j)] + 2 \sum_{v_i, v_j \notin E(G)} [\mathfrak{R}_G(v_i) + \mathfrak{R}_G(v_j)] + |E(\overline{G})| \\
&= 4M_2(G) + 2M_1(G) + \frac{1}{2}(n^2 - n - 2m).
\end{aligned} \tag{12}$$

The total contribution of nonadjacent vertex pairs of type 2 in  $\overline{M}_1(G^*)$  is given by

$$\begin{aligned}
\sum_{x_i, y_j \notin E(G^*)} [d_{G^*}(x_i) + d_{G^*}(y_j)] &= \sum_{y_i, x_j \notin E(G^*)} [d_{G^*}(y_i) + d_{G^*}(x_j)] \\
&= \sum_{v_i, v_j \notin E(G)} [(2\mathfrak{R}_G(v_i) + 1) + (2\mathfrak{R}_G(v_j) + 1)] \\
&= 2 \sum_{v_i, v_j \notin E(G)} [\mathfrak{R}_G(v_i) + \mathfrak{R}_G(v_j)] + 2|E(\overline{G})| \\
&= 2M_1(G) - 2m + n^2 - n,
\end{aligned} \tag{13}$$

and  $\overline{M}_2(G^*)$  is given by

$$\begin{aligned}
\sum_{x_i, y_j \notin E(G^*)} [d_{G^*}(x_i) \cdot d_{G^*}(y_j)] &= \sum_{y_i, x_j \notin E(G^*)} [d_{G^*}(x_i) + d_{G^*}(y_j)] \\
&= \sum_{v_i, v_j \notin E(G)} [(2\mathfrak{R}_G(v_i) + 1) \cdot (2\mathfrak{R}_G(v_j) + 1)] \\
&= 4 \sum_{v_i, v_j \notin E(G)} [\mathfrak{R}_G(v_i) \cdot \mathfrak{R}_G(v_j)] + 2 \sum_{v_i, v_j \notin E(G)} \mathfrak{R}_G(v_i) + \mathfrak{R}_G(v_j) + |E(\overline{G})| \\
&= 4M_2(G) + 2M_1(G) + \frac{1}{2}(n^2 - n - 2m).
\end{aligned} \tag{14}$$

Therefore, by using equations (11) and (13), we have

$$\begin{aligned}
 \overline{M}_1(G^*) &= \sum_{x_i, x_j \notin E(G^*)} [d_{G^*}(x_i) + d_{G^*}(x_j)] = \sum_{y_i, y_j \notin E(G^*)} [d_{G^*}(y_i) + d_{G^*}(y_j)] \\
 &+ \sum_{x_i, y_j \notin E(G^*)} [d_{G^*}(x_i) + d_{G^*}(y_j)] + \sum_{y_i, x_j \notin E(G^*)} d_{G^*}(y_i) + d_{G^*}(x_j) \\
 &= (2M_1(G) - 2m + n^2 - n) + (2M_1(G) - 2m + n^2 - n) \\
 &+ (2M_1(G) - 2m + n^2 - n) + (2M_1(G) - 2m + n^2 - n) \\
 &= 8M_1(G) - 8m + 4n^2 - 4n.
 \end{aligned} \tag{15}$$

By using equations (12) and (14), we also have

$$\begin{aligned}
 \overline{M}_2(G^*) &= \sum_{x_i, x_j \notin E(G^*)} [d_{G^*}(x_i) \cdot d_{G^*}(x_j)] = \sum_{y_i, y_j \notin E(G^*)} [d_{G^*}(y_i) \cdot d_{G^*}(y_j)] \\
 &+ \sum_{x_i, y_j \notin E(G^*)} [d_{G^*}(x_i) \cdot d_{G^*}(y_j)] + \sum_{y_i, x_j \notin E(G^*)} d_{G^*}(y_i) \cdot d_{G^*}(x_j) \\
 &= \left(4M_2(G) + 2M_1(G) + \frac{1}{2}(n^2 - n - 2m)\right) + \left(4M_2(G) + 2M_1(G) + \frac{1}{2}(n^2 - n - 2m)\right) \\
 &+ \left(4M_2(G) + 2M_1(G) + \frac{1}{2}(n^2 - n - 2m)\right) + \left(4M_2(G) + 2M_1(G) + \frac{1}{2}(n^2 - n - 2m)\right) \\
 &= 16M_2(G) + 8M_1(G) + 2(n^2 - n - 2m).
 \end{aligned} \tag{16}$$

Now, we present the first and second indices and coindices of  $k$ -iterated strong double graphs.  $\square$

**Theorem 3.** Let  $G$  be a nontrivial graph of order  $n$  and size  $m$ , and let  $G^{k*}$  be its  $k$ -iterated strong double graph. Then,

- (i)  $M_1(G^{k*}) = 8^k M_1(G) + 2^{2(k+1)}(2^k - 1)m + 2^k(2^k - 1)^2 n$
- (ii)  $M_2(G^{k*}) = 3 \cdot 2^{3k-1} \cdot (2^k - 1)M_1(G) + 4^{2k}M_2(G) + 3 \cdot 2^{2k} \cdot (2^k - 1)^2 m + 2^{k-1}(2^k - 1)^3 n$
- (iii)  $\overline{M}_1(G^{k*}) = 8^k \overline{M}_1(G) + (2^k - 1)4^k(n^2 - n - 2m)$
- (iv)  $\overline{M}_2(G^{k*}) = 2^{4k} \overline{M}_2(G) + 2^{3k} \cdot (2^k - 1) \overline{M}_1(G) + 2^{2k-1} \cdot (2^k - 1)^2(n^2 - n - 2m)$

*Proof.* For any nontrivial graph  $G$  with  $n$  vertices and  $m$  edges, the number of vertices in  $G^*$  is  $2n$  and the number of edges in  $G^*$  is  $2m$  plus those edges between the sets  $\{x_1, x_2, \dots, x_n\}$  and  $\{y_1, y_2, \dots, y_n\}$ , that is,  $4^k m + n$ .

Now, we deduce that  $G^{k*}$  has  $2^k m$  vertices and  $4^k m + (2^{2k-1} - 2^{k-1})n$  edges.

- (i)  $M_1(G^{k*}) = 8^k M_1(G) + 2^{2(k+1)}(2^k - 1)m + 2^k(2^k - 1)^2 n$ .

As we know,

$$M_1(G^*) = 8M_1(G) + 16m + 2n. \tag{17}$$

Using the size of strong double graph  $m = 4^k m + (2^{2k-1} - 2^{k-1})n$ , we have

$$\begin{aligned}
 M_1(G^*) &= 8M_1(G) + 16\{4^k m + (2^{2k-1} - 2^{k-1})n\} + 2n, \\
 M_1(G^{k*}) &= 8M_1(G^{(k-1)*}) + 4 \cdot 2^{2k} m + (2^{2k-1} - 2^{k-1} + 2)n.
 \end{aligned} \tag{18}$$

By Theorem 1 and the definition of the  $k$ -iterated strong double graph, for  $k \geq 1$ , we have

$$\begin{aligned}
M_1(G^{k*}) &= 8M_1(G^{(k-1)*}) + 4 \cdot 2^{2k}m + (8 \cdot 2^{2k-2} - 8 \cdot 2^{k-1} + 2^k)n \\
M_1(G^{k*}) &= 8\{8M_1(G^{(k-2)*}) + 4 \cdot 2^{2k-2}m + (8 \cdot 2^{2k-4} - 8 \cdot 2^{k-2} + 2^{k-1})n\} \\
&\quad + 4 \cdot 2^{2k}m + (8 \cdot 2^{2k-2} - 8 \cdot 2^{k-1} + 2^k)n \\
&= 8^2M_1(G^{(k-2)*}) + 12 \cdot 2^{2k}m + 2^{2k-1}(6 \cdot 2^{2k} - 15 \cdot 2^k)n \\
&= 8^2\{8M_1(G^{(k-3)*}) + 4 \cdot 2^{2k-4}m + (8 \cdot 2^{2k-6} - 8 \cdot 2^{k-3} + 2^{k-2})n\} \\
&\quad + 12 \cdot 2^{2k}m + 2^{2k-1}(6 \cdot 2^{2k} - 15 \cdot 2^k)n \\
&= 8^3M_1(G^{(k-3)*}) + 28 \cdot 2^{2k}m + (14 \cdot 2^{2k} - 63 \cdot 2^k)n \\
M_1(G^{*k}) &= 8^k M_1(G) + 2^{2(k+1)}(2^k - 1)m + 2^k(2^k - 1)^2 n.
\end{aligned} \tag{19}$$

$$(ii) M_2(G^{*k}) = 3 \cdot 2^{3k-1} \cdot (2^k - 1)M_1(G) + 4^{2k}M_2(G) + 3 \cdot 2^{2k} \cdot (2^k - 1)^2 m + 2^{k-1}(2^k - 1)^3 n.$$

As we know,

$$M_2(G^*) = 16M_2(G) + 12M_1(G) + 12m + n. \tag{20}$$

Using  $M_1(G^*) = 8M_1(G) + 4 \cdot 2^{2k}m + (2^{2k-1} - 2^{k-1} + 2)n$  and the number of edges of strong double graph  $m = 4^k m + (2^{2k-1} - 2^{k-1})n$ , we have

$$\begin{aligned}
M_2(G^*) &= 16M_2(G) + 12\{8M_1(G) + 4 \cdot 2^{2k}m + (2^{2k-1} - 2^{k-1} + 2)n\} + 12\{4^k m + (2^{2k-1} - 2^{k-1})n\} + n, \\
M_2(G^*) &= 16M_2(G) + 96M_1(G) + (192 + 12 \cdot 2^{2k})m + (6 \cdot 2^{2k} - 6 \cdot 2^k + 25)n.
\end{aligned} \tag{21}$$

By Theorem 1 and the definition of the  $k$ -iterated strong double graph, for  $k \geq 1$ , we have

$$\begin{aligned}
M_2(G^*) &= 16M_2(G^{(k-1)*}) + 12 \cdot 2^{3(k-1)}M_1(G) + (6 \cdot 2^{3(k-1)} + 6 \cdot 2^{5(k-1)})m + (6 \cdot 4^{k-1} - 6 \cdot 2^{k-1} + 5^{2(k-1)})n \\
&= 16\{16M_2(G^{(k-2)*}) + 12 \cdot 2^{3(k-2)}M_1(G) + (6 \cdot 2^{3(k-2)} + 6 \cdot 2^{5(k-2)})m\} \\
&\quad + 16 \cdot (6 \cdot 4^{k-2} - 6 \cdot 2^{k-2} + 5^{2(k-2)})n + 12 \cdot 2^{3(k-1)}M_1(G) \\
&\quad + (6 \cdot 2^{3(k-1)} + 6 \cdot 2^{5(k-1)})m + (6 \cdot 4^{k-1} - 6 \cdot 2^{k-1} + 5^{2(k-1)})n \\
&= 16^2 M_2(G^{(k-1)*}) + \frac{9 \cdot 2^{3(k)}}{2} M_1(G) + \left(\frac{9 \cdot 2^{3k}}{4} + \frac{9 \cdot 2^{5k}}{32}\right)m + \left(\frac{15 \cdot 2^{2k}}{2} - \frac{41 \cdot 5^{2k}}{625} + 27 \cdot 2^k + 1\right)n, \\
M_2(G^{*k}) &= 16^2\{16M_2(G^{(k-3)*}) + 12 \cdot 2^{3(k-3)}M_1(G) + (6 \cdot 2^{3(k-3)} + 6 \cdot 2^{5(k-3)})m\} \\
&\quad + 16^2 \cdot (6 \cdot 4^{k-3} - 6 \cdot 2^{k-3} + 5^{2(k-3)})n + \frac{9 \cdot 2^{3(k)}}{2} M_1(G) \\
&\quad + \left(\frac{9 \cdot 2^{3k}}{4} + \frac{9 \cdot 2^{5k}}{32}\right)m + \left(\frac{15 \cdot 2^{2k}}{2} - \frac{41 \cdot 5^{2k}}{625} + 27 \cdot 2^k + 1\right)n, \\
M_2(G^*) &= 16^3 M_2(G^{(k-3)*}) + \frac{21 \cdot 2^{3k}}{2} M_1(G) + \left(\frac{21 \cdot 2^{3k}}{4} + \frac{21 \cdot 2^{5k}}{64}\right)m + \left(\frac{63 \cdot 2^{2k}}{2} + \frac{1281 \cdot 5^{2k}}{15625} + 219 \cdot 2^k + 1\right)n, \\
&\vdots \\
M_2(G^{*k}) &= 3 \cdot 2^{3k-1} \cdot (2^k - 1)M_1(G) + 4^{2k}M_2(G) + 3 \cdot 2^{2k} \cdot (2^k - 1)^2 m + 2^{k-1}(2^k - 1)^3 n.
\end{aligned} \tag{22}$$

$$\begin{aligned} \text{(iii)} \quad \overline{M}_1(G^{*k}) &= 8^k \overline{M}_1(G) + (2^k - 1)4^k(n^2 - n - 2m). \\ M_1(G^*) &= 8\overline{M}_1(G^*) - 8m + 4n^2 + 4n. \end{aligned} \quad (23)$$

By Theorem 1 and the definition of the  $k$ -iterated strong double graph, for  $k \geq 1$ , we have

$$\begin{aligned} M_1(G^{k*}) &= 8\overline{M}_1(G^{(k-1)*}) - 2^{2k+1}m + 2^{2k}n^2 + 2^{2k}n \\ M_1(G^{k*}) &= 8\{8\overline{M}_1(G^{(k-2)*}) - 2^{2(k-1)+1}m + 2^{2(k-1)}n^2 + 2^{2(k-1)}n\} \\ &\quad - 2^{2k+1}m + 2^{2k}n^2 + 2^{2k}n \\ &= 8^2 M_1(G^{(k-2)*}) - 6 \cdot 2^{2k}m + 3 \cdot 2^{2k}n^2 + 3 \cdot 2^{2k}n \\ &= 8^2 \{8\overline{M}_1(G^{(k-3)*}) - 2^{2(k-2)+1}m + 2^{2(k-2)}n^2 + 2^{2(k-2)}n\} - 6 \cdot 2^{2k}m \\ &\quad + 3 \cdot 2^{2k}n^2 + 3 \cdot 2^{2k}n \\ &= 8^3 \overline{M}_1(G^{(k-3)*}) - 14 \cdot 2^{2k}m + 7 \cdot 2^{2k}n^2 + 7 \cdot 2^{2k}n \\ &\quad \vdots \\ M_1(G^{k*}) &= 8^k \overline{M}_1(G) + (2^k - 1)4^k(n^2 - n - 2m). \end{aligned} \quad (24)$$

$$\text{(iv)} \quad \overline{M}_2(G^{*k}) = 2^{4k} \overline{M}_2(G) + 2^{3k} \cdot (2^k - 1) \overline{M}_1(G) + 2^{2k-1} \cdot (2^k - 1)^2 (n^2 - n - 2m).$$

$$\overline{M}_2(G^{k*}) = 16\overline{M}_2(G^{(k-1)*}) + 8\overline{M}_1(G^{(k-1)*}) + 2(n^2 - n - 2m), \quad (26)$$

and using  $\overline{M}_1(G^*) = 8\overline{M}_1(G) - 8m + 4n^2 + 4n$ , we have

$$\overline{M}_2(G^*) = 16\overline{M}_2(G) + 8\overline{M}_1(G) + 2(n^2 - n - 2m). \quad (25)$$

By Theorem 1 and the definition of the  $k$ -iterated strong double graph, for  $k \geq 1$ , we have

$$\begin{aligned} \overline{M}_2(G^{k*}) &= 16\overline{M}_2(G^{(k-1)*}) + 8\{8\overline{M}_1(G) - 8m + 4n^2 + 4n\} + 2(n^2 - n - 2m) \\ &= 16\overline{M}_2(G^{(k-1)*}) + 64\overline{M}_1(G) + 32(n^2 - n - 2m) + 2(n^2 - n - 2m). \end{aligned} \quad (27)$$

By rearranging the terms, we have

$$\begin{aligned}
\overline{M}_2(G^{k*}) &= 16\overline{M}_2(G^{(k-1)*}) + 8 \cdot 8^{(k-1)}\overline{M}_1(G) + 32^{(k-1)}(n^2 - n - 2m) \\
&\quad + 2^{(3k-3)}(n^2 - n - 2m) \\
&= 16\{16\overline{M}_2(G^{(k-2)*}) + 8 \cdot 8^{(k-2)}\overline{M}_1(G) + 32^{(k-2)}(n^2 - n - 2m)\} \\
&\quad + 16 \cdot 2^{(3k-6)}(n^2 - n - 2m) + 8 \cdot 8^{(k-1)}\overline{M}_1(G) \\
&\quad + 32^{(k-1)}(n^2 - n - 2m) + 2^{(3k-3)}(n^2 - n - 2m) \\
&= 16^2\overline{M}_2(G^{(k-2)*}) + 3 \cdot 2^{(3k)}\overline{M}_1(G) + \frac{3 \cdot 2^{(5k)}}{64}(n^2 - n - 2m) \\
&\quad + \frac{3 \cdot 2^{(3k)}}{8}(n^2 - n - 2m) \\
&= 16^2\{16\overline{M}_2(G^{(k-3)*}) + 8 \cdot 8^{(k-3)}\overline{M}_1(G) + 32^{(k-3)}(n^2 - n - 2m)\} \\
&\quad + 16^2 \cdot 2^{(3k-9)}(n^2 - n - 2m) + 3 \cdot 2^{(3k)}\overline{M}_1(G) \\
&\quad + \frac{3 \cdot 2^{(5k)}}{64}(n^2 - n - 2m) + \frac{3 \cdot 2^{(3k)}}{8}(n^2 - n - 2m) \\
&= 16^3\overline{M}_2(G^{(k-3)*}) + 7 \cdot 2^{(3k)}\overline{M}_1(G) + \frac{7 \cdot 2^{(5k)}}{128}(n^2 - n - 2m) \\
&\quad + \frac{7 \cdot 2^{(3k)}}{8}(n^2 - n - 2m) \\
&\quad \vdots \\
\overline{M}_2(G^{k*}) &= 2^{4k}\overline{M}_2(G) + 2^{3k} \cdot (2^k - 1)\overline{M}_1(G) + 2^{2k-1} \cdot (2^k - 1)^2(n^2 - n - 2m).
\end{aligned} \tag{28}$$

Here, we present an algorithm to generate and verify the first and second Zagreb indices and coindices of any finite simple connected graph  $G$ . This algorithm is based on the adjacency matrix of  $G$  (Algorithm 1).  $\square$

*Example 1.* Let  $A$ ,  $B$ , and  $C$  be the matrices of path graph  $P_4$  and strong double graphs  $SD^{1*}(P_4)$  and  $SD^{2*}(P_4)$ , respectively. These matrices are square and symmetric, and

choose value 1 (one) at the  $i$ th row and  $j$ th column if  $v_i$  and  $v_j$  are adjacent vertices in a graph; otherwise, it is 0. The suggested algorithm is applied on these matrices to compute the first Zagreb index  $IM_1$ , second Zagreb index  $IM_2$ , first Zagreb coindex  $CM_1$ , and second Zagreb coindex  $CM_2$ . These adjacency matrices have been obtained by drawing the respective graphs in "GraphTea" software; this software is easily available, and it is free of cost.

Input:  $A$  is an adjacency matrix of a finite simple connected graph  
 Output:  $IM_1, IM_2, CM_1, CM_2$   
 Variables used:  $nr$  = number of rows in  $A$ ,  $nc$  = number of columns in  $A$ ,  
 (1)  $IM_1 := 0, IM_2 := 0, CM_1 := 0, CM_2 := 0$   
 (2) for  $i = 1$  to  $nr$   
 (3) for  $j = i$  to  $nc$   
 (4)  $s_i :=$  sum of  $i$ th row of  $A$ ,  
 (5)  $s_j :=$  sum of  $j$ th column of  $A$ .  
 (6) if  $A(i, j) = 1$   
 (7)  $IM_1 := IM_1 + (S_i + S_j)$   
 (8)  $IM_2 := IM_2 + (S_i * S_j)$   
 (9) end if  
 (10) if  $A(i, j) = 0$  and  $i \neq j$   
 (11)  $CM_1 := CM_1 + (S_i + S_j)$   
 (12)  $CM_2 := CM_2 + (S_i * S_j)$   
 (13) end if  
 (14) end for  $j$   
 (15) end for  $i$

ALGORITHM 1: Computing the first Zagreb index  $IM_1$ , second Zagreb index  $IM_2$ , first Zagreb coindex  $CM_1$ , and second Zagreb coindex  $CM_2$ .

$$\begin{aligned}
 A &= \begin{bmatrix} 0 & 1 & 0 & 0 \\ 1 & 0 & 1 & 0 \\ 0 & 1 & 0 & 1 \\ 0 & 0 & 1 & 0 \end{bmatrix}, \\
 B &= \begin{bmatrix} 0 & 1 & 0 & 0 & 1 & 1 & 0 & 0 \\ 1 & 0 & 1 & 0 & 1 & 1 & 1 & 0 \\ 0 & 1 & 0 & 1 & 0 & 1 & 1 & 1 \\ 0 & 0 & 1 & 0 & 0 & 0 & 1 & 1 \\ 1 & 1 & 0 & 0 & 0 & 1 & 0 & 0 \\ 1 & 1 & 1 & 0 & 1 & 0 & 1 & 0 \\ 0 & 1 & 1 & 1 & 0 & 1 & 0 & 1 \\ 0 & 0 & 1 & 1 & 0 & 0 & 1 & 0 \end{bmatrix}, \\
 C &= \left\{ \begin{array}{l} 0 & 1 & 0 & 0 & 1 & 1 & 0 & 0 & 1 & 1 & 0 & 0 & 1 & 1 & 0 & 0 & 0 & 0 & 0 \\ 1 & 0 & 1 & 0 & 1 & 1 & 1 & 0 & 1 & 1 & 1 & 0 & 0 & 0 & 0 & 0 & 0 & 0 & 0 \\ 0 & 1 & 0 & 1 & 0 & 1 & 1 & 1 & 0 & 1 & 1 & 1 & 0 & 0 & 0 & 0 & 0 & 0 \\ 0 & 0 & 1 & 0 & 0 & 0 & 1 & 1 & 0 & 0 & 1 & 1 & 0 & 0 & 0 & 0 & 0 & 0 \\ 1 & 1 & 0 & 0 & 0 & 1 & 0 & 0 & 1 & 0 & 0 & 0 & 1 & 1 & 0 & 0 & 0 & 0 \\ 1 & 1 & 1 & 0 & 1 & 0 & 1 & 0 & 0 & 0 & 0 & 0 & 1 & 1 & 1 & 0 & 0 & 0 \\ 0 & 1 & 1 & 1 & 0 & 1 & 0 & 1 & 0 & 0 & 0 & 0 & 0 & 1 & 1 & 1 & 0 & 0 \\ 0 & 0 & 1 & 1 & 0 & 0 & 1 & 0 & 0 & 0 & 0 & 0 & 0 & 0 & 0 & 1 & 1 & 0 \\ 1 & 1 & 0 & 0 & 1 & 0 & 0 & 0 & 0 & 1 & 0 & 0 & 1 & 1 & 0 & 0 & 0 & 0 \\ 1 & 1 & 1 & 0 & 0 & 0 & 0 & 0 & 1 & 0 & 1 & 0 & 1 & 1 & 1 & 0 & 0 & 0 \\ 0 & 1 & 1 & 1 & 0 & 0 & 0 & 0 & 0 & 1 & 0 & 1 & 0 & 1 & 1 & 1 & 0 & 0 \\ 0 & 0 & 1 & 1 & 0 & 0 & 0 & 0 & 0 & 0 & 1 & 0 & 0 & 0 & 0 & 1 & 1 & 0 \\ 1 & 0 & 0 & 0 & 1 & 1 & 0 & 0 & 1 & 1 & 0 & 0 & 0 & 1 & 0 & 0 & 0 & 0 \\ 0 & 0 & 0 & 0 & 1 & 1 & 1 & 0 & 1 & 1 & 1 & 0 & 1 & 0 & 1 & 0 & 1 & 0 \\ 0 & 0 & 0 & 0 & 0 & 1 & 1 & 1 & 0 & 1 & 1 & 1 & 0 & 1 & 0 & 1 & 0 & 1 \\ 0 & 0 & 0 & 0 & 0 & 0 & 1 & 1 & 0 & 0 & 1 & 1 & 0 & 0 & 1 & 0 & 0 & 1 \end{array} \right\}.
 \end{aligned} \tag{29}$$

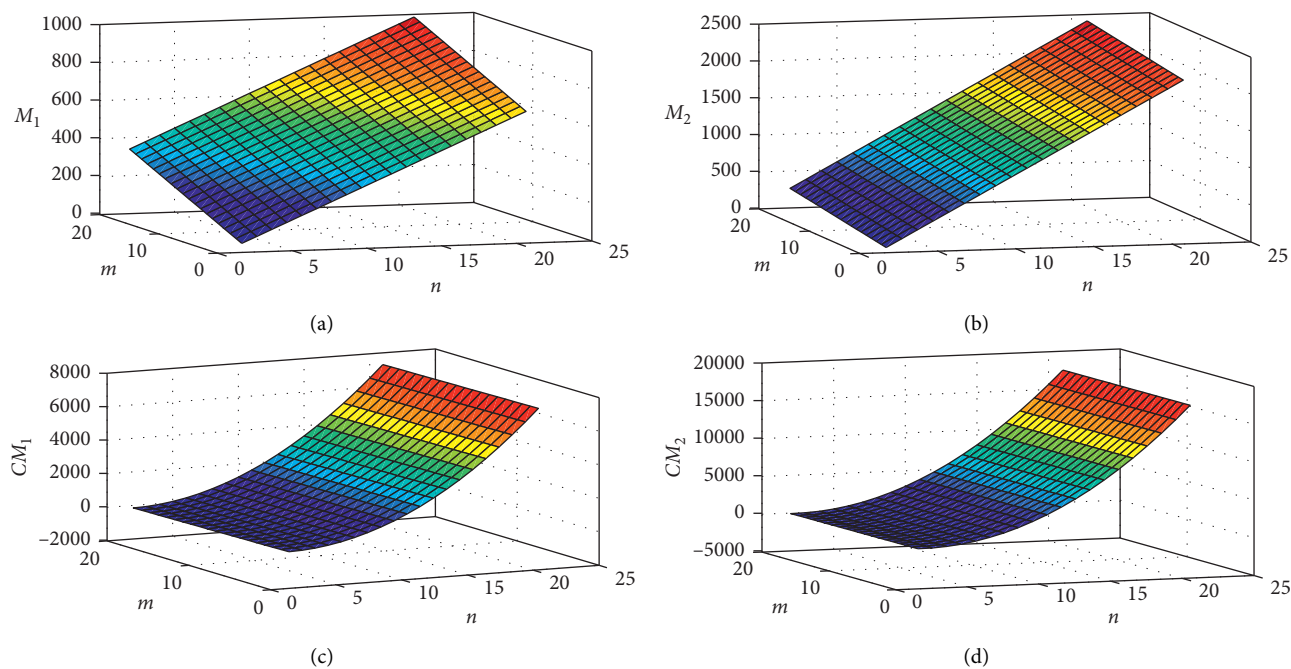


FIGURE 3: 3D surface plot of Zagreb indices and coincides of  $SD(P_n)$ .

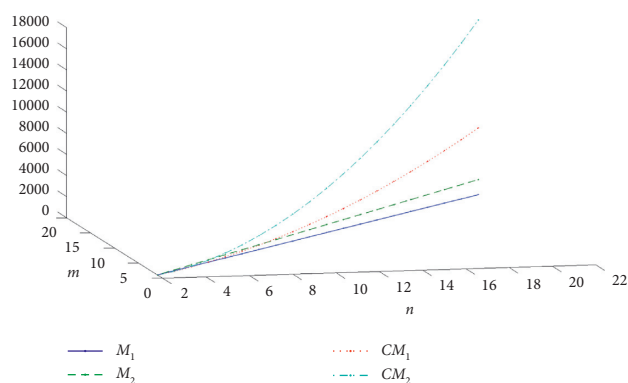


FIGURE 4: 3D curve plot of Zagreb indices and coincides of  $SD(P_n)$ .

The result of the algorithm is given as follows:

Graph	Matrix	$AM_1$	$AM_2$	$CM_1$	$CM_2$
$P_4$	A	10	8	8	5
$SD^{1*}(P_4)$	B	136	288	88	156
$SD^{2*}(P_4)$	C	756	2652	864	2802

Now, we provide graphs of Zagreb indices and coincides. Such type of graphical representation will be more helpful to study the dynamics of topological descriptors of the molecular graphs. Here, we present the strong double graph of the path graph,  $SD(P_n)$ , where  $2 \leq n \leq 21$  and  $m = n - 1$ . In Figure 3, the behaviour of the first Zagreb index  $M_1$  and second Zagreb index  $M_2$  is linear as the straight plane, and the behaviour of the first Zagreb coindex  $CM_1$  and second Zagreb coindex  $CM_2$  is nonlinear as the curved form. In

Figure 4, we have drawn the curves of these indices and coincides for  $SD(P_n)$  to understand their dynamics. This figure shows the relation between Zagreb indices and coincides as  $M_1 \leq M_2 \leq CM_1 \leq CM_2$ .

### 3. Conclusion

We have presented generalized explicit formulas to calculate the first Zagreb index  $M_1(G)$ , second Zagreb index  $M_2(G)$ , first Zagreb coindex  $\overline{M}_1(G)$ , and second Zagreb coindex  $\overline{M}_2(G)$  of the strong double graph  $SD(G)$  and  $k$ -iterated strong double graph  $SD^{k*}(G)$ . The relation between these indices and coincides is also presented as  $M_1 \leq M_2 \leq CM_1 \leq CM_2$ . We have also presented an algorithm with a given adjacency matrix to verify these indices and coincides by programming and numerically. Computer-generated graphs are also given to understand the dynamics of these indices and coincides.

This family of graphs can be considered for other degree-based and distance-related topological indices for further studies.

### Data Availability

No data were used to support this study.

### Conflicts of Interest

The authors declare that there are no conflicts of interest.

### Authors' Contributions

All authors contributed equally to this work.

## References

- [1] B. Danail and D. H. Rouvray, *Chemical Graph Theory: Introduction and Fundamentals*, CRC Press, Boca Raton, FL, USA, 1991.
- [2] R. Todeschini and V. Consonni, *Handbook of Molecular Descriptors*, Wiley-VCH, Weinheim, Germany, 2000.
- [3] R. Todeschini and V. Consonni, "New local vertex invariants and molecular descriptors based on functions of the vertex degrees," *MATCH Communications in Mathematical and in Computer Chemistry*, vol. 64, pp. 359–372, 2010.
- [4] H. H. Lowell and K. B. Lemont, *Molecular Connectivity in Chemistry and Drug Research*, Academic Press, Cambridge, MA, USA, 1976.
- [5] H. Wiener, "Structural determination of paraffin boiling points," *Journal of the American Chemical Society*, vol. 69, no. 1, pp. 17–20, 1947.
- [6] A. R. Ashrafi, T. Došlić, and A. Hamzeh, "The Zagreb coindices of graph operations," *Discrete Applied Mathematics*, vol. 158, no. 15, pp. 1571–1578, 2010.
- [7] L. Yang, X. Ai, and L. Zhang, "The Zagreb coindices of a type of composite graph," *Hacetatepe Journal of Mathematics and Statistics*, vol. 45, pp. 1135–1142, 2016.
- [8] I. Gutman and N. Trinajstić, "Graph theory and molecular orbitals. Total  $\phi$ -electron energy of alternant hydrocarbons," *Chemical Physics Letters*, vol. 17, no. 4, pp. 535–538, 1972.
- [9] S. Nikolic, G. Kovacevic, A. Milicevic, and N. Trinajstic, "The Zagreb indices 30 years after," *Croatica Chemica Acta*, vol. 76, pp. 113–124, 2003.
- [10] I. Gutman, "Multiplicative Zagreb indices of trees," *Bulletin of the Society of Mathematicians Banja Luka*, vol. 18, pp. 17–23, 2011.
- [11] M. Eliasi, A. Iranmanesh, and I. Gutman, "Multiplicative versions of first Zagreb index," *MATCH Communications in Mathematical and in Computer Chemistry*, vol. 68, pp. 217–230, 2012.
- [12] K. Xu and K. C. Das, "Trees, unicyclic, and bicyclic graphs extremal with respect to multiplicative sum Zagreb index," *MATCH Communications in Mathematical and in Computer Chemistry*, vol. 68, pp. 257–272, 2012.
- [13] K. C. Das, "On comparing Zagreb indices of graphs," *MATCH Communications in Mathematical and in Computer Chemistry*, vol. 63, pp. 433–440, 2010.
- [14] T. Doslic, "Vertex-weighted wiener polynomials for composite graphs," *Ars Mathematica Contemporanea*, vol. 1, pp. 66–80, 2008.
- [15] A. R. Ashrafi, T. Doslic, and A. Hamzeh, "Extremal graphs with respect to the Zagreb coindices," *MATCH Communications in Mathematical and in Computer Chemistry*, vol. 65, pp. 85–92, 2011.

## Research Article

# Study of Hardness of Superhard Crystals by Topological Indices

**Xiujun Zhang** <sup>1</sup>, **Muhammad Naeem** <sup>2</sup>, **Abdul Qudair Baig** <sup>2</sup>,  
**and Manzoor Ahmad Zahid** <sup>3</sup>

<sup>1</sup>School of Computer Science, Chengdu University, Chengdu, China

<sup>2</sup>Department of Mathematics and Statistics, Institute of Southern Punjab, Multan, Pakistan

<sup>3</sup>Department of Mathematics, COMSATS University Islamabad, Sahiwal, Pakistan

Correspondence should be addressed to Muhammad Naeem; naeempkn@gmail.com

Received 2 June 2021; Accepted 10 July 2021; Published 20 July 2021

Academic Editor: Dario Pasini

Copyright © 2021 Xiujun Zhang et al. This is an open access article distributed under the Creative Commons Attribution License, which permits unrestricted use, distribution, and reproduction in any medium, provided the original work is properly cited.

Topological indices give immense information about a molecular structure or chemical structure. The hardness of materials for the indentation can be defined microscopically as the total resistance and effect of chemical bonds in the respective materials. The aim of this paper is to study the hardness of some superhard  $BC_x$  crystals by means of topological indices, specifically Randić index and atom-bond connectivity index.

## 1. Introduction

Hardness measures the crystal property of resistance into its deformation. In crystal-type materials, the resistance depends on the chemical bonds between its atoms. In the case of common metals and materials, there exists a delocalized form of bonding. For the domination of the hardness value, the dislocation density which is stored in metals is sufficient. There are many strategies that exist to establish the microscopic theory for the hardness level, and the main ideas are to analyze the experimental material (or metal). There also exist some microscopic hardness models for the prediction of hardness, and these can be applied to covalent (and in some cases to ionic type) crystals (see Gao et al. [1]). A technique to relate the hardness of Vickers for a large class of crystals of covalent type to their microscopic properties has been studied in [2]. To energetically break an electron pair bond has the meaning that two electrons excite from the valence band to the conduction band in covalent crystals. In [3], Gilman proved that the activation energy that is required for a plastic slip is double the band gap denoted as  $E_g$ . The force of resistance of a bond can be computed by studying respective  $E_g$  of the materials. The form of the hardness for pure covalent-type crystals consists of three variables, and it is formulated as

$$H \text{ (Gpa)} = AN_a E_g, \quad (1)$$

where  $A$  is the constant of proportionality and  $N_a$  represents the covalent bond number, and it is per unit area; this area is such that it can be computed from the valence electron density  $N_e$  as

$$N_a = \left( \frac{\sum_i n_i Z_i}{2V} \right) = \left( \frac{N_e}{2} \right)^{2/3}, \quad (2)$$

where  $n_i$  is the position in the form of a number of the  $i$ th atom in the unit cell,  $Z_i$  is the valence electron number of the  $i$ th atom crediting to the covalent bond, and  $V$  is the volume of the unit cell. More results on the hardness (various definitions of hardness) study of crystals can be referred to Suzuki et al. [4], Armstrong et al. [5], Mamun et al. [6], Shkir et al. [7], and Palatnikov et al. [8].

Now, if we talk about the unit crystals studied in this article, then the first one is  $BC_2$ , and by the first-principles computations,  $BC_2$  was predicted originally from (a kind of tetragonal phase) the cubic diamond structure. The lattice of the  $BC_2$  structure is tetragonal, and this structure possesses the simple kind of the stacking sequence such as  $BC_2BC_2 \dots$  along with the  $c$ -axis. Monitoring different states of the electronic densities of  $BC_2$  shows that, in the crystal, all the  $B - C$ - and  $C - C$ -type bonds are purely metallic. The known

hardness level of  $BC_2$  is 56 GPa (gigapascal), and this level is very close to that of cubic boron nitride.

Now, compound  $BC_3$  has a different type of crystal structure which is more like and similar to graphite, and so, it has a hexagonal crystal-type structure. A study was performed in [2] to investigate some improved oxidation resistance in a graphitic material that contains very high collections of secondary boron. The procedure to create and find such samples is a reaction between boron trichloride and benzene to examine for chemical composition and crystal structure.

Another class of recently discovered compounds, which has almost the same structure as that of the diamond, is the crystal structure of  $BC_5$ . For the purpose of correlation, compound  $BC_5$  is very important, and it is also very useful to know under which type of conditions this compound can be extracted. As a function of pressure, the stability of compound  $BC_5$  is relative to a solution of compound  $BC_3$  and graphite.

Another similar but different compound is the  $BC_7$  crystal structure which is more like to both compound structures of graphite and diamond. By computing the constants of elasticity and frequencies of phonon, the structural stability of the assumed compound crystal structure  $BC_7$  has been confirmed. Similar to the direction for tensile strength of the diamond-like  $BC_7$ , its ideal tensile strength was 155.2 GPa; this strength is about 52% more than that of the recent diamond-like predicted structure  $BC_5$ . The theoretical Vickers hardness of the diamond crystals like  $BC_7$  was 78 GPa which indicates that it is a superhard material; these readings show that  $BC_7$  is a superhard material (see in [2]).

We can formulate the Vickers hardness in the form of  $f_i$ ,  $N_e$ , and  $d$  as follows:

$$H_v \text{ (GPa)} = 556 \frac{N_e e^{-1.191 f_i}}{d^{2.5}} = 350 \frac{N_e^{2/3} e^{-1.191 f_i}}{d^{2.5}}, \quad (3)$$

where  $f_i$  is the ionicity of the chemical bond in a crystal scale and  $d$  is the bond length in angstroms [9].

In the 70's, one of the famous degree-based indices is the Randić index which was introduced by Randić [10] in 1975, and it is characterized as

$$R_{-(1/2)}(G) = \sum_{uv \in E(G)} \frac{1}{\sqrt{d_u d_v}} \quad (4)$$

In 1998, Bollobás and Erdos [11] and Amić et al. [12] proposed the general Randić index which is stated as

$$R_\alpha(G) = \sum_{uv \in E(G)} (d_u d_v)^\alpha \quad (5)$$

Das et al. [13] studied the relationship between the Randić index and other degree-based indices. Milivojević and Pavlović [14] presented the extremal value and graphs for the variation of the Randić index with regard to minimum and maximum degrees.

Atom-bond connectivity index (in short, ABC index) was introduced by Estrada et al. [15] to measure the stability

of alkanes and the strain energy of cycloalkanes which can be formulated by

$$ABC(G) = \sum_{uv \in E(G)} \sqrt{\frac{d_u + d_v - 2}{d_u d_v}} \quad (6)$$

Dimitrov [16] provided an affirmative answer of a strengthened version of the previous conjecture and presented that a tree with a minimal ABC index cannot contain a pendent path of length 3 if its order is larger than 415. Dimitrov and Milosavljević [17] manifested several properties of the degree sequences of the trees with minimal ABC index, and a new algorithm for minimal-ABC trees is given. The definitions of more topological indices and results can be referred to Gao et al. [18–22]. Some more literature studies are also available in [23, 24].

The applications of moving correlation coefficient technique enable us to examine the variation in the degree of correlation between correlation stratigraphic sequence and analysis the measure of variables within the framework of a single stratigraphic sequence. Cumulative correlation technique allows to determining more precisely, where such variation took place and it influences every member within the sequence of the preceding ones.

Since both hardness properties and topological indices are important topics in crystal science, it inspired us to study the relationship between them. The main contribution of this paper is to study the hardness of some superhard  $BC_x$  crystals in the light of topological indices.

## 2. Main Results

Many  $B-C$  binary systems show high resistance to oxidation and reaction with ferrous metals, compared with the carbon-based materials. In Figure 1, we present selected  $BC_x$  systems with specific crystal structures found in [2]. The Randić and atom-bond connectivity indices of these 12 types of  $BC$  crystals are computed as follows.

From Figure 1(a), we can see that the number of edges in the unit cell of  $BC_2/41/amd$  is 36. We present the edge partition of  $BC_2/41/amd$  in Table 1 based on the degree of vertices of each edge. The Randić index and ABC index for the  $BC_2/41/amd$  crystal are computed using Table 1, and they are 14.136584 and 25.3452096, respectively.

The number of edges of  $BC_3P4m2$ , from Figure 1(b), is 12, and 8 of its edges are of type (1, 3), and 4 are of type (3, 4). This gives us the Randić and ABC indices 5.773502692 and 9.113961545, respectively.

The number of edges in both  $BC_3Pmmma$  and  $BC_3Pmmab$  is 12 by Figures 1(c) and 1(d). The edge type of these two structures is also the same, containing 4 edges of type (1, 3), 2 edges of type (3, 3), 4 edges of type (2, 3), and 2 edges of type (2, 2). So, the Randić and ABC indices of  $BC_3Pmmma$  and  $BC_3Pmmab$  are the same. They are 5.6090609 and 8.84196034, respectively.

From Figure 1(e), we can see that  $BC_5I4m2$  consists of 20 edges. The degree-based edge partition of this structure is given by 10 edges of type (2, 2), 8 edges of type (2, 3), and 2

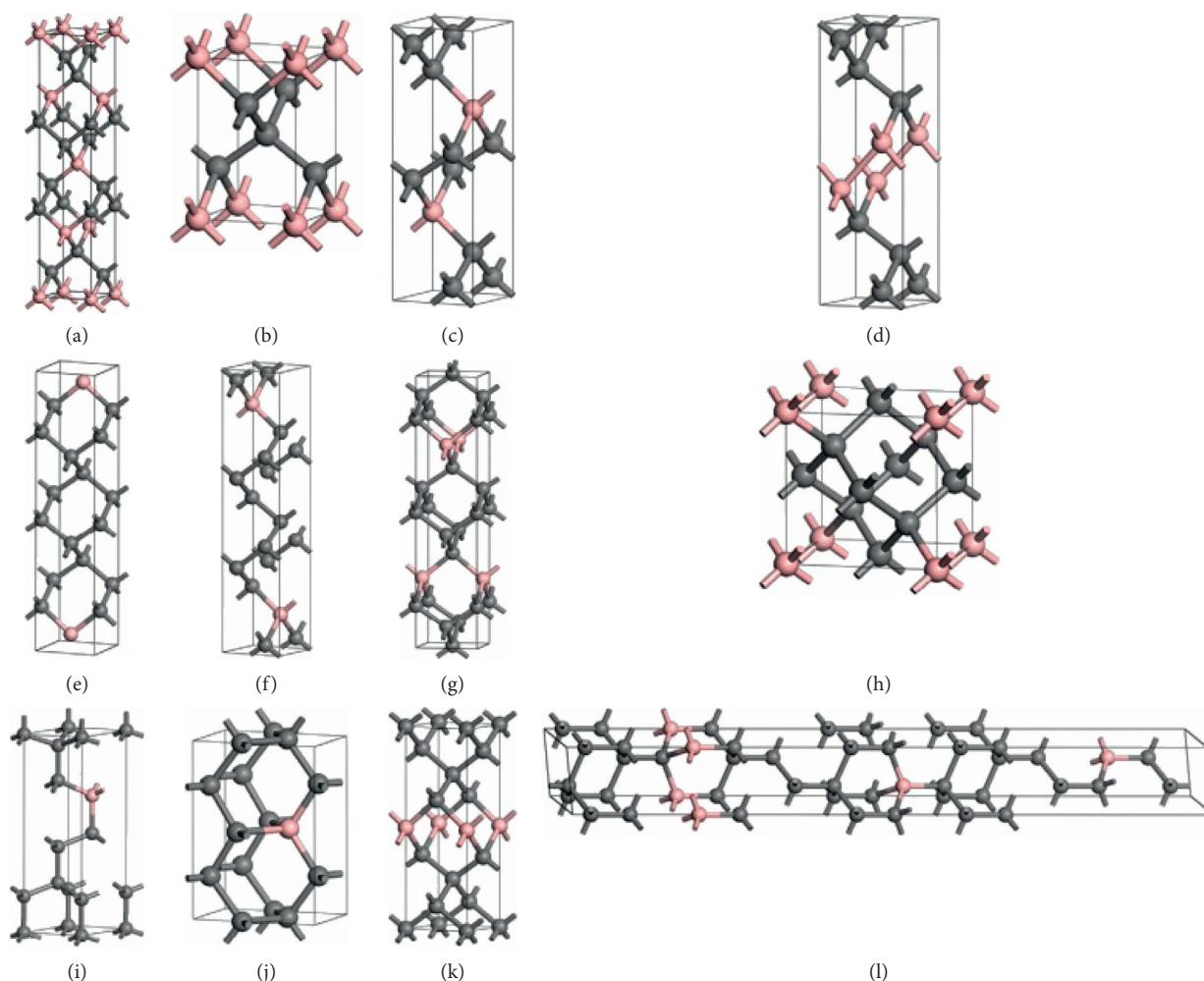


FIGURE 1: Crystal structures of (a)  $BC_2I41/amd$ , (b)  $BC_2P4m2$ , (c)  $BC_3Pmma-a$ , (d)  $BC_3Pmma-b$ , (e)  $BC_2I41/amd$ , (f)  $BC_5Pmma-1$ , (g)  $BC_5Pmma-2$ , (h)  $BC_7P4\ 3m$ , (i)  $BC_7P3m1$ , (j)  $BC_7Pmm2$ , (k)  $BC_7P4m2$ , and (l)  $BC_7R3m$ . Boron atoms are shown in orange.

TABLE 1: Edge partition of  $BC_2I41/amd$ .

$d_u, d_v$	Frequency
(1, 3)	8
(2, 3)	12
(3, 4)	16

edges of type (3, 3). This gives us the Randić and ABC indices as 8.93265299 and 14.0612554, respectively.

The number of edges of  $BC_5Pmma1$ , from Figure 1(f), is 15. Its degree-based edge partition is given by 4 edges of type (1, 3), 2 edges of type (2, 3), 2 edges of type (1, 1), and 7 edges of type (2, 2). So, the Randić and ABC indices are 12.4282032 and 9.62994735, respectively.

The number of edges of  $BC_5Pmma2$ , from Figure 1(g), is 36. Its degree-based edge partition contains 4 edges of type (2, 3), 24 edges of type (3, 3), and 8 edges of type (3, 4). So, the Randić and ABC indices are 11.9423942 and 23.9924049, respectively. From Figure 1(h), the number of edges of

$BC_7P4\ 3m$  is 16. Its degree-based edge partition contains 4 edges of type (1, 4) and 12 edges of type (2, 4). So, the Randić and ABC indices for this crystal are 6.24264069 and 11.949383, respectively.

The number of edges of  $BC_7P3m1$ , from Figure 1(i), is 15. Its degree-based edge partition is given by 1 edge of type (1, 1), 3 edges of type (1, 2), 5 edges of type (2, 4), 3 edges of type (1, 4), and 3 edges of type (2, 3). So, the Randić and ABC indices are 7.61383217 and 10.3762508, respectively. From Figure 1(j), the number of edges of is 18.  $BC_7Pmm2$  Its degree-based edge partition is given by 12 edges of type (2, 3), 2 edges of type (3, 3), and 4 edges of type (2, 2). So, the Randić and ABC indices are 7.56564615 and 12.6470418, respectively.

The number of edges of  $BC_7P4m2$ , from Figure 1(k), is 24. Its degree-based edge partition contains 8 edges of type (1, 3), 8 edges of type (3, 4), and 8 edges of type (2, 3). So, the Randić and ABC indices are 10.1941896 and 17.3528047, respectively. From Figure 1(l), the number of edges of  $BC_7R3m$  is 51. Its degree-based edge partition contains 2

TABLE 2: Hardness (H) of crystals  $BC_2I41/amd$ ,  $BC_3P4m2$ ,  $BC_3Pmhma-a$ ,  $BC_3Pmhma-b$ ,  $BC_5I41/amd$ ,  $BC_5Pmhma-1$ ,  $BC_5Pmhma-2$ ,  $BC_7P43m$ ,  $BC_7P3m1$ ,  $BC_7Pmm2$ ,  $BC_7P4m2$ , and  $BC_7Pmm2$ .

Crystal	Symmetry	Hardness	Reference
$BC_2$	$I4_1/amd$	56	[28]
$BC_3$	$P\bar{4}m2$	65.8	[26]
	$Pmma - a$	61.9	[26]
	$Pmma - b$	64.8	[26]
$BC_5$	$I\bar{4}m2$	80	[30]
	$Pmma - 1$	74	[25]
	$Pmma - 2$	70	[25]
$BC_7$	$P\bar{4}3m$	77.6	[29]
	$P3m1$	65.3	[27]
	$Pmm2$	80.7	[27]
	$P\bar{4}m2$	75.2	[27]
	$R3m$	65.4	[27]

TABLE 3: Structure symmetry, Randić index (R), atom-bond connectivity (ABC) index, calculated hardness (H), and their cumulative correlations (Cor) between (R, H) and (ABC, H).

Crystal	Symmetry	Randić index (R)	ABC index	Hardness of crystals	Cor (R, H)	Cor (ABC, H)
$BC_2$	$I4_1/amd$	14.136584	25.3452096	56.0	—	—
$BC_3$	$P\bar{4}m2$	5.77350269	9.11396154	65.8	-1	-1
	$Pmma - a$	5.6090609	8.84196034	61.9	-0.911790078	-0.9128016
	$Pmma - b$	5.60906090	8.84196034	64.8	-0.921902798	-0.92264538
$BC_5$	$I\bar{4}m2$	8.93265299	14.0612554	80.0	-0.267918644	-0.33848122
	$Pmma - 1$	12.4282032	9.62994735	74.0	-0.028477805	-0.39185327
	$Pmma - 2$	11.9423942	23.9924049	70.0	0.019298886	-0.23407776
$BC_7$	$P\bar{4}3m$	6.24264069	11.949383	77.6	-0.11272915	-0.26114031
	$P3m1$	7.61383217	10.3762508	65.3	-0.092422184	-0.2263985
	$Pmm2$	7.56564615	12.6470418	80.7	-0.134370355	-0.22184915
	$P\bar{4}m2$	10.1941896	17.3528047	75.2	-0.096163473	-0.17150281
	$R3m$	22.8743687	34.3374432	65.4	-0.197758916	-0.24340232

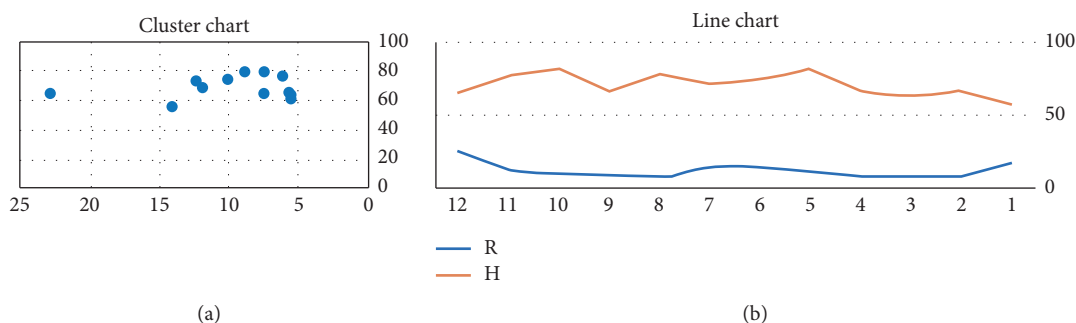


FIGURE 2: Cluster and line chart of R and H.

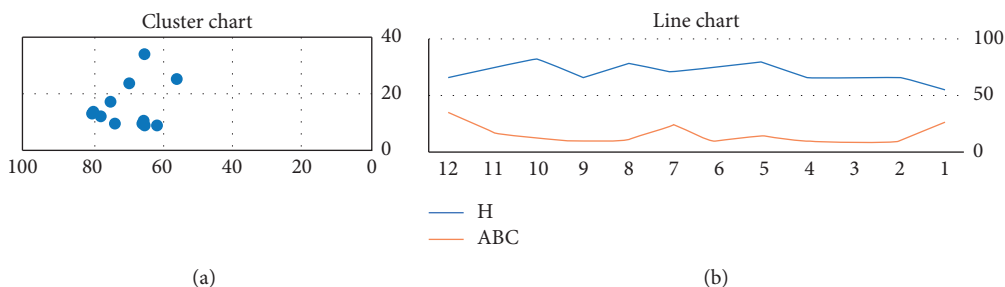


FIGURE 3: Cluster and line chart of ABC and H.

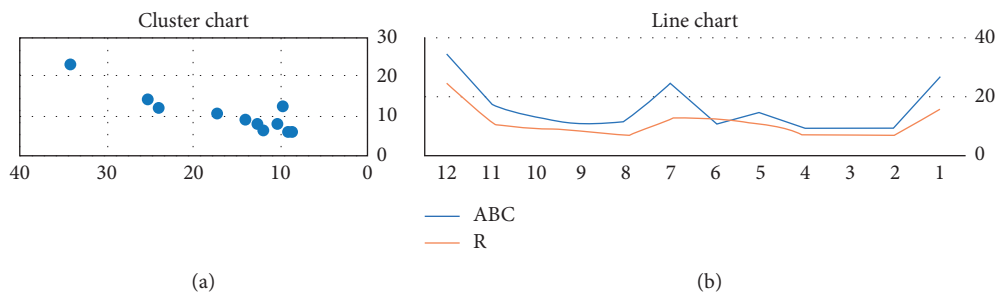


FIGURE 4: Cluster and line chart of R and ABC.

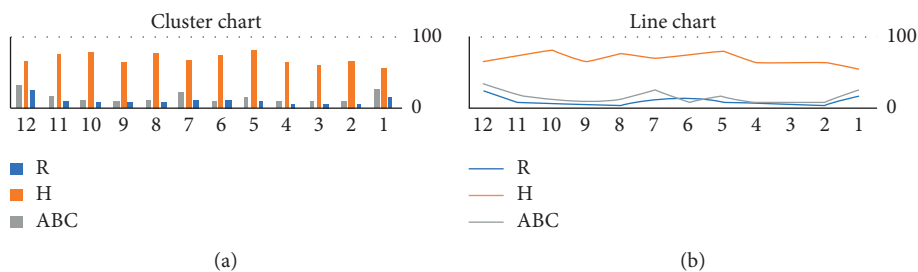


FIGURE 5: Cluster and line chart of ABC, R, and H.

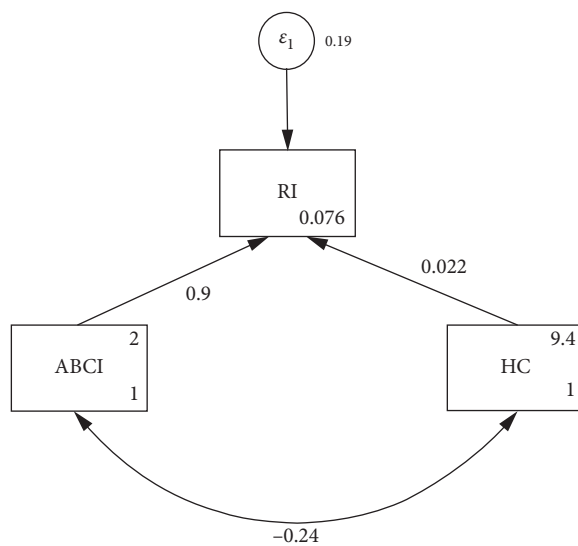


FIGURE 6: The magnitude of the effectiveness of ABCI and HC over RI.

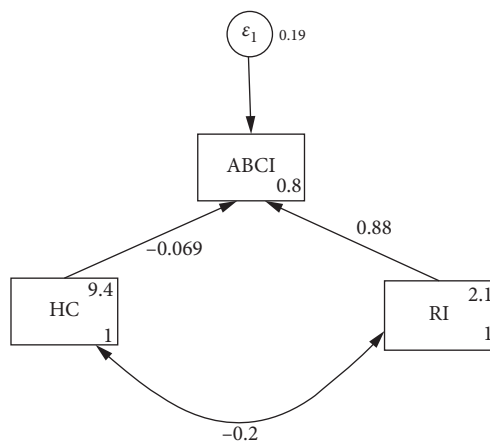


FIGURE 7: The magnitude of the effectiveness of RI and HC over ABCI.

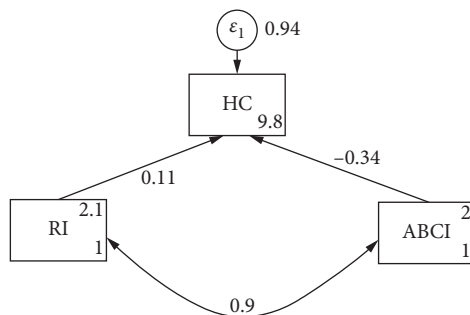


FIGURE 8: The magnitude of the effectiveness of ABCI and RI over HC.

SEM

Endogenous variables

Observed : RI

Exogenous variables

Observed : ABCI HC

Fitting target model :

Iteration 0 : log likelihood = -108.5116

Iteration 1 : log likelihood = -108.5116

Structural equation model

Number of obs = 12

Estimation method = ml

Log likelihood = -108.5116

Standardized	OIM					
	Coef.	Std. Err.	z	P >  z	[95% conf. interval]	
<b>Structural</b>						
RI <-						
ABCI	0.9025842	0.0636826	14.17	0.000	0.7777685	1.0274
HC	0.0219322	0.1313459	0.17	0.867	-0.2355011	0.2793655
_cons	0.0757925	1.32599	0.06	0.954	-2.523101	2.674686
Mean (ABCI)	1.978639	0.4964462	3.99	0.000	1.005622	2.951655
Mean (HC)	9.373905	1.935094	4.84	0.000	5.581191	13.16662
Var (e.RI)	0.1944974	0.1007828			0.0704443	0.5370088
Var (ABCI)	1	.			.	.
Var (HC)	1	.			.	.
Cov (ABCI, HC)	-0.2434024	0.2715727	-0.90	0.370	-0.775675	0.2888702

LR test of model vs. saturated:  $\chi^2(0) = 0.00$ ,  $\text{prob} > \chi^2 = .$

FIGURE 9: Tabular form of the magnitude of the effectiveness of ABCI and HC over RI as shown in Figure 6.

Endogenous variables

Observed : ABCI

Exogenous variables

Observed : HC RI

Fitting target model :

Iteration 0 : log likelihood = -108.5116

Iteration 1 : log likelihood = -108.5116

Structural equation model

Number of obs = 12

Estimation method = *ml*

Log likelihood = -108.5116

Standardized	OIM					
	Coef.	Std.	Err.	<i>z</i>	<i>P</i> >   <i>z</i>	[95% conf. interval]
Structural ABCI <-						
HC	-0.0686487	0.1293607		-0.53	0.596	-0.3221911 0.1848937
RI	0.88367	0.0664661		13.30	0.000	0.7533988 1.013941
_cons	0.7953603	1.311625		0.61	0.544	-1.775377 3.366097
Mean (HC)	9.373905	1.935094		4.84	0.000	5.581191 13.16662
Mean (RI)	2.067271	0.5112733		4.04	0.000	1.065194 3.069348
Var (e.ABCI)	0.1904215	0.0989202				0.0687914 0.5271064
Var (HC)	1	.				.
Var (RI)	1	.				.
Cov (HC, RI)	-0.197759	0.2773855		-0.71	0.476	-0.7414245 0.3459065

LR test of model vs. saturated:  $\chi^2(0) = 0.00$ ,  $\text{prob} > \chi^2 = .$

FIGURE 10: Tabular form of the magnitude of the effectiveness of RI and HC over ABCI as shown in Figure 7.

Endogenous variables

Observed : HC

Exogenous variables

Observed : RI ABCI

Fitting target model :

Iteration 0 : log likelihood = -108.5116

Iteration 1 : log likelihood = -108.5116

Structural equation model

Number of obs = 12

Estimation method = ml

Log likelihood = -108.5116

Standardized	OIM			z	P >  z	[95% conf. interval]	
	Coef.	Std.	Err.				
Structural							
HC <-							
RI	0.1058366	0.6327297		0.17	0.867	-1.134291	1.345964
ABCI	-0.3383638	0.6263131		-0.54	0.589	-1.565915	0.8891874
_cons	9.824612	1.935909		5.07	0.000	6.030301	13.61892
Mean (RI)	2.067271	0.5112733		4.04	0.000	1.065194	3.069348
Mean (ABCI)	1.978639	0.4964462		3.99	0.000	1.005622	2.951655
Var (e.HC)	0.9385716	0.1343048				0.7090303	1.242424
Var (RI)	1	.				.	.
Var (ABCI)	1	.				.	.
Conv (RI, ABCI)	0.8972459	0.0562772		15.94	0.000	0.7869446	1.007547

LR test of model vs. saturated:  $\chi^2(0) = 0.00$ ,  $\text{prob} > \chi^2 = .$

FIGURE 11: Tabular form of the magnitude of the effectiveness of ABCI and RI over HC as shown in Figure 8.

edges of type (1, 1), 5 edges of type (1, 2), 14 edges of type (2, 2), 2 edges of type (4, 4), 25 edges of type (2, 4), and 3 edges of type (3, 3). So, the Randić and ABC indices for this crystal are 22.8743687 and 34.3374432, respectively.

In [25–30], Li et al., Liu et al., L. Xu et al., and Yao et al. computed the hardness of the above selected crystals shown in Figure 1. The hardness of all the crystals is given in Table 2.

Table 3 shows the crystal structures of Figure 1 along with their Randić index (R), atom-bond connectivity (ABC) index, calculated hardness (H) from Table 2, and cumulative correlations (Cor) between (R, H) and (ABC, H).

### 3. Comparison

In this section, we have compared the hardness of subjected materials with Randić and ABC indices. Figure 2 shows the comparison between the Randić index and hardness of the subjected materials given in Table 3. Figure 3 shows the comparison between the ABC index and hardness.

Figure 4 shows the comparison between the Randić index and ABC index of the subjected materials given in Figure 1.

Figure 5 shows the comparison between the hardness, Randić index, and ABC index of the subjected materials given in Figure 1.

#### 4. Conclusion and Discussion

We have investigated the association among the Randić index (RI), hardness of the crystal (HC), and atom-bond connectivity index (ABCI). For this purpose, the structural equation model (SEM) has been applied by the structure of three equations. Figures 6–8 show us the magnitude of the effectiveness of ABCI and HC over RI, of RI and HC over ABCI, and of ABCI and RI over HC, respectively. Figures 9–11 give us the tabular form of the magnitude of the effectiveness of ABCI and HC over RI as shown in Figure 6, of RI and HC over ABCI as shown in Figure 7, and of ABCI and RI over HC as shown in Figure 8, respectively. Estimates of three equations depict that ABCI is positively and significantly associated with RI, and 1 unit increase in ABCI improves 0.90 units of RI, while HC is positively and insignificantly related with RI. Negative and insignificant magnitude of HC is observed with ABCI. However, RI is positively and significantly related with ABCI. Contradictory results are observed about the impact of RI and ABCI on HC; both RI and ABCI are insignificantly linked with HC. In this article, we have started a new study which relates the hardness and topological indices of superhard crystals; which can contribute to some futuristic applications, and we encourage others to do more research in this area.

#### Data Availability

All the data used to support the findings of this study are included within the article.

#### Conflicts of Interest

The authors declare no conflicts of interest.

#### Authors' Contributions

All the authors contributed equally to this study. M. Naeem and A. Q. Baig completed all the computations, wrote the manuscript, and added all figures. X. Zhang checked and corrected the initial manuscript. M. A. Zahid added some final remarks and improved the overall paper. All authors read and approved the final draft.

#### Acknowledgments

This work was supported by the National Key Research and Development Program (Grant no. 2018YFB0904205).

#### References

- [1] F. Gao, J. He, E. Wu et al., "Hardness of covalent crystals," *Physical Review Letters*, vol. 91, no. 1, Article ID 015502, 2003.
- [2] Y. Tian, B. Xu, and Z. Zhao, "Microscopic theory of hardness and design of novel superhard crystals," *International Journal of Refractory Metals and Hard Materials*, vol. 33, pp. 93–106, 2012.
- [3] J. J. Gilman, "Flow of covalent solids at low temperatures," *Journal of Applied Physics*, vol. 46, no. 12, pp. 5110–5113, 1975.
- [4] R. Suzuki, T. Kishi, S. Tsukashima, M. Tachibana, K. Wako, and K. Kojima, "Hardness and slip systems of orthorhombic hen egg-white lysozyme crystals," *Philosophical Magazine*, vol. 96, no. 28, pp. 2930–2942, 2016.
- [5] R. Armstrong, S. Walley, and W. Elban, "Crystal indentation hardness," *Crystals*, vol. 7, no. 1, 21 pages, 2017.
- [6] A. A. Mamun, Y. Mohammed, T. T. Ava, G. Namkoong, and A. A. Elmustafa, "Influence of air degradation on morphology, crystal size and mechanical hardness of perovskite film," *Materials Letters*, vol. 229, pp. 167–170, 2018.
- [7] M. Shkir, V. Ganesh, S. AlFaify, A. Black, E. Dieguez, and K. K. Maurya, "Large size crystal growth, photoluminescence, crystal excellence, and hardness properties of in-doped cadmium zinc telluride," *Crystal Growth & Design*, vol. 18, no. 4, pp. 2046–2054, 2018.
- [8] M. N. Palatnikov, N. V. Sidorov, O. V. Makarova, S. L. Panasyuk, E. R. Kurkamgulova, and I. V. Yudin, "Relationship between the optical damage resistance and radiation hardness and the influence of threshold effects on the radiation hardness of ZnO-doped LiNbO<sub>3</sub> crystals," *Inorganic Materials*, vol. 54, no. 1, pp. 55–59, 2018.
- [9] J. C. Phillips, "Ionicity of the chemical bond in crystals," *Reviews of Modern Physics*, vol. 42, no. 3, pp. 317–356, 1970.
- [10] M. Randić, "Characterization of molecular branching," *Journal of the American Chemical Society*, vol. 97, no. 23, pp. 6609–6615, 1975.
- [11] B. Bollobás and P. Erdős, "Graphs of extremal weights," *Ars Combinatoria*, vol. 50, pp. 225–233, 1998.
- [12] D. Amić, D. Bešlić, B. Lučić, S. Nikolić, and N. Trinajstić, "The vertex-connectivity index revisited," *Journal of Chemical Information and Computer Sciences*, vol. 38, pp. 819–822, 1998.
- [13] K. Das, S. Balachandran, and I. Gutman, "Inverse degree, Randić index and harmonic index of graphs," *Applicable Analysis and Discrete Mathematics*, vol. 11, no. 2, pp. 304–313, 2017.
- [14] M. Milivojević and L. Pavlović, "The variation of the Randić index with regard to minimum and maximum degree," *Discrete Applied Mathematics*, vol. 217, pp. 286–293, 2017.
- [15] E. Estrada, L. Torres, L. Rodríguez, and I. Gutman, "An atom-bond connectivity index: modelling the enthalpy of formation of alkanes," *Indian Journal of Chemistry*, vol. 37(A), pp. 849–855, 1998.
- [16] D. Dimitrov, "On structural properties of trees with minimal atom-bond connectivity index IV: solving a conjecture about the pendent paths of length three," *Applied Mathematics and Computation*, vol. 313, pp. 418–430, 2017.
- [17] D. Dimitrov and N. Milosavljević, "Efficient computation of trees with minimal atom-bond connectivity index revisited," *MATCH Communications in Mathematical and in Computer Chemistry*, vol. 79, pp. 431–450, 2018.
- [18] W. Gao, Z. Iqbal, M. Ishaq, R. Sarfraz, M. Aamir, and A. Aslam, "On eccentricity-based topological indices study of a class of porphyrin-cored dendrimers," *Biomolecules*, vol. 8, no. 3, 71 pages, 2018.
- [19] W. Gao and W. F. Wang, "The fifth geometric-arithmetic index of bridge graph and carbon nanocones," *Journal of Difference Equations and Applications*, vol. 23, no. 1–2, pp. 100–109, 2016.
- [20] W. Gao and W. Wang, "The eccentric connectivity polynomial of two classes of nanotubes," *Chaos, Solitons & Fractals*, vol. 89, pp. 290–294, 2016.
- [21] W. Gao, W. Wang, D. Dimitrov, and Y. Wang, "Nano properties analysis via fourth multiplicative ABC indicator

- calculating,” *Arabian Journal of Chemistry*, vol. 11, no. 6, pp. 793–801, 2018.
- [22] W. Gao, H. Wu, M. K. Siddiqui, and A. Q. Baig, “Study of biological networks using graph theory,” *Saudi Journal of Biological Sciences*, vol. 25, no. 6, pp. 1212–1219, 2018.
- [23] J.-B. Liu, M. Siddiqui, M. Zahid, M. Naeem, and A. Baig, “Topological properties of crystallographic structure of molecules,” *Symmetry*, vol. 10, no. 7, 265 pages, 2018.
- [24] J.-B. Liu, I. Khalid, M. T. Rahim, M. U. Rehman, F. Ali, and M. Salman, “Eccentric topological properties of a graph associated to a finite dimensional vector space,” *Main Group Metal Chemistry*, vol. 43, no. 1, pp. 164–176, 2020.
- [25] Q. Li, H. Wang, Y. J. Tian et al., “Superhard and superconducting structures of  $BC_5$ ,” *Journal of Applied Physics*, vol. 108, 2010.
- [26] H. Liu, Q. Li, L. Zhu, and Y. Ma, “Superhard and superconductive polymorphs of diamond-like  $BC_3$ ,” *Physics Letters A*, vol. 375, no. 3, pp. 771–774, 2011.
- [27] H. Liu, Q. Li, L. Zhu, and Y. Ma, “Superhard polymorphs of diamond-like,” *Solid State Communications*, vol. 151, no. 9, pp. 716–719, 2011.
- [28] L. Xu, Z. Zhao, L.-M. Wang et al., “Prediction of a three-dimensional conductive superhard material: diamond-like  $BC_2$ ,” *The Journal of Physical Chemistry C*, vol. 114, no. 51, pp. 22688–22690, 2010.
- [29] L. Xu, Z. Zhao, Q. Wang et al., “Prediction of a superconductive superhard material: diamond-like  $BC_7$ ,” *Journal of Applied Physics*, vol. 110, no. 1, Article ID 013501, 2011.
- [30] Y. Yao, J. S. Tse, and D. D. Klug, “Crystal and electronic structure of superhard  $BC_5$ : first-principles structural optimizations,” *Physical Review B*, vol. 80, Article ID 094106, 2009.

## Research Article

# On Analysis and Computation of Degree-Based Topological Invariants for Cyclic Mesh Network

Nida Zahra,<sup>1</sup> Muhammad Ibrahim,<sup>1</sup> Muhammad Kamran Siddiqui,<sup>2</sup>  
and Hajar Shooshtri <sup>3</sup>

<sup>1</sup>Centre for Advanced Studies in Pure and Applied Mathematics, Bahauddin Zakariya University, Multan, Pakistan

<sup>2</sup>Department of Mathematics, Comsats University Islamabad, Lahore Campus, Islamabad, Pakistan

<sup>3</sup>Department of Mathematics, Azarbaijan Shahid Madani University, Tabriz, Iran

Correspondence should be addressed to Hajar Shooshtri; hajarshooshtri91@gmail.com

Received 31 May 2021; Accepted 9 July 2021; Published 15 July 2021

Academic Editor: Muhammad Kamran Jamil

Copyright © 2021 Nida Zahra et al. This is an open access article distributed under the Creative Commons Attribution License, which permits unrestricted use, distribution, and reproduction in any medium, provided the original work is properly cited.

Recently, there has been increasing attention on the system network due to its promising applications in parallel hanging architectures such as distributed computing (Day (2004), Day and Al-Ayyoub (2002)). Related networks differ in the circumstances of topology, and the descriptors were freshly examined by Hayat and Imran (2014) and Hayat et al. (2014). Distance-based descriptors, counting-related descriptors, and degree-based descriptors are all examples of topological descriptors. These topological characteristics are linked to chemical features of a substance, such as stability, strain energy, and boiling point. The specifications for the 1st Zagreb alpha, 1st Zagreb beta, 2nd Zagreb, sum-connectivity, geometric-arithmetic, Randic, harmonic, and atom-bond connectivity indices for mesh networks ( $MN_{m \times n}$ ) based on VE and EV degree are discussed in this paper.

## 1. Introduction

Cheminformatics is a relatively new field that combines chemistry, mathematics, and information science. Cheminformatics is primarily used to store, index, and retrieve information on chemicals. In index factors, graph theory is very essential. Biological activity is used as an introduction to numerous structural properties of molecules in the study of (QSAR) models. Topological indicators are a fascinating subset of these factors. Topological indices can be calculated using simply nodes (atoms) and edges in a graph representation (chemical bonds) [1, 2]. A series of numbers, a polynomial, or a numeric number can all be used to identify a graph. A complete graph is represented by numbers or an array, and for those graphs, these interpretations are supposed to be unique. The topological index is a mathematical term that belongs to a graph and is unaffected by graph automorphism. It identifies the structure of the graph. Degree-based topological indices, counting-related polynomials, and graph indices are some of the most common types of topological indices in [3, 4]. A topological index is a function “Top” from  $\Sigma$  to the set of real

numbers. Topological indicators in a network are, of course, the number of nodes and links present in the network. Numerous networks having an atomic or molecular structure, such as honeycomb, grid networks, and hexagonal, are comparable. Topological properties of this network are very interesting, which are studied in various aspects in [5, 6]. Hexagonal and honeycomb structures have also been identified as important in biological evolution, where intersecting triangles are critical for transmission of aid in societal problems, particularly for the development of collaboration [7, 8]. Appropriate research on this topic and further benefit from the new research findings are given in [9–12]. While working on paraffin breaking, Wiener’s approach [13] gave the impression of being a topological description. This identifier is known as the route number. After this, Wiener index is used to remember the route number. In terms of theory and practice, this topological descriptor served as the foundation for the topological index, see [14, 15] for details. Therefore, the topological lesions in the chemical and quantitative literature are Wiener, Zagreb, and Randic [16, 17]. By using the previous degree concepts, all of the above works were completed. In grid history, Chellali et al. [18] developed

two additional degree theories, namely, VE degrees and EV degrees, after some time. These concepts are a twist on the previous degree-based concept.

## 2. Preliminaries

In this section, we recall some fundamental definitions concerned to network which is usually represented by  $N = (P, C)$ , where  $P$  is the set of points and  $C$  is the set of connections of network. The degree of a point is the number of connections joined to that point. The open neighborhood, indicated as  $N(v)$ , for a point  $v$ , is written as  $N(v) = u \in P | u, v \in C$  in networks. If we add the point  $v$  to the set of  $N(v)$ , we get the same as the closed neighborhood of  $v$ , represented by  $N[v]$ . The number of connections that are connected to any points from the closed neighbourhood of  $v$  is equal to the vertex-edge degree, denoted by  $\phi_{ve}(v)$ , specified in [19], of the point  $v \in P$ . Furthermore, the number of points in the union of the closed neighbourhoods of  $u$  and  $v$  is equal to the edge-vertex degree of the connection  $e = uv \in C$ , indicated by  $\phi_e v(e)$  specified in [19]. Let  $N$  be a simple network and  $e = uv \in C(N)$ . The EV and VE degree topological descriptor-related details can be seen in [18, 19].

Consider  $N$  to be a basic network in all of the illustrations and  $v \in V(N)$ .

The Zagreb indices for edge-vertex degree are specified as

$$\mathcal{M}^{ev}(N) = \sum_{e \in C(N)} \phi_{ev}(e)^2. \quad (1)$$

The first Zagreb alpha indices for vertex-edge degree are specified as

$$\mathcal{M}_1^{\alpha ve}(N) = \sum_{u \in P(N)} \phi_{ve}(u)^2. \quad (2)$$

The first Zagreb beta indices for vertex-edge degree are specified as

$$\mathcal{M}_1^{\beta ve}(N) = \sum_{uv \in C(N)} (\phi_{ve}(u) + \phi_{ve}(v)). \quad (3)$$

The second Zagreb indices for vertex-edge degree are specified as

$$\mathcal{M}_2^{ve}(N) = \sum_{uv \in C(N)} (\phi_{ve}(u) \times \phi_{ve}(v)). \quad (4)$$

The Randic indices for vertex-edge degree are specified as

$$\mathcal{R}^{ve}(N) = \sum_{uv \in C(N)} (\phi_{ve}(u) \times \phi_{ve}(v))^{-1/2}. \quad (5)$$

The Randic indices for edge-vertex degree are specified as

$$\mathcal{R}^{ev}(N) = \sum_{e \in C(N)} \phi_{ve}(e)^{-1/2}. \quad (6)$$

The atom-bond connectivity indices for vertex-edge degree are specified as

$$\mathcal{BAC}^{ve}(N) = \sum_{uv \in C(N)} \sqrt{\frac{\phi_{ve}(u) + \phi_{ve}(v) - 2}{\phi_{ve}(u) \times \phi_{ve}(v)}}. \quad (7)$$

The geometric-arithmetic ( $ve - GA$ ) indices for vertex-edge degree are specified as

$$\mathcal{GA}^{ve}(N) = \sum_{uv \in C(N)} \frac{2\sqrt{\phi_{ve}(u) \times \phi_{ve}(v)}}{\phi_{ve}(u) + \phi_{ve}(v)}. \quad (8)$$

The harmonic ( $ve - H$ ) indices for vertex-edge degree are specified as

$$\mathcal{H}^{ve}(N) = \sum_{uv \in C(N)} \frac{2}{\phi_{ve}(u) + \phi_{ve}(v)}. \quad (9)$$

The sum-connectivity ( $ve - \chi$ ) indices for vertex-edge degree are specified as

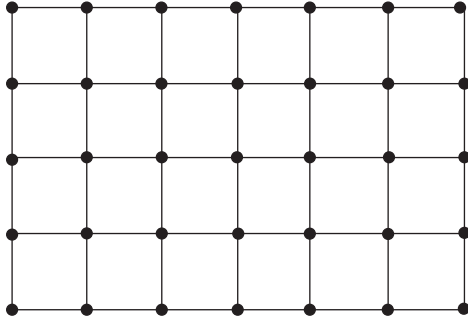
$$\chi^{ve}(N) = \sum_{uv \in C(N)} (\phi_{ve}(u) + \phi_{ve}(v))^{-1/2}. \quad (10)$$

## 3. Result for Mesh Network ( $MN_{m \times n}$ )

In this part, we calculate several mesh network ( $MN_{m \times n}$ ) topological indices based on EV and VE degree, seen in Figure 1. Let ( $MN_{m \times n}$ ) be a mesh network. ( $MN_{m \times n}$ ) has  $mn$  points and  $2mn - (m + n)$  connections. Table 1 shows how we partition the set of connections of ( $MN_{m \times n}$ ) into four components on the behalf of degrees of end points. Similarly, partition the collection of points into three components based on the degrees of points, as shown in Table 2.

Depending on the EV degree of the links of ( $MN_{m \times n}$ ) for  $n \geq 5$ , we separate them in Table 3 and partition the points and connections in Table 4 and Table 5 depending on the VE degree of ( $MN_{m \times n}$ ) for  $n \geq 5$ .

**3.1. Edge-Vertex Degree-Based Indices.** Now, we will calculate Zagreb and Randic indices for the mesh network ( $MN_{m \times n}$ ) depending on the EV degree.

FIGURE 1: Mesh network  $(MN)_{5 \times 7}$ .TABLE 1: Connection division of  $(MN)_{m \times n}$ .

No. of connections	$(\deg(u), \deg(v))$
8	(2, 3)
$2m + 2n - 12$	(3, 3)
$2m + 2n - 8$	(3, 4)
$2mn - 5m - 5n + 12$	(4, 4)

TABLE 2: Points partitioning of  $(MN)_{m \times n}$ .

No. of points	$\deg(u)$
4	2
$2(m + n - 4)$	3
$mn - 2(m + n) + 4$	4

TABLE 3: Link partitioning of  $(MN)_{m \times n}$ .

No. of connections	Degree of end points	EV degrees
8	(2, 3)	5
$2m + 2n - 12$	(3, 3)	6
$2m + 2n - 8$	(3, 4)	7
$2mn - 5(m + n) + 12$	(4, 4)	8

TABLE 4: Points partitioning of  $(MN)_{m \times n}$ .

No. of points	Degree (u)	VE degrees
4	2	6
8	3	9
$2(m + n) - 16$	3	10
4	4	14
$2(m + n) - 16$	4	15
$mn - 4(m + n) + 16$	4	16

TABLE 5: The VE degree of the end points of connections of  $(MN)_{m \times n}$ .

No. of connections	Degree of end points	VE degree of end points
8	(2, 3)	(6, 9)
8	(3, 3)	(9, 10)
$2(m + n) - 20$	(3, 3)	(10, 10)
8	(3, 4)	(9, 14)
$2(m + n) - 16$	(3, 4)	(10, 15)
8	(4, 4)	(14, 15)
$2(m + n) - 20$	(4, 4)	(15, 15)
$2(m + n) - 16$	(4, 4)	(15, 16)
$2mn - 9(m + n) + 40$	(4, 4)	(16, 16)

3.1.1. *Zagreb Index.* Employing Table 3, the Zagreb index is calculated as follows:

$$\begin{aligned} \mathcal{M}^{ev}(MN_{m \times n}) &= \sum_{e \in E(MN_{m \times n})} \phi_{ev}(e)^2, \\ \mathcal{M}^{ev}(MN_{m \times n}) &= 8 \times 5^2 + (2(m + n) - 12) \times 6^2 + (2(m + n) - 8) \times 7^2 + (2mn - 5(m + n) + 12) \times 8^2 \\ &= 200 + 72(m + n) - 432 + 98(m + n) - 392 + 128mn - 320(m + n) + 768 \\ &= 128mn - 150(m + n) + 144. \end{aligned} \quad (11)$$

3.1.2. *The Randic Index.* Employing Table 3, the Randic index is calculated as follows:

$$\begin{aligned} \mathcal{R}^{ev}(MN_{m \times n}) &= \sum_{e \in E(MN_{m \times n})} \phi_{ev}(e)^{-1/2}, \\ \mathcal{R}^{ev}(MN_{m \times n}) &= 8 \times 5^{-1/2} + (2(m + n) - 12) \times 6^{-1/2} + (2(m + n) - 8) \times 7^{-1/2} + (2mn - 5(m + n) + 12) \times 8^{-1/2} \\ &= \frac{1}{\sqrt{2}}mn + \left( \frac{2}{\sqrt{6}} + \frac{2}{\sqrt{7}} - \frac{5}{2\sqrt{2}} \right)(m + n) + \left( \frac{8}{\sqrt{5}} - \frac{12}{\sqrt{6}} - \frac{8}{\sqrt{7}} + \frac{6}{\sqrt{2}} \right) \\ &= 0.707mn - 0.195(m + n) - 0.102. \end{aligned} \quad (12)$$

3.2. *Vertex-Edge Degree-Based Indices.* Now, we will calculate the 1st Zagreb alpha, 1st Zagreb beta, 2nd Zagreb, geometric-arithmetic, sum-connectivity, Randic, harmonic, and atom-bond connectivity indices for the mesh network ( $MN_{m \times n}$ ) depending on VE.

3.2.1. *The 1st Zagreb Alpha Index.* Employing Table 4, the 1st Zagreb alpha index is calculated as follows:

$$\begin{aligned} \mathcal{M}_1^{\alpha ve}(MN_{m \times n}) &= \sum_{u \in V(MN_{m \times n})} \phi_{ve}(u)^2, \\ \mathcal{M}_1^{\alpha ve}(MN_{m \times n}) &= 4 \times 6^2 + 8 \times 9^2 + (2(m+n) - 16) \times 10^2 + 4 \times 14^2 + (2(m+n) - 16) \times 15^2 + (mn - 4(m+n) + 16) \times 16^2 \\ &= 144 + 648 + 200(m+n) - 1600 + 784 + 450(m+n) - 3600 + 256mn - 1024(m+n) + 4096 \\ &= 256mn - 374(m+n) + 472. \end{aligned} \tag{13}$$

3.2.2. *The 1st Zagreb Beta Index.* Employing Table 5, the 1st Zagreb beta index is calculated as follows:

$$\begin{aligned} \mathcal{M}_1^{\beta ve}(MN_{m \times n}) &= \sum_{uv \in E(MN_{m \times n})} (\phi_{ve}(u) + \phi_{ve}(v)), \\ \mathcal{M}_1^{\beta ve}(MN_{m \times n}) &= 8 \times 15 + 8 \times 19 + (2(m+n) - 20) \times 20 + 8 \times 23 + (2(m+n) - 16) \times 25 + 8 \times 29 \\ &\quad + (2(m+n) - 20) \times 30 + (2(m+n) - 16) \times 31 + (2mn - 9(m+n) + 40) \times 32 \\ &= 120 + 152 + 40(m+n) - 400 + 184 + 50(m+n) - 400 + 232 + 60(m+n) - 600 \\ &\quad + 62(m+n) - 496 + 64mn - 288(m+n) + 1280 \\ &= 64mn - 76(m+n) + 72. \end{aligned} \tag{14}$$

3.2.3. *The 2nd Zagreb Index.* Employing Table 5, the 2nd Zagreb index is calculated as follows:

$$\begin{aligned} \mathcal{M}_2^{ve}(MN_{m \times n}) &= \sum_{uv \in E(MN_{m \times n})} (\phi_{ve}(u) \times \phi_{ve}(v)), \\ \mathcal{M}_2^{ve}(MN_{m \times n}) &= 8 \times 54 + 8 \times 90 + (2(m+n) - 20) \times 100 + 8 \times 126 + (2(m+n) - 16) \times 150 \\ &\quad + 8 \times 210 + (2(m+n) - 20) \times 225 + (2(m+n) - 16) \times 240 + (2mn - 9(m+n) + 40) \times 256 \\ &= 432 + 720 + 200(m+n) - 2000 + 1008 + 300(m+n) - 2400 + 1680 + 450(m+n) \\ &\quad - 4500 + 480(m+n) - 3840 + 512mn - 2304(m+n) + 10240 \\ &= 512mn - 874(m+n) + 1340. \end{aligned} \tag{15}$$

3.2.4. *The Randic Index.* Employing Table 5, the Randic index is calculated as follows:

$$\begin{aligned}
\mathcal{R}^{ve}(MN_{m \times n}) &= \sum_{uv \in E(MN_{m \times n})} (\phi_{ve}(u) \times \phi_{ve}(v))^{-(1/2)}, \\
\mathcal{R}^{ve}(MN_{m \times n}) &= 8 \times 54^{-(1/2)} + 8 \times 90^{-(1/2)} + (2(m+n) - 20) \times 100^{-(1/2)} + 8 \times 126^{-(1/2)} \\
&\quad + (2(m+n) - 16) \times 150^{-(1/2)} + 8 \times 210^{-(1/2)} + (2(m+n) - 20) \times 225^{-(1/2)} \\
&\quad + (2(m+n) - 16) \times 240^{-(1/2)} + (2mn - 9(m+n) + 40) \times 256^{-(1/2)} \\
&= \frac{1}{8}mn + \left( \frac{1}{5} + \frac{2}{5\sqrt{6}} + \frac{2}{15} + \frac{1}{2\sqrt{15}} - \frac{9}{16} \right) (m+n) \\
&\quad + \left( \frac{8}{3\sqrt{6}} + \frac{8}{3\sqrt{10}} - 2 + \frac{8}{3\sqrt{14}} - \frac{16}{5\sqrt{6}} + \frac{8}{\sqrt{210}} - \frac{4}{3} - \frac{4}{\sqrt{15}} + \frac{5}{2} \right) \\
&0.125mn + 0.063(m+n) + 0.0241.
\end{aligned} \tag{16}$$

3.2.5. *The Atom-Bond Connectivity Index.* Employing Table 5, we calculate the above said index as follows:

$$\begin{aligned}
\mathcal{BC}^{ve}(MN_{m \times n}) &= \sum_{uv \in E(MN_{m \times n})} \sqrt{\frac{\phi_{ve}(u) + \phi_{ve}(v) - 2}{\phi_{ve}(u) \times \phi_{ve}(v)}}, \\
\mathcal{BC}^{ve}(MN_{m \times n}) &= 8 \times \sqrt{\frac{15-2}{54}} + 8 \times \sqrt{\frac{19-2}{90}} + (2(m+n) - 20) \times \sqrt{\frac{20-2}{100}} + 8 \times \sqrt{\frac{23-2}{126}} \\
&\quad + (2(m+n) - 16) \times \sqrt{\frac{25-2}{150}} + 8 \times \sqrt{\frac{29-2}{210}} + (2(m+n) - 20) \times \sqrt{\frac{30-2}{225}} \\
&\quad + (2(m+n) - 16) \times \sqrt{\frac{31-2}{240}} + (2mn - 9(m+n) + 40) \times \sqrt{\frac{32-2}{256}} \\
&= \frac{\sqrt{30}}{8}mn + \left( \frac{3\sqrt{2}}{5} + \frac{2\sqrt{23}}{5\sqrt{6}} + \frac{4\sqrt{7}}{15} + \frac{\sqrt{29}}{2\sqrt{15}} - \frac{9\sqrt{30}}{16} \right) (m+n) \\
&\quad + \left( \frac{8\sqrt{13}}{3\sqrt{6}} + \frac{8\sqrt{17}}{3\sqrt{10}} - 6\sqrt{2} + \frac{8\sqrt{3}}{3\sqrt{2}} - \frac{16\sqrt{23}}{5\sqrt{6}} + \frac{24}{\sqrt{70}} - \frac{4\sqrt{28}}{3} - \frac{4\sqrt{29}}{\sqrt{15}} + \frac{5\sqrt{30}}{2} \right) \\
&= 0.68mn - 0.048(m+n) - 0.138.
\end{aligned} \tag{17}$$

3.2.6. *The Geometric-Arithmetic Index.* Employing Table 5, the above said index is calculated as follows:

$$\begin{aligned}
\mathcal{GA}^{ve}(MN_{m \times n}) &= \sum_{uv \in E(MN_{m \times n})} \frac{2\sqrt{\phi_{ve}(u) \times \phi_{ve}(v)}}{\phi_{ve}(u) + \phi_{ve}(v)}, \\
\mathcal{GA}^{ve}(MN_{m \times n}) &= 8 \times \frac{2\sqrt{54}}{15} + 8 \times \frac{2\sqrt{90}}{19} + (2(m+n) - 20) \times \frac{2\sqrt{100}}{20} + 8 \times \frac{2\sqrt{126}}{23} \\
&\quad + (2(m+n) - 16) \times \frac{2\sqrt{150}}{25} + 8 \times \frac{2\sqrt{210}}{29} + (2(m+n) - 20) \times \frac{2\sqrt{225}}{30} \\
&\quad + (2(m+n) - 16) \times \frac{2\sqrt{240}}{31} + (2mn - 9(m+n) + 40) \times \frac{2\sqrt{256}}{32} \\
&= 2mn + \left( 2 + \frac{4\sqrt{6}}{5} + 2 + \frac{16\sqrt{15}}{31} - 9 \right) (m+n) \\
&\quad + \left( \frac{16\sqrt{6}}{5} + \frac{48\sqrt{10}}{19} - 20 + \frac{48\sqrt{14}}{23} - \frac{32\sqrt{6}}{5} + \frac{16\sqrt{210}}{29} - 20 - \frac{128\sqrt{15}}{31} + 40 \right) \\
&= 2mn - 1.041(m+n) - 0.037.
\end{aligned} \tag{18}$$

3.2.7. *The Harmonic Index.* Employing Table 5, the harmonic index is calculated as follows:

$$\begin{aligned}
\mathcal{H}^{ve}(MN_{m \times n}) &= \sum_{uv \in E(MN_{m \times n})} \frac{2}{\phi_{ve}(u) + \phi_{ve}(v)}, \\
\mathcal{H}^{ve}(MN_{m \times n}) &= 8 \times \frac{2}{15} + 8 \times \frac{2}{19} + (2(m+n) - 20) \times \frac{2}{20} + 8 \times \frac{2}{23} + (2(m+n) - 16) \times \frac{2}{25} + 8 \times \frac{2}{29} \\
&\quad + (2(m+n) - 20) \times \frac{2}{30} + (2(m+n) - 16) \times \frac{2}{31} + (2mn - 9(m+n) + 40) \times \frac{2}{32} \\
&= \frac{1}{8}mn + \left( \frac{1}{5} + \frac{4}{25} + \frac{2}{15} + \frac{4}{31} - \frac{9}{16} \right) (m+n) \\
&\quad + \left( \frac{16}{15} + \frac{16}{19} - 2 + \frac{16}{23} - \frac{32}{25} + \frac{16}{29} - \frac{4}{3} - \frac{32}{\sqrt{31}} + \frac{5}{2} \right) \\
&= 0.125mn + 0.063(m+n) + 0.0241.
\end{aligned} \tag{19}$$

3.2.8. *The Sum-Connectivity Index.* Employing Table 5, the sum-connectivity index is calculated as follows:

$$\begin{aligned} \chi^{ve}(MN_{m \times n}) &= \sum_{uv \in E(MN_{m \times n})} (\phi_{ve}(u) + \phi_{ve}(v))^{-(1/2)}, \\ \chi^{ve}(MN_{m \times n}) &= 8 \times 15^{-(1/2)} + 8 \times 19^{-(1/2)} + (2(m+n) - 20) \times 20^{-(1/2)} + 8 \times 23^{-(1/2)} + (2(m+n) - 16) \times 25^{-(1/2)} \\ &\quad + 8 \times 29^{-(1/2)} + (2(m+n) - 20) \times 30^{-(1/2)} + (2(m+n) - 16) \times 31^{-(1/2)} \\ &\quad + (2mn - 9(m+n) + 40) \times 32^{-(1/2)} \\ &= \frac{1}{2\sqrt{2}}mn + \left( \frac{1}{\sqrt{5}} + \frac{2}{5} + \frac{2}{\sqrt{30}} + \frac{2}{\sqrt{31}} - \frac{9}{4\sqrt{2}} \right) (m+n) \\ &\quad + \left( \frac{8}{\sqrt{15}} + \frac{8}{\sqrt{19}} - \frac{10}{\sqrt{5}} + \frac{8}{\sqrt{23}} - \frac{16}{5} + \frac{8}{\sqrt{29}} - \frac{20}{\sqrt{30}} - \frac{16}{\sqrt{31}} + \frac{10}{\sqrt{2}} \right) \\ &= 0.3533mn - 0.0194(m+n) - 0.071. \end{aligned} \tag{20}$$

#### 4. Conclusion

It's crucial to explore the structure using graphs, and topological indicators are crucial for grasping the network's core topology. This sort of analysis has a wide range of applications in computer science, where different indexes based on graph invariance are used to evaluate multiple stimulation summaries. Invariants stats are essential factors for analyzing and predicating the features of chemical structures in the quantitative structure-property relationship (QSPR) and quantitative structure-activity relationship (QSAR) explorations. We offer several finished products for VE degree and EV degree-based indices, such as the indices depending on the vertex-edge degree are the 1st Zagreb alpha, 1st Zagreb beta, 2nd Zagreb, geometric-arithmetic, sum-connectivity, Randic, harmonic, and atom-bond connectivity indices, in this article, for the mesh network ( $MN_{m \times n}$ ), and EV degree Randic and Zagreb indices. There will be some who are involved in designing new grids in the future, and we are examining their topological indices in order to grasp their core topology.

#### Data Availability

The data used to support the findings of this study are cited at relevant places within the text as references.

#### Conflicts of Interest

The authors declare that they have no conflicts of interest.

#### Authors' Contributions

All authors contributed equally to this work.

#### References

- [1] K. Day, "Optical transpose  $k$ -ary  $n$ -cube networks," *Journal of Systems Architecture*, vol. 50, no. 11, pp. 697–705, 2004.
- [2] K. Day and A.-E. Al-Ayyoub, "Topological properties of OTIS-networks," *IEEE Transactions on Parallel and Distributed Systems*, vol. 13, no. 4, pp. 359–366, 2002.
- [3] P. Manuel, R. Bharati, I. Rajasingh, and C. Monica, "On minimum metric dimension of honeycomb networks," *Journal of Discrete Algorithms*, vol. 6, no. 1, pp. 20–27, 2008.
- [4] P. Manuel and I. Rajasingh, "Minimum metric dimension of silicate networks," *Ars Combinatoria*, vol. 98, pp. 501–510, 2011.
- [5] P. Manuel and I. Rajasingh, "Topological properties of silicate networks," in *Proceedings of the 2009 5th IEEE GCC Conference & Exhibition*, vol. 15, pp. 15–25, Kuwait City, Kuwait, March 2009.
- [6] B. Rajan, A. William, C. Grigorious, and S. Stephen, "On certain topological indices of silicate, honeycomb and hexagonal networks," *Journal of Mathematics and Computer Science*, vol. 5, pp. 530–535, 2012.
- [7] S. Hayat and M. Imran, "Computation of topological indices of certain networks," *Applied Mathematics and Computation*, vol. 240, pp. 213–228, 2014.
- [8] S. Hayat, M. Imran, and M. Y. H. Maillk, "On topological indices of certain interconnection networks," *Applied Mathematics and Computation*, vol. 244, pp. 936–951, 2014.
- [9] M. Perc, J. Gómez-Gardeñes, A. Szolnoki, L. M. Floría, and Y. Moreno, "Evolutionary dynamics of group interactions on structured populations: a review," *Journal of the Royal Society, Interface*, vol. 10, 2013.
- [10] M. Perc and A. Szolnoki, "Coevolutionary games-a mini review," *BioSystems*, vol. 99, no. 2, pp. 109–125, 2010.
- [11] A. Szolnoki, M. Perc, and G. Szabó, "Topology-independent impact of noise on cooperation in spatial public goods games," *Physical Review. E, Statistical, Nonlinear, and Soft Matter Physics*, vol. 80, pp. 56109–56166, 2009.
- [12] Z. Wang, A. Szolnoki, and M. Perc, "If players are sparse social dilemmas are too: importance of percolation for evolution of cooperation," *Scientific Reports*, vol. 2, no. 1, pp. 369–379, 2012.
- [13] H. Wiener, "Structural determination of paraffin boiling points," *Journal of the American Chemical Society*, vol. 69, no. 1, pp. 17–20, 1947.
- [14] A. A. Dobrynin, R. Entringer, and I. Gutman, "Wiener index of trees: theory and applications," *Acta Applicandae Mathematicae*, vol. 66, no. 3, pp. 211–249, 2001.

- [15] I. Gutman and O. E. Polansky, *Mathematical Concepts in Organic Chemistry*, Springer-Verlag, New York, NY, USA, 1986.
- [16] Y. Li, F. Li, Z. Zhou, and Z. Chen, "SiC<sub>2</sub> silagraphene and its one-dimensional derivatives: where planar tetracoordinate silicon happens," *Journal of the American Chemical Society*, vol. 133, no. 4, pp. 900–908, 2010.
- [17] L.-J. Zhou, Y.-F. Zhang, and L.-M. Wu, "SiC<sub>2</sub> siligraphene and nanotubes: novel donor materials in excitonic solar cells," *Nano Letters*, vol. 13, no. 11, pp. 5431–5436, 2013.
- [18] M. Chellali, T. W. Haynes, S. T. Hedetniemi, and T. M. Lewis, "On ve-degrees and ev-degrees in graphs," *Discrete Mathematics*, vol. 340, no. 2, pp. 31–38, 2017.
- [19] M. Cancan, "On edge-vertex degree and vertex-edge degree topological properties of tickysim spiking neural network," *Computational Intelligence and Neuroscience*, vol. 8, pp. 11–31, 2019.